Universitat Autònoma de Barcelona

Novel therapeutic approaches for Cutaneous Lupus Erythematosus (CLE): The role of microRNAs and Thalidomide

Sandra Domingo Bover

Novel therapeutic approaches for Cutaneous Lupus Erythematosus (CLE): The role of microRNAs and Thalidomide

Doctoral Thesis presented by

Sandra Domingo Bover

To obtain the degree of

Doctor for the Universitat Autònoma de Barcelona

Doctoral thesis performed at Vall d'Hebron Institut de Recerca (VHIR) under the supervision of

Dr. Josefina Cortés-Hernández

Universitat Autònoma de Barcelona, February 2022

Dra. Josefina Cortes-Hernández (Director)

Sandra Domingo (PhD Student)

Dra. Anna Meseguer (Tutor)

Universitat Autònoma de Barcelona

Vall d'Hebron Institut de Recerca VHIR

Vall d'Hebron

“¿Fronteras? Nunca he visto una. Pero he oído que existen en la mente de algunas personas.”

— Thor Heyerdahl

CONTENTS

ABSTRACT

Cutaneous Lupus Erythematosus (CLE) is a chronic autoimmune disease that includes heterogenous cutaneous manifestations and can be presented as an individual disease or as a manifestation of Systemic Lupus Erythematosus (SLE). CLE pathogenesis is multifactorial and involves genetic predisposition, environmental factors and immune response abnormalities. However, etiology of CLE still remains unknown as well as the complete pathological and molecular mechanisms of CLE subtypes: Subacute Cutaneous Lupus Erythematosus (SCLE) and Discoid Lupus Erythematosus (DLE) which are the most prevalent forms, and despite sharing histological similarities, clinically they differ in their course and prognosis, suggesting different pathogenesis. The fact that the mechanisms in CLE pathogenesis are currently unknown, implies that therapeutic options for this condition do not include approved specific drugs and need to be empirically determined for individual patients. Thalidomide, is an highly effective drug for CLE, showing clinical efficacy that ranges between 80-90%. However its use is restricted due to its important side effects such as teratogenicity and peripheral neuropathy. Therefore, an enhanced understanding of the molecular and genetic basis of the disease as well as thalidomide mechanism of action is a requirement to improve the search for novel therapeutic targets.

In this project, the chapter 1 has been focused in exploring the role of miRNAs in CLE. MicroRNAs, are small noncoding RNAs that regulate numerous cellular processes in normal physiological conditions and in disease they may be deregulated, promoting aberrant gene expression. By performing a microarray in CLE lesional skin and non-lesional skin from paired patients we have found that the DLE subtype presents a specific miRNA signature compared with SCLE. miR-31 and miR-485-3p have been identified as a miRNAs upregulated in DLE lesional skin and their role has been examined by *in vitro* experiments: miR-31 promotes NF-κB dependent epidermal inflammation and apoptosis, whereas miR-485-3p promotes T cell activation and fibrosis. Next, focusing on the common deregulated miRNAs in CLE (including both DLE and SCLE) we have found that miR-885-5p is downregulated and it promotes epidermal proliferation and also inflammation through PSMB5 and posterior NF-κB upregulation, and immune recruitment through TRAF1.

Next on chapter 2, the role of thalidomide has been examined by performing RNA sequencing in skin biopsies from paired patients before and after receiving thalidomide treatment together with system biology analysis and we have found that it may act by modulating de acts via two CRBN-CRL4A dependent pathways: IRF4/NF-κB and AMPK1/mTOR,

Finally on chapter 3, microRNA expression has been examined after thalidomide and we have found that miR-31 and miR-885-5p, keratinocyte derived microRNAs that regulate NF-κB are modulated in both skin from responder patients treated with thalidomide and *in vitro* with primary cells treated with thalidomide.

Taken together, our findings provide insights into molecular pathogenetic mechanism in CLE and in DLE subtype, as well as molecular mechanism of action of thalidomide in CLE. Novel therapeutic targets have been identified such as the discovered miRNAs or the molecular pathways affected by thalidomide. Moreover, both miRNAs and thalidomide affect NF-κB pathway, highlighting that this pathway is crucial in CLE and support the further study of NF-κB signaling as novel a therapeutic target for CLE.

RESUMEN

El lupus eritematoso cutáneo (LEC) es una enfermedad autoinmune crónica que incluye manifestaciones heterogéneas y puede presentarse como una entidad individual o como una manifestación de lupus eritematoso sistémico (LES). La patogénesis del LEC es multifactorial e intervienen la predisposición genética, los factores ambientales y las anomalías de la respuesta inmune. Sin embargo, la etiología del LEC sigue siendo desconocida, así como los mecanismos patológicos y moleculares completos de sus subtipos más prevalentes: Lupus Eritematoso Cutáneo Subagudo (LSA) y Lupus Eritematoso Discoide (LED) que pesar de compartir similitudes histológicas, clínicamente difieren en su curso y pronóstico, lo que sugiere una patogénesis diferente. El hecho de que los mecanismos en la patogénesis del LEC sean actualmente desconocidos, implica que las opciones terapéuticas para esta afección no incluyan fármacos específicos aprobados y deban determinarse empíricamente para cada paciente. La talidomida, es un fármaco muy eficaz para el LEC, con una eficacia clínica que oscila entre el 80-90%. Sin embargo, su uso está restringido debido a sus importantes efectos secundarios, como la teratogenicidad y la neuropatía periférica. Es necesario conocer mejor las bases moleculares y genéticas del LEC, así como el mecanismo de acción de la talidomida, para la identificación de nuevas dianas terapéuticas.

En este proyecto, el capítulo 1 se ha centrado en explorar el papel de los miRNAs en el LEC. Los microRNAs, son pequeños RNAs no codificantes que regulan numerosos procesos celulares en condiciones fisiológicas normales y pueden estar desregulados, promoviendo una expresión génica aberrante. Mediante la realización de un microarray en la piel lesional y no lesional de pacientes con LEC, se ha hallado que el Lupus Discoide presenta un perfil específico de miRNAs en comparación con el Lupus Subagudo. El miR-31 y miR-485-3p han sido identificados como miRNAs regulados al alza en la piel lesional del LEC y su papel ha sido examinado mediante experimentos *in vitro*: el miR-31 promueve la inflamación epidérmica dependiente de NF-κB y la apoptosis, mientras que miR-485-3p promueve la activación de las células T y la fibrosis. A continuación, centrándonos en los miRNAs comúnmente desregulados en el LEC (incluyendo tanto el LED como el LSA), el miR-885-5p está desregulado y promueve la proliferación epidérmica y también la inflamación a través de PSMB5 y la posterior regulación de NF-κB, y el reclutamiento de leucocitos a través de TRAF1.

A continuación, en el capítulo 2, se ha examinado el papel de la talidomida realizando la secuenciación de ARN en biopsias de piel de pacientes pre y post tratados con talidomida junto con un análisis de biología de sistemas y se ha descubierto que actúa modulando dos vías dependientes de CRBN-CRL4A: IRF4/NF-κB y AMPK1/mTOR,

Por último, en el capítulo 3, se ha examinado la relación de la talidomida con los microARN de interés y hemos descubierto que el miR-31 y miR-885-5p, que regulan el NF-κB, están modulados tanto en la piel de pacientes respondedores tratados con talidomida como *in vitro* con queratinocitos primarios tratados con talidomida.

En conjunto, nuestros hallazgos proporcionan información sobre el mecanismo patogénico molecular en el LEC y en el subtipo de LED, así como el mecanismo molecular de acción de la talidomida en el LEC. Se han identificado nuevas dianas terapéuticas, como los miRNAs descubiertos o las vías moleculares afectadas por la talidomida. Además, tanto los miRNAs como la talidomida afectan a la vía del NF-κB, destacando que esta vía es crucial en el LEC y apoyando el estudio de la señalización del NF-κB como nueva diana terapéutica para el LEC.

LIST OF INCLUDED PUBLICATIONS

1. Solé C, **Domingo S**, Ferrer B, Moliné T, Ordi-Ros J, Cortés-Hernández J. MicroRNA Expression Profiling Identifies miR-31 and miR-485-3p as Regulators in the Pathogenesis of Discoid Cutaneous Lupus. *J Invest Dermatol*. **2019**; 139 :51-61.

2. **Domingo S**, Solé C, Moliné T, Ferrer B, Cortés-Hernández J. MicroRNA-885-5p is downregulated in Cutaneous Lupus Erythematosus lesions and promotes epidermal inflammation and proliferation via PSMB5 and immune recruitment via TRAF1. (Manuscript in revision)

3. Domingo S, Solé C, Moliné T, Ferrer B, Cortés-Hernández J. Thalidomide exerts anti-inflammatory effects in cutaneous lupus by inhibiting the IRF4/NF-κB and AMPK1/mTOR pathways. *Biomedicines.* **2021;** Dec 7;9:1857.

LIST OF RELATED PUBLICATIONS (Annex 5)

1. Domingo S, Solé C, Moliné T, Ferrer B, Cortés-Hernández J. MicroRNAs in Several Cutaneous Autoimmune Diseases: Psoriasis, Cutaneous Lupus Erythematosus and Atopic Dermatitis. *Cells*. **2020**; 9:2656.

2. Domingo S, Solé C, Moliné T, Ferrer B, Ordi-Ros J, Cortés-Hernández J. Efficacy of Thalidomide in Discoid Lupus Erythematosus: Insights into the Molecular Mechanisms. *Dermatology*. **2020**; 236:467-476.

ABREVIATIONS

ACLE: Acute Cutaneous Lupus
AGO: Argonaute
AID: Activation-induced cytidine deaminase
AMPK: AMP-activated protein kinase
ANA: Antinuclear Antibodies
Anti-dsDNA: Anti-double strand DNA
Anti-RNP: Antinuclear Ribonucleoprotein
Anti-SM: Anti-Smith
BAFF: B cell activating factor
Blimp-1: B lymphocyte-induced maturation protein-1
BLyS: B lymphocyte stimulator
BSA: Bovine Serum Albumin
C1qA: Complement C1q Subcomponent Subunit A
C3: Complement component 3
C4: Complement component 4
CCLE: Chronic Cutaneous Lupus
Cereblon: CRBN
cGAMP: Cyclic guanosine monophosphate–adenosine monophosphate.
cGAS: Cyclic GMP-AMP Synthase
ChLE: Chilblain Lupus Erythematosus
CI: Calcineurin inhibitors
CK1: Casein kinase 1A1
CLASI: Cutaneous Lupus Activity and Severity Index
CLE: Cutaneous Lupus Erythematosus
CQ: Chloroquine
CRL4A: CUL4–RBX1–DDB1 complex
$CRL4^{CRBN}$: CRL4 CRBN E3 ubiquitin ligase complex
CS: Corticosteroids
Ct: Cycle Threshold
CTLA4: Cytotoxic T-Lymphocyte Associated Protein 4
CTLS: Cytotoxic T Lymphocytes
CUL4: Cullin-4A
DCs: Dendritic Cells
DDB1: Damage-specific DNA-binding protein 1
DEGs: differentially expressed genes
DGCR8: DiGeorge syndrome critical region gene 8
DI-SCLE: Drug Induced Subacute Cutaneous Lupus Erythematosus
DIF: Direct Immunofluorescence
DLE: Discoid Lupus Erythematosus

DMRs: Differentially Methylated Regions
DMSO: Dimethyl sulfoxide
DNA: Deoxyribonucleic Acid
EC-MPS: Enteric-coated mycophenolate sodium
EUSCLE: European Society of Cutaneous Lupus Erythematosus
FFPE: Formalin-Fixed Paraffin-Embedded
FLOT1: Flotillin 1
FPKM: fragments per kb per million
GM-CSF: Granulocyte-macrophage colony-stimulating factor
GSPT1: G1 To S Phase Transition 1 protein
GWAS: Genome-Wide Association Studies
HCQ: Hydroxychloroquine
HEKa: Healthy primary human epidermal adult Keratinocytes
HLA: Human Lymphocyte Antigen
HMGB1: High-mobility group box 1
IFN: Interferon
Ig: Immunoglobulin
IκB: I kappa B alpha (NFκBI inhibitor)
IKZF1: Ikaros
IKZF3: Aiolos
IL: Interleukin
IMiDs: Immunomodulatory Drugs
iNKT: Invariant Natural Killer
IRF: Interferon Regulatory Factor
ITGAM: Integrin Subunit Alpha M
KCs: Keratinocytes
LCs: Langerhans cells
LE: Lupus Erythematosus
LEP: Lupus Erythematosus Profundus
LET: Lupus Erythematosus Tumidus
MDSC: Myeloid derived suppressor cells
MHC: Major Histocompatibility Complex
MICA: MHC Class I Polypeptide-Related Sequence A
MICB: MHC Class I Polypeptide-Related Sequence B
miRISC: miRNA-induced silencing complex
miRNAs: MicroRNAs
miRs: MicroRNAs
MM: Multiple Myeloma
MMF: Mycophenolate mofetil
MoA: Mechanism of action
mRNA: Messenger RNA

MSH5: MutS Homolog 5
mTOR: Mammalian target of rapamycin
MTX: Methotrexate
NET: Neutrophil Extracellular Trap
NF-κB: Nuclear factor kappa-light-chain-enhancer of activated B cells
NFKBAI: Nuclear Factor Of Kappa Light Polypeptide Gene Enhancer In B-Cells Inhibitor Alpha (IκBα)
NK: Natural Killer
NSAIDS: Non-Steroidal Anti-Inflammatory Drugs
NT: Nucleotide
OCT: Optimal cutting temperature compound
p63:Tumor protein p63
PAS: Periodic Acid-Schiff
PBMCs: Peripheral blood mononuclear cells
PBS: Phosphate buffered saline
PCR: Polymerase chain reaction
pDCs: Plasmacytoid Dendritic cells
PKC-θ : Protein kinase C delta
PMNCs: Polymorphonuclear Neutrophil cells
Pol II: polymerase II
PSMB5: Proteasome 20S Subunit Beta 5
RBX1: RING-box protein 1
RCTs: Randomised Clinical Trials
RISC: RNA-induced silencing complex
RT: Reverse Transcription
Sall4: Sal-like protein 4
SCLE: Subacute Cutaneous Lupus
SLE: Systemic Lupus Erythematosus
SNP: Single-nucleotide polymorphism
SPF: Sun Protective Factor
SSC: Saline- Sodium Citrate
ssDNA: single stranded DNA
shRNA: short hairpin RNA
siRNA: short interfering RNA
STAT: Signal Transducer And Activator Of Transcription
STING: Stimulator of Interferon Response CGAMP Interactor 1
TGF- β: Transforming Growth Factor-β
Th: Thalidomide
Th1: T helper 1
Th2: T helper 2
TLRs: Toll-like receptors

TMPS: Therapeutic Performance Mapping System
TNFR: TNF receptor
TNFα: Tumor Necrosis Factor Alpha
TRAF: TNF receptor associated factor
TRAF1: TNF Receptor Associated Factor 1
TRAIL: TNF-related apoptosis-inducing ligand
Tregs: Regulatory T cells
TREX1: Three Prime Repair Exonuclease 1
TYK2: Tyrosine Kinase
USA: United States of America
UTR: Untranslated region
UV: Ultraviolet
VEGF: Vascular endothelial growth factor
VGLL3: vestigial-like family member 3

1. Introduction

1.1 The Structure and Function of Skin

1.1.1 Skin definition and function

Skin is the largest organ of the human body with a surface that measures around 1.5-2m^2, a thickness of 0.5-4 mm and weights approximately the 15 percent of total body weight in adults [1] (Fig 1). It provides an effective barrier between the organism and the environment [2,3] .

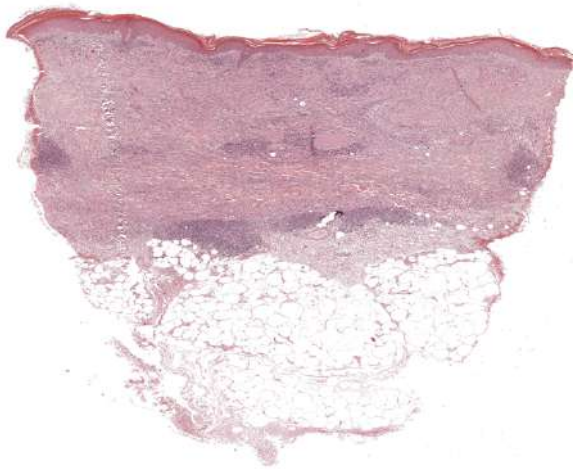

Figure 1. A whole slide image of hematoxylin and eosin staining in human skin. Modified from Kleczek et al. [4]

The skin main function is to act as a protective barrier against infection and mechanical and chemical injuries.

Other important functions include [5,6]

Maintenance of hydrolytic balance: It helps reducing water loss with the water-impermeable stratum corneum.

- Photoprotection: Skin pigment melanin protects the body from damage caused by UV (Ultraviolet) radiation caused by sun exposure.
- Sensory perception: Skin is enriched with free nerve endings and end corpuscles.
- Thermoregulation: Regulation of heat loss is achieved by vasodilatation and vasoconstriction and by the sweat produced by eccrine sweat glands.
- Vitamin D synthesis: The epidermis is the major source of vitamin D for the body. It contributes to bone formation, calcium metabolism, and immune regulation.
- Immunologic surveillance: Skin is infiltrated by immune cells that initiate immune responses against pathogens. Also, cells that are present in the skin are able to

secrete anti-microbial peptides that are active against a variety of bacteria, viruses and fungi and the sweat-derived peptide dermcidin has been shown to have potent anti-microbial activity.

- Self-regeneration: Skin has a regenerative capacity that is of vital importance in case of burns and trauma. It has a vast reserve of stem and progenitor cells that are able to repair wounds and the injured body surface.

1.1.2 Skin structure and cell types

The skin consists of three separated but functionally dependent layers, from the outermost to the innermost are the following: epidermis, dermis, and hypodermis (Fig 2).

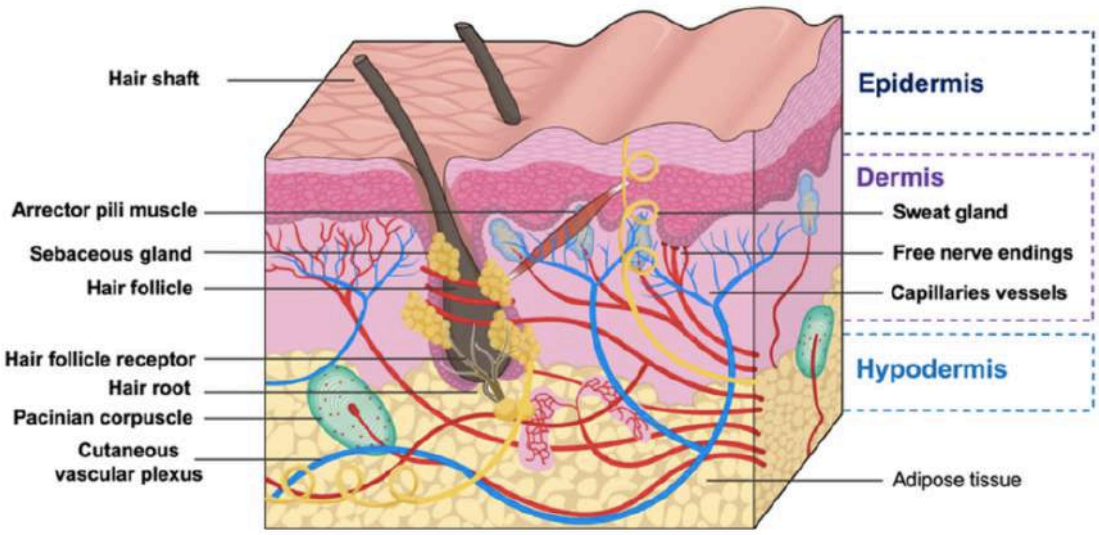

Figure 2: Schematic illustration of the anatomy of the skin. . From Ramadon et al. [7].

Epidermis: It is the most superficial skin layer. Cells that compose the epidermis are mainly keratinocytes (KCs) (95%), but also melanocytes, Langerhans cells (LCs) and Merkel cells are present [8].

Depending on the keratinocyte stage differentiation, the epidermis is organised in five distinct cell levels from the deepest layer to the most superficial are: the stratum basale, stratum spinosum, stratum granulosum, stratum lucidum and stratum corneum [9] (Fig 3) . In the stratum basale, **keratinocytes** have a high proliferative capacity, and cells are continuously proliferating and continue with differentiation by ascending up to the next stratums. When keratinocytes reach the last step of their differentiation convert into cells named corneocytes that are devoid of their nucleus and almost all their water content.

Corneocytes are dead skin cells filled with the tough protein keratin and form the stratum corneum and function as the main element of the skin barrier [10]. In this stratum there are lipid components that integrate between corneocytes to prevent dehydration [11] . It takes around 30 days for a new keratinocyte cell to move up through the epidermis stratums and achieve terminal differentiation state [12]. Keratinocytes are connected by desmosomes that provide cell-to-cell adhesion and help linking cell surface proteins to intracellular keratin cytoskeletal filaments [13]. These junctions are crucial for the correct functioning of the skin, and they anchor the cells to each other to maintain skin integrity [14].

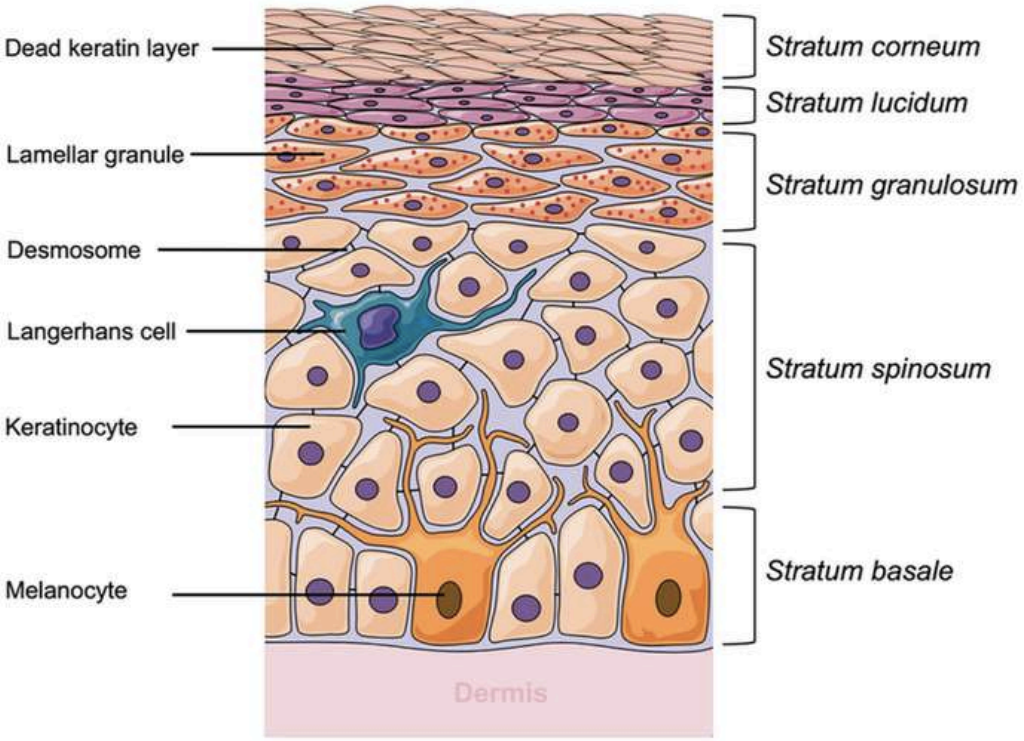

Figure 3: Schematic representation of epidermis layer of human skin. From Ramadon et al. [7].

Keratinocytes also participate in immunity as they can distinguish pathogens due to recognition of pathogen-associated molecular patterns (PAMPs) [15]. As a result, they secrete antimicrobial peptides, Interleukins (IL)-1, IL-6, IL-10, IL-12, IL-17, IL-18, IL-22, tumor necrosis factor alpha (TNFα), major histocompatibility complex (MHC) class I and II glycoproteins, and chemokines such as CXCL1, CXCL8, CXCL9, CXCL10, CCL11 and CXCL20 that promote immune cell recruitment [16-18]. The secreted inflammatory effectors trigger dermal immune responses.

Melanocytes are cells derived from the neural crest and they are found in the basal layer of the epidermis. They are in contact with keratinocytes through cytoplasmic extensions known as dendrites [19]. Melanin is synthetised in their subcellular organelles called melanosomes. The melanosomes are organised in a cap that protects keratinocytes from the harmful ultraviolet radiation [20].

LCs are bone marrow derived antigen presenting cells that provide a state of immune tolerance and in case of infection or skin damage, activate effector T cells [21]. LCs are found in the basal, spinous and granular epidermal layers of the epidermis [22].

Merkel cells are specialised cells located in the basal layer of the epidermis with neuroendocrine and sensory functions as they membrane interacts with nerve endings in the skin and are specialised in the perception of light touch [23].

The zone between the epidermis and the dermis is called the dermal-epidermal junction and it is composed by macromolecules that unite the keratin intermediate filaments of the basal keratinocytes with the collagen fibers of the superficial dermis [24]. The junction maintains the epidermal-dermal adherence and gives mechanical support to the epidermis.

Dermis: It is the middle layer of the skin located below epidermis and above the hypodermis. It is 0.5-5 mm thick and composed of collagen, elastin, salts, water, and a gel of glycosamin proteoglycans that provide density to the dermal layer of the skin [25]. It has two layers: the most superficial is the papillary dermis and the deepest is called reticular dermis. The dermis sustains and supports the epidermis and has thermoregulatory, sensitive and immunological functions. **Fibroblasts** are the predominant cells and control the production and maintenance of the structural components of the dermis such as procollagen and elastic fibers [26]. Procollagen is cleaved by N and C proteinases into collagen that forms the 70% of the dermis. The predominant types are collagen I and III [27]. Collagen provides structure and support to mechanical forces. The elastic fibers are responsible of the flexibility and elasticity.

The dermis presents a complex organization, as there are present blood and lymphatic vessels, nerves, sweat and sebaceous glands and hair follicles. It has also numerous immune cell populations such as **Dendritic Cells** (**DCs), $CD4^+$ T lymphocytes, γδ T lymphocytes, natural killer (NK) T cells, mast cells** and **macrophages** [28] (Fig 4). Dermal fibroblasts are crucially involved in the skin wound healing process; however,

increased fibroblast proliferation and deposition of extracellular matrix components may lead to fibrosis [29].

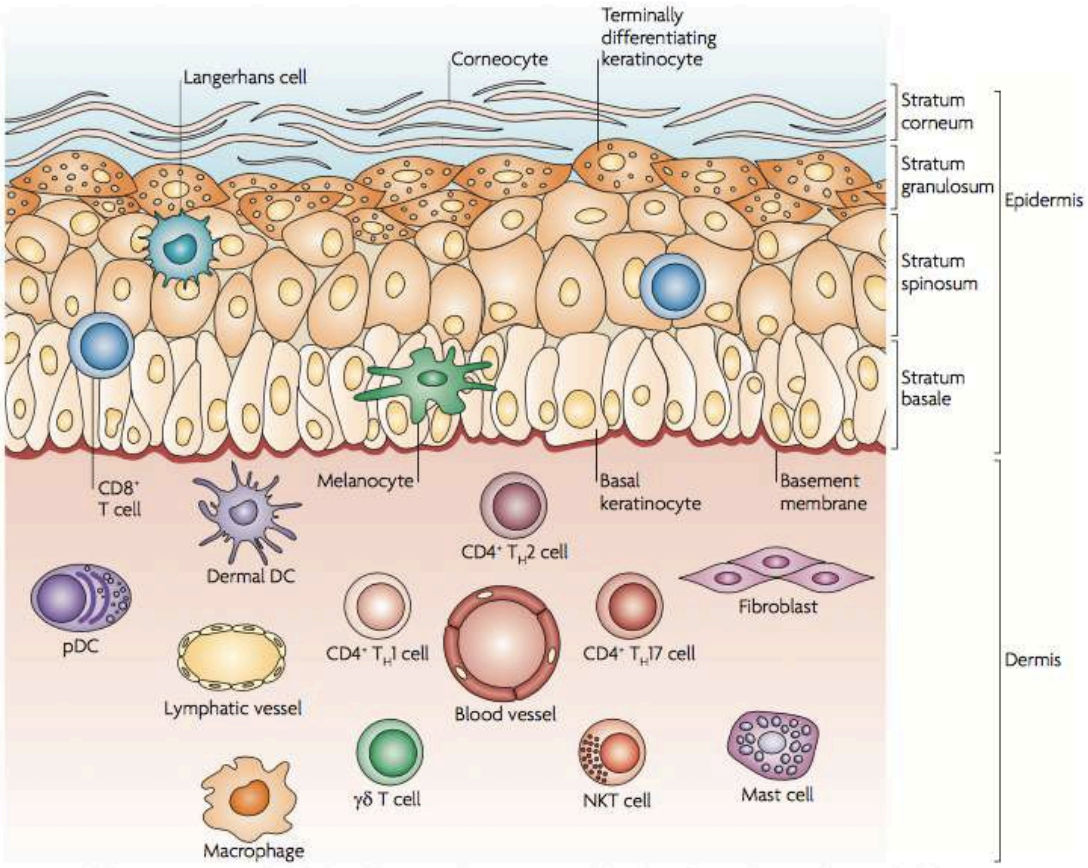

Figure 4: Schematic representation of the cell types present in epidermal and dermal layers of human skin. From Nestle et al. [30].

Hypodermis: It is the deepest skin layer and lies under the dermis. It consists mainly of fat-storing cells called **adipocytes,** but also contains fibroblasts, connective tissue, larger nerves, blood vessels, and macrophages [31]. Its function is to store energy supply. In addition, it allows mobility over underlaying structures. In non-obese subjects, about 80% of all body fat is located within the hypodermis [32]. Drugs can be administrated subcutaneously in hypodermis as it is vascularised and that allows an effective drug absorption and rapid onset of action [33].

1.2 Cutaneous Lupus Erythematosus

1.2.1 CLE definition

Cutaneous Lupus erythematosus (CLE) is an autoimmune chronic disease that includes a broad range of dermatologic manifestations and usually follows a relapsing-remitting

course. It can be presented as an individual disease affecting skin or as a clinical manifestation within the spectrum of systemic lupus erythematosus (SLE).

1.2.2 CLE Types and classification

According to the classification developed by James N. Gilliam and R.D. Sontheimer in 1981, the manifestations of CLE can be divided into two types: Lupus Erythematosus (LE)-specific and LE-nonspecific lesions [34] (Fig 5). LE specific manifestations include symptoms that are not seen in other disorders and are highly characteristic of CLE. On the other hand, LE-nonspecific manifestations are skin lesions that are associated with lupus but not exclusive and may be found in patients with active SLE but also in other autoimmune diseases.

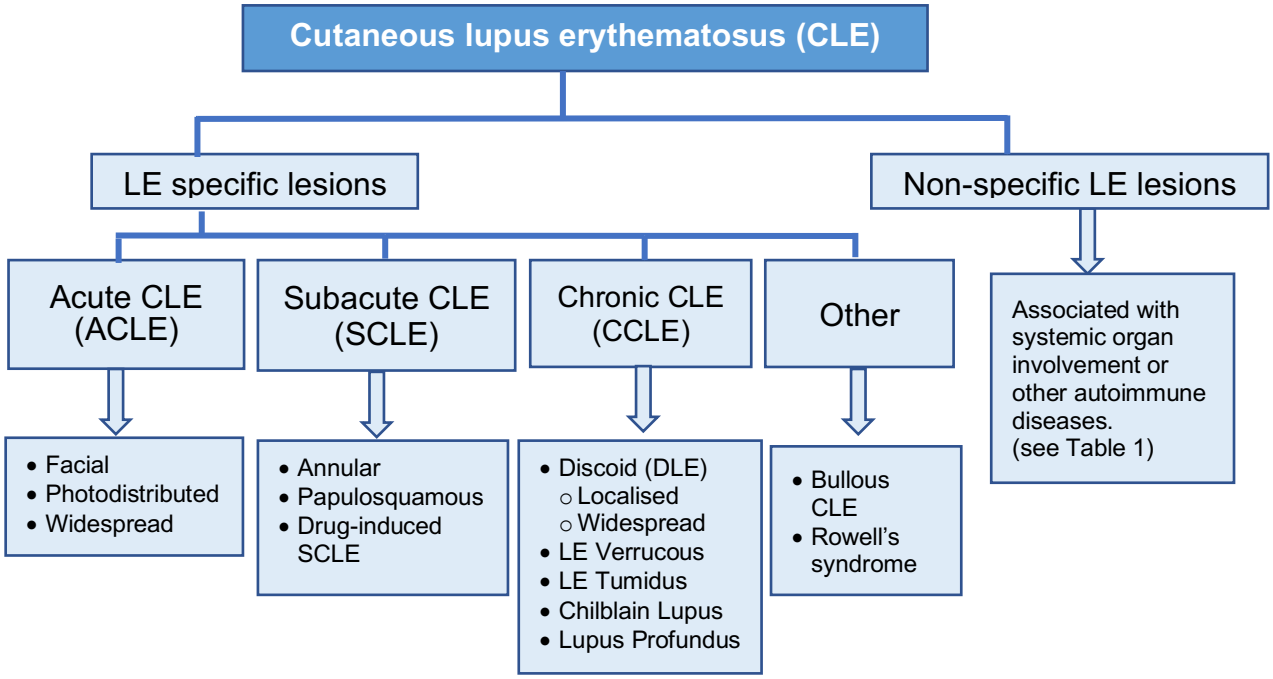

Figure 5. Cutaneous Lupus Erythematosus (CLE) classification according to Gilliam and Sontheimer [34]

1.2.2.1 LE-specific lesions

LE-specific lesions can be classified into three subgroups: Acute Cutaneous Lupus Erythematosus (ACLE), Subacute Cutaneous Lupus Erythematosus (SCLE) and Chronic cutaneous Lupus Erythematosus (CCLE) (Fig 5). An alternative classification has been

proposed with a novel subgroup: Intermittent Cutaneous Lupus Erythematosus that includes Lupus Erythematosus Tumidus (LET) [35].

- **Acute Cutaneous Lupus Erythematosus (ACLE**): ACLE has a very close association with systemic lupus disease [36]. There are localised and generalised forms of ACLE. The localised form is the frequently described malar, or “butterfly” rash, which refers to erythema that occurs over both cheeks, extends over the nasal bridge, and spares the nasolabial folds (Fig 6a). These lesions are classically transient, sun-induced, and non-scarring, although dyspigmentation can occur. Malar rashes have been reported to be present in up to 52% of SLE patients at the time of diagnosis, with clinical activity of the rash paralleling that of the systemic disease [37]. The generalised form of ACLE is rarely observed and this form occurs above and below the neck and has been referred to as a ‘maculopapular rash of lupus’ or ‘photosensitive lupus dermatitis. In addition, it may occur with prolonged generalised organ disease activity [38].

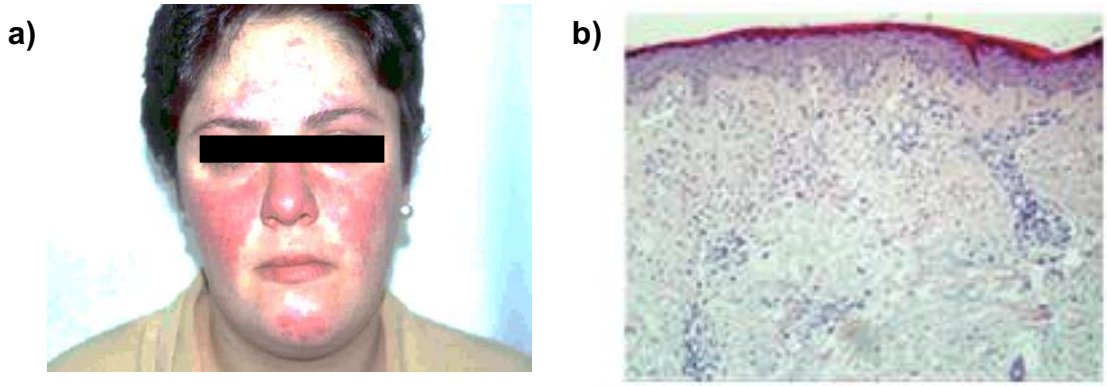

Figure 6. a) Patients with ACLE typically have a butterfly rash on the face. **b)** Skin samples from these patients histologically show moderate interface dermatitis with some infiltrating neutrophils (magnification ×100). Modified from Wenzel et al. [39].

Histologically, ACLE lesions show liquefactive degeneration of the basal layer, oedema of the upper dermis, and a scattered interface, perivascular, and periadnexal lymphocytic infiltrate, all of which are generally less pronounced as compared to other CLE subtypes (Fig 6b) . Immunologically, positive Antinuclear Antibodies (ANA) are found in 95% of ACLE patients, as well as a high incidence of anti-double strand (Anti-ds)DNA and anti-Smith (Anti-Sm) antibodies. Lesional direct immunofluorescence reveals granular immune deposits at the dermal-epidermal junction and perivascular deposits in the upper dermis, most commonly Immunoglobulin (Ig)-M [40].

-**Subacute Cutaneous Lupus Erythematosus (SCLE):** SCLE occurs primarily in young to middle aged women. SCLE is highly photosensitive, with 70-90% of patients having and

abnormal photosensitivity after sun exposition. The lesions are frequently found in the following sun-exposed areas: neck, upper thorax ('V' distribution), upper back, and the extensor surfaces of arms and forearms, and hands, however the face and the scalp are frequently unaffected [41]. The initial SCLE presentation consists of erythematosus macules that turn into extended annular polycyclic plaques, papulosquamous psoriasic-like lesions or combination of both [42]. The annular type is characterised by scaly annular erythematous plaques, which tend to coalesce and produce a polycyclic array. The papulosquamous variant can resemble eczema or psoriasis, as well as pityriasis occasionally. The cutaneous lesions, even though being sizeable, are not indurated and heal without scarring, although hypopigmentation may occur (Fig 7a).

A high proportion SCLE patients present anti-SSA/Ro (70–80%) and anti-SSB/La antibodies (30–40%). In addition, the presence of anti-SSA/Ro antibodies has been associated with SCLE photosensitivity [43]. An estimated 50% of SCLE patients will meet criteria for SLE. Studies found that 70-80% of SCLE patients had ANA positive, but with low prevalence (5%) of anti-dsDNA [44]. SCLE has been found to be frequently associated with the existence of human lymphocyte antigen (HLA)-DR3 [45].

Some drugs have been considered triggering factors of SCLE (drug induced (DI)-SCLE). Commonly used drugs that have been associated with SCLE are angiotensin-converting enzyme inhibitors, anticonvulsants, beta-blockers, and immune modulators, including TNFα inhibitors. There have been case reports of the development of SCLE in malignancies that could be associated to the new check-point inhibitors, mainly. These medications unmask SCLE in immunogenetically susceptible individuals, probably via photosensitizing mechanisms [46].

a) **b)**

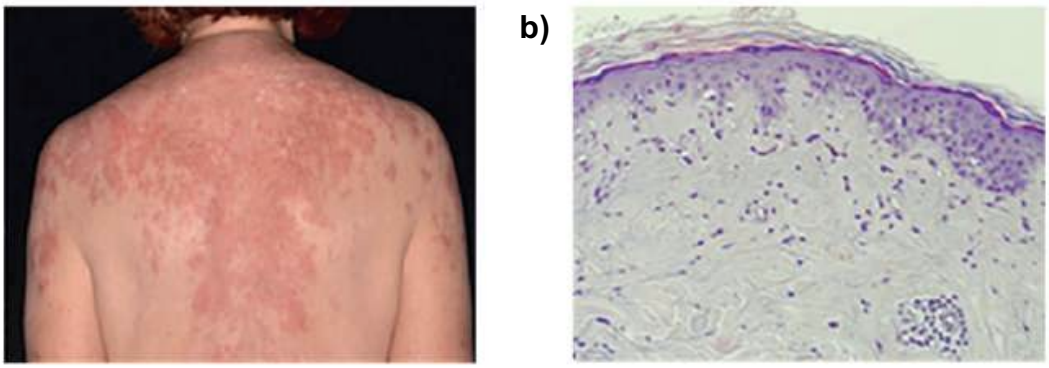

Figure 7. a) Non- scarring erythematosquamous lesions in sun- exposed skin are a typical feature of SCLE. **b)** SCLE presents histologically as mild interface dermatitis (magnification ×100). Modified from Wenzel et al. [39].

Histologic examination of SCLE lesions demonstrates hydropic degeneration of the basal keratinocytes, dermal oedema, hyperkeratosis, follicular plugging, and a sparse superficial and deep inflammatory infiltrate predominantly lymphocytic [37] (Fig 7b). The density and depth of the inflammatory infiltrate are less accentuated and less restricted to periadnexal, and perivascular regions compared with other CCLE subtype such as DLE. Also, the presence of follicular plugging and hyperkeratosis are significantly less pronounced than in DLE. The presence of “dust-like particles” representing IgG deposits on direct immunofluorescence (DIF) is a highly specific but not sensitive finding in SCLE [47].

- **Chronic Cutaneous Lupus Erythematosus (CCLE**): CCLE is the most severe skin manifestation of Lupus. Chronic cutaneous lupus includes discoid LE (DLE), hypertrophic/verrucous LE, LE profundus (LEP), chilblain LE (CHLE), and LE tumidus (LET).

DLE: Discoid lesions are the most common lesions of CCLE and DLE represents 50-98% of the CCLE cases [48]. DLE occurs more frequently in women in their fourth and fifth decade of life. It is characterised by inflammatory, scarring lesions, mainly involving the head or neck, but also elsewhere, mostly on the photoexposed areas. DLE may be localised or generalised [49]. Localised DLE commonly involves the head and neck, and particularly the scalp and ears. However, generalised DLE, which occurs both above and below the neck, is less common and typically involves the extensor forearms and hands [50]. DLE can occur on mucosal surfaces, including lips, and oral, nasal, and genital mucosa.

Clinically DLE is presented as erythematous macule or papules, well-demarcated, scaly and with follicular plugging, which progressively develops into an indurated discoid (coin-shaped) plaque with an adherent scale. The extension into the hair follicle, results in scarring alopecia. Over time, lesions become atrophic and scarring, with central hypopigmentation, peripheral hyperpigmentation and telangiectasias [51] (Fig 8a). Around half of DLE patients will develop significant skin scarring and scarring alopecia is present in one-third of DLE patients.

Serologically, DLE patients have a lower incidence of ANA, anti-dsDNA, anti-Sm, anti-U1 Ribonucleoprotein (RNP), and anti- SSA/Ro antibodies, as compared to other CLE

subtypes [52]. Patients with DLE can progress to a SLE through their disease course, although the rates are low (5-18%) [53].

Histologically long-standing DLE lesions reveal hyperkeratosis, dilated compact keratin-filled follicles, vacuolar degeneration of the basal keratinocytes, and an intensely predominantly lymphocytic infiltrate along the dermal-epidermal junction, around the fair follicles and eccrine ducts, in an interstitial pattern (Fig 8b) [54].

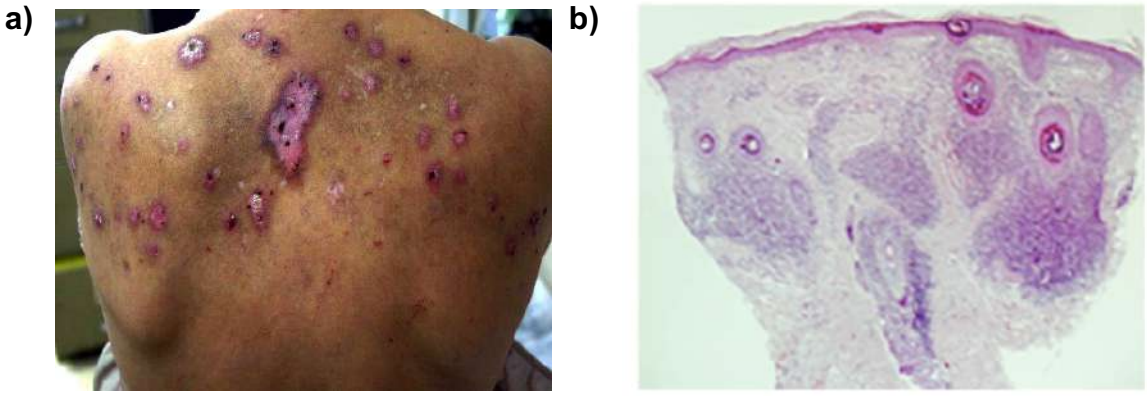

Figure 8. a) DLE lesions begin as well-demarcated erythematous macules or papules with a scaly surface, and frequently evolve into larger coin-shaped plaques. **b)** Histological samples show dense perifollicular and perivascular infiltrates combined with interface dermatitis and follicular plugging (magnification ×50). Modified from Wenzel et al. [39].

The evolutionary phases of DLE are also observed at the histological level:

- In the <u>active phase</u>, the histology shows keratinocyte necrosis/apoptosis, periadnexal and perivascular lymphocytic infiltrate under an interface dermatitis, hyperkeratosis orthokeratosis, edema of papillary dermis and vessels dilatation, erythrocytes extravasation in the superficial dermis, initial atrophy, melanophages in the papillary dermis and an impressive deposit of mucin among the collagen fibers [55]. Follicular hyperkeratosis is a characteristic picture. In this phase, thickening of the basement membrane may be highlighted with periodic acid-Schiff (PAS) straining [56]. Immunofluorescence may be positive for immunoglobulin (IgM, IgG and IgA) and complement at the dermo-epidermal junction and around hair follicles.

- In <u>later phases</u>, the histology shows a reduction in basal vacuolar degeneration, edema and lymphocyte infiltrate and is characterised by epidermal and adnexal atrophy, dermal fibrosis, vessels dilatation and presence of melanophages corresponding to the clinical scarring aspects [57].

Other CCLE variants include (Fig 9):

- **Hypertrophic or verrucous LE:** It is a distinct form of chronic cutaneous (discoid) lupus, which is characterised by hyperkeratotic plaques that typically are observed over sun-exposed areas (frequently face, extensor surfaces of forearms arms, and upper trunk). Lesions vary from squamous violet, painful papules and blackish hyperkeratotic ulcers to depigmented atrophic plaques on the back, hyperkeratotic papules on upper extremities, and disseminated keratoacanthoma-like papulonodular verrucous lesions. Classic discoid lesions and squamous cell carcinoma may be associated [58].
- **Lupus Erythematosus Profundus** (LEP) or panniculitis, is characterised by painful firm subcutaneous nodules in areas of increased fat deposition, such as the upper arms and legs, face, and breasts [59]. LEP tends to have a chronic course, characterised by remission and flares, and ultimately leaving atrophic scars and loss of subcutaneous fat. Histology shows lobular panniculitis with a dense lymphocytic infiltrate.
- **Chilblain lupus erythematosus** (ChLE). It is a rare form of CCLE that resembles frostbite. Lesions are painful, violaceous plaques and nodules in cold-exposed areas. Central erosions or ulcerations may occur on acral surfaces, such as fingers, toes, heels, nose, and ears. Pathology shows epidermal atrophy, interface vacuolization, and a perivascular mononuclear infiltrate [60].
- **Lupus Erythematosus Tumidus** (LET) is a very sensitive form of CCLE with lesions appearing in sun-exposed areas: face, arms, back, V-area of the neck and shoulders. The swollen aspect and the red color are the mainly traits of LET lesions [61]. Histologically is characterised by large clusters of plasmacytoid dendritic cells (pDCs) and mucin deposition [62].

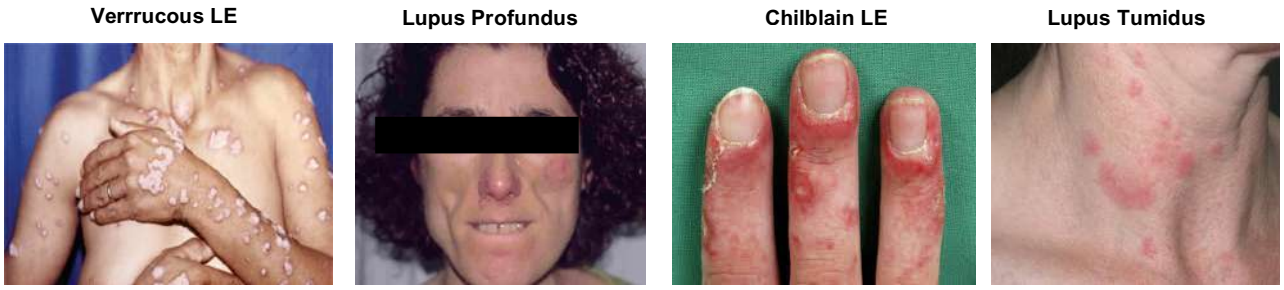

Figure 9. Chronic Cutaneous lupus has different subsets, the most common is Discoid Lupus however other skin affections are seen such as verrucous CCLE, Lupus Profundus, Chilblain LE and Lupus Tumidus.

Other forms of LE-specific lesions include bullous acute lupus erythematosus (characterised by subepidermal bullae) and Rowell syndrome (with erythema multiforme-like target lesions).

1.2.2.2 LE non-specific lesions

The LE non-specific lesions are skin lesions that are associated with lupus but are not specific from the lupus disease. Identical lesions can be seen in other diseases. They are strongly associated with SLE [63]. Table 1 includes all the described non-specific LE lesions in which the most common types are: cutaneous vasculitis, livedo reticularis, alopecia and Raynaud phenomenon.

Non-specific LE skin lesions	
Cutaneous vascular disease **Vasculitis** - **Leukocytoclastic** **Palpable purpura** **Urticarial vasculitis** - **Periarteritis nodosa-like cutaneous lesions** **Vasculopathy** - **Degos' disease-like lesions** - **Secondary atrophie blanche (livedoid vasculitis, livedo vasculitis)** **Periungual telangiectasia** **Livedo reticularis** **Thrombophlebitis** **Raynaud's phenomenon** **Erythromelalgia (erythermalgia)**	**Nonscarring alopecia** "Lupus hair" Telogen effluvium Alopecia areata **Other cutaneous manifestations** Sclerodactyly Rheumatoid nodules Calcinosis cutis LE-nonspecific bullous lesions Urticaria Papulonodular mucinosis Cutis laxa/anetoderma Acanthosis nigricans (type B insulin resistance) Erythema multiforme Leg ulcers Lichen planus

Table 1. Non-specific LE skin lesions.

1.2.2 CLE epidemiology

Only few studies have evaluated the prevalence and incidence of CLE showing consistency between the different studied populations.

Incidence: According to the different studies, the overall CLE incidence ranges from 2.7 to 4.3 per 100.000. In United States, Jarukitsopa et al. [64] described that the incidence of CLE was 4.2 per 100,000; (95% confidence interval [CI] 3.1, 5.2, p= 0.10). They also found that CLE was three times higher than SLE in males (2.4 versus 0.8 per 100,000, p=0.009) and that the prevalence of CLE and SLE in women were similar, but the CLE prevalence was higher in men than in women (56.9 versus 1.6 per 100,000, p<0.001). Durosaro et al [65] , found that in Minnesota (USA), the CLE incidence rate was 4.30 per 100.000 (95% CI, 3.62–4.98). In Sweden, Grödnhagen et al. [66] described that the average annual incidence of CLE in Sweden 2005-2007 was 4.0 per 100,000 (95 % CI 3.9-4.2). Further analysis showed that DLE incidence rate was 3.2 per 100, 000 (95 % CI 3.0-3.4) and 0.6 per 100, 000 (95 % CI 0.5- 0.7) for SCLE. In South Korea, Sang Baek et al. [67] showed that the average annual incidence of cutaneous lupus was 4.36 per 100 000. Finally, in Denmark, Petersen et al. [68] described that the annual incidence rate (IR) of CLE was 2.74 per 100,000 and that the female:male ratio was 4:1 with no differences in the gender distribution between the disease subtypes (p=0.27).

Prevalence: The overall described prevalence of CLE ranges from 73 to 86 per 100 000. Durosaro et al. in USA [65] found to be 73.24 per 100 000 (95% CI, 58.29–88.19). Whereas Jarret et al. [69] in New Zealand found CLE prevalence to be 86.0 per 100,000 (95% CI 78.1-94.7). This study concluded that Māori and Pacific people in Auckland, New Zealand, have greater relative risk of cutaneous lupus compared to the European population and in particularly, high risk of discoid lupus erythematosus. This higher prevalence could be related to the fact that SLE is more common in “Polynesians” compared to other ethnic groups. Moreover, they used capture–recapture technique which accounts for unidentified cases by examining different but overlapping databases.

1.2.2.1 CLE subtypes epidemiology (LE-specific)

DLE is the most common subtype reported in the studies. In the Minnesota study [65], the age- and sex-adjusted incidence rate per 100,000 for DLE was 3.56 (95% CI 2.94–4.18). Jarrett et al. [69] described that the prevalence rate of DLE per 100,000 for Maori/Pacific was 27.24 (95% CI 20.73–35.82) and the European rate was 6.57 (95% CI 3.76–11.49). In French Guiana, the crude average incidence of DLE was 3.56 per 100,000 per year [70].

The incidence of subacute cutaneous lupus erythematosus (SCLE) in Sweden was 0.7 per 100,000 per year [66] consistent with the Minnesota study that described the SCLE incidence rate was of 0.63 per 100.000 (95% CI 0.37–0.89) [65].

The other forms of CLE (hypertrophic, profundus, mucosal, tumidus, chillblain) are unusual. For example, the incidence of lupus tumidus and bullous lupus, is reported as 0.07 per 100.000 (95% CI 0.00–0.16) and 0.03 per 100.000 (95% CI 0.00–0.08), respectively [71].

1.2.2.2 CLE association with SLE

Skin involvement is very common in SLE as it occurs in 70-80% of SLE patients during the course of their disease [72]. Up to 20-25% of patients with SLE will have a skin lesion as a first sign of the systemic disease [73]. A study in 260 SLE patients showed that LE-non-specific cutaneous manifestations were present in 43% of the SLE patients and LE-specific in 23% of the patients [74]. Of the LE-specific, DLE (11%) was the most common followed by SCLE (8%) and ACLE (4%). Of the LE-non-specific skin manifestations Raynaud's phenomenon was the most common (25%), followed by non-scarring alopecia (9%) and vasculitis (8%) [74].

Cutaneous manifestations are so prevalent and relevant, that some of them are included in the classification criteria for SLE. For example, in the Systemic Lupus International Collaborating Clinics (SLICC) classification [75], four of the eleven criteria used for SLE classification are mucocutaneous and include ACLE (also including SCLE), CCLE, oral ulcers and non-scarring alopecia, emphasizing the importance of skin involvement in lupus.

CLE is not always associated to SLE and sometimes patients have some autoantibodies without fulfilling the criteria for SLE. The probability of a CLE patient of being diagnosed of SLE was of 18.1% (95% CI 14.1–22.1%) during the first three years after being diagnosed with CLE. High ANA titters (>1:320), anti-dsDNA, anti-SSA/Ro, anti-SSB/La, leucopenia and arthralgia have been described risk factors of progression [76].

As is showed in table 2, the rate of systemic manifestations varies according to the underlying subtype of CLE.

Type of CLE	Relation with SLE	Ref.
ACLE	A high proportion of ACLE patients present ANAs (~80%) or anti-double-stranded DNA antibodies (30–40%).	[44]
SCLE	Around 20-50% of SCLE patients fulfill the American College of Rheumatology (ACR) criteria for SLE.	[77]
DLE	Around 5-35% of all patients with DLE are ANA- positive, and some patients develop systemic features of SLE (5–18% of DLE patients). SLE patients have a 20–25% risk over their lifetime of developing one or more classic DLE.	[78]
LET	Anti- SSA/Ro and anti-SSB/La antibodies are rare (10–20% of LET patients) and LET patients rarely develop SLE (<5%).	[79]

Table 2. Relation of cutaneous lupus with systemic lupus disease.

Although the prognosis of CLE is often more favourable than SLE, in a significant proportion of patients CLE can be disfiguring and debilitating. For this reason, the impact in our society is pronounced; it is the third most common cause of industrial disability from dermatological diseases, with 45% of patients experiencing some degree of vocational handicap [80].

1.2.3 CLE diagnosis

CLE diagnosis should be based on the findings of patient history, clinical exam, laboratory studies, serology, as well as histology and direct immunofluorescence exam of skin biopsies if the histology is not diagnostic. Detailed skin examination is crucial for classifying the CLE subtype and systemic involvement needs to be excluded.

The cornerstone of CLE diagnosis is a lesional biopsy for histology, and it should be performed in SLE patients mainly if lesions are atypical or refractory [81]. The skin biopsy should be performed in an established lesion (at least 6-month-old) that is still active. Within this features, it provides the highest yield for both hematoxylin eosin-stained sections and direct immunofluorescence technique [82]. An optimal diagnostic specimen should be around 4 mm diameter and can be obtained using the punch biopsy technique extending to the subcutaneous fat. However, in case of lupus panniculitis, a deep incisional biopsy may be required.

Histologic findings vary by subtype, but in general CLE lesions share the features of vacuolar or hydropic change and lymphocytic infiltrates. Direct immunofluorescence of lesional biopsies can supplement non-definitive histologic findings. The lesional lupus

band test refers to the finding of immunoglobulins and complement at the dermal-epidermal junction of a lesional biopsy, a classic finding in CLE [83]. Deposits are typically granular in appearance, and most commonly contain Complement component 3(C3), IgG and IgM, although IgA can be found (Fig 10a, 10b). A lupus band test is interpreted as positive when all the following criteria are met:

1. IgM or IgG must be demonstrated singly or in combination with other immunoglobulin classes at the epidermal or appendageal basement membrane zone. Complement components or alternate pathway proteins may be present.
2. The pattern must consist of either a homogeneous or granular band, or a band made up of closely spaced fibrils, threads, or stipples.
3. The immunofluorescence should be bright.

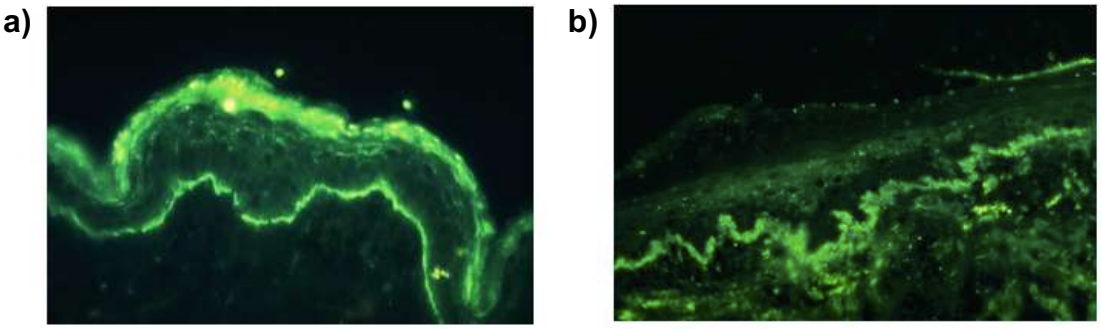

Figure 10. **a)** Linear band- like deposits of IgM along the dermoepidermal junction of a chronic discoid lupus erythematosus lesion. **b)** Granular deposits of C3 along the dermoepidermal junction of a chronic discoid lupus erythematosus lesion. From Meurer et al. [84].

A negative test does not exclude the diagnosis. Also, a positive test does not secure the diagnosis, as false positive tests can occur in sun-damaged skin. A positive lupus band test in non-lesional and non-sun exposed skin is associated with (but not diagnostic for) systemic disease. In most cases, clinical and histologic findings provide sufficient information to make a diagnosis of CLE.

Serological tests for autoantibodies should be performed in CLE newly diagnosed patients to determine the presence of SLE.

1.2.4 CLE activity and severity assessment (CLASI)

Cutaneous Lupus Area and Severity Index (CLASI) was developed by Albrecht et al. [85]. It is a system to measure CLE disease activity and damage. Within this index the lesional morphology and the anatomic location are considered. It consists of two scores, the

CLASI-A that summarizes the activity of the disease and ranges from 0 (mild) to 70 (severe) and include measures for erythema, scale/hypertrophy, mucous membrane lesions, recent hair loss, and nonscarring alopecia. The second part of the score is CLASI-D, a measure of the damage done exclusively by the disease and is scored in terms of dyspigmentation and scarring, including scarring alopecia. The reduction of CLASI score is associated with an improvement in disease. It is widely used in clinical trials and research studies (Annex 1).

1.2.5 CLE pathogenesis

The initial and perpetuating mechanism involved in the pathogenesis of CLE is not well understood yet. It is likely to be multifactorial with a complex interaction occurring between environmental exposures and genetic susceptibility that triggers and/or propagates immune dysregulation, resulting in disease in affected individuals (Fig 11).

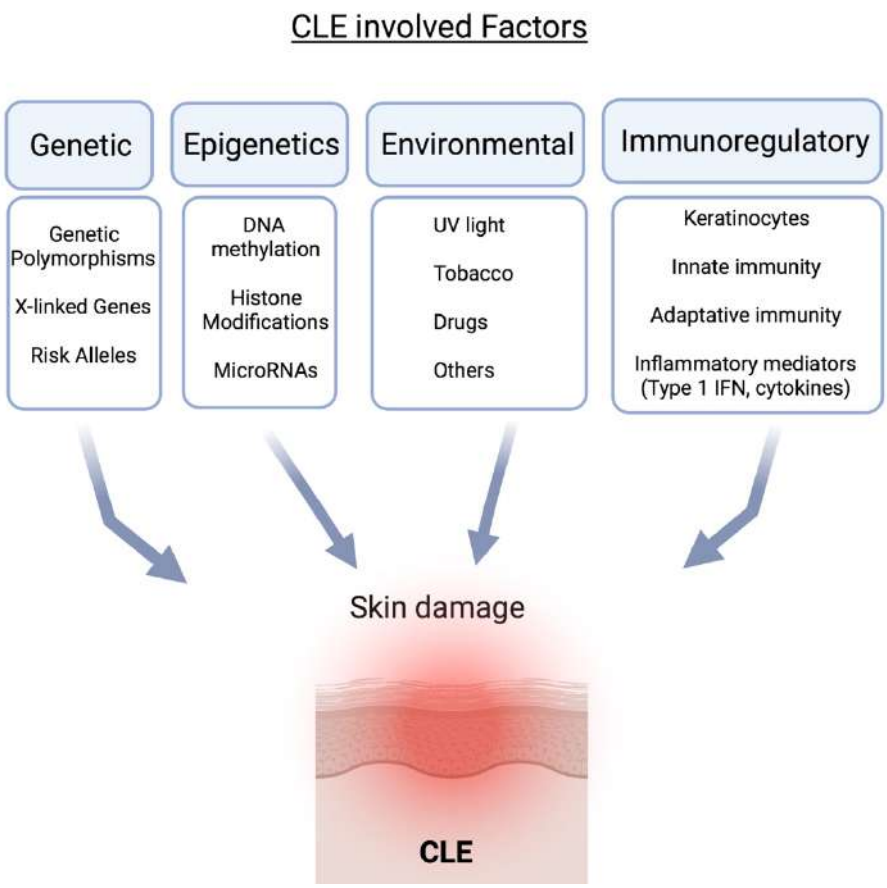

Figure 11. Factors involved in CLE pathogenesis

1.2.5.1 Genetic factors

Genetic studies, including those of families, of affected individuals, and of affected populations in genome-wide association studies (GWAS), have identified genetic

polymorphisms, mutations, and risk alleles in CLE populations [86]. The vast majority of these identified genes are involved in pathways that affect the function of innate and adaptive immune responses, predisposing to immune dysregulation. Among others, these include apoptosis/cell death, deoxyribonucleic acid (DNA) processing, the type I interferon (IFN) pathway, migration of leukocytes, the complement cascade and clearance of cell debris, T-cell immune checkpoints, antigen presentation, and antibody production [87]. Although various risk alleles have been found in CLE, only one monogenic cause had been identified [88]. Mutations in the Three Prime Repair Exonuclease 1 (TREX1) represent the only monogenic cause of cutaneous lupus identified to date, resulting in the rare form of CCLE familial chilblain lupus [89]. These patients develop cold-induced purple-red lesions on acral surfaces, which may ulcerate. TREX1 is a cytosolic DNA exonuclease that plays an essential role in the homeostatic degradation of single stranded DNA (ssDNA), and TREX1 deficiency results in intracellular ssDNA accumulation. Recognition of these accumulated nucleic acids by innate immune receptors results in chronic hyperactivation of the type I interferon pathway [90].

X-Linked Genes

Female gender is a known risk factor for CLE as supported by the preponderance of disease in females. Sex hormone differences may explain this increased risk as estrogen may enhance autoantibody production via B cell and monocyte activity [91]. However, the effects of estrogens and androgens are still unclear with conflicting results as patients with anti-estrogen treatment have been reported to develop SCLE skin lesions [92].

Recent investigation into human skin sexual dimorphism identified the putative transcription factor vestigial-like family member 3 (VGLL3) as an essential regulator of female-biased genes that may contribute to an autoimmune phenotype in women [93]. VGLL3 influences type I interferon responses and promotes the expression of genes encoding inflammatory molecules, many of which are genetic risk variants previously identified in autoimmune diseases including SLE. In normal skin, VGLL3 is more highly expressed in female-derived tissue. In addition, skin-directed overexpression of VGLL3 in mice causes a lupus-like disease with cutaneous manifestations. When analysing, skin expression of VGLL3 and their targets including BAFF (B cell activating factor) and ITGAM (Integrin Subunit Alpha M) in SCLE, no differences were observed between males and females, suggesting that VGLL3 is a sex-biased risk factor prior to disease manifestation

and a general regulator brought to comparable functional levels in the two sexes as autoimmune conditions arise.

Risk Alleles

Several genes related to apoptosis, DNA processing, type I IFNs, immune stimulation, and antibody production identified by genome-wide association studies have been associated with CLE.

HLA variants are associated with numerous immune diseases as they orchestrate antigen presentation and immune activation. HLA-B8, HLA-DR, and HLA-DQ have been associated with SLE, and HLA-DR2 and HLA-DR3 have been associated with SCLE [86].

Regarding DLE susceptibility MHC *HLA DQA1, DQA1*0102, HLA A*03, B*07, DRB1*15* alleles have been described [94]. A predictive role may exist for HLA-B8 as DLE females with this haplotype progress to SLE [95]. The role of the HLA variants is important as they may allow for the forecast of severity and ultimately disease progression.

Polymorphisms in cell death genes ITGAM, MHC Class I Polypeptide-Related Sequence A (MICA) and B (MICB), DNA repair gene MSH5, vesicle trafficking Flotillin 1 (FLOT1) and interferon pathway genes TRIM39-RPP21, Interferon Regulatory Factor (IRF)5, Signal Transducer And Activator of Transcription (STAT)4, and Tyrosine Kinase (TYK)2 have all been associated with CLE. IRF5 and TYK2 have been associated specifically with both SCLE and DLE subtypes and their expression is upregulated after UV exposure and are known to promote type I IFN [96] .

Subtype differences may exist, with SCLE associated with C1qA, C2, C4, TNF 308A [97]. The TNF308A single-nucleotide polymorphism (SNP) transcript is increased with UVB radiation and participates in autoantigen presentation, cytokine production, and immune recruitment, suggesting a photosensitivity predisposition in SCLE [98]. CCLE is associated with STAT4, ITGAM, Cytotoxic T-Lymphocyte Associated Protein (CTLA)4, and TREX1, with recent molecular profiling highlighting IFNγ as well. Early complement deficiencies are associated with autoimmunity and in particular in individual and familial cases of DLE [99].

Epigenetics

In addition to genetic mutations and polymorphisms that predispose to CLE, external stimuli may interact with the genome in susceptible individuals to cause epigenetic variation, leading to dysregulated gene expression via DNA methylation, histone modification, and microRNA-mediated gene silencing.

- **DNA Methylation**: In SLE, DNA hypomethylation in T cells has been identified resulting in increased inflammatory gene expression [100]. Regarding lupus skin manifestations, malar rash and DLE have been associated with differentially methylated regions (DMRs) of naïve $CD4^+$ T cells in SLE patients [101]. These DMRs were affecting genes that mediate cell proliferation, apoptosis, and antigen presentation, suggesting that DNA methylation plays a role in CLE pathogenesis. Studies on SCLE, DNA methylation analyses revealed demethylation of the promoters of perforin and CD70, a B-cell costimulatory molecule, expressed in $CD4^+$ T cells. Both perforin and CD70, are overexpressed in SCLE T cells, suggesting a possible pathogenic link [102,103].

- **Histone modifications:** In SLE patients, histone modifications in peripheral blood mononuclear cells [104, 105] are found and their correlation with disease activity and nephritis manifestations has been established. No studies have been performed in CLE patients yet. Interestingly, the inhibition of histone deacetylase, an enzyme involved in the removal of acetyl groups from lysine residues in histones, can upregulate B-cell microRNAs (miRNAs) that silence Activation-induced cytidine deaminase (AID) and B lymphocyte-induced maturation protein-1 (Blimp-1) [106], contributing to B-cell differentiation processes that underpin antibody and autoantibody responses in lupus MRL/Faslpr/lpr mice a lupus model mice that presents spontaneously lesions that resemble CLE. Further research may be needed to elucidate the histone modifications in CLE.

- **microRNAs:** Several microRNAs are dysregulated in SLE, and some of them have been extensively investigated. Among the most studied, miR-21 was found upregulated in T cells from SLE patients and promotes hypomethylation [107]. mir-146a is downregulated in SLE PBMCs

(Peripheral blood mononuclear cells) and when downregulated promotes inflammation via NF- κB regulation [108]. And miR-150, that inhibits both T cell and B cell activation and proliferation and is downregulated in B cells and $CD4^+$ T Helper (Th) 1 cells from SLE patients [109]. At the time of this thesis, no miRNAs in CLE had been described.

In this thesis, the role of miRNAs in CLE has been explored as there were no previous studies investigating their role in CLE. Further investigation in the role of miRNAs in CLE can provide a better understanding of the pathogenic mechanisms involved in this condition and may yield targets for therapy to restore normal epigenetic patterns.

microRNAs definition

microRNAs, also known as miRs or miRNAs, are abundant, small, highly conserved, non-coding RNA sequences that are about 19-22 nucleotides in length [110]. Its main function is to regulate gene expression post-transcriptionally by binding to mRNA. The miRNA-mRNA complementary union promotes the gene expression regulation is by preventing mRNA from being translated or inducing mRNA degradation [111] The interaction of the miRNA with the mRNA is short, around 6 to 8 nucleotides. Therefore, multiple genes can be targeted by the same miRNA and therefore, a single miRNA can regulate simultaneously different cellular pathways and biological processes. They approximately regulate 60% of all the protein- coding genes and they can modulate the gene expression in the same cell where are being synthetised or can be enveloped in extracellular vesicles, secreted, transported to neighboring cells and regulate gene expression in recipient cells [112]. For this reason, they are considered fundamental regulators of gene expression. In recent years, more than 2,000 human miRNAs have been described employing new advances in molecular biology and bioinformatics, achieving relevance in translational research.

microRNAs in skin

miRNAs are involved in development, organogenesis, proliferation and apoptosis, among other cell processes. In skin physiology, the role of miRNAs is well-known as they are involved in epidermal and dermal proliferation, pigmentation, aging, wound healing, skin microbiome and skin immunity [113].

microRNAs in skin disease.

Under normal physiological conditions, microRNAs are regulating correct cell functions. However, in disease, microRNAs may change, inducing an altered gene expression that leads into an aberrant phenotype when they are dysregulated, they may alter relevant cellular processes, favoring pathogenic conditions. On the other hand, they may also play protective roles by trying to re-establish cell homeostasis. A miRNA balance is key for the correct functioning of cell and tissue physiology.

As microRNAs play crucial roles in development, homeostasis and regeneration of the skin, their deregulated expression may result in skin disorders (Fig 12). Recent findings show that miRNAs are involved in skin carcinogenesis [114] and also, in the pathogenesis of chronic inflammatory skin diseases, as lesional skin from chronic inflammatory skin diseases such as psoriasis or atopic dermatitis presents specific miRNA expression profiles that differ from healthy skin [115].

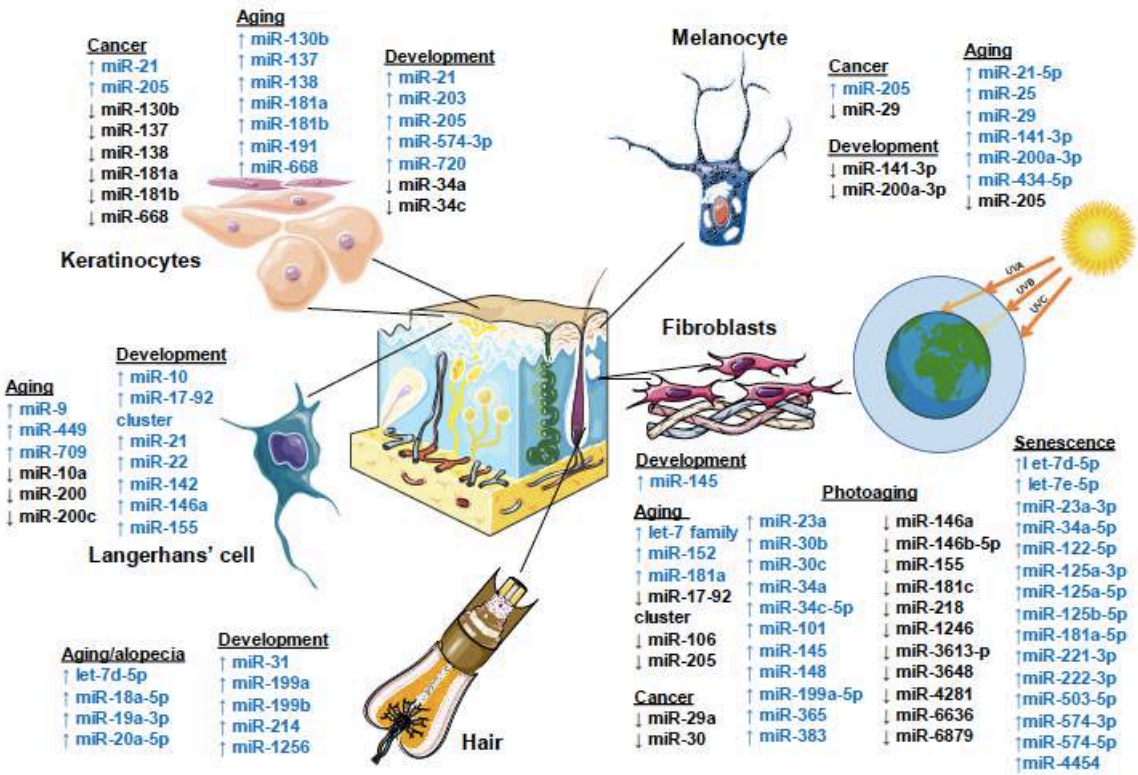

Figure 12. microRNAs are involved in several cellular processes in the skin. From Gerasymchuk M et al, [116].

1.2.5.2 Environmental factors

Ultraviolet (UV) light

Photosensitivity is a well-known phenomenon in lupus, as 60–80% patients with SLE have photosensitive skin lesions [117]. In addition, evaluation of CLE skin shows that lesions are commonly found in the sun-exposed areas indicating that UV is an important environmental factor. UV light exposure is the most well-known factor in triggering skin injury in CLE. UV irradiation directly induces chemokine production by epithelial cells, and it also causes DNA damage, resulting in keratinocyte apoptosis and necrosis. Dying keratinocytes release inflammatory cytokines and chemokines, which in turn recruit lymphocytes and pDCs. Keratinocyte death may also result in release of nuclear debris, which can stimulate pDCs via Toll-like receptors (TLRs) and can also serve as a reservoir of autoantigen for autoreactive T and B cells.

Spectrum differences in ultraviolet exposure may exist as UVA penetrates the dermis and activates metalloproteinases to evoke immune infiltration, whereas UVB induces cell proliferation in the epidermis and increases FAS–FASL interactions in hair follicle [118]. Recently the role of UVB in SLE skin lesions has been investigated by Skopelja-Gardner et al. [119] and they found that a single exposure to UVB light triggers not only an early exaggerated cutaneous IFN-I response in female mice but also a systemic IFN-I response in the blood and kidneys. Characterization of the generated IFN response in the skin showed that it was dependent on the stimulator of Interferon Response CGAMP Interactor 1 (STING) and cytosolic DNA sensing adaptor protein downstream of cyclic GMP-AMP (cGAMP) synthase (cGAS) but independent of pDCs recruitment, suggesting a mechanism for CLE initiation and flares.

Another mechanism by which UV can induce CLE may be dependent of epidermal IFNκ production by keratinocytes. IFNκ has been found increased in epidermis from CLE lesional skin and it plays a pathogenic role in CLE by amplifying and accelerating responsiveness of epithelia to IFNα and increasing keratinocyte sensitivity to UV irradiation [120]. Therefore, IFNκ is a critical IFN in CLE pathology via promotion of enhanced IFN type I responses and photosensitivity.

In addition, UV light protection has been shown to prevent skin injury in CLE [121]. Currently, the only treatment for photosensitivity is sunlight avoidance and broad-

spectrum, high sun protective factor (SPF) sunscreen, which prevents the development of disease-specific skin lesions in CLE patients exposed to UVA/UVB.

Tobacco

Cigarette smoking is associated with CLE, and it is suggested that tobacco smoke contributes to CLE disease activity by increasing inflammatory cytokines, apoptosis, autoantibodies, and the development of free radicals. Compared with non-smokers, smokers with CLE have worse quality of life and worse skin disease, as measured by the CLASI Index [122]. There is conflicting data regarding whether smokers respond to antimalarials as well as non-smokers, but smokers exhibit more recalcitrant disease than non-smokers if both antimalarials and immunomodulators are required [123]. It is still unknown whether decreased treatment efficacy in smokers is due to direct interference of cigarette smoke with the treatment or to the higher disease severity in smokers. It is also possible that some smokers may have lower medication adherence rates.

Drugs

Some drugs have been reported to induce SLE and CLE. Drug-induced skin-limited SCLE (DI-SCLE) is much more common than drug induced CCLE of which very few cases have been reported. Table 3 shows the most frequently drugs associated with the development of DI-SCLE [124]. A systematic review of drug induced SCLE found the most frequently reported causative medications to be antihypertensives (most commonly hydrochlorothiazide and calcium channel blockers) and terbinafine, with less frequent reports of many other medications including chemotherapeutics, antihistamines, leflunomide, interferon, antiepileptics, statins, lansoprazole, and non-steroidal anti-inflammatory drugs (NSAIDs) such as naproxen and piroxicam [125]. Medications highly associated with DI-SLE are thought to enhance innate immune responses, particularly of neutrophils, resulting in increased neutrophil extracellular trap (NET) formation and autoantigen exposure. It is hypothesised that DI-SLE/SCLE due to TNFα inhibitors may be in part due to the immunogenicity of the medications themselves, though more recent formulations have lower immunogenicity and DI-SLE/SCLE continue to be reported to these agents. There may also be a component of “unmasking” rather than causing the SLE or SCLE, as some patients treated with TNFα inhibitors have conditions that are associated with a higher baseline risk of SLE, such as rheumatoid arthritis [126].

Drugs associated with Subacute Cutaneous Lupus Erythematosus
ACE inhibitors (e.g. captopril)
Antiepileptics (e.g. phenytoin)
Antimicrobial agents (e.g. griseofulvin, terbinafine and tretracycline)
B.Aderenoreceptor antagonists (e.g. acebutolol)
Calcium channel blockers (e.g. diltiazem and nifedipine)
Chemotherapeutic agents (e.g. tamoxifen and docetaxel)
NSAIDs (e.g. naproxem and piroxicam)
Proton pump inhibitors (e.g. omeprazole
Sulfonylureas (e.g. glyburide)
Thiazide diuretics (e.g. hydrichlorothiazide)
Others (eg. Bupropion, leftunomide, interferon α …)

Table 3. Medications associated with triggering subacute cutaneous lupus erythematosus patterns.

Others

Other possible proposed factors implicated in CLE are viral infections, stress and diet but no significant evidence has been found yet. Studies investigating the microbiome in SLE patients have suggested that host-microbe interactions contribute to the development of disease [127]. Molecular mimicry is proposed to play a role in the development and propagation of autoimmunity in SLE and SCLE patients with anti-SSA/Ro antibodies. Evolutionarily conserved Ro60 protein orthologues were identified in a subset of human skin, oral, and gut commensal bacteria, which was found to be cross-reactive with both the SCLE/SLE patient's anti-Ro antibodies as well as their Ro60 autoreactive T cell clones [128].

1.2.5.3 Immunoregulatory related factors

Insights from genetic studies and environmental triggers in lupus pathogenesis implicate both innate and adaptive immune components. Overall, CLE is a disease of dysregulated immune homeostasis, resulting in unwanted innate immune stimulation and adaptive immune activation (Fig 13). The autoimmune pathways involved in CLE development and pathogenesis remain incompletely understood. It must also be emphasised that the complete sequence of events from environmental trigger, if any, to immune activation to disease is also unknown. However, there is substantial data that suggests the following:

Initiating the damage: Keratinocytes

Keratinocytes play an important role in the cutaneous lupus pathogenesis and appear to be involved in the initiation and sustainment of the lesions. They interact with host immunity and often serve as innate immune cells by releasing “alarmins” and danger signals that activate neighbouring immune sentinels and recruit adaptive immune lymphocytes to areas of stress or damage [129]. As a consequence of UVB light in genetic predisposed individuals together with other unknown triggers, as stated previously, keratinocytes start an aberrant apoptosis [130]. CLE keratinocytes are known to be more susceptible to apoptosis. This enhanced epidermal apoptosis in CLE lesions has been demonstrated by the increase level of proteins that mediate apoptotic processes such as Fas (CD95), TNF-related apoptosis-inducing ligand (TRAIL) and TRAIL-R1 [131,132]. Within keratinocyte apoptosis, epidermal nuclear debris and autoantigens are resealed and are recognised by autoantibodies, resulting in the release of additional proinflammatory cytokines and skin inflammation. In addition, CLE keratinocytes exposed to UVB light produce several cytokines such as IL-1β, IL-6, TNFα, IFNα, IFNκ, IFNλ, and chemo attractants such as CXCL10 [133]. As a consequence, the immune system is activated, and immune cells are recruited to the skin. Together, keratinocytes and IFNs appear to initiate and sustain CLE disease activity.

Sensing the damage: Innate immunity

Into detail, all nuclear debris such as RNA and DNA resulting from the apoptotic keratinocytes, are recognised by Antigen Presenting Cells (APCs) that in turn activate T cell responses. One of the most important DC type in CLE pathogenesis are pDCs which are relatively abundant in CLE, especially in DLE and are known to be recruited in the skin after UVB exposure. CLE lesions are characterised by a strong IFN type 1 signature in which pDCs are the main producers [134].

Neutrophils mediate the presence of NETs, which are networks of chromosomal DNA, histones, and granule proteins that are released by neutrophils [135]. Lupus skin lesions show evidence of infiltration by netting neutrophils in the dermis and subcutis of several subtypes such as discoid lupus, acute cutaneous lupus, subacute cutaneous lupus, and lupus panniculitis. Netosis was most frequently seen in DLE (32%) than in SCLE (5%) [136].

TLRs may be involved in the initiation of pDCs and neutrophil activity in CLE. In CLE, there is an activation of TLR7 and TLR9 by endogenous nucleic acids [137]. Moreover, neutrophils are known to be activated by TLR7 agonists [138].

Macrophages have been slightly studied in CLE, mainly in DLE. They modulate T-cell differentiation and facilitate antigen presentation. DLE lesional skin presented a transcriptome analysis of an M1 macrophage gene signature that may contribute to local inflammation and damage and Th1 differentiation [139]. On the other hand, M2 macrophage-related proteins were also detected by immunohistochemistry, suggesting that diversity of macrophage subtypes may be due to their gene expression plasticity and a mixture of acute and chronic phases in the DLE skin.

Regarding epidermal Langerhans cells, they are reduced in CLE lesions, which may reflect dendritic cell activation and migration into the regional lymph nodes [140]. In contrast, it is known that LCs interaction with apoptotic Keratinocytes has anti-inflammatory effects and is critical for resolution of UVB-induced cutaneous inflammation [141]. Therefore, low levels of LCs may decrease its tissue protective function from UVB and contribute to CLE pathogenesis.

Effectors: Adaptive Immunity

T cells

T cells are the most abundant immune cell type within CLE. The inflammation in CLE seems to be predominantly mediated by a Th1 response, especially in DLE, in which high numbers of $CD4^+$ Th1 cells are infiltrated in the lesional sites [142]. Type I IFNs produced by the pDCs recruit Th1 lymphocytes into CLE lesions by increasing the production of CXCL10 in CLE skin, specifically in keratinocyte cells [143]. CXCL10 is known to correlate with the presence of pDCs and lymphocytes in CLE [144] .

CLE lesions have shown less Th17 genes compared with psoriasis and SLE but some authors like Oh et al. [145] and Tanasescu et al. [146] have observed elevated expression of IL-17 in the CLE lesion sites. Yet, others as Jabbari et al. [147] found little evidence of Th17 in lesions and IFNγ regulated genes were upregulated whereas IL-17 gene expression was not increased in DLE. However, most recently, CLE patients that are non-responders to antimalarials expressed more STAT3, a Th17-associated marker suggesting some role in refractoriness [148]. So far, the role of Th17 responses in CLE is not completely established and further studies are needed.

Cytotoxic $CD8^+$ T cells are the driver of keratinocyte death and disruption of the dermal-epidermal junction. Cytotoxic $CD8^+$ T cells (CTLs) express granzyme B that is involved in promoting cell apoptosis via activating caspases. In DLE, decreased circulating $CD8^+$ $CXCR3^+$ cells have been found. It has been postulated that extravasation to the skin and over-recruitment of the cytotoxic T cell pool leads to low circulating populations. These $CD8^+$ T cells seem to be activated based on expression of granzyme B and correlation with type I IFN–dominant signature in scarring DLE lesions [149].

Finally, regulatory T cells are involved in the inhibition of inflammation by secreting inhibitory cytokines such as IL-10 and transforming growth factor-β (TGF-β) and by suppressing other T cells through direct contact [150]. Franz et al [151]. reported that LE lesional skin displays reduced numbers of $FoxP3^+$ Regulatory T cells (Tregs) and that may contribute to insufficient suppression of inflammation.

B cells

B cells act as autoantibody producers and inflammatory cytokine secretors. Accumulation of necrotic debris in CLE is thought to contribute to autoantibody production. Keratinocytes are known to upregulate autoantigens such as Ro52 in CLE [152]. UV radiation induces translocation from nucleus and cytoplasm to the cell surface of SSA/Ro, SSB/La, RNP, and Sm. Studies have demonstrated that antigens Ro and La re-localize into apoptotic bodies in UV-irradiated KCs undergoing programmed cell death [153]. B cells may then produce autoantibodies. Presence of antibodies against these antigens are common in CLE, especially anti- SSA/ Ro in SCLE subtype. ACLE is strongly associated with anti-dsDNA antibodies and ANA and CCLE is negatively associated with anti-extractable nuclear antigens (ENA) and anti-dsDNA antibodies [154]. Studies are being conducted to explore the contribution of b cells in CLE pathogenesis. In that sense it has been has identified a transcriptional B cell signature that is more prominent in DLE patients and more prominent when the CLE lesions occur without associated SLE, and concluded that B cell function in skin may be an important link between cutaneous lupus and systemic disease activity [155]

Although autoantibodies play a significant role in CLE pathogenesis, there are individuals without autoantibodies that present CLE. When autoantibodies bind to autoantigens in the skin there is a release of cytokines and subsequent inflammation, however their exact implications remain to be defined. Another reason to think that B cells may be involved in CLE producing autoantibodies and perpetuating inflammation, but may not be the

essential pathogenic players, is the fact that B cell therapies approved in SLE do not show high clinical efficacy when treating CLE.

NK T cells

NK cells may also play a role in cytotoxicity and can overlap with T cells as NK T cells. In DLE blood samples, there are decreased NK T cells, suggesting their recruitment to skin [156, 157].

Inflammatory mediators

Type I Interferon

Studies found that type I IFN–related genes are highly upregulated in CLE and correlate with CLASI scores [158]. IFNα is thought to play an important role, as elevated levels have been found in the serum of patients with SLE in addition to their family members without SLE, suggesting heritability. Type I IFNs have pleiotropic effects on the immune system by affecting survival, differentiation, and proliferation [159]. IFNα has been shown to promote production of chemokines CXCL9 and CXCL10 to recruit immune cells to the skin [160]. Despite its crucial known implication in disease, the initial source of IFNs in CLE is still uncertain. It is hypothesised that keratinocytes may be an initial source as they have been shown to produce type I IFNκ upon UVB irradiation as well as type III IFNλ in response to immunostimulatory nuclear acids. Importantly, these type I IFNs have autocrine effects on keratinocytes and result in the production of cytokines and chemokines such as IL-6, IFNα, CXCL9, and CXCL10 to recruit $CXCR3^+$ immune cells. Keratinocyte-induced IFN may be the initial insult, but propagation of IFN may be sustained by the recruited immune cells such as neutrophils, macrophages, and pDCs via their responses to cellular debris [161]. Taken together, IFN signaling appears to contribute to CLE disease pathogenesis and is one of most critical immune pathways involved

Cytokines

Cytokines such as TNFα, IL-1, IL-6, IL-10, IL-12, IL-17, IL-18 have been detected in CLE and are involved in the initiation and perpetuation of CLE skin lesions [162] . Their implication is detailed in Table 4:

Cytokine	Source	Function	Role in CLE
TNFα	Keratinocytes Fibroblasts Mast cells	Proinflammatory	- - Stimulates production of inflammatory cytokines, chemokines and adhesion molecules such as IL-1, IL-6, CXCL8, CCL20, VCAM-1 and ICAM-1. - Activates B cells antibody production. - Upregulates keratinocyte surface expression of lupus antibodies.
IL-1	Keratinocytes	Proinflammatory	- Amplifies production of TNFα and the inflammatory chemokines CCL5, CCL20, CCL22 and CXCL8.
IL-6	Keratinocytes	Proinflammatory	- Triggers B cell maturation an Immunoglobulin secretion. - Increases cytotoxic T cell production and differentiation.
IL-10	B cells Monocytes $CD4^+$ T cells $CD8^+$ T cells	Proinflammatory Anti-inflammatory	- Suppresses Th1 cells, macrophages and dendritic cells. - Stimulates B cell hyperactivity.
IL-12	B cells DCs Macrophages	Anti-inflammatory	- Regulates T cell function - Reduces immunoglobulin production - Protects keratinocytes from UV induced apoptosis.
IL-17	Th17 cells	Proinflammatory	- Stimulates T cells - Increases the production of autoantibodies. - Triggers the production of inflammatory cytokines and chemokines including IL-1, IL-6, CCL2, CCL7, CCL20, CXCL1 and CXCL5.
IL-18	Macrophages	Proinflammatory	- Stimulates the production of the inflammatory cytokines IFNs, TNF α and IL-1β. - Potentiates IFNs-induced production of CXCL9, CXCL10 and CXCL11.

Table 4. Cytokines in CLE. Modified from Robinson et al. [162]

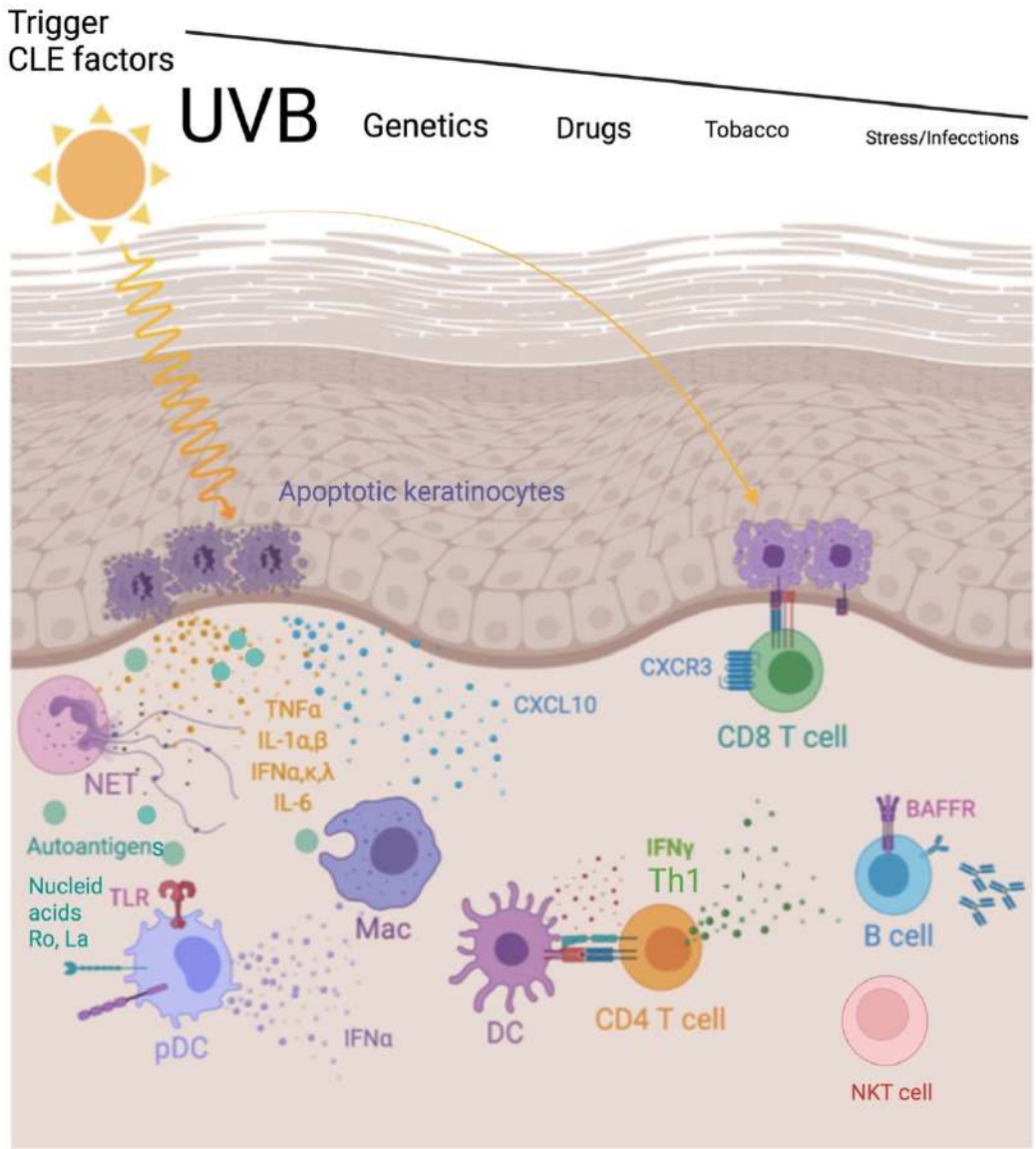

Figure 13. **Pathogenesis of cutaneous lupus erythematosus (CLE)**. Triger CLE factors include: Ultraviolet (UVB) radiation, genetics, drugs, tobacco, stress and infections. The combination of these factors in particular UVB exposure induces keratinocyte apoptosis, resulting in the release of autoantigens together with proinflammatory cytokines such as TNFα, IL-1, IFNs and IL-6 and chemokines such as CXCL10. Autoantigen release from dying keratinocytes may be trapped in neutrophil extracellular traps (NETs). In addition, autoantigens are recognised by Antigen presenting cells (APCs) such as plasmacytoid dendritic cells (pDCs) that are activated and as a result release IFNα. Dendritic cells (DC) activate $CD4^+$ T Th1 cells to secrete IFN γ. CD8+ T cells expressing CXCR3 are recruited to dermal-epidermal junction via CXCL10 and attack keratinocytes, resulting in enhanced keratinocyte apoptosis. Activation of TLR7 and TLR9 by endogenous nucleic acids results in DC and neutrophil activation. B cells expressing BAFF (B cell activating factor) receptor and may secrete autoantibodies. Natural Killer T Cells (NKT) are increased in the lesional sites. Macrophages (Mac) phagocytose autoantigens released from dying keratinocytes and help prime adaptive immune lymphocytes. Modified from Little A, et al. [87]

1.2.5.4 Pro-inflammatory self-amplifying cycle in CLE

A pro-inflammatory amplifying cycle in CLE lesions has been proposed by some authors and could explain the continuous reactivation of the immune system in CLE lesional sites (Fig 14).

In genetically predisposed individuals, together with distinct environmental factors in which UVB light is crucial, keratinocytes are damaged, and apoptosis occurs. The accumulation of DNA from keratinocytes implies the prolonged activation of TLR and subsequent initiation of innate and adaptive immune responses. Within this pro-inflammatory scenario, the IFNα secreted by pDCs is known to enhance the expression of TRAIL1 in keratinocytes, suggesting that it may be involved in the increase and prolongation of the apoptotic death of keratinocytes in CLE [163]. Moreover, the endogenous nucleic acids released from apoptotic keratinocytes, are recognised by autoantibodies that form immune complexes.

Some examples of autoantigens include Ro52 and High-mobility group box 1 (HMGB1). Ro 52 is an E3 ubiquitin ligase with regulatory role in inflammation. Specific Ro52 autoantibodies can be found in CLE skin lesions and keratinocytes from non-lesional skin of CLE patients that show increased Ro52 expression after UV exposure, confirming UV as a triggering factor for skin lesions in patients with Ro52 antibodies [164]. HMGB1 is a protein located in nuclei under normal conditions and increased amounts of HMGB1 expression and translocation have been observed in CLE skin lesions [165]. Moreover, UV irradiation is able to lead HMGB1 translocation to the cytoplasm. In apoptotic or necrotic keratinocytes, HMGB1 is translocated to the cytoplasm and binds DNA to form immune complex [166]. The immunocomplexes can be taken up by pDCs via CD32-mediated endocytosis and as a result, the nucleic acid components of these immune complexes may reactivate type I interferon production that contributes to enhanced inflammation [167].

In parallel, the recruited Th1 cells, produce IFNγ, which perpetuates the upregulation of CXCR3 ligands [168]. This promotes more immune recruitment and upregulation of downstream inflammatory effectors that are responsible for lesion formation and persistence in CLE.

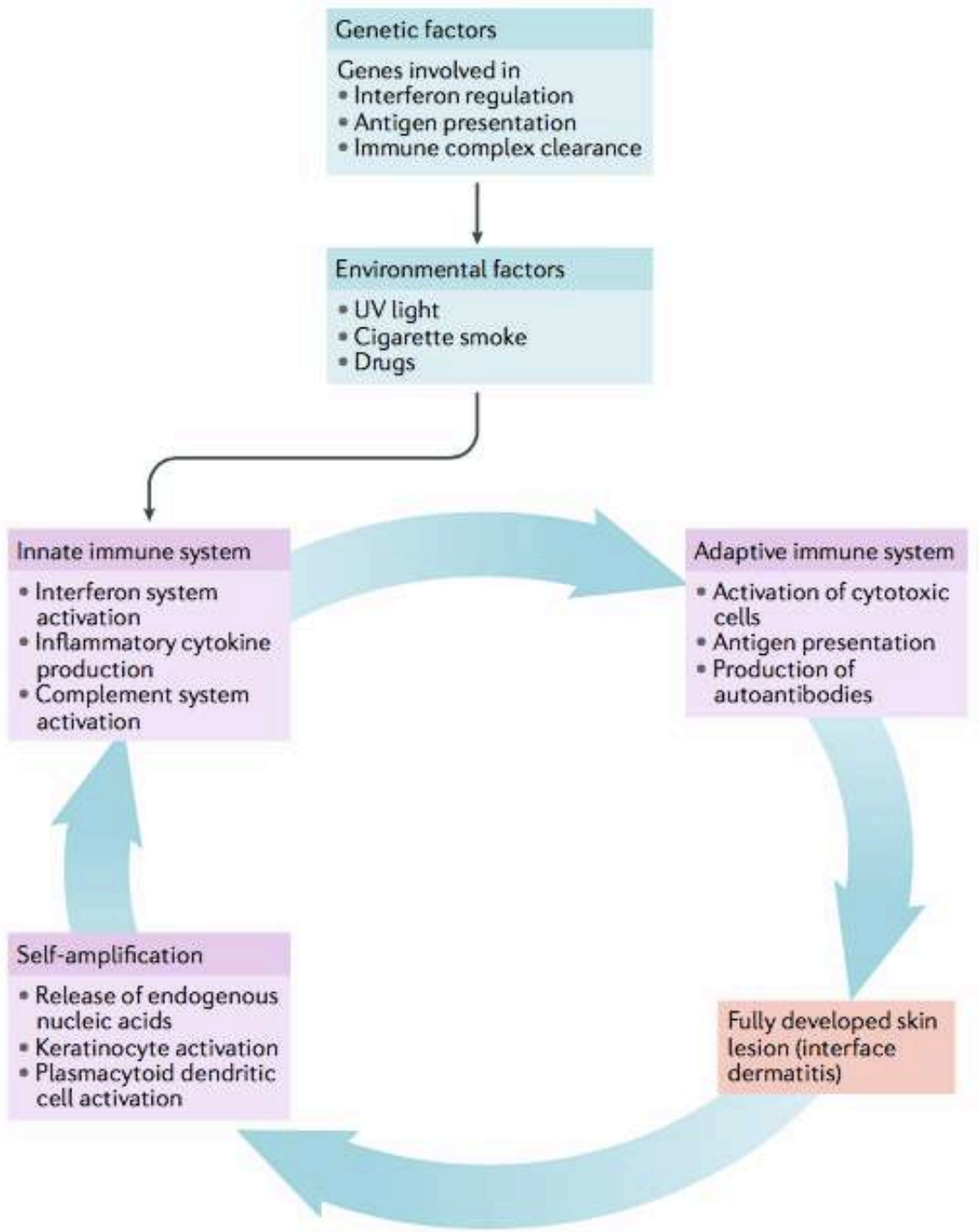

Figure 14. **Pro-inflammatory self-amplifying cycle in CLE**. The innate immune system is activated in genetic susceptible individuals exposed to environmental factors. Subsequently there is an activation of adaptive immune responses and cutaneous lupus erythematosus (CLE) skin lesions appear. These CLE lesions are characterised by a self-amplification inflammatory loop: epidermal keratinocyte stress and death cause the release of autoantigens and immunostimulatory endogenous nucleic acids that reactivate innate immune responses. As a result, the skin inflammation is perpetuated and maintained in time. From Wenzel J [39].

1.2.6 CLE treatment

CLE management involves combinations of local and systemic agents requiring adjustment to the activity and course of the disease. The treatment options are fairly similar for the different subtypes; however, before treating patients with CLE, it is essential to evaluate them for signs of systemic disease.

To date, many drugs have been evaluated for patients with SLE in clinical trials, however, only few randomised, placebo-controlled trials have been performed in CLE. One of them is a small randomised, double-blind, intraindividual trial comparing 0.1% tacrolimus cream with 0.05% clobetasol propionate cream in patients with CLE and malar erythema of SLE [169]. Another is a multicentre, double-blind, randomised, placebo-controlled phase II trial that demonstrated the efficacy and safety of 0.5% R-salbutamol cream versus placebo [170]. However, no medication has been approved specifically for the treatment of CLE, although several agents licensed for SLE, and other autoimmune diseases are currently used. Thus, off-label-use of topical and systemic agents is observed in most patients with CLE.

Figure 15 shows a still valid algorithm of treatment for CLE proposed by Kuhn et al [171]:

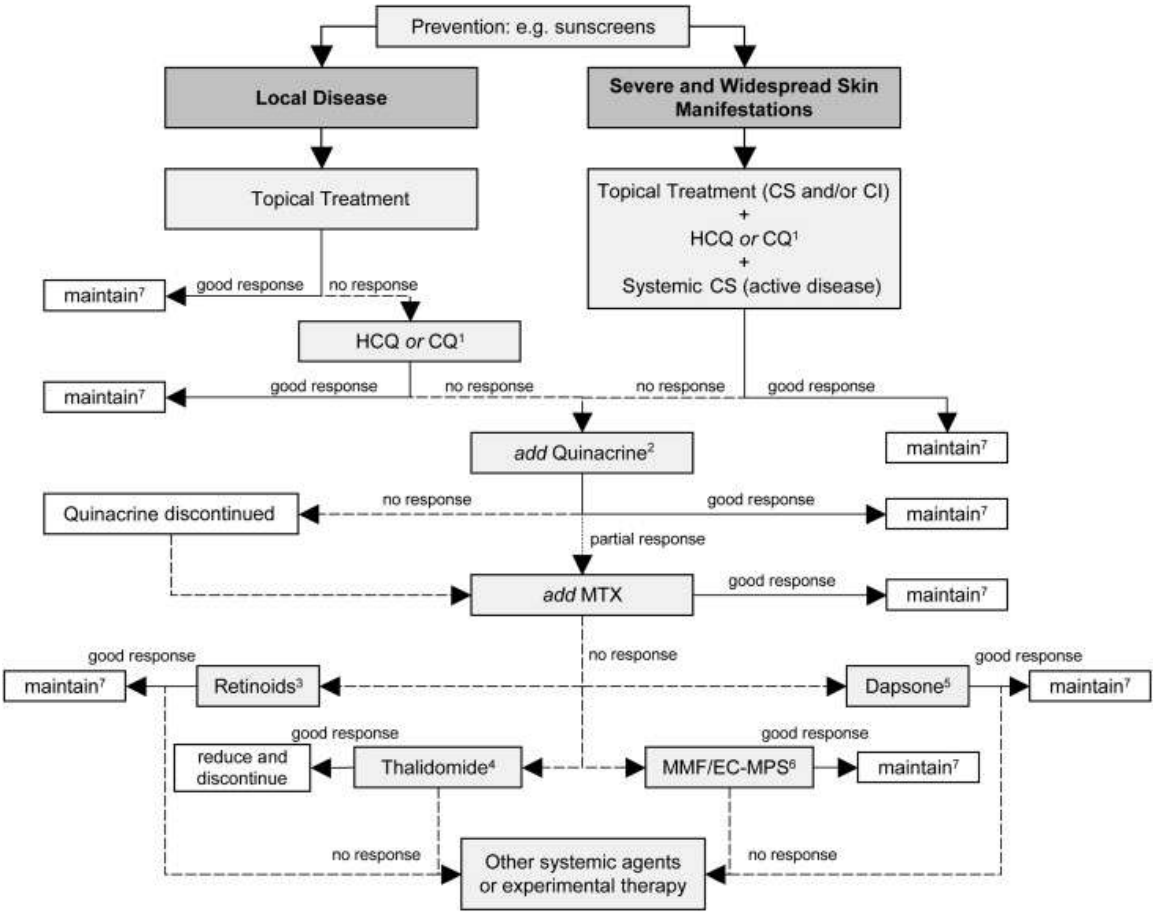

Figure 15. Algorithm of treatment for CLE. [1]Systemic treatment is usually initiated with hydroxychloroquine (HCQ), if no response, chloroquine (CQ) can be used. [2]If there is partial response with quinacrine, methotrexate (MTX) may be added; if there is no response with antimalarials, these drugs are discontinued and MTX is started. [3]Retinoids are primarily used in hypertrophic discoid lupus erythematosus (LE), refractory subacute CLE (SCLE) and CLE/lichen planus overlap (discontinue MTX). [4]Thalidomide should only be applied in severe refractory CLE as remission-inducing agent (discontinue MTX). [5]Dapsone is recommended for urticarial vasculitis, LE panniculitis, SCLE, and oral ulcers (discontinue MTX). [6]Mycophenolate mofetil (MMF) or mycophenolate sodium (EC-MPS) is primarily indicated in refractory SCLE (discontinue MTX). [7]Note that ''maintain'' only refers to a certain period of time depending on agent, efficacy, and CLE subtype. After clearing of skin lesions, agents should be reduced to minimum effective dose or discontinued; however, sunscreens should be used for prevention of skin lesions. CI, Calcineurin inhibitors; CS, corticosteroids. From Kuhn et al. [171].

1.2.6.1. First-Line Treatment

Prevention and sunscreens

CLE patients frequently present photosensitivity (60–80%); therefore, patients should avoid sun-exposure time and use sun protection as prevention. In all patients with CLE and SLE, it is important to provide instructions concerning methods of protection from sunlight and artificial sources of UV radiation, and avoidance of potentially photosensitizing drugs. Consistent UV protection may also involve photo-resistant clothing and thorough application of light-shielding substances with highly potent chemical (organic) and/or physical (inorganic) UVA and UVB protective filters [172].

Topical treatment

Topical corticosteroids (CS): Topical CS have proven to be a very effective treatment for skin lesions in all subtypes of CLE. The main symptoms, such as redness and scaling, are reduced by CS. Topical steroids are indicated mainly in patients with localised CLE [173].

The treatment of CLE usually starts with topical steroids that can be of low, mild or high potency. Choice of the CS class should consider the area of the body and the activity of the skin lesion. In the face: short application of low- to mid-potency CS (such as: methylprednisolone); trunk and extremities: mid-potency CS (such as: mometasone furoate, betamethasone valerate, triamcinolone acetonide); scalp, palms, and soles of the foot: super-potent CS (such as: Clobetasol). For hairy areas, CS solution, lotion, or foam may be used. High potency CS result in improved efficacy however, patients developed more common side effects such as atrophy and telangiectasia [174]. Because of this well-known side effects treatment with CS should be time-limited and preferably intermittent.

Calcineurin inhibitors (CI): In CLE, several reports have shown efficacy of calcineurin inhibitors, such as tacrolimus and pimecrolimus, which down-regulate T-cell activity by inhibiting the phosphatase calcineurin, responsible for dephosphorylation of the nuclear factor of activated T cells [175]. A randomised, double-blind, vehicle-controlled trial of tacrolimus 0.1% ointment was evaluated in a 12-week twice-daily treatment of 30 patients with different CLE subtypes, resulting in a significantly higher response rate than in patients treated with placebo [176]. Because of the absence of atrophic side effects, tacrolimus and pimecrolimus are suitable as topical treatment of CLE, especially in the face [177].

Other topical treatments: other topical therapies include mainly retinoids that are used for refractory cases, especially in hypertrophic DLE lesions [178].

Systemic treatment:

CLE patients with generalised lesions, potential scarring disease and refractoriness to topical treatment can benefit from systemic therapy. When systemic treatments are indicated, topical therapy usually is continued as an adjunctive therapy.

Antimalarials: Antimalarial drugs include hydroxychloroquine (HCQ), chloroquine (CQ) and quinacrine. Current guidelines consider antimalarials as first line systemic treatment for CLE patients with active or extensive skin lesions [179]. Since long time ago, antimalarials have been considered the first-line systemic treatment in all CLE subtypes; however, only two randomised, double-blinded trials in CLE or SLE with skin lesions have been performed until now, showing its efficacy. Ruiz-Irastorza et al. [180] found high evidence supporting the global safety of HCQ and CQ, with HCQ having a safer profile than CQ. Therefore, HCQ is usually the first prescribed treatment in CLE patients with severe or widespread skin lesions, in particular in patients with the risk of scarring and development of systemic disease.

A systematic review by Shipman et al. [181] including 852 patients treated with HCQ from 10 different studies (five retrospective studies, three prospective, two case series and the two randomised clinical trials) identified HCQ dosage up to 400 mg/day to be effective for most CLE patients with 50 – 97% of clinical response and few adverse effects. However, there was a decline in efficacy (45%) in long-term HCQ responders. In the event of progressive loss of efficacy and refractoriness to HCQ or CQ, it is necessary to ensure adherence to treatment before considering therapeutic changes, since around 40% of patients, according to different studies, do not comply with medications as recommended

[182]. Measurement of HCQ levels in serum is not routinely performed. Intriguingly, patients with a more TLR9-driven disease pathology may have more benefit from HCQ [183, 184]. Currently, biomarkers are lacking to predict HCQ treatment response.

The main side-effect of antimalarials is retinal toxicity, more frequent in CQ-treated patients than with HCQ. HCQ retinal toxicity is far more common than previously considered; an overall prevalence of 7.5% was identified in patients taking HCQ for more than 5 years, rising to almost 20% after 20 years of treatment [185]. Early retinal changes (premaculopathy) are subclinical and only detected in regular controls. However, with continued drug exposure, there is progressive development of a bilateral atrophic bull's-eye maculopathy and paracentral scotomata which cause widespread retinal atrophy and visual loss [186]. Analysis of almost 2500 patients using long-term HCQ showed that risk rises markedly with over-dosage (>5 mg/kg real weight) or durations beyond 10 years [187]. There are two other major risk factors that accelerate toxicity: renal disease (since the drugs are largely cleared by the kidneys) and use of the breast cancer drug tamoxifen.

Intervals for screening of retinal changes should follow the guidelines of the American Academy of Ophthalmology [188]. Based on these data, it is recommended to prescribe a maximum daily dose of 5.0 mg HCQ/kg real bodyweight.

If monotherapy with HCQ or CQ is not successful, quinacrine (100 mg/day) may be added, resulting in synergistic efficacy, without increasing the risk of retinopathy [189].

Systemic corticosteroids: In severe or widespread active CLE lesions, systemic corticosteroids are recommended as first-line treatment in addition to antimalarials. In a prospective, cross-sectional, multicentre study performed by the European Society of Cutaneous Lupus Erythematosus (EUSCLE) [190], systemic corticosteroids showed the highest efficacy in comparison with all other systemic drugs used for CLE therapy, providing efficacy in 94.3% of the 413 treated patients. Long-term therapy with corticosteroids in CLE without systemic involvement is not recommended due to the well-known serious side-effects.

1.2.6.2. Second Line Treatment/Refractory CLE

Immunosuppressants: Approximately half patients refractory to antimalarials respond to immunosuppressants. In the presence of high disease activity, long-stablished disease, and refractoriness to antimalarials, immunosuppressive are recommended. Methotrexate (MTX) is considered second-line treatments whereas, third-line therapies include other

immunosuppressants such as Mycophenolate mofetil (MMF), Azathioprine, Cyclosporine or Cyclophosphamide that are mainly recommended for CLE with systemic involvement [191].

MTX is recommended at 7.5 to 25mg orally or subcutaneously once a week [178]. A retrospective analysis of 43 treatment-refractory CLE patients treated with oral or subcutaneous methotrexate found improvement in 98% of cases. Seven patients developed severe side-effects that required treatment withdrawal [192]. Potential side effects include gastrointestinal toxicity, bone marrow suppression, nephrotoxicity, hepatotoxicity, and interstitial pneumonitis.

MMF and mycophenolate sodium have been shown to be effective in treating all CLE subtypes in multiple case reports and small studies. A retrospective analysis showed that MMF was effective in antimalarial-resistant CLE when added to antimalarial therapy [193], although treatment response was often delayed, but sustained. Out of 24 patients with a variety of CLE subtypes, 9 patients (37%) demonstrated a complete response to MMF therapy and 9 (37%) showed some improvement. Six of them (25%) flare-up after response. Azathioprine has been also shown to successfully treat DLE in several small case series.

Chang et al. [194] evaluated the quality of life of CLE following different treatments and showed that methotrexate and MMF were more effective than azathioprine for CLE management as evaluated by CLASI index. Overall, studies assessing the efficacy of immunosuppressants in CLE are small and limited in the ability to draw a conclusion and further work needs to be carried out.

Oral dapsone and retinoids are recommended as second-line systemic treatment in selected CLE patients unresponsive to other treatments, preferable in addition to antimalarials [178]. Dapsone can cause agranulocytosis, haemolysis, methemoglobinemia, or a hypersensitivity reaction, and therefore monitoring for hematologic and hepatic toxicity is critical. Patients with glucose-6-phoshate dehydrogenase deficiency should not take dapsone [195].

Biologics: The unique biologic agent approved for SLE is belimumab, a human monoclonal antibody that inhibits B-cell activating factor, also known as B-lymphocyte stimulator (BLyS). Belimumab has demonstrated improved SLE disease activity on musculoskeletal and mucocutaneous parameters in data pooled from two phase III trials. [196], but the trials were not designed or powered to determine its efficacy in any specific

organ domain. Therefore, according to the European guidelines belimumab is not recommended for the treatment of CLE without systemic involvement [178].

The other anti-B cell therapy is Rituximab, an anti-CD20 monoclonal antibody, showed efficacy in case reports of refractory lupus profundus and SCLE [197,198] but not in the Randomised Clinical Trials (RCTs). For this reason, it is not either recommended by guidelines. Recently, anifrolumab, a human monoclonal antibody to type I interferon receptor subunit 1, has been approved for SLE showing discrete efficacy [199]. However, improvements in skin conditions were observed. Among patients with at least moderately active skin disease (CLASI ≥10) at baseline, a reduction of 50% or more in the CLASI at week 12 occurred in 49.0% of the patients (24 of 49) receiving anifrolumab and in 25.0% (10 of 40) receiving placebo (adjusted difference, 24.0 percentage points; 95% CI, 4.3 to 43.6; adjusted P=0.04).

Novel biological treatments may appear in the next years as several molecules are being currently evaluated in different clinical trials specific for CLE.

Immunomodulators: Several case series support the use of immunomodulatory drugs (IMiDs) such as thalidomide or analogs like lenalidomide for erythema nodosum leprosum, Behcet´s disease and refractory CLE. In CLE, both drugs have shown a marked efficacy, achieving clinical remission in 80–90% of the refractory SCLE or DLE patients [200].

Although thalidomide is considered a third line of treatment in CLE, for the PhD purposes this section will be described in more detail.

1.3 Thalidomide definition

Thalidomide is a derivative of glutamic acid, an oral non-barbituric drug, developed by Chemie Gruenenthal GmbH in West German in 1954. It is formed by S(–) and R(+) enantiomers that interconvert under physiological conditions. The S(–) form potently inhibits release of TNFα from peripheral mononuclear blood cells, whereas the R(+) form seems to act as a sedative [201]. In late 1950s and early 1960s it was prescribed as a sedative and hypnotic. Patients with hyperthyroidism and thyrotoxicosis, labile hypertension, bronchial asthma, and “nervous gastric troubles” were treated with thalidomide. Moreover, it was especially effective for the treatment of morning sickness and nausea of pregnant woman.

1.3.1 History of thalidomide

Thalidomide rapidly became a popular sedative and antiemetic, marketed under at least 37 names worldwide. However, shortly, its high teratogenicity was described, newborns of women who took thalidomide during gestation were born with important congenital birth defects such as phocomelia [202]. Thalidomide was then withdrawn for the market in 1962, however, it is estimated that around 7000-8000 births were affected with congenital defects in at least 14 countries.

1.3.2 Thalidomide current indications

In 1965, Sheskin et al [203], reported that thalidomide was administered to a patient with erythema nodosum leropsum because of his insomnia and conversely, had an impressive therapeutic response in his skin condition. Within this discovery, thalidomide was then selectively reintroduced for the treatment other immune-mediated skin disorders during the 1970s and 1980s. Thalidomide beneficial effects were reported in the treatment of patients with actinic prurigo, prurigo nodularis and chronic aphthosis [204–206]. In 1975, Barba-Rubio and Franco-González [207] reported good clinical response in patients with discoid lupus erythematosus treated with thalidomide.

Thalidomide is also an anticarcinogenic agent both as a single agent or in combination with dexamethasone or other chemotherapeutic agents [208]. The best response rates had been observed in hematological malignancy, especially in relapsing or refractory multiple myeloma with a clinical response ranging 25-69% [209].

1.3.3 Thalidomide efficacy in CLE

Since beneficial effects in CLE were reported, multiple studies have been performed. Studies show that thalidomide's efficacy in CLE patients is significant, with 80–90% reaching clinical remission [210–212] . The majority of CLE patients included had DLE, to a lesser extent SCLE and much less frequently acute lupus, lupus profundus and lupus tumidus. The response rates were significantly higher in DLE and SCLE (98%), whereas in the other CLE subtypes the response rates only reached 50%. Recurrence in CLE reaches 70% occurring when decreasing or interrupting treatment. Relapse is frequent after thalidomide's withdrawal and most common in DLE. Among patients with DLE, the generalised subtype tended to recur more than the localised one. All cases responded to the drug reintroduction; therefore, a minimal maintenance dose is required in some patients to avoid relapse. Clinical improvement was observed within the first 2 weeks of treatment, although a complete response usually occurred between weeks 4 and 8.

Although no studies have established an induction and maintenance dosage for the control of skin lesions, the different studies have used between 100 and 400 mg/day.

1.3.4 Thalidomide side effects

Thalidomide drug has important side effects such as teratogenicity, peripheral neuropathy in 20-30% of patients and thromboembolic events [213]. Minor side effects include constipation, somnolence and amenorrhea. For this reason, the clinical benefits in CLE need to be balanced against thalidomide potential side effects. Its use is restricted to severe CLE disabling conditions and only after the failure of several previous treatments.

1.3.5 Thalidomide described mechanism of action

In 2010, Ito et al [214], discovered that the Cereblon (CRBN) protein was the primary target of thalidomide and its analogues lenalidomide and pomalidomide. CRBN forms part of E3 ubiquitin ligase complex ($CRL4^{CRBN}$) composed by Cullin-4A(CUL4), damage-specific DNA-binding protein 1 (DDB1) and RING-box protein 1 (RBX1), and its function is to target substrates for degradation via ubiquitin-proteasome pathway. When IMiDs bind to CRBN, there is an alteration for the substrate specificity of E3 ligase $CRL4^{CRBN}$, displacing endogenous substrates, and as a result, other substrates are recruited and degraded, leading to the beneficial immunomodulatory effects of thalidomide, but also to its undesirable teratogenic effects.

Ikaros (IKZF1) and Aiolos (IKZF3) are well-known described substrates of $CRL4^{CRBN}$ in presence of IMiDs. These two proteins are transcription factors that regulate gene expression, and their degradation promotes a downregulation of c-MYC and IRF4 (Interferon Regulatory Factor 4) [215]. Both c-MYC and IRF4 are factors that sustain multiple myeloma cells growth and survival, and their modulation by IMiDs has been shown to be beneficial with anti-proliferative and pro-apoptotic effects [216].

Moreover IKZF1/3 are involved in the modulation of immune response. IKZF1 modulates dendritic cell development and function, specifically pDCs and DCs numbers [217] in humans. Moreover, IMiDs-CRBN-IKZF1/3-IRF4 axis is also involved in NK-cell activating ligand by multiple myeloma cells [218]. IKZF transcription factors act as regulators of T cell homeostasis by negatively regulating Th1 cell polarization and promoting Th17 and Treg responses [219]. Also, Th1 cytokines IFNγ and IL-2, and inflammatory cytokines, TNFα and Granulocyte-macrophage colony-stimulating factor (GM-CSF) and, IFN type I genes are negatively regulated by IKZF1 [220].

Other recent novel but less explored identified substrates of $CRL4^{CRBN}$ in presence of IMiDs are Casein kinase 1A1 (CK1), Sal-like protein 4 (Sall4), Tumor protein p63 (p63) and G1 To S Phase Transition 1 protein (GSPT1) [221–224].

1.3.6 Thalidomide biological properties

Thalidomide is known to have beneficial therapeutic effects mediated by its anti-inflammatory, immunomodulatory and anti-angiogenic properties (Fig 16):

- *Anti-inflammatory*. In 1991, it was discovered that thalidomide inhibited the synthesis of TNFα [225]. TNFα induces an increased vascular permeability leading to a greater recruitment of inflammatory cells, immunoglobulins, and complement, as well as causing activation of T and B lymphocytes [226]. Activated macrophages are the main producers of TNFα and also highly reactive to it, although it can be produced by many other cell types. It has been demonstrated that thalidomide inhibits the alternative activation of macrophages accompanied by a reduction of TNFα, IL-4, IL-5, IL-13, and IL-17 [227]. Moreover, thalidomide anti-inflammatory effect is mediated by the modulation of other inflammatory cytokines such as IL-1, IL-2, IL-6, IL-8, IL-10, IL-12, and IFNγ [228].

- *Immunomodulatory.* To date, the immunomodulatory effect of thalidomide is poorly understood. In 1998, it was discovered that thalidomide could co-stimulate T cells independently of the secondary interaction between B7 and CD28 molecules [229]. Immunomodulatory effects of thalidomide analogues, lenalidomide and pomalidomide, have been studied and they promote stimulatory effects in both $CD4^+$ and in $CD8^+$ T cells [230]. IMiDs exert their effects by activating protein kinase C delta (PKC-θ) and acting o1 AP-1 DNA-binding activity in T cells, resulting in augmented IL-2 synthesis and activation of IL-2-dependent downstream effectors, such as NK cells [231].

- *Anti-angiogenic.* It was in 1994 when the anti-angiogenic effect of thalidomide was discovered. Using a rabbit model, it was demonstrated that thalidomide could inhibit the fibroblast growth factor and vascular endothelial growth factor (VEGF) induced in angiogenesis [232]. Due to its anti-angiogenic effects, thalidomide is able to alter fetal development in pregnant women, which leads to fetal deformity. However, at the same time this effect is one of the mechanisms for its antitumour activity. *In vitro* and *in vivo* studies suggest that IMiDs may inhibit angiogenesis by anti-migratory mechanisms [233, 234]. Thalidomide reduces metastasis by reducing the expression of proangiogenic cytokines such as VEGF that decreases both capillary density and the number of adhesion cells [235].

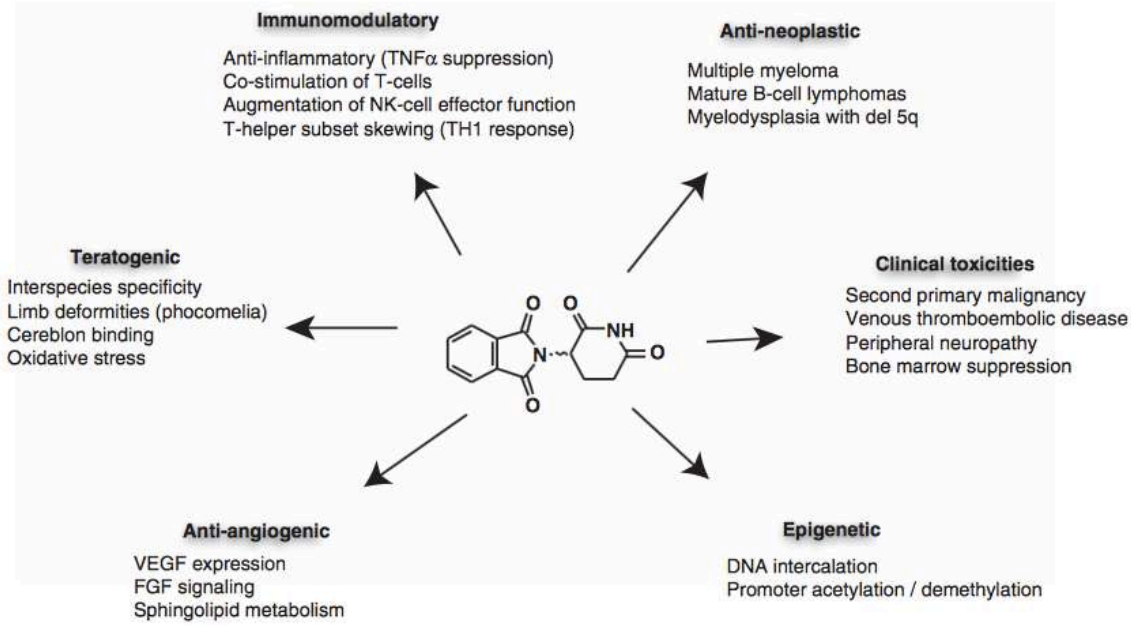

Figure 16. The pleotropic effects of thalidomide. From Shortt et al. [236]

1.4 Differences between SCLE and DLE subtypes

Although CLE shares common histological and pathophysiological features, its clinical heterogeneity has been largely established. Clinically they differ in the type of lesion, duration and outcomes. SLCE resolve without scarring whereas DLE is prone to leave irreversible fibrotic scars with pigmentary changes (Fig 17).

In 1992 David-Bajar et al. proposed that SCLE and DLE may have different pathological mechanisms [237]. Immunofluorescence studies show a different distribution of IgG deposits with a predominance in the dermal-epidermal junction (DEJ) in DLE lesional skin, whereas in SCLE, IgG patterns were predominantly found in the epidermis. IgM and IgA were both found in the DEJ of both subtypes. In addition, serologically, SCLE is strongly associated with anti-SSA/Ro and SSB/La antibodies and the presence of SLE, whereas many DLE do not have detectable circulating antibodies and the progression rates to a systemic disease are low.

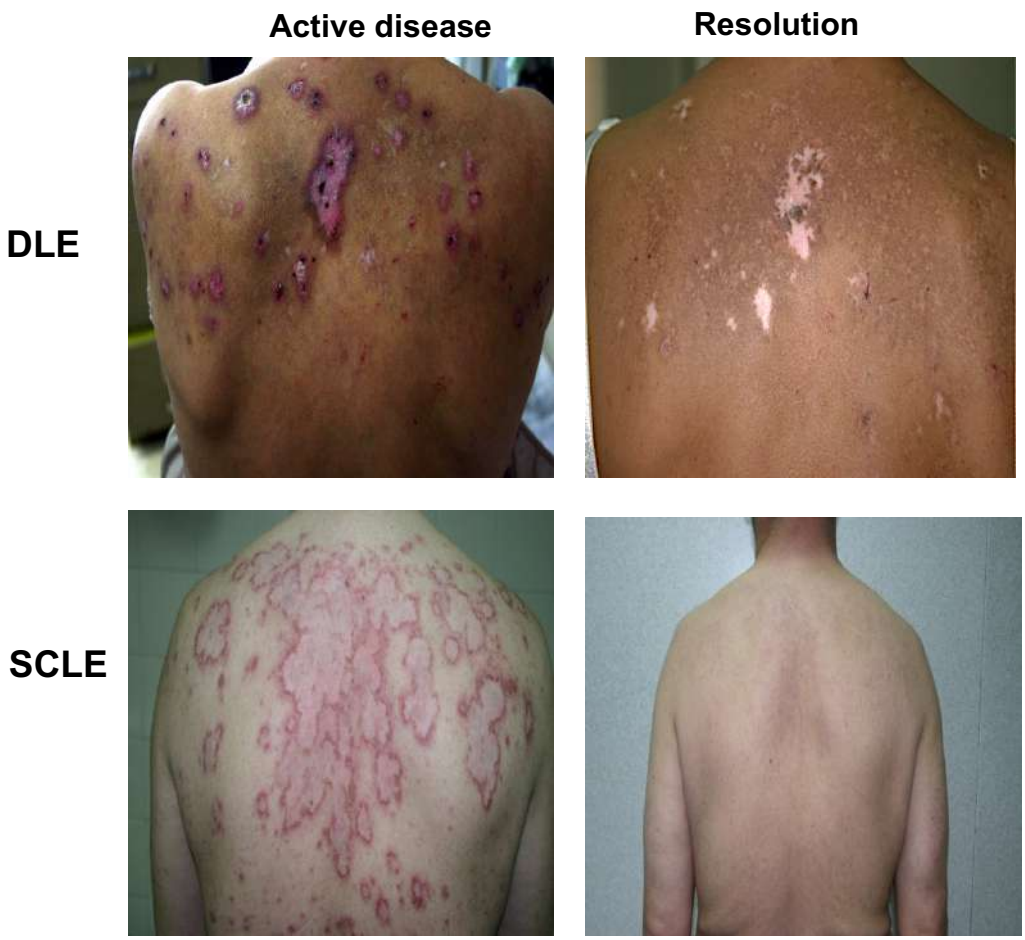

Figure 17. DLE and SCLE patients before and after treatment. After treatment, in DLE permanent scarring occurs in lesional sites. In contrast in SCLE, lesions completely resolved without sequelae.

In recent years, the use of next-generation transcriptomic techniques has led to the study of the molecular heterogeneity of DLE and SCLE. Gene microarray analysis of DLE and SCLE lesional skin compared with non-lesional skin from paired patients performed by our group showed that DLE and SCLE lesional skin present differentially transcriptional prolife from their respective non-lesional CLE subtype. However, direct comparison of DLE and SCLE differentially expressed genes, showed that there were no uniquely differentiated genes in SCLE. Analyzing the identified differentially expressed genes in the DLE lesional skin, $CD4^+$T cell enrichment with an imbalance towards T helper 1 predominance and an increase FoxP3 response was observed. Also, it was shown a TGF-β-dependent pathway inducing fibrosis in DLE [142]. All this data suggests there are differences in pathogenesis in the DLE subtype.

Cytokine assessment in $CD4^+$ T cells from DLE and SCLE present in the skin, showed that IL-17, IL-22 and IFNγ were significantly higher expressed in DLE compared in SCLE,

expression levels in SCLE were higher when compared with healthy controls. Similar results has been described in In circulation, suggesting that T cell responses are more intense in DLE compared with SCLE [238].

B cells have been recently studied in gene expression programs showing a significant enrichment in numbers and subsets in the lesional skin of DLE lesions compared to SCLE, suggesting a most pronounced role of B cells in DLE pathogenesis compared with SCLE. However, the study did not deepen into the role of B cells, their recruitment and their differentiation in lesional skin in CLE [155].

Finally, it is suggested that there is heterogeneity of clinical response to therapy between subtypes, as DLE tends to be more refractory to standard treatment than other CLE subtypes [239]. However, the only evidence-based study comparing medication response by subtype or race did not find statistically significant difference when comparing SCLE vs DLE ($p > 0.05$). Whereas DLE forms tended to relapse and required a long-term maintenance dose of thalidomide, SCLE forms showed a sustained remission after withdrawal. In addition, although response to thalidomide is similar between the two types of CLE, DLE forms tended to relapse and required a long-term maintenance dose of thalidomide, SCLE forms showed a sustained remission after withdrawal [240].

2. Hypothesis and Objectives

2.1 Hypothesis

The pathogenesis of CLE is not completely understood. MiRNAs, are fine regulators of gene expression and have been described to be involved in the pathogenesis of other autoimmune chronic skin diseases, therefore, our first hypothesis is that:

- There are differentially expressed miRNAs between CLE lesional and CLE non-lesional skin and that they contribute to CLE pathogenesis.

Moreover, the DLE subtype develops inflammatory lesions that progress into hypopigmented scarring areas. Therefore, our second hypothesis is that:

- There are miRNAs that differ from DLE and SCLE subtypes and may be involved in the DLE pathogenesis and may explain the characteristic DLE features.

In addition, up to 40% of patients are refractory to standard treatment and for these cases there is no consensus algorithm and a trial-and-error approach using multiple systemic immunosuppressive agents with a variable poor clinical response is being used. Thalidomide, although used as a third line of therapy, is an effective drug for refractory CLE cases, with a proven clinical efficacy of 80-90%. However, its use is restricted due to its severe side effects. Its mechanisms of action in skin inflammatory diseases and specifically in CLE it is not elucidated. And our third hypothesis is that:

- Identification of thalidomide's mechanism of action in CLE may help us to identify novel therapeutic targets in order to develop in the future new drugs as effective as thalidomide but with fewer adverse effects.

2.2 Objectives

In order to demonstrate the hypothesis, the project has been divided in three parts and the following objectives associated to a chapter have been established:

- **Chapter 1: microRNAs in CLE**
  - **Objective 1**: To Identify a specific DLE miRNA profile compared with SCLE, and to study the role of the differentially expressed miRNAs in DLE pathogenesis.
  - **Objective 2:** To identify the miRNA profile in CLE lesional skin in comparison with CLE non-lesional skin, and to study the role of the differentially expressed miRNAs in CLE pathogenesis.

- **Chapter 2: Thalidomide mechanism of action in CLE**
  - **Objective 3**: To Identify the Thalidomide mechanism of action in CLE and novel putative therapeutic targets.

- **Chapter 3: Thalidomide – miRNAs**
  - **Objective 4:** To study the expression of the discovered miRNAs in skin from CLE patients before and after thalidomide treatment and also *in vitro* within primary cells treated with thalidomide.

3. Materials and Methods

In order to conduct this thesis, the following methods cited in table 5 have been performed. Some methods are common in the different scientific manuscripts (Paper I, II and III) and some of them are specific for each work. They are detailed below in this section and also in the materials and methods section of each paper.

Chapter 1. microRNAs in CLE		**Chapter 2. Thalidomide Mechanism of action in CLE**
Paper I. miR-31 and miR-485-3p in DLE.	Paper II. miR-885-5p in CLE	Paper III. Thalidomide mechanism of action in CLE.
3.1 Common methodology between Paper I and Paper II:		3.3 Specific methods for Paper III
3.1.1 Baseline characteristics of the patients. 3.1.2. Biological samples collection 3.1.3. miRNA extraction from skin biopsies 3.1.4. miRNA screening of lesional and non-lesional skin samples 3.1.5. Statistical Analysis of miRNA microarray data. 3.1.6. miRNA RT-qPCR 3.1.7. *In situ* Hybridization 3.1.8 ELISA (Enzyme-Linked ImmunoSorbent Assay) 3.1.9 Anti-miRNA or mimics-miRNA (Paper I and II)		3.3.1 Baseline characteristics of the patients 3.3.2. Biological samples collection 3.3.3. RNA extraction from skin biopsies 3.3.4. RNA-sequencing in thalidomide pre and post treated samples and library construction 3.3.5 Identification of the thalidomide mechanism of action by applying TPMS protocols 3.3.6 Immunohistochemistry 3.3.7 Protein extraction from skin biopsies 3.3.8.Western blot 3.3.9 Ubiquitination assay *in vitro* 3.3.10 Ubiquitination assay *in vivo* 3.3.11 Thalidomide preparation

	3.2 Specific methods for paper II 3.2.1 Gene microarray in anti-885-5p transfected keratinocytes. 3.2.2 Statistical analysis of the mIR-885-p transfected keratinocytes microarray 3.2.3 Kinetic study of the expression levels of mIR-885-p following stimulation 3.2.4 Luciferase assay	
Chapter 3: Thalidomide – miRNA		
3.4.1 Hydroxychloroquine preparation. Notes: - Thalidomide was prepared as detailed in Chapter 2 (3.3.11) - RT-qPCR of microRNAs of interest was performed as detailed in Chapter 1 (3.1.6) - Skin samples used were the same as in Chapter 2. (3.3.1, 3.3.3)		
3.5 Common methodology for Chapter 1, 2, 3 (Paper I,II and III)		
3.5.1 Cell culture 3.5.2 Cell stimulation 3.5.3 siRNA transfection 3.5.4. Migration experiments 3.5.5 Gene expression analysis 3.5.6 Immunofluorescence analysis of cultured cells 3.5.7 Functional cell assays (Proliferation and Apoptosis) 3.5.8 Flow Cytometry 3.5.9 Immunofluorescence in skin biopsy 3.5.10 Statistical Analysis of the obtained data		

Table 5: Experimental Methods performed in the thesis

3.1. Chapter 1: Common methodology in the study of microRNAs in CLE

3.1.1 Baseline characteristics of the CLE patients included in the study (Paper I and II)

In order to conduct the microRNA profiling study in CLE skin, CLE patients were recruited from the Rheumatology Department at Vall d'Hebron University Hospital (Barcelona, Spain). A total of 20 patients were enrolled of whom 10 were diagnosed with DLE and 10 with SCLE. The patient inclusion criteria were: 1) age ≥ 18 years; 2) the presence of active cutaneous lupus lesions bigger than 3cm; 3) the presence of lesions classified by the CLE Disease Area and Severity Index (CLASI) > 4; 4) no previous treatment with immunosuppressants for ≥1 month or topical corticoids for at least ≥2 weeks.

The study was approved by the local Vall d'Hebrón ethics committee and written informed consent was obtained from all subjects before enrolment. The diagnosis and classification of CLE were based on clinical and histological criteria according to the 2004 Dusseldorf classification [35].

The baseline, clinical and laboratory characteristics of the patients that participated in the study are summarised in the Table 6:

Clinical features*	**DLE (n=10)**	**SCLE (n=10)**	***P* value**
AGE, mean (SD), in years	44 (10.3)	51 (15.9)	0.25
Female, n (%)	7 (70%)	8 (80%)	0.79
Photosensitivity, n (%)	3 (30%)	5 (50%)	0.47
Smoking, (%)	6 (60%)	1 (10%)	0.05
CLASI ACTIVITY, mean (SD)	9.8±3.7	6.54±2.16	0.03
Skin Lesion Location • Back • Arm • Face • V-neck area	 4 (40%) 2 (20%) 4 (40%) 0 (0%)	 5 (50%) 3 (30%) 0 (0%) 2 (20%)	 0.11 0.65 0.04 0.15
CLASI DAMAGE, mean (SD)	1.78±1.76	0.18±0.60	0.01
SLE	4 (40%)	6 (60%)	0.52
Duration of cutaneous lesions, months, mean (SD)	8.9 (3.7)	6.2 (5.57)	0.21
ANA positive, n (%)	5 (50%)	7 (70%)	0.56
Anti-Ro positive, n (%)	1 (10%)	5 (50%)	0.10
Previous CLE medication • Topical Steroids • Antimalarials	 10 (100%) 10 (100%)	 10 (100%) 10 (100%)	 0.99 0.99

• Immunosupressants - Methotrexate - Azathioprine - Mycophenolate • Dapsone • Retinoids • Thalidomide • Oral Steorids	 4 (40%) 3 (30%) 2 (20%) 0 (0%) 0 (0%) 5 (50%) 4 (40%)	 4 (40%) 2 (20%) 0 (0%) 0 (0%) 0 (0%) 5 (50%) 6(60%)	 0.99 0.50 0.75 0.99 0.99 0.99 0.52

Table 6: Baseline characteristics for 20 patients diagnosed with CLE that participated in the microRNAs in CLE skin research project (DLE= 10, SCLE= 10).* Patients were not receiving treatment with immunosuppressants for ≥1 month or topical corticoids for at least ≥2 weeks before inclusion.

3.1.1.2. Biological samples collection (Paper I and II)

Two six-milliliter skin punch biopsies were taken from lesional active skin and non-lesional skin of CLE paired patients. The first skin biopsy was divided into two sections: the first was used for miRNA microarray experiments and the second section was fixed in 5% formalin and paraffin-embedded in order to perform immunohistochemistry technique. The second six-millimeter skin punch biopsy was immediately processed for keratinocyte and fibroblast primary cell isolation or frozen at -180ºC for immunofluorescence studies. In order to validate the results obtained in the miRNA screening, a new cohort of formalin-fixed paraffin embedded (FFPE) lesional samples obtained from DLE (n=20) and SCLE (n=18) patients was included (Table 7).

Clinical features*	**DLE (n=20)**	**SCLE (n=18)**	***P* value**
AGE, mean (SD), in years	51 (9.7)	44 (12.8)	0.05
Female, n (%)	14 (70%)	10 (55,5%)	0.66
Photosensitivity, n (%)	6 (30%)	9 (50%)	0.43
Smoking, (%)	14 (70%)	2 (11,1%)	0.002
CLASI ACTIVITY, mean (SD)	8.89±4.6	6.53±2.2	0.07
Skin Lesion Location • Back • Arm • Face • V-neck area	 8 (40%) 4 (20%) 8 (40%) 0 (0%)	 9 (50%) 3 (16,6%) 0 (0%) 6 (33,3%)	 0.80 0.70 0.004 0.01
CLASI DAMAGE, mean (SD)	2.01±1.86	0.15±0.50	0.001
SLE	8 (40%)	12 (66,6%)	0.37

Duration of cutaneous lesions, months, mean (SD)	10.1 (5.7)	7.2 (6.7)	0.15
ANA positive, n (%)	8 (40%)	12 (66,6%)	0.37
Anti-Ro positive, n (%)	2 (10%)	9 (50%)	0.03
Previous CLE medication • Topical Steroids • Antimalarials • Immunosupressants - Methotrexate - Azathioprine - Mycophenolate • Dapsone • Retinoids • Thalidomide • Oral Steroids	 20 (100%) 20 (100%) 5 (25%) 5 (25%) 2 (10%) 0 (0%) 0 (0%) 7 (35%) 10 (50%)	 18 (100%) 18 (100%) 2 (11,1%) 1 (5,5%) 1 (5,5%) 0 (0%) 0 (0%) 3 (16,6%) 12 (66,6%)	 0.99 0.99 0.89 0.61 0.87 0.99 0.99 0.17 0.66

Table 7: Baseline characteristics for the validation cohort (DLE= 20, SCLE= 18).* Patients were not receiving treatment with immunosuppressants for ≥1 month or topical corticoids for at least ≥2 weeks before inclusion.

At the time of skin biopsy, blood samples were also collected from CLE patients to isolate peripheral blood mononuclear cells (PBMCs) that were stored at -180ºC for further experiments. Serum and plasma were also obtained and stored at -80ºC.

3.1.3. miRNA extraction from skin biopsies (Paper I and II)

a) miRNA extraction from fresh skin samples

Total miRNA from fresh skin biopsies was obtained based on sample disruption and organic extraction using *mir*Vana Isolation Kit (Applied Biosystems, Foster City, CA, USA). We selected this kit because is a rapid procedure to isolate small RNAs from tissue and cells using an efficient glass fiber filter based method. The method isolates total RNA ranging in size from kilobases down to 10-mers. Although the *mir*Vana miRNA Isolation Kit efficiently purifies all RNA larger than 10 nt, it also includes procedures for isolating RNA fractions, specifically enriched or depleted in small RNA species. RNA molecules of ~200 nt and less can be efficiently purified away from the larger RNA species. The resulting RNA preparation is highly enriched for miRNAs. Small RNA enrichment allows more sensitive small RNA detection with less background as compared to the same assay used with total RNA.

Firstly, skin biopsies were homogenised by polytron and lysed with 300 µL of Lysis/Binding Buffer which aims to stabilize RNA and inactivate RNases. Then, 1/10 volume (30 µL) of miRNA homogenate was added to optimize microRNA extraction. After incubation on ice for 10 minutes, an equal volume to the lysate of Acid Phenol:Chloroform was added and the tubes were vortexed for 30 minutes and centrifuged for 5 minutes at 10.000 rpm. The aqueous phase (upper) containing a semi-pure RNA samples was clearly visualised from the organic phase (lower) and transferred into a fresh tube with 1/3 volumes of 100% ethanol. Then, the enrichment procedure for small RNA enrichment was performed. The enrichment is accomplished by first immobilizing large RNAs on a Filter Cartridge with a 1/3 volume 100% ethanol concentration and collecting the flow-through containing mostly small RNA species. Then, 2/3 volume 100% ethanol was added to the collected flow-through and the solution was placed into a second Filter Cartridge and centrifuged at 10.000rpm for 15 seconds in order to retain the miRNAs. The flow-through is discarded and washes are performed with miRNA wash solution 1 and 2 (buffers with ethanol). Finally, miRNAs were eluted from the filter with 100 µL of nuclease free water (Invitrogen, Carlsbad, CA, USA) pre-heated to 95ºC.

Agilent 2100 bioanalyzer (Agilent Technologies, Santa Clara, CA, USA) was used to perform quality control and only samples with RNA integrity number ≥ 8 were selected for the miRNA microarray.

b) miRNA extraction from FFPE samples

Validation of microarray results was performed in another cohort of FFPE skin samples from patients with CLE. Sample blocks were cut in 20µm sections using a microtome. Three of the obtained sections were used to isolate the total miRNA with the PureLink FFPE RNA Isolation Kit (Applied Biosystems, Foster City, CA, USA). The sectioned pieces of FPPE skin were placed into RNase free microcentrifuge tube in which 300µl Melting Buffer were added. The tube was incubated 10 min at 72ºC with gentle shaking to melt the paraffin. 20 µl of proteinase K were added to digest the contaminating proteins present in the sample for 10 min at 60ºC. Then, the sample was centrifuged at maximum speed for 1 minute and the tissue lysate was easily separated from the paraffin and transferred into a clean RNase free tube. Binding buffer (400 µl) was added to lysate the sample together with 800 µl of 100% ethanol and mixed thoroughly. The solution was placed into a Filter Cartridge and centrifuged. A total of three washes were performed with ethanol buffers to remove impurities. Finally, elution of the miRNAs was done with 50µl of RNAse

free water (Invitrogen, Carlsbad, CA, USA) pre-heated at 65ºC. Isolated miRNA was stored at -80ºC until further use.

The yield and the quality of RNA were determined by measuring its absorbance at 260nm and 280nm by using Nanodrop-2000 UV-Vis Spectrophotometer (ThermoFisher Scientific, Waltham, MA, USA), using 3µl of sample. Ratios of A_{260}/A_{280} between 1.8 and 2.1 were considered acceptable to use the RNA for the subsequent experiments.

3.1.4. miRNA screening of lesional and non-lesional skin samples (Paper I and II)

High-throughput microRNA expression profiling of CLE lesional and non-lesional skin was acquired using TaqMan MicroRNA A+B Cards Set v2,0. (Applied Biosystems, Foster City, CA, USA) following manufacturing instructions. The TaqMan® Array Human MicroRNA Card Set v2.0 is a two-card set containing a total of 384 TaqMan® MicroRNA Assays per card. A total of 754 human microRNAs can be detected by using two 384-well microfluidic cards, where each well represents a miRNA of interest. Three endogenous controls are included as positive controls for data normalization and one not human microRNA is included as a negative control to assure the correct functioning of the technique.

The procedure begins with the transcription of 350 ng of isolated miRNA to cDNA by using Taqman MicroRNA Reverse transcription kit in combination with the stem-loop Megaplex primer pool (Applied Biosystems, Foster City, CA, USA), allowing simultaneous reverse transcription of 450 miRNAs and endogenous controls. After RT, the cDNA was diluted with RNase free water to have 50 µL total volume. Then, 50 µL of TaqMan® Universal PCR Master Mix (2×) were added and the mixture was transferred into one of the eight loading ports on a micro fluidic card. The cards were centrifuged in a Sorvall Legend™ centrifuge (Kendro Scientific, Asheville, USA) for 2 min at 1200 rpm to distribute the samples from the loading port into each well. Following centrifugation, the cards were sealed with a TaqMan Low Density array sealer (Applied Biosystems, Foster City, CA, USA) to prevent cross-contamination. Each card was placed in the micro fluidic card sample block of an ABI Prism® 7900HT sequence detection system (Applied Biosystems, Foster City, CA, USA) and polymerase chain reaction (PCR) amplification was performed. Thermal Cycling conditions were as follows in table 8:

Step	Time	Temperature
Step 1	10 min	95 ºC
Step 2: 40 cycles	15 sec	95 ºC
	60 sec	60 ºC
Hold	∞	4 ºC

Table 8. qPCR conditions.

Raw Cq (quantification cycle: the crossing point between the baseline corrected amplification curve and threshold line) values were calculated using the SDS software v.2.3. Array experiments were performed in four replicates.

3.1.5 Statistical Analysis of miRNA microarray data (Paper I and II)

The obtained data from the Taqman MicroRNA arrays were analysed by the Statistics and Bioinformatics Unit of Vall d'Hebron Research Institute (VHIR). The statistical analyses corresponding to arrays were performed using the R statistical software package (www.R-project.org) (R Core Team, 2014) and the libraries developed for microarray data analysis by the Bioconductor Project (www.bioconductor.org).
The biological significance of the differential expressed microRNAs and their involvement in cellular signaling pathways were studied using the Ingenuity Pathway Analysis (IPA®, QIAGEN Redwood City, www.qiagen.com/ingenuity).

3.1.6. miRNA RT-qPCR (Paper I and II)

The specific detection of each miRNA of interest was conducted in the miRNA isolated from another cohort of FFPE samples. The total isolated miRNA was reverse transcribed into cDNA using specific miRNA primers with TaqMan MicroRNA Reverse Transcription Kit (Applied Biosystems, Foster City, CA, USA) and then PCR products were amplified from cDNA samples.

The obtained miRNA was diluted to 50ng of RNA per RT-reaction. Then 0.15 µl of dNTPs, 1 µL of Reverse Transcriptase, 1.5 µl of 10x Reverse Transcription Buffer, 0.19 µl RNAse inhibitor, 4.16 µl of Nuclease free water and 3µl 5x of specific miRNA RT primer were added. The following Reverse Transcription (RT) primers for hsa-miR-31, hsa-miR-485-3p, hsa-miR-885-5p and hsa-miR-139-5p quantification were used and also endogenous control miR-U6 expression was assessed for data normalization (Applied Biosystems,

Foster City, CA, USA). Master mix with all the reagents was prepared in order to assure properly consistency and avoid pipetting bias errors. The RT-reaction tubes were placed in a thermocycler (Biometra, Göttingen, Germany) and incubated using standard cyclin the following settings in Table 9:

Step	Time	Temperature
Step 1	30 min	16 ºC
Step 2	30 min	42 ºC
Step 3	5 min	85 ºC
Hold	∞	4 ºC

Table 9. miRNA reverse transcription conditions.

After that, the quantification of each miRNA was performed by real time quantitative PCR. The obtained cDNA was placed into 96 well plaques and 1 µl of Specific PCR primers for hsa-miR-31, hsa-miR-485-3p, hsa-miR-885-5p and hsa-miR-139-5p and for the endogenous control miR-U6 (Applied Biosystems, Foster City, CA, USA) were added in each appropriate well together with 10 µl of TaqMan® Universal Master Mix II, no UNG (Applied Biosystems, Life Technologies, CA, USA). Again, a master mix with all the reagents was prepared in order to assure properly consistency. Once prepared, the plate was sealed with adhesive PCR film (ThermoFisher Scientific, Waltham, MA, USA) and placed into ABI7000 (Applied Biosystems, Life Technologies, CA, USA) with the following conditions (Table 10). All the assays were performed in triplicate.

Step	Time	Temperature
Step 1	10 min	95 ºC
Step 2: 40 cycles	15 sec	95ºC
	60 sec	60 ºC
Hold	∞	4 ºC

Table 10. qPCR conditions.

The quantification of the miRNAs was based on the fluorescence in each reaction, expressed in terms of threshold cycle (Ct) values provided by the thermal cycler at the end of the PCR reactions. To analyze the data the ΔCT method was used. Within this method it is assumed that the target and the reference miRNAs have similar amplification efficiencies, therefore it is crucial that the expression of the endogenous control (U6

snRNA) does not change due to the different biological and experimental. In our study the expression of U6 snRNA did not change between lesional and non-lesional skin or between different experimental conditions in cell culture. Target miRNAs were normalised with the reference U6 snRNA and finally the expression ration was calculated. Fold change was calculated dividing the obtained relative expression with the control or calibrator sample/condition. In the skin, the calibrator condition was the non-lesional skin and in the cell culture experiments was the transfected control or non-stimulated condition.

3.1.7. *In situ* Hybridization studies (Paper I and II)

In order to locate the differentially expressed miRNAs in the skin, *in situ* hybridization was performed on the second-cohort patients (validation cohort) in PFEE sections (6-4 µm thickness) from lesional and non-lesional areas of DLE and SCLE patients using miRCURY LNA microRNA ISH Optimization Kit (FFPE) (Qiagen, Hilden, Germany). Sections were deparaffinised submerged in Xylene for 15 minutes and then in 99,9% ethanol, 96% ethanol, 70% ethanol for 5 minutes each. Then, they were treated with proteinase K (20µg/ml) during 10 minutes at 37ºC for protein digestion. After being washed twice with PBS, 50µL of hybridization mix containing LNA microRNA probe of specific miRNAs (20nM) (miR-31, miR-485-3p, miR-885-5p, miR-139-5p) (Qiagen, Hilden, Germany) was incubated overnight at 55ºC in the DAKO humidified hybridization chamber (Agilent, Santa Clara, CA, USA). LNA Scramble miR probe and LNA U6 snRNA (25nM) were also hybridised as negative and positive controls respectively. On the next day, the slides were stringently washed with 5x Saline- Sodium Citrate buffer (SSC), 1xSSC and 0.2xSSC at hybridization temperature (55ºC) for 5 minutes each. Another wash was done with 0.2xSSC for 10 minutes at room temperature. The sections were then placed into a humidified chamber and incubated with blocking solution (Bovine Serum Albumin, BSA 5%) to avoid unspecific bindings at room temperature. The blocking solution was removed, and the sections were incubated with the alkaline phosphatase-conjugated sheep antidigoxigenin Fab fragments (1:800) (Roche, Basel, Switzerland) overnight at 4ºC. The probe was visualised by an incubation of 2 hours at 30ºC with the AP substrate (NBT-BCIP tablets in Milli-Q water with 0.2mM of Levamisole) (Sigma-Aldrich, Sant Louis, MO, USA) followed by a double incubation of KTBT (AP stop solution, prepared with 50mM Tris-Cl, 150 mM NaCl and 10 mM KCl) at room temperature during 5 min. The slices were then dehydrated with rising ethanol concentration buffers (70%, 96%, 99,9% ethanol each for 5 minutes) and mounted with mounting medium. The staining was observed with Olympus IX71 (TH4-200) U-RFL-T microscope. Optimization of concentration of the

reagents and incubation timings was achieved previously by assessing miR-31 *in situ* hybridization in psoriasis lesional and non-lesional samples.

3.1.8. ELISA (Enzyme-Linked ImmunoSorbent Assay) (Paper I and II)

The supernatant (culture medium) of all the *in vitro* experiments was collected and stored at -80ºC. For cytokine measurement ELISA (Abcam, Cambridge, UK) was performed. The supernatants were thawed at 37ºC in the water bath and centrifuged for 10 minutes at 2000 rpm to remove the possible presence cellular debris. 100µL of each standard and sample were added to the appropriate wells of the ELISA plaque. Then 50 µL of 1X Biotinylated antibody (Table 11) was added to all wells and the plaque was covered and incubated for 3 hours at room temperature. After incubation, the plaque was washed tree times with 1x Wash Buffer. 100 µL of 1X Streptavidin-HRP solution was added into each well. The plaque was re-covered and incubated at room temperature for 30 minutes. Three washes were repeated and 100 µL of Chromogen TMB substrate solution were added into each well. After incubation in the dark for 20 minutes at room temperature the substrate was visible and 100 µL of stop reagent was added. The plaque was immediately analysed with a spectrophotometer using 450 nm as the primary wavelength. Triplicates were performed. The mean absorbance for each set of standards, controls and samples, and the average zero standard optical density was subtracted.

Biotinylated antibody	Supplier	Paper
Anti-IL-12	Abcam	Paper I
Anti-IL-1β	Abcam	Paper I and II
Anti-IL-8/CXCL8	Abcam	Paper I and II
Anti-CCL5	Abcam	Paper II
Anti-CCL20	Abcam	Paper II
Anti-TNFα	Abcam	Paper II
Anti-S100A7	Abcam	Paper II

Table 11. Antibodies used in ELISA assay.

3.1.9 Anti-miRNA or mimics-miRNA (Paper I and II)

After 24 hours at 37ºC 5% CO_2, miRNA inhibition or overexpression was performed following mirVana™ miRNA Transfection protocols. In brief, cells were visualised under the microscope before starting to confirm that they were around 60% of confluence. Then,

3 µl of Lipofectamine 2000 (Thermofisher scientific, Waltham, MA, USA) was diluted into 50 µL of Opti-MEM Medium (Thermofisher scientific, Waltham, MA, USA). On a separate Eppendorf tube, 1 µl of the synthetic anti-miRNA or miRNA-mimics (10µM) (Thermofisher scientific, Waltham, MA, USA) was diluted with 50 µL of Opti-MEM. Next 450 µL of complete media was added to the wells Opti-MEM media presents a 50% serum reduction which facilitates the cationic lipid transfections. Both tubes were combined into one single tube and the mix was incubated for 5 minutes at room temperature for miRNA-lipid complex generation.

3.2. Specific methodology in the study of miR-885-5p (paper II)

3.2.1 Gene microarray in anti-885-5p transfected keratinocytes (Paper II)

Gene microarrays are designed for profiling the expression of predefined or customised sets of genes in tissues, cells or fluids. They consist in solid surfaces in which a collection of microscopic spots is attached. These spots are specific proves complementary to the genes that we aim to detect. Since mRNA is degraded easily, it is necessary to convert it into a more stable cDNA form. The process in which the cDNA binds to its complementary probe is named hybridization. The hybridization level of the specific probe with the target cDNA will determine a fluorescent intensity measurable by image analysis and therefore, the gene expression is quantifiable in the processed samples.

In order to evaluate the effect of miR-885-5p in keratinocytes after anti miR-885-5p inhibition and stimulation, RNA was extracted and gene microarrays were carried out using the Clariom™ S Array Assay (Thermofisher scientific, Waltham, MA, USA)), human an array with 20.000 well-characterised human genes used to explore human biology and disease processes. Within this array, the probes are distributed across the full length of the gene, providing a complete and accurate picture of overall gene expression.

The arrays were performed at the Unitat d'Alta Tecnologia (UAT) of Vall d'Hebron Institut de Recerca (VHIR). First, samples were processed using the Affymetrix GeneChip WT PLUS Reagent kit (Thermofisher scientific, Waltham, MA, USA). Then the obtained cDNA (500ng) was labeled by exploiting the 3' hydroxyl end by T4 RNA ligase-mediated ligation of a p-CU-Cy3 dinucleotide (TriLink, BioTech, San Diego, CA). Labeled samples were then dried, resuspended in RNAse free water and co-hybridised with the Clariom™ S Array. Once the hybridization was completed, samples were subsequently washed, and slides were scanned on an appropriate microarray scanner and quantified with the Affymetrix analysis software (Thermofisher scientific, Waltham, MA, USA).

3.2.2 Statistical analysis of the mIR-885-p transfected keratinocytes microarray (Paper II)

Data obtained from the microarrays were analysed by the Statistics and Bioinformatics Unit of our institute Vall d'Hebrón Institut de Recerca (VHIR). The statistical analyses corresponding to arrays were performed using the R statistical software package (www.R-project.org) (R Core Team, 2014) and the libraries developed for microarray data analysis by the Bioconductor Project (www.bioconductor.org) (Gentleman et al, 2004).

3.2.3 Kinetic study of the expression levels of mIR-885-p following stimulation (Paper II)

Primary keratinocytes were cultured in 96 well-plates treated with Poly-D-Lysine that facilitates cells adhesion (Sarstedt, Nümbrecht, Germany). After letting keratinocytes adhere for 24h, cells were stimulated with IL-1 α (5 ng/μL) or TNFα or TGFβ or IFNα (10 ng/μL, Life Technologies, Thermofisher scientific, Waltham, MA, USA) or 25-50mJ/cm^2 UVB (Westinghouse Electric, Pittsburgh, PA, USA). RNA was extracted 0h, 2h, 4h, 6h, 8h, 12h, 18h and post-stimulation and miR-885-5p expression was evaluated.

3.2.4 Luciferase assay

To demonstrate putative target genes of miRNA 885-5p, Firefly/Renilla Dual Luciferase Assay (Promega, Wisconsin, USA) was performed. Within this assay, a reported gene is cloned with a DNA sequence of interest into an expression vector that is transferred into the cells. Then, the cells are assayed for the presence of the reporter. Luciferase assays consist in bioluminescent reporters which present exceptional sensitivity, moreover, there is no endogenous activity in the host cells to interfere with quantifications. Renilla was used as an endogenous control for the normalization of the Luciferase in order to reduce the variability that could be present between samples due to differences in the transfection efficiency. Each experiment was done in five replicates.

In order to do it, 1x10^4 primary keratinocytes were seeded into 96 well plates and were co-transfected with 3 μl Dharmafect transfection reagent (Invitrogen, Carlsbad, CA, USA) with the plasmids pEZX-MT01-PSMB5 3′UTR or pEZX-MT01-TRAF1 3′ UTR and the following:

- Negative Control
- mir-885-5p mimics 10 μM
- miRNA scrambled (control) 10 μM

After 24h, cells were lysed with 20 µL cell lysis buffer and incubated with Luciferase substrate. After lecture in the luminometer LUMIstar Omega (Ortenberg,Germany), Renila substrate was added a second lecture was performed. Data is normalised by the average ratio (Firefly/Renilla) and shown as percent activity by multiplying the fold change in activity by 100.

3.3. Chapter 2. Thalidomide mechanism of action in CLE

3.3.1 Baseline characteristics of the patients (Paper III and Chapter 3)

A total of 10 patients were included in the study. Demographic characteristics are shown in Table 12 . The patient inclusion criteria were: 1) age ≥ 18 years; 2) the presence of active cutaneous lupus lesions bigger than 3cm; 3) the presence of lesions classified by the CLE Disease Area and Severity Index (CLASI) > 4 at the time of the skin biopsy; 4) no previous treatment with immunosuppressants for ≥1 month or topical corticoids for at least ≥2 weeks. 5) At inclusion all patients received oral thalidomide (100 mg/day) at night for 4 weeks. The study was approved by the Local Vall d'Hebrón Ethics Committee and informed consent was obtained from all subjects before the study

Baseline characteristics	**CLE (n=10)**
AGE, mean (SD), years	44 (10.3)
Female, n (%)	10 (100%)
Photosensitivity, n (%)	3 (30%)
Smoking, (%)	4 (40%)
Type of CLE	
DLE	8 (80%)
SCLE	2 (20%)
CLASI ACTIVITY, mean (SD)	11.0±2.5
CLASI DAMAGE, mean (SD)	4.3±1.45
Systemic Lupus Erythematosus	4 (40%)
Clinical response to Thalidomide (4 weeks) Complete response (CLASI=0)	7 (70%)
ANA antibodies positive, n (%)	8 (80%)
Anti-SSA/Ro antibodies positive, n (%)	1 (10%)
Previous CLE medication • Topical Steroids • Antimalarials	 10 (100%) 10 (100%)

• Immunosupressants - Methotrexate - Azathioprine - Mycophenolate • Dapsone • Retinoids • Oral Steroids	7 (70%) 2 (20%) 4 (40%) 1 (10%) 0 (0%) 4 (40%)

Table 12: Baseline characteristics for 10 patients diagnosed with CLE that participated in the CLE thalidomide skin research project.

3.3.2. Biological samples collection (Paper III)

A six-millimeter punch biopsy was taken from lesional skin from CLE untreated patients and another six-millimeter punch biopsy was taken from paired patient's post-thalidomide treatment. The skin punch was divided into three sections: the first section was used for RNA-sequencing experiments, the second was immediately frozen in liquid nitrogen in OCT compound for immunofluorescence studies and the third was fixed in 5% formalin and paraffin-embedded in order to perform immunohistochemistry techniques.

At the same moment, blood samples were also collected from CLE patients to isolate PBMCs that were stored at -180ºC for further experiments. Serum and plasma were also obtained and stored at -80ºC.

3.3.3 RNA extraction from skin biopsies (Paper III)

Total RNA from skin biopsies was obtained using RNeasy Mini Kit (Qiagen, Hilden, Germany) and Ribosomal RNA was removed using Epicentre's Ribo-Zero rRNA Removal kit (Illumina, San Diego, USA). Within RNeasy Mini Kit there is no phenol/chloroform extraction. Skin samples were first lysed and homogenised as previously described in the presence of a highly denaturing guanidine-thiocyanate–containing buffer, which immediately inactivates RNases to ensure purification of intact RNA. Ethanol is next added to provide appropriate binding conditions, and the sample is then applied to RNeasy Mini spin column, where the total RNA binds to the membrane and contaminants are efficiently washed away. Finally, high-quality RNA is eluted in 30–100 µl water.

RNA integrity was evaluated using Bioanalyzer 2100 obtaining values ≥8.5 (Agilent Technologies, Santa Clara, CA, USA). Therefore, all samples were considered for the study.

3.3.4 RNA-sequencing in thalidomide pre- and post-treated patients and library construction (Paper III)

Samples were converted to cDNA and subsequently subjected to fragmentation, linker adapter ligation and amplification using TruSeq library generation kits (Illumina, San Diego, USA) according to manufacturer's instructions. The constructed libraries were amplified using 8 cycles of PCR. The resulting libraries were subjected to Illumina Hiseq 2000 sequencing platform version 3 producing 2x75 bp run with >65 M reads (Illumina, San Diego, USA).

Image analysis, sequencing quality evaluation, and data production summarisation were performed using the Illumina/Solexa pipeline (Illumina, San Diego, USA). Sequences were analysed for quality control (FASTQC) and aligned to the Human genome (GRCh38) using STAR program (version 2.5.2a) (Wingett et al., 2018; Dobin et al., 2013). RSEM program (version 1.2.28) (Li et al., 2011) was used to determine transcript assembly, and the abundance and expression levels were determined based on the fragments per kb per million (FPKM) values, a way of normalizing read counts by calculating the number of reads mapped to each transcript divided by its length and the total number of mapped reads in the sample. To find differentially expressed genes and transcripts, the logarithmic ratios of FPKMs were calculated by pairwise comparisons of the expression between pre- and post-skin thalidomide samples with tests for significant differences using DESeq2 (Love et al., 2014). To obtain high-quality differentially expressed genes (DEGs), we set the threshold for the false-discovery rate at < 0.05 and for fold change at ≥ 2 or ≤ 05 ($|\log2FC| \geq 1$) in the comparison analysis.

Data obtained from the RNA-seq before and after being processing are available in the Gene Expression Omnibus (GEO) database with the following identification code (GSE162424) (https://www.ncbi.nlm.nih.gov/geo/query/acc.cgi?acc=GSE162424)

3.3.5 Identification of the thalidomide mechanism of action by applying TPMS protocols (Paper III)

The Therapeutic Performance Mapping System (TPMS) is a tool that creates mathematical models of a drug/pathology protein pathways to explain a clinical outcome or phenotype (Anaxomics Biotech, Barcelona, Spain). These mathematical models find

mechanism of action (MoAs) that explain how a Stimulus (i.e., proteins activated or inhibited by a drug) produces a Response (i.e., proteins active or inhibited in a phenotype). The detailed steps are explained below:

Molecular characterization of CLE disease and thalidomide

To apply the TPMS approach and create the mathematical models of MoAs, a characterization of CLE disease and thalidomide is needed. We manually curated a list of proteins and motives relevant for cutaneous lupus erythematosus (CLE) pathogenesis and targets for thalidomide's mechanism of action. Manual curation was performed through an extensive and careful review of full-length articles in the PubMed database, Drug Bank, Stitch and Supertarget (Knehisa et al., 2014; Gilson et al., 2016; Chatr-Aryamontri et al., 2017; Croft et al., 2014). The search was expanded using the "related articles" function and article reference list. For CLE characterization, we included 206 proteins. For thalidomide molecular drug characterization, eight main molecules have been identified (CRBN, IKZF1, IKZF3, IRF4, MEIS2, ORM1, ORM2, FGF2) and 36 proteins were related to them.

Generation of mathematical models

We generated a biological map between CLE proteins and thalidomide targets using public information about protein-to-protein interactions, physical interactions and modulations, signaling, metabolic relationships and gene expression regulation that are founded in: KEGG, Binding Database, BioGRID and REACTOME (Jorba et al., 2020; Wishart et al., 2008; Szklarzyk et al., 2016; Hecker et al., 2012).

The algorithm of TPMS for generating the mathematical models is similar to a Multilayer Perceptron of an Artificial Neural Network over the biological map (where neurons are the proteins, and the edges of the network are used to transfer the information). It takes as input signals the activation (+1) and inactivation (-1) of the drug target proteins and as output proteins implicated in CLE pathogenesis.
The models have to be able to weigh the relative value of each protein (node) relation. Since the number of links is very high, the number of parameters to solve also increases exponentially. Anaxomics applied Artificial Intelligence (AI) technologies for modelling complex network behaviors, including graph theory and statistical pattern recognition technologies; genetic algorithms; artificial neural networks; dimensionality reduction

techniques; and stochastic methods like Simulated Annealing, Monte Carlo among others (Anaxomics Biotech, Barcelona, Spain).

Molecular mechanism construction

Then a collection of restrictions, defined as the true set of edges and nodes with the property of being active or inactive, are used for validating the mathematical models obtained with TPMS (Truth table). Two type of restrictions are used: 1) information found in microarray database (GEO, PHOSIDA, 2D gel database, BED) and drug database (DrugBank); 2) data obtained from our RNA-seq analysis using skin biopsies of CLE patients pre- and post-thalidomide treatment.

As the number of restrictions is always smaller than the number of parameters required by the algorithm, any process modelled by TPMS has a “population” of different solutions, which is set around 106–109, since this interval is estimated to faithfully portray nature. From this set of solutions, only the best ones (showing acceptable accuracy values for the Truth Table) are used to construct a “global” or “average” molecular mechanism, which represents the most probable molecular mechanism according to the current biological knowledge.

3.3.6 Immunohistochemistry (Paper III)

Immunohistochemistry was performed on paraffin-embedded skin sections according to standard procedures. Sections were deparaffined by incubation at 15 min at 60ºC and then 15 min in Xylene and 5 min in ethanol decreasing concentrations (99%, 96% and 70%). Endogenous peroxidase activity was blocked using 0.3% H2O2 in methanol. Then, slides were incubated at for antigen retrieval for 20min at 92 ºC 10mM Sodium Citrate, pH 6.0. After blocking for 1h with BSA 5% in PBS (phosphate buffered saline) , primary monoclonal antibodies were incubated overnight at 4ºC. Incubation with the secondary antibody was carried out for 30 minutes at room temperature, followed by washing in distilled water and two changes of PBS. Sections were incubated in avidin-biotin complex (ABC, Dako) for 30 minutes at room temperature, followed by washes in distilled water and two changes in PBS. The antigen-antibody reaction was visualised using di-aminobenzidine (DAB, Sigma) as the chromogen. The slides were observed with Olympus IX71 (TH4-200) U-RFL-T microscope (Olympus, Tokyo, Japan). Images were processed with Image J (NIH, USA). Antibodies are detailed in the following table (Table 13).

Primary Antibody	Supplier	Code
Anti-CD4	Roche	SP35
Anti-CD8	Agilent	DK25
Anti-CD56	Fisher Scientific	56C04
Anti-Phospho-Raptor (Ser863)	Invitrogen	PA5-64849
Secondary Antibody	**Supplier**	**Code**
Goat Anti-Rabbit IgG H&L (HRP)	Abcam	ab6721

Table 13. Antibodies used for immunohistochemistry

3.3.7 Protein extraction from skin biopsies (Paper III)

Protein was extracted from skin tissue following the instructions of PARIS kit (Thermo Fisher, Waltham, MA, USA). The skin was homogenised with the lysis buffer and samples were centrifuged at 12000 rpm at 4ºC for 3 minutes. The supernatant was collected, and 200 mL of chloroform was added. After 5 minutes on ice, samples were centrifuged 12000 rpm at 4ºC for 15 min. Then, the organic phase was collected, and isopropanol was added for 10 min at room temperature for protein precipitation. After centrifugation at 12000 rpm for 4ºC, 0.3 M of guanidine hydrochloride solution was added and centrifuged at 12000 rpm at 4ºC twice. Supernatant was discarded and the protein pellet was washed with ethanol and dried for 5-10 minutes. Finally, 1% SDS solution was added to dissolve the protein by repeated pipetting. The protein concentration was determined using the Bio-Rad Protein Assay (Bio-Rad, Hercules, CA, USA) according to the manufacturer's instructions.

3.3.8 Western blot (Paper III)

A total of 60 µg of protein was loaded into 12% SDS-PAGE and transferred to PVDF membranes (Millipore, Billerica, MA, USA) by Semi-Dry Electrophoretic Transfer (Bio-Rad, Hercules, CA, USA). Membranes were blocked with 5% BSA (RT, 1 h) followed by overnight incubation (4°C) with specific primary antibodies and on the next day, Secondary HRP-labelled antibodies were added for 2h at room temperature (1:500) (Table 14) and visualised using ECL Detection System (Santa Cruz Biotechnology).

Primary Antibody	Supplier	Code
Anti-CRBN	Abcam	ab244223
Anti-IRF4 (MUM1)	Abcam	ab133590

Anti-MTOR	Abcam	ab45989
Anti-NF-KB p65	Abcam	ab16502
Anti-AMPK alpha-1	Invitrogen	AHO1332
Anti-Ubiquitin	Abcam	Ab7780
Anti-alpha-actin	Abcam	Ab203696
Secondary Antibody	**Supplier**	**Code**
Donkey Anti-Mouse IgG (HRP)	Invitrogen	A16011
Goat anti-Rabbit IgG (HRP)	Invitrogen	31460

Table 14. Antibodies used in western blot.

3.3.9. Ubiquitination assay *in vitro* (Paper III)

Recombinant Human CRBN + DDB1 + CUL-4A + RBX1 (Abcam, Cambridge, UK) (1 uM), Human AMPK1 Fisher (ThermoFisher, Waltham, MA, USA) (1.5 μM) and Thalidomide (100 μM) were used with the E3 Ligase Auto-Ubiquitilylation Assay Kit (Abcam, Cambridge, UK) following the manufacturer's instructions. Reactions were incubated at 37º C for 2 h before separation by SDS–PAGE followed by western blot analysis.

3.3.10. Ubiquitination assay *in vivo* (Paper III)

Epidermal keratinocytes were stimulated with UVB for 6h and then treated with thalidomide. After 24 h, cells were washed twice with PBS and lysed with RIPA buffer (Sigma Aldrich, St. Louis, MI, USA) together with protease inhibitor cocktail (Sigma Aldrich, St. Louis, MI, USA). After centrifugation at 10,000 rpm for 15 min, supernatant was collected. Concurrently, Dynabeads™ Protein G for Immunoprecipitation (Invitrogen, Waltham, MA, USA), were washed and incubated with anti-AMPK antibody (1:250) (Abcam, Cambridge, UK) in PBS 0.02% Tween™ 20 for 15 min at room temperature in order to obtain the Antibody-bead complex. Then, the mix was incubated with the obtained supernatant from the cell lysis. After 1 h at room temperature, the antibody-bead-AMPK protein complexes were obtained. Finally, AMPK protein was eluted with elusion buffer (50 mM glycine pH 2.8) for 2 min at room temperature. Supernatants were subjected to western blot analysis for AMPK and ubiquitin protein analysis.

3.3.11. Thalidomide preparation (Paper III and Chapter 3)

For *in vitro* cell culture, thalidomide (Celgene) was grinded and dissolved in 10% dimethyl sulfoxide (DMSO) (Sigma) and stored at -20°C until use. Concentrations of 100 ng of Thalidomide per mL were used in cell culture experiments.

3.4 Chapter 3: Thalidomide - miRNAs

3.4.1. Hydroxychloroquine preparation

For *in vitro* cell culture, Dolquine (Celgene) was grinded and dissolved in 10% dimethyl sulfoxide (DMSO) (Sigma) and stored at -20°C until use. Concentrations of 1µg of Dolquine (Hydroxychoroloquine) per mL were used in cell culture experiments.

3.5. Common methods for Chapter 1, 2 and 3 (miRNA and thalidomide projects).

3.5.1 Cell culture (Paper I, II and III)

In order to perform *in vitro* functional experiments, the following primary cells were used:

3.5.1.1. Primary cells isolated from patients or healthy controls

- Keratinocyte isolation from skin biopsies

The skin punch biopsy was placed in EpiLife medium (Gibco, Thermofisher scientific, Waltham, MA, USA) containing 5% Penicillin/Streptomycin (Pen/Strep) in order to disinfect the tissue and avoid future cell contaminations.

In the cell culture cabinet, the tissue was placed into a plaque and using forceps and scissors the fat and connective tissue (hypodermis) were removed. The cleaned biopsy was placed into a falcon tube containing 2u/mL of dispase and placed at 4ºC overnight. On the next day, dispase solution was discarded and the biopsy was placed in a plate and washed three times with PBS. Then, epidermis could be easily separated from the dermis with forceps. The isolated epidermis was cut into small pieces (around 1mm) and placed into a 24 well plate specifically treated with Poly-D-Lysine that facilitates cells adhesion (Sarstedt, Nümbrecht, Germany). Then, 2mL of t TrypLE Express (1X) (Gibco, Thermofisher scientific, Waltham, MA, USA) already warmed at 37ºC were added and the epidermal pieces were incubated for 18 minutes at 37ºC. After that, the cell suspension was collected into a Falcon tube containing EpiLife with 10% FBS to inhibit the trypsin

activity. The cellular suspension was taken avoiding the collection of the remaining skin tissue pieces and centrifuged for 5 minutes at 4ºC.

Cells were resuspended, counted and seeded with EpiLife supplemented with 1% Human Keratinocyte Growth Supplement (HKGS) (Gibco, Thermofisher scientific, Waltham, MA, USA). The seeding concentration of cells was $1x10^6$ per 25 cm^2 flask (Corning Inc, Acton, MA, USA). The media was changed every 2-3 days.

- Fibroblasts isolation from skin biopsies (Paper I)

After placing the skin biopsy with dispase at 4ºC overnight and separating epidermis of the dermis, the dermal layer was cut into 0.5-1.0mm pieces and placed into a cell culture dish 21 cm^2 (Sarstedt, Nümbrecht, Germany) containing Dulbecco's Modified Eagle Medium (DMEM) (Gibco, Thermofisher scientific, Waltham, MA, USA) supplemented with 5% Pen/Strep antibiotics and assuring that the media did not cover completely the pieces, no pieces were floating and all remained attached to the dish. The dish was incubated at 37ºC 5% CO_2 in an incubator and every day the culture was evaluated. Medium was replaced every 3-4 days and within 7-10 days fibroblasts started to grow nicely. After 14-21 days, the media was discarded and two washes with PBS were performed. 5mL of 0.05% Trypsin/EDTA solution (Gibco, Thermofisher scientific, Waltham, MA, USA) were added and incubated for 5 minutes at 37ºC. Once fibroblasts were rounded and detached, the tissue dish was tapped and the cells were collected and centrifuged at 1500 rpm for 5 minutes. The cells were subcultured in standard 25 cm^2 tissue culture flasks (Corning Inc, Acton, MA, USA) in a 37°C, 5% CO2 tissue-culture incubator and were passaged every 6-7 days at a ratio of 1:4 in 150 mm^2 tissue culture dishes. The media was changed every 3 days.

- PBMCs/PMNCs isolation from total blood

Blood from CLE and healthy donors was collected using venipuncture technique into Cellular Preparation Vacutainer blood draw tubes (BD, Franklin Lanes, NJ, USA). The tubes contain Ficoll solution followed by a gel plug which contacts the blood to be drawn. The tubes were inverted 8-10 times and centrifuged for 3000 rpm during 30 min at room temperature with deceleration. Human neutrophils were isolated from fresh peripheral blood using Polymorphprep (Axis-Shield diagnostics, Dundee, UK) with centrifugation at 3000 rpm during 30 min at room temperature with deceleration (purity ≥85%).

After centrifugation the white phase containing PBMCs/PMNCs was clearly visible and collected using a Pasteur pipette. The collected cell suspension was transferred into conical tube and washed three times with PBS.

Cells were counted and resuspended in complete RPMI 1640 Media (Gibco, Thermofisher scientific, Waltham, MA, USA) supplemented with 5% Pen/Strep and 2mM L-Glutamine (Sigma-Aldrich, Sant Louis, MO, USA). The majority of *in vitro* experiments were conducted on freshly isolated cells. When not possible, cells were frozen with cryomedium Fetal Bovine Serum (FBS, Sigma-Aldrich, Sant Louis, MO, USA) with 10% Dimethyl sulfoxide (DMSO, Sigma-Aldrich, Sant Louis, MO, USA) and stored in -180ºC liquid nitrogen for forward studies.

- T cells isolation from blood

After obtaining the PBMCs as previously described, T cells were subsequently isolated by using Dynabeads Untouched T cells kit (Invitrogen, Carlsbad, CA, USA) according to manufacturing instructions. Within this kit, T cells are isolated from PBMCs by negative selection, with an antibody mix that contains monoclonal antibodies towards human CD14, CD16 (a and b), CD19, CD36, CD56, CD123 and CD235a which allows depleting B cells, NK cells, monocytes, platelets, dendritic cells, granulocytes and erythrocytes.

Cells were resuspended at $1x10^8$ cells per mL with an Isolation buffer (0.1% PBS and 2mM BSA). An antibody mix against the “non-T cells” and 100 µL of heat inactivated Fetal Calf Serum (FCS) were added. After 20 minutes incubation at 4ºC, cells were centrifuged and 500 µL of pre-washed Dynabeads were added for 15 minutes at RT. The Dynabeads bind to the antibody-labeled cells during the incubation. The suspension was placed on the magnet and T cells were obtained by negative selection. This step was repeated twice. The non-desired bead-bound cells remained on the magnet and were discarded. The obtained supernatant containing T cells was washed in PBS and cells were counted and seeded for cell culture experiments. Purification of isolated T cells was analysed by FSR Fortessa cytometer (BD Biosciences, Franklin Lakes, NJ) with anti-CD3, anti-CD4 and anti-CD8 antibodies (BD Biosciences, Franklin Lakes, NJ).

3.5.1.2. Commercial Primary cells

- **Healthy human epidermal adult Keratinocytes (HeKa)**

Healthy primary human epidermal adult Keratinocytes (HEKa) were purchased from Life Technologies (Carlsbad, CA, USA) and cultured in EpiLife serum-free media supplemented with 1% HSGK (Thermofisher scientific, Waltham, MA, USA). Into detail, upon the vial arrival, it was thawed rapidly at 37ºC in a water bath for 1-2 minutes. Then, cells were counted and resuspended at a concentration of $1.25x10^4$ cells/mL in T-75 Cell+ Flasks (Sarstedt, Nümbrecht, Germany). Following inoculation, the medium in the flasks was distributed equally due to keratinocytes attach surfaces quickly and uneven patterns need to be avoided. The cells were incubated at 37ºC 5% CO_2 in the cell culture incubator and not disturbed for at least 24h. The media was changed every 2-3 days and passages were done before reaching 80% of confluence. At high confluence rates, cells arrest and leave the proliferating pool, reducing the long-term potential yield.

Centrifugation was not performed at the initiation of the cultures due to damage to HEKa culture are common with centrifugation. For subsequent passages cells were trypsinised by adding 3 mL of TrypLE Express (1X) at 37ºC for 2-3 minutes and cell suspension was collected and added into a tube containing EpiLife and 10% FBS (Thermofisher scientific, Waltham, MA, USA) for trypsin inactivation. Cells were centrifuged at 1200 rpm for 3 minutes and subcultured. In case we were facing contaminations, the cell culture was discarded and on the next keratinocyte-initiated culture 0.1% of Pen/Strep was added.

3.5.1.3. Cell culture conditions (Paper I, II and III)

Primary cells (Keratinocytes, Fibroblasts, PBMCs, T cells) were seeded at $1x10^5$ cells per mL in 24-well plaques or $1X10^4$ cells/mL in 96-well plates for functional experiments with their respective media:
- Keratinocytes: EpiLife serum-free media supplemented with 1% HSGK.
- Fibroblasts: DMEM supplemented with 10%FBS and 5% of Pen/Strep.
- PBMCs and T cells: RPMI 1640 supplemented with 5% Pen/Strep and 2mM L-Glutamine.

3.5.2 Cell stimulation (Paper I, II and III)

After 24 hours of being seeded or after 24 of miRNA transfection/gene silencing, cells were treated with several cytokines and inflammatory stimulus for 6h in order to simulate inflammation and be able to study the gene and protein expression.

The following conditions were established:
- 5 ng/µL IL-1 α (Life Technologies, Thermofisher scientific, Waltham, MA, USA).
- 10 ng/µL TNF α (Life Technologies, Thermofisher scientific, Waltham, MA, USA).
- 10 ng/µL TGF β (Life Technologies, Thermofisher scientific, Waltham, MA, USA).
- 5 ng/µL PMA/Ionomycin (Life Technologies, Thermofisher scientific, Waltham, MA, USA).
- 10 ng/µL IFN α (Life Technologies, Thermofisher scientific, Waltham, MA, USA).
- 25-50mJ/cm^2 UVB.

3.5.3 siRNA transfection (Paper II and III)

Keratinocytes were plated at a density of 1x10^5 cells per mL in 24 well-plates overnight at 37ºC 5%. On the next day, silencing of gene of interest was performed using CRISPRMAX tm Reagent Cas9 nuclease transfection protocol (Thermofisher Scientific, Waltham, MA, USA). Cells were around 60% of confluence at the time of the transfection. A mixture containing 25 µL of Opti-MEM, 1250 ng Cas9 nuclease, 240 ng of the PSMB5/TRAF1 or control siRNA and 2.5 µL of Cas9 Plus reagent was prepared in an Eppendorf Tube. In another separate tube, 25µL of Opti-MEM and 1.5 µL of CrisprMAX reagent were added. Immediately after preparation, the solution from the first tube was transferred to the second tube and mixed well. After 5 minutes of incubation, the 50 µL of solution containing siRNA complexes was added to the cells and 450µL of complete media per well were added.

3.5.4. Migration experiments (Paper I, II and III)

Two approaches have been conducted:

- The supernatant from transfected keratinocytes was thawed and placed on the bottom of a 24-well plate (Paper I)

- Stimulated keratinocytes were cultured in the bottom of 24-well plates at 1x10^5 cells/mL and were transfected or treated with thalidomide as described previously for 6h or 24h. (Paper II and III)

Then the co-culture was performed, PBMCs were isolated from healthy controls as described, marked with DAPI and added in the insert (3.0mm pore; BD Biosciences, Franklin Lakes, NJ) placed in the upper side of the well (1x10^6 cells/mL). After 6, 24 and 48 hours migrated PBMCs that were located in the bottom of the well were under a confocal inverted fluorescence microscope (Leica, Wetzlar, Germany). Cell number was counted in five random microscopic fields per well.

3.5.5 Gene expression analysis

3.5.5.1. mRNA extraction from cultured cells (Paper I, II and III)

In order to isolate miRNA and mRNA from cultured cells, the miRNA easy Mini kit (Qiagen, Hilden, Germany) was used according to manufacturing instructions. This kit is used for low-throughput RNA purification using spin columns. In brief, after transfection and stimulation cells were trypsinised using TrypLE Express (1X) ThermoFisher Scientific, Waltham, MA, USA) for 3 to 6 minutes at 37ºC. For experiments with PBMCs, the cell suspension was collected, and the adherent monocytes were trypsinised with TrypLE Express (1X) for 5 minutes at 37ºC. The supernatant of all the experiments was frozen and stored at -80ºC for further ELISA experiments.

The collected cells were centrifuged, and the pellet was lysed by adding 700 µL of Qiazon lysis reagent (Qiagen, Hilden, Germany) and vortexing for 1 minute. Then, the samples were incubated for 5 minutes at room temperature and 140µL chloroform per sample was added. After centrifugation for 15 minutes at 12.000 rpm 4ºC, phases were visible, and the upper aqueous phase was transferred into a new collection tube with 1.5 volumes of 100% ethanol. After vortexing 1 minute, the sample was placed into an RNAeasy mini column in a collection tube. Successive spinning with ethanol wash buffers were performed. Finally, a centrifuge at a full speed is done to dry the membrane and the mature miRNA and RNA are eluted with 35 µL of RNAse free water and centrifuging for 1 minute at 13.000 rpm.

The integrity and purity of the isolated RNA was measured in the Nanodrop-2000 UV-Vis Spectrophotometer (ThermoFisher Scientific, Waltham, MA, USA). Ratios of A_{260}/A_{280} between 1.8 and 2.1 were considered acceptable to use the RNA for the subsequent experiments.

3.5.5.2. RT-qPCR (Paper I, II and III)

Quantification of gene expression from cultured cells after being transfected with anti-miRNAs and miRNA-mimics or being treated with thalidomide or siRNA silencing and being stimulated was done by real-time reverse-transcriptase quantitative polymerase chain reaction (RT-qPCR) according to the manufacturer using the High-Capacity RNA-to-cDNA Kit (Applied Biosystems, Foster City, CA, USA). First, isolated RNA was converted to cDNA with reverse transcription reaction and the cDNA expression was quantified with PCR. In order to perform the RT, RNA was diluted into 500 ng in 10 µL of RNAse free water in microcentrifuge tubes. Then, 2.0µL of RT buffer, 0.8 µL of dNTP mix,

2µL of random primers, 1µL of reverse transcriptase enzyme, 1 µL of RNase inhibitor and 4.2µL of RNAse water were added. A master mix on ice was prepared in order to avoid pipetting errors and assure accuracy between conditions. After setting the RT-reactions, tubes were spun to down the contents and eliminate air bubbles and loaded in the thermal cycler within the following conditions (Table 15):

Step	Time	Temperature
Step 1	10 min	25 ºC
Step 2	120 min	37 ºC
Step 3	5 min	85 ºC
Hold	∞	4 ºC

Table 15. Reverse Transcription conditions.

After that, samples were ready for PCR amplification. A dilution with RNAse free water was done in order to have a total of 20 µg of cDNA per well. Then, 10 µL of TaqMan Universal Master Mix II (Thermofisher scientific, Waltham, MA, USA) was added with 1µL of primer. 96 well plates or 384 well plates were used and after being prepared, they were sealed with sealing tape (Thermofisher scientific, Waltham, MA, USA) and then immediately processed in the ABI PRISM 7000 or ABI PRISM 7900 thermocyclers respectively (Table 16):

Step	Time	Temperature
Step 1	2 min	50 ºC
Step 2	10 min	95ºC
Step 3: 40 cycles	15 sec	95 ºC
	1 min	60ºC
Hold	∞	4 ºC

Table 16. qPCR conditions

Gene expression was assessed by TaqMan gene expression assays gene expression assays (FAM dye labeled MGB probe, Applied Biosystems, Foster City, CA, USA) (Table 17). Obtained data was normalised based on the expression the endogenous control gene GAPDH (Hs02786624_g1, Thermofisher scientific, Waltham, MA, USA). Gene expression was calculated as previously described, following the 2ΔCt method. Fold changes were obtained by dividing the experimental conditions with the transfection controls or non-

stimulated conditions as applicable. A minimum of triplicates per condition were performed.

Gene	Assay ID (TaqMan)	Paper
GADPH	Hs02786624_g1	I, II, III
NFKB1	Hs00765730_m1	I, II, III
MTOR	Hs00234508_m1	III
CXCL1	Hs00236937_m1	I
IL1B	Hs01555410_m1	I, II, III
CCL3	Hs00234142_m1	III
GATA3	Hs00231122_m1	I, III
TBX21 (T-bet)	Hs00894392_m1	I, III
TGFB1	Hs00998133_m1	I, III
TGFBR1	Hs00610322_m1	I, III
IL-2	Hs00174114_m1	I, III
CXCL8 (IL8)	Hs00174103_m1	I, II, III
TNF	Hs00174128_m1	I, II, III
PRKAA1 (AMPK1)	Hs01562308_m1	III
IL-10	Hs00961622_m1	I, III
IFNA1	Hs04189288_g1	III
BIM (BCL2L11)	Hs01076940_m1	I
BAX	Hs00180269_m1	I
P53 (TP53)	Hs01034249_m1	I
Caspase3	Hs00234387_m1	I
PPP6C	Hs00254827_m1	I
CXCL10	Hs01124252_g1	I
STK40	Hs00894269_m1	I
PIK3CA	Hs00907957_m1	I
PRKCD	Hs01090047_m1	I
Smad3	Hs00969210_m1	I
Smad2	Hs00998187_m1	I
TIMP3	Hs00165949_m1	I
PRF1	Hs00169473_m1	III
GRNZ	Hs00188051_m1	III
IL-4	Hs00174122_m1	I, III
IL-17A	Hs00174383_m1	I
COL3A1	Hs00943809_m1	I
SMA (ACTA2)	Hs00426835_g1	I
CXCL9	Hs00171065_m1	I

INFG	Hs00989291_m1	I, III
HCN1	Hs01085412_m1	I
CD28	Hs01007422_m1	I
ICOS	Hs00359999_m1	I
ZAP70	Hs00896345_m1	I
LCK	Hs00178427_m1	I
SLP-76 (LCP2)	Hs01092638_m1	I
PGC1A	Hs00173304_m1	I
PSMB5	Hs01002826_g1	II
KRT16	Hs00373910_g1	II
BIRC5	Hs04194392_s1	II
TP63	Hs00978340_m1	II
CCL5	Hs00982282_m1	II
TRAF1	Hs01090170_m1	II
CCL20	Hs00355476_m1	II
S100A7	Hs01923188_u1	II
NFKBIA	Hs01123969_g1	II

Table 17. Taqman assays used in the studies.

3.5.6 Immunofluorescence analysis of cultured cells (Paper I, II and III)

First, cells were washed with PBS and then fixed for 15 minutes in 4% Paraformaldehyde (PFA) followed by permeabilization with 0.1% Triton X-100 for 10 minutes in order to let the antibodies penetrate the cell membranes and combine to the target molecules. Then, blocking solution (BSA 5%) was added for 1 hour at RT in order to avoid unspecific unions.

Then, Primary antibodies in blocking solution was incubated overnight at 4ºC. Secondary antibody was prepared in PBS and 200 µL were added in each well for 2 hours at RT (Table 18). Coverslips were mounted with mounting media containing Dapi (Fluoromount-G™ eBioscience™, Thermofisher Scientific, Waltham, MA, USA) which was used to visualize the nuclei of the cells. Immunofluorescent staining was observed with inverted fluorescent microscope (Leica, Wetzlar, Germany). Images were processed with Image J (NIH, USA).

Primary Antibody	Supplier	Code	Paper
Anti-IRF4 (MUM1)	Abcam	ab133590	III
Anti-MTOR	Abcam	ab45989	III
Anti-NF-KB p65	Abcam	ab16502	I, II, III

Anti-Phospho-Raptor (Ser863)	Invitrogen	PA5-64849	**III**
Anti-AMPK alpha-1	Invitrogen	AHO1332	**III**
Anti-Ubiquitin	Abcam	Ab7780	**III**
Anti-TGFBR1	Abcam	ab31013	**I**
Anti-PSMB5	GeneTex,	GTX23330	**II**
Anti-TRAF1	Abcam	Ab203316	**II**
Anti-IKBa (NFKBIA)	Abcam	ab7217	**II**
Secondary Antibody	**Supplier**	**Code**	**Paper**
Alexa-680-conjugated anti-goat IgG	Abcam	ab175776	**I**
Alexa-488-conjugated anti-rabbit IgG	Abcam	ab150077	**II, III**
Alexa-647-conjugated anti-mouse IgG	Abcam	ab150115	**I, II, III**

Table 18. Antibodies used for immunofluorescence in cells.

3.5.7. Functional cell assays (Proliferation and Apoptosis)

3.5.7.1. Proliferation Assay (Paper I, II and III)

Proliferation was measured after transfection of cultured keratinocytes and PBMCs with the CyQUANT™ Cell Proliferation Assay (Thermofisher scientific, Waltham, MA, USA). Within this kit, cells are lysed, and their proliferation is assessed with highly sensitive fluorescence-based methods. Moreover, it requires to freeze the samples, which permits getting data from different experimental timepoints and analyze all together once you have all the experimental conditions completed. Cells were transfected and/or stimulated in 96-well plates at a density of $1x10^4$ cells/mL. Then, for adherent cells, the media was removed, and plate were frozen at -80ºC covered with foul. Regarding suspension cells, the plates were centrifuged at 1500 rpm for 5 minutes and the supernatant was discarded, and cells were frozen as described. When all the different experimental timepoints were achieved, all the samples were assayed together. The plates were thawed at room temperature and 200 µL of CyQUANT® GR dye/cell-lysis buffer previously prepared was added. After mixing gently, the samples were incubated 5 minutes at room temperature protected from light. Finally, the sample fluorescence using a microplate reader (Luminex, Austin, TX, USA) was measured using filters for 480 nm excitation and 520 emission maxima.

3.5.7.2. Apoptosis Assay (Paper I, II and III)

Apoptosis was measured in cultured transfected and/or stimulated cells by flow cytometry within the Dead Cell Apoptosis Kit Annexin V APC and SYTOX™ Green (Thermofisher scientific, Waltham, MA, USA). Adherent Cells were trypsinised as described and in case of PBMCs, they were collected, and adherent monocytes were trypsinised and added to the collected cell suspension. Then, cells were centrifuged and washed with 1x Annexin Binding buffer. Then, 5µl of 1x Annexin V and 1µL of SYTOX Green solutions previously prepared were added to 100µL of each cell suspension. Cells were incubated at 37ºC 5% of CO_2 for 15 minutes. After incubation, cells were washed and resuspended in 200 µL of 1x annexin binding buffer and analysed in FSR Fortessa cytometer measuring the fluorescence emission at 530 nm and 660 nm. A positive control for necrosis was done by incubating cells with 2 mM hydrogen peroxide for 15 minutes to assure that the technique is working and set the flow cytometry gating strategy. A total of 10.000 cells per condition were analysed.

3.5.8 Flow Cytometry analysis (Paper I and III)

Immune phenotyping and cell activation was measured by flow cytometry. Isolated T cells were transfected and stimulated and after 24h, they were centrifuged at 2000 rpm for 5 minutes, washed with PBS and then resuspended with 100 µL of PBS with 1%BSA containing antibodies (Table 19). The antibodies were incubated for 20 minutes at 4ºC protected from light. After incubation, stained cells were centrifuged and resuspended with 200 µL of PBS. A total of 10.000 cells per condition were analysed in FSR Fortessa cytometer. Negative controls with incubation without antibodies were performed in order to set the flow cytometry gating. Data were analysed using FCS Express 4 Flow Research software (BD Biosciences, Erembodegem, Belgium).

B cell subsets	**Supplier**	**Code**	**Paper**
CD19	BD Biosciences	345788	III
CD27	BD Biosciences	558664	III
CD38	BD Biosciences	555460	III
IgD	BD Biosciences	555779	III
Tcell subsets/ activation	**Supplier**	**Code**	**Paper**
CD3	BD Biosciences	340662	I, III
CD4	BD Biosciences	561842	I, III
CD8	BD Biosciences	555369	I, III

CCR3	BD Biosciences	561745	III
CCR4	BD Biosciences	744140	III
CCR5	BD Biosciences	560932	III
CCR6	BD Biosciences	564479	III
CXCR3	BD Biosciences	740183	III
CD25	BD Biosciences	340939	III
FOXP3	BD Biosciences	560046	III
CD69	BD Bioscience	562617	I
Dendritic Cell and Monocytes	**Supplier**	**Code**	**Paper**
CD11c	BD Biosciences	559877	I
CD14	BD Biosciences	557154	I
CD16	BD Biosciences	555406	I
NK cell subsets	**Supplier**	**Code**	**Paper**
CD3	BD Biosciences	340662	I, III
CD16	BD Biosciences	561842	I, III
CD56	BD Biosciences	555369	I, III
6B11	BD Biosciences	552825	III

Table 19. Antibodies used in flow cytometry.

3.5.9 Immunofluorescence in skin biopsy (Paper II and III)

Skin biopsies were mounted in Optimal cutting temperature compound (OCT embedding compound) and frozen rapidly by with nitrogen liquid by quick taps and immersions in liquid nitrogen. Once OCT turned white and solidified, the OCT bloc containing the skin biopsy was placed in the cryostat at -20ºC (Leica CM3050 S Research Cryostat (Leica, Wetzlar, Germany). The sections were cut in 6-10 µm of thickness. Once the skin was cut, the tissue section was adhered by contact Superfrost slides (FisherScientific, Waltham, MA, USA). Finally, the obtained slides were stored at -80 ºC.

The obtained sections were unfrozen and air-dried for 30 minutes at room temperature to prevent the tissue to fall off the slides during antibody incubations. Then, the skin section was fixed with 4% PFA in PBS for 15 minutes followed by three washes of PBS. A blocking solution containing 5% BSA was added for 1 hour at room temperature. Primary antibody was diluted with blocking solution and incubated overnight at 4ºC. On the next day, the slides were washed with PBS and secondary antibody was added for 2h at room temperature (Table 20). Finally, slides were washed with PBS and then were mounted with mounting media containing Dapi (Fluoromount-G™ eBioscience™, Thermofisher Scientific, Waltham, MA, USA) for nuclear staining. The slides were observed with Olympus IX71 (TH4-200) U-RFL-T microscope (Olympus, Tokyo, Japan). Images were processed with Image J (NIH, USA).

Primary Antibody	Supplier	Code	Paper
Anti-CRBN	Abcam	ab244223	III
Anti-IRF4 (MUM1)	Abcam	ab133590	III
Anti-MTOR	Abcam	ab45989	III
Anti-NF-KB p65	Abcam	ab16502	III
Anti-6B11	Invitrogen	14-5806-82	III
Anti-Phospho-Raptor (Ser863)	Invitrogen	PA5-64849	III
Anti-AMPK alpha-1	Invitrogen	AHO1332	III
Anti-PSMB5	GeneTex,	GTX23330	II
Anti-TRAF1	Abcam	Ab203316	II
Anti-Ki67	Abcam	ab15580	II
Secondary Antibody	**Supplier**	**Code**	**Paper**
Alexa-488-conjugated anti-rabbit IgG	Abcam	ab150077	II, III
Alexa-647-conjugated anti-mouse IgG	Abcam	ab150115	II, III

Table 20. Antibodies used in immunofluorescence in skin sections.

Skin sections were evaluated on blinded specimens by the Vall d'Hebron pathology unit. The staining of the epidermis, dermis and inflammatory infiltrate was evaluated semi-quantitatively as 0 (<10% positive cells), 0.5 (10-20% positive cells), 1 (20-40% positive cells), 1.5 (40-60% positive cells), 2 (60-80% positive cells), 2.5 (80-90% positive cells) or 3 (>90% positive cells).

3.5.10 Statistical Analysis (Paper I, II and III)

All experiments have been performed at least three independent times in three replicates. Data are represented as mean ± standard error of the mean (SEM). Comparison between groups and conditions was calculated with paired t tests or unpaired t tests as applicable. All tests were done using Prism GraphPad version 7.0 (GraphPad Software, v 7.0, San Diego, CA, USA). P values of less than 0.05 were considered statistically significant. In the graphs and figures, the significant statistical values were indicated as following: *$p < 0.05$, **$p < 0.01$, ***$p < 0.001$.

4. Results

Chapter 1. microRNAs in CLE

Paper I: microRNA Expression Profiling Identifies miR-31 and miR-485-3p as Regulators in the Pathogenesis of Discoid Cutaneous Lupus

The first part of the thesis focused on studying a differential pathogenesis between DLE and SCLE subtypes based on miRNA expression profiles. In this study, 10 DLE and 10 SCLE patients were included, and a skin biopsy from non-lesional and lesional skin was obtained. Using the TaqMan human array, differentially expressed miRNAs were identified. *In vitro* experiments were performed to validate the obtained results and investigate the role of the differentially expressed miRNAs.

DLE skin presents a differential microRNA profile from SCLE lesional skin

Direct comparison the miRNA data of lesional DLE versus lesional SCLE generated a list of 12 differentially expressed miRNAs (fold change >|1.5|, $P < 0.05$) of which 8 were upregulated and 4 downregulated. We focused on the top two upregulated miRNAs in DLE vs SCLE, miR-31 and miR-485-3p that presented a Fold change of 11.21 and 10.09, respectively. Their upregulation was first validated by Rt-qPCR. Next, to identify the cell type in the skin involved in their deregulation, in situ hybridization was performed and it was found that miR-31 expression was mostly increased in DLE lesional epidermis compared with SCLE epidermis ($P < 0.001$) and upregulation of miR-485-3p was found in dermal inflammatory infiltrates and fibroblasts of DLE skin vs SCLE ($P < 0.0001$). These results indicate that in DLE, miR-31 deregulation was mainly in keratinocytes, and it was a keratinocyte-specific miRNA, whereas miR-485-3p was in immune infiltrates and fibroblasts.

miR-31 upregulation promotes keratinocyte apoptosis, NF-κB pathway activation and neutrophil and monocyte recruitment

We next aimed to study the biological role of miR-31 in keratinocytes in *in vitro* studies, by inhibiting or overexpressing miR-31. After several stimulations, TGF-β1 and UVB were identified strong miR-31 inducers *in vitro* in primary keratinocytes from DLE patients, therefore further experiments were conducted stimulating keratinocytes with these conditions. Proliferation and apoptosis were assessed, and it was found that miR-31 mimics keratinocytes present increased apoptotic rates ($P < 0.0001$). No changes in epidermal proliferation were observed.

As miR-31 is known to modulate the NF-κB pathway which in turn regulates multiple aspects of immune functions serving as a pivotal mediator of inflammatory response, and it has been found to be upregulated in the skin of autoimmune conditions, we next assessed by immunofluorescence NF-κB protein levels. We found that NFKB1 was increased after miR-31 mimics (3.2 – fold change; $p<0.001$) along with NF-κB related inflammatory mediators. IL-12, IL-8, and TGF-β1 were significantly upregulated in pre-miR 31-transfected cells and cell culture supernatants, indicating that upregulation of miR-31 contributes to inflammation in CLE skin by promoting NF-κB pathway.

Because of the interaction between epithelial cells and the immune system is crucial in CLE, cross-talking functional studies were performed. Briefly, the supernatant from anti-miR-31 and pre-miR-31 keratinocytes was placed in the low-chamber and PBMCs/ PMNCs were plated on the upper-chamber. Neutrophils were selected for this experiment as IL-8 is an important neutrophil chemoattractant and was the most upregulated chemokine in pre-miR-31 transfected keratinocytes ($p<0.001$). A significant increase of intermediate and non-classical monocytes and neutrophil migration were observed, suggesting that upregulation of epidermal miR-31 promotes immune recruitment in DLE lesional sites by upregulating inflammatory effectors in keratinocytes that recruit immune cells.

miR-485-3p upregulation in DLE is responsible for T cell activation

We next focused on the other differentially expressed miRNA, miR-485-3p. As it was highly detected in immune infiltrated and fibroblasts, experiments inhibiting and overexpressing this miR were performed in PBMCs and fibroblasts. IL-1 α and TGF- β1 were identified as a strong miR-485-3p inducers in peripheral mononuclear blood cells from DLE patients (14- and 4.9-fold change, $P < 0.0001$, respectively) and fibroblasts (1.9- and 2.1-fold change, respectively). Further experiments were carried out stimulating cells in those conditions.

As DLE is characterised by a deep lymphocytic infiltrate in which T cells are the most abundant cells, miR-485-3p mimics transfected PBMCs were assessed for T cell activation. A significant increase of activation, measured by CD69 expression, was found in CD8 and CD4 T cells (>80% of the cells). Similar results were obtained transfecting isolated T cells: Data suggests that miR-485-3p contributes to T cell activation in DLE.

Upregulation of miR-485-3p promotes skin fibrosis in DLE

Since the study showed and increased expression of this miRNA in the dermis, and DLE has a characteristic TGF β -dependent fibrotic signature, we next assessed the potential role of miR-485-3p in fibroblasts. Resolution of skin inflammation differs between DLE and SCLE because DLE is characterised by scarring and the development of fibrotic irreversible sequelae. We studied the miR-485-3p role in the development of fibrosis. Pre-miR-485-3p fibroblasts presented increased gene expression levels of fibrotic genes COL3A1, α-SMA, TGFBR1, and Smad3 (2.3-, 2.6-, 2.3-, and 2.7-fold change, respectively). In addition, protein levels of TGF-βRI ($p<0.001$), a crucial protein implicated in fibrosis were also upregulated. Data suggests that upregulation of miR-485-3p contributes to fibrosis in DLE.

ORIGINAL ARTICLE

MicroRNA Expression Profiling Identifies miR-31 and miR-485-3p as Regulators in the Pathogenesis of Discoid Cutaneous Lupus

Cristina Solé[1], Sandra Domingo[1], Berta Ferrer[2], Teresa Moliné[2], Josep Ordi-Ros[1] and Josefina Cortés-Hernández[1]

Cutaneous lupus erythematosus is a common and disfiguring manifestation in systemic lupus erythematosus. Subacute cutaneous lupus erythematosus and discoid lupus erythematosus (DLE) are the most prevalent forms. Despite sharing histological similarities, clinically they differ in their course and prognosis, suggesting different pathogenesis. Here, we show that DLE-affected skin has a specific microRNA expression profile when compared with subacute cutaneous lupus erythematosus. Among the DLE-specific microRNAs, we identified one keratinocyte-derived microRNA, miR-31, and one leukocyte-derived microRNA, miR-485-3p. We show that UV and transforming growth factor-β1 stimulation up-regulates miR31 expression in DLE. Specific miR-31 overexpression induces keratinocyte apoptosis and NF-κB pathway activation with the production of related inflammatory cytokines and contributes to the recruitment of neutrophils and intermediate monocytes at the inflammation site. IL-1α and TGF-β1 stimulation increased the expression of miR-485-3p in peripheral mononuclear blood cells from DLE patients and induced T-cell activation, mainly of CD8 lymphocytes. In addition, miR-485-3p overexpression in dermal fibroblasts contributes to fibrosis by targeting peroxisome PGC-1α. Collectively, our findings suggest that overexpression of miR-31 and miR-485-p contribute to skin inflammation in DLE lesions by regulating the production of inflammatory mediators and attracting neutrophils and intermediate monocytes to the skin.

Journal of Investigative Dermatology (2019) **139**, 51–61; doi:10.1016/j.jid.2018.07.026

INTRODUCTION

Cutaneous involvement in lupus erythematosus is an autoimmune disease with a wide range of dermatologic manifestations. Skin involvement is very frequent in systemic lupus erythematosus (SLE), with up to 70% of patients developing skin lesions at some point during the course of the disease (Onkon, 2013). Cutaneous lupus erythematosus (CLE) is divided into different subtypes according to clinical and histological characteristics, of which discoid lupus erythematosus (DLE) and subacute cutaneous lupus erythematosus (SCLE) are the most prevalent forms, representing approximately 80% of cases. Although these two clinical subtypes share histological similarities, clinically they differ in their course and prognosis, suggesting a different pathogenesis (Baltaci and Fritsch, 2009; Yu et al., 2013).

[1]*Department of Medicine, Systemic Autoimmune Diseases Unit, Hospital Universitari Vall d'Hebron, Institut de Recerca (VHIR), Universitat Autònoma de Barcelona, Barcelona, Spain; and* [2]*Department of Pathology, Hospital Universitari Vall d'Hebron, Universitat Autònoma de Barcelona, Barcelona, Spain*

Correspondence: Cristina Solé Marcé, Research Unit in Systemic Autoimmune Diseases, Vall d'Hebron Research Institute, Hospital Vall d'Hebron, Passeig Vall d'Hebron 119-129. 08035, Barcelona, Spain. E-mail: cristina.sole@vhir.org

Abbreviations: CLE, cutaneous lupus erythematosus; DLE, discoid lupus erythematosus; miRNA, microRNA; PBMC, peripheral blood mononuclear cell; PMNC, neutrophil polymorphonuclear cell; SCLE, subacute cutaneous lupus erythematosus; SLE, systemic lupus erythematosus; Th, T helper

Received 18 April 2018; revised 10 July 2018; accepted 12 July 2018; accepted manuscript published online 18 August 2018; corrected proof published online 19 October 2018

The pathophysiology of CLE is not fully elucidated and involves complex genetic, environmental, and immune cell interactions (Actman and Werth, 2015). Microarray studies have provided further understanding of key pathogenic pathways. Initial studies identified a predominance of dendritic and natural killer cells, toll-like receptor–, and SLE-related signaling pathways, along with evidence for a T helper (Th) type 1-related signature in lesional DLE when compared with healthy and involved DLE skin (Dey-Rao et al., 2014; Jabbari et al., 2014). Later, by comparing lesional DLE and SCLE skin, we identified a distinctive T-cell and a fibrotic TGF-β–dependent signature in DLE (Solé et al., 2016). Despite recent advances, further studies are required to understand the interactions between pathways and the mechanisms of initiation and perpetuation of inflammation.

MicroRNAs (miRNAs) are approximately 22-nucleotide RNA molecules that cause translation repression by interacting simultaneously with different target mRNAs within one cell type (Krek et al., 2005). They play an essential role in the regulatory mechanisms in immune homeostasis, and their deregulation has been described in a wide variety of human diseases. Consequently, there is a growing interest in their role as potential therapeutic targets or diagnostic and prognostic biomarkers (Baltimore et al., 2008; Czech, 2006; O'Connell et al., 2010). In SLE, although no individual dysregulated miRNAs had been found, the aberrant expression of distinct groups of miRNAs has been associated with perturbed type I interferon signaling, DNA hypomethylation, and T/B cell hyperactivation (Yan et al., 2014). In skin diseases, miRNAs have been shown to play a pathogenic role in

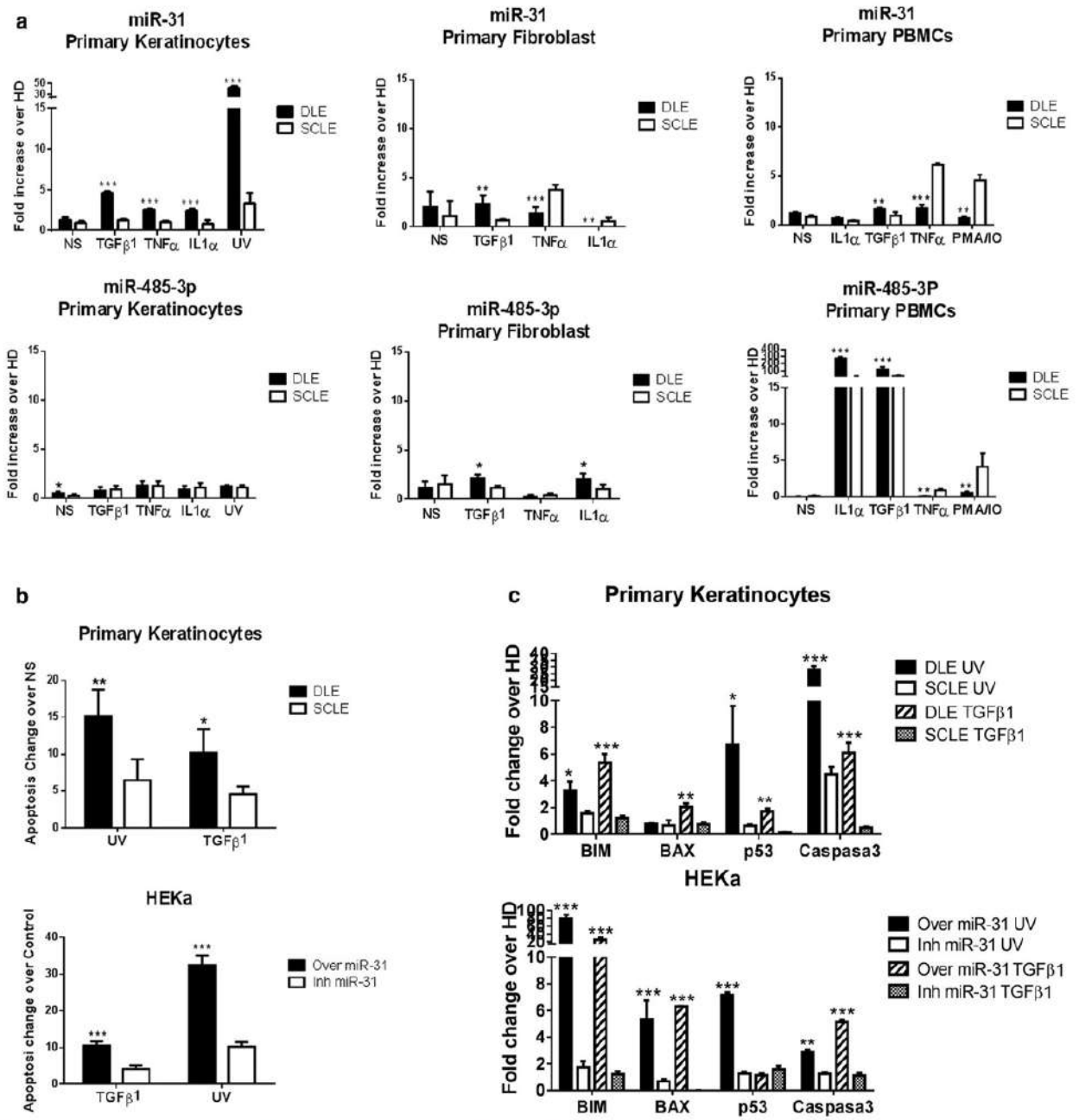

Figure 2. Expression of miR-31 and miR-485-3p after stimulatory conditions and during apoptosis. (**a**) Expression of miR-31 and miR-485-3p were analyzed in the cellular constituents of the skin including primary adult keratinocytes, dermal fibroblasts, and PBMCs using quantitative real-time PCR. (**b**) Expression of miR-31 and miR-485-3p in apoptotic primary keratinocytes and in transfected adult epidermal keratinocytes (HEKa cells) after UV and TGF-β1 stimulation. (**c**) BAX, BIM, p53, and caspase3 expression levels in apoptotic primary keratinocytes and in transfected adult epidermal keratinocytes (HEKa cells) after UV and TGF-β1 stimulation. Gene expression for miRNAs and mRNAs was normalized, respectively, using U6 or GADPH as endogenous control. Fold change in expression level was calculated using the $2^{-\Delta\Delta Ct}$ method. $^{*}P < 0.05$, $^{**}P < 0.005$, $^{***}P < 0.0005$. HD, healthy donors; Inh, inhibited; miR, microRNA; NS, not stimulated; Over, overexpressed; PBMC, peripheral blood mononuclear cell.

levels of PPP6c and STK40 increased in anti-miR31 treated keratinocytes after TGF-β1 (2.4- and 2.3-fold change, respectively) and UV radiation (3.7- and 2.3-fold change, respectively) (Figure 3c).

miR-485-3p regulates T-cell activation

After IL-1α and TGF-β1, we observed an increased proliferative response of pre-miR-485−3p−transfected PBMCs (2.5 and 4.5 fold-change proliferation, respectively) (see Supplementary Figure S2 online) but no effect on apoptosis. By cytometry, pre-miR-485-3p−transfected PBMCs expressed $CD69^{+}$ as a marker of T-cell activation (see Supplementary Figure S3 online). We further isolated T cells from PBMCs by flow cytometry and found that approximately 80%−90% of pre-miR-485-3p−transfected CD8 or CD4 cells expressed $CD69^{+}$ (Figure 4a). miRNA-485-3p overexpression in

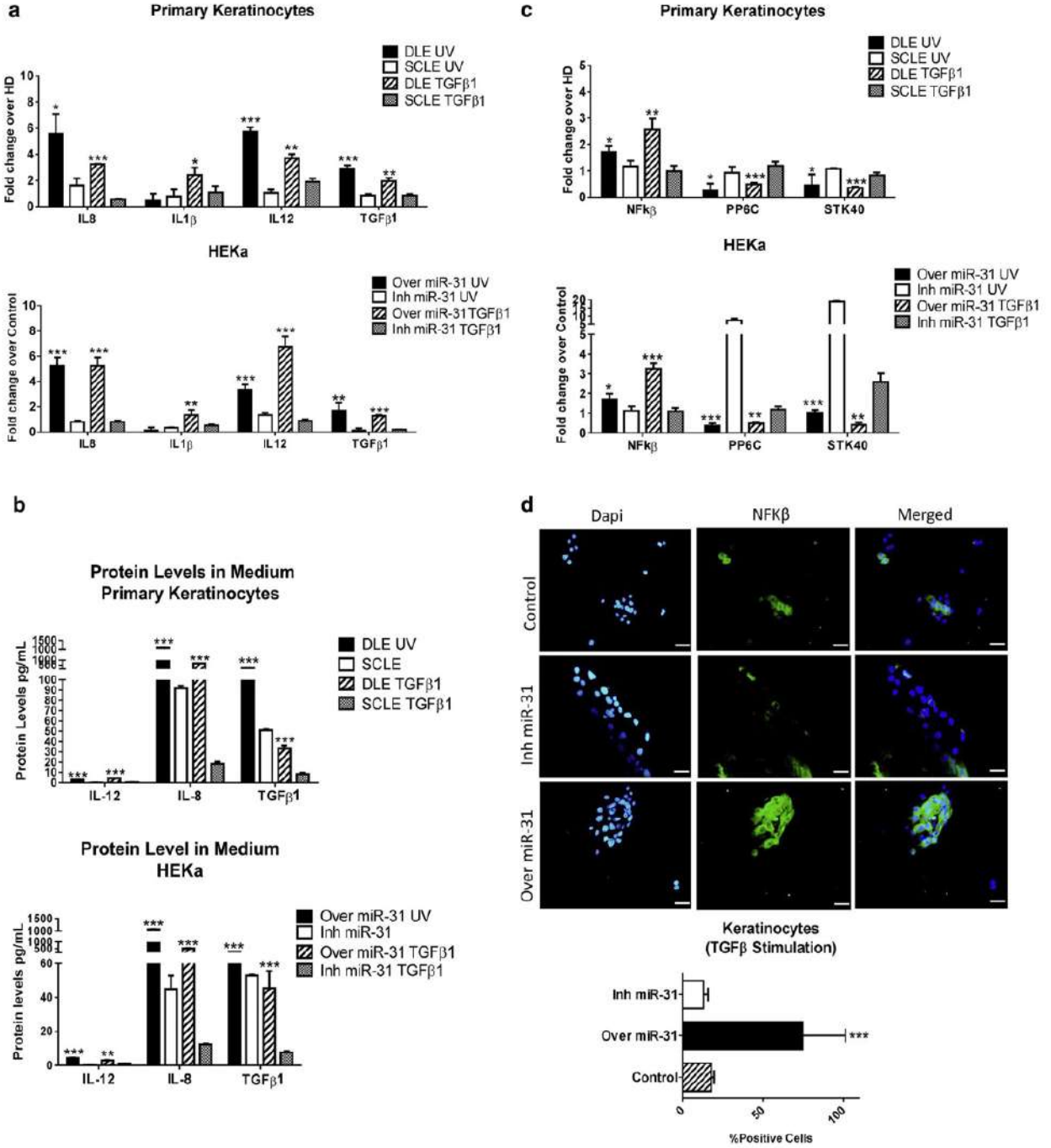

Figure 3. Overexpression of miRNA-31 increases the production of inflammatory cytokines by keratinocytes. UV or TGF-β1 stimulation of DLE keratinocytes and HEKa cells overexpressing miR-31 induces an increased expression and secretion of IL-8, IL-1β, IL-12, and TGF-β1 as measured by (**a**) qRT-PCR and (**b**) ELISA. (**c**) miR-31 regulates the NF-κB pathway in keratinocytes. Expression levels of NF-κB and of PPP6C and STK40, negative regulators, were measured by qRT-PCR in DLE keratinocytes and in transfected HEKa cells after UV and TGF-β1 stimulation. Gene expression was normalized using GADPH as endogenous gene control. Fold change in expression level was calculated using the $2^{-\Delta\Delta Ct}$ method. (**d**) NF-κB expression was measured by immunofluorescence in overexpressed or inhibited miR-31 HEKa cells after 6 hours of treatment with TGF-β1. Scale bar = 20 μm. $^{*}P < 0.05$, $^{**}P < 0.005$, $^{***}P < 0.0005$. DLE, discoid lupus erythematosus; HD, healthy donors; Inh, inhibited; miRNA, microRNA; Over, overexpressed; qRT-PCR, real-time quantitative reverse transcription–PCR; SCLE, subacute cutaneous lupus erythematosus.

isolated T cells produced a significant up-regulation of PIK3CD, NF-κB1, and PRKCD ($P < 0.0001$) (Figure 4b). No changes in the TCR proximal signaling complex (ZAP70, Lck, SLP-76) and costimulatory molecules (CD28, inducible T-cell costimulator) were observed. Furthermore, we used TargetScan miRNA target prediction algorithm (TargetScan Release 7.2, www.targetscan.org) and Ingenuity Pathway Analysis (Qiagen Silicon Valley, Redwood, CA) to generate a list of potential target genes for miR-485-3p (see Supplementary Table S4 online). Only down-regulation of

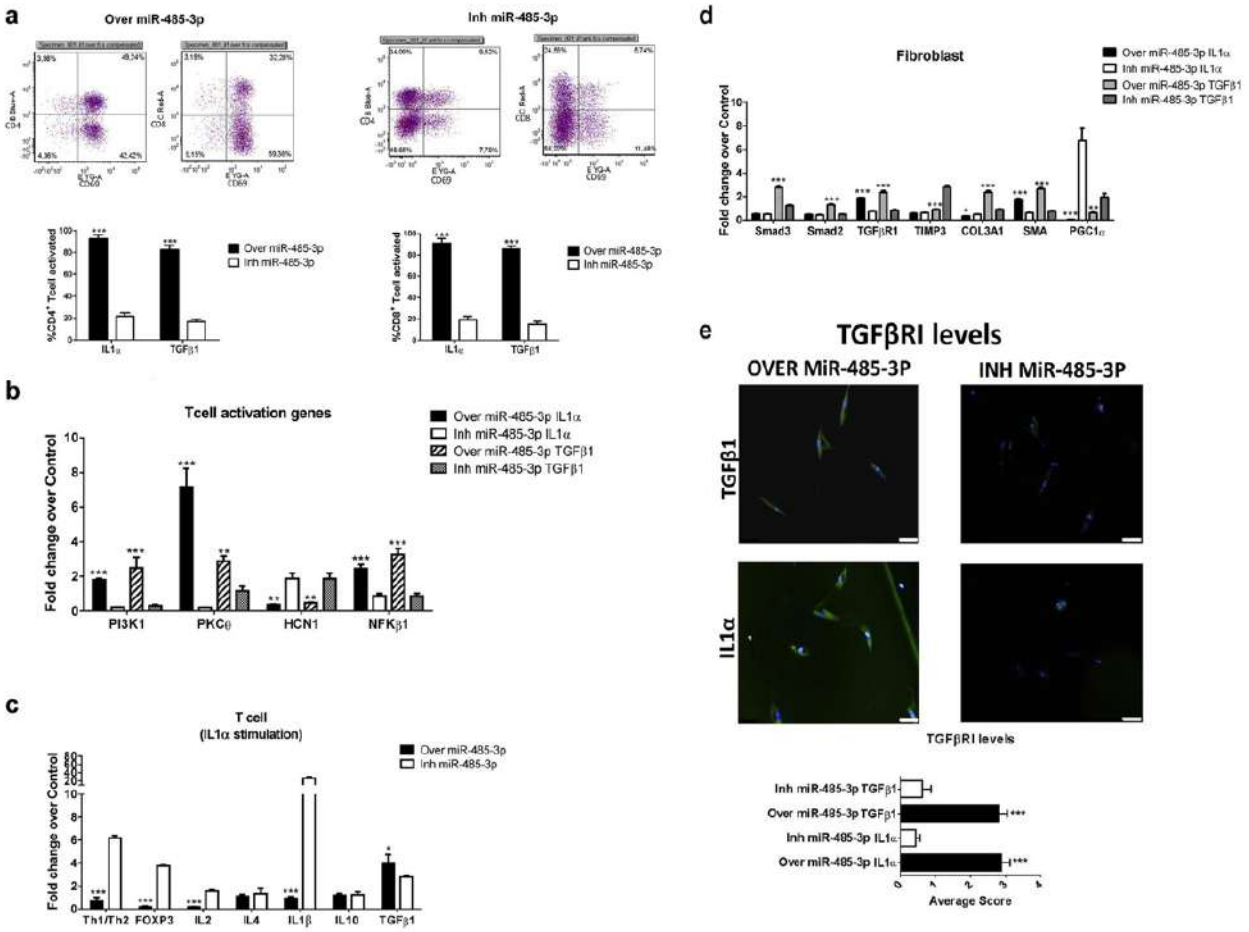

Figure 4. Effect of miR-485-3p on expression of T-cell activation markers, T-cell differentiation, and fibrosis formation in primary fibroblast. Transfected miR-485-3p T cell stimulated with IL-1α or TGF-β1. (**a**) Flow cytometry diagram and percentages of $CD69^+CD4^+$ and $CD69^+CD8^+$. (**b**) qRT-PCR of T-cell activation genes and (**c**) transcription factor genes of Th1, Th2, and regulatory T cells and related cytokines. Overexpressed or inhibited miR-485-3p in fibroblast after stimulation with IL-1α or TGF-β1. (**d**) Gene expression analysis by qRT-PCR. (**e**) Immunofluorescence of TGF-βR1 protein levels. Scale bar = 20 μm. Data represent the mean ± standard error of the mean from three independent experiments. Genes were normalized to GADPH gene, and transfected controls were used for the fold changes. $^*P < 0.05$, $^{**}P < 0.005$, $^{***}P < 0.0005$. Inh, inhibited; miR, microRNA; Over, overexpressed; qRT-PCR, real-time quantitative reverse transcription–PCR; Th, T helper.

HCN1 was observed in pre-miR-485-3p–transfected T cells after IL-1α and TGF-β1 stimulation (−2.73 and −2.13-fold changes) (see Figure 4b). Stimulated transfected T cells also induced a differentiation toward a Th2 phenotype (−6.2-fold change in Th1/Th2 ratio) with a reduction of FoxP3 (−3.8 fold change) (Figure 4c).

miR-31–transfected PBMCs induced cell proliferation and a skew toward the Th1 phenotype after TGF-β1 stimulation. FoxP3 and related cytokine (IL-10 and TGF-β1) expression levels were reduced (Figure 4c).

Fibroblast miR-485-3p overexpression promotes fibrosis

Because miR-485-3p was overexpressed in fibroblasts, we studied its role in the development of fibrosis. After TGF-β1 stimulation, pre-miR-485-3p mimic–transfected dermal fibroblasts enhanced the fibrogenic activity of TGF-β1 by increasing the mRNA expression levels of COL3A1, α-SMA, TGF-βRI, and Smad3 (2.3-, 2.6-, 2.3-, and 2.7-fold change, respectively) (Figure 4d). Increased protein levels of TGF-βRI in transfected fibroblasts were confirmed by immunofluorescence (Figure 4e). Reduced expression of PGC-1α, an antifibrotic gene and target of miR-485-3p, was observed ($P < 0.001$, −1.6 and −20-fold change) (Figure 4d).

Pre-miR-31 mimic–transfected keratinocytes mediate neutrophil/monocyte recruitment and a shift toward Th1/regulatory T-cell response at the site of inflammation

Because the interaction between epithelial cells and the immune system is tightly regulated, we performed cross-talking functional studies to evaluate the effect of miRNA-transfected keratinocytes on skin PBMCs/neutrophil polymorphonuclear cells (PMNCs). IL-8, a neutrophil chemotactic (Barker et al., 1991), was one of the prevalent cytokines found in the supernatant of transfected keratinocytes. For this reason, freshly isolated neutrophils were co-cultured in inserts with pre-miR-31–transfected or –inhibited or control keratinocytes (see Supplementary Figure S4 online). After stimulation with TGF-β1, IL-1α, and UV radiation, a significant number of migrating neutrophils were observed (48%, 12%, and 65% of migration relative to control, respectively) (Figure 5a). The migration rate was

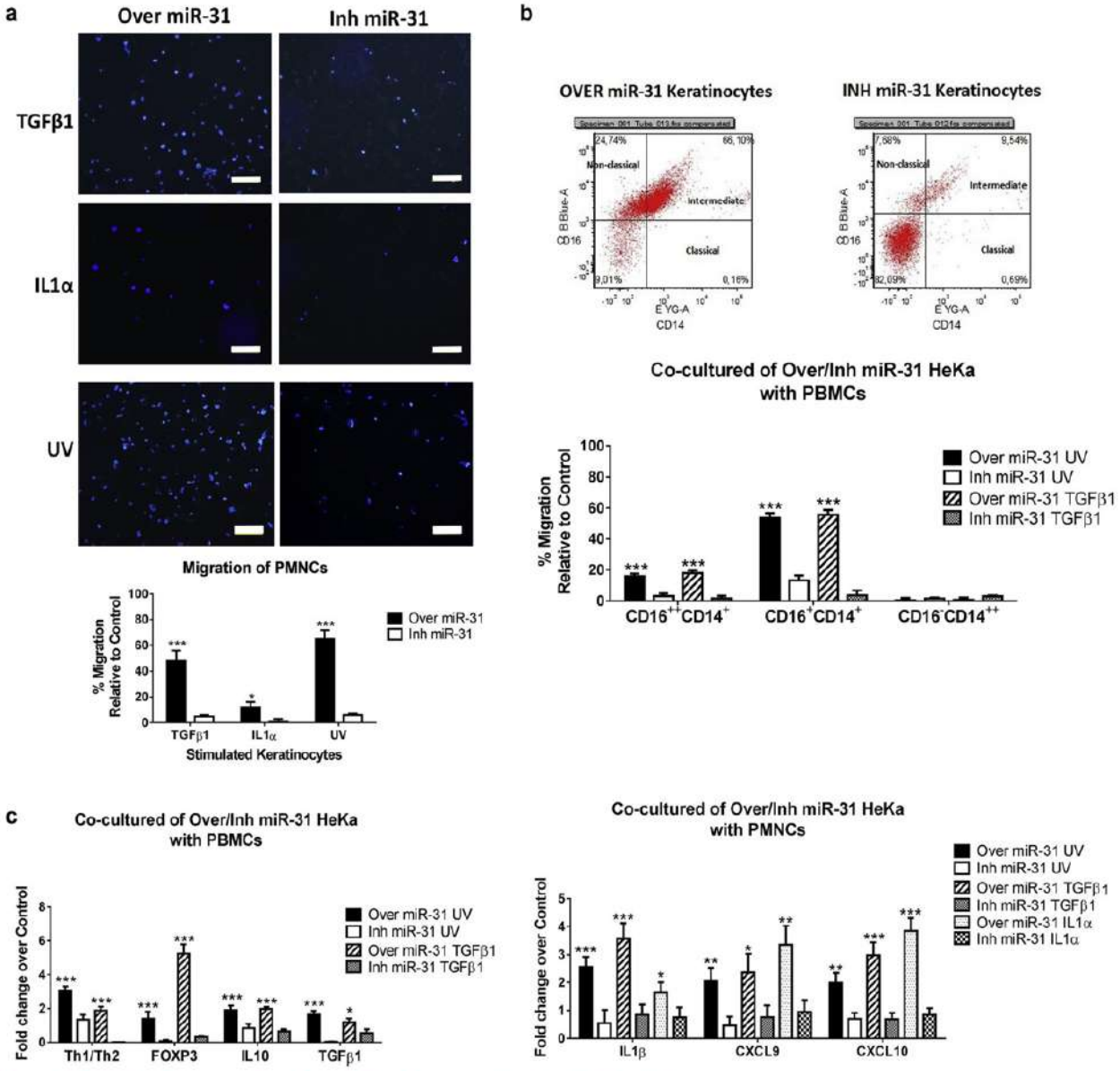

Figure 5. miR-31 keratinocytes mediated neutrophil and monocyte migration and effect to their gene expression. PMNCs or primary PBMCs were placed into the upper of insert and transfected stimulated keratinocytes were in the bottom. (**a**) After 6 hours, the migrated primary neutrophil cells were counted. A representative image of the migrated primary neutrophil cells labeled with DAPI on the bottom of the Transwell membrane (Sarstedt, Nümbrecht, Germany) is shown. Percent migration of primary neutrophils relative to the transfected controls. Scale bar = 20 μm. (**b**) Migration of PBMCs were evaluated by flow cytometry. Representative dot blots indicating the percentages of migrated monocytes (nonclassical, intermediate, and classical) are shown. (**c**) Gene expression analysis by qRT-PCR were done for PMNC and PBMC co-culture with transfected stimulated keratinocytes. Comparisons were done by Student *t* test between overexpression and inhibition conditions. $^{*}P < 0.05$, $^{**}P < 0.005$, $^{***}P < 0.0005$. Inh, inhibited; miR, microRNA; Over, overexpressed; PBMC, peripheral blood mononuclear cell; PMNC, neutrophil polymorphonuclear cell; qRT-PCR, real-time quantitative reverse transcription–PCR.

strongly correlated with the supernatant IL-8 levels ($r = 0.968$, $P = 0.007$) (see Supplementary Figure S5 online). Migrated neutrophils overexpressed IL1-β, CXCL9, and CXCL10 (Figure 5b). No change in neutrophil apoptosis was observed (see Supplementary Figure S6 online). Co-culture conditions also produced intermediate ($CD14^{+}CD16^{+}$) and nonclassical ($CD14^{+}CD16^{++}$) monocyte migration after TGF-β1 stimulation (58% and 18% migration relative to control, respectively) and UV (53% and 13% migration relative to control, respectively) (Figure 5b). No lymphocyte, dendritic cell, and natural killer cell migration was observed (see Supplementary Figure S7 online). After TGF-β1 and UV stimulation, a shift toward a Th1 response, with an increased Th1/Th2 ratio (1.8- and 3.1-fold change, respectively) and in FoxP3 levels and related cytokines (IL-10 and TGF-β1) (5.2-, 1.9-, and 1.2-fold change and 1.3-, 1.9-, and 1.6-fold change, respectively), was observed.

DISCUSSION

DLE-affected skin has a specific differential microRNA expression profile compared with SCLE-affected skin, with a

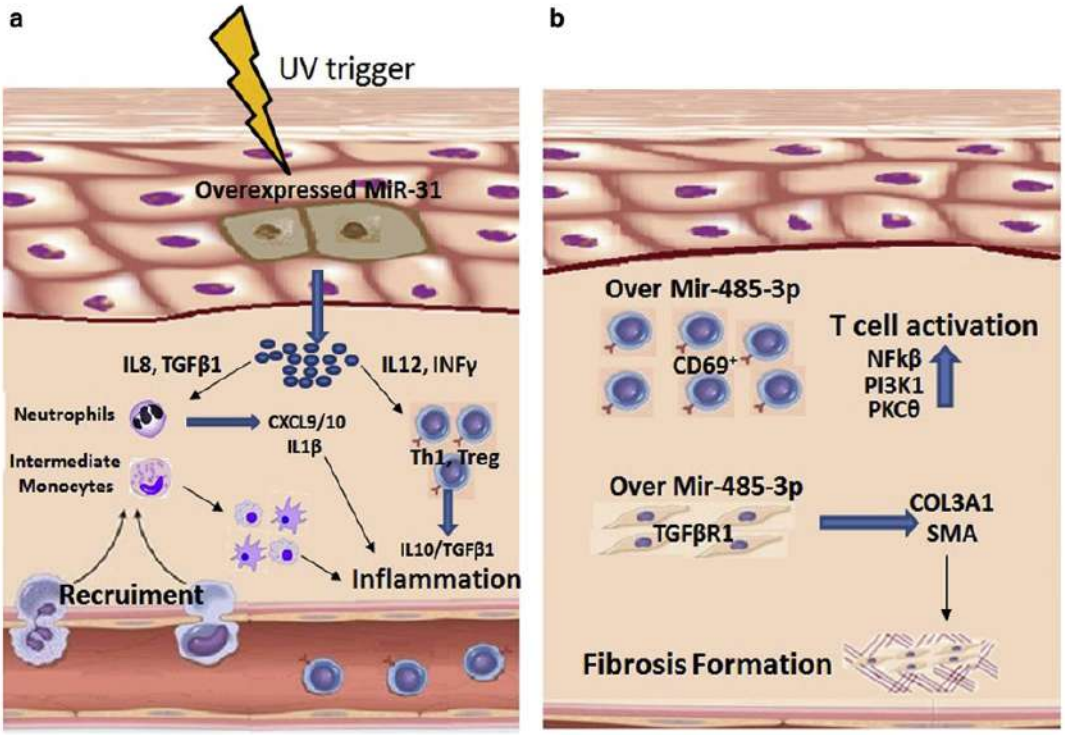

Figure 6. Proposed mechanism for miR-31 and miR-485-3p involvement in the pathogenesis of cutaneous lupus. (**a**) miR-31 overexpression in keratinocytes induced apoptosis and the production of inflammatory cytokines that in turn attract neutrophils/intermediate monocytes (IL-8, TGF-β1) and enhanced toward a Th1/regulatory T lymphocyte differentiation (IL-12, INFγ). Attracted neutrophils overexpressed IL-1β, CXCL9, and CXCL10, which could promote more leukocyte chemotaxis. Intermediate monocytes could be transformed into dendritic cells or macrophages to contribute to the maintenance of the inflammatory response. (**b**) Overexpression of miR-485-3p contributes to the inflammatory response by inducing T-cell activation by NF-κβ/PI3K1/PKCθ up-regulation. Overexpression of miR-485-3p in fibroblasts contributed to fibrosis formation by increasing levels of TGF-βR1, collagen (COL3A1), and smooth muscle actin (SMA). miR, microRNA; Th, T helper.

predominant overexpression of miR-31 in keratinocytes and miR-485-3p in PMBCs.

miR-31 is a major keratinocyte miRNA with minimal expression in other cell types. It is hardly expressed in normal skin but is significantly up-regulated in other skin diseases (Stepicheva and Song, 2016), with a role in restoring epidermal homeostasis or driving hyperproliferation. We identified in vitro TGFβ-1 and UV radiation as the main regulators of miR-31 expression in primary DLE keratinocytes. Both stimuli are known to play an important role in the pathogenesis of CLE. Our previous work showed the relevance of TGF-β1R in the pathogenesis of DLE by identifying impaired TGF-β1 signaling in those patients (Solé et al., 2016). Similarly, UV exposure has been associated with keratinocyte apoptosis, production of inflammatory cytokines, and autoantigen exposure in CLE (Furukawa et al., 1999). miR-31 is a prominent mediator of radiation-induced cell death in higher eukaryotes (Lynam-Lennon et al., 2012). Radiation-induced miR-31 overexpression alters BIM-mediated regulation of BAX translocation that, in turn, results in the post-irradiation mitochondrial cytochrome-c release, increasing apoptosis by a yet-to-be identified mechanism (Kuma et al., 2015). Our study also showed miR-31 to play a role in keratinocyte apoptosis by showing UV radiation and TGF-β1–induced miR-31 overexpression to increase rates of apoptosis in a capsase-3–dependent pathway and by regulating the BIM/BAX axis. miR-31 overexpression in stimulated keratinocytes also induced production of proinflammatory cytokines and chemokines, which in turn contribute to the initiation and maintenance of the inflammatory process in DLE. The main cytokines produced by stimulated primary DLE and miRNA-transfected keratinocytes were TGF-β1, NF-κB, and NF-κB–related cytokines such as IL-8, IL-12, and IL-1β. Our study confirmed the contribution of miR-31 in the pathogenesis of DLE by regulating the NF-κB activity in keratinocytes. NF-κB is a key signaling pathway, shown also to be constitutively activated in psoriatic epidermis (Xu et al., 2013), that commonly regulates proinflammatory cytokines, adhesion molecules, and chemokines (Bonizzi and Karin, 2004). In turn, this can contribute to endothelial cell activation, leukocyte attraction, and maintenance of inflammation. As previously reported, we confirmed that miR-31 overexpression can lead to the increased NF-κB activity, partially through the suppression of STK40 and PPP6C, negative regulators of the pathway (Yan et al., 2015).

The cross-talk study showed that human epidermal miR-31 mimic–transfected keratinocytes, after appropriate cytokine stimulation, had neutrophil and intermediate/nonclassical monocyte chemotactic activity, leading to an activation of the innate immune response (Figure 6a). IL-8 is a chemokine that attracts and activates neutrophils and regulates angiogenesis (Tecchio and Cassatella, 2014).

Unlike psoriasis, DLE skin lesions are characterized by a dense lymphocyte infiltrate, and neutrophil infiltration is hardly seen (Baltaci and Fritsch, 2009). However, irradiated uninvolved skin of patients with photosensitive lupus erythematosus has shown a gradual increase of epidermal neutrophils over time after irradiation, suggesting that neutrophil influx appears at early stages of the condition (Janssens et al., 2005). We showed that those attracted neutrophils could contribute to the amplification of the immune response by the production of T-cell chemoattractant molecules (CXCL9 and CXCL10) (Ogawa et al., 2002) and the production of IL-1β. In addition to neutrophils, intermediate/nonclassical monocytes were also attracted by keratinocytes overexpressing miR-31. TGF-β1 has been described as a potent chemoattractant of human peripheral blood monocytes in vitro (Wahl et al., 1987). These intermediate monocytes could participate in the inflammatory process by its role in antigen presentation, proinflammatory cytokine/chemokine production, wound healing (Turner et al., 2014), and fibrosis formation, in view of their accumulation in the damaged tissue (Thomas et al., 2015). Also, the co-stimulation influenced leukocytes by inducing a differentiation toward a Th1 response, probably in relation to the presence of IL-12 in the supernatant and an increased production of regulatory T cells. Our data suggest an early innate immune response at the initiation of inflammation in DLE that would lead to a leukocyte chemoattraction that, in turn, would contribute to the perpetuation of the inflammatory process (Figure 6a).

Previous studies have shown miR-485-3p to be involved in the regulation, apoptosis, migration, and invasion of metastatic cancer, but little is known of its role as a regulator of the immune system. miR-485-3p overexpression induced T-cell activation, with a significant increase in activated $CD8^+$ T cells and up-regulation of the NF-κB and PI3Kδ gene expression. High levels of PI3Kδ expression promote the production of proinflammatory cytokines through NF-κB activation downstream of AKT and are critical for effector T- and regulatory T-cell differentiation (Han et al., 2012). One of the predicted targets of miR-485-3p is HCN1, related negatively to PKCθ activity (Williams et al., 2015). Our study showed that overexpression of miR-485-3p in T cells induced down-regulation of HCN1 with an up-regulation of PKCθ. T-cell activation observed could be a result of PKCθ activation. PKCθ is also described as a regulator of NF-κB activation, but the specifics of how PKCθ activation leads to nuclear import of NF-κB in T cells is still being elucidated (Smith-Garvin et al., 2009). In addition, miR-485-3p overexpression modulated Th1/Th2 response by inducing a differentiation toward a Th2 phenotype. Our study also showed miR-485-3p to enhance the TGF-β signaling pathway, probably by targeting the PGC-1α gene (Lou et al., 2016). Previous studies showed the PGC-1α gene to be a known miR-485-3p target gene with a protective role in the development of fibrosis (Dinulovi et al., 2016).

Taken together, we show that in DLE, miR-31 overexpression in keratinocytes contributes to increased apoptosis and skin inflammation by enhancing neutrophil and monocyte migration into the skin and the cytokine production (Figure 6a). miR-485-3p may also contribute to skin inflammation by inducing T-cell activation. Finally, the high production of cytokines and the overexpressed miR-485-3p in fibroblasts contribute to fibrosis formation by a TGF-β/Smad3–dependent pathway (Figure 6b).

MATERIALS AND METHODS

Additional details are available in the Supplementary Materials online.

Patients and skin samples

After written informed consent, two 6-mm punch biopsy samples were taken from lesional and nonlesional skin of untreated patients with active disease and from healthy control individuals (n = 10 for each group) (see Supplementary Table S5 online). Validation was performed in a new cohort of paraffin-embedded lesional and nonlesional samples from DLE (n = 20) and SCLE (n = 18) and healthy control individuals (n = 10). All samples were evaluated by histology. At the time of biopsy, blood samples were also extracted for PBMCs/T-cell isolation. The study was approved by the local ethics committee.

miRNA screening and validation

Total RNA and miRNA were extracted and purified using the mirVana miRNA Isolation Kit (Applied Biosystems, Foster City, CA) or the PureLink FFPE RNA Isolation Kit (Applied Biosystems) according to the manufacturer's instructions. The miRNA screening was performed using TaqMan MicroRNA Array (Applied Biosystems), which enables quantification of 667 human microRNAs (see Supplementary Table S6). For validation, quantification of miRNAs by TaqMan real-time PCR was carried out using the Taqman MicroRNA Reverse Transcription Kit and MicroTaqman gene expression assays (Applied Biosystems) (see Supplementary Table S7 online).

In situ hybridization

Hybridization was performed on paraffin-embedded skin biopsy samples from lesional and nonlesional DLE and SLCE (n = 5 for each group), lesional psoriasis (n = 5), and healthy individuals (n = 5). Hybridization with hsa-miR-31, hsa-miR-485-3p, and has-miR-30c with 5′-DIG and 3′-DIG–labeled miRCURY LNA detection probe (Exiqon, Copenhagen, Denmark) was performed overnight at 50°C. The probe binding was detected by incubating sections with anti-DIG-alkaline phosphatase antibody (1:800; Roche, Basel, Switzerland) for 2 hours at room temperature.

Cell culture and stimulation

Functional miRNA studies were performed in isolated primary human cells and adult epidermal keratinocytes (HEKa cells) purchased from Cascade Biologics (Eugene, OR). Primary epidermal and fibroblast cells were isolated and characterized from punch skin biopsy samples (see Supplementary Figure S8 online). PBMCs and T cells were obtained from patients and healthy donors. Cells were transfected with miRNA mimics or anti-miR miRNA inhibitors (Thermo Fisher Scientific, Waltham, MA) using Lipofectamine RNAiMAX Reagent (Invitrogen, Waltham, MA). All cells were stimulated with recombinant human TGF-β1 (10 ng/ml), TNF-α (10 ng/ml), IL-1α (10 ng/ml), phorbol 12-myristate 13-acetate/ionomycin (50ng/mL and 10ng/mL, respectively), or UVB (25mJ/cm^2) for 6 hours. After that, total RNA was extracted with PureLink RNA Mini Kit (Invitrogen), and relative gene expression was measured by

real-time quantitative reverse transcription–PCR (Applied Biosystems) (see Supplementary Table S8 online).

Immunofluorescence

After stimulation, cells were washed with phosphate buffered saline and fixed with 4% paraformaldehyde. Permeabilization was done with 0.1% Triton and subsequently blocked with 5% bovine serum albumin. Primary antibodies were incubated overnight (1:1000), and secondary antibodies were incubated for 2 hours at room temperature (1:500) (Abcam, Cambridge, UK).

Cytokine measurement

The culture medium was collected from transfected keratinocytes after stimulation and stored at −80°C. ELISA kits were used to quantify protein levels of IL-8 (Invitrogen), IL-12, and TGF-β1 (Abcam) following the manufacturer's instructions.

Apoptosis and proliferation assay

Cells were plated in 96-well plates, and after treatment, apoptosis was determined using CellEvent Caspase-3/7 Green Detection Reagent (Invitrogen) and proliferation using CyQUANT NF Cell Proliferation Assay Kit (Invitrogen), following manufacturer's instructions.

Migration assay and co-culture experiments

The migration assays and co-culture experiments were performed in a modified 24-well plate with cell culture inserts (3.0- and 0.4-μm pore; BD Biosciences, Franklin Lakes, NJ). Transfected stimulated keratinocytes were cultured in the bottom of 24-well plates, and their supernatant was used as a chemoattractant for PMNC or PBMC migration. PMNCs were isolated from blood. PMNCs were marked with DAPI and plated in the upper well. After 6 hours, the upper surface of the filter was washed and swabbed with cotton to remove nonmigratory cells. Migrated PMNCs were fixed with 4% paraformaldehyde and observed under a fluorescence microscope. Cell number was counted in five random microscopic fields per well. Migration assay for PBMCs was evaluated by flow cytometry. The culture medium was also collected for cytokine measurement and RNA from cells were extracted following the instruction manual of PureLink RNA Mini Kit (Invitrogen).

Flow cytometry

Cell phenotype was analyzed by seven-color flowcytometry (LSRFortessa, BD Biosciences). For cell surface staining, conjugated monoclonal antibodies were used (BD Biosciences) (see Supplementary Table S9 online. Isotype controls were used for gate setting. Data were analyzed using FCS Express 4 Flow Research software (BD Biosciences, Erembodegem, Belgium).

Statistical analysis

GraphPad Prism software (GraphPad, La Jolla, CA) was used for statistical analysis. Numerical variables with normal distribution were compared with unpaired *t* test or paired *t* test. Non-normal distribution data were compared with Wilcoxon rank sum test. Data were expressed as mean ± standard error of the mean. *P* less than 0.05 was considered statistically significant.

CONFLICT OF INTEREST

The authors state no conflict of interest.

ACKNOWLEDGMENTS

This work was financed by Instituto de Salud Carlos III (Spain Government, PI10/02234), Catalan Lupus Foundation, and A. Bosch Foundation.

SUPPLEMENTARY MATERIAL

Supplementary material is linked to the online version of the paper at www.jidonline.org, and at https://doi.org/10.1016/j.jid.2018.07.026.

REFERENCES

Actman JC, Werth VP. Pathophysiology of cutaneous lupus erythematosus. Arthritis Res Ther 2015;17:182–93.

Baltaci M, Fritsch P. Histologic features of cutaneous lupus erythematosus. Autoimmun Rev 2009;8:467–73.

Baltimore D, Boldin MP, O'Connell RM, Rao DS, Taganov KD. MicroRNAs: new regulators of immune cell development and function. Nat Immunol 2008;9:839–45.

Barker JN, Jones ML, Mitra RS, Crockett-Torabe E, Fantone JC, Kunkel SL, et al. Modulation of keratinocyte-derived interleukin-8 which is chemotactic for neutrophils ant T lymphocytes. Am J Pathol 1991;139:869–76.

Bonizzi G, Karin M. The two NF-κB activation pathways and their role in innate and adaptive immunity. Trends Immunol 2004;25:280–8.

Botchkareva NV. The molecular revolution in cutaneous biology: noncoding RNAs: new molecular players in dermatology and cutaneous biology. J Invest Dermatol 2017;137(5):e105–11.

Czech MP. MicroRNAs as therapeutic targets. N Engl J Med 2006;354:1194–5.

Dey-Rao R, Smith JR, Chow S, Sinha AA. Differential gene expression analysis in CCLE lesions provides new insights regarding the genetics basis of skin vs. systemic disease. Genomics 2014;104:144–55.

Dinulovi I, Furrer R, Di Fulvio S, Ferry A, Beer M, Handschin C. PGC-1α modulates necrosis, inflammatory response, and fibrotic tissue formation in injured skeletal muscle. Skelet Muscle 2016;6:38–48.

Furukawa F, Itoh T, Wakita H, Yagi H, Tokura Y, Norris DA, et al. Keratinocytes from patients with lupus erythematosus show enhanced cytotoxicity to ultraviolet radiation and to antibody-mediated cytotoxicity. Clin Exp Immunol 1999;118:164–70.

Han JM, Patterson SJ, Levings MK. The role of the PI3K signaling pathway in $CD4^+$ T cell differentiation and function. Front Immunol 2012;3:245–56.

Jabbari A, Suarez-Fariñas M, Fuentes-Duculan J, Gonzalez J, Cueto I, Franks AG Jr, et al. Dominant Th1 and minimal Th17 skewing in discoid lupus revealed by transcriptomic comparison with psoriasis. J Invest Dermatol 2014;134:87–95.

Janssens AS, Lashley EE, Out-Luiting CJ, Willemze R, Pavel S, de Gruijl FR. UVB-induced leucocyte trafficking in the epidermis of photosensitive lupus erythematosus patients: normal depletion of Langerhans cells. Exp Dermatol 2005;14:138–42.

Krek A, Grun D, Poy MN, Wolf R, Rosenberg L, Epstein EJ, et al. Combinatorial microRNA target predictions. Nat Genet 2005;37:495–500.

Kuma A, Gosh S, Chandna S. Evidence for microRNA-31 dependent Bim-Bax interaction preceding mitochondrial Bax translocation during radiation-induced apoptosis. Sci Rep 2015;5:15923–36.

Lou C, Xiao M, Cheng S, Lu X, Jia S, Ren Y, et al. MiR485-3p and miR-485-5p suppress breast cancer cell metastasis by inhibiting PGC-1α expression. Cell Death Dis 2016;7:e2159.

Lynam-Lennon N, Reynolds JV, Marignol L, Sheils OM, Pidgeon GP, Maher SG. MicroRNA-31 modulates tumour sensitivity to radiation in oesophageal adenocarcinoma. J Mol Med (Berl) 2012;90:1449–58.

Mannucci C, Casciaro M, Minciullo PL, Calapai G, Navarra M, Gangemi S. Involvement of microRNAs in skin disorders: a literature review. Allergy Asthma Proc 2017;38:9–15.

O'Connell RM, Rao DS, Chaudhuri AA, Baltimore D. Physiological and pathological roles for microRNAs in the immune system. Nat Rev Immunol 2010;10:111–22.

Ogawa N, Ping L, Zhenjun L, Takada Y, Sugai S. Involvement of the interferon-gamma-induced T cell-attracting chemokines, inteferon-gamma-inducible 10-kd protein (CXCL10) and monokine induced by interferon-gamma (CXCL9), in the salivary gland lesions of patients with Sjögren's syndrome. Arthritis Rheum 2002;46:2730–41.

Onkon LG. Cutaneous lupus erythematosus: diagnosis and treatment. Best Pract Res Clin Rheumatol 2013;27:391–404.

Smith-Garvin JE, Koretzky GA, Jordan MS. T cell activation. Annu Rev Immunol 2009;27:591–619.

Solé C, Gimenez-Barcons M, Ferrer B, Ordi-Ros J, Cortés-Hernández J. Microarray study reveals a transforming growth factor-β-dependent mechanism of fibrosis in discoid lupus erythematosus. Br J Dermatol 2016;175:302–13.

Stepicheva NA, Song JL. Function and regulation of microRNA-31 in development and disease. Mol Reprod Dev 2016;83:654–74.

Tecchio C, Cassatella MA. Neutrophil-derived cytokines involved in physiological and pathological angiogenesis. Chem Immunol Allergy 2014;99:123–37.

Thomas G, Tacke R, Hedrick CC, Hanna RN. Non-classical patrolling monocyte function in the vasculature. Arterioscler Thromb Vasc Biol 2015;35:1306–16.

Turner JD, Bourke CD, Meurs L, Mbow M, Dièye TN, Mboup S, et al. Circulating $CD14^{bright}CD16^{+}$ 'intermediate' monocyte exhibit enhanced parasite pattern recognition in human helminth infection. PLoS Negl Trop Dis 2014;8:e2817.

Wahl SM, Hunt DA, Wakefiel LM, McCarteny-Francis N, Wahl LM, Roberts AB, et al. Transforming growth factor type beta induces monocytes chemotaxis and growth factor production. Proc Natl Acad Sci USA 1987;84:5788–97.

Wang MJ, Xu YY, Huang RY, Chen XM, Chen HM, Han L, et al. Role of an imbalanced miRNAs axis in pathogenesis of psoriasis: novel perspectives based on review of the literature. Oncotarget 2017;8:5498–507.

Williams AD, Jung S, Poolos NP. Protein kinase C bidirectionally modulates I_h and hyperpolarization-activated cyclic nucleotide-gated (HCN) channel surface expression in hippocampal pyramidal neurons. J Physiol 2015;13:2779–92.

Xu N, Meisgen F, Butler LM, Han G, Wang XJ, Söderberg-Nauclér C, et al. MicroRNA-31 is overexpressed in psoriasis and modulates inflammatory cytokine and chemokine production in keratinocytes via targeting serine/threonine kinase 40. J Immunol 2013;190:678–88.

Yan S, Xu Z, Lou F, Zhang L, Ke F, Bai J, et al. NF-κB-induced microRNA-31 promotes epidermal hyperplasia by repressing protein phosphatase 6 in psoriasis. Nat Commun 2015;6:7652–66.

Yan S, Yim LY, Lu L, Lau CS, Chan VS. MicroRNA regulation in systemic lupus erythematosus pathogenesis. Immune Netw 2014;14:138–48.

Yu C, Chang C, Zhang J. Immunologic and genetic considerations of cutaneous lupus erythematosus: a comprehensive review. J Autoimmun 2013;41:34–45.

Supporting Information

MicroRNA expression profiling identifies miR-31 and miR-485-3p as a novel regulators in the pathogenesis of Discoid Cutaneous Lupus

Cristina Solé [1], Sandra Domingo [1], Berta Ferrer[2], Teresa Moliné[2], Josep Ordi-Ros[1], Josefina Cortés-Hernández[1]

[1]Department of Medicine, Systemic Autoimmune Diseases Unit, Hospital Universitari Vall d'Hebron, Institut de Recerca (VHIR), Universitat Autònoma de Barcelona, Barcelona, Spain. [2]Department of Pathology, Hospital Universitari Vall d'Hebron, Universitat Autònoma de Barcelona, Barcelona, Spain.

INDEX

SI Materials and Methods

Patients and samples

Two six-millimetre punch biopsies were taken from lesional skin from 10 DLE and 10 SCLE untreated patients with active disease for the miRNAs screening and *in vitro* experiments (Supplementary Table S2). The first 6mm punch of lesional and non-lesional skin biopsy was bisected in two parts immediately, one part was frozen in liquid nitrogen for miRNA isolation and the other one was fixed in 5% formalin and embedded in paraffin blocks for the histological examination, immunohistochemistry or hybridization *in situ*. The second 6mm punch of lesional skin biopsy and skin biopsies from healthy donors (n=10) were immediately processed to obtain their primary fibroblast/keratinocytes. To validate the miRNAs screening, a new cohort of paraffin-embedded (FFPE) lesional samples obtained from DLE (n=20) and SCLE (n=18) patients was used. The diagnosis and classification of CLE were based on clinical and histological criteria according to the 2004 Dusseldorf classification (Khun and Ruzicka, 2004). Disease activity and degree of scarring was assessed by the validated modified CLE Disease Area and Severity Index (CLASI) (Albrecht et al, 2005).

Blood samples were also extracted for PBMCs isolation. Blood samples were collected in mononuclear cell preparation tubes with sodium citrate (Vacutainer CPT, BD Bioscences). After 25 min of centrifugation at 3000 rpm the section containing PBMCs was clearly visible and cells were collected using a pipette and washed twice in phosphate buffered saline (PBS). The cellular pellet was frozen at -80ºC for the miRNA extraction and also frozen with cell culture freezing medium for *in vitro* experiments. The study was approved by the Local Vall d'Hebrón Ethics Committee and informed consent was obtained from all subjects before the study.

Histology and immunofluorescence

FFPE tissue sections were evaluated for routine hemoxolin and endosing (H&E) staining and immunofluorescence. Each specimen was scored for the presence or absence of the following histologic features: hyperkeratosis; parakeratosis; acanthosis; epidermal and pilosebaceous atrophy; oedema; colloid bodies; liquefaction; basement-membrane thickening; dermal melanosis; follicular plugging; type, location and density of the inflammatory infiltrate; vascular changes; and myxoid degeneration. Each feature was scored semiquantitatively as follows: 0 (no presence), 1 (1%-10%), 2 (11-50%), or 3 (>50%). Fluorescent staining of the epidermis, dermal-epidermal junction and dermis was evaluated semiquantitatively as 0 (no staining), 1 (weakly positive), 2 (moderately positive), or 3 (strongly positive) and the pattern of staining was noted. The results of histology and immunofluorescence were evaluated on blinded specimens by the Vall d'Hebrón pathologist unit under the supervision of one the most experienced dermatopathologist (Dr. Berta Ferrer).

Isolation of Primary fibroblast/keratinocytes from the skin biopsy

Human fibroblasts/keratinocytes were isolated following the optimised protocol from Belmonte (Trond and Belmonte, 2010). Briefly, punch skin biopsies of 6 mm from lupus cutaneous patients (DLE n=10 and SCLE n=10) and healthy controls (n=10) were obtained, then incubated with dispase overnight at 4ºC to peel off the dermis from epidermis and they were cut into 2-3-mm^2 pieces to be digested with TrypLE Express Enzyme (1X) at 37°C during 18min, separately. Then the dermis and epidermis skin pieces were mechanically dissociated and filtered through a 40-µm cell strainer (Falcon, BD Biosciences). The filtrate was centrifuged at 1600g during 5min at 4ºC. The cellular pellets were resuspended in DMEM (10 mL) supplemented with 10% SFB and 5% antibiotics (for dermis cellular pellet, fibroblast culture) and in 10mL Epilife Medium supplemented with 10% HGSK and 5% antibiotics (for epidermis cellular pellet, keratinocyte culture). The cells were cultured in 25 cm^2 tissue culture flasks (Corning Inc, Acton, MA) at 37°C in 5% CO_2 and the medium cells were change every 2-3 days. In the present study, keratinocytes and fibroblasts at passage 2 were used for all experiments.

Isolation of Primary T cells from blood

Blood samples were collected in mononuclear cell preparation tubes with sodium citrate (Vacutainer CPT, BD Bioscences) and after 25 min of centrifugation at 3000 rpm the section containing PBMCs was clearly visible. Following the manufacturer's instructions of Dynabeads Untouched Human T cells (Invitrogen), T cell isolation were obtained from PBMCs pellet. Magnetic beads were prewashed with isolation buffer (PBS supplemented with 0.1% BSA and 2mM EDTA). After that, PBMCs pellet were re-suspended in isolation buffer and incubated with antibody mix/heat inactivated fetal calf serum during 20 minutes at 4ºC. Cells were washed two times with isolation buffer and washed magnetic beads were added. After 15 minutes in rotation at room temperature, the mixture were in the magnet for two minutes and purified T cells were isolated in supernatant. Purification and characterization of them were analyzed using LSR Fortessa cytometer with CD3-PE, CD4-FITC and CD8-APC as markers (BD biosciences).

RNA extraction for all samples

In this study several kind of samples were used to carry out the microarray analysis (punch skin biopsies), its validation (Formaldehyde Fixed-Paraffin Embedded (FFPE) skin samples) and the *in vitro* studies (primary fibroblast cells).

Punch skin biopsy specimens were homogenised by polytron and purified with the mirVANA miRNA Isolation Kit (Applied Biosystems) following the manufacturer's instructions to obtain total mRNA. Before to use them for microarray analysis, the integrity and the quantity of the RNA samples were determined using Agilent 2100 Bioanalyzer (RIN values ≥ 8). RNA samples with low RNA Integrity Number (RIN) were repurified to obtain RIN ≥ 8.

FFPE samples were cut in 20 µm sections using a microtome. Three of these sections were used to obtain the total RNA following the manufacturer's instructions of the PureLink FFPE

RNA Isolation Kit (Applied Biosystems). Xylene treatment was used to remove paraffin from the sections. The yield and the quality of RNA were determined by measuring its absorbance at 260nm and 280nm. Ratios of A_{260}/A_{280} between 1.8 and 2.1 were accepted to use the RNA for the subsequent experiments.

RNA and protein from primary isolated fibroblast were obtained after the lysis of the cells and using the PureLink RNA mini kit (Applied Biosystem) according the manufacturer's instructions. Similar to the FFPE samples, the quality and yield of RNA was determined by spectrophometry.

MiRNAs analysis – Statistical Analysis

Data obtained from the Taqman MicroRNA arrays were analyzed by the Statistics and Bioinformatics Unit of our research institute. The statistical analyses corresponding to microarrays were performed using the R statistical software package (www.R-project.org) (R Core Team, 2014) and the libraries developed for microarray data analysis by the Bioconductor Project (www.bioconductor.org) (Gentleman et al, 2004). The biological relationship of the results obtained in the microarray was studied using the Ingenuity Pathway Analysis (IPA®, QIAGEN Redwood City, www.qiagen.com/ingenuity).

Quantitative Reverse Transcription-PCR

To quantification of mRNAs, 1.5µg total RNA was reverse-transcribed using the High-Capacity Cdna Reverse Transcription Kit (Applied Biosystems) with the thermal cycler program: 25ºC for 5min, 37ºC for 2hours and 82ºC for 5min.

To quantify miRNAs, 200ng microRNA was reverse-transcribed using the Taqman MicroRNA Reverse Transcription Kit (Applied Biosystems) with the thermal cycler program: 16ºC for 30min, 42ºC for 30min and 85ºC for 5min.

MRNAs or miRNAs were quantified by TaqMan gene expression assays or MicroTaqMan gene exrpression assays (FAM dye-labeled MGB probe, Applied Biosystems) using the ABI PRISM 7000 termocycler at 50ºC for 2 min, 95ºC for 10min, followed by 40 cycles of 95ºC for 15s and 60ºC for 1 min. Data was normalised based on the expression of the endogenous control GAPDH for mRNA quantification (Hs02786624_g1) and U6 snRNA for miRNA quantification (4427975).

Evaluation of hybridization in situ

After antibody incubation, the results were evaluated on blinded specimens by the Vall d'Hebrón pathologist unit under the supervision of one the most experienced dermatopathologist (Dr. Berta Ferrer). The percentage of cells expressing the different probes was scored semiquantitatively as follows: 0 (no expression), 1 (11-20%), 2 (40-60%), or 3

(>80%). Staining intensity was scored semiquantitatively as 0 (no staining), 1 (weakly positive), 2 (moderately positive), or 3 (strongly positive).

In vitro experiments performed with primary human isolated cells from the skin biopsy

Isolated Human fibroblast or keratinocytes at passage 2 were plated onto 24-well Cell+ Sarstedt culture slides at a concentration of $1 \cdot 10^4$ cells/mL Epilife Medium supplemented with 10% HGSK and 5% antibiotics was used for primary keratinocytes cells. DMEM or RPMI supplemented with 10% serum fetal bovine and 5% antibiotics was used for primary fibroblasts or PBMCs (respectively). After 24 hours, primary cells were transfected with anti-miR, pre-mimic-miR or their relative negative-control using Lipofectamine RNAiMAX (Thermo Fisher) following the manufacturer's instructions. After 36hours, primary cells were stimulated with the corresponding stimulation conditions: recombinant human TGF-β1 (10 ng/mL), TNF-α (10 ng/mL), IL-1α (10 ng/mL), UVB (25mJ/cm^2) during 6 hours. For "non-stimulation" conditions (NS), phosphate-buffered saline were use in the place of the cytokines. Different concentrations of stimuli (5-100 ng/mL and 5-250mJ/cm^2) were used to evaluate the optimal concentration for each type of cell by cytotoxicity assay using LIVE/DED Viability/Cyttoxicity Kit (Applied Biosystem).

After incubation, total RNA and protein were extracted with PureLink RNA mini kit (Applied Biosystem) following the manufacturer's instructions. Relative gene expression was determined by quantitative real-time PCR using Taqman gene expression assays according to the manufacturer's protocol. GAPDH (Hs02786624_g1) was used as endogenous control to normalise the data. Western Blot or immunofluorescence were carried out using antibodies from Abcam.

In vitro experiment performed with primary human PBMCs or T cells extracted from blood samples

Blood samples were collected in mononuclear cell preparation tubes with sodium citrate (Vacutainer CPT, BD Bioscences) and after 25 min of centrifugation at 3000 rpm the section containing PBMCs was clearly visible.Cells were plated onto 24-well Sarstedt culture slides with a concentration of $1 \cdot 10^4$ cells/mL using RPMI media with 10% serum fetal bovine and 5% antibiotics or were used for T cell isolation using "Dynabeads Untouched Human T Cells" (described previously). After 24 hours, PBMCs or T cells were transfected with anti-miR, pre-mimic-miR or their relative negative-control using Lipofectamine RNAiMAX (Thermo Fisher) following the manufacturer's instructions. After 36hours, they were stimulated with IL-1α (10 ng/mL), TNF-α (10 ng/mL) and PMA/ionomycin (50ng/mL and 1ug/mL, respectively) during 6 hours. After incubation, total RNA and protein were extracted with PureLink RNA mini kit (Applied Biosystem) following the manufacturer's instructions. Relative gene expression was determined by quantitative real-time PCR using Taqman gene expression assays according to the manufacturer's protocol. GAPDH (Hs02786624_g1) was used as endogenous control to normalise the data. Western Blot or immunofluorescence were carried out using antibodies from Abcam.

In vitro experiments: Immunofluorescence

Cells were plated onto sterile *glass* cover slips and incubate overnight at 37ºC. Then they were transfected and stimulated. After that, cells were washed briefly with PBS, fixed with PFA 10% for 20min and permeabilised with 0.1% Triton for 10min. Cells were incubated with BSA 5% during 1hour and later incubated with primary antibody for NF-kβ (Abcam, 1/250) and VCAM-1 (Abcam, 1/250) overnight at 4ºC. Alexa-488-conjugated anti-rabbit IgG (Abcam, 1/500) and Alexa-680-conjugated anti-goat IgG (Abcam 1/500) were used as secondary antibodies. They were incubated for 2hours at room temperature. DAPI was used to visualise the nucleus cells.

SI References

Albrecht J, Taylor L, Berlin JA *et al.* (2005) The CLASI (Cutaneous Lupus Erythematosus Disease Area and Severity Index): an outcome instrument for cutaneous lupus erythematosus. *J Invest Dermatol.* 125:889–94.

Gentleman RC, Carey VJ, Bates DM, Bolstad B *et al.* (2004) Bioconductor: open software development for computational biology and bioinformatics. *Genome Biol.* 5 : R80.

Khun A, Ruzicka T (2004) Classification of cutaneous lupus erythematosus. In: Khun A, Lehmann P, Ruzicka T, editors. Cutaneous lupus erythematosus. Heidelberg: Springer Verlag; P. 53-59.

R Core Team (2014). R: A language and environment for statistical computing. R Foundation for Statistical Computing, Vienna, Austria. URL http://www.R-project.org/.

Trond A, Belmonte JC (2010) Isolation and cultivation of human keratinocytes from skin or plucked hair for the generation of induced pluripotent stem cells. *Nat. Protoc* 5:371-382.

Supplementary Figure 1

Figure S1. Validation of differential expressed miRNAs between lesional and non-lesional skin from DLE and SCLE patients. Expression of differentially expressed miRNAs was validated using quantitative real-time PCR (qRT-PCR) in lesional skin of DLE **(a)** and SCLE **(b)** from non-lesional skin of these patients. The results for individual patients and mean are shown. Gene expression was normalised using U6 as endogenous control. Fold change in expression level was calculated using the $2^{-\Delta\Delta Ct}$ method. **P*<0.05; ***P*<0.005; ****P*<0.0005.

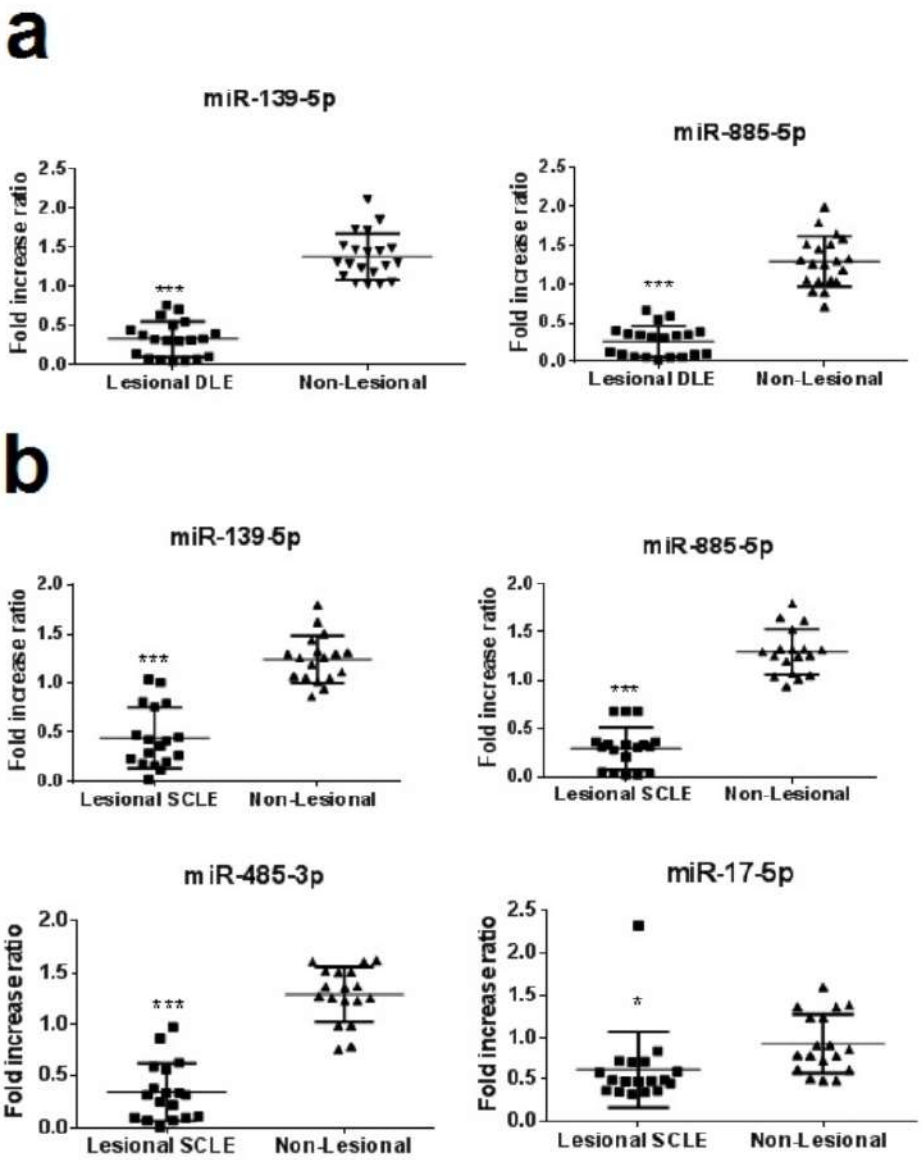

Supplementary Figure 2

Figure S2. Overexpression of miR-485-3p in PBMCs increase the rate of proliferation. PBMCs were transfected with 40 nM of pre-miR-485-3p or anti-miR-485-3p for 24hours and proliferation change (a) and apoptosis (b) were evaluated using fluorescence commercial kits. Six independent experiments were done in 96-well plates. Data represent the mean ±SEM. **P*<0.05; ***P*<0.005; ****P*<0.0005.

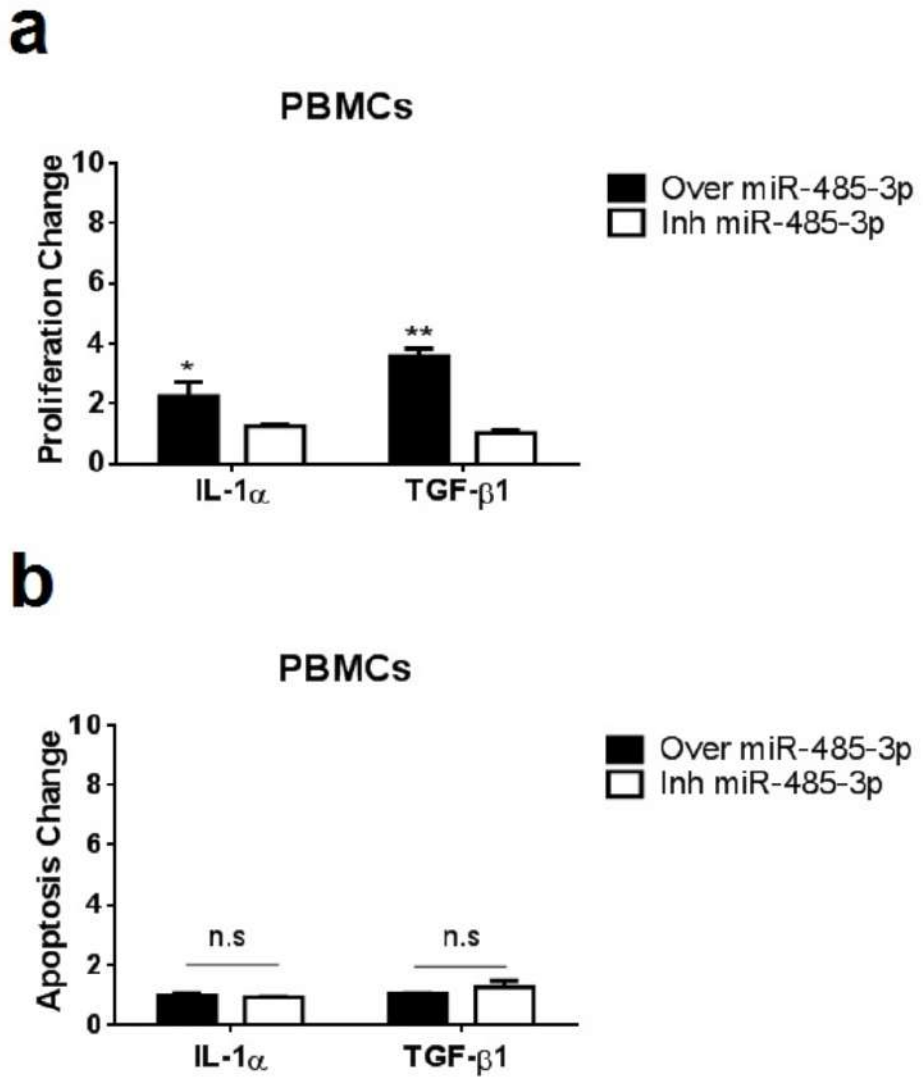

Supplementary Figure 3

Figure S3. Transfected miR-485-3p PBMCs stimulated with IL-1α or TGF-β1. (a) Flow cytometry diagram and percentage of $CD69^{+}CD4^{+}$ and $CD69^{+}CD8^{+}$. **(b)** Quantitative reverse transcriptase-PCR (qPCR-RT) of T cell activation genes and **(c)** transcription factors genes of Th1, Th2 and Treg and related cytokines. Data represent the mean ±SEM from three independent experiments. Gene were normalised to GADPH gene and transfected controls were used for the fold changes. **P*<0.05; ***P*<0.005; ****P*<0.0005.

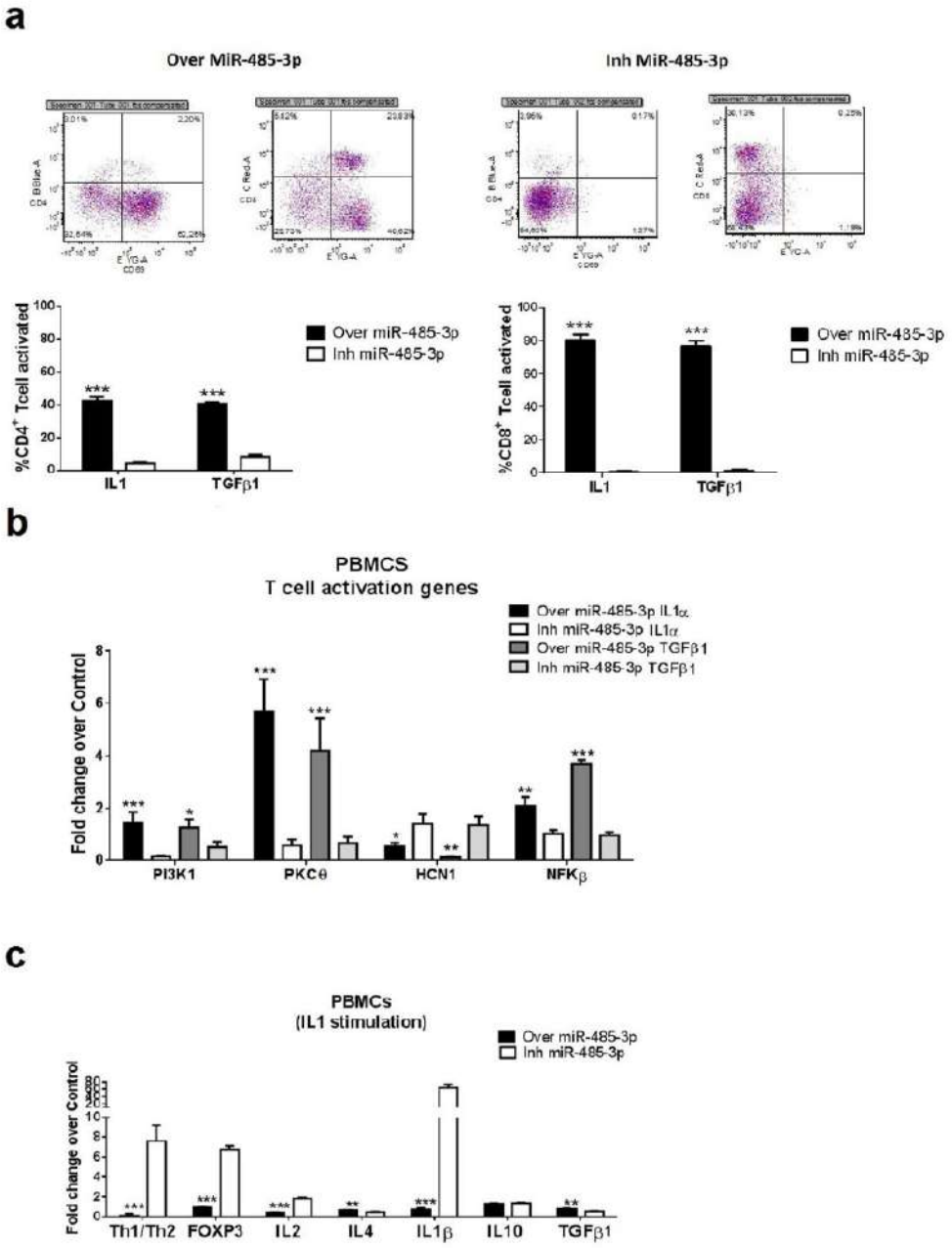

Supplementary Figure 4

Figure S4. Schematic illustration of co-culture experiments with keratinocytes and PMNCs or PBMCs. Keratinocytes were transfected with anti-miR-31, pre-miR-31 or the corresponding negative control and platted in the bottom of 24-well plate. After 24hours, they were stimulated with TGF-β1 (10 ng/mL), TNF-α (10 ng/mL), IL-1α (10 ng/mL) or UVB (25mJ/cm^2) during 6 hours. An insert was added and primary mononuclear neutrophil cells (PMNCs) or primary peripheral blood mononuclear cells (PBMCs) were placed into the upper of insert (3μm or 0.4μm). Migration of PMNCs or PBMCs were evaluated by flow cytometry after 6-24hours of incubation using the 3μm insert. Apoptosis of PMNCs or PBMCs were evaluated using the 0.4μm insert; however, it was not observed.

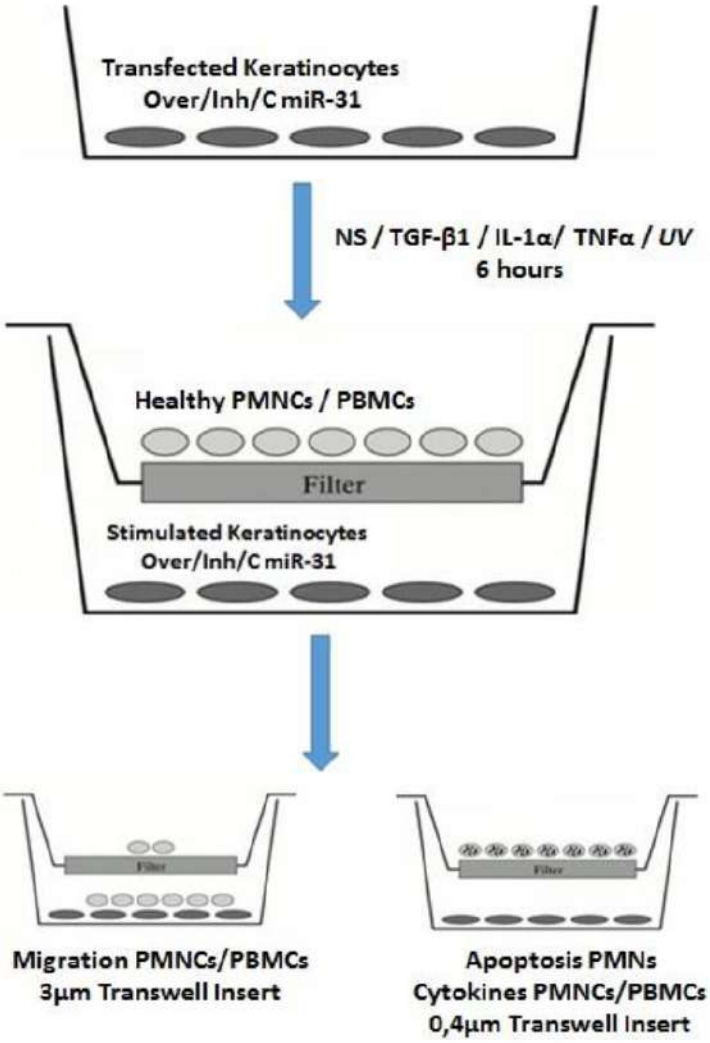

Supplementary Figure 5

Figure S5. Correlation with IL-8 protein levels in cultured medium and %migration neutrophils. A strong correlation was found between IL-8 protein levels found in the medium and the percentage of neutrophils migration in co-cultured keratinocytes-PMNCs experiments.

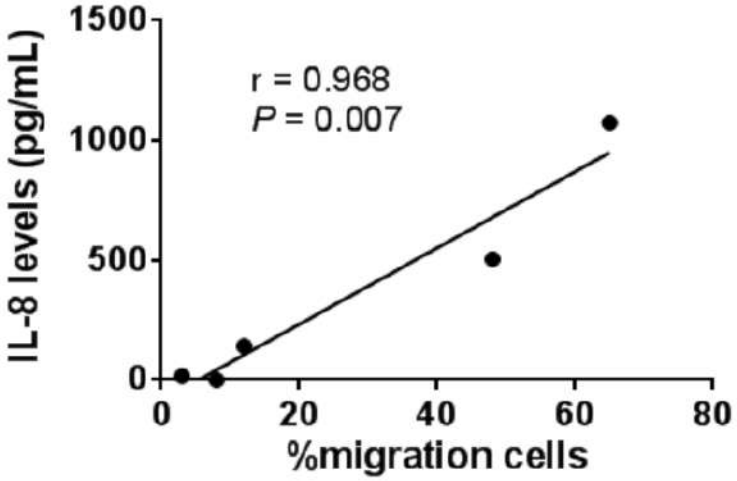

Supplementary Figure 6

Figure S6. Apoptosis assay in co-cultured of neutrophils and transfected stimulated keratinocytes. Transfected miR-31 keratinocytes were platted on 24-well and stimulated with TGF-β1, IL-1α, TNF-α, *UV* or NS (no-stimulation conditions). An insert of 0.4μm was added with isolated neutrophils. After 24-48hours, apoptosis was evaluated using a fluorometric assay and expressed has a fold change in comparison with transfected negative controls. No significate apoptosis change were observed.

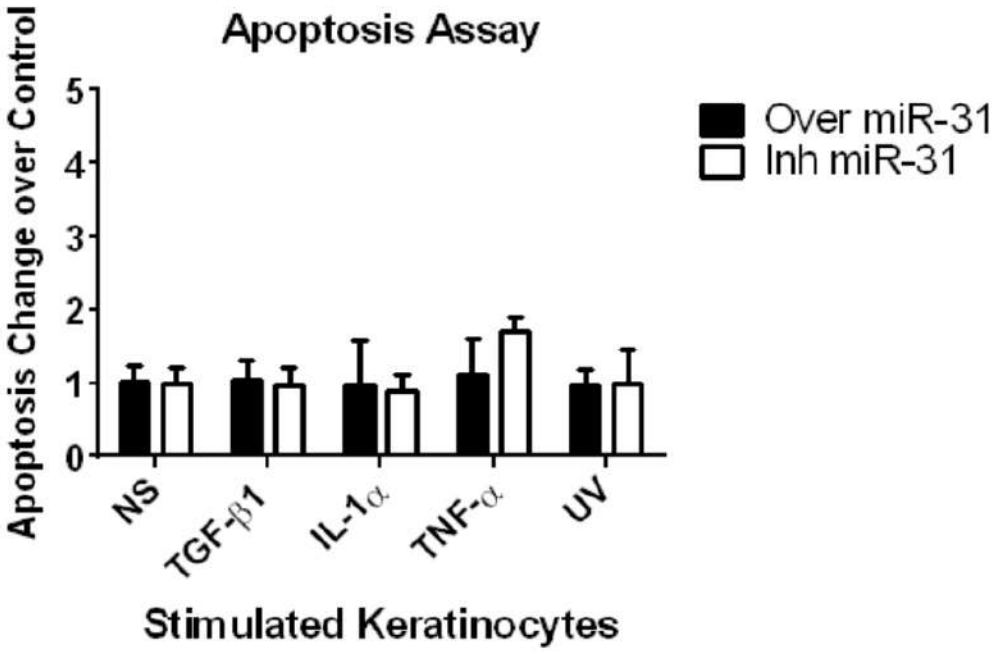

Supplementary Figure 7

Figure S7. Migration of dendritic cells(DC) / natural killer cells (NK) or lymphocytes cells (CD4$^+$ or CD8$^+$). Transfected miR-31 keratinocytes were platted on 24-well and stimulated with TGF-β1 or *UV*. Insert of 3µm was added with DC, NK or lymphocytes. Flow cytometry analysis was used to evaluated their migration. Flow cytometry diagram not reveals significant different migration of DC **(a)**, NK **(b)** or lymphocytes **(c)** between the conditions with overexpressed miR-31 or inhibited miR-31 keratinocytes.

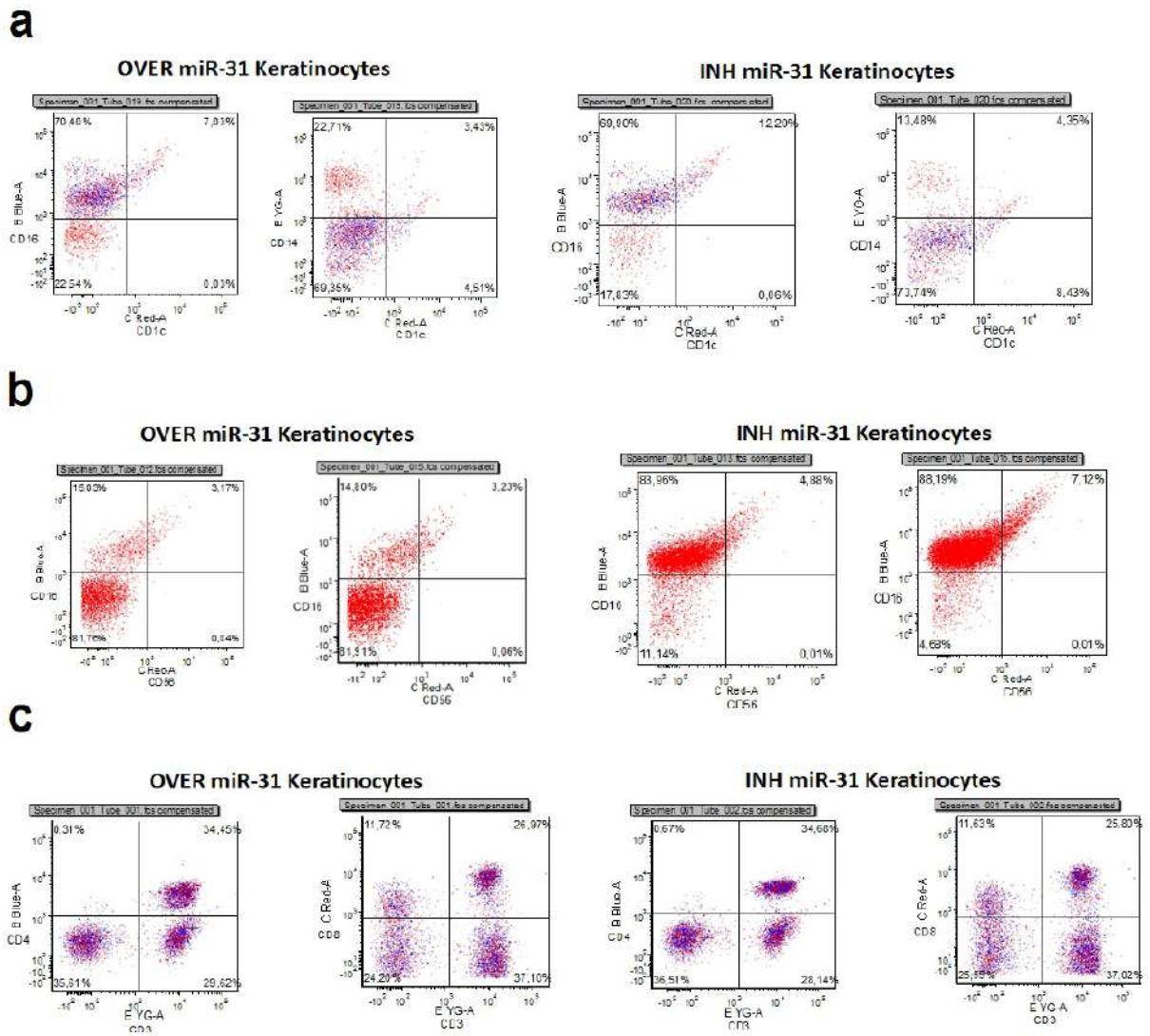

Supplementary Figure 8

Figure S8. Evaluation of the purity of primary cell cultures isolated from lesional DLE or SCLE skin biopsy or blood. a) The purity of keratinocytes was assessed by light microscopy and anti-cytokeratin14 staining. b) The purity of fibroblast was assessed by light microscopy and 6-diamidino-2-pphenylindole (DAPI) staining. c) The purity of PBMCs was assessed by flow cytometry.

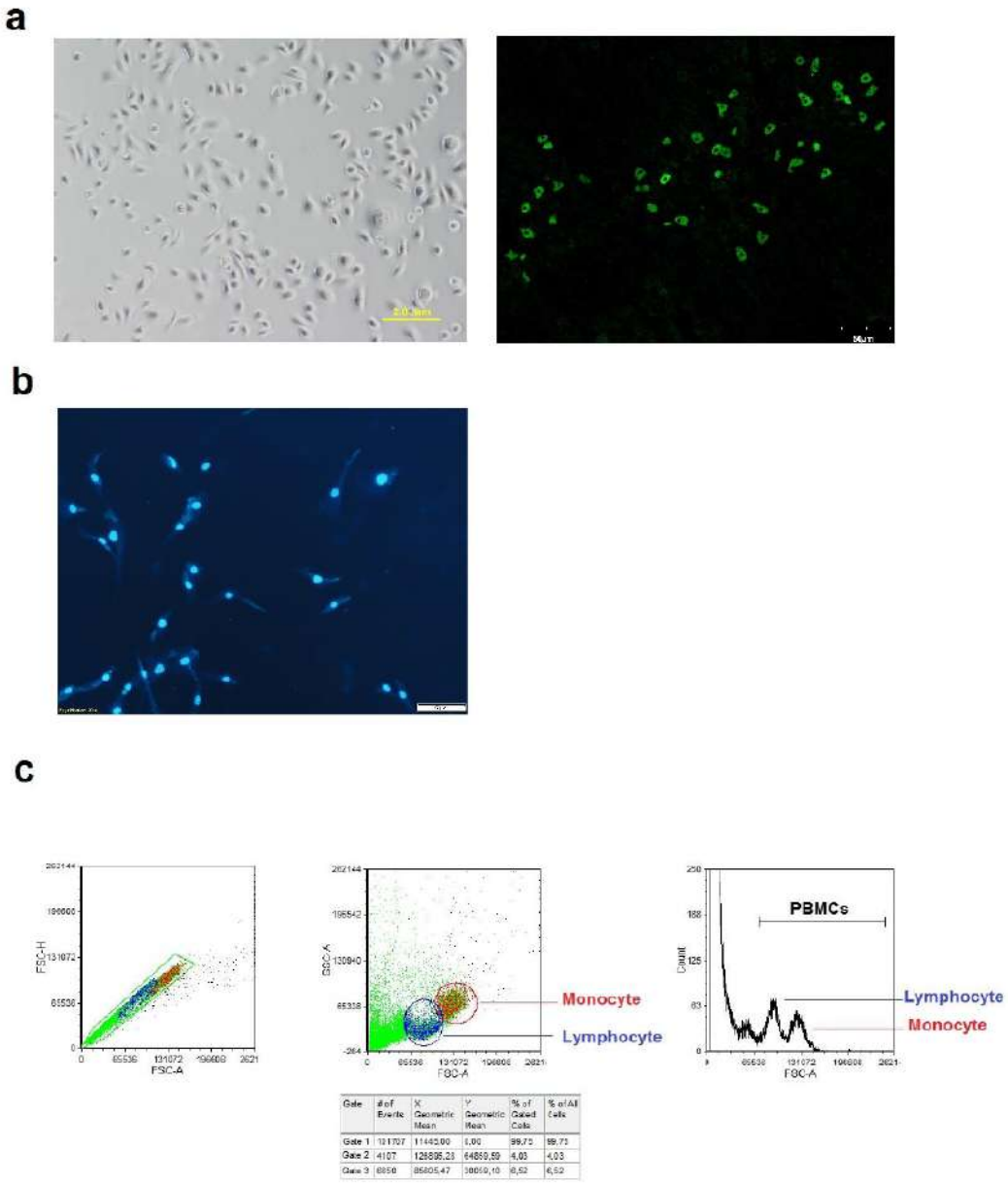

Gate	# of Events	X Geometric Mean	Y Geometric Mean	% of Gated Cells	% of All Cells
Gate 1	131707	11442,00	0,00	99,73	99,73
Gate 2	4107	128895,23	64859,59	4,03	4,03
Gate 3	6858	85805,47	38859,10	6,52	6,52

Supplementary Table S1

Table S1. Common and differenced expressed miRNAs in the comparation between "DLE versus non-lesional skin" and "SCLE versus non-lesional skin" and "DLE versus SCLE"

Lesional DLE versus non-lesional DLE skin

feature.ID	t.test	p.value	adj.p.value	B	ddCt	ExprFold	RQ
hsa-miR-885-5p-002296	6,10136566	1,58E-06	0,00012669	5,08911313	3,35105714	0,09800118	1 / 10.204
hsa-miR-139-5p-002289	5,79135053	3,60E-06	0,00014394	4,35601648	2,70005714	0,15388696	1 / 6.498
hsa-miR-744-002324	3,84387208	0,00066321	0,01768552	-0,3458046	2,50771429	0,17583397	1 / 5.687
hsa-miR-889-002202	3,72158293	0,00091404	0,01828079	-0,6345404	3,12262857	0,11481408	1 / 8.71

Lesional SCLE versus non-lesional SCLE skin

feature.ID	t.test	p.value	adj.p.value	B	ddCt	ExprFold	RQ
hsa-miR-885-5p-002296	4,14485613	0,00029875	0,02390006	0,37458989	2,3542	0,19557583	1 / 5.113
hsa-miR-485-3p-001277	3,12091628	0,00462615	0,14585614	-2,0255834	4,41841667	0,04676534	1 / 21.383
hsa-miR-486-001278	2,90984202	0,00713569	0,14585614	-2,4508895	2,95106667	0,12931247	1 / 7.733
hsa-miR-139-5p-002289	2,83396864	0,00857117	0,14585614	-2,6113158	1,36636667	0,38786684	1 / 2.578
hsa-miR-574-3p-002349	2,80828354	0,00911601	0,14585614	-2,6651373	2,70183333	0,15369761	1 / 6.506
hsa-miR-20b-001014	2,63159835	0,01457758	0,19436776	-3,0328345	9,0269	0,00191705	1 / 521.636
mmu-miR-451-001141	2,49085082	0,0191521	0,21888117	-3,3079063	2,9922	0,12567765	1 / 7.957

Supplementary Table S2

Table S2. Common and differenced expressed miRNAs in the comparation between "DLE versus SCLE"

feature.ID	t.test	p.value	adj.p.value	B	ddCt	ExprFold	RQ
hsa-miR-139-5p	3,01072796	0,00557691	0,29993301	-2,8417833	1,33369048	0,39675203	1 / 2.52
hsa-miR-485-3p	-2,7336659	0,01153859	0,29993301	-3,1910745	-3,3356666	10,0956834	1 x 10.096
hsa-miR-31	-2,7192833	0,01192741	0,29993301	-3,206887	-3,4960952	11,2831285	1 x 11.283
hsa-miR-889	2,58992341	0,01525228	0,29993301	-3,3247033	2,0647619	0,23902577	1 / 4.184
hsa-miR-30c	2,48717012	0,01986295	0,29993301	-3,4956018	5,53908571	0,02150647	1 / 46.498
hsa-miR-222	-2,4197951	0,02249498	0,29993301	-3,5118251	-1,7376666	3,33495355	1 x 3.335
hsa-miR-636	-2,2487142	0,0328463	0,36976795	-3,6937667	-2,3469523	5,0874841	1 x 5.087
hsa-miR-30a-5p-000417	-2,1876659	0,03679543	0,65586054	-4,5863320	-2,5830833	5,99218985	1 x 5.992
hsa-miR-625#-002432	-2,2063493	0,03702106	0,65586054	-4,5886632	-2,94045	7,67650701	1 x 7.677
hsa-miR-628-5p	-2,1680793	0,03908369	0,36976795	-3,7770505	-2,5050238	5,67658711	1 x 5.677
hsa-miR-193a-3p	2,13880447	0,04159889	0,36976795	-3,806863	1,5025	0,35294126	1 / 2.833
hsa-miR-657-001512	2,09756526	0,04497274	0,65586054	-4,5869728	2,5482	0,17096821	1 / 5.849

Supplementary Table S3

Table S3. Predicted Targets of hsa-miR-31. Using miRNAs database (TargetScanHuman and miRTarBase) and Ingenuity Pathway Analysis, a table of predicted and reported targets of miR-31 was generated.

Predicted Targets

Target gene	Representative transcript	Gene name	3P-seq tags + 5
RSBN1	ENST00000261441.5	round spermatid basic protein 1	54
SH2D1A	ENST00000371139.4	SH2 domain containing 1A	5
AK4	ENST00000545314.1	adenylate kinase 4	116
PAX9	ENST00000361487.6	paired box 9	53
LPP	ENST00000312675.4	LIM domain containing preferred translocation partner in lipoma	1894
NR5A2	ENST00000367362.3	nuclear receptor subfamily 5, group A, member 2	121
ARHGEF 2	ENST00000368315.4	Rho/Rac guanine nucleotide exchange factor (GEF) 2	313
WDR5	ENST00000425041.1	WD repeat domain 5	889
PSMB11	ENST00000408907.2	proteasome (prosome, macropain) subunit, beta type, 11	5
SYDE2	ENST00000341460.5	synapse defective 1, Rho GTPase, homolog 2 (C. elegans)	72
PDZD2	ENST00000438447.1	PDZ domain containing 2	5
SSH1	ENST00000360239.3	slingshot protein phosphatase 1	115
TFRC	ENST00000540528.1	transferrin receptor	296
IL34	ENST00000429149.2	interleukin 34	5
CIAPIN1	ENST00000565961.1	cytokine induced apoptosis inhibitor 1	423
PC	ENST00000529047.1	pyruvate carboxylase	798
TMPRSS 11F	ENST00000356291.2	transmembrane protease, serine 11F	5
CRYBG3	ENST00000389622.2	beta-gamma crystallin domain containing 3	46
EGLN3	ENST00000250457.3	egl-9 family hypoxia-inducible factor 3	71
TBXA2R	ENST00000375190.4	thromboxane A2 receptor	169
HIAT1	ENST00000370152.3	hippocampus abundant transcript 1	1473
UCN2	ENST00000273610.3	urocortin 2	44
TESK2	ENST00000372084.1	testis-specific kinase 2	11
SERTAD 2	ENST00000313349.3	SERTA domain containing 2	119
C17orf78	ENST00000586700.1	chromosome 17 open reading frame 78	5
MGAT1	ENST00000333055.3	mannosyl (alpha-1,3-)-glycoprotein beta-1,2-N-acetylglucosaminyltransferase	831
KHDRBS 3	ENST00000355849.5	KH domain containing, RNA binding, signal transduction associated 3	11
RGS4	ENST00000531057.1	regulator of G-protein signaling 4	489
FAM73A	ENST00000370791.3	family with sequence similarity 73, member A	837
AHCYL1	ENST00000369799.5	adenosylhomocysteinase-like 1	1279
SPARC	ENST00000231061.4	secreted protein, acidic, cysteine-rich (osteonectin)	2467
KANK1	ENST00000382303.1	KN motif and ankyrin repeat domains 1	6
DCBLD2	ENST00000326840.6	discoidin, CUB and LCCL domain containing 2	798

FAM53B	ENST00000337318.3	family with sequence similarity 53, member B	27
FLOT1	ENST00000376389.3	flotillin 1	809
AP000695.1	ENST00000595927.1		5
LBH	ENST00000406087.1	limb bud and heart development	1956
TMED10	ENST00000303575.4	transmembrane emp24-like trafficking protein 10 (yeast)	1753
SEMA6D	ENST00000355997.3	sema domain, transmembrane domain (TM), and cytoplasmic domain, (semaphorin) 6D	179
AMER1	ENST00000330258.3	APC membrane recruitment protein 1	11
FAM60A	ENST00000539409.1	family with sequence similarity 60, member A	58
SEPHS1	ENST00000545675.1	selenophosphate synthetase 1	281
PAX5	ENST00000358127.4	paired box 5	5
RASA1	ENST00000456692.2	RAS p21 protein activator (GTPase activating protein) 1	1700
HOMER1	ENST00000508576.1	homer homolog 1 (Drosophila)	394
CD28	ENST00000324106.8	CD28 molecule	5
GXYLT1	ENST00000398675.3	glucoside xylosyltransferase 1	126
NDRG3	ENST00000373803.2	NDRG family member 3	960
MMP16	ENST00000286614.6	matrix metallopeptidase 16 (membrane-inserted)	12

Reported Targets (Igenuity Pathway Analysis)

Target gene	Gene name
TIAM1	T-lymphoma invasion and metastasis-inducing protein 1
PPP6C	Protein Phosphatase 6 Catalytic Subunit
STK40	Serine/Threonine Kinase 40
RHOA	Ras Homolog Family Member A
FOXP3	Forkhead box P3

Reported Targets (miRTarBase, strong evidence)

ID	Species (miRNA)	Species (Target)	miRNA	Target
MIRT000088	Homo sapiens	Homo sapiens	hsa-miR-31-5p	RHOA
MIRT000490	Homo sapiens	Homo sapiens	hsa-miR-31-5p	PPP2R2A
MIRT000491	Homo sapiens	Homo sapiens	hsa-miR-31-5p	LATS2
MIRT001180	Homo sapiens	Homo sapiens	hsa-miR-31-5p	FOXP3
MIRT004019	Homo sapiens	Homo sapiens	hsa-miR-31-5p	SELE
MIRT004968	Homo sapiens	Homo sapiens	hsa-miR-31-5p	YY1
MIRT004969	Homo sapiens	Homo sapiens	hsa-miR-31-5p	RET
MIRT004970	Homo sapiens	Homo sapiens	hsa-miR-31-5p	NUMB
MIRT004971	Homo sapiens	Homo sapiens	hsa-miR-31-5p	NFAT5
MIRT004972	Homo sapiens	Homo sapiens	hsa-miR-31-5p	KLF13
MIRT004973	Homo sapiens	Homo sapiens	hsa-miR-31-5p	JAZF1
MIRT004974	Homo sapiens	Homo sapiens	hsa-miR-31-5p	HOXC13
MIRT004975	Homo sapiens	Homo sapiens	hsa-miR-31-5p	ETS1

MIRT004976	Homo sapiens	Homo sapiens	hsa-miR-31-5p	ITGA5
MIRT004977	Homo sapiens	Homo sapiens	hsa-miR-31-5p	MPRIP
MIRT004978	Homo sapiens	Homo sapiens	hsa-miR-31-5p	MMP16
MIRT004979	Homo sapiens	Homo sapiens	hsa-miR-31-5p	RDX
MIRT004980	Homo sapiens	Homo sapiens	hsa-miR-31-5p	CXCL12
MIRT004981	Homo sapiens	Homo sapiens	hsa-miR-31-5p	ARPC5
MIRT004984	Homo sapiens	Homo sapiens	hsa-miR-31-5p	FZD3
MIRT005456	Homo sapiens	Homo sapiens	hsa-miR-31-5p	DMD
MIRT005566	Homo sapiens	Homo sapiens	hsa-miR-31-5p	TIAM1
MIRT005707	Homo sapiens	Homo sapiens	hsa-miR-31-5p	ICAM1
MIRT005874	Homo sapiens	Homo sapiens	hsa-miR-31-5p	DKK1
MIRT005875	Homo sapiens	Homo sapiens	hsa-miR-31-5p	DACT3
MIRT004981	Homo sapiens	Homo sapiens	hsa-miR-31-5p	ARPC5
MIRT006026	Homo sapiens	Homo sapiens	hsa-miR-31-5p	WASF3
MIRT006468	Homo sapiens	Homo sapiens	hsa-miR-31-5p	HIF1AN
MIRT006567	Homo sapiens	Homo sapiens	hsa-miR-31-5p	SATB2
MIRT007065	Homo sapiens	Homo sapiens	hsa-miR-31-3p	RHOA
MIRT007286	Homo sapiens	Homo sapiens	hsa-miR-31-5p	PRKCE
MIRT007292	Homo sapiens	Homo sapiens	hsa-miR-31-5p	RASA1
MIRT007319	Homo sapiens	Homo sapiens	hsa-miR-31-5p	STK40
MIRT007327	Homo sapiens	Homo sapiens	hsa-miR-31-5p	MCM2
MIRT007328	Homo sapiens	Homo sapiens	hsa-miR-31-5p	CDK1
MIRT007367	Homo sapiens	Homo sapiens	hsa-miR-31-5p	CREG1
MIRT035519	Homo sapiens	Homo sapiens	hsa-miR-31-5p	MLH1
MIRT035528	Homo sapiens	Homo sapiens	hsa-miR-31-5p	MET

Supplementary Table S4

Table S4. Predicted Targets of hsa-miR-485-3p. Using miRNAs database (TargetScanHuman and miRTarBase) and Ingenuity Pathway Analysis, a table of predicted and reported targets of miR-485-3p was generated.

Predicted Targets

Target gene	Representative transcript	Gene name	3P-seq tags + 5
CREBRF	ENST00000540014.1	CREB3 regulatory factor	24
ST6GAL2	ENST00000361686.4	ST6 beta-galactosamide alpha-2,6-sialyltranferase 2	5
ELAVL2	ENST00000380110.4	ELAV like neuron-specific RNA binding protein 2	78
SMPX	ENST00000379494.3	small muscle protein, X-linked	19
CCDC68	ENST00000591504.1	coiled-coil domain containing 68	72
HS3ST3B1	ENST00000360954.2	heparan sulfate (glucosamine) 3-O-sulfotransferase 3B1	1489
SRSF2	ENST00000392485.2	serine/arginine-rich splicing factor 2	9241
WIF1	ENST00000286574.4	WNT inhibitory factor 1	28
TMEM184B	ENST00000361906.3	transmembrane protein 184B	1362
NRF1	ENST00000393230.2	nuclear respiratory factor 1	321
GJA9	ENST00000454994.2	gap junction protein, alpha 9, 59kDa	85
VAPB	ENST00000395802.3	VAMP (vesicle-associated membrane protein)-associated protein B and C	391
ZNF197	ENST00000383745.2	zinc finger protein 197	53
OSTC	ENST00000512478.2	oligosaccharyltransferase complex subunit (non-catalytic)	8403
CD46	ENST00000358170.2	CD46 molecule, complement regulatory protein	5846
KATNBL1	ENST00000256544.3	katanin p80 subunit B-like 1	105
UBE2Q1	ENST00000292211.4	ubiquitin-conjugating enzyme E2Q family member 1	3046
CHTOP	ENST00000368694.3	chromatin target of PRMT1	2499
PAG1	ENST00000220597.4	phosphoprotein associated with glycosphingolipid microdomains 1	53
FLJ20306	ENST00000601673.1	CDNA FLJ20306 fis, clone HEP06881; Putative uncharacterized protein FLJ20306; Uncharacterized protein	5
KLF6	ENST00000542957.1	Kruppel-like factor 6	4644
RCN2	ENST00000394885.3	reticulocalbin 2, EF-hand calcium binding domain	4448
FBXO45	ENST00000311630.6	F-box protein 45	72
FAM26E	ENST00000368599.3	family with sequence similarity 26, member E	32
SEPT2	ENST00000391971.2	septin 2	1445
ASCL4	ENST00000342331.4	achaete-scute complex homolog 4 (Drosophila)	5

FAM133B	ENST00000438306.1	family with sequence similarity 133, member B	32
CTBP1	ENST00000382952.3	C-terminal binding protein 1	573
TTC39A	ENST00000530004.1	tetratricopeptide repeat domain 39A	174
FAM76A	ENST00000373954.6	family with sequence similarity 76, member A	173
YAF2	ENST00000327791.4	YY1 associated factor 2	413
NUS1	ENST00000368494.3	nuclear undecaprenyl pyrophosphate synthase 1 homolog (S. cerevisiae)	302
HCN1	ENST00000303230.4	hyperpolarization activated cyclic nucleotide-gated potassium channel 1	5
STX2	ENST00000392373.2	syntaxin 2	216
RUNX1T1	ENST00000523629.1	runt-related transcription factor 1; translocated to, 1 (cyclin D-related)	9
USP27X	ENST00000508866.2	ubiquitin specific peptidase 27, X-linked	260
SOX7	ENST00000554914.1	Transcription factor SOX-7; Uncharacterized protein; cDNA FLJ58508, highly similar to Transcription factor SOX-7	47
AK3	ENST00000381809.3	adenylate kinase 3	323
HNRNPA3	ENST00000411529.2	heterogeneous nuclear ribonucleoprotein A3	329
ITM2B	ENST00000378565.5	integral membrane protein 2B	10367
PI4K2A	ENST00000370649.3	Phosphatidylinositol 4-kinase type 2-alpha; Uncharacterized protein	1489
MYCT1	ENST00000367245.5	myc target 1	5
ARHGAP29	ENST00000260526.6	Rho GTPase activating protein 29	451
SMIM14	ENST00000295958.5	small integral membrane protein 14	601
UBE2E3	ENST00000410062.4	ubiquitin-conjugating enzyme E2E 3	15
ANKS1B	ENST00000546960.1	ankyrin repeat and sterile alpha motif domain containing 1B	21
POM121C	ENST00000257665.5	POM121 transmembrane nucleoporin C	5
NXPH1	ENST00000405863.1	neurexophilin 1	5
ZFAND5	ENST00000237937.3	zinc finger, AN1-type domain 5	2522

Reported Targets (Igenuity Pathway Analysis)

Target gene	Gene name
HCN1	Hyperpolarization Activated Cyclic Nucleotide Gated Potassium Channel 1
KMT2C	Lysine Methyltransferase 2C

Reported Targets (miRTarBase, strong evidence)

ID	Species (miRNA)	Species (Target)	miRNA	Target
MIRT000045	Homo sapiens	Homo sapiens	hsa-miR-485-3p	NTRK3
MIRT005607	Homo sapiens	Homo sapiens	hsa-miR-485-3p	NFYB
MIRT054252	Homo sapiens	Homo sapiens	hsa-miR-485-3p	SLC40A1
MIRT102191	Homo sapiens	Homo sapiens	hsa-miR-485-3p	NAPEPLD
MIRT147294	Homo sapiens	Homo sapiens	hsa-miR-485-3p	KPNA2
MIRT255969	Homo sapiens	Homo sapiens	hsa-miR-485-3p	WDR17
MIRT318224	Homo sapiens	Homo sapiens	hsa-miR-485-3p	RREB1
MIRT731334	Homo sapiens	Homo sapiens	hsa-miR-485-3p	PPARGC1A
MIRT735513	Homo sapiens	Homo sapiens	hsa-miR-485-3p	PBRM1
MIRT749054	Homo sapiens	Homo sapiens	hsa-miR-485-3p	IFNLR1

Supplementary Table S5

Table S5. Clinical and laboratory characteristics of the study subjects.

	DLE (n=10)	SCLE (n=10)
AGE, mean (SD), yrs	44 (10.3)	51 (15.9)
Female, n (%)	7 (70%)	8 (80%)
Photosensitivity, n (%)	3 (30%)	5 (50%)
Smoking, (%)	6 (60%)	1 (10%)
CLASI ACTIVITY, mean (SD)	9.8±3.7	6.54±2.16
CLASI DAMAGE, mean (SD)	1.78±1.76	0.18±0.60
SLE	4 (40%)	6 (60%)
Duration of cutaneous lesions, months, mean (SD)	8.9 (3.7)	6.2 (5.57)
ANA positive, n (%)	7 (70%)	7 (70%)
Anti-Ro positive, n (%)	1 (10%)	5 (50%)

Values are number of patients and between brackets the percent of total number patients. The other values are means ± SD. CLASI: Cutaneous Lupus Erythematosus Disease Area and Severity Index; ANA: Antinuclear Antibodies; Ant-Ro: autoantibody Ro protein.

Supplementary Table S6

Table S6. Taqman Array Human MicroRNA A+B Cards Set v3.0 gene list for each 384-well microfluidic card

Card A

Well location	Assay ID	Assay Name	Target Sequence
A1	000377	hsa-let-7a	UGAGGUAGUAGGUUGUAUAGUU
A2	000379	hsa-let-7c	UGAGGUAGUAGGUUGUAUGGUU
A3	002283	hsa-let-7d	AGAGGUAGUAGGUUGCAUAGUU
A4	002406	hsa-let-7e	UGAGGUAGGAGGUUGUAUAGUU
A5	000382	hsa-let-7f	UGAGGUAGUAGAUUGUAUAGUU
A6	002282	hsa-let-7g	UGAGGUAGUAGUUUGUACAGUU
A7	002222	hsa-miR-1	UGGAAUGUAAAGAAGUAUGUAU
A8	000583	hsa-miR-9	UCUUUGGUUAUCUAGCUGUAUGA
A9	000387	hsa-miR-10a	UACCCUGUAGAUCCGAAUUUGUG
A10	002218	hsa-miR-10b	UACCCUGUAGAACCGAAUUUGUG
A11	001973	U6 snRNA	GUGCUCGCUUCGGCAGCACAUAUACUAAAAU*
A12	001973	U6 snRNA	GUGCUCGCUUCGGCAGCACAUAUACUAAAAU*
A13	000389	hsa-miR-15a	UAGCAGCACAUAAUGGUUUGUG
A14	000390	hsa-miR-15b	UAGCAGCACAUCAUGGUUUACA
A15	000391	hsa-miR-16	UAGCAGCACGUAAAUAUUGGCG
A16	002308	hsa-miR-17	CAAAGUGCUUACAGUGCAGGUAG
A17	002422	hsa-miR-18a	UAAGGUGCAUCUAGUGCAGAUAG
A18	002217	hsa-miR-18b	UAAGGUGCAUCUAGUGCAGUUAG
A19	000395	hsa-miR-19a	UGUGCAAAUCUAUGCAAAACUGA
A20	000396	hsa-miR-19b	UGUGCAAAUCCAUGCAAAACUGA
A21	000580	hsa-miR-20a	UAAAGUGCUUAUAGUGCAGGUAG
A22	001014	hsa-miR-20b	CAAAGUGCUCAUAGUGCAGGUAG
A23	000397	hsa-miR-21	UAGCUUAUCAGACUGAUGUUGA
A24	000398	hsa-miR-22	AAGCUGCCAGUUGAAGAACUGU
B1	000399	hsa-miR-23a	AUCACAUUGCCAGGGAUUUCC
B2	000400	hsa-miR-23b	AUCACAUUGCCAGGGAUUACC
B3	000402	hsa-miR-24	UGGCUCAGUUCAGCAGGAACAG
B4	000403	hsa-miR-25	CAUUGCACUUGUCUCGGUCUGA
B5	000405	hsa-miR-26a	UUCAAGUAAUCCAGGAUAGGCU
B6	000407	hsa-miR-26b	UUCAAGUAAUUCAGGAUAGGU
B7	000408	hsa-miR-27a	UUCACAGUGGCUAAGUUCCGC
B8	000409	hsa-miR-27b	UUCACAGUGGCUAAGUUCUGC
B9	002446	hsa-miR-28-3p	CACUAGAUUGUGAGCUCCUGGA
B10	000411	hsa-miR-28	AAGGAGCUCACAGUCUAUUGAG
B11	001973	U6 snRNA	GUGCUCGCUUCGGCAGCACAUAUACUAAAAU*
B12	001973	U6 snRNA	GUGCUCGCUUCGGCAGCACAUAUACUAAAAU*
B13	002112	hsa-miR-29a	UAGCACCAUCUGAAAUCGGUUA
B14	000413	hsa-miR-29b	UAGCACCAUUUGAAAUCAGUGUU
B15	000587	hsa-miR-29c	UAGCACCAUUUGAAAUCGGUUA
B16	000602	hsa-miR-30b	UGUAAACAUCCUACACUCAGCU
B17	000419	hsa-miR-30c	UGUAAACAUCCUACACUCUCAGC
B18	002279	hsa-miR-31	AGGCAAGAUGCUGGCAUAGCU
B19	002109	hsa-miR-32	UAUUGCACAUUACUAAGUUGCA
B20	002085	hsa-miR-33b	GUGCAUUGCUGUUGCAUUGC
B21	000426	hsa-miR-34a	UGGCAGUGUCUUAGCUGGUUGU
B22	000428	hsa-miR-34c	AGGCAGUGUAGUUAGCUGAUUGC
B23	000431	hsa-miR-92a	UAUUGCACUUGUCCCGGCCUGU
B24	001090	mmu-miR-93	CAAAGUGCUGUUCGUGCAGGUAG
C1	000433	hsa-miR-95	UUCAACGGGUAUUUAUUGAGCA
C2	000186	mmu-miR-96	UUUGGCACUAGCACAUUUUUGCU
C3	000577	hsa-miR-98	UGAGGUAGUAAGUUGUAUUGUU
C4	000435	hsa-miR-99a	AACCCGUAGAUCCGAUCUUGUG
C5	000436	hsa-miR-99b	CACCCGUAGAACCGACCUUGCG
C6	000437	hsa-miR-100	AACCCGUAGAUCCGAACUUGUG
C7	002253	hsa-miR-101	UACAGUACUGUGAUAACUGAA
C8	000439	hsa-miR-103	AGCAGCAUUGUACAGGGCUAUGA
C9	002167	hsa-miR-105	UCAAAUGCUCAGACUCCUGUGGU
C10	002169	hsa-miR-106a	AAAAGUGCUUACAGUGCAGGUAG
C11	001094	RNU44	CCUGGAUGAUGAUAGCAAAUGCUGACUGAAC*
C12	000442	hsa-miR-106b	UAAAGUGCUGACAGUGCAGAU

C13	000443	hsa-miR-107	AGCAGCAUUGUACAGGGCUAUCA
C14	002245	hsa-miR-122	UGGAGUGUGACAAUGGUGUUUG
C15	001182	mmu-miR-124a	UAAGGCACGCGGUGAAUGCC
C16	002199	hsa-miR-125a-3p	ACAGGUGAGGUUCUUGGGAGCC
C17	002198	hsa-miR-125a-5p	UCCCUGAGACCCUUUAACCUGUGA
C18	000449	hsa-miR-125b	UCCCUGAGACCCUAACUUGUGA
C19	002228	hsa-miR-126	UCGUACCGUGAGUAAUAAUGCG
C20	000452	hsa-miR-127	UCGGAUCCGUCUGAGCUUGGCU
C21	002229	hsa-miR-127-5p	CUGAAGCUCAGAGGGCUCUGAU
C22	002216	hsa-miR-128a	UCACAGUGAACCGGUCUCUUU
C23	001184	mmu-miR-129-3p	AAGCCCUUACCCCAAAAAGCAU
C24	000590	hsa-miR-129	CUUUUUGCGGUCUGGGCUUGC
D1	000454	hsa-miR-130a	CAGUGCAAUGUUAAAAGGGCAU
D2	000456	hsa-miR-130b	CAGUGCAAUGAUGAAAGGGCAU
D3	000457	hsa-miR-132	UAACAGUCUACAGCCAUGGUCG
D4	002246	hsa-miR-133a	UUUGGUCCCCUUCAACCAGCUG
D5	002247	hsa-miR-133b	UUUGGUCCCCUUCAACCAGCUA
D6	001186	mmu-miR-134	UGUGACUGGUUGACCAGAGGGG
D7	000460	hsa-miR-135a	UAUGGCUUUUUAUUCCUAUGUGA
D8	002261	hsa-miR-135b	UAUGGCUUUUCAUUCCUAUGUGA
D9	000592	hsa-miR-136	ACUCCAUUUGUUUUGAUGAUGGA
D10	001129	mmu-miR-137	UUAUUGCUUAAGAAUACGCGUAG
D11	002284	hsa-miR-138	AGCUGGUGUUGUGAAUCAGGCCG
D12	002313	hsa-miR-139-3p	GGAGACGCGGCCCUGUUGGAGU
D13	002289	hsa-miR-139-5p	UCUACAGUGCACGUGUCUCCAG
D14	002234	hsa-miR-140-3p	UACCACAGGGUAGAACCACGG
D15	001187	mmu-miR-140	CAGUGGUUUUACCCUAUGGUAG
D16	000463	hsa-miR-141	UAACACUGUCUGGUAAAGAUGG
D17	000464	hsa-miR-142-3p	UGUAGUGUUUCCUACUUUAUGGA
D18	002248	hsa-miR-142-5p	CAUAAAGUAGAAAGCACUACU
D19	002249	hsa-miR-143	UGAGAUGAAGCACUGUAGCUC
D20	002278	hsa-miR-145	GUCCAGUUUUCCCAGGAAUCCCU
D21	000468	hsa-miR-146a	UGAGAACUGAAUUCCAUGGGUU
D22	002361	hsa-miR-146b-3p	UGCCCUGUGGACUCAGUUCUGG
D23	001097	hsa-miR-146b	UGAGAACUGAAUUCCAUAGGCU
D24	002262	hsa-miR-147b	GUGUGCGGAAAUGCUUCUGCUA
E1	000470	hsa-miR-148a	UCAGUGCACUACAGAACUUUGU
E2	000471	hsa-miR-148b	UCAGUGCAUCACAGAACUUUGU
E3	002255	hsa-miR-149	UCUGGCUCCGUGUCUUCACUCCC
E4	000473	hsa-miR-150	UCUCCCAACCCUUGUACCAGUG
E5	000475	hsa-miR-152	UCAGUGCAUGACAGAACUUGG
E6	001191	mmu-miR-153	UUGCAUAGUCACAAAAGUGAUC
E7	000477	hsa-miR-154	UAGGUUAUCCGUGUUGCCUUCG
E8	000480	hsa-miR-181a	AACAUUCAACGCUGUCGGUGAGU
E9	000482	hsa-miR-181c	AACAUUCAACCUGUCGGUGAGU
E10	002334	hsa-miR-182	UUUGGCAAUGGUAGAACUCACACU
E11	001006	RNU48	GAUGACCCCAGGUAACUCUGAGUGUGUCGCU*
E12	002269	hsa-miR-183	UAUGGCACUGGUAGAAUUCACU
E13	000485	hsa-miR-184	UGGACGGAGAACUGAUAAGGGU
E14	002271	hsa-miR-185	UGGAGAGAAAGGCAGUUCCUGA
E15	002285	hsa-miR-186	CAAAGAAUUCUCCUUUUGGGCU
E16	001193	mmu-miR-187	UCGUGUCUUGUGUUGCAGCCGG
E17	002106	hsa-miR-188-3p	CUCCCACAUGCAGGGUUUGCA
E18	000489	hsa-miR-190	UGAUAUGUUUGAUAUAUUAGGU
E19	002299	hsa-miR-191	CAACGGAAUCCCAAAAGCAGCUG
E20	000491	hsa-miR-192	CUGACCUAUGAAUUGACAGCC
E21	002250	hsa-miR-193a-3p	AACUGGCCUACAAAGUCCCAGU
E22	002281	hsa-miR-193a-5p	UGGGUCUUUGCGGGCGAGAUGA
E23	002367	hsa-miR-193b	AACUGGCCCUCAAAGUCCCGCU
E24	000493	hsa-miR-194	UGUAACAGCAACUCCAUGUGGA
F1	000494	hsa-miR-195	UAGCAGCACAGAAAUAUUGGC
F2	002215	hsa-miR-196b	UAGGUAGUUUCCUGUUGUUGGG
F3	000497	hsa-miR-197	UUCACCACCUUCUCCACCCAGC
F4	002273	hsa-miR-198	GGUCCAGAGGGGAGAUAGGUUC
F5	000498	hsa-miR-199a	CCCAGUGUUCAGACUACCUGUUC
F6	002304	hsa-miR-199a-3p	ACAGUAGUCUGCACAUUGGUUA
F7	000500	hsa-miR-199b	CCCAGUGUUUAGACUAUCUGUUC
F8	000502	hsa-miR-200a	UAACACUGUCUGGUAACGAUGU
F9	002251	hsa-miR-200b	UAAUACUGCCUGGUAAUGAUGA
F10	002300	hsa-miR-200c	UAAUACUGCCGGGUAAUGAUGGA
F11	002363	hsa-miR-202	AGAGGUAUAGGGCAUGGGAA
F12	000507	hsa-miR-203	GUGAAAUGUUUAGGACCACUAG

F13	000508	hsa-miR-204	UUCCCUUUGUCAUCCUAUGCCU
F14	000509	hsa-miR-205	UCCUUCAUUCCACCGGAGUCUG
F15	002290	hsa-miR-208b	AUAAGACGAACAAAAGGUUUGU
F16	000512	hsa-miR-210	CUGUGCGUGUGACAGCGGCUGA
F17	002306	hsa-miR-214	ACAGCAGGCACAGACAGGCAGU
F18	000518	hsa-miR-215	AUGACCUAUGAAUUGACAGAC
F19	002220	hsa-miR-216a	UAAUCUCAGCUGGCAACUGUGA
F20	002326	hsa-miR-216b	AAAUCUCUGCAGGCAAAUGUGA
F21	002337	hsa-miR-217	UACUGCAUCAGGAACUGAUUGGA
F22	000521	hsa-miR-218	UUGUGCUUGAUCUAACCAUGU
F23	000522	hsa-miR-219	UGAUUGUCCAAACGCAAUUCU
F24	000524	hsa-miR-221	AGCUACAUUGUCUGCUGGGUUUC
G1	002276	hsa-miR-222	AGCUACAUCUGGCUACUGGGU
G2	002295	hsa-miR-223	UGUCAGUUUGUCAAAUACCCCA
G3	002099	hsa-miR-224	CAAGUCACUAGUGGUUCCGUU
G4	002101	hsa-miR-296-3p	GAGGGUUGGGUGGAGGCUCUCC
G5	000527	hsa-miR-296	AGGGCCCCCCCUCAAUCCUGU
G6	001015	hsa-miR-299-3p	UAUGUGGGAUGGUAAACCGCUU
G7	000600	hsa-miR-299-5p	UGGUUUACCGUCCCACAUACAU
G8	000528	hsa-miR-301	CAGUGCAAUAGUAUUGUCAAAGC
G9	002392	hsa-miR-301b	CAGUGCAAUGAUAUUGUCAAAGC
G10	000529	hsa-miR-302a	UAAGUGCUUCCAUGUUUUGGUGA
G11	000338	ath-miR159a	UUUGGAUUGAAGGGAGCUCUA
G12	000531	hsa-miR-302b	UAAGUGCUUCCAUGUUUUAGUAG
G13	000533	hsa-miR-302c	UAAGUGCUUCCAUGUUUCAGUGG
G14	002277	hsa-miR-320	AAAAGCUGGGUUGAGAGGGCGA
G15	002227	hsa-miR-323-3p	CACAUUACACGGUCGACCUCU
G16	002161	hsa-miR-324-3p	ACUGCCCCAGGUGCUGCUGG
G17	000539	hsa-miR-324-5p	CGCAUCCCCUAGGGCAUUGGUGU
G18	000542	hsa-miR-326	CCUCUGGGCCCUUCCUCCAG
G19	000543	hsa-miR-328	CUGGCCCUCUCUGCCCUUCCGU
G20	001101	hsa-miR-329	AACACACCUGGUUAACCUCUUU
G21	000544	hsa-miR-330	GCAAAGCACACGGCCUGCAGAGA
G22	002230	hsa-miR-330-5p	UCUCUGGGCCUGUGUCUUAGGC
G23	000545	hsa-miR-331	GCCCCUGGGCCUAUCCUAGAA
G24	002233	hsa-miR-331-5p	CUAGGUAUGGUCCCAGGGAUCC
H1	000546	hsa-miR-335	UCAAGAGCAAUAACGAAAAAUGU
H2	002156	hsa-miR-337-5p	GAACGGCUUCAUACAGGAGUU
H3	002252	hsa-miR-338-3p	UCCAGCAUCAGUGAUUUUGUUG
H4	002184	hsa-miR-339-3p	UGAGCGCCUCGACGACAGAGCCG
H5	002257	hsa-miR-339-5p	UCCCUGUCCUCCAGGAGCUCACG
H6	002258	hsa-miR-340	UUAUAAAGCAAUGAGACUGAUU
H7	002623	hsa-miR-155	UUAAUGCUAAUCGUGAUAGGGGU
H8	002619	hsa-let-7b	UGAGGUAGUAGGUUGUGUGGUU
H9	002260	hsa-miR-342-3p	UCUCACACAGAAAUCGCACCCGU
H10	002147	hsa-miR-342-5p	AGGGGUGCUAUCUGUGAUUGA
H11	002186	hsa-miR-345	GCUGACUCCUAGUCCAGGGCUC
H12	000554	hsa-miR-361	UUAUCAGAAUCUCCAGGGGUAC
H13	002117	hsa-miR-362-3p	AACACACCUAUUCAAGGAUUCA
H14	001273	hsa-miR-362	AAUCCUUGGAACCUAGGUGUGAGU
H15	001271	hsa-miR-363	AAUUGCACGGUAUCCAUCUGUA
H16	001020	hsa-miR-365	UAAUGCCCCUAAAAAUCCUUAU
H17	000555	hsa-miR-367	AAUUGCACUUUAGCAAUGGUGA
H18	000557	hsa-miR-369-3p	AAUAAUACAUGGUUGAUCUUU
H19	001021	hsa-miR-369-5p	AGAUCGACCGUGUUAUAUUCGC
H20	002275	hsa-miR-370	GCCUGCUGGGGUGGAACCUGGU
H21	002124	hsa-miR-371-3p	AAGUGCCGCCAUCUUUUGAGUGU
H22	000560	hsa-miR-372	AAAGUGCUGCGACAUUUGAGCGU
H23	000561	hsa-miR-373	GAAGUGCUUCGAUUUUGGGGUGU
H24	000563	hsa-miR-374	UUAUAAUACAACCUGAUAAGUG
I1	001319	mmu-miR-374-5p	AUAUAAUACAACCUGCUAAGUG
I2	000564	hsa-miR-375	UUUGUUCGUUCGGCUCGCGUGA
I3	000565	hsa-miR-376a	AUCAUAGAGGAAAAUCCACGU
I4	001102	hsa-miR-376b	AUCAUAGAGGAAAAUCCAUGUU
I5	000566	hsa-miR-377	AUCACACAAAGGCAACUUUUGU
I6	001138	mmu-miR-379	UGGUAGACUAUGGAACGUAGG
I7	000569	hsa-miR-380-3p	UAUGUAAUAUGGUCCACAUCUU
I8	000571	hsa-miR-381	UAUACAAGGGCAAGCUCUCUGU
I9	000572	hsa-miR-382	GAAGUUGUUCGUGGUGGAUUCG

I10	000573	hsa-miR-383	AGAUCAGAAGGUGAUUGUGGCU
I11	002331	hsa-miR-409-5p	AGGUUACCCGAGCAACUUUGCAU
I12	001274	hsa-miR-410	AAUAUAACACAGAUGGCCUGU
I13	001610	hsa-miR-411	UAGUAGACCGUAUAGCGUACG
I14	002297	hsa-miR-422a	ACUGGACUUAGGGUCAGAAGGC
I15	002340	hsa-miR-423-5p	UGAGGGGCAGAGAGCGAGACUUU
I16	000604	hsa-miR-424	CAGCAGCAAUUCAUGUUUUGAA
I17	001516	hsa-miR-425-5p	AAUGACACGAUCACUCCCGUUGA
I18	001024	hsa-miR-429	UAAUACUGUCUGGUAAAACCGU
I19	001979	hsa-miR-431	UGUCUUGCAGGCCGUCAUGCA
I20	001028	hsa-miR-433	AUCAUGAUGGGCUCCUCGGUGU
I21	001030	hsa-miR-449	UGGCAGUGUAUUGUUAGCUGGU
I22	001608	hsa-miR-449b	AGGCAGUGUAUUGUUAGCUGGC
I23	002303	hsa-miR-450a	UUUUGCGAUGUGUUCCUAAUAU
I24	002208	hsa-miR-450b-3p	UUGGGAUCAUUUUGCAUCCAUA
J1	002207	hsa-miR-450b-5p	UUUUGCAAUAUGUUCCUGAAUA
J2	001141	mmu-miR-451	AAACCGUUACCAUUACUGAGUU
J3	002329	hsa-miR-452	AACUGUUUGCAGAGGAAACUGA
J4	002318	hsa-miR-453	AGGUUGUCCGUGGUGAGUUCGCA
J5	002323	hsa-miR-454	UAGUGCAAUAUUGCUUAUAGGGU
J6	002244	hsa-miR-455-3p	GCAGUCCAUGGGCAUAUACAC
J7	001280	hsa-miR-455	UAUGUGCCUUUGGACUACAUCG
J8	002338	hsa-miR-483-5p	AAGACGGGAGGAAAGAAGGGAG
J9	001821	hsa-miR-484	UCAGGCUCAGUCCCCUCCCGAU
J10	001277	hsa-miR-485-3p	GUCAUACACGGCUCUCCUCUCU
J11	001036	hsa-miR-485-5p	AGAGGCUGGCCGUGAUGAAUUC
J12	002093	hsa-miR-486-3p	CGGGGCAGCUCAGUACAGGAU
J13	001278	hsa-miR-486	UCCUGUACUGAGCUGCCCCGAG
J14	001279	hsa-miR-487a	AAUCAUACAGGGACAUCCAGUU
J15	001285	hsa-miR-487b	AAUCGUACAGGGUCAUCCACUU
J16	002357	hsa-miR-488	UUGAAAGGCUAUUUCUUGGUC
J17	002358	hsa-miR-489	GUGACAUCACAUAUACGGCAGC
J18	001037	hsa-miR-490	CAACCUGGAGGACUCCAUGCUG
J19	002360	hsa-miR-491-3p	CUUAUGCAAGAUUCCCUUCUAC
J20	001630	mmu-miR-491	AGUGGGGAACCCUUCCAUGAGG
J21	002364	hsa-miR-493	UGAAGGUCUACUGUGUGCCAGG
J22	002365	hsa-miR-494	UGAAACAUACACGGGAAACCUC
J23	001663	mmu-miR-495	AAACAAACAUGGUGCACUUCUU
J24	001953	mmu-miR-496	UGAGUAUUACAUGGCCAAUCUC
K1	002427	hsa-miR-499-3p	AACAUCACAGCAAGUCUGUGCU
K2	001352	mmu-miR-499	UUAAGACUUGCAGUGAUGUUU
K3	002428	hsa-miR-500	UAAUCCUUGCUACCUGGGUGAGA
K4	002435	hsa-miR-501-3p	AAUGCACCCGGGCAAGGAUUCU
K5	001047	hsa-miR-501	AAUCCUUUGUCCCUGGGUGAGA
K6	002083	hsa-miR-502-3p	AAUGCACCUGGGCAAGGAUUCA
K7	001109	hsa-miR-502	AUCCUUGCUAUCUGGGUGCUA
K8	001048	hsa-miR-503	UAGCAGCGGGAACAGUUCUGCAG
K9	002084	hsa-miR-504	AGACCCUGGUCUGCACUCUAUC
K10	002089	hsa-miR-505	CGUCAACACUUGCUGGUUUCCU
K11	001051	hsa-miR-507	UUUUGCACCUUUUGGAGUGAA
K12	001052	hsa-miR-508	UGAUUGUAGCCUUUUGGAGUAGA
K13	002092	hsa-miR-508-5p	UACUCCAGAGGGCGUCACUCAUG

K14	002235	hsa-miR-509-5p	UACUGCAGACAGUGGCAAUCA
K15	002241	hsa-miR-510	UACUCAGGAGAGUGGCAAUCAC
K16	001823	hsa-miR-512-3p	AAGUGCUGUCAUAGCUGAGGUC
K17	001145	hsa-miR-512-5p	CACUCAGCCUUGAGGGCACUUUC
K18	002090	hsa-miR-513-5p	UUCACAGGGAGGUGUCAU
K19	002369	hsa-miR-515-3p	GAGUGCCUUCUUUUGGAGCGUU
K20	001112	hsa-miR-515-5p	UUCUCCAAAAGAAAGCACUUUCUG
K21	002416	hsa-miR-516a-5p	UUCUCGAGGAAAGAAGCACUUUC
K22	001150	hsa-miR-516b	AUCUGGAGGUAAGAAGCACUUU
K23	002402	hsa-miR-517a	AUCGUGCAUCCCUUUAGAGUGU
K24	001153	hsa-miR-517c	AUCGUGCAUCCUUUUAGAGUGU
L1	002397	hsa-miR-518a-3p	GAAAGCGCUUCCCUUUGCUGGA
L2	002396	hsa-miR-518a-5p	CUGCAAAGGGAAGCCCUUUC
L3	001156	hsa-miR-518b	CAAAGCGCUCCCCUUUAGAGGU
L4	002401	hsa-miR-518c	CAAAGCGCUUCUCUUUAGAGUGU
L5	001159	hsa-miR-518d	CAAAGCGCUUCCCUUUGGAGC
L6	002389	hsa-miR-518d-5p	CUCUAGAGGGAAGCACUUUCUG
L7	002395	hsa-miR-518e	AAAGCGCUUCCCUUCAGAGUG
L8	002388	hsa-miR-518f	GAAAGCGCUUCUCUUUAGAGG
L9	002415	hsa-miR-519a	AAAGUGCAUCCUUUUAGAGUGU
L10	002403	hsa-miR-519d	CAAAGUGCCUCCCUUUAGAGUG
L11	002370	hsa-miR-519e	AAGUGCCUCCUUUUAGAGUGUU
L12	001167	hsa-miR-520a	AAAGUGCUUCCCUUUGGACUGU
L13	001168	hsa-miR-520a#	CUCCAGAGGGAAGUACUUUCU
L14	002393	hsa-miR-520d-5p	CUACAAAGGGAAGCCCUUUC
L15	001121	hsa-miR-520g	ACAAAGUGCUUCCCUUUAGAGUGU
L16	001122	hsa-miR-521	AACGCACUUCCCUUUAGAGUGU
L17	002413	hsa-miR-522	AAAAUGGUUCCCUUUAGAGUGU
L18	002386	hsa-miR-523	GAACGCGCUUCCCUAUAGAGGGU
L19	001982	hsa-miR-524-5p	CUACAAAGGGAAGCACUUUCUC
L20	002385	hsa-miR-525-3p	GAAGGCGCUUCCCUUUAGAGCG
L21	001174	hsa-miR-525	CUCCAGAGGGAUGCACUUUCU
L22	002382	hsa-miR-526b	CUCUUGAGGGAAGCACUUUCUGU
L23	002355	hsa-miR-532-3p	CCUCCCACACCCAAGGCUUGCA
L24	001518	hsa-miR-532	CAUGCCUUGAGUGUAGGACCGU
M1	001286	hsa-miR-539	GGAGAAAUUAUCCUUGGUGUGU
M2	002201	hsa-miR-541	UGGUGGGCACAGAAUCUGGACU
M3	001284	hsa-miR-542-3p	UGUGACAGAUUGAUAACUGAAA
M4	002240	hsa-miR-542-5p	UCGGGGAUCAUCAUGUCACGAGA
M5	002265	hsa-miR-544	AUUCUGCAUUUUUAGCAAGUUC
M6	002267	hsa-miR-545	UCAGCAAACAUUUAUUGUGUGC
M7	001538	hsa-miR-548a	CAAAACUGGCAAUUACUUUUGC
M8	002412	hsa-miR-548a-5p	AAAAGUAAUUGCGAGUUUUACC
M9	001541	hsa-miR-548b	CAAGAACCUCAGUUGCUUUUGU
M10	002408	hsa-miR-548b-5p	AAAAGUAAUUGUGGUUUUGGCC
M11	001590	hsa-miR-548c	CAAAAAUCUCAAUUACUUUUGC
M12	002429	hsa-miR-548c-5p	AAAAGUAAUUGCGGUUUUUGCC
M13	001605	hsa-miR-548d	CAAAAACCACAGUUUCUUUUGC
M14	002237	hsa-miR-548d-5p	AAAAGUAAUUGUGGUUUUUGCC
M15	001535	hsa-miR-551b	GCGACCCAUACUUGGUUUCAG
M16	002345	hsa-miR-556-3p	AUAUUACCAUUAGCUCAUCUUU
M17	002344	hsa-miR-556-5p	GAUGAGCUCAUUGUAAUAUGAG

M18	001528	hsa-miR-561	CAAAGUUUAAGAUCCUUGAAGU
M19	002347	hsa-miR-570	CGAAAACAGCAAUUACCUUUGC
M20	002349	hsa-miR-574-3p	CACGCUCAUGCACACACCCACA
M21	002351	hsa-miR-576-3p	AAGAUGUGGAAAAAUUGGAAUC
M22	002350	hsa-miR-576-5p	AUUCUAAUUUCUCCACGUCUUU
M23	002398	hsa-miR-579	UUCAUUUGGUAUAAACCGCGAUU
M24	002399	hsa-miR-582-3p	UAACUGGUUGAACAACUGAACC
N1	001983	hsa-miR-582-5p	UUACAGUUGUUCAACCAGUUACU
N2	002409	hsa-miR-589	UGAGAACCACGUCUGCUCUGAG
N3	001984	hsa-miR-590-5p	GAGCUUAUUCAUAAAAGUGCAG
N4	001551	hsa-miR-597	UGUGUCACUCGAUGACCACUGU
N5	001988	hsa-miR-598	UACGUCAUCGUUGUCAUCGUCA
N6	001960	mmu-miR-615	UCCGAGCCUGGGUCUCCCUCUU
N7	002353	hsa-miR-615-5p	GGGGGUCCCCGGUGCUCGGAUC
N8	002414	hsa-miR-616	AGUCAUUGGAGGGUUUGAGCAG
N9	001593	hsa-miR-618	AAACUCUACUUGUCCUUCUGAGU
N10	002430	hsa-miR-624	CACAAGGUAUUGGUAUUACCU
N11	002431	hsa-miR-625	AGGGGGAAAGUUCUAUAGUCC
N12	001560	hsa-miR-627	GUGAGUCUCUAAGAAAAGAGGA
N13	002433	hsa-miR-628-5p	AUGCUGACAUAUUUACUAGAGG
N14	002436	hsa-miR-629	UGGGUUUACGUUGGGAGAACU
N15	002088	hsa-miR-636	UGUGCUUGCUCGUCCCGCCCGCA
N16	001592	hsa-miR-642	GUCCCUCUCCAAAUGUGUCUUG
N17	001604	hsa-miR-651	UUUAGGAUAAGCUUGACUUUUG
N18	002352	hsa-miR-652	AAUGGCGCCACUAGGGUUGUG
N19	002292	hsa-miR-653	GUGUUGAAACAAUCUCUACUG
N20	002239	hsa-miR-654-3p	UAUGUCUGCUGACCAUCACCUU
N21	001611	hsa-miR-654	UGGUGGGCCGCAGAACAUGUGC
N22	001612	hsa-miR-655	AUAAUACAUGGUUAACCUCUUU
N23	001515	hsa-miR-660	UACCCAUUGCAUAUCGGAGUUG
N24	002322	hsa-miR-671-3p	UCCGGUUCUCAGGGCUCCACC
O1	002327	hsa-miR-672	UGAGGUUGGUGUACUGUGUGUGA
O2	002021	hsa-miR-674	GCACUGAGAUGGGAGUGGUGUA
O3	002341	hsa-miR-708	AAGGAGCUUACAAUCUAGCUGGG
O4	002324	hsa-miR-744	UGCGGGGCUAGGGCUAACAGCA
O5	001990	hsa-miR-758	UUUGUGACCUGGUCCACUAACC
O6	002354	hsa-miR-871	UAUUCAGAUUAGUGCCAGUCAUG
O7	002264	hsa-miR-872	AAGGUUACUUGUUAGUUCAGG
O8	002356	hsa-miR-873	GCAGGAACUUGUGAGUCUCCU
O9	002268	hsa-miR-874	CUGCCCUGGCCCGAGGGACCGA
O10	002204	hsa-miR-875-3p	CCUGGAAACACUGAGGUUGUG
O11	002225	hsa-miR-876-3p	UGGUGGUUUACAAAGUAAUUCA
O12	002205	hsa-miR-876-5p	UGGAUUUCUUUGUGAAUCACCA
O13	002372	hsa-miR-885-3p	AGGCAGCGGGGUGUAGUGGAUA
O14	002296	hsa-miR-885-5p	UCCAUUACACUACCCUGCCUCU
O15	002194	hsa-miR-886-3p	CGCGGGUGCUUACUGACCCUU
O16	002193	hsa-miR-886-5p	CGGGUCGGAGUUAGCUCAAGCGG
O17	002374	hsa-miR-887	GUGAACGGGCGCCAUCCCGAGG
O18	002212	hsa-miR-888	UACUCAAAAAGCUGUCAGUCA
O19	002202	hsa-miR-889	UUAAUAUCGGACAACCAUUGU
O20	002209	hsa-miR-890	UACUUGGAAAGGCAUCAGUUG
O21	002191	hsa-miR-891a	UGCAACGAACCUGAGCCACUGA

O22	002210	hsa-miR-891b	UGCAACUUACCUGAGUCAUUGA
O23	002195	hsa-miR-892a	CACUGUGUCCUUUCUGCGUAG
O24	000469	hsa-miR-147	GUGUGUGGAAAUGCUUCUGC
P1	000511	hsa-miR-208	AUAAGACGAGCAAAAAGCUUGU
P2	000514	hsa-miR-211	UUCCCUUUGUCAUCCUUCGCCU
P3	000515	hsa-miR-212	UAACAGUCUCCAGUCACGGCC
P4	002095	hsa-miR-219-1-3p	AGAGUUGAGUCUGGACGUCCCG
P5	002390	hsa-miR-219-2-3p	AGAAUUGUGGCUGGACAUCUGU
P6	000523	hsa-miR-220	CCACACCGUAUCUGACACUUU
P7	002206	hsa-miR-220b	CCACCACCGUGUCUGACACUU
P8	002211	hsa-miR-220c	ACACAGGGCUGUUGUGAAGACU
P9	002190	hsa-miR-298	AGCAGAAGCAGGGAGGUUCUCCCA
P10	000540	hsa-miR-325	CCUAGUAGGUGUCCAGUAAGUGU
P11	000553	hsa-miR-346	UGUCUGCCCGCAUGCCUGCCUCU
P12	002122	hsa-miR-376c	AACAUAGAGGAAAUUCCACGU
P13	000574	hsa-miR-384	AUUCCUAGAAAUUGUUCAUA
P14	001023	hsa-miR-412	ACUUCACCUGGUCCACUAGCCGU
P15	001029	hsa-miR-448	UUGCAUAUGUAGGAUGUCCCAU
P16	001039	hsa-miR-492	AGGACCUGCGGGACAAGAUUCUU
P17	001050	hsa-miR-506	UAAGGCACCCUUCUGAGUAGA
P18	002155	hsa-miR-509-3-5p	UACUGCAGACGUGGCAAUCAUG
P19	001111	hsa-miR-511	GUGUCUUUUGCUCUGCAGUCA
P20	001152	hsa-miR-517b	UCGUGCAUCCCUUUAGAGUGUU
P21	001163	hsa-miR-519c	AAAGUGCAUCUUUUUAGAGGAU
P22	001116	hsa-miR-520b	AAAGUGCUUCCUUUUAGAGGG
P23	001119	hsa-miR-520e	AAAGUGCUUCCUUUUUGAGGG
P24	001120	hsa-miR-520f	AAGUGCUUCCUUUUAGAGGGUU

Card B

Well location	Assay ID	Assay Name	Target Sequence
A1	000268	dme-miR-7	UGGAAGACUAGUGAUUUUGUUGU
A2	002909	hsa-miR-548l	AAAAGUAAUUGCGGAUUUUGCC
A3	000416	hsa-miR-30a-3p	CUUUCAGUCGGAUGUUUGCAGC
A4	000417	hsa-miR-30a-5p	UGUAAACAUCCUCGACUGGAAG
A5	000420	hsa-miR-30d	UGUAAACAUCCCCGACUGGAAG
A6	000422	hsa-miR-30e-3p	CUUUCAGUCGGAUGUUUACAGC
A7	000427	hsa-miR-34b	UAGGCAGUGUCAUUAGCUGAUUG
A8	000451	hsa-miR-126#	CAUUAUUACUUUUGGUACGCG
A9	000478	hsa-miR-154#	AAUCAUACACGGUUGACCUAUU
A10	000483	hsa-miR-182#	UGGUUCUAGACUUGCCAACUA
A11	001973	U6 snRNA	GUGCUCGCUUCGGCAGCACAUAUACU*
A12	001973	U6 snRNA	GUGCUCGCUUCGGCAGCACAUAUACU*
A13	000510	hsa-miR-206	UGGAAUGUAAGGAAGUGUGUGG
A14	000516	hsa-miR-213	ACCAUCGACCGUUGAUUGUACC
A15	000534	hsa-miR-302c#	UUUAACAUGGGGGUACCUGCUG
A16	000535	hsa-miR-302d	UAAGUGCUUCCAUGUUUGAGUGU
A17	000567	hsa-miR-378	CUCCUGACUCCAGGUCCUGUGU
A18	000570	hsa-miR-380-5p	UGGUUGACCAUAGAACAUGCGC
A19	002910	hsa-miR-1257	AGUGAAUGAUGGGUUCUGACC
A20	001011	hsa-miR-200a#	CAUCUUACCGGACAGUGCUGGA
A21	001026	hsa-miR-432	UCUUGGAGUAGGUCAUUGGGUGG
A22	001027	hsa-miR-432#	CUGGAUGGCUCCUCCAUGUCU
A23	001043	hsa-miR-497	CAGCAGCACACUGUGGUUUGU
A24	001046	hsa-miR-500	AUGCACCUGGGCAAGGAUUCUG
B1	002927	hsa-miR-1238	CUUCCUCGUCUGUCUGCCCC
B2	001106	hsa-miR-488	CCCAGAUAAUGGCACUCUCAA
B3	001113	hsa-miR-517#	CCUCUAGAUGGAAGCACUGUCU
B4	001149	hsa-miR-516-3p	UGCUUCCUUUCAGAGGGU
B5	001158	hsa-miR-518c#	UCUCUGGAGGGAAGCACUUUCUG
B6	001166	hsa-miR-519e#	UUCUCCAAAAGGGAGCACUUUC
B7	001170	hsa-miR-520h	ACAAAGUGCUUCCCUUUAGAGU

B8	001173	hsa-miR-524	GAAGGCGCUUCCCUUUGGAGU
B9	001178	mmu-let-7d#	CUAUACGACCUGCUGCCUUUCU
B10	001283	hsa-miR-363#	CGGGUGGAUCACGAUGCAAUUU
B11	001973	U6 snRNA	GUGCUCGCUUCGGCAGCACAUAUACU*
B12	001973	U6 snRNA	GUGCUCGCUUCGGCAGCACAUAUACU*
B13	001338	mo-miR-7#	CAACAAAUCACAGUCUGCCAUA
B14	001510	hsa-miR-656	AAUAUUAUACAGUCAACCUCU
B15	001511	hsa-miR-549	UGACAACUAUGGAUGAGCUCU
B16	001512	hsa-miR-657	GGCAGGUUCUCACCCUCUCUAGG
B17	001513	hsa-miR-658	GGCGGAGGGAAGUAGGUCCGUUGGU
B18	001514	hsa-miR-659	CUUGGUUCAGGGAGGGUCCCCA
B19	001519	hsa-miR-551a	GCGACCCACUCUUGGUUUCCA
B20	001520	hsa-miR-552	AACAGGUGACUGGUUAGACAA
B21	001521	hsa-miR-553	AAAACGGUGAGAUUUUGUUUU
B22	001522	hsa-miR-554	GCUAGUCCUGACUCAGCCAGU
B23	001523	hsa-miR-555	AGGGUAAGCUGAACCUCUGAU
B24	001525	hsa-miR-557	GUUUGCACGGGUGGGCCUUGUCU
C1	001526	hsa-miR-558	UGAGCUGCUGUACCAAAAU
C2	001527	hsa-miR-559	UAAAGUAAAUAUGCACCAAAA
C3	001529	hsa-miR-562	AAAGUAGCUGUACCAUUUGC
C4	001530	hsa-miR-563	AGGUUGACAUACGUUUCCC
C5	001531	hsa-miR-564	AGGCACGGUGUCAGCAGGC
C6	001533	hsa-miR-566	GGGCGCCUGUGAUCCCAAC
C7	001534	hsa-miR-567	AGUAUGUUCUUCCAGGACAGAAC
C8	001536	hsa-miR-569	AGUUAAUGAAUCCUGGAAAGU
C9	001539	hsa-miR-586	UAUGCAUUGUAUUUUUAGGUCC
C10	001540	hsa-miR-587	UUUCCAUAGGUGAUGAGUCAC
C11	001094	RNU44	CCUGGAUGAUGAUAGCAAAUGCUGAC*
C12	001542	hsa-miR-588	UUGGCCACAAUGGGUUAGAAC
C13	001543	hsa-miR-589	UCAGAACAAAUGCCGGUUCCCAGA
C14	001544	hsa-miR-550	UGUCUUACUCCCUCAGGCACAU
C15	001545	hsa-miR-591	AGACCAUGGGUUCUCAUUGU
C16	001546	hsa-miR-592	UUGUGUCAAUAUGCGAUGAUGU
C17	001547	hsa-miR-593	AGGCACCAGCCAGGCAUUGCUCAGC
C18	001550	hsa-miR-596	AAGCCUGCCCGGCUCCUCGGG
C19	001553	hsa-miR-622	ACAGUCUGCUGAGGUUGGAGC
C20	001554	hsa-miR-599	GUUGUGUCAGUUUAUCAAAC
C21	001555	hsa-miR-623	AUCCCUUGCAGGGGCUGUUGGGU
C22	001556	hsa-miR-600	ACUUACAGACAAGAGCCUUGCUC
C23	001557	hsa-miR-624	UAGUACCAGUACCUUGUGUUCA
C24	001558	hsa-miR-601	UGGUCUAGGAUUGUUGGAGGAG
D1	001559	hsa-miR-626	AGCUGUCUGAAAAUGUCUU
D2	001562	hsa-miR-629	GUUCUCCCAACGUAAGCCCAGC
D3	001563	hsa-miR-630	AGUAUUCUGUACCAGGGAAGGU
D4	001564	hsa-miR-631	AGACCUGGCCCAGACCUCAGC
D5	001566	hsa-miR-603	CACACACUGCAAUUACUUUUGC
D6	001567	hsa-miR-604	AGGCUGCGGAAUUCAGGAC
D7	001568	hsa-miR-605	UAAAUCCCAUGGUGCCUUCUCCU
D8	001569	hsa-miR-606	AAACUACUGAAAAUCAAAGAU
D9	001570	hsa-miR-607	GUUCAAAUCCAGAUCUAUAAC
D10	001571	hsa-miR-608	AGGGGUGGUGUUGGGACAGCUCCGU
D11	001573	hsa-miR-609	AGGGUGUUUCUCUCAUCUCU
D12	001574	hsa-miR-633	CUAAUAGUAUCUACCACAAUAAA
D13	001576	hsa-miR-634	AACCAGCACCCCAACUUUGGAC
D14	001578	hsa-miR-635	ACUUGGGCACUGAAACAAUGUCC
D15	001581	hsa-miR-637	ACUGGGGGCUUUCGGGCUCUGCGU
D16	001582	hsa-miR-638	AGGGAUCGCGGGCGGGUGGCGGCCU
D17	001583	hsa-miR-639	AUCGCUGCGGUUGCGAGCGCUGU
D18	001584	hsa-miR-640	AUGAUCCAGGAACCUGCCUCU
D19	001585	hsa-miR-641	AAAGACAUAGGAUAGAGUCACCUC
D20	001586	hsa-miR-613	AGGAAUGUUCCUUCUUUGCC
D21	001587	hsa-miR-614	GAACGCCUGUUCUUGCCAGGUGG
D22	001589	hsa-miR-616	ACUCAAAACCCUUCAGUGACUU
D23	001591	hsa-miR-617	AGACUUCCCAUUUGAAGGUGGC
D24	001594	hsa-miR-643	ACUUGUAUGCUAGCUCAGGUAG
E1	001596	hsa-miR-644	AGUGUGGCUUUCUUAGAGC
E2	001597	hsa-miR-645	UCUAGGCUGGUACUGCUGA
E3	001598	hsa-miR-621	GGCUAGCAACAGCGCUUACCU
E4	001599	hsa-miR-646	AAGCAGCUGCCUCUGAGGC
E5	001600	hsa-miR-647	GUGGCUGCACUCACUUCCUUC
E6	001601	hsa-miR-648	AAGUGUGCAGGGCACUGGU
E7	001602	hsa-miR-649	AAACCUGUGUUGUUCAAGAGUC

E8	001603	hsa-miR-650	AGGAGGCAGCGCUCUCAGGAC
E9	001606	hsa-miR-661	UGCCUGGGUCUCUGGCCUGCGCGU
E10	001607	hsa-miR-662	UCCCACGUUGUGGCCCAGCAG
E11	001006	RNU48	GAUGACCCCAGGUAACUCUGAGUGUG*
E12	001613	hsa-miR-571	UGAGUUGGCCAUCUGAGUGAG
E13	001614	hsa-miR-572	GUCCGCUCGGCGGUGGCCCA
E14	001615	hsa-miR-573	CUGAAGUGAUGUGUAACUGAUCAG
E15	001617	hsa-miR-575	GAGCCAGUUGGACAGGAGC
E16	001619	hsa-miR-578	CUUCUUGUGCUCUAGGAUUGU
E17	001621	hsa-miR-580	UUGAGAAUGAUGAAUCAUUAGG
E18	001622	hsa-miR-581	UCUUGUGUUCUCUAGAUCAGU
E19	001623	hsa-miR-583	CAAAGAGGAAGGUCCCAUUAC
E20	001624	hsa-miR-584	UUAUGGUUUGCCUGGGACUGAG
E21	001625	hsa-miR-585	UGGGCGUAUCUGUAUGCUA
E22	001818	rno-miR-29c#	UGACCGAUUUCUCCUGGUGUUC
E23	001986	hsa-miR-766	ACUCCAGCCCCACAGCCUCAGC
E24	001987	hsa-miR-595	GAAGUGUGCCGUGGUGUGUCU
F1	001992	hsa-miR-668	UGUCACUCGGCUCGGCCCACUAC
F2	001993	hsa-miR-767-5p	UGCACCAUGGUUGUCUGAGCAUG
F3	001995	hsa-miR-767-3p	UCUGCUCAUACCCCAUGGUUUCU
F4	001996	hsa-miR-454#	ACCCUAUCAAUAUUGUCUCUGC
F5	001998	hsa-miR-769-5p	UGAGACCUCUGGGUUCUGAGCU
F6	002002	hsa-miR-770-5p	UCCAGUACCACGUGUCAGGGCCA
F7	002003	hsa-miR-769-3p	CUGGGAUCUCCGGGGUCUUGGUU
F8	002004	hsa-miR-802	CAGUAACAAAGAUUCAUCCUUGU
F9	002005	hsa-miR-675	UGGUGCGGAGAGGGCCCACAGUG
F10	002087	hsa-miR-505#	GGGAGCCAGGAAGUAUUGAUGU
F11	002094	hsa-miR-218-1#	AUGGUUCCGUCAAGCACCAUGG
F12	002096	hsa-miR-221#	ACCUGGCAUACAAUGUAGAUUU
F13	002097	hsa-miR-222#	CUCAGUAGCCAGUGUAGAUCCU
F14	002098	hsa-miR-223#	CGUGUAUUUGACAAGCUGAGUU
F15	002100	hsa-miR-136#	CAUCAUCGUCUCAAAUGAGUCU
F16	002102	hsa-miR-34b	CAAUCACUAACUCCACUGCCAU
F17	002104	hsa-miR-185#	AGGGGCUGGCUUUCCUCUGGUC
F18	002105	hsa-miR-186#	GCCCAAAGGUGAAUUUUUUGGG
F19	002107	hsa-miR-195#	CCAAUAUUGGCUGUGCUGCUCC
F20	002108	hsa-miR-30c-1#	CUGGGAGAGGGUUGUUUACUCC
F21	002110	hsa-miR-30c-2#	CUGGGAGAAGGCUGUUUACUCU
F22	002111	hsa-miR-32#	CAAUUUAGUGUGUGUGAUAUUU
F23	002113	hsa-miR-31#	UGCUAUGCCAACAUAUUGCCAU
F24	002114	hsa-miR-130b#	ACUCUUUCCCUGUUGCACUAC
G1	002115	hsa-miR-26a-2#	CCUAUUCUUGAUUACUUGUUUC
G2	002116	hsa-miR-361-3p	UCCCCCAGGUGUGAUUCUGAUUU
G3	002118	hsa-let-7g#	CUGUACAGGCCACUGCCUUGC
G4	002119	hsa-miR-302b#	ACUUUAACAUGGAAGUGCUUUC
G5	002120	hsa-miR-302d#	ACUUUAACAUGGAGGCACUUGC
G6	002121	hsa-miR-367#	ACUGUUGCUAAUAUGCAACUCU
G7	002125	hsa-miR-374a#	CUUAUCAGAUUGUAUUGUAAUU
G8	002126	hsa-miR-23b#	UGGGUUCCUGGCAUGCUGAUUU
G9	002127	hsa-miR-376a#	GUAGAUUCUCCUUCUAUGAGUA
G10	002128	hsa-miR-377#	AGAGGUUGCCCUUGGUGAAUUC
G11	000338	ath-miR159a	UUUGGAUUGAAGGGAGCUCUA
G12	002129	hsa-miR-30b#	CUGGGAGGUGGAUGUUUACUUC
G13	002130	hsa-miR-122#	AACGCCAUUAUCACACUAAAUA
G14	002131	hsa-miR-130a#	UUCACAUUGUGCUACUGUCUGC
G15	002132	hsa-miR-132#	ACCGUGGCUUUCGAUUGUUACU
G16	002134	hsa-miR-148a#	AAAGUUCUGAGACACUCCGACU
G17	002135	hsa-miR-33a	GUGCAUUGUAGUUGCAUUGCA
G18	002136	hsa-miR-33a#	CAAUGUUUCCACAGUGCAUCAC
G19	002137	hsa-miR-92a-1#	AGGUUGGGAUCGGUUGCAAUGCU
G20	002138	hsa-miR-92a-2#	GGGUGGGGAUUUGUUGCAUUAC
G21	002139	hsa-miR-93#	ACUGCUGAGCUAGCACUUCCCG
G22	002140	hsa-miR-96#	AAUCAUGUGCAGUGCCAAUAUG
G23	002141	hsa-miR-99a#	CAAGCUCGCUUCUAUGGGUCUG
G24	002142	hsa-miR-100#	CAAGCUUGUAUCUAUAGGUAUG
H1	002143	hsa-miR-101#	CAGUUAUCACAGUGCUGAUGCU
H2	002144	hsa-miR-136-2#	GCUAUUUCACGACACCAGGGUU
H3	002145	hsa-miR-141#	CAUCUUCCAGUACAGUGUUGGA
H4	002146	hsa-miR-143#	GGUGCAGUGCUGCAUCUCUGGU
H5	002148	hsa-miR-144#	GGAUAUCAUCAUAUACUGUAAG
H6	002149	hsa-miR-145#	GGAUUCCUGGAAAUACUGUUCU
H7	002150	hsa-miR-920	GGGGAGCUGUGGAAGCAGUA

H8	002151	hsa-miR-921	CUAGUGAGGGACAGAACCAGGAUUC
H9	002152	hsa-miR-922	GCAGCAGAGAAUAGGACUACGUC
H10	002154	hsa-miR-924	AGAGUCUUGUGAUGUCUUGC
H11	002157	hsa-miR-337-3p	CUCCUAUAUGAUGCCUUUCUUC
H12	002158	hsa-miR-125b-2#	UCACAAGUCAGGCUCUUGGGAC
H13	002159	hsa-miR-135b#	AUGUAGGGCUAAAAGCCAUGGG
H14	002160	hsa-miR-148b#	AAGUUCUGUUAUACACUCAGGC
H15	002163	hsa-miR-146a#	CCUCUGAAAUUCAGUUCUUCAG
H16	002164	hsa-miR-149#	AGGGAGGGACGGGGGCUGUGC
H17	002165	hsa-miR-29b-1#	GCUGGUUUCAUAUGGUGGUUUAGA
H18	002166	hsa-miR-29b-2#	CUGGUUUCACAUGGUGGCUUAG
H19	002168	hsa-miR-105#	ACGGAUGUUUGAGCAUGUGCUA
H20	002170	hsa-miR-106a#	CUGCAAUGUAAGCACUUCUUAC
H21	002171	hsa-miR-16-2#	CCAAUAUUACUGUGCUGCUUUA
H22	002172	hsa-let-7i#	CUGCGCAAGCUACUGCCUUGCU
H23	002173	hsa-miR-15b#	CGAAUCAUUAUUUGCUGCUCUA
H24	002174	hsa-miR-27b#	AGAGCUUAGCUGAUUGGUGAAC
I1	002176	hsa-miR-933	UGUGCGCAGGGAGACCUCUCCC
I2	002177	hsa-miR-934	UGUCUACUACUGGAGACACUGG
I3	002178	hsa-miR-935	CCAGUUACCGCUUCCGCUACCGC
I4	002179	hsa-miR-936	ACAGUAGAGGGAGGAAUCGCAG
I5	002180	hsa-miR-937	AUCCGCGCUCUGACUCUCUGCC
I6	002181	hsa-miR-938	UGCCCUUAAAGGUGAACCCAGU
I7	002182	hsa-miR-939	UGGGGAGCUGAGGCUCUGGGGGUG
I8	002183	hsa-miR-941	CACCCGGCUGUGUGCACAUGUGC
I9	002185	hsa-miR-335#	UUUUUCAUUAUUGCUCCUGACC
I10	002187	hsa-miR-942	UCUUCUCUGUUUUGGCCAUGUG
I11	002188	hsa-miR-943	CUGACUGUUGCCGUCCUCCAG
I12	002189	hsa-miR-944	AAAUUAUUGUACAUCGGAUGAG
I13	002196	hsa-miR-99b#	CAAGCUCGUGUCUGUGGGUCCG
I14	002197	hsa-miR-124#	CGUGUUCACAGCGGACCUUGAU
I15	002200	hsa-miR-541#	AAAGGAUUCUGCUGUCGGUCCCACU
I16	002203	hsa-miR-875-5p	UAUACCUCAGUUUUAUCAGGUG
I17	002213	hsa-miR-888#	GACUGACACCUCUUUGGGUGAA
I18	002214	hsa-miR-892b	CACUGGCUCCUUUCUGGGUAGA
I19	002231	hsa-miR-9#	AUAAAGCUAGAUAACCGAAAGU
I20	002238	hsa-miR-411#	UAUGUAACACGGUCCACUAACC
I21	002243	hsa-miR-378	ACUGGACUUGGAGUCAGAAGG
I22	002254	hsa-miR-151-3p	CUAGACUGAAGCUCCUUGAGG
I23	002259	hsa-miR-340#	UCCGUCUCAGUUACUUUAUAGC
I24	002263	hsa-miR-190b	UGAUAUGUUUGAUAUUGGGUU
J1	002266	hsa-miR-545#	UCAGUAAAUGUUUAUUAGAUGA
J2	002270	hsa-miR-183#	GUGAAUUACCGAAGGGCCAUAA
J3	002272	hsa-miR-192#	CUGCCAAUUCCAUAGGUCACAG
J4	002274	hsa-miR-200b#	CAUCUUACUGGGCAGCAUUGGA
J5	002286	hsa-miR-200c#	CGUCUUACCCAGCAGUGUUUGG
J6	002287	hsa-miR-155#	CUCCUACAUAUUAGCAUUAACA
J7	002288	hsa-miR-10a#	CAAAUUCGUAUCUAGGGGAAUA
J8	002293	hsa-miR-214#	UGCCUGUCUACACUUGCUGUGC
J9	002294	hsa-miR-218-2#	CAUGGUUCUGUCAAGCACCGCG
J10	002298	hsa-miR-129#	AAGCCCUUACCCCAAAAAGUAU
J11	002301	hsa-miR-22#	AGUUCUUCAGUGGCAAGCUUUA
J12	002302	hsa-miR-425#	AUCGGGAAUGUCGUGUCCGCCC
J13	002305	hsa-miR-30d#	CUUUCAGUCAGAUGUUUGCUGC
J14	002307	hsa-let-7a#	CUAUACAAUCUACUGUCUUUC
J15	002309	hsa-miR-424#	CAAAACGUGAGGCGCUGCUAU
J16	002310	hsa-miR-18b#	UGCCCUAAAUGCCCCUUCUGGC
J17	002311	hsa-miR-20b#	ACUGUAGUAUGGGCACUUCCAG

J18	002312	hsa-miR-431#	CAGGUCGUCUUGCAGGGCUUCU
J19	002314	hsa-miR-7-2#	CAACAAAUCCCAGUCUACCUAA
J20	002315	hsa-miR-10b#	ACAGAUUCGAUUCUAGGGGAAU
J21	002316	hsa-miR-34a#	CAAUCAGCAAGUAUACUGCCCU
J22	002317	hsa-miR-181a-2#	ACCACUGACCGUUGACUGUACC
J23	002325	hsa-miR-744#	CUGUUGCCACUAACCUCAACCU
J24	002330	hsa-miR-452#	CUCAUCUGCAAAGAAGUAAGUG
K1	002332	hsa-miR-409-3p	GAAUGUUGCUCGGUGAACCCCU
K2	002333	hsa-miR-181c#	AACCAUCGACCGUUGAGUGGAC
K3	002336	hsa-miR-196a#	CGGCAACAAGAAACUGCCUGAG
K4	002339	hsa-miR-483-3p	UCACUCCUCUCCUCCCGUCUU
K5	002342	hsa-miR-708#	CAACUAGACUGUGAGCUUCUAG
K6	002343	hsa-miR-92b#	AGGGACGGGACGCGGUGCAGUG
K7	002346	hsa-miR-551b#	GAAAUCAAGCGUGGGUGAGACC
K8	002362	hsa-miR-202#	UUCCUAUGCAUAUACUUCUUUG
K9	002366	hsa-miR-193b#	CGGGGUUUUGAGGGCGAGAUGA
K10	002368	hsa-miR-497#	CAAACCACACUGUGGUGUUAGA
K11	002371	hsa-miR-518e#	CUCUAGAGGGAAGCGCUUUCUG
K12	002376	hsa-miR-543	AAACAUUCGCGGUGCACUUCUU
K13	002378	hsa-miR-125b-1#	ACGGGUUAGGCUCUUGGGAGCU
K14	002379	hsa-miR-194#	CCAGUGGGGCUGCUGUUAUCUG
K15	002380	hsa-miR-106b#	CCGCACUGUGGGUACUUGCUGC
K16	002381	hsa-miR-302a#	ACUUAAACGUGGAUGUACUUGCU
K17	002384	hsa-miR-519b-3p	AAAGUGCAUCCUUUUAGAGGUU
K18	002387	hsa-miR-518f#	CUCUAGAGGGAAGCACUUUCUC
K19	002391	hsa-miR-374b#	CUUAGCAGGUUGUAUUAUCAUU
K20	002400	hsa-miR-520c-3p	AAAGUGCUUCCUUUUAGAGGGU
K21	002404	hsa-let-7b#	CUAUACAACCUACUGCCUUCCC
K22	002405	hsa-let-7c#	UAGAGUUACACCCUGGGAGUUA
K23	002407	hsa-let-7e#	CUAUACGGCCUCCUAGCUUUCC
K24	002410	hsa-miR-550	AGUGCCUGAGGGAGUAAGAGCCC
L1	002411	hsa-miR-593	UGUCUCUGCUGGGGUUUCU
L2	002417	hsa-let-7f-1#	CUAUACAAUCUAUUGCCUUCCC
L3	002418	hsa-let-7f-2#	CUAUACAGUCUACUGUCUUUCC
L4	002419	hsa-miR-15a#	CAGGCCAUAUUGUGCUGCCUCA
L5	002420	hsa-miR-16-1#	CCAGUAUUAACUGUGCUGCUGA
L6	002421	hsa-miR-17#	ACUGCAGUGAAGGCACUUGUAG
L7	002423	hsa-miR-18a#	ACUGCCCUAAGUGCUCCUUCUGG
L8	002424	hsa-miR-19a#	AGUUUUGCAUAGUUGCACUACA
L9	002425	hsa-miR-19b-1#	AGUUUUGCAGGUUUGCAUCCAGC
L10	002432	hsa-miR-625#	GACUAUAGAACUUUCCCCCUCA
L11	002434	hsa-miR-628-3p	UCUAGUAAGAGUGGCAGUCGA
L12	002437	hsa-miR-20a#	ACUGCAUUAUGAGCACUUAAAG
L13	002438	hsa-miR-21#	CAACACCAGUCGAUGGGCUGU
L14	002439	hsa-miR-23a#	GGGGUUCCUGGGGAUGGGAUUU
L15	002440	hsa-miR-24-1#	UGCCUACUGAGCUGAUAUCAGU
L16	002441	hsa-miR-24-2#	UGCCUACUGAGCUGAAACACAG
L17	002442	hsa-miR-25#	AGGCGGAGACUUGGGCAAUUG
L18	002443	hsa-miR-26a-1#	CCUAUUCUUGGUUACUUGCACG
L19	002444	hsa-miR-26b#	CCUGUUCUCCAUUACUUGGCUC
L20	002445	hsa-miR-27a#	AGGGCUUAGCUGCUUGUGAGCA
L21	002447	hsa-miR-29a#	ACUGAUUUCUUUUGGUGUUCAG

L22	002642	hsa-miR-151-5P	UCGAGGAGCUCACAGUCUAGU
L23	002643	hsa-miR-765	UGGAGGAGAAGGAAGGUGAUG
L24	002658	hsa-miR-338-5P	AACAAUAUCCUGGUGCUGAGUG
M1	002672	hsa-miR-620	AUGGAGAUAGAUAUAGAAAU
M2	002675	hsa-miR-577	UAGAUAAAAUAUUGGUACCUG
M3	002676	hsa-miR-144	UACAGUAUAGAUGAUGUACU
M4	002677	hsa-miR-590-3P	UAAUUUUAUGUAUAAGCUAGU
M5	002678	hsa-miR-191#	GCUGCGCUUGGAUUUCGUCCCC
M6	002681	hsa-miR-665	ACCAGGAGGCUGAGGCCCCU
M7	002743	hsa-miR-520D-3P	AAAGUGCUUCUCUUUGGUGGGU
M8	002752	hsa-miR-1224-3P	CCCCACCUCCUCUCUCCUCAG
M9	002867	hsa-miR-1305	UUUUCAACUCUAAUGGGAGAGA
M10	002756	hsa-miR-513C	UUCUCAAGGAGGUGUCGUUUAU
M11	002757	hsa-miR-513B	UUCACAAGGAGGUGUCAUUUAU
M12	002758	hsa-miR-1226#	GUGAGGGCAUGCAGGCCUGGAUGGGG
M13	002761	hsa-miR-1236	CCUCUUCCCCUUGUCUCUCCAG
M14	002763	hsa-miR-1228#	GUGGGCGGGGGCAGGUGUGUG
M15	002766	hsa-miR-1225-3P	UGAGCCCCUGUGCCGCCCCCAG
M16	002768	hsa-miR-1233	UGAGCCCUGUCCUCCCGCAG
M17	002769	hsa-miR-1227	CGUGCCACCCUUUUCCCCAG
M18	002773	hsa-miR-1286	UGCAGGACCAAGAUGAGCCCU
M19	002775	hsa-miR-548M	CAAAGGUAUUUGUGGUUUUUG
M20	002776	hsa-miR-1179	AAGCAUUCUUUCAUUGGUUGG
M21	002777	hsa-miR-1178	UUGCUCACUGUUCUUCCCUAG
M22	002778	hsa-miR-1205	UCUGCAGGGUUUGCUUUGAG
M23	002779	hsa-miR-1271	CUUGGCACCUAGCAAGCACUCA
M24	002781	hsa-miR-1201	AGCCUGAUUAAACACAUGCUCUGA
N1	002783	hsa-miR-548J	AAAAGUAAUUGCGGUCUUUGGU
N2	002784	hsa-miR-1263	AUGGUACCCUGGCAUACUGAGU
N3	002785	hsa-miR-1294	UGUGAGGUUGGCAUUGUUGUCU
N4	002789	hsa-miR-1269	CUGGACUGAGCCGUGCUACUGG
N5	002790	hsa-miR-1265	CAGGAUGUGGUCAAGUGUUGUU
N6	002791	hsa-miR-1244	AAGUAGUUGGUUUGUAUGAGAUGGUU
N7	002792	hsa-miR-1303	UUUAGAGACGGGGUCUUGCUCU
N8	002796	hsa-miR-1259	AUAUAUGAUGACUUAGCUUUU
N9	002798	hsa-miR-548P	UAGCAAAAACUGCAGUUACUUU
N10	002799	hsa-miR-1264	CAAGUCUUAUUUGAGCACCUGUU
N11	002801	hsa-miR-1255B	CGGAUGAGCAAAGAAAGUGGUU
N12	002803	hsa-miR-1282	UCGUUUGCCUUUUUCUGCUU
N13	002805	hsa-miR-1255A	AGGAUGAGCAAAGAAAGUAGAUU
N14	002807	hsa-miR-1270	CUGGAGAUAUGGAAGAGCUGUGU
N15	002810	hsa-miR-1197	UAGGACACAUGGUCUACUUCU
N16	002815	hsa-miR-1324	CCAGACAGAAUUCUAUGCACUUUC
N17	002816	hsa-miR-548H	AAAAGUAAUCGCGGUUUUUGUC
N18	002818	hsa-miR-1254	AGCCUGGAAGCUGGAGCCUGCAGU
N19	002819	hsa-miR-548K	AAAAGUACUUGCGGAUUUUGCU
N20	002820	hsa-miR-1251	ACUCUAGCUGCCAAAGGCGCU
N21	002822	hsa-miR-1285	UCUGGGCAACAAAGUGAGACCU
N22	002823	hsa-miR-1245	AAGUGAUCUAAAGGCCUACAU
N23	002824	hsa-miR-1292	UGGGAACGGGUUCCGGCAGACGCUG
N24	002827	hsa-miR-1301	UUGCAGCUGCCUGGGAGUGACUUC
O1	002829	hsa-miR-1200	CUCCUGAGCCAUUCUGAGCCUC

O2	002830	hsa-miR-1182	GAGGGUCUUGGGAGGGAUGUGAC
O3	002832	hsa-miR-1288	UGGACUGCCCUGAUCUGGAGA
O4	002838	hsa-miR-1291	UGGCCCUGACUGAAGACCAGCAGU
O5	002840	hsa-miR-1275	GUGGGGGAGAGGCUGUC
O6	002841	hsa-miR-1183	CACUGUAGGUGAUGGUGAGAGUGGGCA
O7	002842	hsa-miR-1184	CCUGCAGCGACUUGAUGGCUUCC
O8	002843	hsa-miR-1276	UAAAGAGCCCUGUGGAGACA
O9	002844	hsa-miR-320B	AAAAGCUGGGUUGAGAGGGCAA
O10	002845	hsa-miR-1272	GAUGAUGAUGGCAGCAAAUUCUGAAA
O11	002847	hsa-miR-1180	UUUCCGGCUCGCGUGGGUGUGU
O12	002850	hsa-miR-1256	AGGCAUUGACUUCUCACUAGCU
O13	002851	hsa-miR-1278	UAGUACUGUGCAUAUCAUCUAU
O14	002852	hsa-miR-1262	AUGGGUGAAUUUGUAGAAGGAU
O15	002854	hsa-miR-1243	AACUGGAUCAAUUAUAGGAGUG
O16	002857	hsa-miR-663B	GGUGGCCCGGCCGUGCCUGAGG
O17	002860	hsa-miR-1252	AGAAGGAAAUUGAAUUCAUUUA
O18	002861	hsa-miR-1298	UUCAUUCGGCUGUCCAGAUGUA
O19	002863	hsa-miR-1290	UGGAUUUUUGGAUCAGGGA
O20	002868	hsa-miR-1249	ACGCCCUUCCCCCCCCUUCUUCA
O21	002870	hsa-miR-1248	ACCUUCUUGUAUAAGCACUGUGCUAAA
O22	002871	hsa-miR-1289	UGGAGUCCAGGAAUCUGCAUUUU
O23	002872	hsa-miR-1204	UCGUGGCCUGGUCUCCAUUAU
O24	002873	hsa-miR-1826	AUUGAUCAUCGACACUUCGAACGCAAU
P1	002874	hsa-miR-1304	UUUGAGGCUACAGUGAGAUGUG
P2	002877	hsa-miR-1203	CCCGGAGCCAGGAUGCAGCUC
P3	002878	hsa-miR-1206	UGUUCAUGUAGAUGUUUAAGC
P4	002879	hsa-miR-548G	AAAACUGUAAUUACUUUUGUAC
P5	002880	hsa-miR-1208	UCACUGUUCAGACAGGCGGA
P6	002881	hsa-miR-548E	AAAAACUGAGACUACUUUUGCA
P7	002883	hsa-miR-1274A	GUCCCUGUUCAGGCGCCA
P8	002884	hsa-miR-1274B	UCCCUGUUCGGGCGCCA
P9	002885	hsa-miR-1267	CCUGUUGAAGUGUAAUCCCCA
P10	002887	hsa-miR-1250	ACGGUGCUGGAUGUGGCCUUU
P11	002888	hsa-miR-548N	CAAAAGUAAUUGUGGAUUUUGU
P12	002890	hsa-miR-1283	UCUACAAAGGAAAGCGCUUUCU
P13	002893	hsa-miR-1247	ACCCGUCCCGUUCGUCCCCGGA
P14	002894	hsa-miR-1253	AGAGAAGAAGAUCAGCCUGCA
P15	002895	hsa-miR-720	UCUCGCUGGGGCCUCCA
P16	002896	hsa-miR-1260	AUCCCACCUCUGCCACCA
P17	002897	hsa-miR-664	UAUUCAUUUAUCCCCAGCCUACA
P18	002901	hsa-miR-1302	UUGGGACAUACUUAUGCUAAA
P19	002902	hsa-miR-1300	UUGAGAAGGAGGCUGCUG
P20	002903	hsa-miR-1284	UCUAUACAGACCCUGGCUUUUC
P21	002904	hsa-miR-548L	AAAAGUAUUUGCGGGUUUUGUC
P22	002905	hsa-miR-1293	UGGGUGGUCUGGAGAUUUGUGC
P23	002907	hsa-miR-1825	UCCAGUGCCCUCCUCUCC
P24	002908	hsa-miR-1296	UUAGGGCCCUGGCUCCAUCUCC

* More nucleotides to complete sequence

Supplementary Table S7

Table S7. Primer IDs used in MicroTaqman RT-PCR from Applied Biosystem

Gene	Assay ID
U6 snRNA	Hs00984809_m1
hsa-miR-139	002289
hsa-miR-885-5p	002296
hsa-miR-31	002279
hsa-miR-485-3p	001277
hsa-miR-30a-5p	000417
hsa-miR-30c	000419
hsa-miR-17-5p	002308

Supplementary Table S8

Table S8. Primer IDs used in Taqman RT-PCR from Applied Biosystem

Gene	Primer ID
GAPDH	Hs02786624_g1
BIM (BCL2L11)	Hs01076940_m1
BAX	Hs00180269_m1
P53 (TP53)	Hs01034249_m1
FOXp3	Hs01085834_m1
Caspasa3	Hs00234387_m1
IL8 (CXCL8)	Hs00174103_m1
IL1B	Hs01555410_m1
IL12	Hs01073447_m1
NFKB1	Hs00765730_m1
PPP6C	Hs00254827_m1
CXCL10	Hs01124252_g1
STK40	Hs00894269_m1
PIK3CA	Hs00907957_m1
PRKCD	Hs01090047_m1
Smad3	Hs00969210_m1
Smad2	Hs00998187_m1
TGFBR1	Hs00610320_m1
TIMP3	Hs00165949_m1
IL4	Hs00174122_m1
IL17A	Hs00174383_m1
IL2	Hs00174114_m1
IL10	Hs00961622_m1
TGFβ1	Hs00998133_m1
COL3A1	Hs00943809_m1

Gene	Primer ID
SMA (ACTA2)	Hs00426835_g1
CXCL9	Hs00171065_m1
INFG (IFNG)	Hs00989291_m1
HCN1	Hs01085412_m1
CD28	Hs01007422_m1
CTNNB1	Hs00355049_m1
iCOS	Hs00359999_m1
ZAP70	Hs00896345_m1
LCK	Hs00178427_m1
SLP-76 (LCP2)	Hs01092638_m1
COL3A1	Hs00943809_m1
T-Bet (TBX21)	Hs00894392_m1
GATA3	Hs00231122_m1
PGC1A	Hs00173304_m1
HCN1	Hs01085412_m1

Supplementary Table S9

Table S9. Conjugated mAbs used in flow cytometry analysis (Biosciences)

mAbs	Conjugated	ID product BDBiosciences
CD3	PE	552127
CD8	APC	561421
CD4	FITC	561842
CD69	PE	562617
CD11c	APC	559877
CD14	PE	557154
CD16	FITC	555406
CD56	APC	555518

PE=Phycoerythrin; APC=Allophycocyanin; FITC=Fluorescein

Paper II: MicroRNA-885-5p is downregulated in Cutaneous Lupus Erythematosus lesions and promotes epidermal inflammation and proliferation via PSMB5 and immune recruitment via TRAF1

The next part of the thesis was focused on the study of CLE pathogenesis by analyzing the common deregulated miRNAs in CLE (both DLE and SCLE subtypes). In order to do it, the data from the previous microarray was analysed by grouping both DLE and SCLE in a single group (CLE). Deregulated miRNAs were identified and *in vitro* experiments have been performed to evaluate their role in CLE skin and identify putative target genes.

CLE skin (DLE and SCLE) presents differentially expressed microRNAs vs non-lesional CLE skin

Comparison of miRNA expression between lesional and non-lesional skin from 20 patients with CLE (10 DLE and 10 SCLE) showed only significant differentially down-regulated miRNAs. Down-regulation of miR-885-5p and miR-139-5p was shared by both CLE types. In SCLE (miR-885-5p: -5.83 fold change $p<0.001$ and miR-139-5p: -2.57 fold change $p<0.01$) and in DLE (miR-885-5p -10.20 fold change $p<0.0001$ and miR-139-5p -6.49 fold change $p<0.0001$).

miR-885-5p is expressed in epidermal keratinocytes of non-lesional CLE skin

We next performed *in situ* hybridization in CLE skin biopsies and found that miR-885-5p was highly expressed in the epidermis of both DLE and SCLE non-lesional skin. Regarding miR-139-5p, no staining was observed even though increasing prove concentration from 20 nM up to 100 nM (Annex 2) therefore, we decided to focus on miR-885-5p for the next steps of the project. We next isolated primary keratinocyte from healthy donors and we found that miR-885-5p was specifically detected in keratinocytes. Next, healthy primary keratinocyte were stimulated and miR-885-5p expression was examined within different timepoints. We observed that there was a decrease of miR-885-5p expression in all stimulations, suggesting that the miR-885-5p downregulation depends on inflammatory/damage stimulus. Significant long-lasting downregulation of miR-885-5p, which remained suppressed 18 hours after treatment was achieved with a single treatment with IFNα and UVB. Therefore all the subsequent experiments were performed within these two conditions.

miR-885-5p downregulation promotes epidermal proliferation and inflammation via PSMB5 modulation.

In order to know the implicated molecular signaling pathways and genes in miR-885-5p downregulation in CLE, we next performed microarray in anti-miR-885-5p transfected

keratinocytes. The transfection of anti-miR-885-5p resulted in 65 differentially expressed genes (DEGs) in non-stimulatory conditions, 128 DEGs post IFNα stimulation and 208 DEGs post UVB exposure (p value <0.05, logFC > |1.5|). The gene *PSMB5* (Proteasome 20S Subunit Beta 5) was the unique common gene up upregulated in all conditions with anti-885-5p. Target Scan revealed that the 3'untranslated region (3'UTR) of human *PSMB5* mRNA contains a potential binding site for miR-885-5p, which was further confirmed by luciferase assay (p<0.001).

We next aimed to investigate the role of miR-885-5p modulation *PSMB5* in CLE. As miR-885-5p and proteasome are strongly associated with cell cycle [241, 242] we analysed proliferation and apoptosis. We found that anti-miR-885-5p increased epidermal proliferation (p<0.05) within an significant increase in epidermal proliferative genes *P63*, *KRT16, BIRC5* and *CDK4*. Silencing of PSMB5 in keratinocytes showed reduced proliferation rates (p<0.05) and genes indicating that miR-885-5p may modulate epidermal proliferation via PSMB5. No changes in apoptosis were observed.

Next, we focused in analyzing PSMB5 effect in inflammation as it has been described to interact with NF-κB signaling [243]. Anti-miR-885-5p transfected keratinocytes showed an a decrease of IκBα (NFKBIA), a NF-κB inhibitor and an increase of NF-κB and inflammatory related mediators IL1β and TNFα, especially when exposed to UVB. Regarding siPSMB5 cells opposite effects were observed with an increase of the inhibitor NFKBIA and a subsequent decrease of NF-κB and related mediators at both protein and RNA level. Altogether, suggests that in CLE low levels of miR-885-5p increase epidermal inflammation in CLE, by modulating *PSMB5* and subsequent reduction of NFKBIA and that contributes to NF-κB activation.

Low levels of miR-885-5p promotes immune recruitment via TRAF1 modulation.

An increase of immune mediators and chemokines were observed in the microarray data from UVB stimulated anti-miR-885-5p keratinocytes. First, it was confirmed that high levels of CCL20, CCL5, CXCL8 and S100A7 were observed in both RNA and supernatant of anti-miR-885-5p UVB keratinocytes.

Therefore, we next performed co-culture experiments with miR-885-5p transfected keratinocytes and PBMCs to evaluate immune migration. After 6h of co-culture, a significant number of migrating PBMCs were observed (p<0.01) and this migration was sustained over time within 24h (p<0.001) and 48h (p<0.001) of co-culture, indicating that

inhibition of miR-885-5p plays a role in immune cell recruitment in CLE lesional sites. We next aimed to identify target gene of miR-885-5p which is responsible for immune migration as silencing of PSMB5 did not modulate immune migration. By comparing the genes upregulated on UVB condition with the predicted target genes of miR-885-5p in target scan, 16 candidate genes were found of which only one TRAF1 has been described to be involved in immune recruitment [244]. TRAF1 RNA and protein levels were found upregulated in anti-miR-885-5p keratinocytes. Moreover, TRAF1 RNA and protein were upregulated in CLE lesional skin. Luciferase assay confirmed that TRAF1 is a direct target of miR-885-5p. Finally, silencing of TRAF1 decreased immune recruitment in co-culture experiments and decreased immune mediators such as CCL20, CCL5, CXCL8 and S100A7 indicating that miR-885-5p modulates immune recruitment in CLE via TRAF1 modulation.

MicroRNA-885-5p is downregulated in Cutaneous Lupus Erythematosus lesions and promotes epidermal inflammation and proliferation via PSMB5 and immune recruitment via TRAF1

Sandra Domingo [1], Laura Porres[1], Cristina Solé [1*], Teresa Moliné[2], Berta Ferrer [2] , Josefina Cortés-Hernández[1]

[1] Rheumatology Research Group - Lupus Unit, Vall d'Hebrón University Hospital, Vall d'Hebrón Research Institute (VHIR), Universitat Autònoma de Barcelona (UAB), Barcelona, Spain.

[2] Department of Pathology, Vall d'Hebrón University Hospital, Barcelona, Spain.

Abstract

Cutaneous lupus erythematosus (CLE) is an autoimmune chronic condition that includes a broad range of dermatological manifestations. Its pathogenesis is multifactorial and involves genetic predisposition, environmental factors and immune response abnormalities. In this context, the participation of microRNAs in CLE remains to be completely understood. Here, we found that miR-885-5p is markedly downregulated in CLE lesional keratinocytes. IFNα and UVB are identified as strong modulators of miR-885-5p. Next, gene microarray of anti-miR-885-5p keratinocytes revealed that proteasome subunit 5 (PSMB5) may be a potential novel target gene which was further validated by Luciferase assay. MiR-885-5p was found to be implicated in epidermal proliferation by modulating K16, BIRC5, TP63 and CDK4 proliferative genes, and in epidermal inflammation via promotion of NF-κB activation by decreasing IκBα (NF-κB inhibitor, NFKBIA) via PSMB5 modulation. In addition, inhibition miR-885-5p in keratinocytes promotes immune recruitment independently of PSMB5 and identified TRAF1, as a second direct target responsible for the immune migration to the inflammation site. Collectively, our findings suggest that UVB and IFNα downregulate miR-885-5p in CLE keratinocytes leading to epidermal inflammation via enhanced NF-κB activity and proliferation through PSMB5 and immune recruitment through TRAF1.

Introduction

Cutaneous Lupus Erythematosus (CLE) includes a wide range of heterogeneous dermatologic manifestations which may or may not be associated with Systemic Lupus Erythematosus (SLE) (Okon and Werth, 2013). In SLE, up to 80% of patients will develop skin manifestations during the disease course and in 20% of them, cutaneous lesions will be the first sign of systemic disease (Tebbe and Orfanos, 1997). CLE is divided into specific and non-specific CLE lesions according to clinical and histological characteristics (Gilliam and Sontheimer, 1981). Within CLE-specific manifestations, Discoid Lupus Erythematosus (DLE) and Subacute Cutaneous Lupus Erythematosus (SCLE) are the most prevalent (Grönhagen et al., 2014).

The pathophysiology of CLE is not fully elucidated and encompasses complex genetic, environmental, and immune cell interactions (Achtman and Werth, 2015). CLE skin lesions are characterised by an anti-epithelial cytotoxic immune response, orchestrated in part by type I and type III interferon- regulated cytokines and chemokines, which promote the release of cell debris that in turn re-activates innate immune pathways, leading to a pro-inflammatory self-amplifying cycle (Deng and Tsokos, 2015; Wenzel, 2019). High

throughput sequencing screening technologies have provided further insights into the molecular features of most common CLE subtypes. DLE and SCLE lesions share a high expression of type 1 IFN molecules, whereas DLE is characterised by distinctive T-cell and TGF-β gene signatures. (Berthier et al., 2019; Lazar et al., 2018; Sinha et al., 2017; Solé et al., 2016)

MicroRNAs (miRNAs) are small non-coding RNA sequences of 20-25 nucleotides length (Ambros, 2004). Their main function is to regulate gene expression post-transcriptionally by blocking transcription and promoting mRNA degradation (Baek et al., 2008). They play an essential role in the regulatory mechanisms of immune homeostasis, and their deregulation has been described in a wide variety of human diseases, including psoriasis and atopic dermatitis (Sonkoly et al., 2007; 2010a). Moreover, their role is also well documented in skin physiology and development, contributing to wound healing, skin microbiota and aging (Yi and Fuchs, 2010; Yi et al., 2006). Their preclinical and clinical applications include their use as biomarkers or therapeutic agents. To date, few studies have evaluated the role of miRNAs in CLE (Domingo et al., 2020). Our recent microarray expression profile study identified miR-31 and miR-485-3p as regulators of DLE pathogenesis by promoting inflammation, keratinocyte apoptosis and skin fibrosis (Solé et al., 2019).
In this study, by comparing lesional and non-lesional CLE skin samples, we also found miR-885-5p downregulated in CLE lesional skin in both DLE and SCLE subtypes, suggesting a role for this miRNA in the pathogenesis of CLE. In oncology, studies have found miR-885-5p to play a role as a tumor promoter in hepatocellular carcinoma and a tumor suppressor in colorectal cancer and glioma (Su et al., 2018; Xu et al., 2019) Our study aimed to verify whether miR-885-5p exhibits abnormal expression in CLE and further decipher its molecular mechanism in this condition. We demonstrate that downregulation of miR-885-5p induces epidermal inflammation and proliferation by targeting PSMB5 and promotes the recruitment of leucocytes into the inflammatory site by targeting TRAF1.

Materials and methods

Additional details are available in the Supplementary Materials.

Patients and skin samples

After written informed consent, two 6-mm punch biopsy samples were taken from lesional and nonlesional skin of untreated patients with active disease (n=20). (see Supplementary Table S1). The patient inclusion criteria were age≥ 18 years, a CLE Disease Area and

Severity Index (CLASI) > 4, presence of a cutaneous lesion bigger than 3cm, and no systemic o local therapy for at least 4 weeks prior inclusion. Blood samples for PBMCs isolation were obtained from patients with CLE at the time of biopsy and healthy donors (n=20 in each group). The study was approved by the local Vall d'Hebrón ethics committee.

***In situ* hybridization or immunofluorescence in skin biopsies**

Hybridization was performed on paraffin embedded 6µm skin sections from paired lesional and non-lesional CLE skin samples using the protocol described in miRCURY LNA microRNA ISH Optimization Kit (FFPE) (Qiagen, Hilden, Germany). Immunofluorescence in skin biopsies were performed as described on paraffin-embedded (Guttman-Yassky et al., 2019) using purified monoclonal antibodies listed in Table S2. Stained samples were evaluated by two blinded dermatopathologists and cells counts were quantified using Image J V1.42 (see Supporting Information).

Epidermal primary keratinocytes and PBMCs isolation

Primary keratinocytes were obtained from CLE skin biopsies following the optimised methodology described before (Trond and Belmonte, 2010). Peripheral blood mononuclear cells (PBMCs) from patients with CLE and healthy donors were isolated from blood collected in mononuclear cell preparation tubes with sodium citrate (Vacutainer CPT, BD Bioscience, NJ, USA) (more details in Supporting Information).

Immunofluorescence in culture cells

After transfection and stimulation with UVB or IFNα, cells were washed with phosphate buffered saline, fixed with 4% paraformaldehyde an permeabilised with 0.1% triton. Primary antibodies were incubated overnight and secondary antibody for 2 hours at room temperature (Table S2).

miRNA and RNA quantification

Skin and cultured cells RNA was obtained with RNAeasy Mini Kit (Qiagen, Hilde, Germany). For quantification of miRNAs or mRNAs, a total of 50 ng for miRNAs and 1µg for RNA was reverse transcribed into cDNA using the MicroRNA Reverse Transcription Kit (Applied biosystems, Foster City, CA, USA) and the High-Capacity cDNA Reverse Transcription Kit (Applied biosystems, Foster City, CA, USA) respectively. Gene expression was assessed by TaqMan gene expression assays gene expression assays (FAM dye labeled MGB probe, Applied Biosystems, Foster City, CA, USA, Table S3) using

96 well plates or 384 well plates in the ABI PRISM 7000 or ABI PRISM 7900 thermocyclers respectively.

***In vitro* evaluation of miR-885-5p**

Human epidermal keratinocytes (HEKa cells, Life Technologies, Carlsbad, CA) were cultured and stimulated with different cytokines (TNFα, IFNα, IL1α, TGFβ, 10 ng/mL) or UVB (25 mJ/cm^2) at single dose. The stimulation was stopped at 2, 4, 6, 8, 12 and 18 hours to obtain cellular pellet and perform miRNAs quantification of miR-885-5p (described above).

Cell transfection

Functional miRNA studies were performed in healthy Human epidermal keratinocytes (HEKa cells, Life Technologies, Carlsbad, CA). Cells at ~ 70% confluence were transfected with miRNA mimics or anti-miR miRNA inhibitors (mirVanaTM, Life technologies, Carlsbad, CA, USA) using Lipofectamine RNAiMAX Reagent (Life Technologies, Carlsbad, CA, USA). Silencing of PSMB5 and TRAF1 was performed using CRISPRMAX tm Reagent Cas9 nuclease transfection protocol (Thermofisher Scientific, Waltham, MA, USA).

Apoptosis and Proliferation assay

Cells were plated in 96-well plates, and after treatment, apoptosis was determined using CellEvent Caspase-3/7 Green Detection Reagent (Invitrogen) and proliferation using CyQUANT NF Cell Proliferation Assay Kit (Invitrogen, Carlsbad, CA, USA), following manufacturer's instructions (more details in supporting information).

Cytokine measurement

The culture medium was collected from transfected keratinocytes after stimulation and stored at –80°C. ELISA kits were used to quantify protein levels of CXCL8, CCL5, CCL20 and S100A7 (Diaclone, Besancon, France) following the manufacturer's instructions.

miRNA microarray and pathway analysis

To comprehensively characterize the miR-885-5p regulatory network and to precisely map the miRNA target sites, we performed a Genechip Human Gene 1.0 ST Array (Thermofisher, Waltham, MA, USA), using anti-885-5p transfected keratinocytes, non-stimulated and stimulated with IFNα or UVB (more details in supporting information).

Luciferase assay

Primary keratinocytes were co-transfected with the vector pEZX-MT01-PSMB5 3′UTR or pEZX-MT01-TRAF1 3′ UTR and 10 μM miR-885-5p mimics (mirVanaTM, Life technologies, Carlsbad, CA, USA) using DharmaFECT Duo transfect reagent (Thermo Fisher Scientific, Waltham, MA, USA) according to manufacturer protocols. After 24 h, luciferase activity was measured using a Dual-Luciferase Reporter Assay System (Promega, Madison, WI, USA).

Migration Transwell assay

The migration assays and co-culture experiments were performed in a modified 24-well plate with cell culture inserts (3.0- and 0.4-μm pore; BD Biosciences, Franklin Lakes, NJ). keratinocytes (1×10^5 cells/well) were transfected with anti-miR-885-5p (10μM), siTRAF1 (240 ng) or the corresponding negative control and platted in the bottom of 24-well plate. After 24hours, they were stimulated with UVB (25mJ/cm2). Then, primary PBMCs from healthy controls were stained with DAPI (5 μL) (Invitrogen, Waltham, MA, DAPI), and plated in the upper well. Migration of PBMCs was evaluated with inverted fluorescence microscope Leica DMi1 (Leica, Wetzlar, Germany) after 6, 24 and 48 hours of incubation.

Statistical Analysis

Data are represented as mean ± SEM. Paired an unpaired T-tests were used for the analysis of the data as applicable using Prism GraphPad version 7.0 (GraphPad Software, v 7.0, San Diego, CA, USA). P values of less than 0.05 were considered statistically significant. RT-qPCR analysis was done by calculating Fold Change differences $2^{-\Delta\Delta Ct}$ method.

Results

miR-885-5p is suppressed in the epidermis of lesional CLE skin

We described that miR-885-5p expression levels, measured by RT-qPCR, were downregulated in lesional skin from CLE patients, in both DLE and SCLE subtypes (Solé et al. 2019). In the present study we performed an *in situ* hybridization to locate miR-885-5p in sections of lesional and non-lesional skin from CLE patients (DLE (n=5) and SCLE (n=5)). We found miR-885-5p expressed in nonlesional CLE skin, mainly in the basal and spinous layers of the epidermis. In contrast, in lesional skin from the same patients, miR-885-5p was downregulated (DLE p=0.003; SCLE p=0.018) (Figure 1a). To identify the cell types expressing miR-885-5p in the skin, we also performed RT-qPCR on a panel of

isolated primary human skin cells. Results showed that miR-885-5p was mainly expressed by keratinocytes ($p<0.001$, Figure 1b).

IFNα and UVB regulate miR-885-5p expression in keratinocytes

Next, we sought to explore the mechanisms underlying decreased miR-885-5p expression in CLE epidermis. To investigate whether its decreased expression is due to the inflammatory cytokine milieu in CLE and UVB radiation, primary human keratinocytes from healthy individuals (Heka) were treated with a single dose of either TNFα, IFNα, IL1α, TGFβ (10 ng/mL) and UVB (25 mJ/cm2), and the expression of miR-885-5p was analysed. Expression started to decline significantly after 6 hours in most stimuli ($p<0.05$). Of all tested conditions, a single treatment with IFNα and UVB exposure led to a significant long-lasting downregulation of miR-885-5p, which remained suppressed 18 hours after treatment (Figure 1c). Therefore, for later experiments we chose IFNα and UVB as stimuli for miR-885-5p modulation for their marked effect.

To further investigate the regulation of miR-885-5p, we analysed *in vitro* the effects of IFNα and UVB in primary keratinocytes isolated from CLE patients (Figure 1d). Compared to healthy controls, a more significant downregulation of miR-885-5p was observed in both DLE and SCLE following IFNα stimulation ($p<0.001$, fold decrease of 9.61 and 7.20, respectively) and UVB radiation ($p<0.001$, fold decrease of 7.80 and 9.20, respectively).

miRNA 885-5p targets PSMB5 in keratinocytes

To explore the biological role of miR-885-5p in CLE, we transfected miR-885-5p hairpin inhibitor (anti–miR-885-5p) into primary human keratinocytes to inhibit endogenous miR-885-5p. Inhibition of miR-885-5p was confirmed by qRT-PCR analysis of miR-885-5p expression (Figure S1). We performed a global transcriptome analysis of keratinocytes upon supression of endogenous miR-885-5p using Affymetrix arrays in non-stimulatory conditions and after stimulation with IFNα or UVB exposure. Differentially expressed genes (DEG) were generated using a criteria of > 1.5-fold change and p value < 0.05, and were subsequently interrogated using Ingenuity Pathway Analysis (IPA) (Qiagen, Hilden, Germany). The study identified 65 DEGs in non-stimulatory conditions, 128 DEGs post IFNα stimulation and 208 DEGs post UVB exposure (p value <0.05, logFC > |1.5|) (Figure 2a). Volcano Plots show the top 20 most significant DEGs for each condition (Figure S2, Table S4). Studying the overlap among DEGs with >1.5-fold increase/decrease from each comparison, *PSMB5* (proteasome 20S Subunit Beta 5) was identified as the unique common DEG (Figure 2b). This gene encodes for a protein that contributes to the complete

assembly of 20S proteasome subunit and forms a proteolytic environment for substrate degradation, antigen cell presentation and cell proliferation (Seifert et al., 2010).

Using TargetScan, we detected that the 3'untraslated region (3'UTR) of human PSMB5 mRNA contains a potential binding site for miR-885-5p. To verify whether *PSMB5* is a direct target gene for miR-885-5p, we performed 3′UTR luciferase-binding assays. The transfection of miR-885-5p mimics resulted in the suppression of the luciferase activity of the reporter containing regions of the 3'UTR of human *PSMB5* indicating that *PSMB5* is a direct target of miR-885-5p (74% of reduction $p<0.001$) (Figure 2c).

We next sought to evaluate whether miR-885-5p influences endogenous PSMB5 expression. Notably, in anti-miR-885-5p transfected keratinocytes, *PSMB5* expression was increased both at mRNA level as shown by qRT-PCR (NS: 1.3-fold $p<0.01$; IFN: 2.1-fold $p<0.001$; UVB 1.9-fold $p<0.05$) (Figure S3) and at a protein level by immunofluorescence (Figure 2d) (NS: $p<0.05$; IFN $p<0.05$; UVB: $p<0.05$).
PSMB5 expression negatively correlated with miR-885-5p (r=-0-4905; p=0.0105) (Figure S4). Moreover, mRNA ($p<0.01$) and protein levels of PSMB5 were significantly increased in lesional skin samples from CLE patients (Figure 2e, 2f). In tissue, PSMB5 expression was also detected in the spinous and basal layers of the epidermis (DLE: $p<0.001$; SCLE: $p<0.001$). Together, data from luciferase reporter assay, transfection experiments, immunofluorescence analysis, and clinical samples indicate that PSMB5 is a direct target of miR-885-5p.

miR-885-5p promotes NF-κB pathway activation and proliferation via PSMB5

To explore the biological role and importance of miR-885-5p targeting PSMB5 in CLE, we performed functional assays using anti-miR-885-5p transfected keratinocytes and silenced-PSMB5 keratinocytes. Since miR-885-5p and PSMB5 have been associated with cell cycle progression and survival, we evaluated their effect in keratinocyte proliferation and apoptosis. *In vitro*, anti-miR-885-5p transfected keratinocytes displayed an enhanced cell proliferation in non-stimulatory conditions and following IFNα or UVB stimulation (fold increase of 1.87, 2.23 and 2.42, respectively, Figure 3a).
There was a parallel increase of *P63* and *KRT16* proliferative epidermal markers and *CDK4* and *BIRC5* proliferative genes by RT-qPCR (Figure 3b). Silencing PSMB5 showed the opposite effect on keratinocyte proliferation under all studied conditions (fold decrease of 1.52 for non-stimulation, 1.43 for IFNα stimulation and 1.27 for UVB) (Figure 3a). This effect was also observed in the expression levels of *P63*, *KRT16*, *CDK4* and *BIRC5* (Figure 3b). The presence of keratinocyte proliferation in CLE, mainly observed in DLE

lesional skin (p=0.009, Figure 3c) shown by KI-67 immunofluorescent staining. No effect on apoptosis was observed (Figure S5).

NF-κB plays a central role in CLE and its activation is regulated by a proteasome-dependent degradation of its inhibitory proteins termed inhibitors of nuclear kappa B (IκBs or NFκBIs) (Chen 2007). Since PSMB5 is a proteolytically active subunit of the ubiquitin-proteasome system (UPS), we investigated a possible interaction between miR-885-5p/PSMB5 and NF-κB signaling pathway. First, we demonstrated that anti-miR-885-5p transfected keratinocytes overexpressed *NFKB1* and related cytokines (*IL1A*, *TNF* and *CXCL8*) and that the inhibitor of NF-κB IκBα (*NFKBIA*) expression levels were reduced both at mRNA level by qRT-PCR (Fig. 3d) , and at protein level by immunofluorescence (Fig. 3e). These changes were more pronounced under the UVB stimulatory condition. siPSMB5 keratinocytes showed the opposite effect (Figure 3d, 3e). These data indicate that the regulation miR-885-5p modulates of NF-κB in keratinocytes, and that this modulation is mediated by PSMB5.

miR-885-5p downregulation regulates the leukocyte-attracting capacity of keratinocytes independently of PSMB5

Heat map from microarray results highlights the most relevant common cytokines in stimulatory and non-stimulatory conditions (Figure 4a). *CCL5*, *CCL20*, *CXCL8* and *S1007A* upregulation was validated by RT-qPCR on keratinocytes transfected with anti–miR-885 or anti–miR-Ctrl under UVB stimulatory conditions (Figure 4b). Of all chemokines, *CCL5* and *CCL20* were the most significantly overexpressed (fold change of 10.97 $p<0.001$ and 12.38, $p<0.001$ respectively). Consistently, the amount of these chemokines secreted into the culture medium was increased by anti–miR-885 as shown by ELISA (Figure 4c). Since these chemokines have the ability to recruit leukocytes (20), we examined whether the capacity of keratinocytes to attract leukocytes was affected by miR-885-5p. Migration assays with PBMCs co-cultured with UVB stimulated anti-miR-885-5p transfected keratinocytes showed an increased PBMCs migration (fold increase of 2.27, 2.55 and 2.83 overtime) that was sustained over time but that it was PSMB5 independent (Figure 4d).

miR-885-5p targets TNF Receptor Associated Factor 1 (TRAF1) in keratinocytes promoting leukocyte recruitment

Next, we aimed to identify the molecular mechanism by which miR-885-5p modulates the leukocyte recruitment. Analysis of upregulated genes of anti-885-5p UVB-stimulated keratinocytes in the microarray and the predicted target genes provided by TargetScan

data base data, we identified sixteen predicted genes (Table S5) of which TRAF1 was the only one related with immune recruitment (Figure 5a) (Oyoshi et al 2007). *TRAF1* gene expression (fold change of 6.04, $p<0.001$) and protein levels ($p<0.05$) (Figure 5b and 5c) were upregulated in keratinocytes upon miR-885-5p inhibition. *TRAF1* expression inversely correlated with miR-885-5p expression ($r=-0.36$; $p=0.02$) (Figure S6). To determine whether *TRAF1* is a target of miR-885-5p, we performed 3'-UTR luciferase reporter assays with luciferase reporter gene constructs containing the full-length 3'-UTR of *TRAF1* mRNA in human primary keratinocytes. We observed a significant reduction of luciferase activity using miR-885-5p mimics in comparison with miR-control (27% of reduction, $p=0.005$, Figure 5d).

Silencing of *TRAF1* reduced significantly leucocyte migration overtime (fold decrease of 1.82, 2.35 and 2.38 overtime, Figure 5e). In addition, siTRAF1 reduced the expression of *CCL5*, *CCL20*, *CXCL8* and *S100A7* chemokines (fold decrease of 3.22, 2.21, 6.61 and 2.35, respectively) in UVB-stimulated keratinocytes (Figure 5f). Consistently, the amount of protein in culture medium were also decreased in a similar way (Figure 5g). TRAF1 is described as an inductor of NF-κB pathway (Xie P, 2013). We found that *NFKB1* gene expression is reduced in siTRAF1 (fold decrease of 1.84, $p=0.005$) suggesting a direct link between miR-885-5p/TRAF1 and NF-κB pathway (Figure 5h).

Discussion

In this study, we show that miR 885-5p is downregulated in the epidermis of patients with CLE and we have identified two novel targets that demonstrate this gene to be involved in epidermal inflammation, proliferation and immune regulation. miR-885-5p expression has been reported to be dysregulated in several human cancer types (Zu et al., 2021), however it has not been described previously in skin or other autoimmune diseases. In CLE, miR-885-5p was identified as a keratinocyte-specific miRNA and no differences in expression were found between the most common subtypes of CLE, DLE and SCLE, suggesting that miR-885-5p plays a role in common pathogenic pathways. UVB and IFNα were found two be strong regulators of miR-885-5p in keratinocytes, suggesting that high IFNα levels in CLE skin, and mainly UVB are responsible for the downregulation of miR-885-5p.

Increasing evidence demonstrates keratinocytes to play an important role in the pathogenesis of CLE (Sarkar et al., 2018; Stannard et al., 2017; Tsoi et al., 2019). Photosensitivity is a common characteristic for CLE, ranging from 27-100% according to the subtype of CLE. Ultraviolet (UV) light, particularly UVB (290–320 nm), plays a central role by triggering keratinocyte apoptosis, transport of nucleoprotein autoantigens to the

keratinocyte cell surface and the release of inflammatory cytokines (including interferons (IFNs), tumor necrosis factor (TNF)-α, inter-leukin (IL)-1, IL-6, IL-8, IL-10 and IL-17) which are important for initiation, development and perpetuation of CLE (Robinson and Werth, 2015; Zhou et al., 2021). Increased IFN, particularly type I IFN, is central to the development of CLE lesions. In CLE, type I IFN is produced in response to nuclear antigens, immune complexes and UV light (Kahlenberg, 2021). Type I IFN increases leukocyte recruitment to the skin via inflammatory cytokines, chemokines, and adhesion molecules, thereby inducing a cycle of cutaneous inflammation (Turnier et al.; 2020).

In pathological conditions, miR-885 expression has been reported to be dysregulated in several human cancer types, including liver cancer, neuroblastoma and oncocytic follicular thyroid carcinomes (Dettmer et al., 2012; Su et al., 2018; Xu et al., 2019). When overexpressed this miRNA has been shown to supress cell proliferation, migration and invasion by regulating the cell cycle arrest, senescence and/or apoptosis (Gao et al., 2017; Li et al., 2019). Keratinocyte hyperproliferation is not a hallmark of cutaneous lupus, but DLE lesions, show hyperkeratosis and atrophy, which reflect abnormal epidermal proliferation, combined with normal early differentiation and premature terminal differentiation of keratinocytes (de Jong et al., 1991). Our study showed that inhibition of miR-885-5p promotes aberrant keratinocyte proliferation accompanied by an increase of proliferative genes *KRT16, TP63, BIRC5* and *CDK4 in vitro*. However, no effects were observed on apoptosis. This proliferation was mediated by a novel target gene identified of miR-885-5p, PSMB5 as silencing of PSMB5 reverted the effect of miR-885 on keratinocyte proliferation.

PSMB5 is a subunit of the 20 S proteasome. Into detail, the 20 S proteasome is composed of seven subunits, termed α1-α7 and β1-β7. The α subunits maintain the structure, whereas the core β rings contains proteolytically active subunits such as PSMB5 (β5, chymotrypsin-like), PSMB6 (β1, caspase-like), and PSMB7 (β2, trypsin-like) (Tanaka, 2009). The proteasome activity is controlled stringently and attuned to cellular requirements. Aberrations of this pathway lead to pleiotropic defects in all aspects of cell function and may affect cellular homeostasis and contribute to disease origin and development (Vangala et al., 2014). It mediates the intracellular key proteins including those involved in cell cycle regulation (Tu et al., 2012). Our findings indicate that miR-885-5p was targeting PSMB5 proteasome subunit. In addition, PSMB5 was increased at a gene expression and protein level in lesional epidermal CLE skin compared to non-lesional CLE skin. The ubiquitin-proteasome pathway plays a crucial role in NF-κB pathway activation by promoting the ubiquitination of NF-κB inhibitor IκBα (NFKBIA), promoting its

degradation and the subsequent NF-κB activation (Chen, 2007). Therefore, we aimed to investigate the relation between miR-885-5p/PSMB5 and NF-κB signaling. *In vitro* experiments showed that when miR-885-5p inhibited, there is a decrease of NF-κB inhibitor IκBα (*NFKBIA*) at a protein and gene expression levels and consequently there is an increase of NFKB1 and related cytokines *TNF* and *IL1B.* Contrary results were observed when PSMB5 is inhibited. Taken together, our results indicate that in cutaneous lupus lesional skin low levels of miR-885-5p modulate NF-κB via PSMB5. Low levels of miR-885-5p increase PSMB5 and NFKBIA is decreased and NF-κB is released and active for nuclear translocation to promote epidermal inflammation.

Gene microarray in anti-885-5p UVB keratinocytes revealed an increase of chemokines *CCL5, CXCL8* and *CCL20* and antimicrobial peptide *S100A7.* Inhibition of miR-885-5p in keratinocytes increased migration of immune cells *in vitro* in co-culture experiments. To our knowledge, we are the first to report that low levels of miR-885-5p contribute to immune recruitment. Immune migration was not observed when PSMB5 was inhibited indicating that PSMB5 does not mediate the miR-885-5p immune migration. By luciferase assay we demonstrated that TRAF1 is a direct miR-885-5p target and *in vitro* co-culture studies showed that it mediates immune recruitment. Increased protein and gene expression of TRAF1 in CLE lesional skin was observed. TRAF1 is a member of the TRAF protein family, which regulates the canonical and noncanonical NF-κB signaling cascades and mediates pro-inflammatory cytokine production and inflammatory responses (Edilova et al., 2018; Guo et al., 2009). It has been reported that TRAF1 expression in skin and keratinocytes is upregulated and sustained after UVB exposure (Yamamoto et al., 2018). Our results underline previous studies which found that TRAF1 deficiency impairs attraction of lymphocytes, neutrophils, myeloid dendritic cells and monocyte recruitment and tissue secretion of chemokines and adhesion molecules (Oyoshi et al., 2007; Missou et al., 2010).

Currently there is a lack of efficient targeted treatment for CLE refractory patients. Because of their crucial roles in regulation of gene expression in diverse physiological and pathological conditions, miRNAs are promising therapeutic agents (Christopher et al., 2016). To date, miRNA-based therapies have entered the clinical trial phase, showing promising results (Chakraborty et al., 2020). In addition strategies of topical nanodelivery show few adverse events (Gallant-Behm et al, 2019). Our study suggests that miRNA-885-5p mimics based therapy could be of interest for CLE. Further research on miRNA therapeutics within *in vivo* models or 3D skin equivalent need to be conducted to the development of new strategies for treating this refractory disease.

In conclusion, the present study has shown that miR-885-5p is commonly downregulated in DLE and SCLE. Low levels mediates a role in CLE pathogenesis promoting epidermal inflammation, proliferation and immune recruitment in the CLE lesional sites. Two novel target genes of miR-885-5p PSMB5 and TRAF1 have been identified. As in CLE, miR-885-5p is downregulated, PSMB5 and TRAF1 are in turn upregulated and may promote epidermal inflammation/proliferation and immune recruitment respectively (Figure 6). Further research into the therapeutical role of miR-885-5p in cutaneous lupus should be considered.

Conflict of interest
The authors state no conflict of interest.

Acknowledgments
This work was financed by Instituto de Salud Carlos III (Spain Government, PI10/02234).

Figures

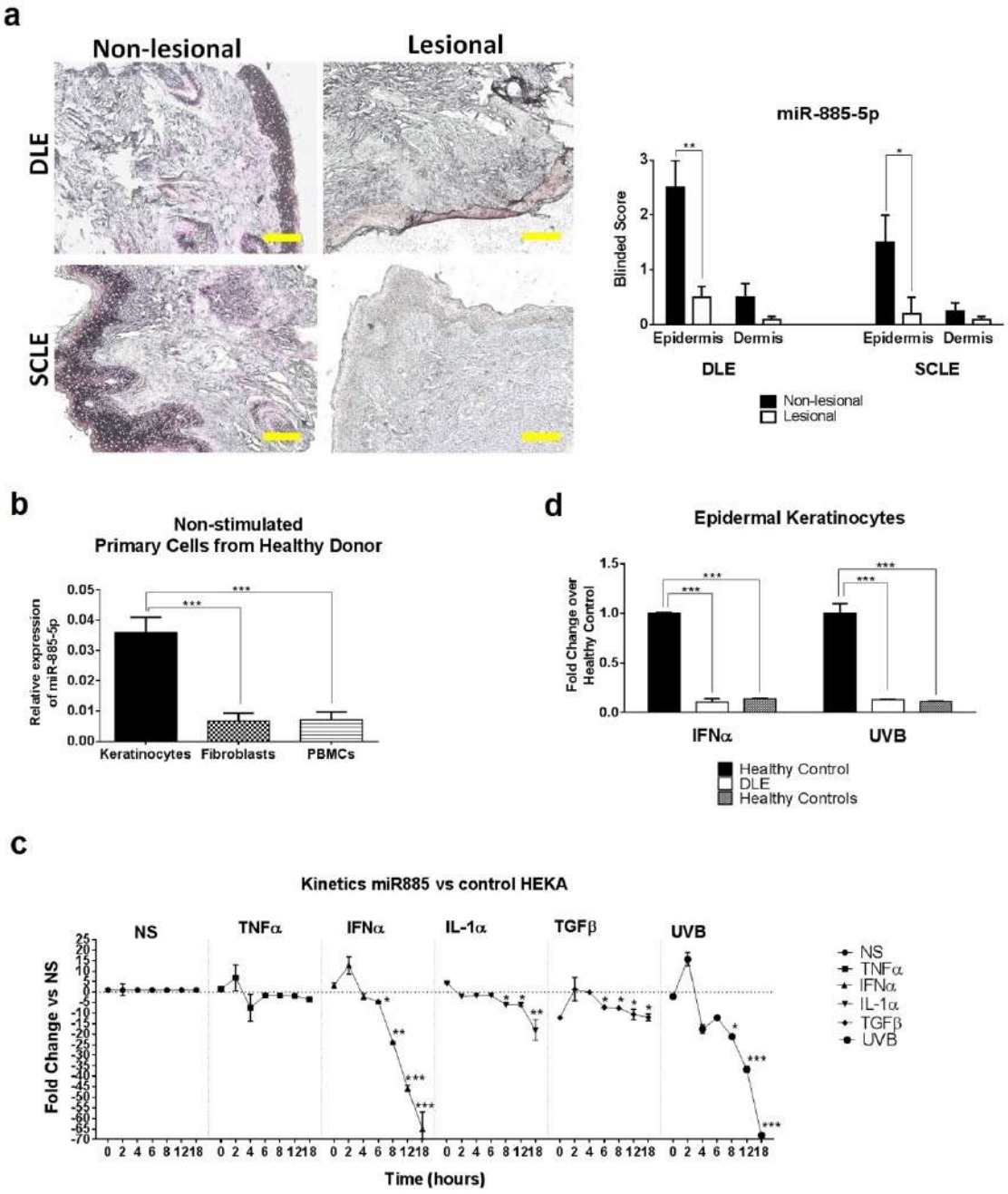

Figure 1. miR-885-5p is downregulated in CLE lesional keratinocytes and it is modulated by IFNα and UVB. A) In situ hybridization of miR-885-5p in CLE skin showed that miR-885-5p is mainly detected in the epidermis of DLE and SCLE lesional skin (n=5 DLE, n=5 SCLE, paired patients). **B)** Keratinocytes from healthy donors express high levels of miR-885-5p compared to other cell types such as dermal fibroblasts of PBMCs (n=3). **C)** miR-885-5p expression by RT-qPCR was evaluated at different timepoints after receiving inflammatory stimulus *in vitro* in keratinocytes. **D)** Keratinocytes from healthy donors, DLE and SCLE (n=3 respectively) were incubated with IFNα or UVB and miR-885-5p expression was analysed by RT-qPCR.

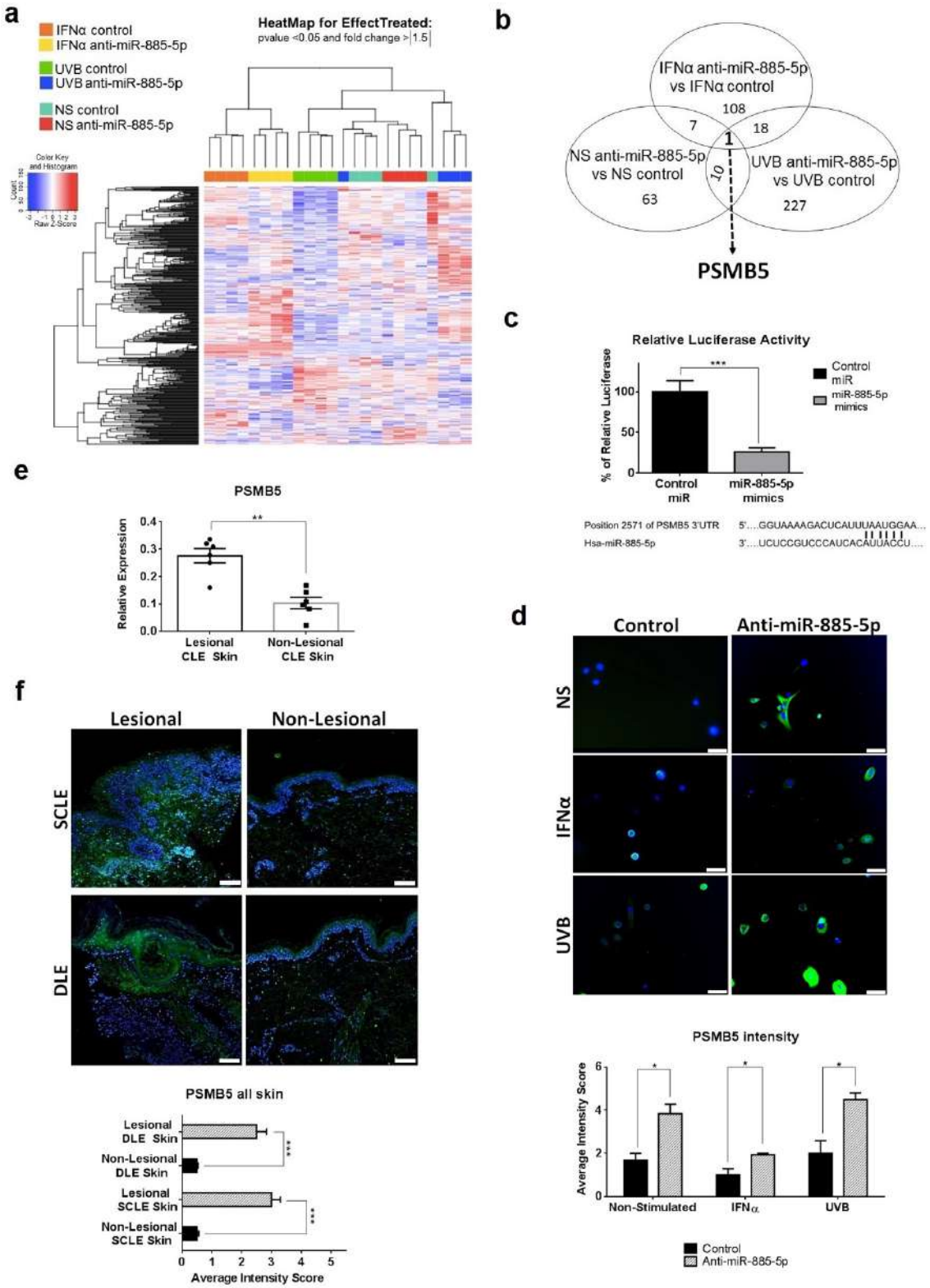

Figure 2. miR-885-5p modulates PSMB5. A) Heatmap of gene expression in microarray of anti-miR-885-5p transfected keratinocytes vs control in Non-stimulated, IFNα and UVB conditions (n=4 each condition). **B)** Venn diagram showing that PSMB5 is the unique gene upregulated in Non-stimulated, IFNα and UVB conditions with miR-885-5p inhibited. **C)** Luciferase assay showed that miR-885-5p targets directly PSMB5. **D)** Anti miR-885-5p increases protein levels of PSMB5 in keratinocytes *in vitro* shown by immunofluorescence. **E)** RT-qPCR of miR-885-5p in CLE lesional and non-lesional skin from paired patients

(n=6). **F)** Immunofluorescence of PSMB5 in CLE lesional and non lesional skin from paired patients n=5. *In vitro* experiments were with performed a minimum of three replicates.

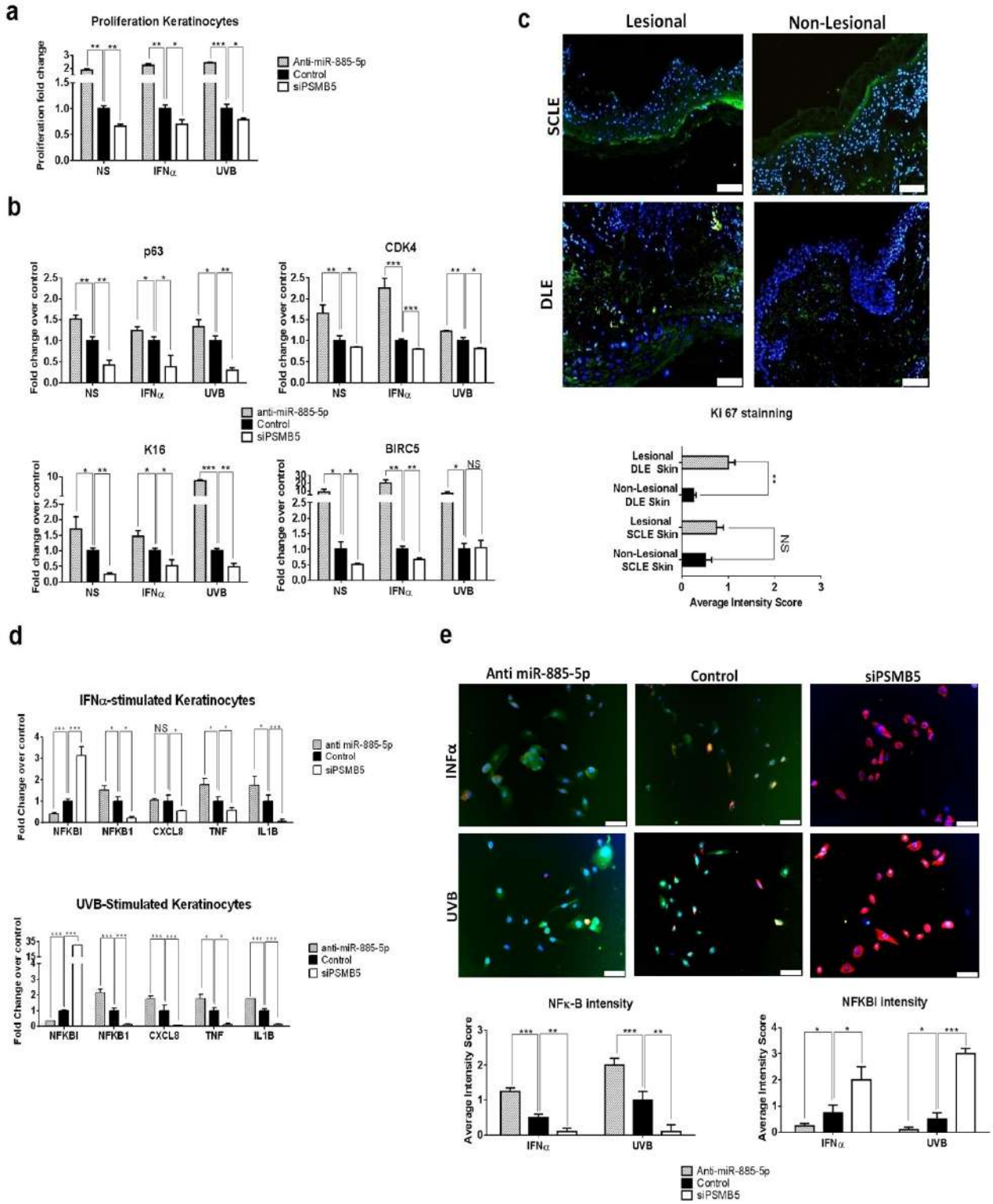

Figure 3. mir-885-5p inhibition promotes epidermal proliferation *in vitro* and NF-κB activation via PSMB5. A) Proliferation assay in anti-miR-885-5p and siPSMB5 transfected keratinocytes. **B)** Gene expression of epidermal proliferation genes anti-miR-885-5p keratinocytes and siPSMB5 keratinocytes. **C)** Immunofluorescence of KI67 in CLE

lesional and non-lesional skin (n=5). **D)** Gene expression of NF-κB signaling pathway molecules in UVB and IFN stimulated keratinocytes transfected with anti-miR-885-5p or siPSMB5. **E)** Merged Immunofluorescence of NF-κB (green), NFκBI inhibitor (red), nuclei (DAPI in blue) in anti-miR-5p and siPSMB5 keratinocytes. All experiments were performed in a minimum of triplicates. For gene expression assays, keratinocytes were transfected for 24h and stimulated for 6h. For protein expression assays, keratinocytes were transfected for 24h and stimulated for 24h.

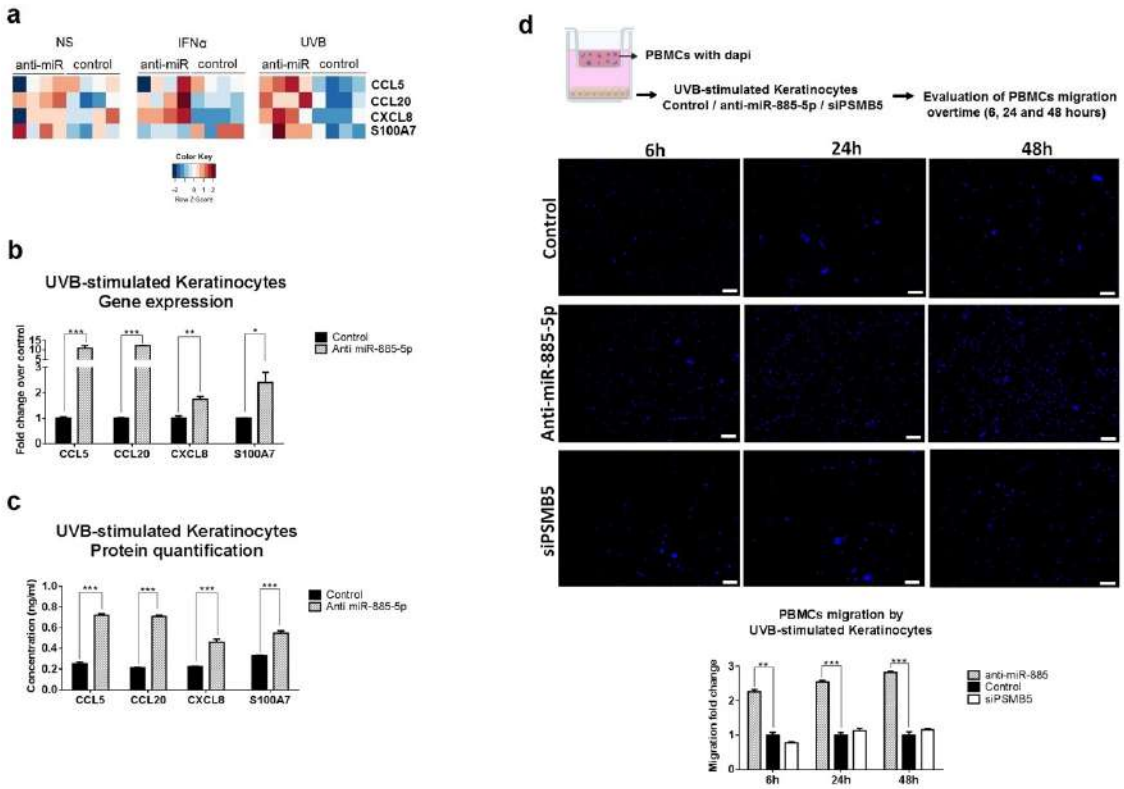

Figure 4. miR-885-5p inhibitions promotes the leukocyte-attracting capacity of keratinocytes independently of PSMB5. A) Heatmap showing differentially expressed chemokines CCL5, CCL20, CXCL8 and antimicrobial peptide S100A7 in anti-miR-885-5p transfected keratinocytes vs control. **B)** RT-qPCR of CCL5, CCL20, CXCL8 and S100A7 in anti-miR-885-5p transfected keratinocytes. **C)** Evaluation of CCL5, CCL20, CXCL8 and S100A7 in supernatant from anti-miR-885-5p keratinocytes. **D)** Migration assays in co-culture experiments. Keratinocytes were transfected (siPSMB5/anti-miR-885-5p) and on the next day UVB stimulated and PBMCs were stained with DAPI and seeded in the upper insert. Migration was evaluated at 6h, 24h and 48h.

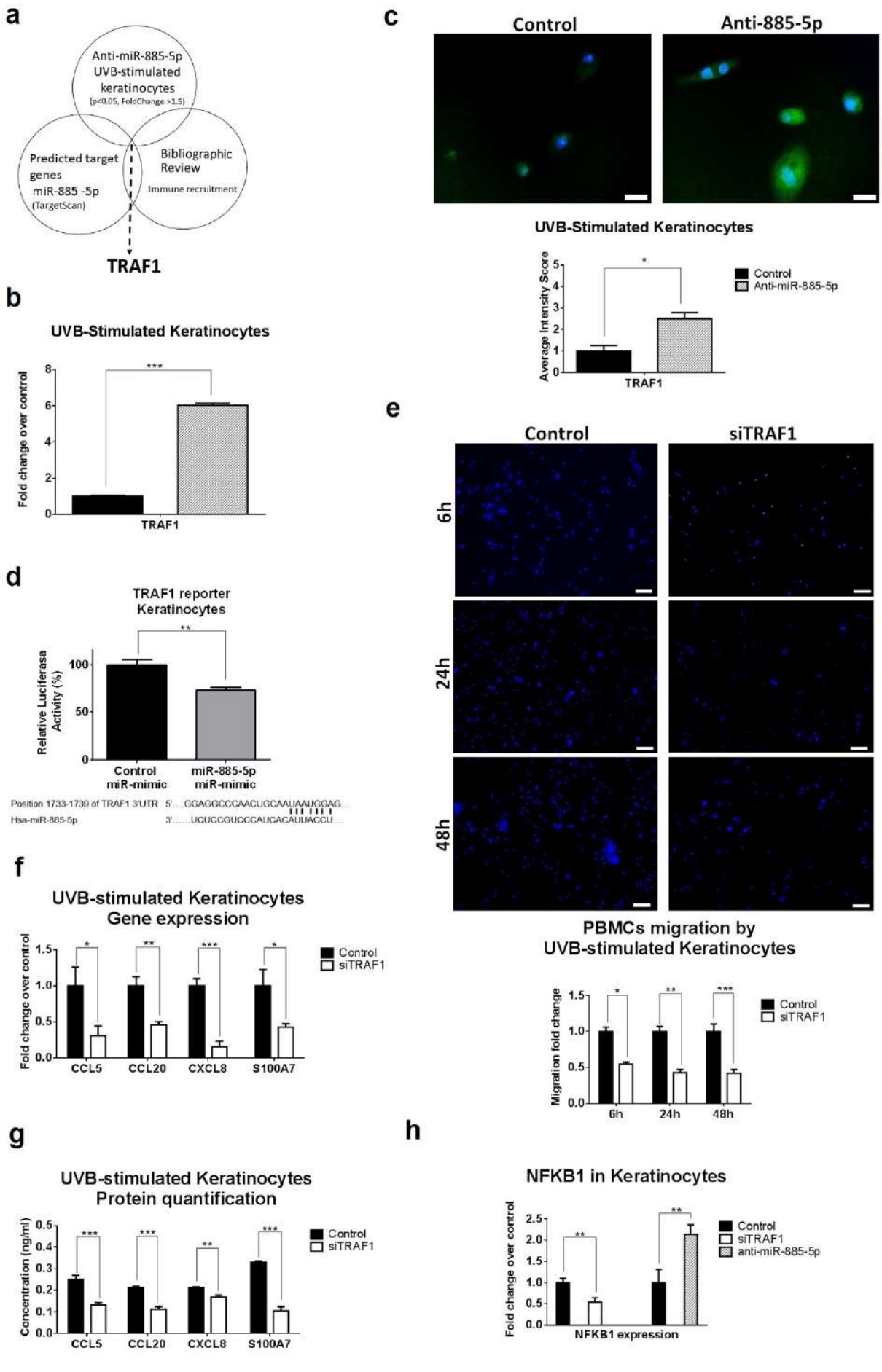
a
Anti-miR-885-5p
UVB-stimulated
keratinocytes
(p<0.05, FoldChange >1.5)
Predicted target
genes
miR-885 -5p
(TargetScan)
Bibliographic
Review
Immune recruitment
TRAF1
b
UVB-Stimulated Keratinocytes
Fold change over control
TRAF1
c
Control
Anti-885-5p
UVB-Stimulated Keratinocytes
Average Intensity Score
Control
Anti-miR-885-5p
TRAF1
d
TRAF1 reporter
Keratinocytes
Relative Luciferasa
Activity (%)
Control
miR-mimic
miR-885-5p
miR-mimic
Position 1733-1739 of TRAF1 3'UTR 5'....GGAGGCCCAACUGCAAUAAUGGAG...
Hsa-miR-885-5p 3'.....UCUCCGUCCCAUCACAUUACCU....
e
Control
siTRAF1
6h
24h
48h
PBMCs migration by
UVB-stimulated Keratinocytes
Migration fold change
Control
siTRAF1
6h
24h
48h
f
UVB-stimulated Keratinocytes
Gene expression
Fold change over control
Control
siTRAF1
CCL5
CCL20
CXCL8
S100A7
g
UVB-stimulated Keratinocytes
Protein quantification
Concentration (ng/ml)
Control
siTRAF1
CCL5
CCL20
CXCL8
S100A7
h
NFKB1 in Keratinocytes
Fold change over control
Control
siTRAF1
anti-miR-885-5p
NFKB1 expression

Figure 5. miR-885-5p targets TNF Receptor Associated Factor 1 (TRAF1) in keratinocytes promoting leukocyte recruitment. A) Venn diagram shows TRAF1 as a potential predicted miR-885-5p target gene related with immune recruitment and upregulated in anti-miR-885-5p transfected keratinocytes stimulates with UVB. **B)** TRAF1 gene expression in anti-miR-88-5p transfected keratinocytes stimulated with UVB. **C)** Immunofluorescence of TRAF1 in UVB-stimulated anti-miR-885-5p keratinocytes. **D)** Luciferase assay showed that TRAF1 is target gene of miR-885-5p. **E)** Migration assay of PBMCs co-cultured with siTRAF1 transfected keratinocytes stimulated with UVB. **F)** RT-qPCR of CCL5, CCL20, CXCL8 and S100A7 in siTRAF1 transfected keratinocytes. **G)** Evaluation of CCL5, CCL20, CXCL8 and S100A7 in supernatant from siTRAF1 keratinocytes. **H)** NFKB1 gene expression in siTRAF1 and anti-miR-885-5p keratinocytes.

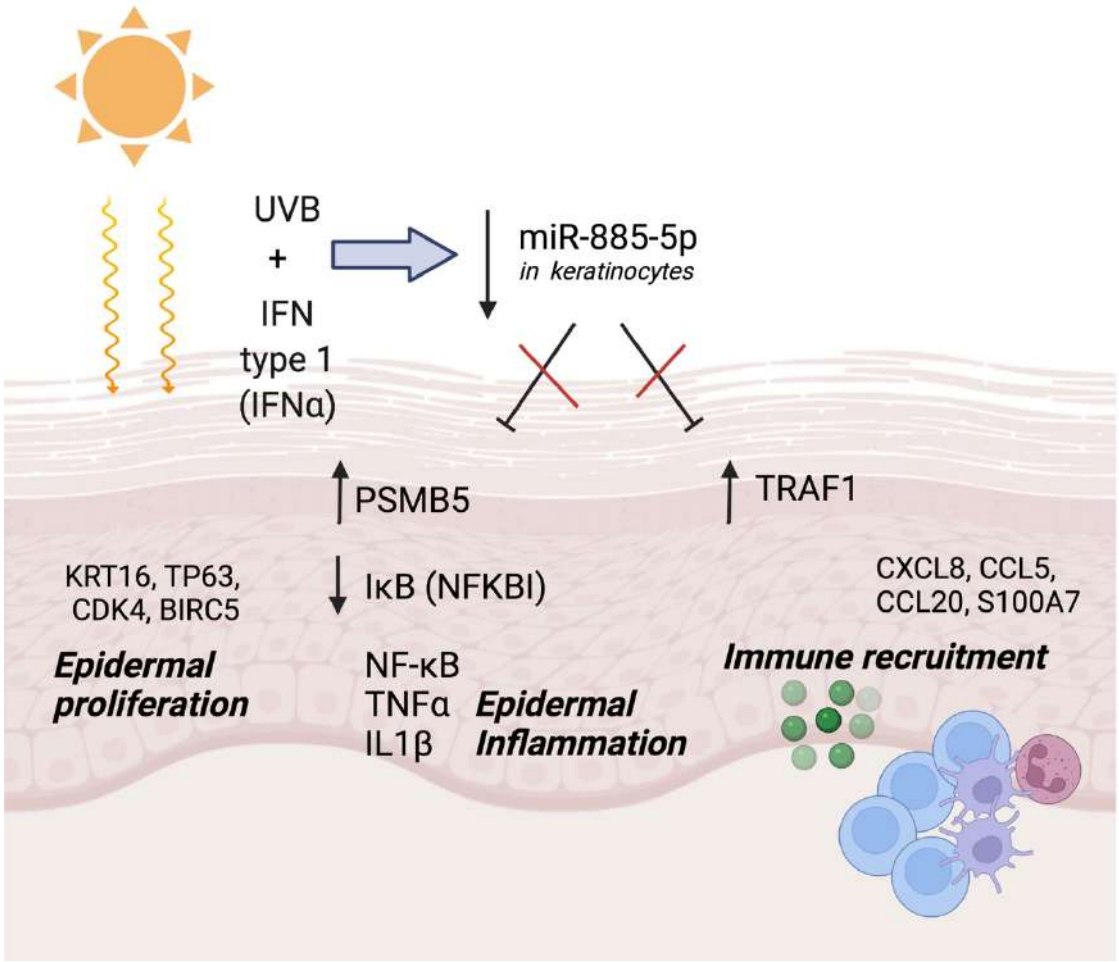

Figure 6. Role of low miR-885-5p levels in CLE. mIR-885-5p is downregulated in CLE epidermal keratinocytes and its downregulated is accentuated after UVB and IFN α. When downregulated it cannot target its two target genes PSMB5 and TRAF1. In turn, PSMB5 is upregulated and therefore IκB (NκFBI) is decreased and NFκB is activated and promotes epidermal inflammation and IL1β and TNFα expression. PSMB5 also promotes epidermal proliferation accompanied by an increase of KRT16, BIRC5, CDK4 and TP63 genes. On the other hand, TRAF1 is upregulated and therefore keratinocytes secrete chemokines CCL5, CCL20, CXCL8 and antimicrobial peptide S100A7 that promote leucocyte attraction and immune recruitment to the CLE lesional site.

References

Achtman JC, Werth VP. Pathophysiology of cutaneous lupus erythematosus. Arthritis Res Ther 2015;17:182.

Ambros V. The functions of animal microRNAs. Nature 2004;431:350–355.

Baek D, Villén J, Shin C, Camargo FD, Gygi SP, Bartel DP. The impact of microRNAs on protein output. Nature 2008;455:64-71.

Berthier CC, Tsoi LC, Reed TJ, Stannard JN, Myers EM, Namas R et al. Molecular Profiling of Cutaneous Lupus Lesions Identifies Subgroups Distinct from Clinical Phenotypes. J Clin Med 2019;8:1244.

Christopher AF, Kaur RP, Kaur G, Kaur A, Gupta V, Bansal P. MicroRNA therapeutics: Discovering novel targets and developing specific therapy. Perspect Clin Res 2016;7:68-74.

Chakraborty C, Sharma AR, Sharma G, Lee SS. Therapeutic advances of miRNAs: A preclinical and clinical update. J Adv Res 2020;28:127-138.

Chen ZJ. Ubiquitin signalling in the NF-kappaB pathway. Nat Cell Biol 2005;7(8):758-765.

de Jong EM, van Erp PE, Ruiter DJ, van de Kerkhof PC. Immunohistochemical detection of proliferation and differentiation in discoid lupus erythematosus. J Am Acad Dermatol 1991;25:1032-1038.

Deng GM, Tsokos G. Pathogenesis and targeted treatment of skin injury in SLE. Nat Rev Rheumatol 2015;11:663–669.

Dettmer M, Vogetseder A, Durso MB, et al. MicroRNA expression array identifies novel diagnostic markers for conventional and oncocytic follicular thyroid carcinomas. J Clin Endocrinol Metab 2013;98:E1-E7.

Domingo S, Solé C, Moliné T, Ferrer B, Cortés-Hernández J. MicroRNAs in Several Cutaneous Autoimmune Diseases: Psoriasis, Cutaneous Lupus Erythematosus and Atopic Dermatitis. *Cells*. 2020;9:2656.

Edilova MI, Abdul-Sater AA, Watts TH. TRAF1 Signaling in Human Health and Disease. Front Immunol 2018;9:2969.

Gallant-Behm CL, Piper J, Lynch JM, et al. A MicroRNA-29 Mimic (Remlarsen) Represses Extracellular Matrix Expression and Fibroplasia in the Skin. J Invest Dermatol 2019;139:1073-1081.

Gao T, Gu G, Tian J, et al. LncRNA HSP90AA1-IT1 promotes gliomas by targeting miR-885-5p-CDK2 pathway. Oncotarget 2017;8:75284-75297.

Gilliam JN, Sontheimer RD. Distinctive cutaneous subsets in the spectrum of lupus erythematosus. J Am Acad Dermatol 1981;4:471-5.

Grönhagen CM, Nyberg F. Cutaneous lupus erythematosus: An update. Indian Dermatol Online J 2014;5:7-13.

Guo F, Sun A, Wang W, He J, Hou J, Zhou P et al. TRAF1 is involved in the classical NF-kappaB activation and CD30-induced alternative activity in Hodgkin's lymphoma cells. Mol Immunol 2009;46:2441-2448.

Kahlenberg JM. Rethinking the Pathogenesis of Cutaneous Lupus. J Invest Dermatol 2021;141:32-35.

Lazar S, Namas R, Berthier CC, Kahlenberg M. IFN-Gene Expression Is Elevated in Subacute Cutaneous Lupus Erythematous and DLE and Decreases with Treatment in DLE [abstract]. Arthritis Rheumatol 2018;70 (suppl 10).

Liu Y, Bao Z, Tian W, Huang G. miR-885-5p suppresses osteosarcoma proliferation, migration and invasion through regulation of β-catenin. Oncol Lett 2019;17:1996-2004.

Missiou A, Köstlin N, Varo N, Rudollf R, Acihele P, Ernst S et al. Tumor necrosis factor receptor-associated factor 1 (TRAF1) deficiency attenuates atherosclerosis in mice by impairing monocyte recruitment to the vessel wall. Circulation 2010;121:2033-2044.

Okon LG, Werth VP. Cutaneous lupus erythematosus: diagnosis and treatment. Best Pract Res Clin Rheumatol 2013; 27:391-404.

Oyoshi MK, Barthel R, Tsitsikov EN. TRAF1 regulates recruitment of lymphocytes and, to a lesser extent, neutrophils, myeloid dendritic cells and monocytes to the lung airways following lipopolysaccharide inhalation. Immunology 2007;120:303-314.

Robinson ES, Werth VP. The role of cytokines in the pathogenesis of cutaneous lupus erythematosus. Cytokine 2015;73:326-334.

Sarkar MK, Hile GA, Tsoi LC, Xing X, Liu J, Liang Y et al. Photosensitivity and type I IFN responses in cutaneous lupus are driven by epidermal-derived interferon kappa. Ann Rheum Dis 2018;77:1653-1664.

Seifert U, Bialy LP, Ebstein F, Bech-Otschir D, Voigt A, Schroter F et al. Immunoproteasomes preserve protein homeostasis upon interferon-induced oxidative stress. Cell 2010; 142: 613–624.

Sinha AA, Dey-Rao R. Genomic Investigation of Lupus in the Skin. J Investig Dermatol Symp Proc 2017;18:S75-S80.

Solé C, Domingo S, Ferrer B, Moliné T, Ordi-Ros J, Cortés-Hernández J. MicroRNA Expression Profiling Identifies miR-31 and miR-485-3p as Regulators in the Pathogenesis of Discoid Cutaneous Lupus. J. Investig. Dermatol 2019;139:51–61.

Solé C, Gimenez-Barcons M, Ferrer B, Ordi-Ros J, Cortés-Hernández J. Microarray study reveals a transforming growth factor-β-dependent mechanism of fibrosis in discoid lupus erythematosus. Br J Dermatol 2016;175:302-13.

Sonkoly E, Wei T, Janson PC, Sääf A, Lundeberg L, Tengvall-Linder M et al. MicroRNAs: novel regulators involved in the pathogenesis of psoriasis?. PLoS One 2007;2:e610.

Stannard JN, Reed TJ, Myers E, Lowe L, Sarkar MK et al. Lupus Skin Is Primed for IL-6 Inflammatory Responses through a Keratinocyte-Mediated Autocrine Type I Interferon Loop. J Invest Dermatol. 2017;137(1):115-122. doi:10.1016/j.jid.2016.09.008

Su M, Qin B, Liu F, Chen Y, Zhang R. miR-885-5p upregulation promotes colorectal cancer cell proliferation and migration by targeting suppressor of cytokine signaling. Oncol Lett 2018;16:65–72.

Tanaka K. The proteasome: overview of structure and functions. Proc Jpn Acad Ser B Phys Biol Sci 2009;85:12-36.

Tebbe B, Orfanos CE. Epidemiology and socioeconomic impact of skin disease in lupus erythematosus. Lupus 1997;6:96–104.
Wenzel, J. Cutaneous lupus erythematosus: new insights into pathogenesis and therapeutic strategies. Nat Rev Rheumatol 2019;15:519–532.

Tsoi LC, Hile GA, Berthier CC, Sarkar MK, Reed TJ, Liu J et al. Hypersensitive IFN Responses in Lupus Keratinocytes Reveal Key Mechanistic Determinants in Cutaneous Lupus. J Immunol 2019;202:2121-2130.

Tu Y, Chen C, Pan J, Xu J, Zhou ZG, Wang CY. The Ubiquitin Proteasome Pathway (UPP) in the regulation of cell cycle control and DNA damage repair and its implication in tumorigenesis. Int J Clin Exp Pathol 2012;5:726-738.

Turnier JL, Kahlenberg JM. The Role of Cutaneous Type I IFNs in Autoimmune and Autoinflammatory Diseases. J Immunol 2020;205:2941-2950.

Vangala JR, Dudem S, Jain N, Kalivendi SV. Regulation of PSMB5 protein and β subunits of mammalian proteasome by constitutively activated signal transducer and activator of transcription 3 (STAT3): potential role in bortezomib-mediated anticancer therapy. J Biol Chem 2014;289:12612-12622.

Xie P. TRAF molecules in cell signaling and in human diseases. J Mol Signal 2013;8:7.

Xu F, Yan JJ, Gan Y, Chang Y, Wang HL, He XX et al. miR-885-5p negatively regulates warburg effect by silencing hexokinase 2 in liver cancer. Mol Ther Nucleic Acids 2019;18:308–19.

Yamamoto H, Ryu J, Min E, et al. TRAF1 Is Critical for DMBA/Solar UVR-Induced Skin Carcinogenesis. J Invest Dermatol 2017;137:1322-1332.

Yi R, Fuchs E. MicroRNA-mediated control in the skin. Cell Death Differ. 2010;17:229–235.

Yi R, O'Carroll D, Pasolli HA, Zhang Z, Dietrich FS, Tarakhovsky A et al. Morphogenesis in skin is governed by discrete sets of differentially expressed miRNAs. Nat. Genet 2006;38:356–362.

Zhou X, Yan J, Lu Q, Zhou H, Fan L. The pathogenesis of cutaneous lupus erythematosus: The aberrant distribution and function of different cell types in skin lesions. Scand J Immunol 2021;93:e12933

Zu Y, Wang Q, Wang H. Identification of miR-885-5p as a Tumor Biomarker: Regulation of Cellular Function in Cervical Cancer. Gynecol Obstet Invest 2021;86:525-532.

Supporting Information

MicroRNA-885-5p is downregulated in Cutaneous Lupus Erythematosus lesions and promotes epidermal inflammation and proliferation via PSMB5 and immune recruitment via TRAF1

Sandra Domingo[1], Laura Porres[1], Cristina Solé[1], Teresa Moliné[2], Berta Ferrer[2], Josefina Cortés-Hernández[1]

[1] Rheumatology Research Group - Lupus Unit, Vall d'Hebrón University Hospital, Vall d'Hebrón Research Institute (VHIR), Universitat Autònoma de Barcelona (UAB), Barcelona, Spain.

[2] Department of Pathology, Vall d'Hebrón University Hospital, Barcelona, Spain.

SI Materials and Methods

Patients' clinical characteristics and samples

A total of 20 CLE patients were included in the study. Demographic characteristics are shown in Table S1. At the time of skin biopsy, disease activity and degree of scarring was assessed by the validated modified CLE Disease Area and Severity Index (CLASI) (Albrecht et al., 2005). Patient's inclusion criteria included: age ≥ 18 years old, the presence of skin lesional area bigger than 3cm, a validated CLE Disease Area and Severity Index (CLASI) greater than 4 and no previous treatment with immunosuppressants for ≥1 month or topical corticoids for at least ≥2 weeks. The study was approved by the Local Vall d'Hebrón Ethics Committee and informed consent was obtained from all subjects before the study.

Two six-millimetre punch biopsies were taken from lesional and non-lesional skin from 20 CLE untreated patients with active disease for histology analysis and *in vitro* experiments (Supplementary Table S1). The first 6mm punch of lesional and non-lesional skin biopsy was fixed in 5% formalin and embedded in paraffin blocks for the histological examination, immunohistochemistry or hybridization *in situ*. The second 6mm punch of lesional skin biopsy and skin biopsies from healthy donors (n=10) were immediately processed to obtain their primary keratinocytes. The diagnosis and classification of CLE were based on clinical and histological criteria according to the 2004 Dusseldorf classification (Khun and Ruzicka, 2004). Disease activity and degree of scarring was assessed by the validated modified CLE Disease Area and Severity Index (CLASI) (Albrecht et al, 2005).

Blood samples were also extracted for PBMCs isolation. Blood samples were collected in mononuclear cell preparation tubes with sodium citrate (Vacutainer CPT, BD Bioscences). After 25 min of centrifugation at 3000 rpm the section containing PBMCs was clearly visible and cells were collected using a pipette and washed twice in phosphate buffered saline (PBS). The cellular pellet was frozen at -80ºC for the miRNA extraction and also frozen with cell culture freezing medium for *in vitro* experiments.

Skin in situ hybridization

Hybridization with hsa-miR-885-5p with 5′-DIG and 3′-DIG–labeled miRCURY LNA detection probe (Exiqon, Copenhagen, Denmark) was performed overnight at 50°C. The probe binding was detected by incubating sections with anti-DIG-alkaline phosphatase

antibody (1:800; Roche, Basel, Switzerland) for 2 hours at room temperature. The staining was blinded evaluated.

Evaluation of in situ hybridization, immunohistochemistry and immunofluorescence in skin sections

In situ hybridization, immunohistochemistry and immunofluorescence results were evaluated on blinded specimens by three independent dermatopathologists from the Vall d'Hebron pathology unit. Positive cells per millimetre were quantified using computer-assisted image analysis software (ImageJ 1.42, National Institutes of Health, Bethesda, MD, USA) and evaluated by Olympus IX71 (TH4-200) U-RFL-T microscope. The staining of the epidermis, dermis and inflammatory infiltrate was evaluated semi-quantitatively using the following blinded score: 0 (<10% positive cells), 0.5 (10-20% positive cells), 1 (20-40% positive cells), 1.5 (40-60% positive cells), 2 (60-80% positive cells), 2.5 (80-90% positive cells) or 3 (>90% positive cells).

Isolation of primary human keratinocytes from the skin biopsy

Primary human keratinocytes were isolated following the optimised protocol from Belmonte (Trond and Belmonte, 2010). Briefly, punch skin biopsies of 6 mm from lupus cutaneous patients (n=20) and healthy controls (n=10) were obtained, then incubated with dispase overnight at 4ºC to peel off the dermis from epidermis and they were cut into 2-3-mm pieces to be digested with TrypLE Express Enzyme (1X) at 37°C during 18min, separately. Then epidermis skin pieces were mechanically dissociated and filtered through a 40-µm cell strainer (Falcon, BD Biosciences). The filtrate was centrifuged at 1600g during 5min at 4ºC. The cellular pellets were resuspended in in 10mL Epilife Medium supplemented with 10% HGSK and 5% antibiotics. The cells were cultured in 25 cm^2 tissue culture flasks (Cell+ Sarstedt) at 37°C in 5% CO_2 and the medium cells were change every 2-3 days. In the present study, keratinocytes at passage 2 were used for all experiments.

PBMCs isolation from blood

Blood from CLE patients before and after thalidomide treatment and healthy controls was collected directly into mononuclear cell preparation tubes with sodium citrate (Vacutainer CPT, BD Biosciences). Tubes were centrifuged at 3000 rpm for 30 minutes at room temperature (RT). After that, the layer containing peripheral blood mononuclear cells was clearly visible and collected using a pipette. Cells were washed twice with PBS and

resuspended in complete RPMI media (RPMI, 10% FBS, 10% Pen/Strep, 2 mM/L-Glutamine) (Gibco, Life Technologies).

Immunofluorescence on primary cells

Healthy Human epidermal keratinocytes (HEKa cells, Life Technologies, Carlsbad, CA) were seeded in sterile glass coverslips in 24 well-plates and incubated overnight at 37ºC for adherence. After anti-miR transfection, keratinocytes were stimulation with IFNα (10 ng/mL, Life Technologies) or 25 mJ/cm^2 or steril PBS (in non-stimulated conditions) during 6 hours. Then, cells were washed with PBS and then fixed for 15 minutes in 4% PFA followed by permeabilization with 0.1% TritonX-100 for 10 minutes. Blocking solution (BSA 5%) was added for 1 hour at RT and primary antibodies were incubated overnight at 4ºC and secondary antibodies were added for 2h at RT (Table S2). DAPI was used to visualize the nucleus. Images were captured using Olympus BX61 microscope.

RNA extraction

Skin biopsies were homogenised by politron and RNA was purified using miRVANA miRNA Isolation Kit (Applied Biosystems) following manufacturer's instructions. Total RNA from cultured cells was extracted after cell lysis with RNeasy Mini Kit (Qiagen). The yield and the quality of RNA from cell cultures were assessed by measuring its absorbance at 260nm and 280nm with Nanodrop. Ratios of A260/A280 between 1.8 and 2.1 were considered acceptable to use the RNA for the subsequent experiments.

Microarray analysis

Microarrays were carried out using Genechip Human Gene 1.0 ST Array (an array with 14,500 well-characterised human genes used to explore human biology and disease processes). The arrays were performed at the Scientific and Technical Support Unit of our Research Institute as described elsewhere (Affymetrix, Santa Clara, CA, www.affymetrix.com). Data obtained from the microarrays were analysed by the Statistics and Bioinformatics Unit of our research institute.

RT-qPCR

Once RNA was obtained, 1ug of total RNA was reverse-transcribed into cDNA using the High Capacity cDNA Reverse Transcription Kit (Applied Biosystems) with the thermal cycler program: 25ºC for 10min, 37ºC for 120 min and 85ºC for 5min. Gene expression

was assessed by TaqMan gene expression assays (FAM dye-labeled MGB probe, Applied Biosystems). Using 96 well plates or 384 well plates in the ABI PRISM 7000 or ABI PRISM 7900 thermocyclers respectively at 50ºC for 2 min, 95ºC for 10min, followed by 40 cycles of 95ºC for 15s and 60ºC for 1 min. Obtained data was normalised based on the expression of the endogenous control gene GAPDH (Hs02786624_g1).

Apoptosis and Proliferation Assays

Cells were plated in 24-well plates, stimulated with 25 mJ/cm2 in case of Keratinocytes or 10 ng/mL TNFα (Life Technologies) for PBMCs and thalidomide was added for 24h. Then, they were stained with Dead Cell Apoptosis Kit with Annexin V APC and SYTOX™ Green (Thermofisher) and measured by flow cytometry. For proliferation assays, cells were plated in 96-well plates, stimulated and thalidomide was added. After 24h, CyQUANT NF Cell Proliferation Assay Kit (Invitrogen) was used following manufacturer's instructions. Relative changes were calculated using "Non-Thalidomide treated cells" as control.

Supplementary Figures

Supplementary Fig 1. Inhibition of miR-885-5p was confirmed by qRT-PCR analysis in keratinocytes before to perform microarray analysis. Four replicates were used for the microarray analysis in each condition. Keratinocytes were stimulated with IFN (10ng/mL) or UVB radiated (25 mJ/cm) or non-stimulated (NS). * p<0.05, ** p<0.005 and ***p>0.001.

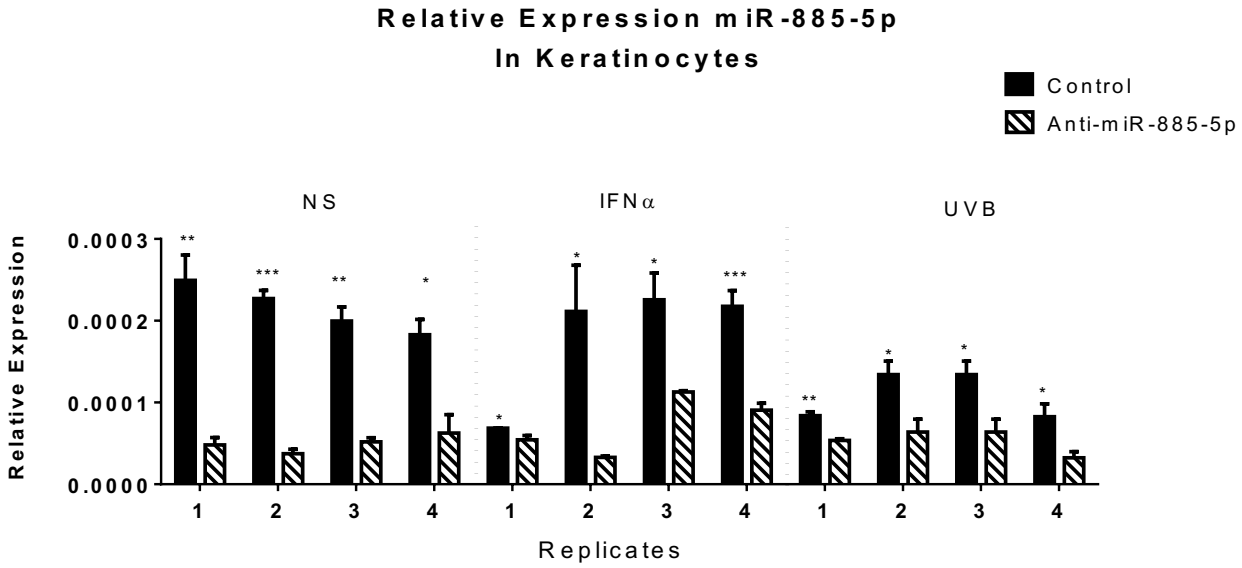

Supplementary Fig 2. Volcano plots from microarray of miR-885-5p inhibited or not inhibited (control) keratinocytes showed the top 20 most significant differentially expressed genes (DEG) for each comparison. Keratinocytes were non-stimulated (NS) or stimulated with interferon (IFNα) or UVB radiation.

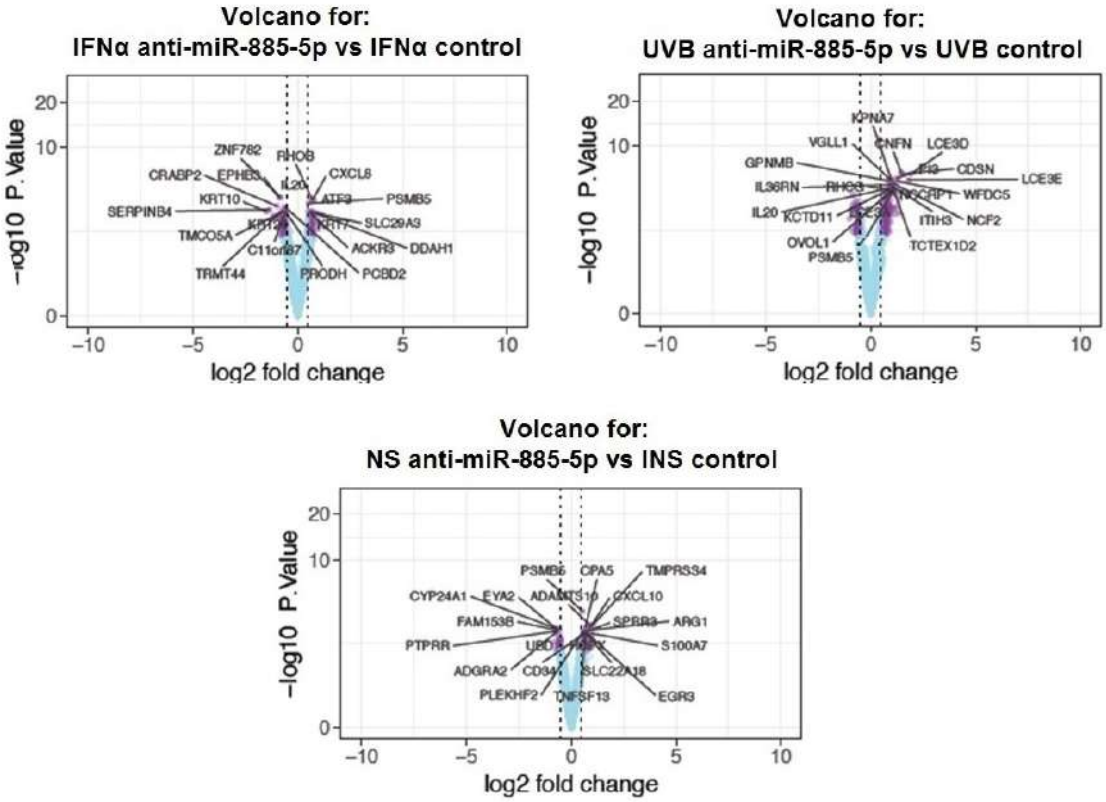

Supplementary Fig 3. Primary keratinocytes were transfected to inhibit miR-885-5p (anti miR-885-5p). Then, they were non-stimulated (NS) or stimulated with interferon alpha or UVB radiation. Gene expression of PSMB5 was evaluated by qRT-PCR showing an upregulation in anti miR-885-5p condition. Fold change over control condition and normalised using GAPDH as endogenous gene. * p<0.05, ** p<0.005 and ***p>0.001.

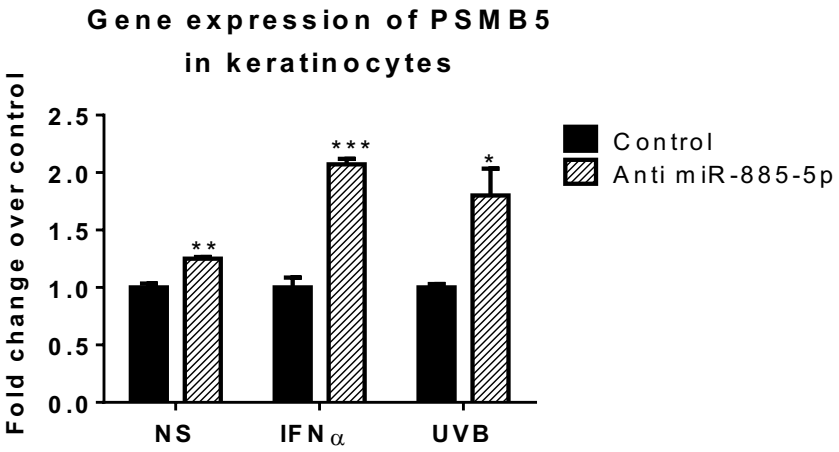

Supplementary Fig 4. A significant inverse correlation was found in the relationship between the relative gene expression (RE) of PSMB5 and the relative gene expression (RE) of miR-885-5p in primary keratinocytes.

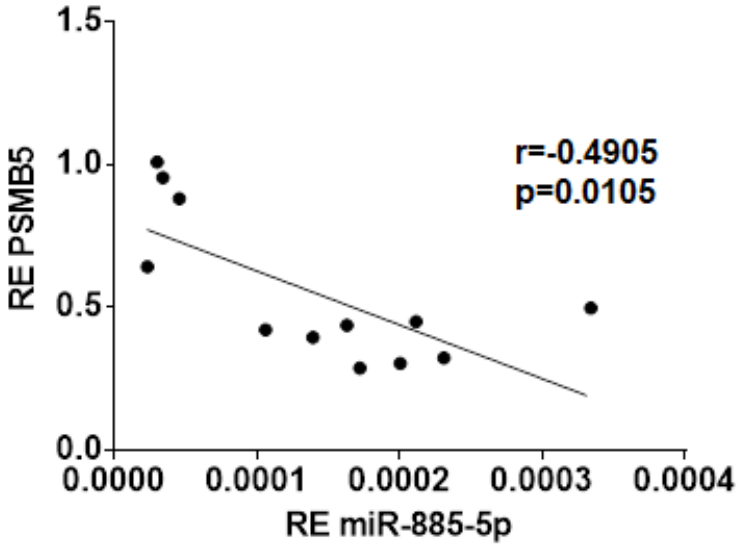

Supplementary Fig 5. Apoptosis of Human epidermal keratinocytes after inhibition of miR-885-5p. Cells were stimulated with IFNα (10ng/mL), non-stimulated (NS) or they were radiated with 25mJ/cm^2 UVB during 6hours after inhibition. Apoptotic cells were calculated by flow cytometry analysis. No significant difference were observed between inhibited (anti-miR-885-5p) and non-inhibited cells (control).

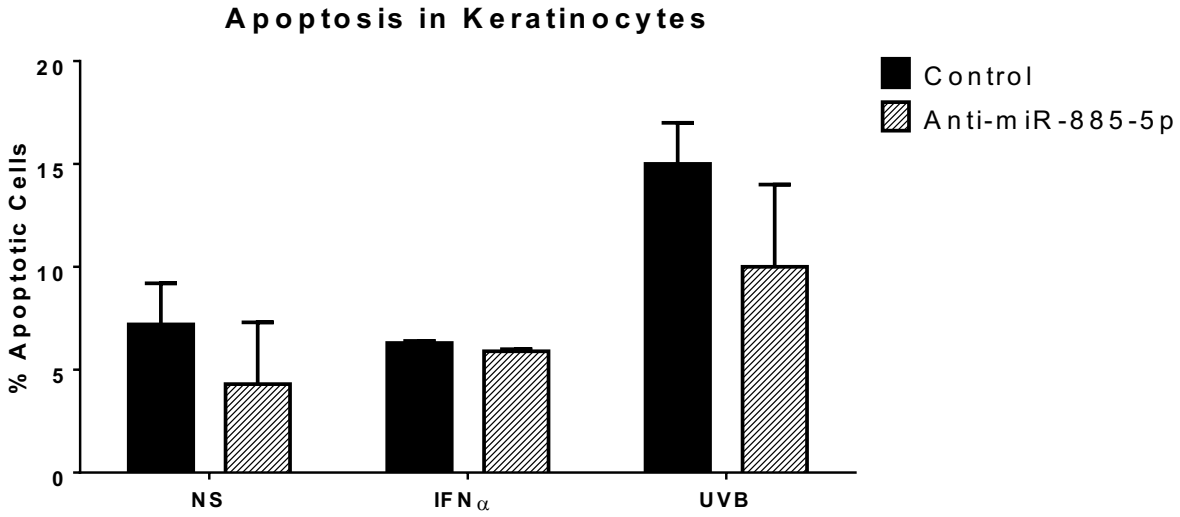

Supplementary Fig 6. A significant inverse correlation was found in the relationship between the relative gene expression (RE) of TRAF1 and the relative gene expression (RE) of miR-885-5p in primary keratinocytes.

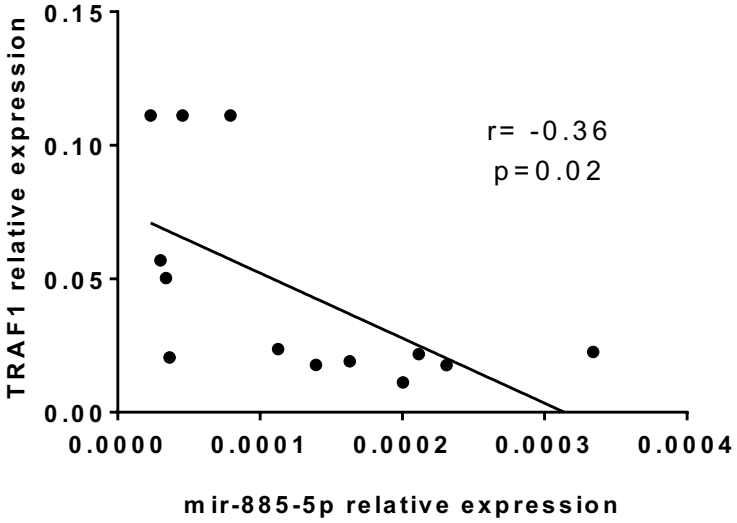

Supplementary Tables

Table S1. Clinical and laboratory characteristics of the study subjects.

	CLE (n=20)
AGE, mean (SD), yrs	47 (13.1)
Female, n (%)	15 (75%)
Photosensitivity, n (%)	8 (40%)
Smoking, (%)	7 (35%)
CLASI ACTIVITY, mean (SD)	8.17 (2.9)
CLASI DAMAGE, mean (SD)	0.98 (1.18)
Type of CLE (DLE/CLE)	10/10
Systemic Lupus Erythematosus	10 (50%)
Duration of cutaneous lesions, months, mean (SD)	7.5 (4.6)
ANA positive, n (%)	12 (60%)
Anti-Ro positive, n (%)	6 (30%)

Values are number of patients and between brackets the percent of total number patients. The other values are means and SD in brackets. CLASI: Cutaneous Lupus Erythematosus Disease Area and Severity Index; CLE: cutaneous lupus erythematosus; DLE: discoid lupus erythematosus; SCLE: subacute cutaneous lupus erythematosus; ANA: Antinuclear Antibodies.

Table S2. Antibodies used in Immunofluorescence analysis.

Primary Antibody	**Supplier**	**Code**
Anti-PSBM5	Genetex	GXT104687
Anti-Ki67	Affinit	AF0198
Anti-TRAF1	Genetex	GXT102372
Anti-NFKB	Genetex	GTX102090
Anti-NFKBIA	Genetex	GTX12138
Secondary Antibody	**Supplier**	**Code**
Alexa-488-conjugated anti-rabbit IgG	Abcam	ab150077

Table S3. Primer IDs used in Taqman RT-qPCR from Applied Biosystems.

miRNAs	Assay ID (TaqMan)
U6 snRNA	001973
miR-885-5p	002296

Gene	Assay ID (TaqMan)
GADPH	Hs02786624_g1
PSBM5	Hs00605652_m1
P63	Hs00978340_m1 (TP63)
K16	Hs00373910_g1 (KRT16)
CDK4	Hs00364847_m1
BIRC5	Hs04194392_s1
CCL5	Hs00982282_m1
CCL20	Hs00355476_m1
CXCL8 (IL8)	Hs00174103_m1
TNF	Hs00174128_m1
IL1B	Hs01555410_m1
S100A7	Hs01923188_u1
TRAF1	Hs01090170_m1
NFKB1	Hs00765730_m1
NFKBIA	Hs00355671_g1

Table S4. Table with the top 20 most significant genes for each condition (IFN alpha stimulation, UBV radiation and Non-stimulation condition) between control and anti-miR-885-5p keratinocytes. Marked in bold the unique common gene (PSMB5).

Condition	Most significant genes
IFNα anti-miR-885-5p vs IFNα control	ANF782, RHOB, IL20, EPHB3, CRABP2, KRT10, KRT2, SERPINB4, TMCO5A, C11orf87, TRMT44, PRODH, PCBD2, ACKR3, KRT7, DDAH1, SLC29A3, ATF2, CXCL8, **PSMB5**
UVB anti-miR-885-5p vs UVB control	VGLL1, GPNMB, IL36RN, RHCG, IL20, KCTD11, OVOL1, ITIH3, NCF2, TCTEX1D2, NSCRP1, KPNA7, CNFN, LCE3D, CDSN, LCE3E, WFDC5, LCE3A, PI3, **PSMB5**
NS anti-miR-885-5p vs NS control	ADAMTS10, EYA2, CYP24A1, FAM153B, PTPRR, ADGRA2, UBD, HOPX, CD34, PLEKHF2, TNFSF13, S100A7, SLC22718, EGFR3, SPRR3, ARG1, CXCL10, TMPRSS4, CPA5, **PSMB5**

Table S5. Detail of the targets identified for miR-885-5p using the upregulated genes of anti-885-5p UVB-stimulated keratinocytes in the microarray and the predicted target genes provided by TargetScan data base. TRAF1 gene is the most related with recruitment and immune response (in bold).

Gene	P.Value	Fold Change	Function
FZD10	0,00048074	1,818524029	Members of this family encode 7-transmembrane domain proteins that are receptors for the Wingless type MMTV integration site family of signaling proteins. Most frizzled receptors are coupled to the beta-catenin canonical signaling pathway
TRPV3	0,000439452	1,810590133	Functions in a variety of processes, including temperature sensation and vasoregulation.
SLC28A3	0,000177666	1,793438903	Nucleoside transporters, such as SLC28A3, regulate multiple cellular processes, including neurotransmission and vascular tone.
RTN2	7,95298E-05	1,740076895	Reticulon proteins play an important role in the replication of positive-strand RNA (ssRNA) viruses
IL6R	0,000641478	1,696482011	Among its related pathways are Autophagy pathway and Cytokine Signaling in Immune system.
S100A7A	0,006271826	1,645514135	Gene Ontology (GO) annotations related to this gene include calcium ion binding and protein self-association.
ACVR1C	0,003456468	1,629626446	Gene Ontology (GO) annotations related to this gene include transferase activity, transferring phosphorus-containing groups and protein tyrosine kinase activity
GSDMA	0,000487379	1,615386424	This form constitutes the precursor of the pore-forming protein: upon cleavage, the released N-terminal moiety (Gasdermin-A, N-terminal) binds to membranes and forms pores, triggering cell death.
GPLD1	0,008885674	1,561920502	The protein encoded by this gene is a glycosylphosphatidylinositol (GPI) degrading enzyme
TRAF1	**0,003070282**	**1,536103429**	**This protein and TRAF2 form a heterodimeric complex, which is required for TNF-alpha-mediated activation of MAPK8/JNK and NF-κB regulation of immune response and immune recruitment.**
IGFBP3	0,000307371	1,534180704	Insulin-like growth factor binding protein (IGFBP) family and encodes a protein with an IGFBP domain and a thyroglobulin type-I domain.
RORA	0,003542912	1,5317749	The encoded protein has been shown to interact with NM23-2, a nucleoside diphosphate kinase involved in organogenesis and differentiation
AQP9	0,001445176	1,525038695	This protein allows passage of a broad range of noncharged solutes and also stimulates urea transport and osmotic water permeability
LYVE1	0,007181546	1,524319893	The encoded protein acts as a receptor and binds to both soluble and immobilised hyaluronan. This protein may function in lymphatic hyaluronan transport and have a role in tumor metastasis.
C15orf62	0,00925998	1,512971676	Annotations related to this gene include small GTPase binding
SLC22A23	0,001068164	1,511087523	SLC22A23 belongs to a large family of transmembrane proteins that function as uniporters, symporters, and antiporters to transport organic ions across cell membranes

Chapter 2: Thalidomide mechanism of action in CLE

Paper III: Thalidomide Exerts Anti-Inflammatory Effects in Cutaneous Lupus by Inhibiting the IRF4/NF-κB and AMPK1/mTOR Pathways

Thalidomide drug has a high clinical efficacy in CLE that ranges between 80-90% in refractory patients. However, despite its proven efficacy its use is restricted due to the severe side effects associated to its use such as teratogenesis and peripheral neuropathy. Since our group has experience with the use of thalidomide in CLE, in this part of the study we aimed to investigate the mechanism of action by which thalidomide improves CLE and to identify novel molecular targets for CLE therapy. We performed RNA sequencing in skin biopsies from CLE patients before and after thalidomide treatment. After that, we included the results together with the information obtained from the literature regarding the immunomodulatory properties of thalidomide and we used TMPS analysis protocols to identify the mechanism of action in CLE. A putative thalidomide mechanism of action was identified, and *in vitro* experiments have been performed to validate the obtained results.

Thalidomide ameliorates skin inflammation by decreasing CD8$^+$ T cells, increasing invariant NKT (iNKT) cells and promoting a TH2 response in CLE.

First, in order to study immunomodulatory properties of thalidomide, circulating immune cells were characterised by flow cytometry in 7 thalidomide treated patients that presented clinical remission (CLASI =0). After thalidomide treatment, we observed a reduction of cytotoxic CD8$^+$ T-cells ($p<0.05$) and an increase of iNKT cells ($p = 0.006$) (Annex 4). Analysis of Th subsets showed that thalidomide treated patients have an imbalance towards a Th2 response ($p<0.05$). Immunohistochemical studies in CLE skin showed similar results, with a significant reduction of CD8$^+$ T-cells ($p<0.05$) and an increase of iNK T-cells post-thalidomide ($p<0.01$).

Thalidomide acts in CLE by modulating two CRL4CRBN-dependent pathways: IRF4-NF-κB and AMPK/mTOR

Next, in order to get insights into the thalidomide mechanism of action (MoA) in cutaneous lupus, a system biology approach was conducted with TPMS analysis which allowed the identification of putative proteins (motives) that mediate the action of thalidomide. Into detail, first, relevant proteins in CLE and Thalidomide were identified through the analysis of published biological information. Next, to obtain further insights into the molecular basis of CLE, we performed an RNA-sequencing in skin of pre and post-thalidomide treated

responder patients (n=7) which revealed 448 differentially expressed transcripts, of which 339 were protein coding genes (|log2(FC)| ≥ 1; Adj. *p* value < 0.05, data available GSE162424). Finally, the data obtained from bibliography and the biological data (RNA-seq data) was used to construct and restrict a model respectively. As a result, it was identified that thalidomide may act in CLE by two $CRL4^{CRBN}$-dependent mechanisms: downregulating IRF4, leading to an inhibition of the NF-κB signaling pathway; and regulating AMPK/mTOR signaling pathway.

Validation of the identified thalidomide mechanism of action

The protein expression pattern of the identified key molecules was evaluated in CLE skin pre and post thalidomide treatment by immunofluorescence. According to the identified mechanism, IRF4 and mTOR (Mammalian target of rapamycin) were significantly upregulated in the pre-treated skin when compared to post-treatment ($p>0.05$ and $p>0.0001$ respectively) and AMPKa1 was upregulated ($p<0.001$). In detail, IRF4 was detected in the dermal inflammatory infiltrate of lesional CLE and mTOR and AMPKa1 were expressed in the epidermal keratinocytes from pre-treated and post-treated skin samples respectively.

- ***Thalidomide modulates IRF4 in PBMCs.***

We next focused on IRF4 pathway in PBMCs, as IRF4 was mainly located in infiltrated immune cells in CLE skin. *In vitro* experiments showed that thalidomide addition decreased IRF4 and NF-κB in PBMCs and also related cytokines such as *CCL3, IL8, IL2, TNF,* and *IL1B*. Similar results were observed in siIRF4 PBMCs, indicating that thalidomide anti-inflammatory effect in PBMCs is dependent on IRF4 modulation

- ***Thalidomide modulates AMPK/mTOR in keratinocytes***

We next focused on AMPK/mTOR pathway in keratinocytes as both molecules were detected in CLE epidermis. *In vitro* experiments showed that thalidomide addition decreased mTOR and increased AMPKa1 in primary keratinocytes and also decreased the expression of related inflammatory mediator *TGFB1*. Effects in NF-κB pathway were also explored and we found that it was also modulated by mTOR and that related cytokines *IL1B, TNF,* and *CXCL1* were decreased in both thalidomide treated and simTOR cells. These results indicate that thalidomide may exert an anti-inflammatory effect in keratinocytes that is mediated by mTOR and that there is a crosstalk between and AMPK/mTOR and NF-κB signaling pathways.

Thalidomide in PBMCs decrease epidermal inflammation by decreasing AMPK/mTOR- N-κB pathway in keratinocytes

As the interaction between epithelial cells and the immune system is tightly regulated and of crucial importance in CLE, *in vitro* coculture functional studies were performed. Keratinocytes were plated on the lower chamber and PBMCs Thalidomide treated or siIRF4 were placed on the upper insert. We observed that thalidomide-treated PBMCs co-cultured with keratinocytes produced a significant downregulation of keratinocyte mTOR protein levels and an increase of AMPKa1 and phosphorylated RPTOR, accompanied by a decrease of *TGFB1* and NF-κB and related mediators (*IL1B* and *TNF*). Same effect was observed in siIRF4 PBMCs, indicating that IRF4 decrease in PBMCs is able to ameliorate inflammation in keratinocyte by AMPK/mTOR and NF-κB modulation.

biomedicines

MDPI

Article

Thalidomide Exerts Anti-Inflammatory Effects in Cutaneous Lupus by Inhibiting the IRF4/NF-κB and AMPK1/mTOR Pathways

Sandra Domingo [1], Cristina Solé [1,*], Teresa Moliné [2], Berta Ferrer [2] and Josefina Cortés-Hernández [1]

[1] Lupus Unit, Rheumatology Departament, Hospital Universitari Vall d'Hebron, Institut de Recerca (VHIR), Universitat Autonoma de Barcelona, 08035 Barcelona, Spain; sandra.domingo@vhir.org (S.D.); fina.cortes@vhir.org (J.C.-H.)

[2] Department of Pathology, Hospital Universitari Vall d'Hebron, Universitat Autònoma de Barcelona, 08035 Barcelona, Spain; teresa.moline@vhir.org (T.M.); bferrer@vhebron.net (B.F.)

* Correspondence: cristina.sole@vhir.org; Tel.: +34-93-489-4045

Abstract: Thalidomide is effective in patients with refractory cutaneous lupus erythematosus (CLE). However, the mechanism of action is not completely understood, and its use is limited by its potential, severe side-effects. Immune cell subset analysis in thalidomide's CLE responder patients showed a reduction of circulating and tissue cytotoxic T-cells with an increase of iNKT cells and a shift towards a Th2 response. We conducted an RNA-sequencing study using CLE skin biopsies performing a Therapeutic Performance Mapping System (TMPS) analysis in order to generate a predictive model of its mechanism of action and to identify new potential therapeutic targets. Integrating RNA-seq data, public databases, and literature, TMPS analysis generated mathematical models which predicted that thalidomide acts via two CRBN-CRL4A- ($CRL4^{CRBN}$) dependent pathways: IRF4/NF-κB and AMPK1/mTOR. Skin biopsies showed a significant reduction of IRF4 and mTOR in post-treatment samples by immunofluorescence. In vitro experiments confirmed the effect of thalidomide downregulating IRF4 in PBMCs and mTOR in keratinocytes, which converged in an NF-κB reduction that led to a resolution of the inflammatory lesion. These results emphasize the anti-inflammatory role of thalidomide in CLE treatment, providing novel molecular targets for the development of new therapies that could avoid thalidomide's side effects while maintaining its efficacy.

Keywords: cutaneous lupus; thalidomide; mechanism of action; new therapy

check for updates

Citation: Domingo, S.; Solé, C.; Moliné, T.; Ferrer, B.; Cortés-Hernández, J. Thalidomide Exerts Anti-Inflammatory Effects in Cutaneous Lupus by Inhibiting the IRF4/NF-κB and AMPK1/mTOR Pathways. *Biomedicines* **2021**, *9*, 1857. https://doi.org/10.3390/biomedicines9121857

Academic Editor: Anna Campanati

Received: 26 October 2021
Accepted: 6 December 2021
Published: 7 December 2021

1. Introduction

Cutaneous Lupus Erythematosus (CLE) is common and encompasses a wide range of dermatologic manifestations. As many as 70–80% of patients can develop skin lesions, which can be an early sign of systemic involvement [1,2]. CLE can be classified into specific and non-specific lesions, of which discoid lupus erythematosus (DLE) and subacute cutaneous lupus erythematosus (SCLE) are the most prevalent forms [3]. Early effective treatment may resolve the lesions, but delayed or inadequate treatment can result in permanent scarring, especially in DLE [4].

First-line therapies for CLE are antimalarial agents and/or topical steroids, together with sun protection [5]. Although most patients respond to this regimen, 30 to 40% of cases will be refractory [6]. For this minority, there is no consensus treatment algorithm, and several systemic agents have shown a variable response [7]. Thalidomide, a glutamic acid derivative with immunomodulatory and anti-inflammatory effects, has been used successfully in several oncological and chronic inflammatory dermatological conditions [8,9]. First prescribed for refractory CLE in 1975 [10], thalidomide use has increased following its reported efficacy, reaching 80–90% [6,10,11]. However, large-scale clinical trials are lacking,

and serious adverse events such as teratogenicity, neurotoxicity, and thrombosis restrict its use [12–15].

Although thalidomide's mechanism of action (MoA) has been studied, little is known of the molecular basis of its immunomodulatory effect in CLE. In vitro studies have demonstrated that thalidomide inhibits neutrophil chemotaxis, phagocytosis, angiogenesis, and production of tumour necrosis factor alpha (TNF-α). It also interacts with the T-helper response and regulation of transcription factor nuclear factor kappa-light-chain-enhancer of activated B cells (NF-κB) [16–19]. In the absence of an effective and safe treatment, a better understanding of thalidomide's MoA can help to identify key target molecules for the development of new therapeutic agents.

Genome-wide gene expression profiling is increasingly used to investigate pathogenetic mechanisms and identify potential disease biomarkers [20]. RNA sequencing (RNA-seq) is a widely used method to study overall transcriptional activity. RNA-seq is a powerful investigative tool using transcriptome changes as a proxy for drug effect and has led to the discovery of potential biomarkers in several diseases, yet standard library construction is costly [21–23]. Using a mathematical model including the comparative RNA-sequencing data, we identified different molecular signalling signatures that provide novel insights into thalidomide's MoA and potential therapeutic targets.

2. Materials and Methods

2.1. Patients

Six-millimetre punch skin biopsies for RNA-seq and blood samples for peripheral blood mononuclear cells (PBMCs) isolation were taken from 10 patients with active CLE, before and 4 weeks after thalidomide treatment (Table S1; see Supplementary Materials). CLE diagnosis and classification was based on clinical and histological criteria according to the 2004 Dusseldorf classification [24]. Disease activity was assessed by the validated modified CLE Disease Area and Severity Index (CLASI) [25]. The study was approved by the Vall d'Hebrón Ethics Committee and informed consent was obtained from all subjects.

2.2. RNA-Seq and System Biology Analysis

Whole skin RNA was extracted following the protein and RNA Isolation kit's instructions (Thermofisher Scientific, Waltham, MA, USA). For library construction, total RNA (1 μg) was used following the Illumina TruSeq™ RNA Sample Prep Kit (Illumina, San Diego, CA, USA) manufacturer's instructions. The resulting libraries were subjected to Illumina Hiseq 2000 sequencing platform version 3, producing 2 × 75 bp run with >65 M reads (Illumina, San Diego, CA, USA). Sequences were analyzed for quality control (FASTQC) and aligned to the Human genome (GRCh38) with STAR program V2.5.2a [26,27]. Sequencing reads were processed using the RSEM program (version 1.2.28) [28] and differential expression calculated by DESeq2 [29]. Data are available from Gene Expression Omnibus (GSE162424). We generate models to predict thalidomide's MoA by a Therapeutic Performance Mapping System (TMPS) approach (Anaxomics Biotech, Barcelona, Spain). TPMS combines RNA-seq data with a complete characterization of CLE/Thalidomide using biological information from KEGG, Binding Database, BioGRID, REACTOME, Pubmed, Drug Bank, Stich and Supertarget [30–37] (See Supplementary Materials).

2.3. Flow Cytometry

PBMCs cell phenotype was analyzed by seven-colour flow cytometry (LSR Fortessa, BD Biosciences, Franklin Lakes, NJ, USA). For cell surface staining, conjugated monoclonal antibodies were used (BD Biosciences) (Table S2; see Supplementary Materials). Isotype controls were used for gate setting. Data were analyzed using FCS Express 4 Flow Research software (BD Biosciences, Erembodegem, Belgium).

2.4. Immunofluorescence and Immunohistochemistry

Immunohistochemistry (IHC) and immunofluorescence (IF) were performed as described on paraffin-embedded and frozen sections, respectively [37,38] using purified monoclonal antibodies listed in Table S3. Stained samples were evaluated by two blinded dermatopathologists and cell counts were quantified using Image J V1.42 (see Supplementary Materials).

2.5. In Vitro Ubiquitination Assay

Recombinant Human CRBN + DDB1 + CUL-4A + RBX1 (Abcam, Cambridge, UK) (1 μM), Human AMPK1 Fisher (ThermoFisher, Waltham, MA, USA) (1.5 μM) and Thalidomide (100 μM) were used with the E3 Ligase Auto-Ubiquitilylation Assay Kit (Abcam, Cambridge, UK) following the manufacturer's instructions. Reactions were incubated at 37 °C for 2 h before separation by SDS–PAGE followed by western blot analysis.

2.6. Co-Immunoprecipitation for Cell-Based Ubiquitination Assay

Epidermal keratinocytes were stimulated with UVB for 6h and then treated with thalidomide. After 24 h, cells were washed twice with PBS and lysed with RIPA buffer (Sigma Aldrich, St. Louis, MI, USA) together with protease inhibitor cocktail (Sigma Aldrich, St. Louis, MI, USA). After centrifugation at 10,000 rpm for 15 min, supernatant was collected.

Concurrently, Dynabeads™ Protein G for Immunoprecipitation (Invitrogen, Waltham, MA, USA), were washed and incubated with anti-AMPK antibody (1:250) (Abcam, Cambridge, UK) in PBS 0.02% Tween™ 20 for 15 min at room temperature in order to obtain the Antibody-bead complex. Then, the mix was incubated with the obtained supernatant from the cell lysis. After 1 h at room temperature, the antibody-bead-AMPKprotein complexes were obtained. Finally, AMPK protein was eluted with elusion buffer (50 mM glycine pH 2.8) for 2 min at room temperature. Supernatants were subjected to western blot analysis for AMPK and ubiquitin protein analysis.

2.7. Protein Extraction and Western Blot

Skin protein samples were obtained using the PARIS kit following manufacturer's instructions (see Supplementary Materials). Protein concentrations were determined using the BCA protein assay kit (Bio-Rad, Hercules, CA, USA). Then, 50 μg of protein was loaded into 12% SDS-PAGE and transferred to PVDF membranes (Millipore, Billerica, MA, USA) by Semi-Dry Electrophoretic Transfer (Bio-Rad, Hercules, CA, USA). Membranes were blocked with 5% BSA (RT, 1 h) followed by overnight incubation (4 °C) with specific primary antibodies (Abcam, Cambridge, UK, Table S3). Secondary HRP-labelled antibodies were added (1:500) and visualized using ECL Detection System (Santa Cruz Biotechnology, Dallas, TA, USA).

2.8. RNA Extraction and RT-qPCR

RNA from cultured lysed cells was obtained with RNeasy Mini Kit (Qiagen, Hilden, Germany). RNA was transcribed into cDNA with High-Capacity cDNA Reverse Transcription Kit (Applied Biosystems, Foster City, CA, USA). Gene expression was assessed by TaqMan assays (Applied Biosystems, Foster City, CA, USA) (Table S4; see Supplementary Materials).

2.9. Proliferation Assays

Proliferation assays were performed using CyQUANT NF Cell Proliferation Assay Kit (Invitrogen), following manufacturer's instructions.

2.10. Cell Culture

Human epidermal adult Keratinocytes (HEKa) were cultured in EpiLife serum-free media with Human Keratinocyte Growth Supplement (Life Technologies, Carlsbad, CA,

USA) and isolated PBMCs from healthy volunteers (Vacutainer CPT, BD Biosciences) in RPMI medium (Life Technologies, Carlsbad, CA, USA; see Supplementary Materials).

2.11. Gene Silencing

Third passage cultured cells at 30–50% confluence were transfected with interferon regulatory factor 4 (IRF4) or mechanistic target of rapamycin (mTOR) small interfering RNA (siRNA, ThermoFisher) or a silencer negative control (ThermoFisher, AM4615) using the lipofectamine CRISPRMAX Cas9 Reagent following the manufacturer's instructions (ThermoFisher, Waltham, MA, USA). After 24 h, cells were treated with TNF-α (10 ng/mL) or U.V for 6 h and analyzed by qPCR-RT or immunofluorescence.

2.12. Co-Culture Experiments

Co-cultures were performed in modified 24-well plates with cell culture inserts (0.4-μm pore; BD Biosciences, Franklin Lakes, NJ, USA). HEKa cells were cultured at the bottom overnight. Isolated healthy donor PBMCs, stimulated with TNF-α for 6 h, were placed in the upper part of the insert and treated with thalidomide (100 ng/mL). After 24 h, the insert was removed, and HEKa cells were analyzed by immunofluorescence or RT-qPCR.

2.13. Statistical Analysis

Data are represented as mean ± SEM. Comparison between groups and differential gene expression was calculated with paired or unpaired t-tests as applicable using Prism GraphPad (GraphPad Software, v7.0, San Diego, CA, USA). p values ≤ 0.05 were considered statistically significant. RT-qPCR analysis was calculated using Fold Change differences with $2^{-\Delta\Delta Ct}$ method.

3. Results

3.1. Immunoregulatory Effects in CLE Peripheral Blood and Skin

Ten thalidomide-treated CLE patients were included (Table S1) (see Supplementary Materials). Seven (70%) achieved clinical remission (CLASI = 0). Following treatment, responder patients had a reduction in peripheral cytotoxic CD8+ T-cells ($p = 0.044$) and an increase of iNK T-cells ($p = 0.006$) (Figure 1a). iNK T-cell related cytokines were not different after treatment; however we observed a tendency to decrease granulate cytokines (perforin A and granzyme B) in post-treatment samples (Figure S1). No significant changes in CD4+ T percentages or in dendritic cells, B-cells, or T regs were observed. Analysis of distinct Th subsets showed a skew towards a Th2 response ($p = 0.018$) (Figure 1b).

The immunohistochemical study results of the skin infiltrating cells mirrored the ones observed in peripheral blood with a significant reduction in the number of CD8+ T-cells ($p = 0.013$, Figure 1c) and an increase in iNK T-cells post-thalidomide ($p = 0.004$, Figure 1d).

3.2. RNA-Sequencing with Therapeutic Performance Mapping System (TMPS) Analysis Revealed Thalidomide's Mechanisms in CLE

We first identified relevant proteins in CLE pathogenesis and thalidomide through the analysis of published biological information that allowed us to establish the protein network (Tables S5 and S6; Figures S2 and S3). To obtain further insight into the molecular basis of CLE, we performed an RNA-seq. Comparative analysis of the skin RNA sequencing of thalidomide responder patients revealed 448 differentially expressed transcripts, of which 339 were protein coding genes ($|\log2(FC)| \geq 1$; Adj. p value < 0.05, data available GSE162424). To construct the Thalidomide's MoA, the RNA-seq data was used to restrict the models (see Supplementary Materials). Finally, we identified twenty-seven differential molecules of which 14 were CLE effectors (Table S7, Figure 2). In our model, we found thalidomide to act by two $CRL4^{CRBN}$-dependent mechanisms: (a) downregulating IRF4 leading to an inhibition of the NF-κB signalling pathway; and (b) regulating AMPK1/mTOR signalling pathway (Figure 2).

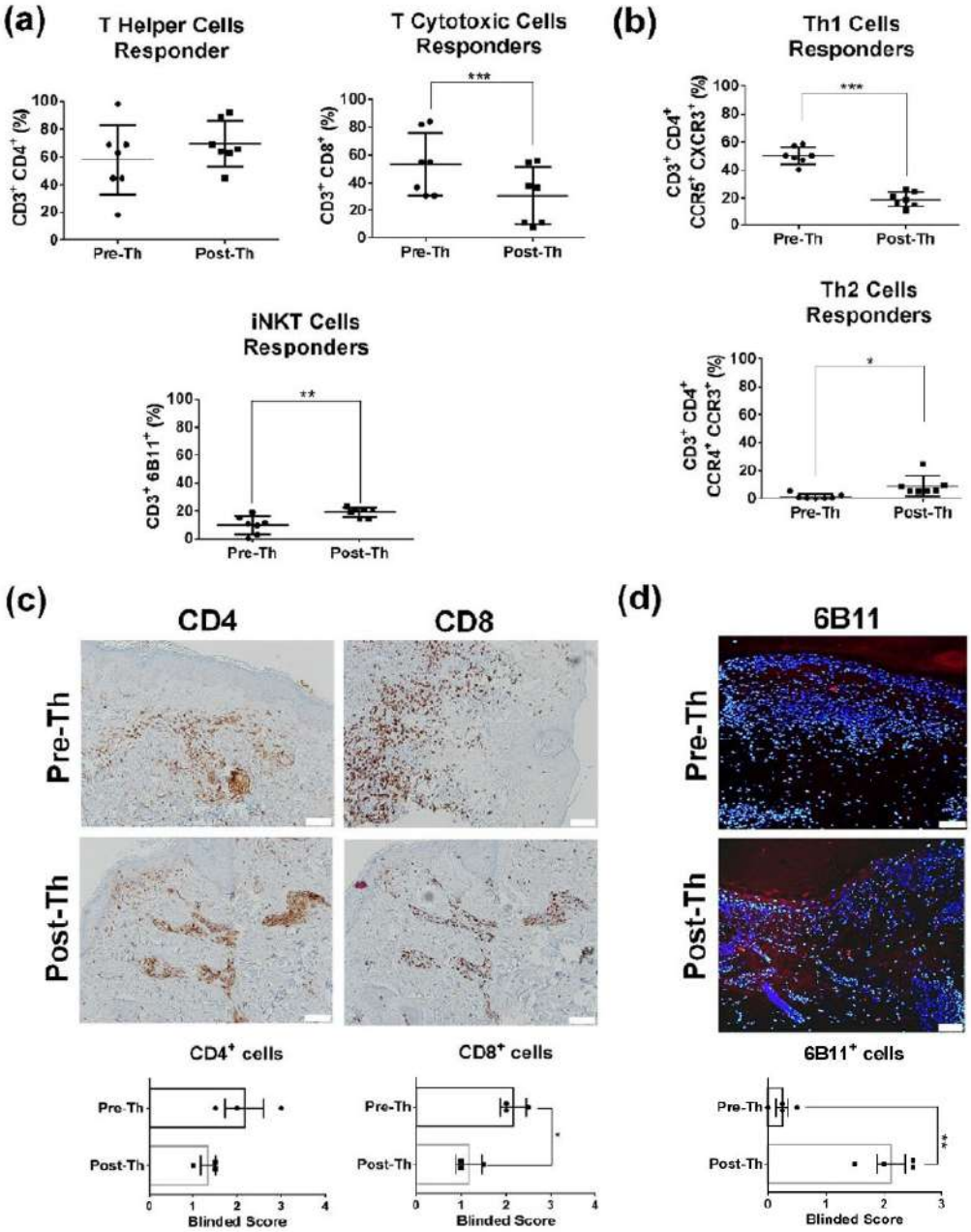

Figure 1. Thalidomide ameliorates skin inflammation by decreasing CD8+ T cells, increasing iNK-Tcells and promoting a Th2 response in CLE. (**a**) Flow cytometry percentages of T helper (CD3+CD4+), T cytotoxic cells (CD3+CD8+) and iNK Tcells (CD3+6B11+) in PBMCs of responder patients ($n = 7$) before and after thalidomide treatment. (**b**) Post-thalidomide, CLE patients had lower percentages of Th1 (CCR5+ CXCR3+) T cells and higher percentages of Th2 (CCR4+CCR3+). (**c**) Skin immunohistochemistry to evaluate infiltrating CD4+ and CD8+ in skin biopsies of CLE. Graphs represent the average signal intensity ($n = 3$). (**d**) Immunofluorescence of post-treatment skin samples showed a significant increase of iNK Tcells (6B11+ cells). Scale bar = 200mm. * $p < 0.05$; ** $p < 0.005$; *** $p < 0.0001$.

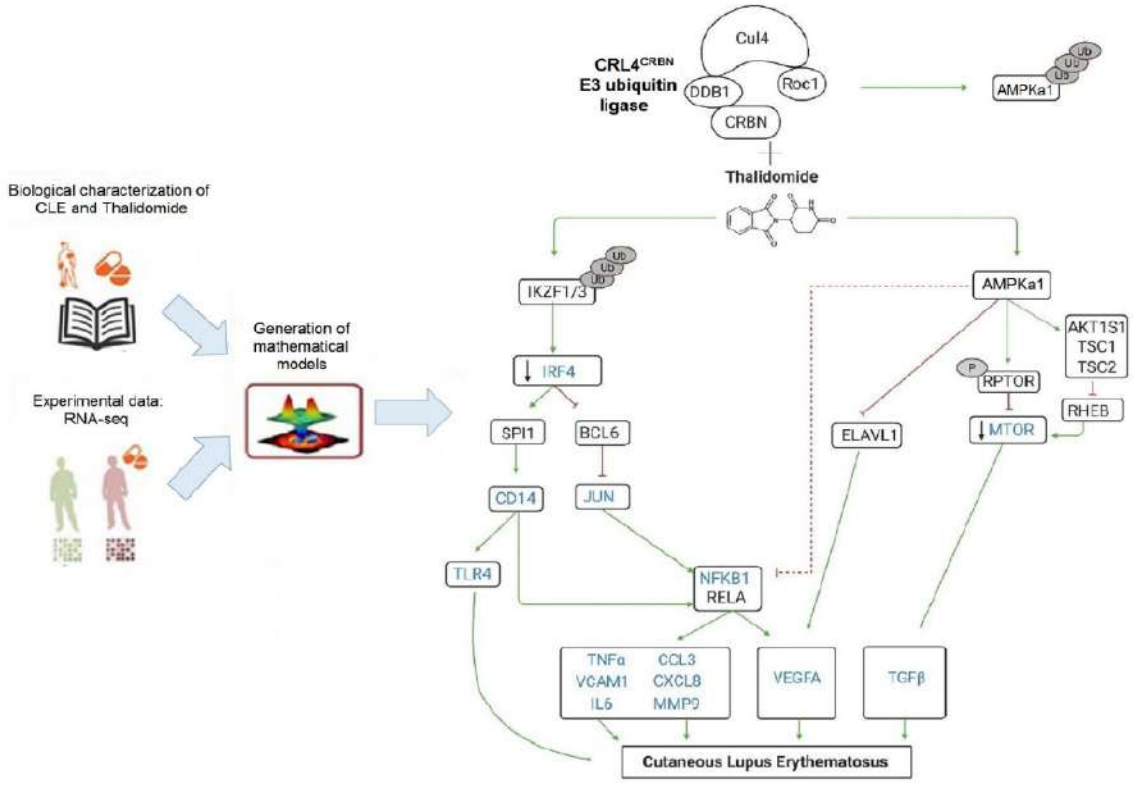

Figure 2. Proposed thalidomide mechanism of action in Cutaneous Lupus Erythematosus (CLE). On the one hand, in the presence of thalidomide, CRL4^{CRBN} complex ubiquitinates IKZF1/3 promoting downstream modulation of IRF4 and, on the other hand, prevents the ubiquitination of AMPKa1, increasing the expression of phosphorylated RPTOR which in turn inhibits mTOR signaling. Therefore, thalidomide modulates IRF4 and AMPK/mTOR pathways and their downstream effector molecules contributing to the resolution of inflammatory lesions in CLE.

In order to confirm the proposed mechanism models, we further investigated the effect of thalidomide in the CRL4^{CRBN}–IKZF1/3 and AMPK1 interaction. It is well-known that in the presence of thalidomide, IKZF1/3 acts as a substrate for the CRL4^{CRBN} complex, and both Ikaros (IKZF1) and Aiolos (IKZF3) are ubiquitinated and targeted for degradation by the ubiquitin–proteasome system [38]; however, the effect of thalidomide in the CRL4^{CRBN}-AMPK1 interaction is not well known. Our in vitro studies showed that in the presence of thalidomide, there was a significant reduction of the ubiquitin-dependent proteasomal degradation of AMPKa1, the catalytic subunit of the 5′-prime-AMP-activated protein kinase (AMPK) (Figure 3a).

Next, we further study the effect of thalidomide treatment in the two signalling pathways by measuring the identified key molecules at a protein level in the skin biopsies of CLE patients. Immunofluorescence in post-thalidomide skin biopsies showed a decrease expression of CRBN ($p = 0.012$ epidermis; $p = 0.008$ dermis), IRF4 ($p = 0.0031$ dermis), and NF-κB ($p < 0.001$ epidermis; $p = 0.001$ dermis), whereas mTOR expression was reduced primarily in the epidermal keratinocytes ($p < 0.001$, Figure 3b). Following thalidomide treatment, there was an increase of AMPKa1 ($p < 0.001$) and phosphorylated RPTOR ($p < 0.001$) protein expression levels in the epidermis (Figure 3b). Results were confirmed also by western blot (Figure S4).

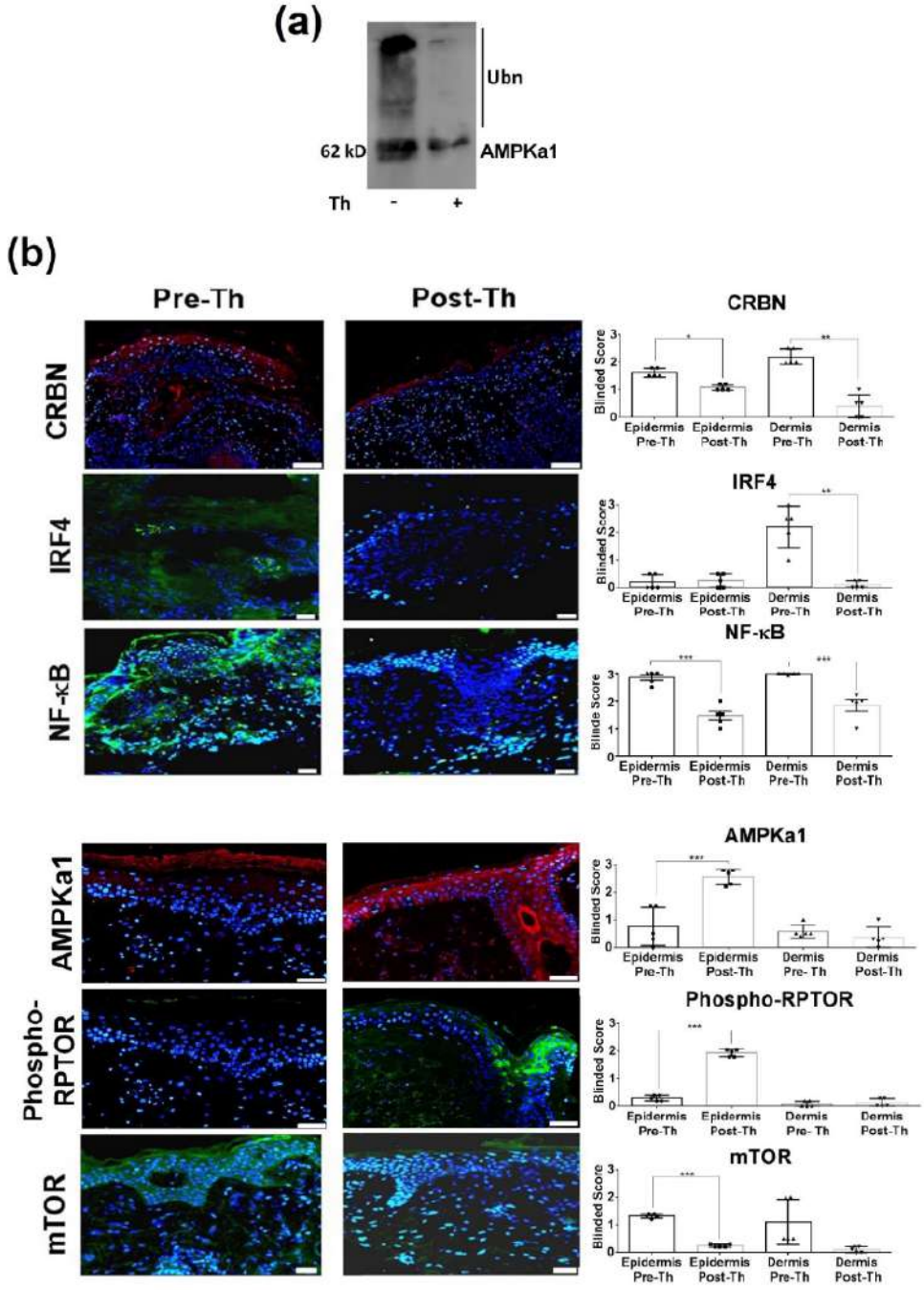

Figure 3. Protein levels of key target molecules identified in the analysis of the thalidomide mechanism of action. (**a**) In vitro ubiquitination of AMPKa1 by the $CRL4^{CRBN}$ showed a reduction of the AMPKa1 ubiquitination in the presence of thalidomide. (**b**) Immunofluorescence of CLE lesional skin of paired patients showed a downregulation of CRBN (red), IRF4, NF-κB, mTOR (green) and upregulation of AMPK1a (red) and phosphorylated RPTOR (Phospho-Rptor, green) after thalidomide treatment. Counterstaining of nuclei is shown in blue. Average intensity fluorescence score evaluated by blinded expert pathologists in the epidermis and the dermis of the CLE skin sections ($n = 5$). Scale bar = 200mm. * $p < 0.05$; ** $p < 0.005$; *** $p < 0.001$.

3.3. Thalidomide Modulates PBMCs via the IRF4/NF-κB Signalling Pathway

Our immunofluorescence findings indicate that thalidomide may modulate the IRF4 pathway in the dermal inflammatory infiltrates. We performed in vitro experiments with stimulated PBMCs treated with thalidomide that showed a significant reduction of IRF4 ($p < 0.01$) and NF-κB ($p < 0.01$) expression but no changes were observed in mTOR (Figures 4a and S5). Gene expression analysis of final effector molecules showed a significant reduction of NF-κB-related cytokines (*IL-1β*, *IL-8* and *TNFα* (9.09, 5.25 and 33.3-fold decrease, respectively) and *CCL3* (6.25-fold decrease). The analysis of the T helper subsets showed an increase of the Th2/Th1 ratio (*GATA3/T-bet*) (1.26 and 1.63-fold increase, respectively) with a significant reduction of *IL-2* levels (1.45-fold decrease, Figure 4b). No significant changes were found in PBMCs proliferation and autophagy (Figures S6 and S7).

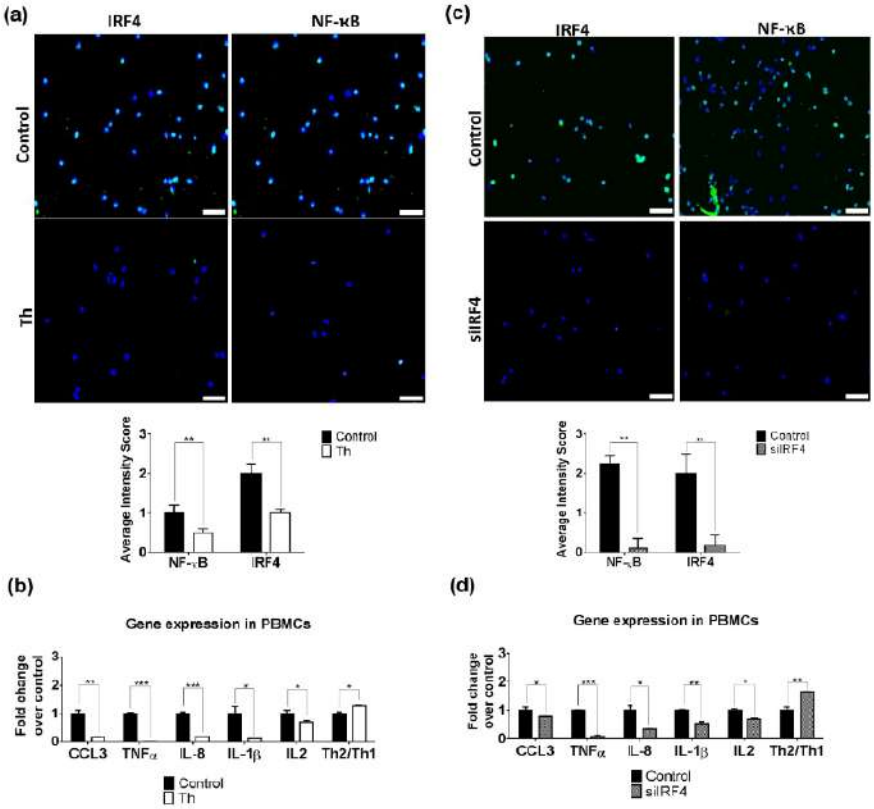

Figure 4. Thalidomide modulates the IRF4/NF-κB pathway in PBMCs. (**a**) Immunofluorescence of NF-κB and IRF4 protein levels (green staining) in PBMCs treated with thalidomide (Th) or with PBS + 1%DMSO (control conditions). Dapi was used to stain nuclei of cells (blue). (**b**) RT-qPCR of NF-κB inflammatory effectors CXCL3, TNFα, IL-8, IL-1β and IL2 was performed in PBMCs treated with or without thalidomide. Ratio T helper 2 vs. 1 was evaluated via gene expression of their transcription factors. (**c**) IRF4-silenced PBMCs were stained in order to evaluate NF-κB and IRF4 protein levels (green). Control condition was performed using a non-targeting siRNA. (**d**) Gene expression in IRF4-silenced PBMCs were determined by RT-qPCR. Fold change was calculated over control conditions. GADPH was used as endogenous control. Scale bar = 50 μm. * $p < 0.05$, ** $p < 0.005$, *** $p < 0.001$.

To demonstrate that the thalidomide anti-inflammatory effect in PBMCs is dependent on IRF4 modulation, we silenced IRF4. We showed that IRF4 silencing induced similar results to the ones observed in thalidomide-treated cells with a reduction of NF-κB protein levels ($p < 0.01$) and a downregulation of *IL-1β*, *IL-8*, *TNFα* (1.87, 2.89 and 11.04-fold decrease, respectively) and *CCL3* expression levels (1.27-fold decrease, Figure 4b). siIRF4

PBMCs showed also a shift of the Th1/Th2 balance with an increase of the Th2/Th1 ratio and a significant reduction of *IL-2* levels.

3.4. Thalidomide Modulates the AMPK1/mTOR-NF-κB Signalling Pathway in Keratinocytes

mTOR epidermal expression in pre-treated samples led us to study thalidomide's effect on keratinocytes through this signalling pathway. First, we demonstrated at a tissue level the effect of thalidomide in AMPK. Keratinocyte cell-based ubiquitination was performed in the presence or absence of thalidomide. A significant increase of AMPKa1 protein levels were observed in thalidomide-treated keratinocytes in comparison to control conditions ($p < 0.001$, Figure 5a). Simultaneously, a significant reduction of ubiquitin-protein conjugates were observed suggesting that ubiquitination of AMPKa1 is more pronounced in the absence of thalidomide ($p = 0.0201$, Figure 5a). This observation was also confirmed by western blot (Figure S8). mTOR expression levels decreased in UVB-stimulated keratinocytes following thalidomide ($p = 0.009$, Figure 5b). Conversely, upregulation of AMPKa1 and phosphorylated RPTOR expression levels were observed ($p = 0.036$ and $p = 0.003$, respectively, Figure 5b). The gene expression analysis of downstream mTOR-dependent cytokines (IL-10, TGFβ and INFα) in thalidomide-treated keratinocytes only showed a significant reduction of TGFβ (6.69-fold decrease, Figure 5c). Keratinocyte proliferation, apoptosis and autophagy after thalidomide were analysed and no changes were observed (Figures S9 and S10).

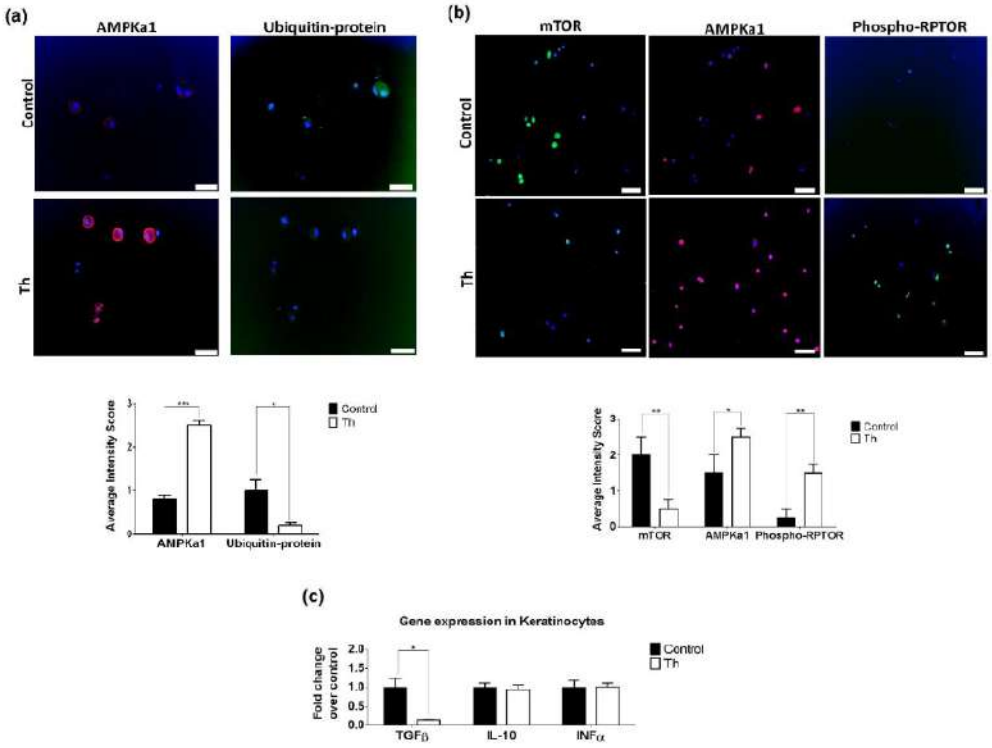

Figure 5. Thalidomide modulates the AMPKa1/mTOR in keratinocytes. (**a**) In vivo ubiquitination was performed in keratinocytes treated or non-treated with thalidomide. Immunofluorescence of AMPKa1 (red) or ubiquitin-proteins conjugates (green) revealed that in the presence of thalidomide AMPKa1 was not degraded. Scale bar = 50 μm. * $p < 0.05$, *** $p < 0.0005$. (**b**) Protein levels of AMPKa1 (red), mTOR and phosphorylated RPTOR (Phospho-RPTOR, green) were measured using immunofluorescence in keratinocytes treated with thalidomide (Th) or with PBS+1%DMSO (control conditions). Nuclei of cells were marked with dapi (blue stainning). Scale bar = 50 μm. * $p < 0.05$, ** $p < 0.005$. (**c**) RT-qPCR of mTOR inflammatory effectors TGFβ, IL-10, INFα was performed in UVB-treated keratinocytes in the presence or not of thalidomide. Fold changes were calculated over control. * $p < 0.05$.

We also studied the ability of thalidomide to modulate NF-κB in keratinocytes, since epidermal NF-κB levels were significantly reduced in skin biopsies following thalidomide treatment. The treatment of these cells with thalidomide reduced significantly the NF-κB protein levels ($p = 0.005$, Figure 6a). Furthermore, gene expression analysis of NF-κB-dependent cytokines (*TNFα*, *IL8*, *IL1β*, *IL6*, *CXCL1* and *MMP9*) showed a reduction of *IL-1β* (5-fold decrease), *TNFα* (6.71-fold decrease) and *CXCL1* (2.67-fold decrease) (Figure 6b). This NF-κB reduction was also observed in keratinocytes when mTOR was silenced, along with an increase of AMPKa1 protein levels ($p < 0.05$) (Figure 6c). Downregulation of *TGFβ* (1.92-fold decrease), *IL-1β* (19.88-fold decrease), TNFα (3.70-fold decrease) and *CXCL1* (4.29-fold decrease) gene expression levels were also observed (Figure 6d).

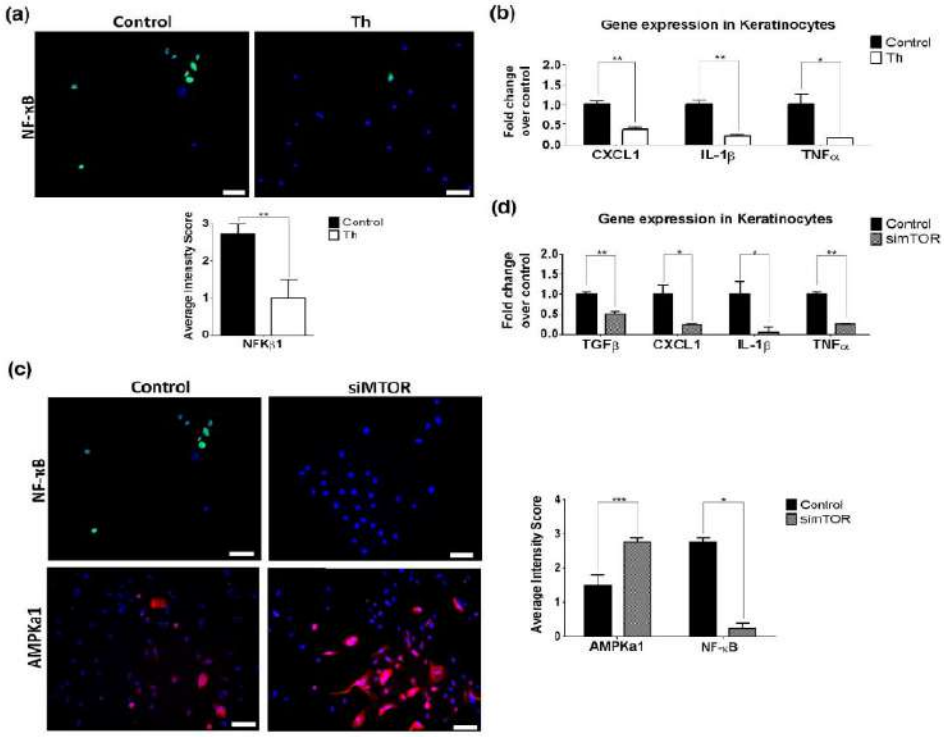

Figure 6. Thalidomide effect in keratinocytes is dependent on mTOR. (**a**) Immunofluorescence showed a reduction of NF-κB protein levels in keratinocytes in the presence of thalidomide (green staining). Scale bar = 50 μm. ** $p < 0.005$. (**b**) A reduction of NF-κB-related cytokine gene expression was confirmed by RT-qPCR analysis. Fold change was calculated over control conditions. GADPH was used as endogenous control. * $p < 0.05$, ** $p < 0.005$. All the experiments were performed in triplicate (**c**) AMPK1a and NF-κB protein levels were measured by immunofluorescence in silenced mTOR keratinocytes and control keratinocytes (non-specific silenced gene). Scale bar = 50 μm. * $p < 0.05$, *** $p < 0.0005$. (**d**) Gene expression of related cytokines were measured by RT-qPCR analysis in silenced mTOR keratinocytes (simTOR). Fold change was calculated over non-silenced mTOR keratinocytes (control conditions). * $p < 0.05$, ** $p < 0.005$.

Silencing IRF4 in keratinocytes had no effect in NF-κB protein levels (Figure S11), reinforcing the evidence of a crosstalk between NF-κB- and AMPK/mTOR-signaling pathway.

3.5. Thalidomide-Treated PBMCs Downregulate Keratinocyte mTOR Signalling Pathway

As the interaction between epithelial cells and the immune system is tightly regulated, we performed cross-talking in vitro functional studies between thalidomide-treated PBMCs and keratinocytes (Figure 7a). Thalidomide-treated PBMCs co-cultured with keratinocytes produced a significant downregulation of keratinocyte mTOR protein levels and an increase of the inhibitor AMPKa1 and phosphorylated mTOR (Figure 7b). Analysis

of gene expression levels showed the reduction of MTOR (6.6-fold decrease), an increase of AMPKa1 (2.20-fold increase), a decrease of NFKB1 (2.94-fold decrease) and related cytokines (TGFβ, IL1β and TNFα) (Figure 7c). Cross-talking studies using IRF4-silenced PBMCs also showed the same effect in mTOR and phosphorylated mTOR protein levels (Figure 7d). Gene expression levels of MTOR, NFKB1, TGFβ, TNFα (4.24, 3.84, 2.36 and 9.13-fold decrease, respectively) and AMPKa1 (2.58-fold increase, Figure 7e).

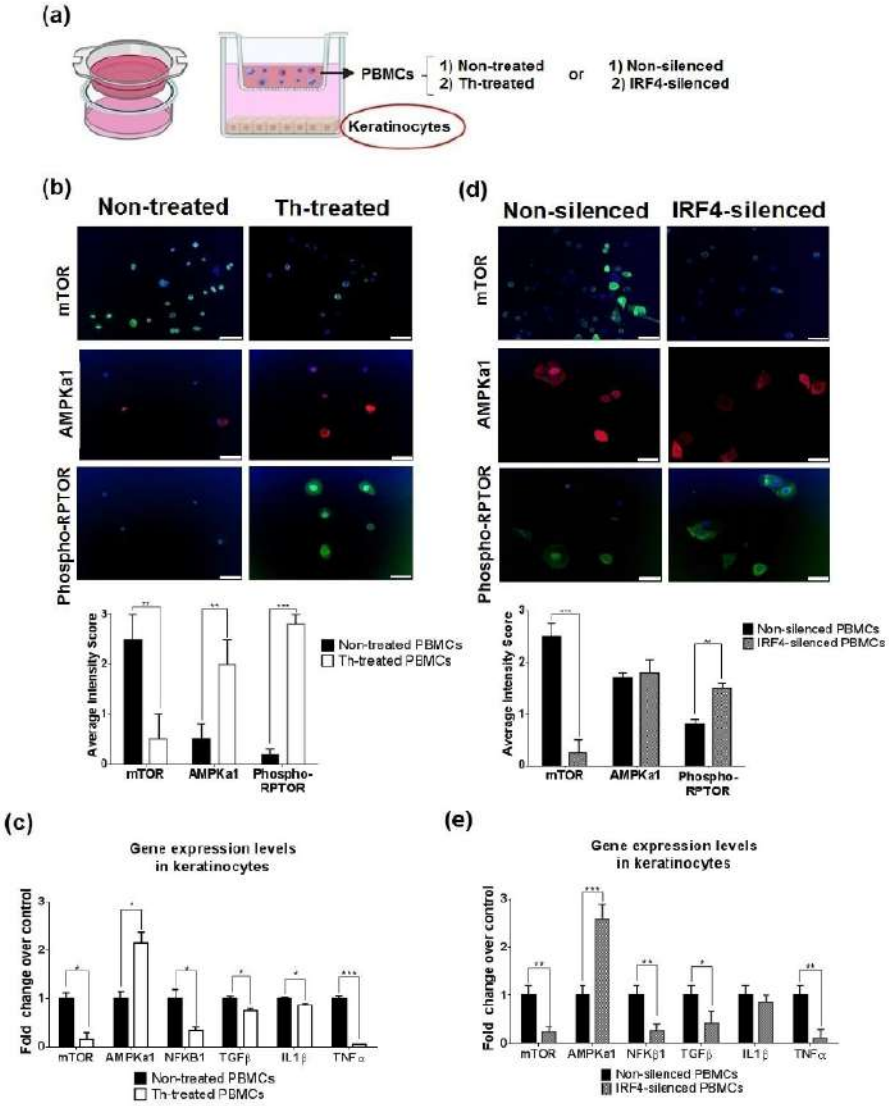

Figure 7. In vitro co-culture of PBMCs and keratinocytes revealed a predominance of IRF4-thalidomide effect. (**a**) PBMCs were stimulated with TNFα and treated or non-treated with thalidomide (Th) and co-cultured with keratinocytes. After 24 h of co-culture, keratinocytes were analysed by immunofluorescence and gene expression assays. A similar experiment was performed using non-silenced or IRF4-silenced PBMCs (siIRF4). (**b**) mTOR protein levels (green) were significantly decreased in the presence of Th-treated PBMCs, whereas AMPKa1 (red) and phosphorylated RPTOR (green) were increased after thalidomide treatment. (**c**) Keratinocyte gene expression levels of the mTOR-related molecules and inflammatory effectors were measured by RT-qPCR. (**d**) mTOR protein levels in keratinocytes also decreased in the presence of IRF4-silenced PBMCs. Phosphorylated-RPTOR increased in keratinocytes after PBMCs were IRF4 silenced (**e**) mTOR related molecules and inflammatory effectors were measured by RT-qPCR in keratinocytes after co-cultured with non-silenced or IRF4-silenced PBMCs. Scale bar = 50 μm. * $p < 0.05$, ** $p < 0.005$, *** $p < 0.001$.

4. Discussion

Our study examined thalidomide's immunomodulatory mechanism in cutaneous lupus. CLE has a distinctive T-cell signature with an imbalance towards a Th1 response [39] and CD8+ T-cell predominance in early inflammatory stages [40]. Thalidomide induced a reduction of cytotoxic CD8+ T-cells and increased the number of iNKT cells both circulating and in tissue. Activated cytotoxic lymphocytes (CTLs), like cytotoxic CD8+ T-cells, contribute to basal keratinocyte damage and inflammatory infiltration in CLE, especially at the dermo-epidermal junction, and correlate with IFN-α expression and damage extension [41]. iNKT cells are a subset of unconventional T-cells which recognise the MHC class I-like CD1d protein with the expression of an invariant TCR chain (Vα24-Jα18) paired with a Vβ11 chain [42]. Lupus patients, especially those with severe cutaneous involvement, have a numerical and functional reduction of circulating iNKT cells, but enrichment has been described in lesional skin. In line with previous IMiDs studies [43], during lesion resolution, we found an increment in both tissue and circulating iNKT cells after thalidomide. The exact role of these cells is not completely understood since they are functionally versatile and may mediate both pathogenic and regulatory immune functions. Whereas, on the one hand, iNKT cells participate in the pathogenesis of several skin inflammatory disorders producing interferon gamma and IL-4 [44], we did not find a difference in their related cytokines. On the other hand, iNKT has been described as potent downregulators of CD8+ cytotoxic T cells [45]; they are implicated in skin would healing [46,47] and they alleviate lupus dermatitis in an MRL-lpr/lpr model [48]. Modulation of the different Th subsets by IMiDs has also generated opposing data [49–51]. In our study, thalidomide induced a Th2 response both in vivo and in vitro. Some Th2 responses are related to the expression of wound healing genes and growth factors involved in tissue regeneration [52], so Th2 enhancement may contribute to skin repair.

To further investigate the thalidomide MoA, we combined machine learning approaches with CLE RNA-sequencing data to obtain a novel predictive model. We showed that thalidomide modulates CLE by targeting two $CRL4^{CRBN}$-dependent pathways, downregulating IRF4 via IKZF1/3 and mTOR through regulation of AMPK1 activity. The study confirmed previous reports describing CRBN as the primary target of thalidomide [15,53] and its expression decreased following treatment both in the dermal inflammatory infiltrates and epidermis. CRBN functions as a substrate receptor for the cullin-4-containing E3 ubiquitin ligase complex CUL4–RBX1–DDB1 (CRL4A) and is responsible for the recruitment of substrates for degradation by the ubiquitin-proteasome pathway. IMiDs bind to CRBN and alter the substrate specificity of $CRL4^{CRBN}$ blocking the degradation of proteins involved in angiogenesis, tumoral activity and inflammation [54,55] but also inducing teratogenicity [56].

As in other inflammatory skin conditions like psoriasis vulgaris, acne, atopic dermatitis, and hidradenitis suppurative [57,58], we found in active lesions of CLE an increased expression of IRF4 in the dermis and mTOR in the epidermis. Following thalidomide there was a reduction in these expression levels. Further in vitro experiments confirmed the effect of thalidomide through the two different signalling pathways according to the skin cell type. Thalidomide reduced IRF4 signalling in lymphocytes whereas the effect on mTOR was observed in keratinocytes.

IRF4 is a member of the IRF family of transcription factors, expressed in immune cells relevant in the IFN signature [59]. IRF4 is required for proper maturation and differentiation of immune cells [60]. IRF4 dysregulation has been described in rheumatoid arthritis and SLE and it is associated with initiation and disease progression [61]. IMiDs can induce $CRL4^{CRBN}$-dependent degradation of the Ikaros family zinc finger protein-1 (IKZF1, Ikaros) and 3 (IKZF3, Aiolos), two transcription factors involved in lymphoid development and differentiation and highly expressed in B cell malignancies, leading to an inhibition of IRF4 expression at transcriptional level [38,62,63]. We showed that thalidomide modulates the IRF4/NF-κB signalling pathway in PMBCs and contributes to the resolution of inflamma-

tion by reducing the expression of NF-κB and its dependent cytokines and chemokines IL-1β, IL-8, TNFα and CCL3.

AMP-activated protein kinase (AMPK) has also been identified as a CRBN-binding protein [64]. AMPK is an important intracellular energy sensor and is activated by phosphorylation of threonine at position 172 (Thr 172) of the α subunit. $CRL4^{CRBN}$ down-regulates the total quantity of the AMPK α subunit by polyubiquitination. Previous reports have shown that thalidomide markedly stimulates the activation of AMPK [63,64] and reduces AMPK α polyubiquitination [65–67]. Accordingly, we demonstrated that thalidomide reduced the AMPK α ubiquitination in a CRBN-dependent manner and increased its expression. Consequently, we observed an increase of RPTOR phosphorylation and a reduction of mTOR signalling. mTOR is a serine threonine kinase crucial in skin homeostasis and morphogenesis, especially in the regulation of keratinocyte differentiation and epidermal stratification [68]. There are two biochemically distinct mTOR complexes, mTORC1 and mTORC2. The activity of mTORC1 is suppressed by AMPK by directly phosphorylating at least two regulator proteins, tuberous sclerosis 2 (TSC2) and RPTOR. In vitro studies showed that treatment with thalidomide or simTOR significantly reduced keratinocyte-derived cytokines TGFβ, IL-1β, TNFα and CXCL1 (Figure 8a) contributing to the resolution of inflammation. In addition, we showed that the specific inhibition of mTOR decreased NF-κB expression in keratinocytes. The existence of a crosstalk between mTOR and NF-κB has been described in other cellular types [69]. Not only have we described a crosstalk between mTOR and NF-κB in keratinocytes, but we have also shown the ability of thalidomide-treated PBMCs to reduce the expression of mTOR and related cytokines in co-culture studies.

Our previous work in DLE [70] and this study confirm the relevance of NF-κB in CLE. NF-κB was the common target molecule in which thalidomide acted through different signalling pathways in their respective skin cells [71]. NF-kB is a key player in the control of both innate and adaptive immunity. NF-kB activity is essential for lymphocyte survival, activation, and mounting normal immune responses. Constitutive activation of the NF-kB pathway is often associated with inflammatory diseases like rheumatoid arthritis, inflammatory bowel disease, multiple sclerosis, and asthma [72]. Activation of NF-κB in keratinocytes has been reported in psoriasis lesions resulting in the production of multiple inflammatory molecules that initiate and sustain the inflammatory process [73–76]. In addition, it has been demonstrated that topical application of an NF-κB inhibitor improved atopic dermatitis in NC/NgaTnd mice [77]. Together, these data support the further study of NF-κB as novel a therapeutic target [78]. While global inhibition may result in profound side effects by selectively targeting specific NF-κB subunits or signalling components relevant to a particular disease, toxicity can be minimized.

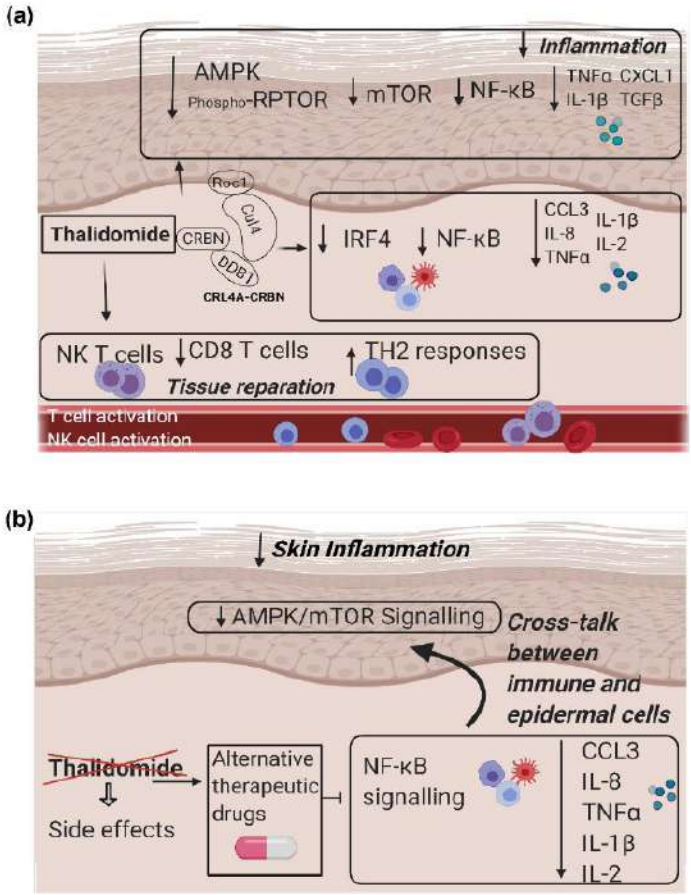

Figure 8. Thalidomide as alternative therapy in CLE. (**a**) Thalidomide binds CRBN in the cullin-4 E3 ubiquitin ligase complex ($CRL4^{CRBN}$) and promotes: A downregulation of mTOR protein, by reducing the AMPK ubiquitination and increasing the RPTOR phosphorylation that downregulated NF-κB and its related cytokines in keratinocytes. Also promoted is a reduction of IRF4 expression in lymphocytes that decreases the expression of NF-κB and related cytokines. In addition, thalidomide enhances tissue reparation promoting Th2 responses, iNK T cells and lower prevalence of CD8+ T cells. (**b**) Alternative therapeutic drugs targeting NF-κB signalling may avoid its important side effects and maintain its anti-inflammatory properties.

5. Conclusions

Taken together, we demonstrated that thalidomide's immunomodulatory anti-inflammatory effect in CLE comprises several mechanisms that include a reduction of predominantly CD8+T cells, and a switch from Th1 to Th2 response. Furthermore, thalidomide reduced NF-κB related inflammatory cytokines and chemokines via the modulation of IRF4- and AMPK/mTOR-signalling pathways. Targeting the function of these key molecules may be an alternative to thalidomide for the treatment of CLE (Figure 8b).

Supplementary Materials: The following are available online at https://www.mdpi.com/article/10.3390/biomedicines9121857/s1, Figure S1: PBMCs from patients were extracted pre and post-thalidomide ($n = 5$), Figure S2: Topological analysis represents the relationships between proteins in the mechanism of action over cereblon modulation, Figure S3: Topological analysis represents the relationships between proteins in the mechanims of action over IRF4, Figure S4: Western blot of lysates from paired skin biopsies, Figure S5: Immunofluorescence of mTOR in thalidomide-treated or non-treated PBMCs, Figure S6: Proliferation in healthy PBMCs after thalidomide treatement,

Figure S7: Immunofluorescence in thalidomide-treated or non-treated PBMCs to monitoring autophagy, Figure S8: Western blot of cell based ubiquitination assay in keratinocytes terated or non-treated with thalidomide, Figure S9: Profiferation and apoptosis of human epidermal keratinocytes after thalidomide addition, Figure S10: Immunofluorescence in thalidomide-treated or non-treated keratinocytes to monitoring autophagy, Figure S11: Immunofluorescence of NF-κB in cultured keratinocytes with thalidomide or silenced IRF4, Table S1: Clinical and laboratory characteristics of the study subjects, Table S2: Conjugated antibodies used in flow cytometry analysis, Table S3: Antibodies used in immunofluorescence, immunohistochemistry and western blot analysis, Table S4: Primer IDs used in Taqman RT-qPCR from Applied Biosystems, Table S5: Characterization of cutaneous lupus erythematosus (CLE) includes 206 proteins distributed in the named motives, Table S6: Detail of the targets identified for thalidomide and the use of the targets in the different project steps, Table S7: MoA included 27 proteins with 14 proteins related directly with CLE.

Author Contributions: Conceptualization: C.S. and J.C.-H.; methodology, S.D., T.M. and C.S.; software, S.D. and C.S.; validation, S.D., T.M. and C.S.; formal analysis, S.D., C.S., T.M., B.F. and J.C.-H.; writing-review and editing, S.D., C.S. and J.C.-H.; visualization, S.D., C.S., T.M., B.F. and J.C.-H.; supervision, J.C.-H.; project administration, J.C.-H.; funding acquisition, J.C.-H. All authors have read and agreed to the published version of the manuscript.

Funding: This research was funded by Instituto de Salud Carlos III, PI15/02145.

Institutional Review Board Statement: The study was conducted according to the guidelines of the Declaration of Helsinki and approved by the Vall d'Hebrón Ethics Committee (protocol code ORDI-02 and date of approval 02/JUL/2012).

Informed Consent Statement: Informed consent was obtained from all subjects involved in the study.

Data Availability Statement: Data are available from Gene Expression Omnibus (GSE162424) at https://www.ncbi.nlm.nih.gov/geo/query/acc.cgi?acc=GSE162424 (accessed on 20 October 2021).

Acknowledgments: We thank all patients and healthy volunteers for participating in the study. The authors wish to acknowledge Associació per la Investigació en el Lupus Eritematós Sistèmic (AILES) for their support.

Conflicts of Interest: The authors declare no conflict of interest.

References

1. Onkon, L.G.; Werth, V.P. Cutaneous lupus erythematosus: Diagnosis and treatment. *Best Pract. Res. Clin. Rheumatol.* **2013**, *27*, 391–404. [CrossRef]
2. Werth, V.P. Clinical manifestations of cutaneous lupus erythematosus. *Autoimmun. Rev.* **2005**, *4*, 293–302. [CrossRef] [PubMed]
3. Gillian, J.N.; Sontheimer, R.D. Distinctive cutaneous subsets in the spectrum of lupus erythematosus. *J. Am. Acad. Derm.* **1981**, *4*, 471–475. [CrossRef]
4. Baltaci, M.; Fritsch, P. Histologic features of cutaneous lupus erythematosus. *Autoimun. Rev.* **2009**, *8*, 467–473. [CrossRef]
5. Sticherling, M.; Bonsmann, G.; Kuhn, A. Diagnostic approach and treatment of cutaneous lupus erythematosus. *J. Dtsch. Derm. Ges.* **2008**, *6*, 48–59. [CrossRef]
6. Cortés-Hernández, J.; Torres-Salido, M.; Castro-Marrero, J.; Vilardell-Tarres, M.; Ordi-Ros, J. Thalidoide in the treatment of refractory cutaneous lupus erythematosus: Prognostic factors of clinical outcome. *Br. J. Derm.* **2012**, *166*, 616–623. [CrossRef] [PubMed]
7. Callen, J.P. Management of "refractory" skin disease in patients with lupus erythematosus. *Best Pract. Res. Clin. Rheumatol.* **2005**, *19*, 767–784. [CrossRef]
8. Hastings, R.C.; Trautman, J.R.; Enna, C.D.; Jacobson, R.R. Thalidomide in the treatment of erythema nodosum leprosum. With a note on slected laboratory abnormalities in erythema nodosum leprosum. *Clin. Pharm.* **1970**, *11*, 481–487.
9. Palumbo, A.; Facon, T.; Sonneveld, P.; Bladè, J.; Offidani, M.; Gay, F.; Moreau, P.; Waage, A.; Spencer, A.; Ludwig, H.; et al. Thalidomide for treatment of multiple myeloma: 10 years later. *Blood* **2008**, *11*, 3968–3977. [CrossRef] [PubMed]
10. Rubio, J.B.; Gonzalez, F.F. Lupus eritematoso discoide & talidomida. *Derm. Rev. Mex* **1975**, *19*, 131–139.
11. Cuadrado, M.J.; Karim, Y.; Sanna, G.; Smith, E.; Khamashta, M.A.; Hughes, G.R.V. Thalidomide for the treatment of resistant cutaneous lupus: Efficacy and safety of different therapeutic regimens. *Am. J. Med.* **2005**, *118*, 246–250. [CrossRef] [PubMed]
12. Duong, D.J.; Spigel, G.T.; Moxley, R.T., 3rd; Gaspari, A.A. American experience with low-dose thalidomide therapy for severe cutaneous lupus erythematosus. *Arch. Dermatol.* **1999**, *135*, 1079–1087. [CrossRef]
13. Bastuji-Garin, S.; Ochonisky, S.; Bouche, P.; Gherardi, R.K.; Duguet, C.; Djerradine, Z.; Poli, F.; Revuz, J.; Thalidomide Neuropathy Study Group. Incidence and risk factors for thalidomide neuropathy: A prospective study of 135 dermatologic patients. *J. Investig. Derm.* **2002**, *119*, 1020–1026. [CrossRef] [PubMed]

14. Bennett, C.L.; Schumock, G.T.; Desai, A.A.; Kwaan, H.C.; Raisch, D.W.; Newlin, R.; Stadler, W. Thalidomide-associated deep vein thrombosis and pulmonary embolism. *Am. J. Med.* **2002**, *113*, 603–606. [CrossRef]
15. Ito, T.; Ando, H.; Handa, H. Teratogenic effects of thalidomide: Molecular mechanisms. *Cell Mol. Life Sci* **2011**, *68*, 1569–1579. [CrossRef]
16. D'Amato, R.J.; Loughnan, M.S.; Flynn, E.; Folkman, J. Thalidomide is an inhibitor of angiogenesis. *Proc. Natl. Acad. Sci. USA* **1994**, *91*, 4082–4085. [CrossRef] [PubMed]
17. Keifer, J.A.; Guttridge, D.C.; Ashburner, B.P.; Baldwin, A.S., Jr. Inhibition of NF-kappa B activity by thalidomide through suppression of IkappaB kinase activity. *J. Biol. Chem* **2001**, *276*, 22382–22387. [CrossRef]
18. Moreira, A.L.; Sampaio, E.P.; Zmuidzinas, A.; Frindt, P.; Smith, K.A.; Kaplan, G. Thalidomide exerts its inhibitory action on tumor necrosis factor α by enhancing mRNA degradation. *J. Exp. Med.* **1993**, *177*, 1675–1680. [CrossRef] [PubMed]
19. Yasui, K.; Kobayashi, N.; Yamazaki, T.; Agematsu, K. Thalidomide as an immunotherapeutic agent: The effects on neutrophil-mediated inflammation. *Curr. Pharm. Des.* **2005**, *11*, 395–401. [CrossRef]
20. Kingsmore, S.F.; Lindquist, I.E.; Mudge, J.; Gessler, D.D.; Beavis, W.D. Genome-wide association studies: Progress and potential for drug discovery and development. *Nat. Rev. Drug Discov.* **2008**, *7*, 221–230. [CrossRef]
21. Avey, D.; Sankararaman, S.; Yim, A.K.Y.; Barve, R.; Milbrandt, J.; Mitra, R.D. Single-Cell RNA-Seq Uncovers a Robust Transcriptional Response to Morphine by Glia. *Cell Rep.* **2018**, *24*, 3619–3629. [CrossRef]
22. Kim, K.T.; Lee, H.W.; Lee, H.O.; Kim, S.C.; Seo, Y.J.; Chung, W.; Hye, H.E.; Do-Hyun, N.; Junhyoung, K.; Kyeung, M.J.; et al. Single-cell mRNA sequencing identifies subclonal heterogeneity in anti-cancer drug responses of lung adenocarcinoma cells. *Genome Biol.* **2015**, *16*, 127. [CrossRef] [PubMed]
23. Wacker, S.A.; Houghtaling, B.R.; Elemento, O.; Kapoor, T.M. Using transcriptome sequencing to identify mechanisms of drug action and resistance. *Nat. Chem. Biol.* **2012**, *8*, 235–237. [CrossRef] [PubMed]
24. Khun, A.; Ruzicka, T. Classification of cutaneous lupus erythematosus. In *Cutaneous Lupus Erythematosus*; Khun, A., Lehmann, P., Ruzicka, T., Eds.; Springer: Berlin/Heidelberg, Germany, 2004; pp. 53–59.
25. Albrecht, J.; Taylor, L.; Berlin, J.A.; Dulay, S.; Ang, G.; Fakharzadeh, S.; Kantor, J.; Kim, E.; Militello, G.; McGinnis, K.; et al. The CLASI (Cutaneous Lupus Erythematosus Disease Area and Severity Index): An outcome instrument for cutaneous lupus erythematosus. *J. Investig. Derm.* **2005**, *125*, 889–894. [CrossRef] [PubMed]
26. Wingett, S.W.; Andrews, S. FastQ Screen: A tool for multi-genome mapping and quality control. *F1000 Res.* **2018**, *7*, 1338. [CrossRef]
27. Dobin, A.; Davis, C.A.; Schlesinger, F.; Drenkow, J.; Zaleski, C.; Jha, S.; Batut, P.; Chaisson, M.; Gingeras, T.R. STAR: Ultrafast universal RNA-seq aligner. *Bioinformatics* **2013**, *29*, 15–21. [CrossRef]
28. Li, B.; Dewey, C.N. RSEM: Accurate transcript quantification from RNA-Seq data with or without a reference genome. *BMC Bioinform.* **2011**, *12*, 323. [CrossRef]
29. Love, M.I.; Huber, W.; Anders, S. Moderated estimation of fold change and dispersion for RNA-seq data with DESeq2. *Genome Biol.* **2014**, *15*, 550. [CrossRef]
30. Jorba, G.; Aguirre-Plans, J.; Junet, V.; Segú-Vergés, C.; Ruiz, J.L.; Pujol, A.; Fernández-Fuentes, N.; Mas, J.M.; Oliva, B. In-silico simulated prototype-patients using TPMS technology to study a potential adverse effect of sacubitril and valsartan. *PLoS ONE* **2020**, *15*, e0228926. [CrossRef]
31. Wishart, D.S.; Knox, C.; Guo, A.C.; Cheng, D.; Shrivastava, S.; Tzur, D.; Gautam, B.; Hassanali, M. DrugBank: A knowledgebase for drugs, drug actions and drug targets. *Nucleic Acids Res.* **2008**, *36*, D901–D906. [CrossRef]
32. Szklarzyk, D.; Santos, A.; von Mering, C.; Jensen, L.J.; Bork, P.; Kuhn, M. STITCH 5: Augmenting protein-chemical interaction networks with tissue and affinity data. *Nucleic Acids Res.* **2016**, *44*, D380–D384. [CrossRef]
33. Hecker, N.; Ahmed, J.; von Eichborn, J.; Dunkel, M.; Macha, K.; Eckert, A.; Gilson, M.K.; Bourne, P.E.; Preissner, R. Super Target goes quantitative: Update on drug-target interactions. *Nucleic Acids Res.* **2012**, *40*, D1113–D1117. [CrossRef]
34. Kanehisa, M.; Goto, S.; Sato, Y.; Kawashima, M.; Furumichi, M.; Tanable, M. Data, information, knowledge and principle: Back to metabolism in KEGG. *Nucleic Acids Res.* **2014**, *42*, D199–D205. [CrossRef] [PubMed]
35. Gilson, M.K.; Liu, T.; Baitaluk, M.; Nicola, G.; Hwang, L.; Chong, J. BindingDB in 2015: A public database for medicinal chemistry, computational chemistry and systems pharmacology. *Nucleic Acids Res.* **2016**, *44*, D1045–D1063. [CrossRef]
36. Chatr-Aryamontri, A.; Oughtred, R.; Boucher, L.; Rust, J.; Chang, C.; Kolas, N.K.; O'Donnell, L.; Oster, S.; Theesfeld, C.; Sellam, A. The BioGRID interaction database: 2017 update. *Nucleic Acids Res.* **2017**, *45*, D369–D379. [CrossRef]
37. Jassal, B.; Matthews, L.; Viteri, G.; Gong, C.; Lorente, P.; Fabregat, A.; Sidiropoulos, K.; Cook, J.; Gillespie, M.; Haw, R.; et al. The Reactome pathway knowledgebase. *Nucleic Acids Res.* **2020**, *48*, D498–D503. [CrossRef]
38. Fionda, C.; Abruzzese, M.; Zingoni, A.; Cecere, F.; Vulpis, E.; Peruzzi, G.; Soriani, A.; Molfetta, R.; Paolini, R.; Ricciardi, M.R.; et al. The IMiDs targets IKZF-1/3 and IRF4 as novel negative regulators of NK cell-activating ligands expression in multiple myeloma. *Oncotarget* **2015**, *6*, 23609–23630. [CrossRef] [PubMed]
39. Solé, C.; Gimenez-Barcons, M.; Ferrer, B.; Ordi-Ros, J.; Cortés-Hernández, J. Microarray study reveals a transforming growth factor-β-dependent mechanism of fibrosis in discoid lupus erythematosus. *Br. J. Derm.* **2016**, *175*, 302–313. [CrossRef]
40. O'Brien, J.C.; Hosler, G.A.; Chong, B.F. Changes in T cell and B cell composition in discoid lupus erythematosus skin at different stages. *J. Derm. Sci.* **2017**, *85*, 247–249. [CrossRef]

41. Li, Q.; Wu, H.; Liao, W.; Zhao, M.; Chan, V.; Li, L.; Zhena, M.; Chen, G.; Zhang, J.; Lau, C.-S.; et al. A comprehensive review of immune-mediated dermatopathology in systemic lupus erythematosus. *J. Autoimmun.* **2018**, *93*, 1–15. [CrossRef] [PubMed]
42. Gadola, S.D.; Dulphy, N.; Salio, M.; Cerundolo, V. Valpha24-JalphaQ-independent, CD1d-restricted recognition of alpha-galactosylceramide by human CD4(+) and CD8alphabeta(+) T lymphocytes. *J. Immunol.* **2002**, *168*, 5514–5520. [CrossRef]
43. Chang, D.H.; Liu, N.; Klimek, V.; Hassoun, H.; Mazumder, A.; Nimer, S.D.; Jagannath, S.; Dhodapkar, M.V. Enhancement of ligand-dependent activation of human natural killer T cells by lenalidomide: Therapeutic implications. *Blood* **2006**, *108*, 618–621. [CrossRef]
44. Elkhal, A.; Pichavant, M.; He, R.; Scott, J.; Meyer, E.; Goya, S.; Geha, R.S.; Umetsu, D.T. CD1d restricted natural killer T cells are not required for allergic skin inflammation. *J. Allergy Clin. Immunol.* **2006**, *18*, 1363–1368. [CrossRef] [PubMed]
45. Goubier, A.; Vocanson, M.; Macari, C.; Poyet, G.; Herbelin, A.; Nicolas, J.F.; Dubois, B.; Kaiserlina, D. Invariant NKT cells suppress CD8(+) T-cell-mediated allergic contact dermatitis independently of regulatory CD4(+) T cells. *J. Investig. Dermatol.* **2013**, *133*, 980–987. [CrossRef] [PubMed]
46. Tanno, H.; Kawakami, K.; Ritsu, M.; Kanno, E.; Suzuki, A.; Kamimatsuno, R.; Takagi, N.; Miyasaka, T.; Ishii, K.; Imai, Y.; et al. Contribution of Invariant Natural Killer T Cells to Skin Wound Healing. *Am. J. Pathol.* **2015**, *185*, 3248–3257. [CrossRef] [PubMed]
47. Tanno, H.; Kawakami, K.; Kanno, E.; Suzuki, A.; Takagi, N.; Yamamoto, H.; Ishii, K.; Imai, Y.; Maruyama, R.; Tachi, M. Invariant NKT cells promote skin wound healing by preventing a prolonged neutrophilic inflammatory response. *Wound Repair Regen.* **2017**, *25*, 805–815. [CrossRef]
48. Godó, M.; Sessler, T.; Hamar, P. Role of invariant natural killer T (iNKT) cells in systemic lupus erythematosus. *Curr. Med. Chem.* **2008**, *15*, 1778–1787. [CrossRef]
49. Lee, H.S.; Kwon, H.S.; Park, D.E.; Woo, Y.D.; Kim, H.Y.; Kim, H.R.; Cho, S.H.; Min, K.U.; Kang, H.R.; Chang, Y.S. Thalidomide inhibits alternative activation of macrophages in vivo and in vitro: A potential mechanism of anti-asthmatic effect of thalidomide. *PLoS ONE* **2015**, *10*, e0123094. [CrossRef]
50. Haslett, P.A.; Corral, L.G.; Albert, M.; Kaplan, G. Thalidomide costimulates primary human T lymphocytes, preferentially inducing proliferation, cytokine production, and cytotoxic responses in the CD8+ subset. *J. Exp. Med.* **1998**, *187*, 1885–1892. [CrossRef]
51. McHugh, S.M.; Rifkin, I.R.; Deighton, J.; Wilson, A.B.; Lachmann, P.J.; Lockwood, C.M.; Ewan, P.W. The immunosuppressive drug thalidomide induces T helper cell type 2 (Th2) and concomitantly inhibits Th1 cytokine production in mitogen- and antigen-stimulated human peripheral blood mononuclear cell cultures. *Clin. Exp. Immunol.* **1995**, *99*, 160–167. [CrossRef]
52. Chan, A.J.; Jang, J.C.; Nair, M.G. Tissue Remodeling and Repair during Type 2 inflammation. In *The Th2 Type Immune Response in Health and Disease*; Gause, W., Artis, D., Eds.; Springer: New York, NY, USA, 2016; ISBN 978-1-4939-2910-8.
53. Ito, T.; Ando, H.; Suzuki, T.; Ogura, T.; Hotta, K.; Imamura, Y.; Yamaguchi, Y.; Handa, H. Identification of a primary target of thalidomide teratogenicity. *Science* **2010**, *327*, 1345–1350. [CrossRef]
54. Amare, G.G.; Meharie, B.G.; Belayneh, Y.M. A drug repositioning success: The repositioned therapeutic applications and mechanisms of action of thalidomide. *J. Oncol. Pharm. Pract.* **2021**, *27*, 673–678. [CrossRef] [PubMed]
55. Mori, T.; Ito, T.; Liu, S.; Ando, H.; Sakamoto, S.; Yamaguchi, Y.; Tokunaga, E.; Shibata, N.; Handa, H.; Hakoshima, T. Structural basis of thalidomide enantiomer binding to cereblon. *Sci. Rep.* **2018**, *8*, 1294. [CrossRef]
56. Kowalski, T.W.; Gomes, J.D.A.; Garcia, G.B.C.; Fraga, L.R.; Paixao-Cortes, V.R.; Recamonde-Mendoza, M.; Sanseverino, M.T.V.; Shuler-Faccini, L.; Vianna, F.S.L. CRL4-Cereblon complex in Thalidomide Embryopathy: A translational investigation. *Sci. Rep.* **2020**, *10*, 851. [CrossRef] [PubMed]
57. Ni, A.; Chen, H.; Wu, Y.; Li, W.; Chen, S.; Li, J. Expression of IRF-4 and IBP in skin lesions of patients with psoriasis vulgaris. *J. Huazhong Univ. Sci. Technol. Med. Sci.* **2012**, *32*, 287–290. [CrossRef]
58. Agnarelli, A.; Chevassut, T.; Mancini, E.J. IRF4 in multiple myeloma-Biology, disease and therapeutic target. *Leuk. Res.* **2018**, *72*, 52–58. [CrossRef]
59. Cretney, E.; Xin, A.; Shi, W.; Minnich, M.; Masson, F.; Miasari, M.; Belz, G.T.; Smyth, G.K.; Busslinger, M.; Nutt, S.L.; et al. The transcription factors Blimp-1 and IRF4 jointly control the differentiation and function of effector regulatory T cells. *Nat. Immunol.* **2011**, *12*, 304–311. [CrossRef] [PubMed]
60. Negishi, H.; Ohba, Y.; Yanai, H. Negative regulation of Toll-like-receptor signaling by IRF-4. *Proc. Natl. Acad. Sci. USA* **2005**, *102*, 15989–15994. [CrossRef]
61. Rodriguez-Carrio, J.; López, P.; Alperi-López, M.; Caminal-Montero, L.; Ballina-Garcia, F.J.; Suárez, A. IRF4 and IRGs delineate clinically relevant gene expression signatures in systemic lupus erythematosus and rheumatoid arthritis. *Front. Immunol.* **2018**, *9*, 3085. [CrossRef]
62. Bjorklund, C.C.; Lu, L.; Kang, J.; Hagner, P.R.; Havens, C.G.; Amatangelo, M.; Wang, M.; Ren, Y.; Couto, S.; Breider, M.; et al. Rate of CRL4(CRBN) substrate Ikaros and Aiolos degradation underlies differential activity of lenalidomide and pomalidomide in multiple myeloma cells by regulation of c-Myc and IRF4. *Blood Cancer J.* **2015**, *5*, e354. [CrossRef]
63. Zhu, Y.X.; Kortuem, K.M.; Stewart, A.K. Molecular mechanism of action of immune-modulatory drugs thalidomide, lenalidomide and pomalidomide in multiple myeloma. *Leuk. Lymphoma* **2013**, *54*, 683–687. [CrossRef]
64. Lee, K.M.; Jo, S.; Kim, H.; Lee, J.; Park, C.S. Functional modulation of AMP-activated protein kinase by cereblon. *Biochim. Biophys. Acta.* **2011**, *1813*, 448–455. [CrossRef]

65. Zhang, H.X.; Yuan, J.; Li, Y.F.; Li, R.S. Thalidomide decreases high glucose-induced extracellular matrix protein synthesis in mesangial cells via the AMPK pathway. *Exp. Med.* **2019**, *17*, 927–934. [CrossRef] [PubMed]
66. Zhang, H.; Yang, Y.; Wang, Y.; Wang, B.; Li, R. Renal-protective effect of thalidomide in streptozotocin-induced diabetic rats through anti-inflammatory pathway. *Drug Des. Dev. Ther.* **2018**, *12*, 89–98. [CrossRef]
67. Kwon, E.; Li, X.; Deng, Y.; Chang, H.W.; Kim, D.Y. AMPK is down-regulated by the CRL4A-CRBN axis through the polyubiquitination of AMPKa isoforms. *FASEB J.* **2019**, *33*, 6539–6550. [CrossRef] [PubMed]
68. Cibrian, D.; Fuente, H.; Sánchez-Madrid, F. Metabolic pathways that control skin homeostasis and inflammation. *Trends Mol. Med.* **2020**, *26*, 975–986. [CrossRef]
69. Li, Y.; Yang, L.; Dong, L.; Yang, Z.W.; Zhang, J.; Zhang, S.L.; Niu, M.J.; Xia, J.W.; Gong, Y.; Zhu, N.; et al. Crosstalk between the Akt/mTORC1 and NF-kb signaling pathways promotes hypoxia-induced pulmonary hypertension by increasing DPP4 expression in PASMCs. *Acta Pharm. Sin.* **2019**, *40*, 1322–1333. [CrossRef] [PubMed]
70. Solé, C.; Domingo, S.; Ferrer, B.; Moliné, T.; Ordi-Ros, J.; Cortés-Hernández, J. MicroRNA Expression Profiling Identifies miR-31 and miR-485-3p as Regulators in the Pathogenesis of Discoid Cutaneous Lupus. *J. Investig. Derm.* **2019**, *139*, 51–61. [CrossRef]
71. Sur, I.; Ulvmar, M.; Toftgard, R. The two-faced NF-kappaB in the skin. *Int. Rev. Immunol.* **2008**, *27*, 205–223. [CrossRef]
72. Verma, I.M. Nuclear factor (NF)-kappaB proteins: Therapeutic targets. *Ann. Rheum Dis.* **2004**, *63* (Suppl. S2), ii57–ii61. [CrossRef]
73. Bell, S.; Degitz, K.; Quirling, M.; Jilg, N.; Page, S.; Brand, K. Involvement of NF-κB signalling in skin physiology and disease. *Cell. Signal* **2003**, *15*, 1–7. [CrossRef]
74. Zhang, C.; Xiao, C.; Dang, E.; Cao, J.; Zhu, Z.; Fu, M.; Yao, X.; Liu, Y.; Jin, B.; Wang, G.; et al. CD100-Plexin-B2 promotes the inflammation in psoriasis by activating NF-kB ant the inflammasome in keratinocytes. *J. Investig. Dermatol.* **2018**, *138*, 375–383. [CrossRef]
75. Homey, B.; Dieu-Nosjean, M.C.; Wiesenborn, A.; Massacrier, C.; Pin, J.J.; Oldham, E.; Catron, D.; Buchanan, M.E.; Müller, A.; Malefyt, R.W.; et al. Up-regulation of macrophage inflammatory protein-3 alpha/CCL20 and CC chemokine receptor 6 in psoriasis. *J. Immunol.* **2000**, *164*, 6621–6632. [CrossRef]
76. Laggner, U.; Meglio, P.D.; Perera, G.K.; Hundhausen, C.; Lacy, K.E.; Ali, N.; Smith, C.H.; Hayday, A.C.; Nickoloff, B.J.; Nestle, F.O. Identificiation of a novel proinflammatory human skin-homing Vgamma9Vdelta2 T cell subset with a potential role in psoriasis. *J. Immunol.* **2011**, *187*, 2783–2793. [CrossRef] [PubMed]
77. Tanaka, A.; Muto, S.; Jung, K.; Itai, A.; Matsuda, H. Topical application with a new NF-kappaB inhibitor improves atopic dermatitis in NC/NgaTnd mice. *J. Investig. Derm.* **2007**, *127*, 855–863. [CrossRef] [PubMed]
78. Yu, H.; Lin, L.; Zhang, Z.; Zhang, H.; Hu, H. Targeting NF-kB pathway for the therapy of diseases: Mechanism an clinical study. *Signal. Transduct. Target. Ther.* **2020**, *5*, 209. [CrossRef] [PubMed]

Supporting Information

Thalidomide exerts anti-inflammatory effects in cutaneous lupus via inhibiting the IRF4/NF-κB and AMPK1/mTOR pathway

Sandra Domingo[1], Cristina Solé[1], Teresa Moliné[2], Berta Ferrer[2], Josefina Cortés-Hernández[1]

[1]Lupus Unit, Rheumatology Department, Hospital Universitari Vall d´Hebron, Institut de Recerca (VHIR), Universitat Autònoma de Barcelona, Barcelona, Spain.

[2]Department of Pathology, Hospital Universitari Vall d´Hebron, Universitat Autònoma de Barcelona, Barcelona, Spain

1. SI Materials and Methods

Patients' clinical characteristics and samples

A total of 10 patients were included in the study. Demographic characteristics are shown in Table S1. At the time of skin biopsy, disease activity and degree of scarring was assessed by the validated modified CLE Disease Area and Severity Index (CLASI) (Albrecht et al., 2005) Patient's inclusion criteria included: age ≥ 18 years old, the presence of skin lesional area bigger than 3cm, a validated CLE Disease Area and Severity Index (CLASI) greater than 4 and no previous treatment with immunosuppressants for ≥1 month or topical corticoids for at least ≥2 weeks. The study was approved by the Local Vall d'Hebrón Ethics Committee and informed consent was obtained from all subjects before the study.

At inclusion all patients received oral thalidomide (100 mg/day) at night for 4 weeks. A six-millimetre punch biopsy was taken from lesional skin from CLE untreated patients and another six-millimetre punch biopsy was taken from paired patient's post-thalidomide treatment. The skin punch was divided into three sections: the first section was used for RNA-sequencing experiments, the second was immediately frozen in liquid nitrogen in OCT compound for immunofluorescence studies and the third was fixed in 5% formalin and paraffin-embedded in order to perform immunohistochemistry techniques.

RNA library construction and sequencing

Total RNA from skin biopsies was obtained using RNeasy Mini Kit (Qiagen, Hilden, Germany) and ribosomal RNA was removed using Epicentre's Ribo-Zero rRNA Removal kit (Illumina, San Diego, USA). RNA integrity was evaluated using Bioanalyzer 2100 obtaining values ≥8.5 (Agilent Technologies, Santa Clara, CA, USA). Samples were converted to cDNA and subsequently subjected to fragmentation, linker adapter ligation and amplification using TruSeq library generation kits (Illumina, San Diego, USA) according to manufacturer's instructions. The constructed libraries were amplified using 8 cycles of PCR. The resulting libraries were subjected to Illumina Hiseq 2000 sequencing platform version 3 producing 2x75 bp run with >65 M reads (Illumina, San Diego, USA).

Image analysis, sequencing quality evaluation, and data production summarisation were performed using the Illumina/Solexa pipeline (Illumina, San Diego, USA). Sequences were analyzed for quality control (FASTQC) and aligned to the Human genome (GRCh38) using STAR program (version 2.5.2a) (Wingett et al., 2018; Dobin et al., 2013). RSEM program (version 1.2.28) (Li et al., 2011) was used to determine transcript assembly, and the abundance and expression levels were determined based on the fragments per kb per million (FPKM) values, a way of normalizing read counts by calculating the number of reads mapped to each transcript divided by its length and the total number of mapped reads in the sample. To find differentially expressed genes and transcripts, the logarithmic ratios of FPKMs were calculated by pairwise comparisons of the expression between pre- and post-skin thalidomide samples with tests for significant differences using DESeq2 (Love et al., 2014). To obtain high-quality DEGs, we set the threshold for the false-discovery rate at < 0.05 and for fold change at ≥ 2 or ≤ 05 (|log2FC| ≥ 1) in the comparison analysis.

TPMS technology [31]

The Therapeutic Performance Mapping System (TPMS) is a tool that creates mathematical models of a drug/pathology protein pathways to explain a clinical outcome or phenotype (Anaxomics Biotech, Barcelona, Spain). These mathematical models find mechanism of action (MoAs) that explain how a *Stimulus* (i.e. proteins activated or inhibited by a drug) produces a *Response* (i.e. proteins active or inhibited in a phenotype). The detailed steps are explained below:

1. Molecular characterization of CLE disease and thalidomide

To apply the TPMS approach and create the mathematical models of MoAs, a characterization of CLE disease and thalidomide is needed. We manually curated a list of proteins and motives relevant for cutaneous lupus erythematosus (CLE) pathogenesis and targets for thalidomide's mechanism of action (Supplemental Table 5 and 6). Manual curation was performed through an extensive and careful review of full-length articles in the PubMed database, Drug Bank, Stitch and Supertarget (Knehisa et al., 2014; Gilson et al., 2016; Chatr-Aryamontri et al., 2017; Croft et al., 2014). The search was expanded using the "related articles" function and article reference list. For CLE characterization, we included 206 proteins. For thalidomide molecular drug characterization, eight main molecules have been identified (CRBN, IKZF1, IKZF3, IRF4, MEIS2, ORM1, ORM2, FGF2) and 36 proteins were related to them.

2. Generation of mathematical models

We generated a biological map between CLE proteins and thalidomide targets using public information about protein-to-protein interactions, physical interactions and modulations, signaling, metabolic relationships and gene expression regulation that are founded in: KEGG, Binding Database, BioGRID and REACTOME (Jorba et al., 2020; Wishart et al., 2008; Szklarzyk et al., 2016; Hecker et al., 2012).

The algorithm of TPMS for generating the mathematical models is similar to a Multilayer Perceptron of an Artificial Neural Network over the biological map (where neurons are the proteins, and the edges of the network are used to transfer the information). It takes as input signals the activation (+1) and inactivation (-1) of the drug target proteins and as output proteins implicated in CLE pathogenesis.

The models have to be able to weigh the relative value of each protein (node) relation. Since the number of links is very high, the number of parameters to solve also increases exponentially. Anaxomics applied Artificial Intelligence (AI) technologies for modelling complex network behaviors, including graph theory and statistical pattern recognition technologies; genetic algorithms; artificial neural networks; dimensionality reduction techniques; and stochastic methods like Simulated Annealing, Monte Carlo among others (Anaxomics Biotech, Barcelona, Spain).

3. Molecular mechanism construction

Then a collection of restrictions, defined as the true set of edges and nodes with the property of being active or inactive, are used for validating the mathematical models obtained with TPMS (Truth table). Two type of restrictions are used: 1) information found in microarray database (GEO, PHOSIDA, 2D gel database, BED) and drug database (DrugBank); 2) data obtained from our RNA-seq analysis using skin biopsies of CLE patient's pre and post-thalidomide treatment

As the number of restrictions is always smaller than the number of parameters required by the algorithm, any process modelled by TPMS has a "population" of different solutions, which is set around 10^6–10^9, since this interval is estimated to faithfully portray nature. From this set of solutions, only the best ones (showing acceptable accuracy values for the Truth Table) are used to construct a "global" or "average" molecular mechanism, which represents the most probable molecular mechanism according to the current biological knowledge. In the present work, two MoAs were detected as the best: molecular response to thalidomide downstream 1) its main target (Cereblon) and 2) indirect modulation of IRF4 activity. The graphical representation of the interactions between the proteins in the two best MoAs are showed in Figure S3 and S4, respectively.

Evaluation of immunohistochemistry and immunofluorescence skin sections

Immunohistochemistry and immunofluorescence results were evaluated on blinded specimens by two independent dermatopathologists from the Vall d'Hebron pathology unit. Positive cells per millimetre were quantified using computer-assisted image

analysis software (ImageJ 1.42, National Institutes of Health, Bethesda, MD, USA). The staining of the epidermis, dermis and inflammatory infiltrate was evaluated semi-quantitatively using the following blinded score: 0 (<10% positive cells), 0.5 (10-20% positive cells), 1 (20-40% positive cells), 1.5 (40-60% positive cells), 2 (60-80% positive cells), 2.5 (80-90% positive cells) or 3 (>90% positive cells).

PBMCs isolation

Blood from CLE patients before and after thalidomide treatment and healthy controls was collected directly into mononuclear cell preparation tubes with sodium citrate (Vacutainer CPT, BD Biosciences). Tubes were centrifuged at 3000 rpm for 30 minutes at room temperature (RT). After that, the layer containing peripheral blood mononuclear cells was clearly visible and collected using a pipette. Cells were washed twice with PBS and resuspended in complete RPMI media (RPMI, 10% FBS, 10% Pen/Strep, 2 mM/L-Glutamine) (Gibco, Life Technologies).

Immunofluorescence on primary cells

Cells were seeded in sterile glass coverslips in 24 well-plates and incubated overnight at 37ºC for adherence. After thalidomide/siRNA treatments and stimulation 25 mJ/cm2 (Bio- Link Crossliner BLX 312; Vilber Lourmat, Germany) in case of Keratinocytes or 10 ng/mL TNFα (Life Technologies) for PBMCs, cells were washed with PBS and then fixed for 15 minutes in 4% PFA followed by permeabilization with 0.1% TritonX-100 for 10 minutes. Blocking solution (BSA 5%) was added for 1 hour at RT and primary antibodies were incubated overnight at 4ºC and secondary antibodies were added for 2h at RT (Table S3). DAPI was used to visualize the nucleus. Images were captured using Olympus BX61 microscope.

RNA extraction

Skin biopsies were homogenized by politron and RNA was purified using miRVANA miRNA Isolation Kit (Applied Biosystems) following manufacturer's instructions. Total RNA from cultured cells was extracted after cell lysis with RNeasy Mini Kit (Qiagen). The yield and the quality of RNA from cell cultures were assessed by measuring its absorbance at 260nm and 280nm with Nanodrop. Ratios of A260/A280 between 1.8 and 2.1 were considered acceptable to use the RNA for the subsequent experiments.

RT-qPCR

Once RNA was obtained, 1ug of total RNA was reverse-transcribed into cDNA using the High Capacity cDNA Reverse Transcription Kit (Applied Biosystems) with the thermal cycler program: 25ºC for 10min, 37ºC for 120 min and 85ºC for 5min. Gene expression was assessed by TaqMan gene expression assays (FAM dye-labeled MGB probe, Applied Biosystems). Using 96 well plates or 384 well plates in the ABI PRISM 7000 or ABI PRISM 7900 thermocyclers respectively at 50ºC for 2 min, 95ºC for 10min, followed by 40 cycles of 95ºC for 15s and 60ºC for 1 min. Obtained data was normalized based on the expression of the endogenous control gene GAPDH (Hs02786624_g1).

Protein extraction and quantification

Protein was extracted from skin tissue following the instructions of PARIS kit (Thermo Fisher, Waltham, MA, USA). The skin was homogenized with the lysis buffer and samples were centrifuged at 12000 rpm at 4ºC for 3 minutes. The supernatant was collected, and 200 mL of chloroform was added. After 5 minutes on ice, samples were centrifuged 12000 rpm at 4ºC for 15 min. Then, the organic phase was collected, and isopropanol was added for 10 min at room temperature for protein precipitation. After centrifugation at 12000 rpm for 4ºC, 0.3 M of guanidine hydrochloride solution was added and centrifuged at 12000 rpm at 4ºC twice. Supernatant was discarded and the protein pellet was washed with ethanol and dried for 5-10 minutes. Finally, 1% SDS solution was added to dissolve the protein by repeated pipetting. The protein concentration was determined using the Bio-Rad Protein Assay (Bio-Rad, Hercules, CA, USA) according to the manufacturer's instructions.

Apoptosis and Proliferation Assays

Cells were plated in 24-well plates, stimulated with 25 mJ/cm2 in case of Keratinocytes or 10 ng/mL TNFα (Life Technologies) for PBMCs and thalidomide was added for 24h. Then, they were stained with Dead Cell Apoptosis Kit with Annexin V APC and SYTOX™ Green (Thermofisher) and measured by flow cytometry. For proliferation assays, cells were plated in 96-well plates, stimulated and thalidomide was added. After 24h, CyQUANT NF Cell Proliferation Assay Kit (Invitrogen) was used following manufacturer's instructions. Relative changes were calculated using "Non-Thalidomide treated cells" as control.

2. Supplementary Figures

Figure S1. PBMCs from patients were extracted pre and post-thalidomide (N=5). We obtained their RNA and we analyzed gene expression of CD8 Tcells (PRF1 and GRNZB) and iNKT (IL4 and INFG) related proteins by RT-qPCR. Relative expression were obtained using $2^{-\Delta\Delta Ct}$ method and GADPH as endogenous control. No significant differences were obtained but we observed a tendency in perforin A (PRF1, p=0.0674) and granzyme B (GRNZB, p=0.068).

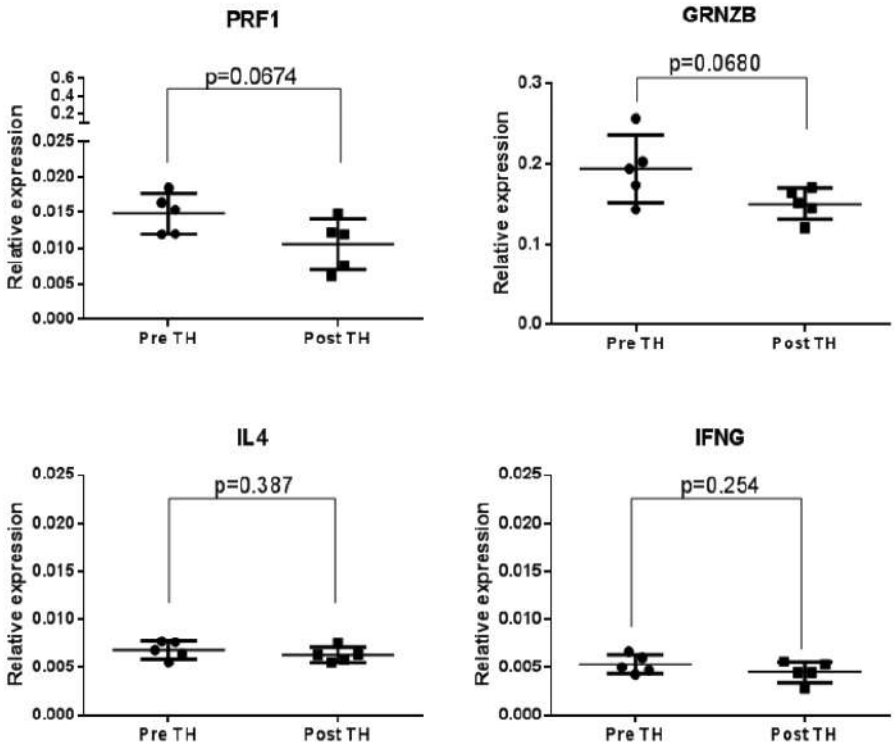
PRF1
p=0.0674
Relative expression
0.6
0.4
0.2
0.025
0.020
0.015
0.010
0.005
0.000
Pre TH
Post TH
GRNZB
p=0.0680
Relative expression
0.3
0.2
0.1
0.0
Pre TH
Post TH
IL4
p=0.387
Relative expression
0.025
0.020
0.015
0.010
0.005
0.000
Pre TH
Post TH
IFNG
p=0.254
Relative expression
0.025
0.020
0.015
0.010
0.005
0.000
Pre TH
Post TH

Figure S2. Topological analysis represents the relationships between proteins in the mechanism of action over cereblon modulation with the proteins identified as differential in RNA-seq analysis.

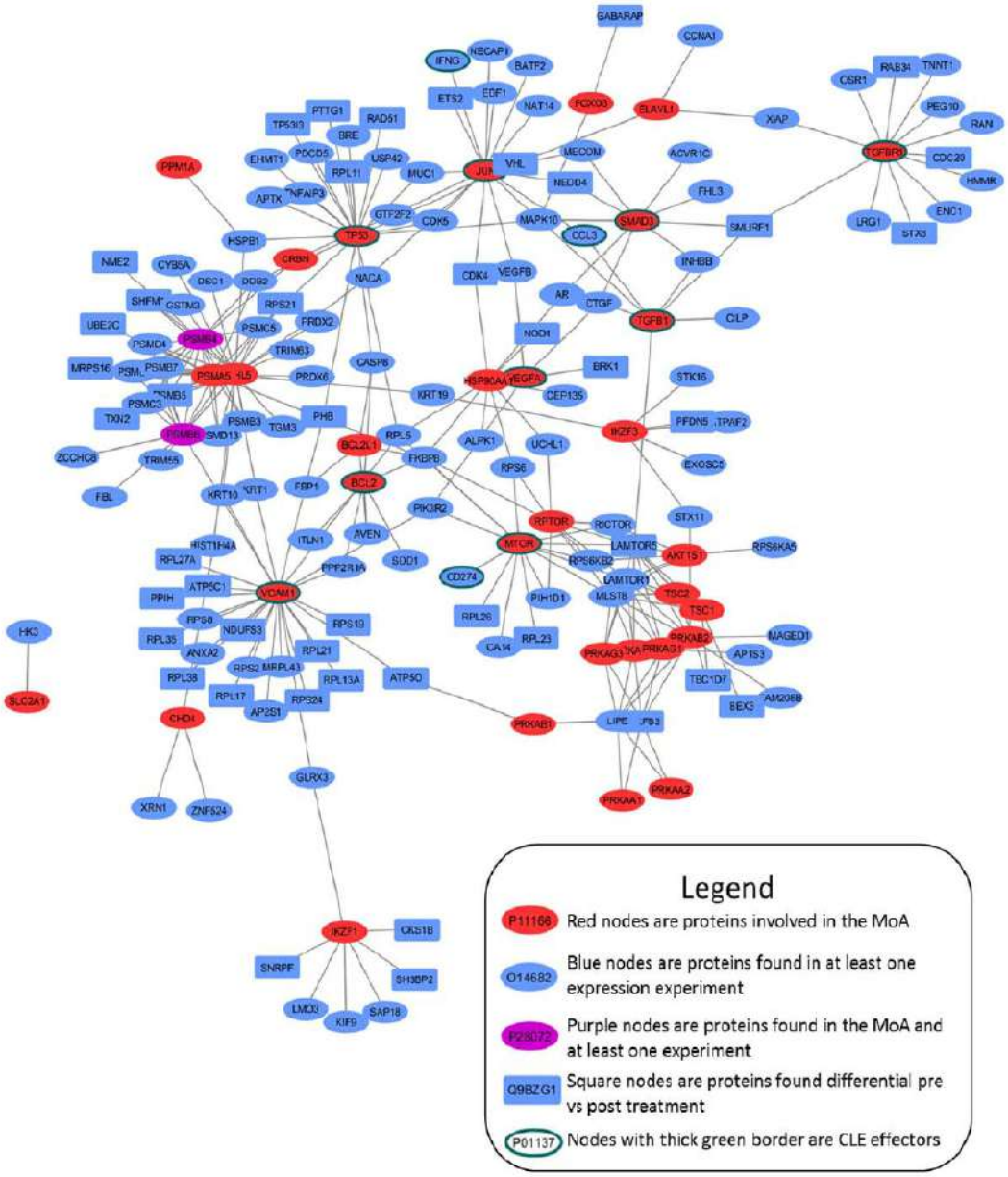

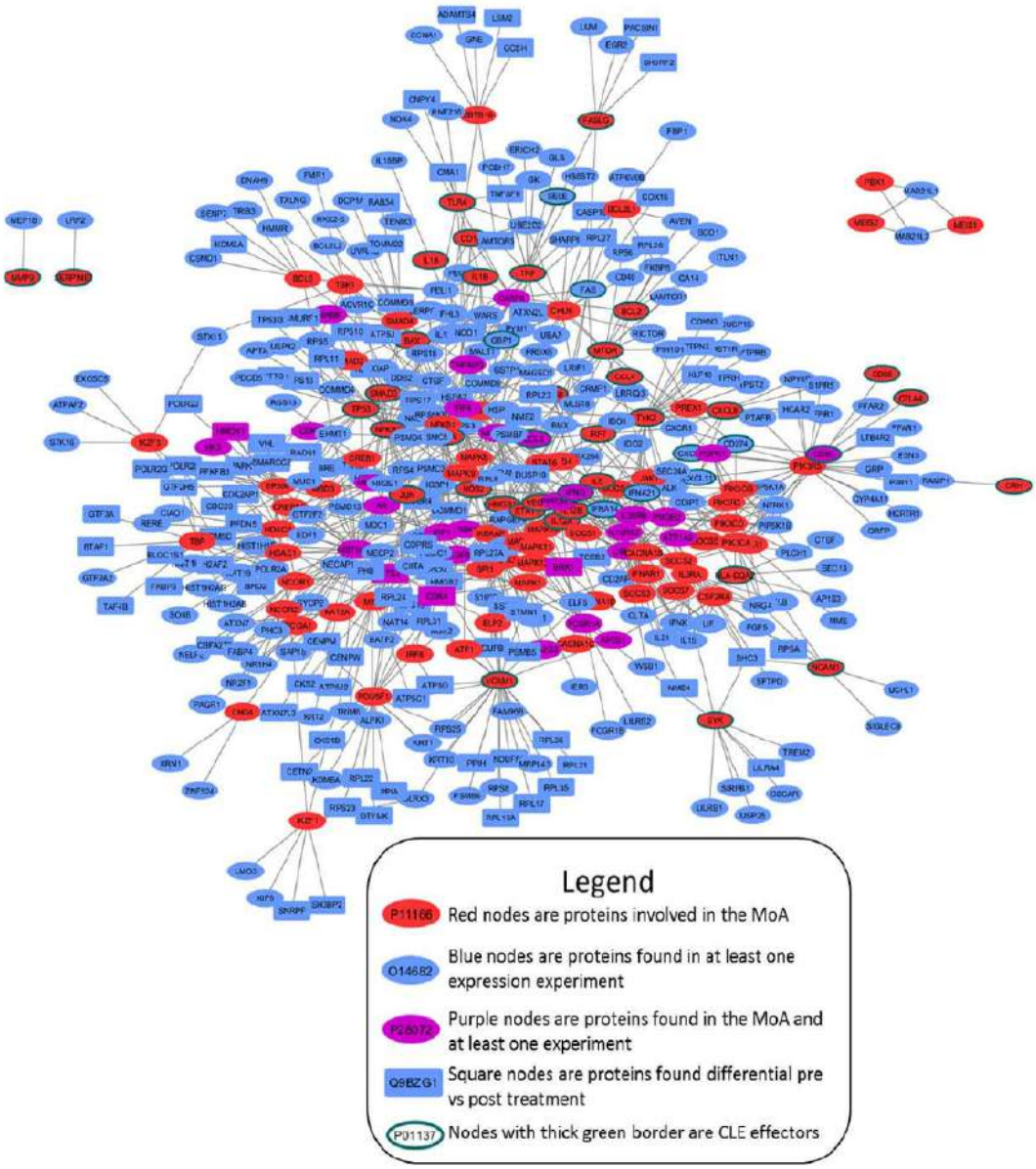

Figure S3. Topological analysis represents the relationships between proteins in the mechanism of action over IRF4 (cereblon-modulated protein) with the proteins identified as differential in RNA-seq analysis.

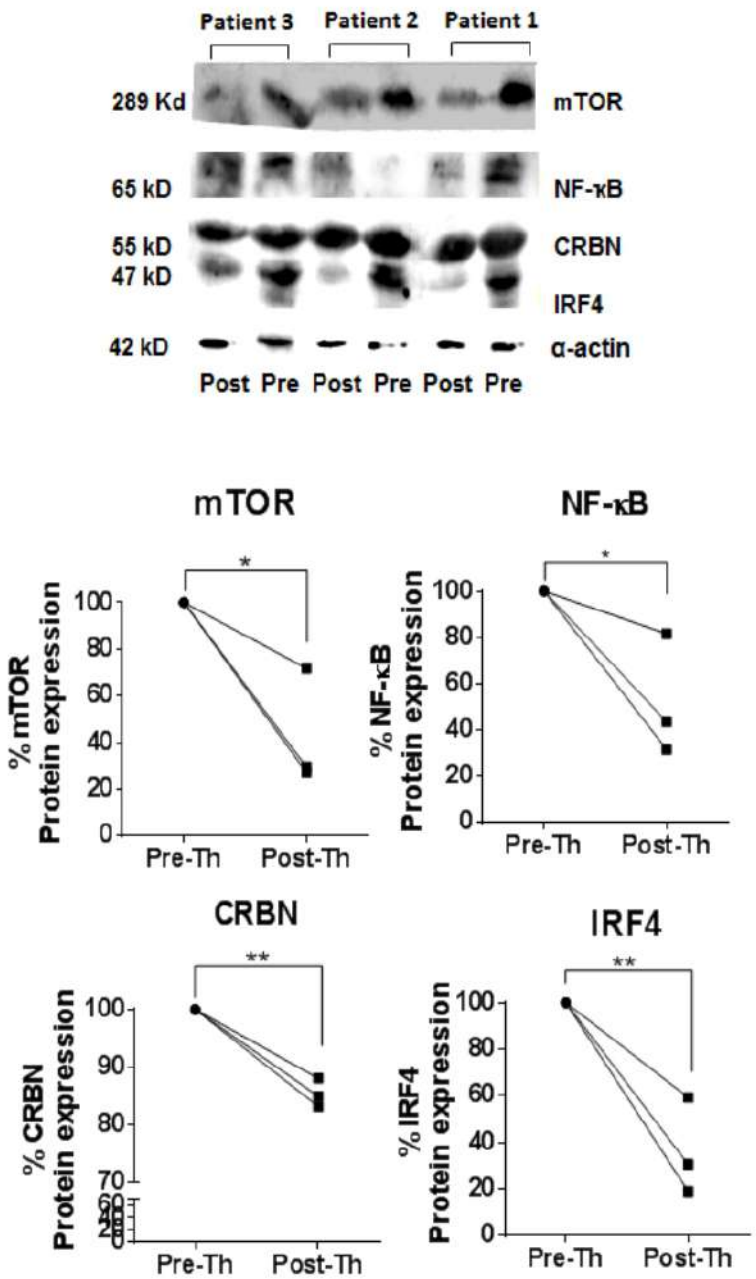

Figure S4. Western Blot of lysates from paired skin biopsies of Post-thalidomide and Pre-thalidomide treated patients for mTOR, NF-κB, CRBN and IRF4 (N= 3). β-actin was used as a control to normalize the levels of protein detected. Graphs show values in normalized band intensities between paired samples. * $p<0.05$ and ** $p<0.005$.

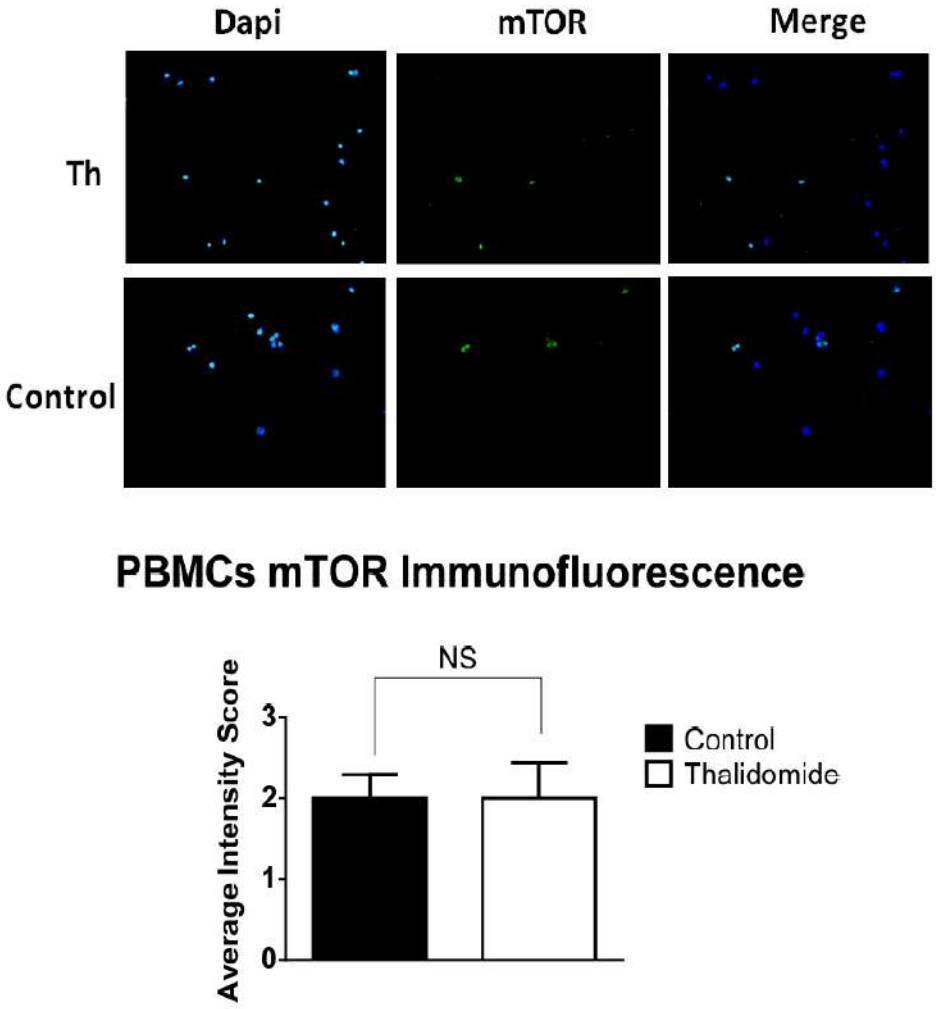

Figure S5. Immunofluorescence of mTOR in thalidomide-treated (Th) or non-treated (control) PBMCs. Nuclei was stained with DAPI (blue) and mTOR has green staining. Before treatment, PBMCs were stimulated with TNFα. No significant differences were observed between conditions (NS).

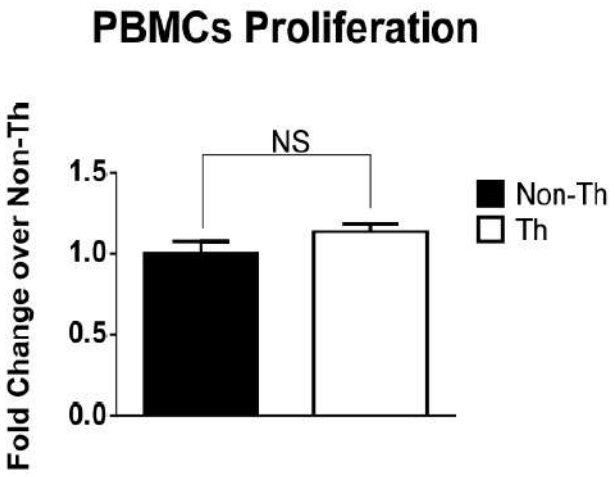

Figure S6. Proliferation in healthy PBMCs after thalidomide treatment. PBMCs were stimulated with TNFα overnight and treated with thalidomide (Th) or with sterile PBS, non-treated condition (Non-Th). After 6 hours, proliferation was quantified, and fold change was calculated over Non-Th condition. No significant differences were observed between conditions (NS).

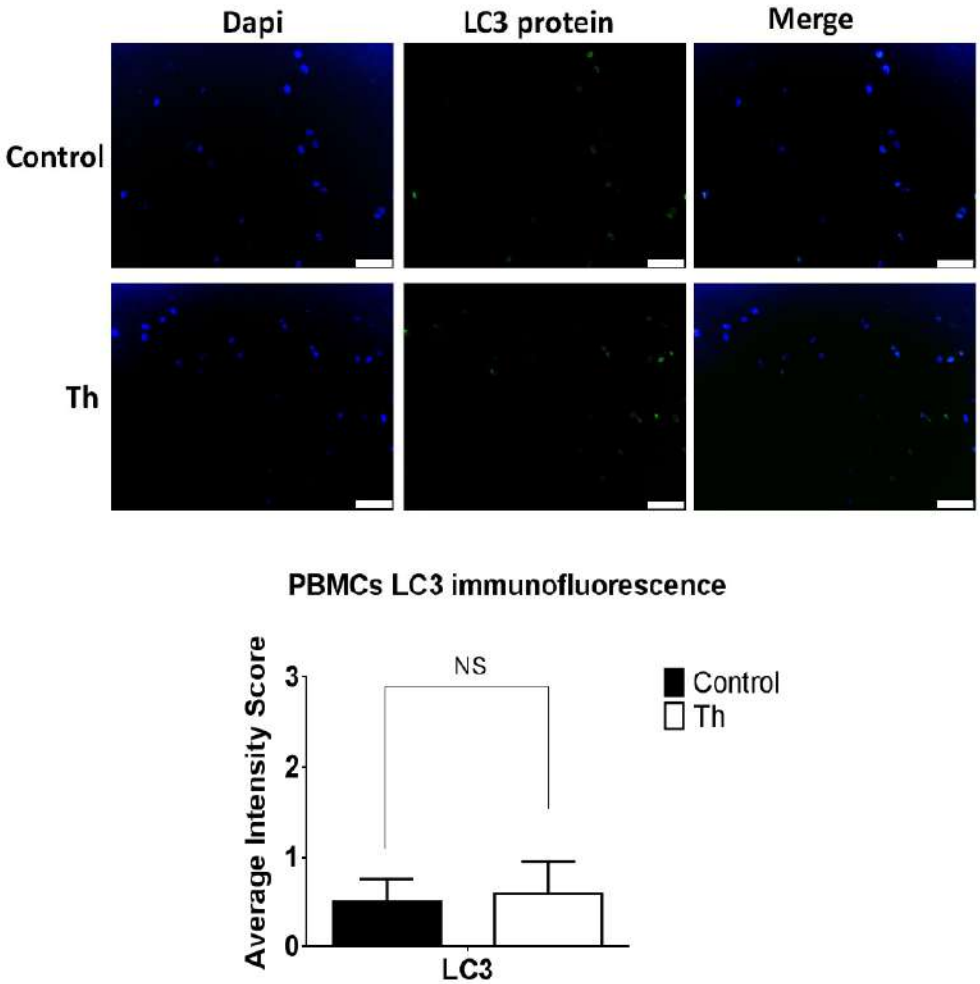

Figure S7. Immunofluorescence in thalidomide-treated (Th) or non-treated (control) PBMCs to monitoring autophagy. Nuclei was stained with DAPI (blue) and LC3 protein has green staining. Before treatment, PBMCs were stimulated with TNFα. No significant differences were observed between conditions (NS).

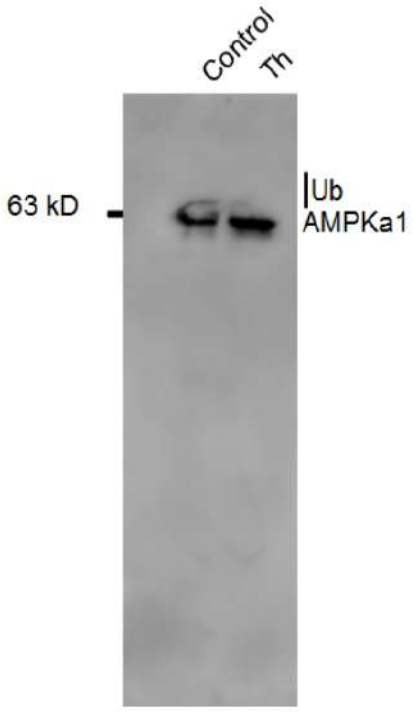

Figure S8. Western blot of cell based ubiquitination assay in keratinocytes treated or non-treated with thalidomide (Th). Results showed that AMPKa1 is ubiquinated in in absence of thalidomide and consequently AMPKa1 levels are decreased in comparison with thalidomide treated cells.

Figure S9. Proliferation and Apoptosis of Human epidermal keratinocytes after thalidomide addition. For proliferation and apoptosis measurement, cells were exposed to 25 mJ/cm^2 UVB and thalidomide was added for 24h (Th). For non-treated thalidomide cells (Non-Th), sterile PBS was added after 24 hours post-UVB stimulation. Fold change was calculated over Non-Th condition.

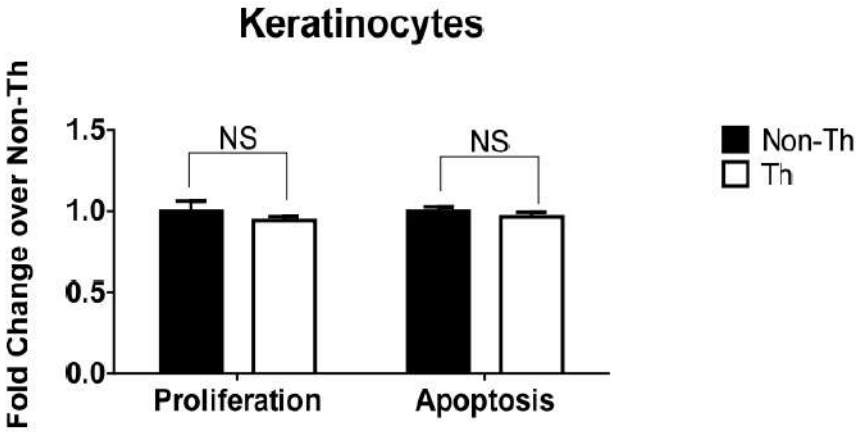

Figure S10. Immunofluorescence in thalidomide-treated (Th) or non-treated (control) keratinocytes to monitoring autophagy. Nuclei was stained with DAPI (blue) and LC3 protein has green staining. Before treatment, keratinocytes were stimulated with UV. No significant differences were observed between conditions (NS).

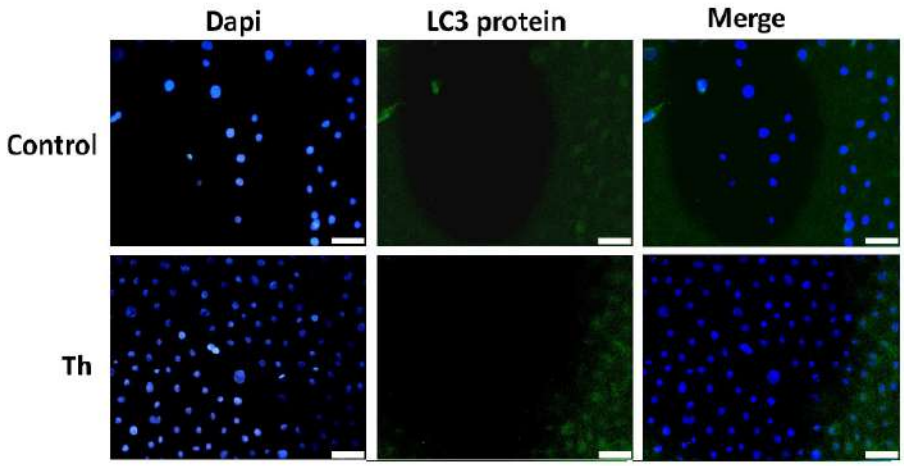

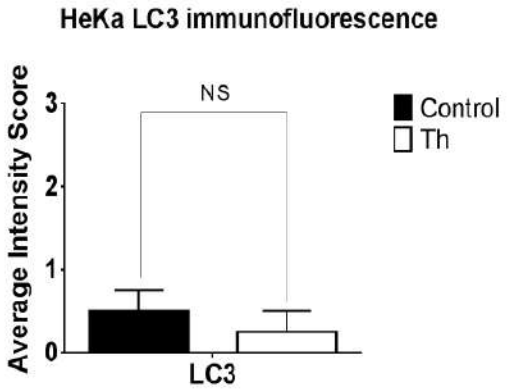

Figure S11. Immunofluorescence of NF-κB (green) in cultured keratinocytes with thalidomide or silenced IRF4. Counterstaining of nuclei is shown with DAPI in blue. No significant differences were observed between conditions (NS).

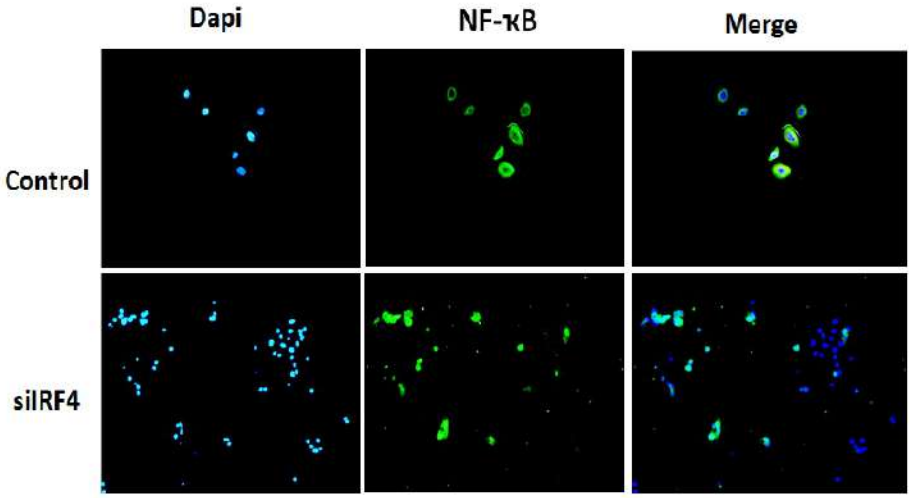

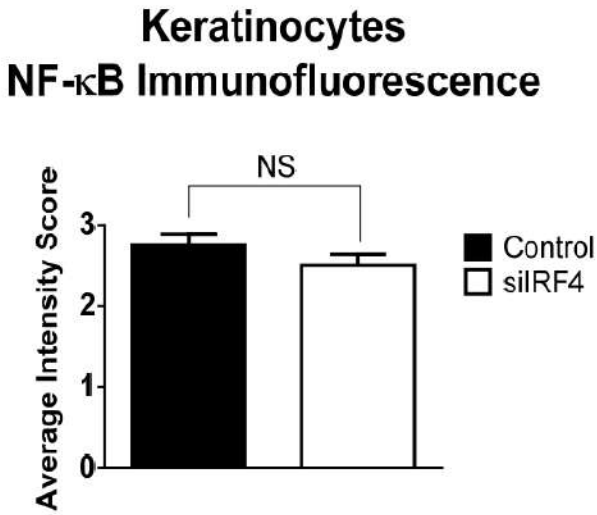

1. Supplementary Tables

Table S1. Clinical and laboratory characteristics of the study subjects.

	CLE (n=10)
AGE, mean (SD), yrs	44 (10.3)
Female, n (%)	10 (100%)
Photosensitivity, n (%)	3 (30%)
Smoking, (%)	4 (40%)
Type of CLE	
DLE	8 (80%)
SCLE	2 (20%)
CLASI ACTIVITY, mean (SD)	11.0±2.5
CLASI DAMAGE, mean (SD)	4.3±1.45
Systemic Lupus Erythematosus	4 (40%)
Clinical response to Thalidomide (4 weeks) Complete response (CLASI=0)	7 (70%)
ANA antibodies positive, n (%)	8 (80%)
Anti-SSA/Ro antibodies positive, n (%)	1 (10%)

Values are number of patients and between brackets the percent of total number patients. The other values are means± SD. CLASI: Cutaneous Lupus Erythematosus Disease Area and Severity Index; CLE: cutaneous lupus erythematosus; DLE: discoid lupus erythematosus; SCLE: subacute cutaneous lupus erythematosus; ANA: Antinuclear Antibodies.

Table S2. Conjugated antibodies used in Flow Cytometry analysis.

B cell subsets	Supplier	Code
CD19	BD Biosciences	345788
CD27	BD Biosciences	558664
CD38	BD Biosciences	555460
IgD	BD Biosciences	555779
T cell subsets **Thelper subsets**	**Supplier**	**Code**
CD3	BD Biosciences	340662
CD4	BD Biosciences	561842
CD8	BD Biosciences	555369
CCR3	BD Biosciences	561745
CCR4	BD Biosciences	744140
CCR5	BD Biosciences	560932
CCR6	BD Biosciences	564479
CXCR3	BD Biosciences	740183
CD25	BD Biosciences	340939
FOXP3	BD Biosciences	560046
NK cell subsets	**Supplier**	**Code**
CD3	BD Biosciences	340662
CD16	BD Biosciences	561842
CD56	BD Biosciences	555369
6B11	BD Biosciences	552825

Table S3. Antibodies used in Immunofluorescence, Immunohistochemistry and Western blot analysis.

Primary Antibody	Supplier	Code
Anti-CRBN	Abcam	ab244223
Anti-IRF4 (MUM1)	Abcam	ab133590
Anti-MTOR	Abcam	ab45989
Anti-NF-KB p65	Abcam	ab16502
Anti-CD4	Roche	SP35
Anti-CD8	Agilent	DK25
Anti-CD56	Fisher Scientific	56C04
Anti-6B11	Invitrogen	14-5806-82
Anti-Phospho-Raptor (Ser863)	Invitrogen	PA5-64849
Anti-AMPK alpha-1	Invitrogen	AHO1332
Anti-Ubiquitin	Abcam	Ab7780
Secondary Antibody	**Supplier**	**Code**
Alexa-488-conjugated anti-rabbit IgG	Abcam	ab150077
Alexa-647-conjugated anti-mouse IgG	Abcam	ab150115

Table S4. Primer IDs used in Taqman RT-qPCR from Applied Biosystems.

Gene	Assay ID (TaqMan)
GADPH	Hs02786624_g1
NFKB1	Hs00765730_m1
MTOR	Hs00234508_m1
CXCL1	Hs00236937_m1
IL1B	Hs01555410_m1
CCL3	Hs00234142_m1
GATA3	Hs00231122_m1
TBX21 (T-bet)	Hs00894392_m1
TGFB1	Hs00998133_m1
IL-2	Hs00174114_m1
CXCL8 (IL-8)	Hs00174103_m1
TNF	Hs00174128_m1
PRKAA1 (AMPKa1)	Hs01562308_m1
IL-10	Hs00961622_m1
IFNA1	Hs04189288_g1
IL4	Hs00174122_m1
IFNG	Hs00989291_m1
PRF1	Hs00169473_m1
GRNZB	Hs00188051_m1

Table S5. Characterization of Cutaneous Lupus Erythematosus (CLE) includes 206 proteins distributed in the named motives.

MOTIVE NAME	Number of proteins
Innate immune system activation	75
Keratinocyte apoptosis	23
Impaired apoptotic clearance	10
Autoantigen exposure	16
Lymphocyte recruitment and activation	44
Complement response and IgG complex formation	15
Fibrosis – Discoid Lupus Erythematosus	22
Angiogenesis	1

Table S6. Detail of the targets identified for thalidomide and the use of the targets in the different project steps.

Protein name	Gene name	UniProt code	Reference	Use
Protein cereblon	CRBL	Q96SW2	PMID: 27460676	Model training and MoA target
DNA-binding protein Ikaros	IKZF1	Q13422	PMID: 27492707	Model training and MoA target
Zinc finger protein Aiolos	IKZF3	Q9UKT9	PMID: 27492707	Model training and MoA target
Interferon regulatory factor 4	IRF4	Q15306	PMID: 26269456	Model training and MoA target
Homeobox protein Meis2	MEIS2	Q14770	PMID: 27492707	Model training and MoA target
Alpha-1-acid glycoprotein 1	ORM1	P02763	PMID: 8755512	Model training
Alpha-1-acid glycoprotein 2	ORM2	P19652	PMID: 8755512	Model training
Fibroblast growth factor 2 (FGF-2)	FGF2	P09038	PMID: 26503997; PMID: 25053990	Model training

Table S7. MoA included 27 proteins with 14 proteins related directly with CLE (in bold).

PROTEIN	Relationship with CLE
VEGFA	Higher VEGF levels in CLE
VCAM1	High VCAM-1 expression on endothelium tissue in CLE lesions
MTOR	MTOR is involved in UVB signaling in keratinocytes and is a potential target for CLE
TLR4	TLR4 increases inflammatory response and has been associated to autoimmunity in CLE
TNF	TNF-α may have both inflammatory and immunomodulatory roles in CLE
IL6	Interleukins are induced by UVB in keratinocytes in CLE
CXCL8	Interleukins are induced by UVB in keratinocytes in CLE
TGFB	High levels in DLE lesions
JUN	In CLE, JUN has been associate to UVB exposure
CD14	CD14+ macrophages are increased in DLE skin
CCL3	CCL3 are found upregulated in CLE
MMP9	MMP9 has been linked to a time-dependent TGF-β-related scarring process in DLE
NFKB1	In CLE, NFKB1 has been associated to UVB exposure, and to UVB-induced TNF-α expression
IRF4	DC dysfunction in lupus-prone mice relies on IRF4 pathways
AMPK	Not related
IKZF1	
IKZF3	
CHD4	
ELAVL1	
RPTOR	
TSC1	
TSC2	
AKT1S1	
CRBN	
SPI1	
BCL6	
RELA	

Chapter 3: Evaluation of the identified miRNAs before and after thalidomide treatment

The modulation of miRNAs expression in CLE following therapy has not been yet investigated. In other skin conditions such as psoriasis, differences in miRNA profiles in serum and in skin have been described after anti-TNFα biological treatment, although not related to disease severity [245, 246]. In this part of the project, we performed a pilot study to determine whether thalidomide therapy affects tissue miRNA levels in patients with CLE. For this purpose, miR-31 and miR-485-3p, miR-885-5p, miR-139-5p expression has been analysed in skin samples before and after thalidomide treatment (Table 12).

Thalidomide modulates miRNAs expression in CLE before and after thalidomide treatment.

Since miR-31 and miR-485-3p were differentially upregulated in DLE (paper I), we performed the analysis in this type of CLE in responder and non-responder patients. Following thalidomide treatment, miR-31 and miR-485-3p expression levels decreased in skin biopsies from paired responder patients, being this reduction more significant in miRNA31 ($p<0.001$) (Fig 18), that is the keratinocyte-dependent miRNA. On the other hand, non-responder DLE patients did not show a significant decrease of miR-31 and miR-485-3p (Fig 18) following thalidomide treatment.

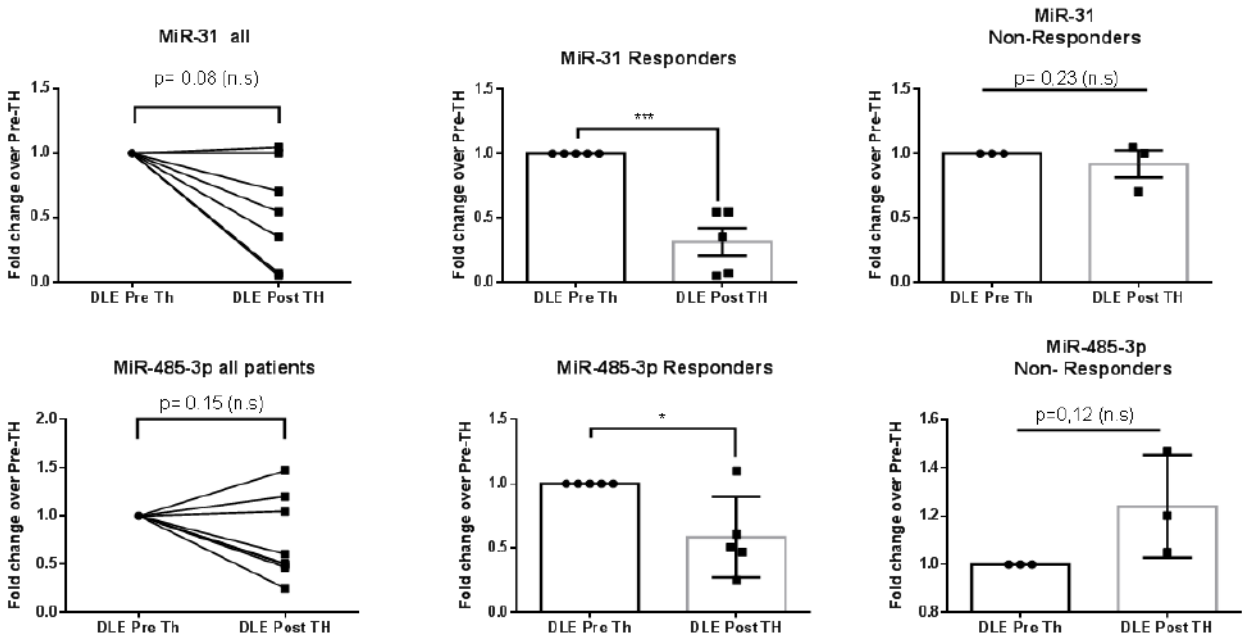

Figure 18. miR-31 and miR-485-3p skin expression levels from DLE al patients (n=8) and divided in responder (n=5) and non-responder (n=3) before and after thalidomide treatment. Th: thalidomide.

The other two miRNAs identified relevant in CLE, miR-885-5p and miR-139-5p were downregulated in CLE both DLE and SCLE. MiR-885-5p was a keratinocyte dependent miRNA whereas miR-139-5p could not be detected in skin following in situ hybridization (paper II). After being treated Thalidomide only showed an upregulation of miR-885-5p ($p<0.01$). Regarding miR-139-5p, a tendency was observed but no significant changes were encountered (Fig 19). On the other hand, non-responder patients did not show a significant change in both miR-885-5p and miR-139-5p (Fig 19).

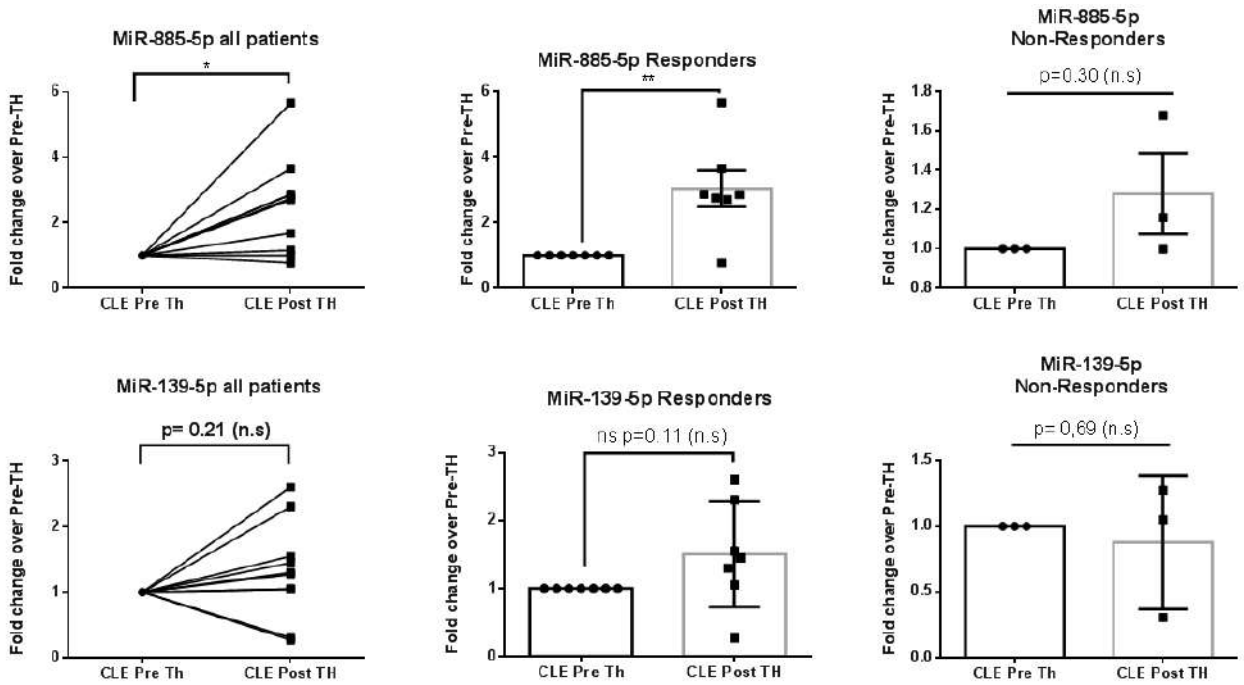

Figure 19. miR-885-5p and miR-139-50 skin expression levels from DLE al patients (n=10) and divided in responder (n=7) and non-responder (n=3) before and after thalidomide treatment . Th: thalidomide.

Taken together, these results indicate that thalidomide exerts an accentuated effect mainly in keratinocyte dependent miRNAs miR-31 and miR-885p and a slight effect in dermal miR-485-3p. The observed changes were significant in the responder group, and non-significant changes were observed in the non-responder group. These data suggest that preliminary studies show these miRNAs as biomarkers of thalidomide response. These results need to be taken with caution since the number of patients evaluated is small.

Differentially expressed miRNAs expression in keratinocytes and PBMCs after treatment in vitro

We next aimed to know if the changes observed in miRNAs following treatment were specific of thalidomide or could be observed following HCQ, the standard treatment for CLE. Healthy keratinocytes and PBMCs were cultured and treated with 100 ng/mL thalidomide or 1 μ g/mL of hydroxychloroquine *in vitro*. The miRNA expression was analysed by RT-qPCR.

We found miR-31 expression levels in keratinocytes to decrease following both treatments, thalidomide ($p<0.0001$) or hydroxychloroquine ($p<0.0001$), suggesting that both treatments contribute to the regulation of this miRNA. However, miR-485-3p decreased slightly in PBMCs only after hydroxychloroquine treatment ($p<0.05$) (Fig 20).

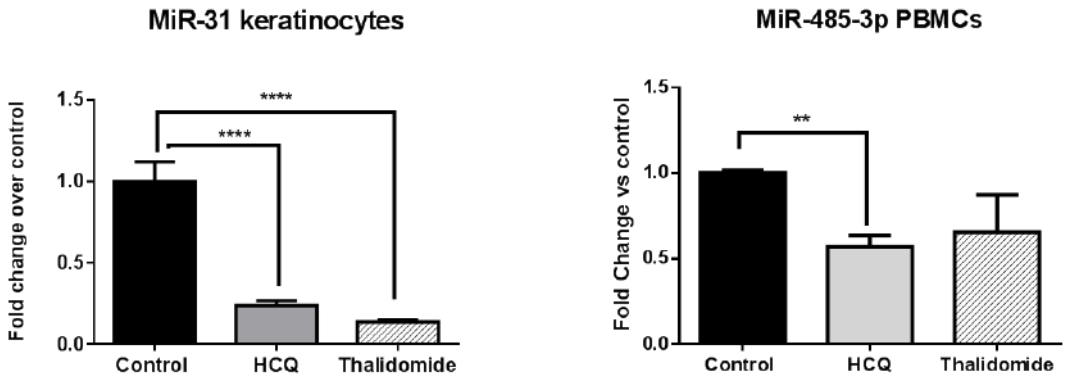

Figure 20. mir-31 and miR-139-5p expression before and after thalidomide treatment in keratinocytes and PBMCs respectively (n=3). HCQ: hydroxychloroquine.

On the other hand, regarding miR-885-5p expression, it was markedly upregulated only when thalidomide was added in keratinocytes (2.3-fold, $p<0.01$). (Fig 21). mir-139 was not further assessed as no significant changes were observed in skin from responder patients treated with thalidomide.

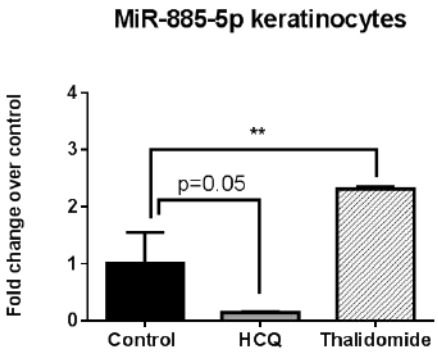

Figure 21. miR-885-5p expression before and after thalidomide treatment in keratinocytes (n=3). HCQ: hydroxychloroquine.

Taking together, the expression keratinocyte derived miRNAs miR-31 and miR-885-5p was modulated by thalidomide addition in skin from responder treated patients and in keratinocytes *in vitro*. Both microRNAs are involved in NF-κB signaling regulation, therefore thalidomide markedly modulates keratinocyte dependent NF-κB microRNAs.

5. Discussion

The pathogenesis of CLE is not fully understood, and it is likely to be multifactorial. Although it is known that there is a genetic predisposition, environmental triggers and abnormalities in the immune response, large gaps in knowledge remain regarding the exact causes, mechanisms and biological interactions leading to the development of the autoimmune attack to the skin. What is clear is the increasing evidence that demonstrates keratinocytes to play an important role in the pathogenesis of CLE [247, 248]. These cells after stimulation in an inflammatory environment or after UV are able to release inflammatory cytokines IFNs, TNFα, IL-1, IL-6, IL-8, IL-10 and IL-17 which are important for initiation, development and perpetuation of CLE [249].

The fact that the mechanisms involved in CLE pathogenesis are not well known, implies that therapeutic options for this condition do not include approved specific drugs and most of the time, treatments need to be empirically determined for individual patients. Currently, approximately 40% of patients will be refractory to conventional therapy with antimalarials and topical corticosteroids. For these patients, there is not a clear treatment algorithm and treatment is based in a trial error, except by the use of thalidomide that has been proved highly effective in CLE. Despite its proven efficacy its use is restricted due to its significant side effects and by the lack of randomised controlled trials. Therefore, an enhanced understanding of the molecular and genetic basis of the disease as well as thalidomide mechanism of action in CLE is a requirement to improve the search for novel therapeutic targets.

It is known that miRNAs are implicated in various cellular processes of both normal and diseased skin. Some miRNAs appear to be consistently deregulated in several different inflammatory skin diseases, including psoriasis and atopic dermatitis, indicating a common role in fundamental biological processes [115]. The clinical implications of miRNAs are intriguing, there is emerging evidence for their clinical potential as both biomarkers and possible therapeutic targets in skin diseases. When we started this thesis, the role of microRNAs in CLE was completely unexplored.

This thesis consisted of three different chapters that involved identifying a miRNA profile in CLE and studying its role in the pathogenesis, exploring the mechanism of action of thalidomide in CLE with the aim of identifying novel therapeutic targets and finally, how this identified miRNA profile was modified by treatment. Each chapter is associated to specific objectives.

This is the first study to report a miRNA profile characteristic of DLE and CLE (paper I).

Although DLE and SCLE subtypes share histological similarities, clinically they differ in their course and prognosis, suggesting a different pathogenesis [54, 140]. The previous microarray study from our group identified a distinctive T-cell and a fibrotic TGF-β–dependent signature in lesional DLE [178]. Similarly, in this study we found DLE-affected skin to have a specific differential microRNA expression profile compared with SCLE-affected skin, with a predominant overexpression of miR-31 in keratinocytes and miR-485-3p in PMBCs and dermal fibroblasts.

miR-31 has been widely studied and it is known to participate in several cellular processes such as embryonic development, myogenesis, bone homeostasis or cancer [250]. In cutaneous conditions is associated with activated keratinocytes such as psoriasis, non-melanoma skin cancer and hair follicle growth [251]. Amongst the different functions , miR-31 plays a role in restoring epidermal homeostasis, promoting keratinocyte proliferation, apoptosis, differentiation as well as and contributing to skin inflammation [252, 253].

We showed miR-31 to be also upregulated in DLE lesional skin, specifically in the epidermis. Using primary DLE keratinocytes, we identified *in vitro* TGFβ-1, like in Psoriasis, but also UVB radiation as the main regulators of miR-31 expression. Ultraviolet (UV) light, particularly UVB (290–320 nm) plays an important role in the initiation, development, and perpetuation of CLE. Exposure to UV light is one of the major factors known to trigger cutaneous disease activity in patients, with photosensitivity ranging from 27-100% according to the clinical subtypes of CLE. UVB promotes development of cutaneous lesions by triggering keratinocyte apoptosis, increasing the transport of nucleoprotein autoantigens to the keratinocyte cell surface, lymphocytic recruitment, and antibody-mediated cytotoxicity.

The specific miR-31 overexpression induced keratinocyte apoptosis in a capsase-3–dependent pathway and by regulating the BIM/BAX axis. However, we did not observe any effect on keratinocyte proliferation. We also showed that miR-31 contributed to skin inflammation by regulating in DLE and SCLE primary keratinocytes the production of inflammatory mediators via NF-κB signaling. As described previously in psoriasis, we confirmed that miR-31 overexpression *in vitro* can lead to the increased NF-κB activity, partially via targeting STK40 and PPP6C, negative regulators of the pathway [254], following TGF-β1 and UVB radiation stimulation in CLE. Our data together with those described in psoriasis [254, 255], show miR-31 as one of the key regulators in both

conditions, with a common role in the development and maintenance of the inflammatory skin process.

miR-31 was also shown to play a role in leukocyte chemotaxis. Following stimulation, miR31 transfected primary a keratinocytes expressed CXCL1, CXCL5, and CXCL8/IL-8, a neutrophil chemotactic factor but no adhesion molecules, such as ICAM-1, VCAM-1, and E- selectin [XU 256]. These chemokines are chemoattractants for multiple subsets of leukocytes, especially neutrophil granulocytes, by binding to the cognate receptors CXCR1 and CXCR2 [257]. By performing cross talking studies between miR31 transfected epidermal keratinocytes and PBMCs we showed an increased recruitment of neutrophils, and intermediate and non-classical monocytes.

DLE lesions are histologically characterized by a strong lymphocytic infiltrate, but neutrophil infiltration is hardly seen [54]. However, previous studies in non-lesional skin from photosensitive SLE patients showed the existence of progressive neutrophil influx at early stages following irradiation [258]. It is possible that the reason for not observing many neutrophils in the skin biopsies is because these are usually performed after a considerable time following the onset of the disease. Neutrophils play a role in CLE pathogenesis as they participate in the formation of neutrophil extracellular traps that may increase autoantigen presentation and the production of inflammatory signals [143]. Data suggests that miR31 is involved in the crosstalk between keratinocytes and immune cells, contributing to the recruitment and amplification of the immune response in CLE.

The analysis of cultured PBMCs with the supernatant resultant from overexpressing miR-31 in keratinocytes showed that miR31 also contributed to perpetuate skin inflammation by promoting a swift towards a Th1 response with an increase of Th1 transcription factor T-BET over GATA-3 (Th1/Th2 ratio) [259]. In addition, we observed an increased expression of FoxP3. Whereas the number of FoxP3^{+} Tregs in CLE has been found significantly reduced compared with other chronic inflammatory diseases but no different amongst CLE subtypes by Franz et al. [151, 260], our previous work showed DLE skin lesions to have an increased number of regulatory T cells [178]. Increased Treg expression might be the result of a regulatory mechanism to control an excessive inflammation or due to an impaired immune suppressive capacity that contributes to the perpetuation of inflammation. Their functionality and contribution in CLE remain to be explored.

miR-485-3p was also differentially expressed in DLE and found to be mainly upregulated in infiltrating lymphocytes and fibroblasts. MiR-485-3p has been described in cancer and neurological diseases and is able to modify memory $CD4^+$ T cells in pancreatic cancer [261-263]. However, its role in skin is unknown. miR-485-5p contributed to DLE skin inflammation by activating T cells. Its overexpression in PMBCs produced an activation of $CD4^+$ and $CD8^+$ T cells together with the an increase T cell activation genes *PI3K1, PKCO and NFKB1*. Data showed that miR-485-3p contributed to DLE not only by activating T cells but also contributing to the development of fibrosis, a signature of DLE. miRNA-485-3p overexpression in fibroblasts induced an upregulation of fibrotic markers SMAD3, COL3A1 and TGFβR. We hypothesized that the fibrotic effect might be via peroxisome *PPARGC1A,* a negative regulator of fibrosis [264], since miR-485-3p targets this gene [265] and was downregulated in dermal fibroblasts overexpressing miR-485-3p.

Taken together we showed that in DLE miR-31 and miR-485-3p are upregulated and contribute to DLE pathogenesis by initiating and perpetuating the inflammatory process and promoting skin damage. miR-31 promotes keratinocyte apoptosis, epidermal inflammation by promoting the NF- κB pathway and increasing the immune recruitment of neutrophils and monocytes into the lesional DLE sites. miR-485-3p contributes to DLE pathogenesis by promoting T cell activation and fibrosis (Fig 22).

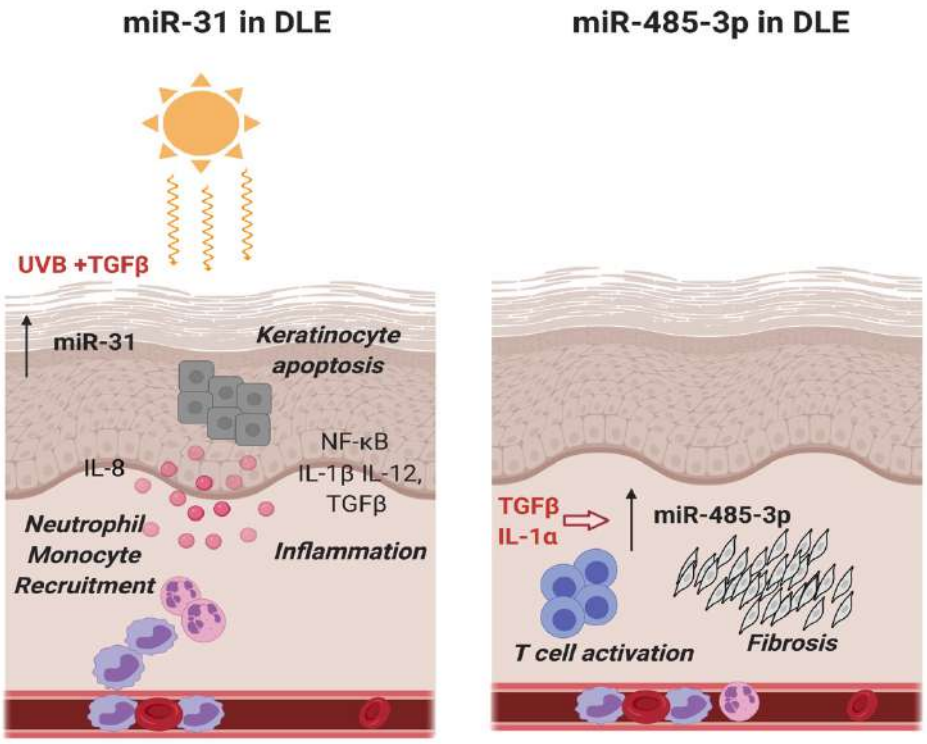

Figure 22. Role of microRNAs in the pathogenesis of DLE (miR-31 and miR-485-3p).

We next focused in the differentially expressed microRNAs in lesional CLE (including DLE and SCLE) when compared to non-lesional skin (Paper II: manuscript in revision).

We found miR-885-5p to be downregulated in CLE epidermis. miR-885-5p was identified as a keratinocyte-specific miRNA and no differences in expression were found between DLE and SCLE subtypes, suggesting that miR-885-5p plays a role in common pathogenic pathways. Its downregulation contributed to skin inflammation by increasing the production of inflammatory mediators, keratinocyte proliferation and attracting leukocytes. We identified PSMB5, a component of the 20S core proteasome complex involved in the proteolytic degradation of most intracellular proteins, as a novel target for miR-885-5p in keratinocytes and demonstrated that silencing PSMB5 reduces the NF-κB pathway activation and keratinocyte proliferation. Furthermore, we identified TRAF1, as another novel target of miR-885-5p in keratinocytes and demonstrated that silencing of TRAF1 can rescue the effect of miR-885-5p on leucocyte migration. Finally, our results suggest a model by which UVB and IFNα downregulate miR-885-5p in CLE keratinocytes leading to an activation of NF-κB pathway through increasing PSMB5 and TRAF1. In turn, the production of chemokines contributes to leukocyte attraction and skin inflammation.

In our study we found UVB and IFNα to be strong regulators of miR-885-5p in keratinocytes *in vitro*. UVB was a regulator of miR-31 and miR-885-5p, both keratinocyte-dependent miRNAs. Type I IFN signatures are increased in CLE lesions and contribute to its pathogenesis [266-268]. Data shows IFNκ is a key regulator of IFN responses in keratinocytes. In CLE, keratinocytes are primed by an abundance of IFNκ to generate robust responses to exogenous type I IFNs, setting up a feed forward loop which promotes exaggerated IFN responses and subsequent activation of the immune system [158].

In pathological conditions, miR-885-5p expression has been reported to be dysregulated in several human cancer types, including liver, neuroblastoma and oncocytic follicular thyroid carcinoma [269-272]. miR-885-5p can supress cell proliferation, migration, invasion by regulating the cell cycle arrest, senescence and/or apoptosis [273]. However, its role in skin diseases, particularly in CLE, was unknown. Inhibition of mIR-885-5p promoted NF-κB and NF-κB-related cytokines and chemokines and contributed to some degree of epidermal proliferation. CLE is not an hyperproliferative disease, but DLE lesions show hyperkeratosis and atrophy, which reflect abnormal epidermal proliferation, combined with normal early differentiation and premature terminal differentiation of keratinocytes [274]. We did not find any effect on apoptosis.

Our findings show that miR-885-5p regulates the activity of NF-κB pathway in keratinocytes. Since activation NF-κB is controlled by proteolysis of its inhibitors (IκBs) via the ubiquitin-proteasome pathway we studied the mechanistic link between increased NF-κB activity and PSMB5 overexpression [243, 275-277]. IκBα expression levels decreased in anti-miR-885-5p transfected keratinocytes *in vitro* whereas NF-κB increased. Silencing PSMB5 rescued the effect observed with anti-885-5p, indicating that the activation of NF-κB pathway observed in keratinocytes is PSMB5 dependent.

Gene microarray in anti-miR-885-5p UVB keratinocytes revealed an increase of *CCL5*, *CCL20*, *CXCL8* and *S1007A*. Inhibition of miR-885-5p in keratinocytes increased migration of leucocytes *in vitro* with co-culture experiments in a PSMB5-independent manner. Study of the mechanisms involved in leucocyte migration in anti-miR-885-5p transfected keratinocytes identified TRAF1 as another target of miR-885-5p responsible of the regulation of migration. TRAF1 is member of the TNF receptor (TNFR) associated factor (TRAF) protein family [278,279]. TRAF1 is upregulated in skin and primary keratinocytes following UVB exposure [280]. When overexpressed in cells, TRAF1 protein regulates inflammation by directly interacting with TNF-R2, TRAF2, TRIF, IKK2, NIK and ASK1 [281]. Therefore, TRAF1 is able to regulate both canonical and non-canonical NF-κB pathways as well as activation of the MAP kinases (JNK, p38, and ERK) to influence pro-inflammatory cytokine production and inflammatory responses [282]. Our results showed that silencing of TRAF1 decreases immune mediators and NFKB1. These data are in line with previous studies which reported that TRAF1 deficiency led to the inhibition of NF-κB-mediated inflammatory responses [283] and impairs attraction of lymphocytes, neutrophils, myeloid dendritic cells and monocyte recruitment [244, 284].

Taken together we showed that in lesional CLE miR-885-p is downregulated, specifically in keratinocytes. Low levels of miR-885-5p contribute to CLE pathogenesis by promoting epidermal proliferation, inflammation and secretion of inflammatory mediators and immune recruitment into the lesional sites through the modulation of two novel target genes of miR-885-5p: PSMB5 and TRAF1 (Fig 23).

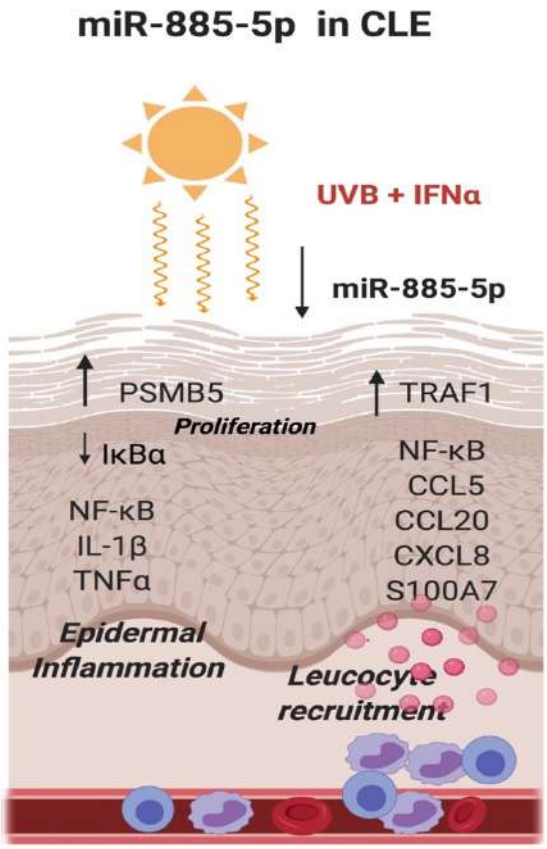

Figure 23. Role of miR-885-5p in the pathogenesis of CLE.

To date, during this period, only one study has also evaluated miRNAs in CLE. The study identified a downregulation of miR-150, miR-1246, and miR-21 in both CLE varieties compared to healthy donors. A difference from our study, they focused in finding differentially expressed miRNAs as circulating biomarkers in PBMCs to distinguish CLE patients and its subtypes but their possible participation in CLE pathogenesis was not demonstrated [285].

<u>In the second chapter, the thalidomide effect in CLE has been explored and a putative mechanism of action has been proposed and validated.</u>

Thalidomide has been used extensively in multiple myeloma (MM) and its mechanism of action has been explored for this condition. In skin diseases thalidomide had been used in HIV associated aphthous ulceration, nodular prurigo, Behçet's disease, CLE, pyoderma gangrenosum, actinic prurigo, graft versus host disease, polymorphic light eruption, lichen planus, bullous pemphigoid and cutaneous sarcoidosis. *In vitro* studies using keratinocytes have shown that thalidomide enhances keratinocyte migration and proliferation [286] and inhibits the activation of Caspase-1 which is required for

unconventional protein secretion of proinflammatory cytokines such as IL-1 [287]. In view of our clinical experience showing thalidomide efficacy in CLE and due to the fact that we do not know the exact mechanism by which thalidomide acts in CLE, we conducted this study.

Studies in MM have shown that IMiDs possess pleiotropic anti-myeloma properties including immune-modulation, anti-angiogenic, anti-inflammatory and anti-proliferative effects. IMiDs enhance the anti-MM immune activity by costimulating T and NK cells resulting in an increased production of Th1-type cytokines, IL-2 and IFNγ [288, 289]. In CLE, we observed that thalidomide induced a reduction of cytotoxic $CD8^+$ T cells, increased the number of tissue and circulating iNKT cells and promote Th2 helper responses. Cytotoxic $CD8^+$ T cells (CTLs) contribute to the inflammatory infiltrate in CLE lesions. These cells express granzyme B, a serine protease which is able to prime cells for apoptosis by activating caspases, contributing to basal keratinocyte damage and inflammatory infiltration, especially at the dermo-epidermal junction. Granzyme B expression is associated with the observed infiltrate and positively correlates with expression of IFNα and damage extension [290]. Therefore, a reduction of cytotoxic T cell numbers in blood and skin of CLE patients after thalidomide will contribute to the amelioration of skin inflammation.

Enhancement of iNKT cells *in vitro and in vivo* following iMiDs treatment has been described [291]. iNTK cells are a subset of unconventional T-cells which recognize the MHC class I-like CD1d protein with the expression of an invariant TCR chain (Vα24-Jα18) paired with a Vβ11 chain [292]. iNKTs have a broad spectrum of functionality and are able to promote or suppress inflammation. Whereas, iNKT cells participate in the pathogenesis of several skin inflammatory disorders producing IFNγ and IL-4 [293], that we did not find, they can also act as potent downregulators of $CD8^+$ cytotoxic T cells [294]; they are implicated in skin would healing [295, 296] and they alleviate lupus dermatitis in an MRL-lpr/lpr model [297]. The increment observed after thalidomide and after achieving clinical remission, supports the beneficial effect of these cells in CLE.

Regarding Th subsets, IMiDs have also generated opposing data on Th modulation. While some reports show that they promote Th1 responses [298], others found that they switched from a Th1 to a Th2 response [299]. In our study, thalidomide induced a Th2 response both *in vivo* and *in vitro*. The Th2-thalidomide induced response may contribute to skin repair as they are related to the expression of wound healing genes and growth

factors such as GF-1, Arg1 and others involved in tissue regeneration [300]. Therefore, in CLE, thalidomide may promote Th2 responses that contribute to skin repair.

We further investigate the thalidomide MoA. After combining system biology approaches with CLE RNA-sequencing data we showed that thalidomide modulates CLE by targeting two $CRL4^{CRBN}$-dependent pathways, downregulating IRF4 via IKZF1/3 and mTOR through regulation of AMPKa1. Within this approach, other drugs' mechanism of action has been identified [301, 302].

The expression of the primary target of thalidomide CRBN decreased following treatment both in the dermis and epidermis of CLE skin. CRBN functions as a substrate receptor for the cullin-4-containing E3 ubiquitin ligase complex CUL4–RBX1–DDB1 (CRL4A) and is responsible for the recruitment of substrates for degradation by the ubiquitin-proteasome pathway [303]. IMiDs bind to CRBN and alter the substrate specificity of $CRL4\text{-}^{CRBN}$ complex blocking the degradation of proteins involved in angiogenesis, tumour activity and inflammation [304, 305], but also inducing teratogenicity [306]. We found in active CLE lesions an increased expression of IRF4 in the dermis and mTOR in the epidermis. IRF4 and mTOR expression has been found in other inflammatory skin conditions like psoriasis vulgaris, acne, atopic dermatitis, and hidradenitis suppurative [307]. Further *in vitro* experiments confirmed the effect of thalidomide through the two different signaling pathways, that was different according to the skin cell type. Thalidomide reduced IRF4 signaling in lymphocytes whereas the effect on mTOR was observed in keratinocytes.

IRF4 is a member of the IRF family that is a group of transcription factors related to the regulation of gene expression and the immune response [308]. IRF4 is expressed in immune cells and plays pivotal roles in the immune response. Its dysregulation has been described in rheumatoid arthritis and SLE, being associated with disease initiation and progression [309]. IMiDs inhibit IRF4 expression at transcriptional level, mainly via downregulation of IKZF1/3 transcription factors [310]. We showed that thalidomide modulates IRF4 in PMBCs *in vitro* and contributes to the resolution of inflammation by reducing the expression of NF-κB and its dependent cytokines and chemokines IL-1β, IL-8, TNFα and CCL3. This data agrees with previous reports that describe that IRF4 inhibition downregulated inflammation by the downregulation of NF-κB activation in inflammation [311].

The other pathway by which thalidomide acts is the mTOR/AMPK signaling pathway. AMP-activated protein kinase (AMPK) is an important intracellular energy sensor and is activated by phosphorylation of threonine at position 172 (Thr 172) of the α subunit [312]. CRBN directly interacts with the catalytic α subunit of AMPK, reducing the phosphorylation of AMPKα1, downregulating the enzymatic activity of AMPK [313]. In addition, the AMPKα subunit and AMPKγ subunit are polyubiquitinated leading to their proteasomal degradation and AMPK downregulation [314, 315]. Previous reports have shown that thalidomide markedly stimulates the activation of AMPK *in vitro* and *in vivo* [316, 317] and it reduced AMPK polyubiquitination [318]. Accordingly, we demonstrated that thalidomide reduced the AMPKα1 ubiquitination in a CRBN-dependent manner and increased its expression. Consequently, we observed an increase of RPTOR phosphorylation and a reduction of mTOR.

mTOR is a serine threonine kinase crucial in skin homeostasis and morphogenesis, especially in the regulation of keratinocyte differentiation and epidermal stratification [319]. mTOR pathway is involved in the pathogenesis of several dermatological conditions such as epithelial tumors, psoriasis, acne, wound healing and hidradenitis suppurativa [320]. Our *in vitro* studies showed that treatment with thalidomide or simTOR significantly reduced keratinocyte-derived cytokines TGF-β, IL-1β, TNFα and CXCL1. In addition, we showed that thalidomide addition and specific inhibition of mTOR decreased NF-κB expression in keratinocytes. The existence of a crosstalk between mTOR and NF-κB has been previously described in other cellular types. Dai et al. demonstrated that mTOR is upstream of NF-κB, and that silencing of mTOR inhibited NF-κB activation, leading to a reduction of inflammation in macrophages [321].

Interactions between keratinocytes and mononuclear cells via cytokines and adhesion molecules are thought to play a crucial part in inflammatory skin diseases. We showed the ability of thalidomide-treated or siIRF4 PBMCs to reduce the expression of mTOR and related cytokines in keratinocytes in co-culture studies.

Taken together, we demonstrated that thalidomide's immunomodulatory anti-inflammatory effect in CLE comprises several mechanisms that include a reduction of predominantly CD8^{+} T cells, an increase of iNKT cells and a switch from Th1 to Th2 response. Furthermore, thalidomide reduced NF-κB related inflammatory cytokines and chemokines via the modulation of IRF4 and AMPK/mTOR-signaling pathways in a CRL4-^{CRBN} dependent manner in immune and epidermal cells (Fig 24).

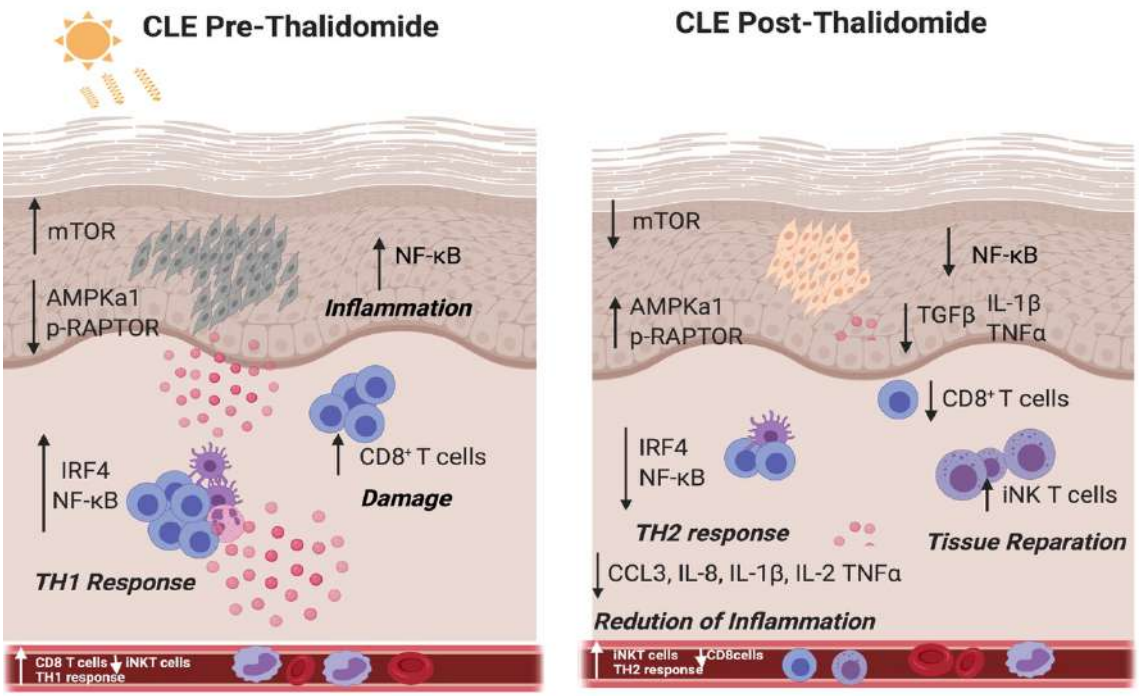

Figure 24. Thalidomide effects in CLE treated skin.

Our work is the first to provide a mechanism of action for thalidomide in CLE. Only one study has examined its role in another dermatological condition, rosacea during this period. In rosacea, thalidomide is not indicated and only few case reports in recalcitrant cases had been reported [322]. In line with our results, Chen et al. [323] showed that thalidomide ameliorates inflammation by suppressing NF-κB activation *in vitro* and in rosacea-like mouse model.

<u>In the 3rd Chapter, the expression of the miRNAs of interested have been analysed in skin samples from CLE patients and *in vitro* in primary cells before and after receiving thalidomide.</u>

So far, our data converge to demonstrate a key role for NF-κB in the pathogenesis of CLE.

The nuclear factor-kappa B (NF-κB) family of transcriptional regulators is essential for transcription of a variety of genes involved in the immune response, cell survival, proliferation, and differentiation [324]. The NF-κB activation pathways are classified as the canonical and non-canonical pathways, depending on whether activation involves IκB degradation or p100 processing [325]. In the canonical pathway, which is the predominant NF-κB signaling pathway, different stimuli, such as cytokines, growth factors, mitogens, microbial components, and stress agents, activate in the cells the IKK complex that is

composed of two catalytic subunits IKKα and IKKβ and a regulatory subunit NEMO (also known as IKKγ). Genetic experiments have demonstrated that IKKβ, but not IKKα, phosphorylates IκBα at two N-terminal serine residues. This signal-induced phosphorylation targets IκBα for polyubiquitination and subsequent degradation by the proteasome, thus releasing NF-κB to be translocated into the nucleus and be active [326]. Whereas NF-κB activation occurs transiently during a normal immune response, it is chronically activated in the affected tissues of autoimmune diseases. A pathological action of NF-κB is the induction of proinflammatory cytokines and chemokines, which mediate the recruitment of immune cells and the establishment of inflammation [327].

Since NF-κB is a key player in CLE pathogenesis its inhibition is an attractive approach as an anti-inflammatory therapy. Although NF-κB inhibition could be beneficial in treating inflammatory diseases, there are obvious questions regarding the balance between efficacy and safety since NF-κB function is also required for maintaining normal immune responses and cell survival. Accumulating studies suggest that global inhibition of NF-κB signalling may cause severe side effects. Several categories of inhibitors have been developed to block different steps of NF-κB signalling: selective IKK inhibitors to block the catalytic activity of IKK and prevent IκBα phosphorylation, proteasome inhibitors, such as Bortezomib which blocks PSMB5 and posterior IκBα degradation in the proteasome, inhibitors that block nuclear translocation of different NF-κB subunits, such as tacrolimus (FK-506) and IκBα super-repressor and drugs that inhibit the DNA-binding activity of NF-κB, such as glucocorticoids [328]. However, while significant progress has been made in designing approaches to inhibit NF-κB, complexities exist for the development of clinically available NF-κB-based drugs.

For these reason, new alternatives need to be explored. In that sense, miRNA therapeutics are the most recent of a range of RNA therapies that have emerged over the last 10-15 years including short interfering RNA (siRNA) and short hairpin RNA (shRNA). Many studies showed that modulating specific miRNAs had therapeutic effect on keratinocytes. Xu et al [329]. reported that downregulated miR-125b was involved in mediating the pathological proliferation and differentiation of keratinocytes in psoriasis, while the overexpression of miR-125b inhibited keratinocyte proliferation and promoted differentiation via inhibiting its direct target, FGFR2, in primary human keratinocytes.

Our study showed that thalidomide could contribute to CLE resolution by modulating keratinocyte derived microRNAs, miR-31 and miR-885-5p, that in turn modulated the NF-κB activity. The modulation of microRNAs by thalidomide has only been previously

investigated by Zheng et al. in which they focused in evaluating the microRNA signatures of paraquat induced lung injury in a rat model. Similarly, they found that that there was a modulation of one microRNA that had protective functions by inhibiting NF-κB pathway. Into detail, thalidomide upregulated miR-141 which suppressed inflammation through IκBα-NF-κB axis [330]. We observed that hydroxychloroquine modified miR-31 and moderately miR-485-3p miRNAs. The fact that thalidomide modified markedly simultaneously the two highly dysregulated miR-31 and miR-885-5p could explain its high efficacy. These preliminary data show that another way to modify NF-κB would be through direct modulation of miRNAs relevant to the disease.

Limitations

One of the limitations is that most of the results were obtained by *in vitro* experiments. *In vitro* experiments present some advantages as control of chemical and physical environment and reduction of environmental variability [331]. However, isolated and cultivated primary cells could differ from the corresponding cell type in an organism, limiting the value of *in vitro* data to predict *in vivo* behavior. The skin is an organ that has several cell types that coexist and communicate in the environment. We attempted to overcome this limitation with co-culture experiments in order to analyze the interaction between epidermal and immune cells [332]. Co-cultures provide a more representative human *in vivo*-like tissue model than animal models, however low complexity was achieved with only two populations settled up in our experiments.

This limitation in the future could be overcome for example, by using *in vivo* experimental models, using a more complex *in vitro* system such as a skin 3D equivalent models which permit to construct the epidermal and dermal layers and also the addition of immune cells, or using skin organoids which may be derived from pluripotent stem cells and present the complexity of native skin [333].

The second limitation is in the thalidomide-miRNA relationship studied in chapter 3, the therapeutic group in which we measured microRNAs is a small sample as a pilot study. Further validation in a larger cohort is required to validate these results. For the same reason there is not enough data to use these miRNAs as a biomarkers of disease or response to therapy.

Novel Research Lines

As a result of the data obtained in this thesis, next steps and new research lines have emerged. We propose:

1. Investigate the potential of the discovered miRNAs as biomarkers. MicroRNAs applicability as biomarkers has been explored, especially in cancer. MiRNAs meet most of the required criteria for being an ideal biomarker, such as accessibility, high specificity, and sensitivity [334], although its applicability in the clinical practice might be difficult because of their fragility and instability overtime. They can be used as biomarkers for differential diagnosis, disease severity/prognosis assessment, and to monitor treatment response. Validation in a larger cohort of patients is required and to establish correlations with parameters of disease activity and severity such as CLASI index, laboratory or co-morbidities.

2. Evaluate the applicability of the identified miRNAs as therapeutics. Several *in vivo* studies have been conducted to evaluate miRs as potential therapeutic agents in skin disorders [335, 336]. There are two strategies to use microRNAs as genetic modulators: miRNA inhibitors and miRNA mimics. miRNA inhibitors bind complementary to the endogenous mature miRNA molecules and as a result the interaction of the miRNA of interest with its target is prevented. Instead, miRNAs that are downregulated in disease may be replaced transiently by miRNA mimics which are chemically synthesized miRs, restoring miRNA expression levels to normal. In addition, to treat dermatological conditions, miRNA therapeutics can be topically administrated to avoid toxicity. If administered in nanoparticles, their degradation is prevented.

3. Novel therapies for CLE based on NF-κB modulation: We have demonstrated the relevance of NF-κB in CLE via the miRNAs studies as well as by revealing the mechanism of action of thalidomide in CLE. Therefore, a NF-κB modulation may be a promising therapy for CLE (Fig 25). Selectively targeting specific NF-κB subunits or signaling components relevant to a particular disease might be of utility minimizing toxicity [337-339]. Topical application of an NF-κB inhibitor improved atopic dermatitis in NC/NgaTnd mice [340]. Therefore, further study of NF-κB signaling as novel a therapeutic target in CLE has emerged.

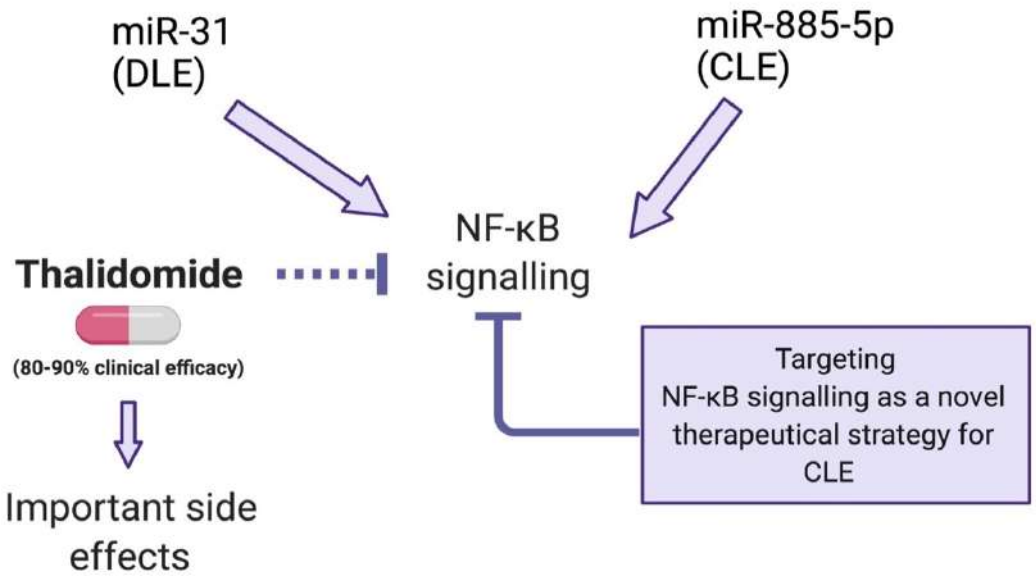

Figure 25. NF- κB signaling pathway a as novel strategy for CLE treatment.

6. Conclusions

CLE is a chronic heterogenic autoimmune disease that affects the skin in which pathogenesis is not completely understood and no specific treatments have yet been developed.

Within this thesis, the role of miRNAs has been examined in CLE and also in one of the most common subtype, DLE. MIcroRNAs may provide insights into disease pathogenesis deregulating cell signaling pathways. A microRNA signature in CLE lesional skin has been identified and three microRNAs have been extensively studied. From this study it can be concluded the following:

- Lesional skin from DLE patients presents a miRNA signature that differs from lesional SCLE.

- mir-31 and miR-485-3p have been identified as the most upregulated miRNAs in DLE lesional skin.

- miR-31 is found in epidermal keratinocytes in DLE lesional skin and its upregulation in DLE promotes keratinocyte apoptosis, epidermal inflammation by NF-κB upregulation and subsequent secretion of inflammatory effectors IL-8, IL-12, IL-1β and monocyte and neutrophil attraction to the DLE lesional sites.

- miR-485-3p is found in immune infiltrates and fibroblasts in DLE lesional skin and its upregulation in DLE promotes T cell activation and fibrosis.

- Lesional skin from CLE patients (DLE and SCLE) present differentially expressed miRNAs when compared with non-lesional skin from paired patients and miR-885-5p and miR-139-5p are downregulated.

- miR-885-5p is downregulated in lesional CLE. From non-lesional skin we found this miRNA to be predominantly expressed in epidermal keratinocytes. Low levels promote epidermal inflammation by promoting NF-κB activation and epidermal proliferation via PSMB5. It also promotes immune cell recruitment to lesional sites via TRAF1 modulation.

Regarding the treatment, thalidomide drug presents a high clinical efficacy around 90% in refractory CLE however its use is restricted to its important side effects. Its mechanism of

action in dermatologic CLE condition was not previously explored. Within this thesis, a mechanism of action in CLE is proposed and validated by *in vitro* functional studies. It can be concluded that:

- Thalidomide immunomodulatory properties in CLE are characterised by a reduction of $CD8^+$ T cells, promotion of Th2 responses and an increase of iNKT cells in both blood and skin from CLE treated patients.

- After RNA-sequencing and TMPS protocol analysis a putative thalidomide mechanism of action in CLE has been identified. It acts in CLE by modulating two CRBN-CRL4 dependent pathways IRF4/NF-κB and mTOR/AMPK.

- IRF4 expression was found in immune infiltrates of lesional CLE skin and decreases significantly after thalidomide treatment. Thalidomide ameliorated inflammation in PBMCs by modulating IRF4 and subsequent modulation of NF-κB and related inflammatory effectors.

- mTOR was found in CLE lesional epidermis and decreased after thalidomide whereas AMPKA1 was found increased after receiving the treatment. Thalidomide anti-inflammatory effect in keratinocytes is mediated by mTOR modulation. In addition, there is a crosstalk of mTOR and NF-κB pathway that results in NFKB1 and related cytokines reduction.

- Co-culture studies showed that modulation of IRF4 by thalidomide reduces inflammation in keratinocytes by reducing mTOR, increasing AMPKa1 and decreasing NF-κB and related cytokines.

- Thalidomide has an effect in NF-κB keratinocyte derived miRNAs modulation in CLE. It promotes a significant downregulation of miR-31 and an upregulation of miR-885-5p in skin lesions from responder patients and in treated cells *in vitro*.

- Both deregulated miRNAs miR-31 in DLE and miR-885-5p promote NF-κB activation. In addition thalidomide anti-inflammatory effect in CLE is mediated by a reduction of NF-κB signaling. Therefore NF-κB seems to be a crucial signaling pathway in CLE and therapies addressed to inhibit this pathway may be beneficial for CLE treatment.

7. Annex

Annex 1. CLASI (Cutaneous LE Disease Area and Severity Index)

Cutaneous LE Disease Area and Severity Index (CLASI) ©

Select the score in each anatomical location that describes the most severely affected cutaneous lupus-associated lesion

activity ⟷ damage

Anatomical Location	Erythema	Scale/ Hypertrophy	Dyspigmentation	Scarring/ Atrophy/ Panniculitis	Anatomical Location
	0-absent 1-pink; faint erythema 2- red; 3-dark red; purple/violaceous/ crusted/ hemorrhagic	0-absent; 1-scale 2-verrucous/ hypertrophic	0-absent, 1-dyspigmentaton	0 – absent 1 – scarring 2 – severely atrophic scarring or panniculitis	
Scalp				See below	Scalp
Ears					Ears
Nose (incl. malar area)					Nose (incl. malar area)
Rest of the face					Rest of the face
V-area neck (frontal)					V-area neck (frontal)
Post. Neck &/or shoulders					Post. Neck &/or shoulders
Chest					Chest
Abdomen					Abdomen
Back, buttocks					Back, buttocks
Arms					Arms
Hands					Hands
Legs					Legs
Feet					Feet

Mucous membrane

Mucous membrane lesions (examine if patient confirms involvement)	
0-absent; 1-lesion or ulceration	

Dyspigmentation

Report duration of dyspigmentation after active lesions have resolved (verbal report by patient – tick appropriate box)
☐ Dyspigmentation usually lasts less than 12 months (dyspigmentation score above remains) ☐ Dyspigmentation usually lasts at least 12 months (dyspigmentation score is doubled)

Alopecia

Recent Hair loss (within the last 30 days / as reported by patient)	
1-Yes 0-No	

NB: if scarring and non-scarring aspects seem to coexist in one lesion, please score both

Divide the scalp into four quadrants as shown. The dividing line between right and left is the midline. The dividing line between frontal and occipital is the line connecting the highest points of the ear lobe. A quadrant is considered affected if there is a lesion within the quadrant.

Alopecia (clinically not obviously scarred)		Scarring of the scalp (judged clinically)	
0-absent 1-diffuse; non-inflammatory 2-focal or patchy in one quadrant; 3-focal or patchy in more than one quadrant		0- absent 3- in one quadrant 4- two quadrants 5- three quadrants 6- affects the whole skull	

Total Activity Score
(For the activity score please add up the scores of the left side i.e. for Erythema, Scale/Hypertrophy, Mucous membrane involvement and Alopecia)

Total Damage Score
(For the damage score, please add up the scores of the right side, i.e. for Dyspigmentation, Scarring/Atrophy/Panniculitis and Scarring of the Scalp)

Annex 2. miR-139-5p in situ hybridization in skin biopsies from CLE lesional and non-lesional skin (10x magnification).

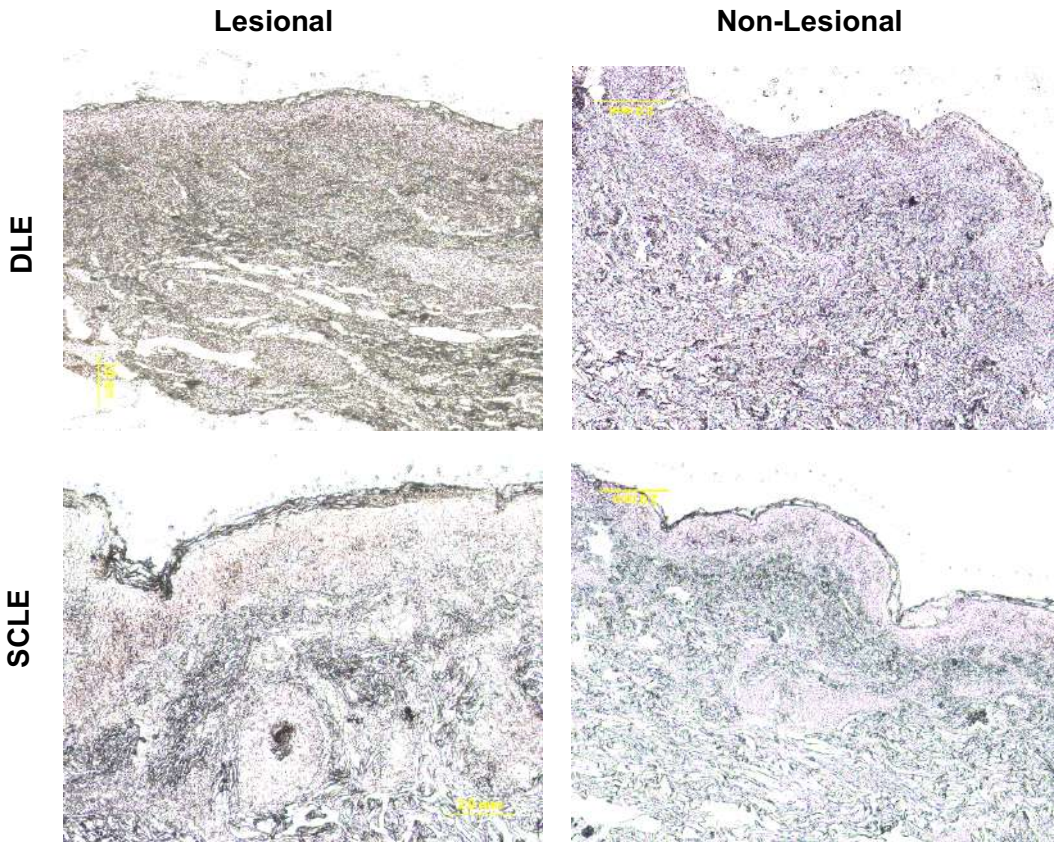

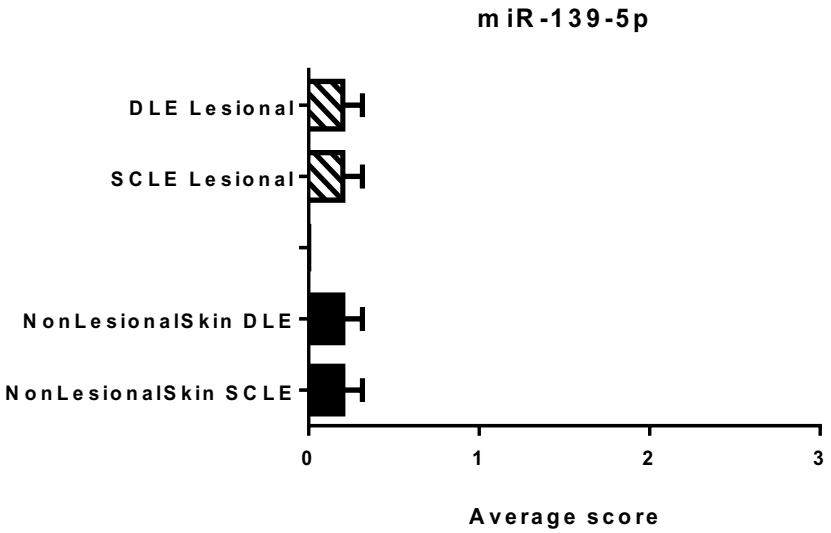

Annex 3. Microscopy images bright field of immune migration experiments in anti-miR-885p and siTRAF1 keratinocytes at 24h (20x magnification).

Control miR

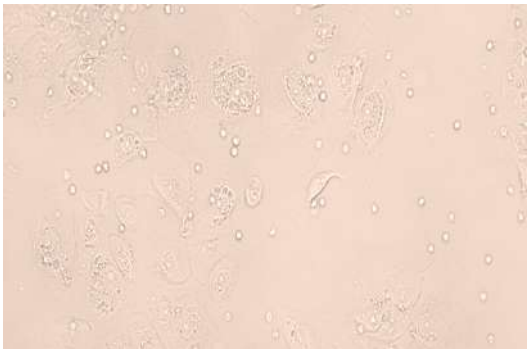

Anti-MiR-885-5p

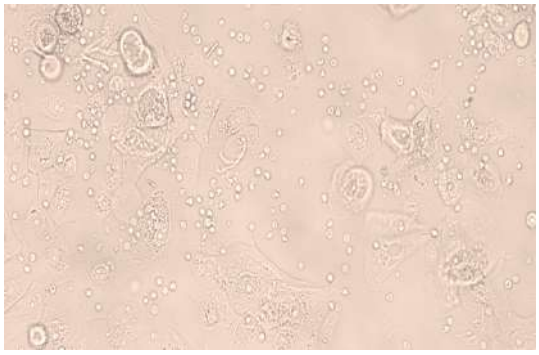

Control siRNA

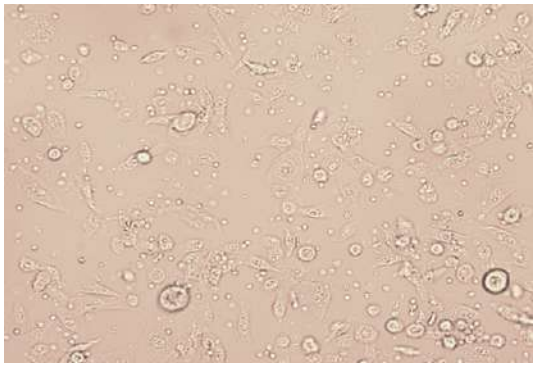

SiTRAF1

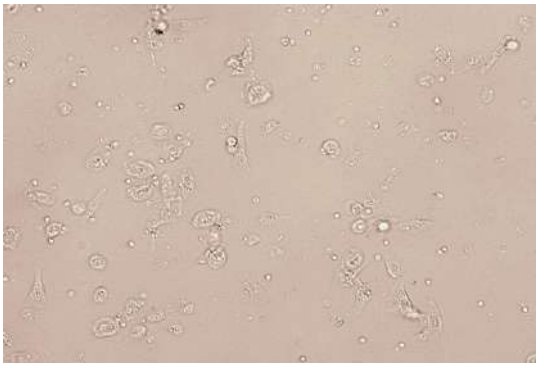

Annex 4. iNKT cells in CLE skin biopsy before and after thalidomide treatment (10x magnification).

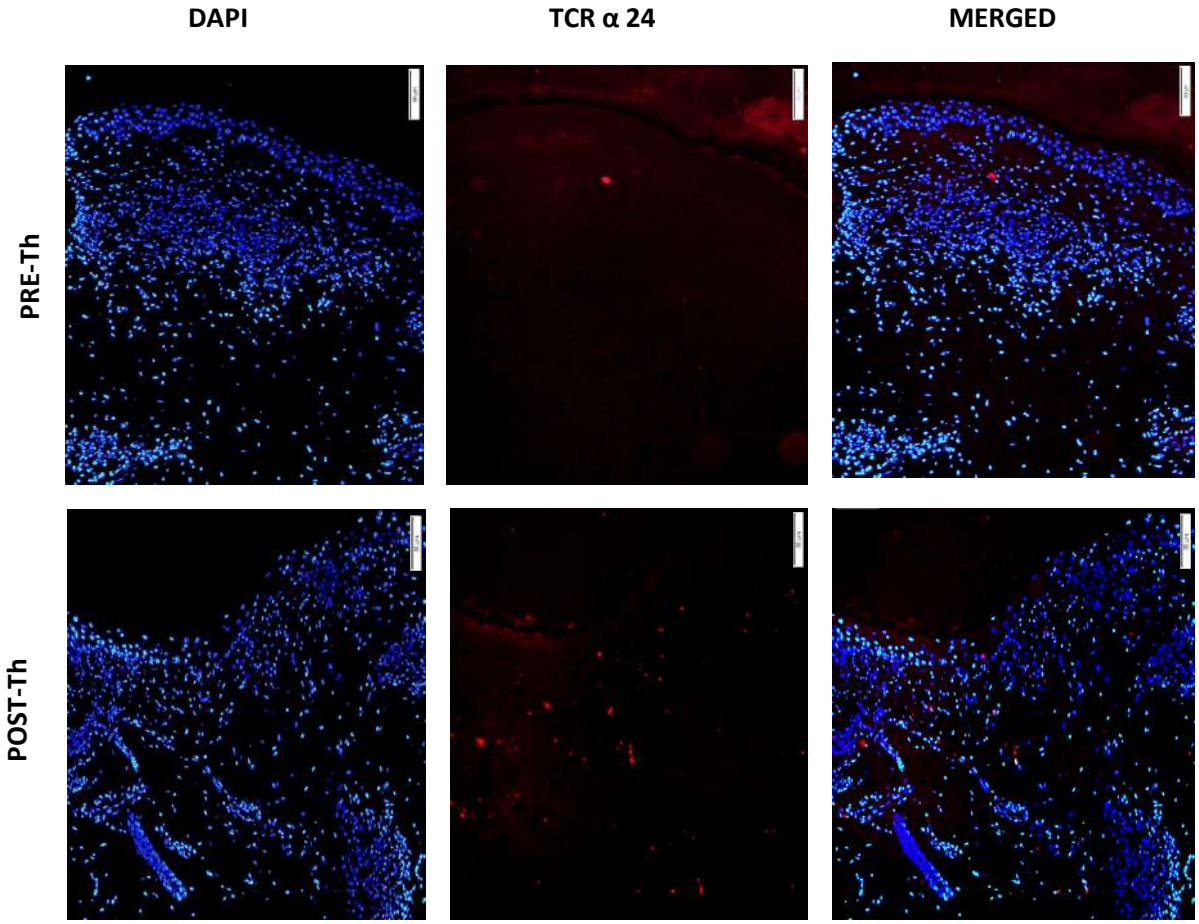

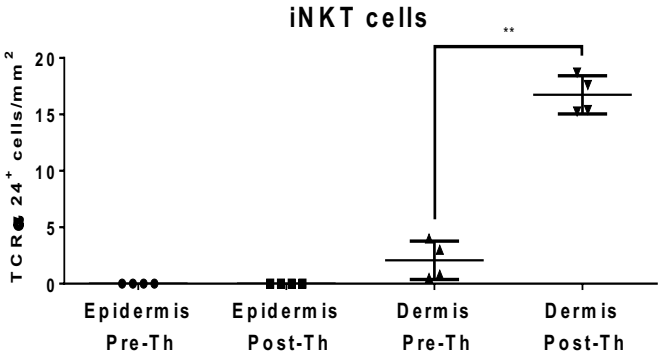

Annex 5. Related Publications

cells

MDPI

Review

MicroRNAs in Several Cutaneous Autoimmune Diseases: Psoriasis, Cutaneous Lupus Erythematosus and Atopic Dermatitis

Sandra Domingo [1], Cristina Solé [1,*], Teresa Moliné [2], Berta Ferrer [2] and Josefina Cortés-Hernández [1]

1 Rheumatology Research Group, Lupus Unit, Hospital Universitari Vall d'Hebron, Institut de Recerca (VHIR), Universitat Autònoma de Barcelona, 08035 Barcelona, Spain; sandra.domingo@vhir.org (S.D.); fina.cortes@vhir.org (J.C.-H.)

2 Department of Pathology, Hospital Universitari Vall d'Hebron, Institut de Recerca (VHIR), Universitat Autònoma de Barcelona, 08035 Barcelona, Spain; teresa.moline@vhir.org (T.M.); ferrerfabrega@yahoo.es (B.F.)

* Correspondence: cristina.sole@vhir.org; Tel.: +34-9-3489-4045

Received: 13 November 2020; Accepted: 5 December 2020; Published: 10 December 2020

check for updates

Abstract: MicroRNAs (miRNAs) are endogenous small non-coding RNA molecules that regulate the gene expression at a post-transcriptional level and participate in maintaining the correct cell homeostasis and functioning. Different specific profiles have been identified in lesional skin from autoimmune cutaneous diseases, and their deregulation cause aberrant control of biological pathways, contributing to pathogenic conditions. Detailed knowledge of microRNA-affected pathways is of crucial importance for understating their role in skin autoimmune diseases. They may be promising therapeutic targets with novel clinical implications. They are not only present in skin tissue, but they have also been found in other biological fluids, such as serum, plasma and urine from patients, and therefore, they are potential biomarkers for the diagnosis, prognosis and response to treatment. In this review, we discuss the current understanding of the role of described miRNAs in several cutaneous autoimmune diseases: psoriasis (Ps, 33 miRNAs), cutaneous lupus erythematosus (CLE, 2 miRNAs) and atopic dermatitis (AD, 8 miRNAs). We highlight their role as crucial elements implicated in disease pathogenesis and their applicability as biomarkers and as a novel therapeutic approach in the management of skin inflammatory diseases.

Keywords: microRNAs; skin autoimmunity; nanoparticles; biomarkers; pathogenesis; psoriasis; atopic dermatitis; cutaneous lupus erythematosus

1. Introduction

MicroRNAs, also known as miRs or miRNAs, are small, highly conserved, non-coding RNA sequences that range from 19 to 25 nucleotides [1]. In recent years, thousands of miRNAs have been discovered employing new advances in molecular biology and bioinformatics, achieving relevance in translational research. miRNA biogenesis has been broadly investigated to establish that most miRNAs are transcribed from DNA sequences in the nucleus by RNA polymerase II (Pol II). Drosha, a member of the RNase III family, with protein DiGeorge syndrome critical region gene 8 (DGCR8), constitute the microprocessor complex that cleaves the primary miRNAs to generate a 70-nucleotide sequence called miRNA precursor [2,3]. This is exported by exportin-5 to the cytoplasm and then processed by RNase III endonuclease dicer. After processing, the terminal loop is removed resulting in a miRNA duplex that will be incorporated into the argonaute (AGO) family of proteins. The directionality of the miRNA determines the name of the mature form. Both 5-p and 3-p strands can be loaded into the AGO

proteins; however, the selection of the 5p or 3p is based on the thermodynamic stability at 5′ ends of the miRNA duplex or a 5′ U at nucleotide position 1. Usually, strands with lower 5′ stability or 5′ uracil are preferentially loaded into AGO and are named "guide strands". The unloaded strand is called a "passenger strand", and it is degraded. After the miRNA duplex is unwound, it is incorporated into the RNA-induced silencing complex (RISC), forming the minimal miRNA-induced silencing complex (miRISC), and then, the miRNA 20 nucleotide's (nt's) mature form is able to recognise and target complementary mRNA sequences (Figure 1).

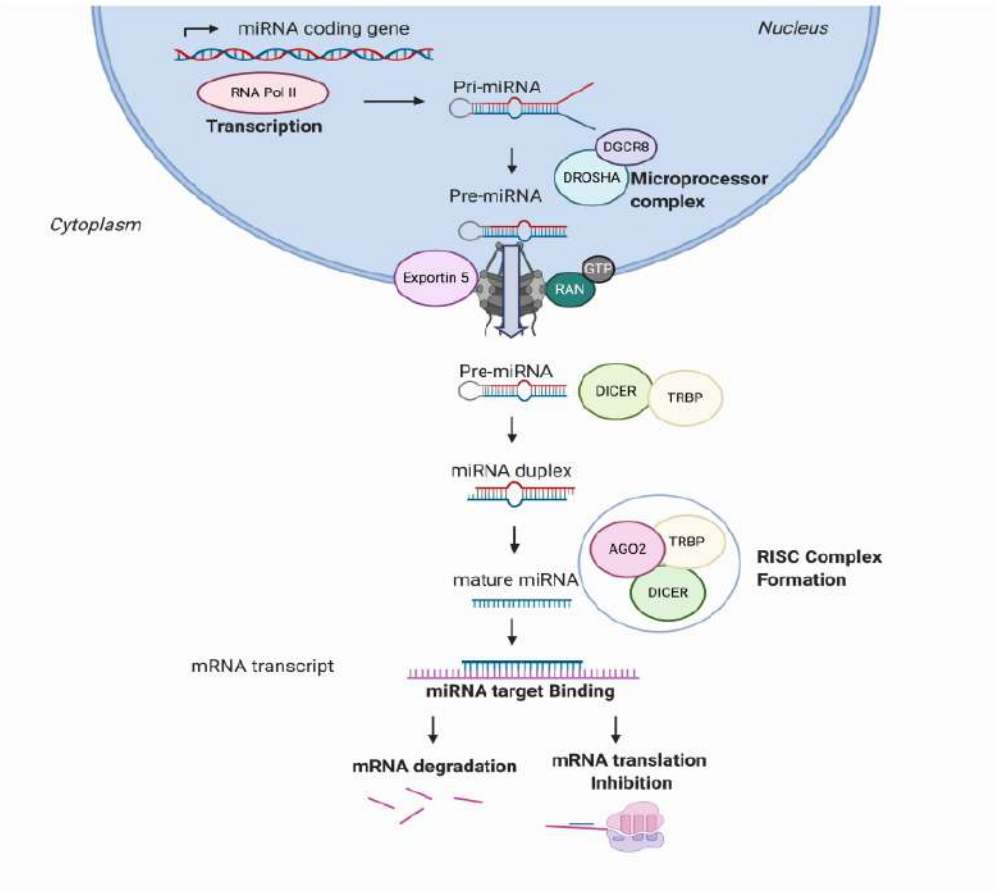

Figure 1. MicroRNA (miRNA) biogenesis and regulation of gene expression. miRNAs are transcribed from the genome into a pre-miRNA. The pre-miRNA is a smaller stem-looped structure that is transported from the nucleus to the cytoplasm by Exportin 5. Once in the cytoplasm, it is cleaved by DICER and TRBP and results into a small mRNA duplex that is around 20–25 nucleotides of length. The duplex is separated, and one of the strands is incorporated into the RISC, formed by AGO member proteins. The mature miRNA is then generated and binds specifically the mRNA transcript by complementary target recognition. The mRNA–miRNA union prevents the mRNA translation or leads into mRNA degradation and subsequent gene silencing. AGO: argonaute protein family and RISC: RNA-induced silencing complex.

MicroRNAs can modulate the gene expression at the same cell where they are being synthetised, or they can be secreted, enveloped in extracellular vesicles (EVs), transported from a parental cell to neighbouring cells and regulate important biological functions in the recipient cells [4]. Moreover, a single miRNA may have multiple target genes, and a single gene may be targeted by multiple

miRNAs [5], making them a powerful system for modulating and adjusting the gene expression, as they approximately regulate around 60% of all the protein-coding genes [6].

miRNAs are involved in development, organogenesis, proliferation and apoptosis, among other cell processes [7,8]. Under normal physiological conditions, microRNAs are regulating correct cell functions. However, in disease, microRNAs may change, inducing an altered gene expression that leads into an aberrant phenotype [9]. When they are dysregulated, they may alter relevant cellular processes, favouring pathogenic conditions. On the other hand, they may also play protective roles by trying to re-establish cell homeostasis. A miRNA balance is key for the correct functioning of cell and tissue physiology.

2. Role of miRNAs in the Skin Pathogenesis of Cutaneous Immune Disorders

Skin is the largest organ in the human body, and its development and morphogenesis require a highly regulated and undisrupted miRNA profile. miRNAs' role in skin physiology is well-known [10,11], as they are involved in epidermal and dermal proliferation, pigmentation, aging, wound healing, skin microbiome and skin immunity, among other processes [12]. Recent findings show that miRNAs have a role in skin carcinogenesis [13] and in the pathogenesis of chronic inflammatory skin diseases, presenting lesional specific miRNA expression profiles that differ from healthy skin [14–16]. A better understanding of the role of miRNAs in autoimmune cutaneous diseases will enhance our knowledge of skin disease pathology. In this section, the most important miRNAs associated with psoriasis, cutaneous lupus disease (CLE) and atopic dermatitis (AD) are described with special emphasis on their role in the disease pathogenesis.

2.1. Psoriasis

Psoriasis is the most prevalent chronic inflammatory skin disease, with an estimated prevalence in adults ranging from 0.91% to 8.5%, varying by country and ethnicity [17]. Genetic and environmental factors in connection with abnormal regulation of the immune system are thought to be involved in pathogenesis of the disease. It is characterised by hyperproliferation and altered differentiation of epidermal keratinocytes and leukocyte infiltration—predominantly, neutrophils, myeloid cells and T cells, causing the secretion of inflammatory mediators such as TNF-α, interferon-γ (IFN-γ), interleukin (IL)-1, IL-17 and IL-22, which contribute to psoriatic inflammation [18]. It has been identified that the IL-23/IL-17 axis is the primary signalling pathway, leading to characteristic molecular and cellular changes in psoriatic skin [18]. It is widely accepted that psoriasis is a consequence of an impaired crosstalk between the immune system and the structural cells of the skin. Several studies have been conducted to reveal the role of miRNAs in psoriasis (Table 1 and Figure 2), highlighting the value of miRNA analysis. The role of miR-203, miR-31, miR-146a, miR-155-5p and miR-21 are described below.

The first study in 2007 that reported a distinctive skin miRNA signature in psoriasis was published by E Sonkoly et al. [14]. The study identified miR-203 as a keratinocyte-derived microRNA related to inflammation by targeting the *SOCS3* gene. After that, further studies have confirmed the direct targeting [19] and its role in the regulation of psoriatic cytokines such as *TNF-α*, *IL-24* and *IL-8* in keratinocytes [20,21]. Moreover, in vitro experiments showed that miR-203 expression is upregulated after IL-17 stimulation in HaCat cells and that miR-203 is involved in the activation of the *JAK2/STAT3* signalling pathway, which contributes to VEGF secretion and the perpetuation of pathological angiogenesis [19]. Recently, it has been described that miR-203 negatively regulates keratinocyte proliferation through the direct targeting of *NR1H3* and *PPARG* [22]. Therefore, in psoriasis, the data suggest that miR-203 may be involved in skin epidermal hyperplasia, inflammation and angiogenesis (Figure 2).

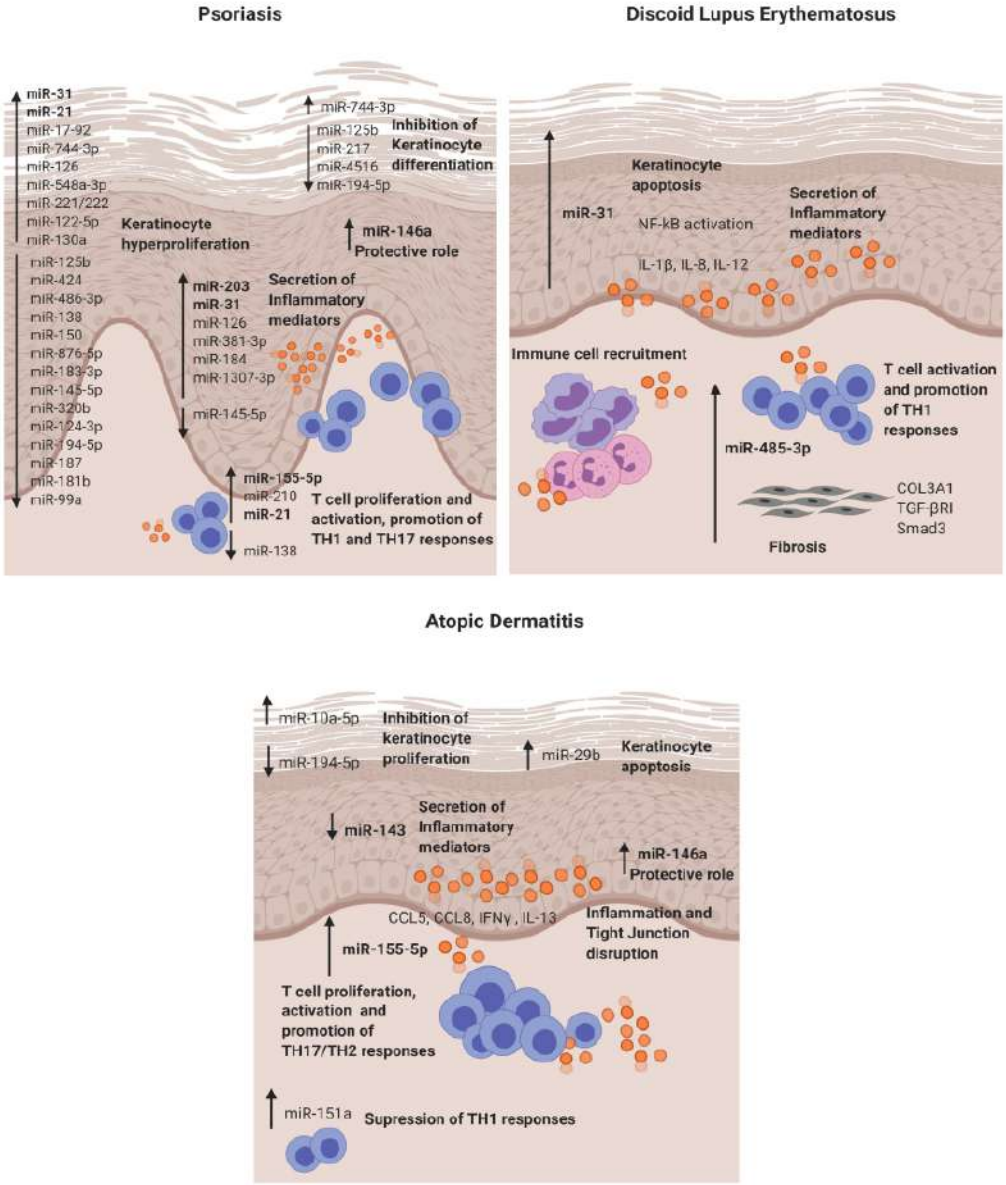

Figure 2. Dysregulated miRNAs involved in Psoriasis, discoid lupus erythematosus and atopic dermatitis and their roles in the disease pathogenesis. DLE: discoid lupus erythematosus and AD: atopic dermatitis.

MiR-31 is known to be involved in normal skin physiology by regulating keratinocyte growth and hair differentiation [23]. High miR-31 levels can be detected in blood and lesional psoriatic epidermis, and its pathogenic role is primarily based on NF-κB signalling alteration [24,25]. NF-κB is a crucial mediator in the pathogenesis of psoriasis and participates in inflammation, cell proliferation, differentiation and apoptosis. Serine/threonine kinase 40 (*STK40*), a negative regulator of NF-κB signalling, has been identified as a direct target for miR-31 [26]. The study demonstrated that miR-31 promotes NF-κB via *STK40* targeting and leads to the secretion of CXLC1, CXCL8, CXCL5 and IL-1β, which promote vascular endothelial cell activation and attract leukocytes via chemotaxis into the skin. Primary keratinocytes treated with TGFβ1, which is highly expressed in psoriatic skin, showed an

upregulation of miR-31 [26]. This effect was also observed when keratinocytes were treated with psoriatic-relevant cytokines: IL-6, IL-22, interferon-γ (IFN-γ) and TNF-α [25], demonstrating its importance in epidermal inflammation. This miRNA is also involved in keratinocyte proliferation, as in vivo studies showed that miR-31 promotes epidermal hyperplasia via the direct targeting of *PPP6C*, a negative regulator of the G1-S phase progression in the cell cycle [25]. Endothelin-1, a peptide involved in cell proliferation and leukocyte chemotaxis, has been positively associated with high levels of miR-31 in blood [24]. MiR-31 may play a role in dermal mesenchymal stem cells (DMSCs) [27], as low levels in DMSCs of psoriasis patients versus healthy controls are found, but this needs further investigation. Taken together, miR-31 has a crucial role in psoriasis by promoting epidermal proliferation and inflammation in lesion sites.

MiR-146a is overexpressed in lesional skin and peripheral blood mononuclear cells (PBMCs) from psoriasis patients [14,28]. It is known for its negative role in epidermal inflammation by targeting NF-κB mediators *IRAK1* and *CARD10* and chemotactic attractant *CCL5* [29–31]. Xia et al. [28] showed that high levels of miR-146a in the skin and in PBMCs of psoriasis patients positively correlate with IL-17 levels in the skin and serum, respectively. However, target gene *IRAK1* was downregulated in PBMCs but not in the skin, showing the asynchronous expression of target genes in local lesions and peripheral PBMCs. In vivo studies using mice models of Psoriasis showed that miR-146a inhibition promoted earlier psoriasis-like onset, epidermal hyperproliferation, IL-17 skin inflammation and IL-8 secretion with the increased infiltration of neutrophils at lesion sites.

MiR-155-5p has been shown upregulated in blood and psoriatic lesional skin [32,33]. It is involved in the keratinocyte cell cycle, as in vitro studies showed that miR-155 inhibition decreases keratinocyte proliferation and increases the expression of *PTEN*, *PIP3*, *AKT*, *BAX* and *BCL2* apoptotic genes [34]. Another study supported this finding by showing that miR-155-5p overexpression impairs keratinocyte apoptosis possibly by targeting *CASP3*, a validated direct target of miRNA-155-5p [35]. This miRNA is also involved in inflammation, as keratinocytes treated with TNF-α upregulated its expression. Moreover, when cells were stimulated with LPS and overexpressed miR-155-5p, there was an increase of *TLR4*; NF-κB proteins together with the levels of secreted TNF-α and IL-18, IL-6 and IL-1β via inflammasome *NLRP3/CASP1* activation [36]. *CXCL8* is also upregulated in miR-155-5p-overexpressed keratinocytes via the *GATA3/IL37* axis [37]. Elevated miR-155 levels have also been observed in DMSCs [38]; however, further research is needed to establish its role. Overall, miR-155-5p is involved in keratinocyte proliferation, apoptosis and inflammation in psoriasis.

Finally, epidermal cells and infiltrated T cells in psoriasis lesions have shown increased miR-21 expression [39]. In vitro, it is regulated by LncRNA *MEG3* and regulates keratinocyte proliferation via the direct targeting of *CASP8* [40]. It also promotes proliferation by regulating the *AKT/PI3K* and TGFβ signalling pathways [41,42]. Regarding its role in inflammation, UVB-exposure promoted miR-21-3p upregulation in keratinocytes. This upregulation led to the production of proinflammatory cytokines IL-6 and IL-1β and chemokines CCL5 and CXCL10 in keratinocytes [42]. The expression of miR-21 is increased in both TH1 and TH2 differentiated T cells after activation with anti-CD3 and anti-CD28, indicating that this miR is involved in T-cell activation regardless the T-cell subtype. Moreover, it has an antiapoptotic effect on the activated T cells [39].

Therefore, this miRNA can contribute to psoriasis pathogenesis by modulating the cell cycle and inflammation in keratinocytes and T cells.

Twenty-seven further miRNAs have also been described in psoriasis pathogenesis. They are detailed in Table 1 [43–70].

Table 1. Differentially expressed mRNAs in skin immune diseases. Tissue/cell/fluids in which microRNAs (miRNAs) are found dysregulated, miRNA expression, validated experimentally target genes, and their biological role in the skin are detailed.

miRNA	Condition	Tissue/Cell/Fluid	Expression	Target Genes	Biological Role	Ref.
miR-203	Psoriasis	Keratinocytes	Upregulated	*SOCS3* *NR1H3* *PPARG*	Keratinocyte proliferation, modulation of cytokines: TNF-α, IL-24 and IL-8 and angiogenesis.	[14,19–22]
miR-31	Psoriasis DLE	Keratinocytes Blood DMSCs	Upregulated (Blood and Keratinocytes) Downregulated (DMSCs)	*PPP6C* *STK40*	Keratinocyte proliferation and apoptosis. Promotes Inflammation via NFKB1 activation and chemokine and cytokine production (CXCL1, CXCL5, IL-8, IL-1B and IL-12). Neutrophile and intermediate monocyte recruitment.	[16,24–26]
miR-146a	Psoriasis AD	Keracinocytes Serum	Upregulated	*CCL5* *IRAK1* *CARD10*	Protective role disminishing keratinocyte proliferation and inflammation supressing IL-17, CCL5, CCL8 and IFNγ.	[14,28–31]
miR-155	Psoriasis AD	Keratinocytes Blood T cells	Upregulated	*CTLA4* *PKIA* *GATA3* *CASP3*	Promoted epidermal proliferation, inflammation, TJ disruption and inhibits apoptosis. T cell proliferation and promotion of TH17 responses.	[32–38,71–74]
miR-21	Psoriasis	Keratinocytes Blood T cells	Upregulated	*CASP8* *SMAD7*	T cell activation and inhibition of apoptosis. Keratinocyte proliferation and inflammation (IL-1β, CCL5 and CXCL10).	[39–42]
miR-125b	Psoriasis	Keratinocytes	Downregulated	*FGFR2*	Keratinocyte proliferation and differentiation.	[43]
miR-424	Psoriasis	Keratinocytes Serum	Downregulated	n.d.	Keratinocyte proliferation via MEK1/cyclin E1.	[44]
miR-486-3p	Psoriasis	Keratinocytes	Downegulated	*K17*	Keratinocyte proliferation.	[45]
miR-138	Psoriasis	Keratinocytes	Downregulated	*K17*	Keratinocyte proliferation and apoptosis reduction.	[46]
miR-744-3p	Psoriasis	Keratinocytes	Upregulated	*KLLN*	Keratinocyte proliferation and differentiation.	[47]

Table 1. *Cont.*

miRNA	Condition	Tissue/Cell/Fluid	Expression	Target Genes	Biological Role	Ref.
miR-150	Psoriasis	Keratinocytes	Downregulated	*HIF1A* *VEGFA*	Keratinocyte proliferation in hypoxic conditions.	[48]
miR-876-5p	Psoriasis	Skin Blood	Downregulated	ANG-1	HaCAT proliferation via PI3K/AKT, cell adhesion and invasion.	[49]
miR-183-3p	Psoriasis	Keratinocytes	Downregulated	*GAB1*	Proliferation and migration of HaCat cells.	[50]
miR-548a-3p	Psoriasis	Keratinocytes	Upregulated	*PPP3R1*	Keratinocyte proliferation.	[51]
miR-217	Psoriasis	Keratinocytes	Downregulated	*GFHL2*	Keratinocyte differentiation.	[52]
miR-4516	Psoriasis	Keratinocytes	Downregulation	*FN1* *ITGA9*	Accelerated migration, resistance to apoptosis and differentiation.	[53]
miR-194-5p	Psoriasis AD	Keratinocytes	Downregulated	*GRHL2* *HS3ST2*	Keratinocyte proliferation and inhibition of differentiation.	[54]
miR-187	Psoriasis	Keratinocytes	Downregulated	*CD276*	Keratinocute proliferation.	[55]
miR-99a	Psoriasis	Keratinocytes	Downregulated	*FZD5/FDZ8*	Keratinocyte proliferation.	[56]
miR-130a	Psoriasis	Keratinocytes	Upregulated	*STK40*	Apoptosis inhibition and cell viability and migration promotion. Direct regulation NFKB pathway via STK40 and inditect regulation of JNK/MAPK pathway via SOX9.	[57]
miR-122-5p	Psoriasis	Keratinocytes	Upregulated	*SPRY2*	Keratinocyte proliferation.	[58]
miR-126	Psoriasis	Keratinocytes	Upregulated	n.d.	Keraintocyte proliferation and inflammation increasing TNFa, IFNg, IL17A, IL-22 and decreasing IL-10. Apoptosis inhibition.	[59]
miR-145-5p	Psoriasis	Keratinocytes	Downregulated	*MLK3*	Cell proliferation and chemokine secretion via NF-kB and STAT 3 activation.	[60]
miR-17-92	Psoriasis	Keratinocytes	Upregulated	*CDKN2B*	Keratinocyte proliferation and immune chemotaxis via secretion CXCL9, CXCL10, supression of SOCS1 and STAT1 activation.	[61]

Table 1. *Cont.*

miRNA	Condition	Tissue/Cell/Fluid	Expression	Target Genes	Biological Role	Ref.
miR-320b	Psoriasis	Keratinocytes	Downregulation	*AKT3*	Keratinocyte proliferation and modulation of STAT3 and SAPK/JNKsingaling pathways.	[62]
miR-124-3p	Psoriasis	Keratinocytes	Downregulated	*FGFR2*	Keratinocyte prolfieration, migration and inflammation.	[63]
miR-184	Psoriasis	Keratinocytes	Upregulated	*AGO2*	Cytokine dependent depletion of AGO2.	[64]
miR-221/222	Psoriasis	Keratinocytes	Upregulated	n.d.	Keratinocyte and immune cells proliferation.	[65]
miR-181-b	Psoriasis	Keratinocytes	Downregulated	*TLR4*	Inflammation and keratinocyte proliferation.	[66]
miR-1307-3p	Psoriasis	Keratinocytes	Upregulated	n.d.	Induces inflammatory mediators IL-8, IL-6 and CCL20.	[67]
miR-381-3p	Psoriasis	Keratinocytes (EVs)	Upregulated	*FOXO1* *UBR5*	Crosslink with T cells inducing TH1/TH17 polarisation.	[68]
miR-210	Psoriasis	$CD4^+$ T cells	Upregulated	*FOXP3*	Induces immune T cell dysfunction.	[69]
miR-138	Psoriasis	$CD4^+$ T cells	Downregulated	*RUNX3*	Modulation of TH1/TH2 balance.	[70]
miR-485-3p	DLE	T cells Fibroblasts	Upregulated	*PPARGC1A*	T cell activation and promotion of fibrotic processes.	[16]
miR-10a-5p	AD	Keratinocytes	Upregulated	*HAS3*	Inhibitis keratinocyte proliferation.	[75]
miR-29b	AD	keratinocytes	Upregulated	*BCL2*	Keratinocyte apoptosis.	[76]
miR-223	AD	Blood	Upregulated	n.d.	Upregulation of HNMT indirectly to degrade excessive histamine.	[77]
miR-151a	AD	Blood	Upregulated	*IL12RB2*	Regulation of TH1 cytokines (IL-2, IFN γ).	[78]
miR-143	AD	Keratinocytes	Downregulatd	*IL13RA1*	Regulation of IL-13 activitu and TH2 inflammation.	[79]

AD, atopic dermatitis; DLE, discoid lupus erythematosus; DMSCs, dermal mesenchymal stem cells; Ref., Reference; n.d., not detailed and TJ, tight junction.

2.2. Cutaneous Lupus Erythematosus (CLE)

Cutaneous lupus erythematosus (CLE) is an autoimmune chronic disease that includes a broad range of dermatologic manifestations. CLE is divided into several subtypes, but discoid lupus erythematosus (DLE) is consistently reported as the most common subtype, and this may be because, as a chronic disorder, it is easier to identify compared to the more evanescent and nonscarring acute cutaneous and subacute cutaneous forms (SCLE) [80]. The CLE overall prevalence is estimated to be around 73.24 per 100,000 according to several USA studies [81]. The pathogenesis of CLE is not completely understood. It seems to be multifactorial and involves genetic predisposition, environmental triggers and abnormalities in the immune response. Findings indicate that UVB may act as a trigger, promoting skin damage and keratinocyte apoptosis. There may be a defective apoptosis/cell clearance, and the immune system is activated against autoantigens.

CLE lesions share extensive lymphocytic infiltrates with a high predominance of CD4 T cells with an imbalance towards T-helper 1, cytotoxic CD8+ T cells, as well as interferon type 1 signature and proinflammatory cytokines, IL-1α, IL-1β, IL-8, TNF-α and IL-6 [82]. To date, we have published the only microRNA study in CLE—in particular, discoid lupus [16]. The study identified in DLE lesions a different microRNA signature (miR-31 and miR-485-3p) when compared to nonlesional sites. The relevant identified miRNAs and their potential role in CLE pathogenesis are detailed below.

MiR-31 was identified as a keratinocyte-derived miR located in the DLE lesional epidermis. It is involved in epidermal apoptosis by promoting the upregulation of apoptotic genes (*BIM*, *BAX*, *P53* and *CASP3*) when overexpressed. Moreover, as in previous reports, we also found that it enhances NF-κB activation and the secretion of inflammatory cytokines such as IL-1β, IL-12 and IL-8 in keratinocytes. The crosslink between keratinocytes and lymphocytes is of critical importance in cutaneous autoimmune diseases, and it was found that miR-31 promotes the attraction of neutrophils and intermediate monocytes; therefore, it enhances the recruitment of immune cells into the DLE lesion sites, perpetuating inflammation.

MiR-485-3p was found in the infiltrating lymphocytes and fibroblasts in DLE lesions. It is involved in the activation of CD4+ and CD8+ T cells and, also, in promoting fibrosis by enhancing fibrotic genes *SMAD3*, *COL3A1* and *TGFβR* in fibroblasts. This fibrosis may occur, as miR-485-3p may be targeting peroxisome *PPARGC1A*, which is known for exerting a protective function of fibrosis development [83] and was found downregulated in fibroblasts that overexpressed miR-485-3p. Studies showing the direct target of *PPARGC1A* by miR-485-3p support this finding [71].

2.3. Atopic Dermatitis (AD)

Atopic dermatitis is a complex, systemic inflammatory disorder associated with a variety of clinical features [72]. It is the most common chronic inflammatory skin disease, with a prevalence of 15–20% of children and 1–3% of adults worldwide. It has high heritability; occurs frequently with other atopic diseases (asthma, allergic rhinitis and food allergies) and its incidence has increased two to three-fold in recent years in industrialised countries [73].

AD is characterised by an epidermal barrier disruption, activation of a T-helper 2 response and alteration of the skin microbiome [72]. IgE and eosinophils are increased, which, in turn, are thought to boost inflammation and skin damage through the production of reactive oxygen species, inflammatory cytokines and the release of toxic granule proteins [74]. miRNA expression profiles in the skin lesions of AD patients have been determined by microarray. The elevated expression of let-7i, miR-24, miR-27a, miR-29a, miR-193a, miR-199a and miR-222 was reported [15]. Gu et al. also reported a multitude of dysregulated miRNAs (e.g., upregulation: miR-4270, miR-211, miR-4529-3p and miR-29b and downregulation: miR-184, miR-135a and miR-4454) in AD skin biopsies [76]. From the identified miRNAs, we describe below the functional role of some of the most relevant in the skin pathogenesis of AD.

MiR-155-5p in AD lesional skin is predominantly expressed in infiltrating immune cells. This miR plays a role in the regulation of allergen-induced inflammation by targeting *CTLA4*, a negative regulator

of T-cell activation [15]. It affects T-cell proliferation and differentiation by shifting towards a TH17 response [84]. The expression of this miR has been analysed in different disease stages in an AD mice model, and it was found to be increased in the elicited phase of the disease compared to controls [85]. Increased levels of miR-155-5p have also been detected in vitro in HaCAT cells stimulated with TNF-α, and it promotes inflammation and epithelial tight junction (TJ) changes by the direct binding of *PKIA* [86]. Taken together, miR-155-5p promotes T-cell activation, epidermal inflammation and TJ disruption in AD.

Previous studies have demonstrated that miR 146a is involved in the inflammatory response of atopic dermatitis (AD). MiR-146a expression is increased in keratinocytes and the chronic lesional skin of patients with AD expression. MiR-146a may have an anti-inflammatory role, alleviating chronic skin inflammation in atopic dermatitis through the suppression of innate immune responses in keratinocytes. It inhibited the expression of numerous proinflammatory factors, including IFN-γ-inducible and AD-associated genes *CCL5*, *CCL8*, and ubiquitin D (*UBD*) in human primary keratinocytes stimulated with IFN-γ, TNF-α or IL-1β. Studies demonstrated that miR-146a-mediated suppression in allergic skin inflammation partially occurs through the direct targeting of the upstream NF-κB signal transducers caspase recruitment domain, containing protein 10 and IL-1 receptor-associated kinase 1. In addition, *CCL5* was identified as a novel, direct target of miR-146a [31]. It is worth mentioning that the upregulation of miR-10a-5p, miR-29b, miR-223 and miR-151a have also been described in the inflammatory response and keratinocyte apoptosis for AD patients [75–78] (Table 1).

Finally, miR-143 has been found downregulated in the lesional skin from AD patients [79]. It targets IL-13 receptor alpha 1 (*IL13R*), modulating IL-13 activity. IL-13 is a cytokine involved in TH2 responses that is highly expressed in AD skin lesions. Therefore, miR-143 may contribute to AD pathogenesis by favouring TH2 responses.

3. Common Deregulated miRNAs in Skin Autoimmune Conditions

Skin lesion transcriptome studies in different autoimmune skin diseases have described unique expression signatures for specific diseases but have also established a common cross-disease gene set among inflammatory skin diseases [87]. The comparative transcriptomic analyses of atopic dermatitis and psoriasis conducted by Choy D.F et al. revealed a shared neutrophil-attracting profile, which may be due to the underlying commonalities in IL-17 signalling [88]. The comparison of DLE and psoriatic lesions revealed differential clustering upon dimensionality reduction, although a certain overlap was observed, pointing toward the existence of a common cross-disease profile. Through a gene set enrichment analysis, the differential T-cell polarisation toward Th17 in psoriasis and Th1 in DLE was supported [89].

Since miRNA studies have become of interest in inflammatory skin disease research; we sought to clarify common and unique molecular and pathophysiologic features in inflamed skin by comparing psoriasis, CLE and AD. The comparison showed miR-31 to be upregulated in both psoriasis and DLE lesional skin, suggesting a shared NF-κB signalling inflammation pathway, a dysregulated keratinocyte apoptosis process and epidermal hyperplasia. On the other hand, miR-155 and miR-146a were found to be upregulated in psoriasis and AD. It seems they may share a regulation of Th17 and the production of chemoattractant cytokines such us CXCL8 fundamental for these conditions.

As miRNA expression profiles are tissue-specific and, in many cases, define the physiological nature of cells, the fact that they are commonly dysregulated among skin conditions (Figure 3) indicates that miRNAs may exert similar pathogenic roles, and dysregulated signalling pathways may be shared between skin conditions. Studies comparing the miRNA profile between autoimmune skin disorders may be of value to understand their pathogenesis and to promote novel therapies.

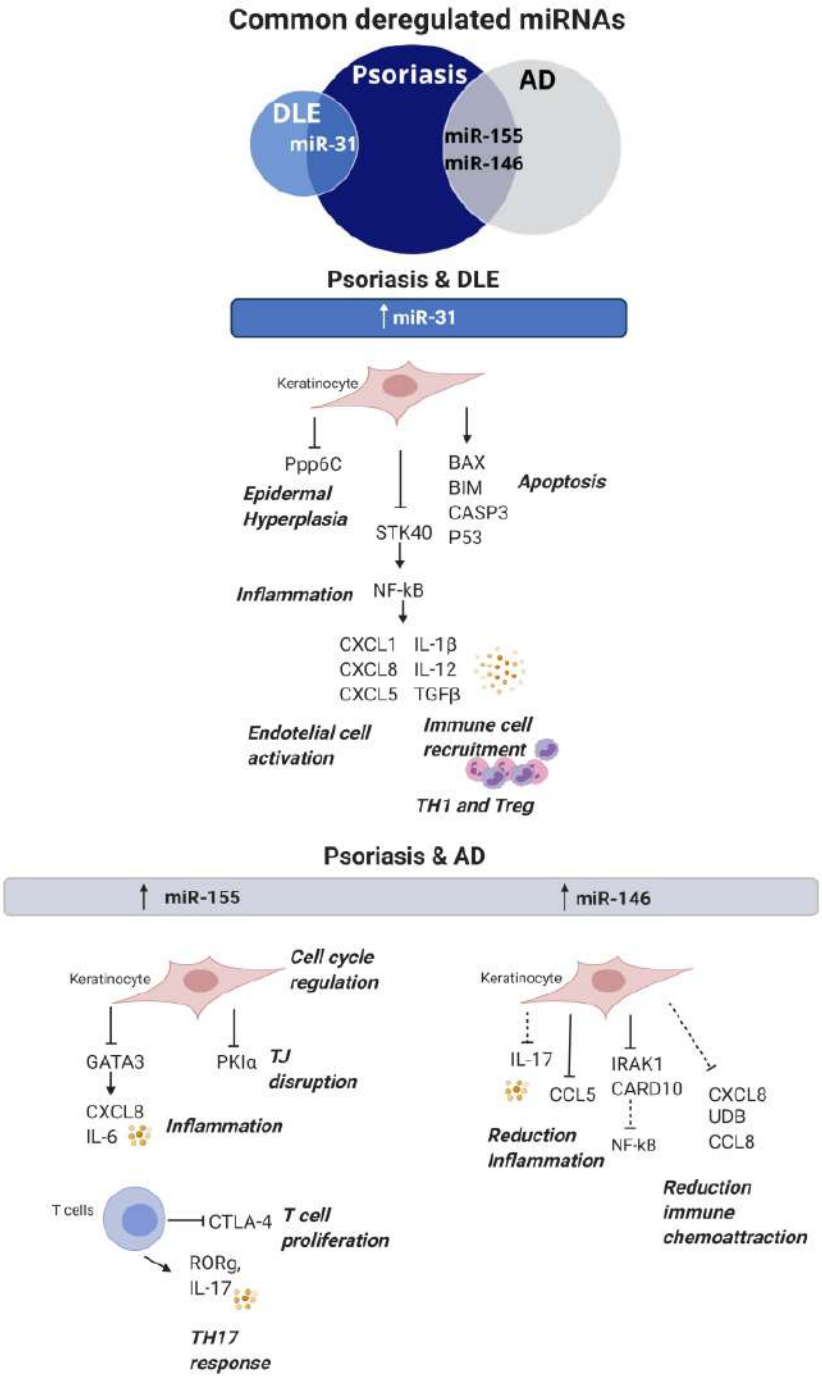

Figure 3. Commonly dysregulated miRNAs and their role in skin autoimmune diseases. MiR-31 is upregulated in both DLE and psoriasis; it participates in keratinocyte proliferation, apoptosis, inflammation and immune cell recruitment. MiR-155 and miR-146 are upregulated in both psoriasis and atopic dermatitis. MiR-155 is involved in keratinocyte proliferation, inflammation and TJ disruption, whereas, in T cells, it promotes proliferation and TH17 responses. MiR-146 has a protective effect and, when upregulated in keratinocytes, promotes a reduction of inflammation and immune chemoattraction. DLE: discoid lupus erythematosus, AD: atopic dermatitis and TJ: tight junction.

4. miRNAs as Potential Biomarkers in Skin Inflammatory Diseases

Circulating miRNAs have been described as biomarkers, since they are found in different body fluids such as serum, plasma, urine, saliva, tears, amniotic and cerebrospinal fluid. Some of the innate properties of miRNAs make them highly attractive as potential biomarkers. They are accessible, stable and resistant to ribonuclease degradation and easily detected in small volumes of samples using standard RT-qPCR [90]. It is not yet clear their origin or function; however, changes in a circulating miRNA profile have correlated with a large number of medical conditions, like gastrointestinal and cardiovascular diseases and primary and metastatic cancers [91]. However, miRNAs with important immunological modulation effects in pathogenesis are not necessarily the best biomarkers; for example, miRNAs in circulation show limited or no correlation with miRNA expression in skin, a difference from other conditions. Moreover, whether the dysregulated miRNAs in blood are disease-specific or related to systemic inflammation is unclear. To date, despite several miRNAs being studied, none of them are used as biomarkers in routine clinical practice.

In this section, we review potential miRNAs as biomarkers in skin inflammatory diseases for early diagnosis, assessment of disease severity/activity, treatment response monitoring and associated comorbidities.

4.1. miRNAs as Diagnostic Biomarkers

Studies in pathogenesis and biomarker research are most developed in psoriasis. Since there is a specific miRNA expression profile different from other skin diseases and healthy controls, miRNAs may be used as diagnostic markers. MiR-223 and miR-143 were found to be significantly upregulated in PBMCs from patients with psoriasis. A ROC analysis showed that miR-223 and miR-143 have the potential to distinguish between psoriasis and healthy controls [92], suggesting that miR-223 and miR-143 may serve as novel diagnostic biomarkers for psoriasis. In the same way, high levels of miR-369-3p in the serum and skin were also distinctive in psoriasis patients compared with healthy controls [93]. Hair studies have shown miR-424 levels to be significantly upregulated in the hair shaft of only patients with psoriasis compared with normal controls and those with atopic dermatitis. A receiver–operator curve analysis of hair shaft miR-424 to distinguish psoriatic patients from normal subjects showed an area under the curve of 0.77 [94]. Hair root levels of miR-19a were also significantly upregulated only in psoriasis compared with normal controls. In a characteristic (ROC) curve analysis for hair root miR-19a, to distinguish psoriasis patients from normal subjects, the area under the curve (AUC) was 0.87 [95]. The results support a putative use as noninvasive diagnostic markers for psoriasis. Finally, another study found that, by real-time PCR study, levels of miR-125b, miR-146a, miR-203 and miR-205 in the serum were significantly decreased in patients with psoriasis compared with normal subjects [96].

Several studies have been performed analysing the microRNA profile in systemic lupus erythematosus patients but fewer in CLE. In SLE, miRNAs have been analysed in the serum, plasma and urine, and their relation has been established with several lupus manifestations, such as nephritis, oral ulcers and lupus anticoagulant, among others [97]. Concerning cutaneous lupus, only one study that included SCLE and DLE patients and healthy donors screened a selected panel of miRNAs related with inflammation and fibrosis in the serum [98]. The study showed that miR-150, miR-1246 and miR-21 are downregulated in both SCLE and DLE compared to healthy controls; therefore, these miRNAs could be of use for CLE diagnosis. Regarding differences between CLE subtypes, no DLE-specific miRNAs were discovered; however, low levels of miR-23b and miR-146 appear characteristic of SCLE [99].

While miRNAs have been extensively investigated as biomarkers in allergic inflammatory conditions like asthma and allergic rhinitis, only a few studies have been conducted in atopic dermatitis. Lv Y et al. [100] focused on paediatric AD and found that miR-203 and miR-483-5p were upregulated in the serum from children with AD and showed areas under the ROC curve (AUC) > 0.7. Surprisingly, miR-203 was also found differentially expressed in urine from these patients, but in this case, it was downregulated. Another study analysing miRNAs in the plasma of children with AD concluded that

miR-194-5p was downregulated in AD when compared with the control group, suggesting that it may be a valuable biomarker for AD diagnosis [101]. MiR-155 plays an important role in AD pathogenesis. Its expression was analysed in peripheral CD4+ T cells, and they found that miR-155 was significantly elevated in AD patient CD4+ T cells compared with healthy subjects, indicating that it may be a useful biomarker of the disease as well [15].

4.2. miRNA as Disease Activity and Severity Biomarkers

The present data suggest that certain miRNAs could potentially serve as psoriasis activity markers. To date, the disease severity of psoriasis is assessed by a PASI score and BSA [102]. However, serum markers reflecting disease activity have not been of clinical use in psoriasis. MiR-223 and miR-143, as previously described, are increased in PBMCs from psoriasis patients and positively correlated with the PASI score and with an area under the ROC curve (AUC) > 0.8 [92]. MiR19a upregulated in hair roots inversely correlated with duration onset and first visit to the hospital [95]. High levels of miR-1266 in the serum [103], reduction of miR-126 and upregulation of miR-200c in plasma [104,105] and elevated miR-146a and miR-155 in PBMCs can also be indicators of psoriasis activity [33,103]. On the other hand, miR-99a in PBMCs are negatively correlated with disease severity [103]. Finally, the serum and skin miR-369-3p levels were detected, and their correlations with disease severity were confirmed [106], in which miR-369-3p levels in skin had a positive linear relationship with the PASI scores [93,106]. Conversely, low miR-369-3p and miR-135b levels in the skin have been associated with disease improvement and lower severity [93,107].

To date, the disease activity in CLE is assessed by the Cutaneous Lupus Erythematosus Disease Area and Severity Index (CLASI) [108]. Only serum miR-150 levels have been identified to be inversely correlated with a CLASI activity score in SCLE patients. Since this miRNA has been associated with dermal and renal fibrotic processes, we can also infer that it may be involved in the activation of inflammatory and profibrotic pathways [109,110]. Therefore, miR-150 may be a good candidate to assess disease severity in SCLE. Further analyses of miRNAs in the plasma or in other biological fluids may yield interesting biomarker targets in CLE.

One study aimed to identify a prognostic miRNA signature in children with AD from serum and urine by a genome-wide miRNA profiling analysis. MiR-203 levels were significantly upregulated in the serum of children with AD compared with healthy controls, and they were significantly associated with increased sTNFRI and sTNFRII. However, miR-203 was markedly decreased in the urine of children with AD [100]. Therefore, miR-203 is proposed as a potential biomarker for the severity of inflammation in childhood AD. It is not clear if the data can be extrapolated to adults, since children with AD may have different miRNA expression profiles compared to their adult counterparts. Research is needed in order to establish biomarkers in the adult population, to be able to predict disease prognosis and, importantly, AD biomarkers may help in the rapid detection of the relapse phase of the disease and treatment outcomes.

4.3. miRNA Levels to Monitor Therapeutic Effects

Changes in miRNA expression following therapy have been studied in psoriasis. Pathological T cells and dendritic cells can trigger abnormal keratinocyte proliferation in psoriasis progression via many cytokines, especially TNF-α. Thus, TNF-α is essential for the pathogenesis of psoriasis. The anti-TNF-α biological drug etanercept significantly suppressed a panel of 38 miRNAs, and validated serum levels of miR-106b, miR-26b, miR-142-3p, miR-223 and miR-126 were significantly downregulated [111]. On the other hand, adalimumab increased miR-23b. These data indicate that changes in the miRNA level can reflect a previously unknown effect of anti-TNF-α therapy [112]. Interestingly, levels of those miRNAs were not altered when patients were treated with methotrexate. Additionally, miR-146a-5p in PBMCs has been described to correlate with clinical efficacy in psoriatic patients treated with anti-TNF-α adalimumab [113] and miR-125a levels in plasma increased in etanercept-treated responder patients [114].

There are no studies evaluating the changes in miRNA levels in response to therapies in CLE or AD. Prognostic or early response miRNAs in DLE may be useful to monitor the disease and avoid the development of irreversible fibrotic scarring lesions.

4.4. Associated Comorbidity Biomarkers

Cardiovascular disease, obesity, diabetes and hypertension have been found at a higher prevalence in psoriasis patients compared to the general population, suggesting that, although psoriasis affects mainly skin, comorbid conditions are related with the underlying chronic systemic inflammation. Studies have been conducted to evaluate miRNAs as biomarkers of comorbidities in psoriasis. Garcia-Rodriguez S. et al. described the upregulation of miR-33 in the plasma of psoriatic patients when compared to controls and correlated with elevated insulin blood levels [115]. Serum levels of miR-126 are negatively associated with carotid intima-media thickness in psoriatic patients [104]. Plasma levels of miR-200c are upregulated in psoriasis and correlated with cardiovascular risk [105]. These results indicate miRNAs may be of value to assess possible comorbidities in psoriasis.

In AD children, miR-483-5p expression in serum has been found as an independent marker of IgE levels. However, the upregulation of miR-483-5p has been significantly associated with the presence of other simultaneous atopic conditions, such as rhinitis and/or asthma, in comparison with healthy controls [100]. Therefore, miR-483-5p may reflect the multiorgan/tissue involvement of AD (Table 2).

Table 2. miRNAs as biomarkers and potential applications in autoimmune skin conditions (psoriasis, cutaneous lupus erythematosus and atopic dermatitis).

miRNA	Condition	Tissue/Cell/Fluid	Expression	Potential Application	Ref.
miR-223 **miR-143**	Psoriasis	PBMCs	Upregulated	Diagnosis, assess disease severity and monitor treatment (metotrexate) response	[92]
miR-424	Psoriasis	Hair shaft	Upregulated	Diagnosis	[94]
miR-19a	Psoriasis	Hair root	Upregulated	Diagnosis and duration of disease	[95]
miR-369-3p	Psoriasis	Serum Skin	Upregulated	Diagnosis (skin and serum) and severity of disease (skin)	[93,106]
miR-1266	Psoriasis	Serum	Upregulated	Diasease activity	[116]
miR-126	Psoriasis	Plasma	Downregulated	Disease Severity Comorbidities (carotid thickness)	[104]
miR-200c	Psoriasis	Plasma	Upregulated	Diseaase activity and Comorbidities (cardiovascular disease)	[105]
miR-155	Psoriasis	PBMCs	Upregulated	Disease activity	[33]
miR-146a	Psoriasis	PBMCs	Upregulated	Disease activity Monitor treatment response (adalimumab)	[96,103]
miR-99a	Psoriasis	PBMCs	Downregulated	Disease activity	[103]
miR-135b	Psoriasis	Skin	Upregulated	Disease improvement	[107]
miR-125a	Psoriasis	Plasma	Downregulated	Diagnosis, and Monitor treatment response (etanercept)	[114]
miR-33	Psoriasis	Plasma	Upregulated	Detection of comorbidities (elevated insulin levels)	[115]
miR-150 **miR-1246** **miR-21**	CLE (SCLE and DLE)	Serum	Downregulation	Diagnosis	[98]
miR-23b **miR1246** **miR-146**	SCLE	Serum	Downregulated	Diagnosis	[99]
miR-150	SCLE	Serum	Downregulated	Disease Seveity	[109,110]
miR-203	AD in children	Serum Urine	Upregulated in serum Downregulated in urine	Diagnosis and Disease severity	[100]
miR-483-5p	AD in children	Serum	Upregulated	Diagnosis and Detection of comorbidities (asthma/rhinitis)	[100]
miR-194-5p	AD in children	Plasma	Downregulated	Diagnosis	[101]
miR-155	AD	$CD4^+$ T cells	Upregulated	Diagnosis	[15]

CLE, cutaneous lupus erythematosus; DLE, discoid lupus erythematosus; SCLE, subacute cutaneous lupus erythematosus; AD, atopic dermatitis and PBMCs, peripheral blood mononuclear cells.

5. Targeting miRNAs to Treat Skin Autoimmune Diseases

To date, there is no fully effective therapy for several skin autoimmune diseases, and the drugs used are not exempt from significant side effects. In addition, there are refractory cases that do not respond to conventional treatment, and their therapeutic options are limited. Most drugs may reverse local skin inflammation, like in DLE, but they do not avoid the progression of fibrosis or irreversible sequelae. Therefore, there is a need for novel specific and safe therapeutic agents to treat these chronic skin inflammatory diseases. miRNA therapeutics are the most recent of a range of RNA therapies that have emerged over the last 10–15 years [117].

There has been an increase of miRNA profiling studies in skin inflammatory diseases, leading to the identification of differentially expressed miRNAs, key in disease pathogenesis. Data supports the concept that miRNAs represent valid drug targets for treatment [118]. There are two strategies to use microRNAs as genetic modulators: miRNA inhibitors and miRNA mimics [119]. miRNA inhibitors or anti-miRNAs are chemically synthesised single-stranded nucleic acids designed to specifically bind to endogenous mature miRNA molecules. When a miRNA inhibitor is administered, there is a reduction of the targeted endogenous miRNA, and as a result, the interaction of the miRNA of interest with its targets is prevented. This approach is used for those aberrant expressed miRs that are upregulated in disease. Conversely, miRNAs that are downregulated in disease may be replaced transiently by using miRNA mimics. The miRNA mimics are chemically synthesised miRs that mimic endogenous miRNAs and are able to restore miRNA expression levels to normal. Therefore, when administered, they can modulate the gene expression correctly and achieve appropriate cell functioning.

5.1. In Vivo Approaches of miRNA Therapy for Skin Autoimmune Diseases

In vivo studies have been conducted to evaluate miRs as potential therapeutic agents in skin disorders, mainly in psoriasis. MiR-21 expression is increased in epidermal lesions of patients with psoriasis, and this leads to reduced epidermal *TIMP3* (tissue inhibitor of matrix metalloproteinase 3) expression and the activation of *ADAM17* (tumour necrosis factor-α-converting enzyme), which induces TNF-α shedding. The inhibition of miR-21 by locked nucleic acid (LNA)-modified anti-miR-21 compounds ameliorated disease, reducing hyperplasia in patient-derived psoriatic skin xenotransplants in mice and in a psoriasis-like mouse model, suggesting that anti-miR-21 is a promising therapy for psoriasis [120]. Similarly, in an imiquimod-induced psoriasis mouse model, the subcutaneous administration of anti-miR-31 decreased acanthosis, dermal cellular infiltration and epidermal thickness hyperplasia [25]. Treatment with mimic-340 alleviated the psoriasis severity in the same mouse model through the downregulation of cytokine *IL17A* [121]. In addition, an intradermal injection of synthetic miR-146 mimics efficiently inhibited the development of psoriasiform skin and reduced the epidermal thickening and the number of infiltrating neutrophils [122]. These results highlight the potential of miRNA mimics as a therapy to alleviate skin inflammation. The topical administration of nanocarrier miRNA-210 antisense ameliorated the psoriasis-like dermatitis in mice, providing a potentially effective topical drug for psoriasis [123]. The delivery of mimic-145-5p into the skin also decreased the epidermal hyperplasia and ameliorated psoriasis-like dermatitis in mice [60].

In AD mice models, the treatment with anti-miR-155-5p inhibitors clearly reduced the thinning of the epidermis and reduction of the inflammatory skin cell infiltrates accompanied by decreasing levels of Th2 cytokines (IL-4, IL-5, IL-9 and IL-13) [85]. The results suggest that antimir-155 therapy would help reducing AD-associated inflammation. The IL-32γ inhibition of miR-205 led to an inactivation of NF-κB in AD mice models, suggesting a promising therapy for further study [124].

Other miRs have been investigated as a therapy in skin diseases. miR-132 plays a role in the wound-healing processes, and when liposome-formulated miR-132 mimics were topically applied in human ex-vivo skin wounds, they promoted healing [125]. miR-203 also plays a role in scarring and anti-miR-203 treatment accelerated wound closure and reduced scar formation in vivo in mice skin wound models [126].

So far, no in vivo miRNA therapy studies have been performed in CLE. miRNAs involved in skin fibrotic processes may be potential targets in DLE in order to avoid scarring.

In vivo experiments have reported good results in Ps and AD, giving excellent expectative of the clinical applicability of miRNAs therapy for autoimmune skin diseases. However, experiments performed using animal models not always translating the same positive results in human trials is an important limitation. Currently, novel technologies are applied, such as 3D skin models (skin organoids) using patients samples to validate in vivo results before performing human clinical trials.

5.2. Clinical Trials Using miRNA as a Therapy for Treating Skin Diseases

Since the discovery of miRNAs in 1993, a number of preclinical studies have been conducted. Consequently, there has been an increase in the number of patient treatments over the last decade, and some of them have progressed translationally, and phase I and phase II clinical trials are currently ongoing. There are only two clinical trials involving the applicability of miR-29 mimics to treat lesional skin. MiR-29 is known to have an antifibrotic role, and it may be helpful for the treatment of fibrotic skin diseases. It is found at a lower level in cutaneous scars, keloids and in the lesional dermis of scleroderma patients, as compared with healthy controls [127]. A double-blinded, placebo-randomised, within-subject controlled clinical trial (ClinicalTrials.gov, ID NCT02603224) was performed with Remlarsen (miR-29 Mimic) administrated intradermally in healthy volunteers. The study showed a downregulation in collagen expression and a reduction in the development of fibroplasia in incisional skin wounds, accompanied by a downregulation of miR-29 target genes *COL1A1*, *COL1A2* and *COL3A1*, strongly involved with fibrosis [128]. A phase II trial (ClinicalTrials.gov, ID NCT03601052) is ongoing to study the efficacy and safety of Remlarsen, as well as its pharmacokinetics in patients with a history of keloid scars.

However, there are not any clinical trials going on for psoriasis, atopic dermatitis or cutaneous lupus. It would be necessary to perform complete clinical trials in order to guarantee the possible clinical implementation of miRNA therapy into skin diseases treatments.

5.3. Topical Nanodelivery of miRNA

Topical-based miRNA administration may be an attractive approach for applying miRNA therapy in skin diseases [129]. Off-target effects, dilution and toxicity, often associated with systemic administration, may be avoided when miRNA formulation is applied directly on the lesional skin area. The most significant limitation in the transdermal application of miRNAs is the skin barrier, since the natural function of the skin is to protect the body from unwanted effects from the environment [130]. The stratum corneum is the primary barrier to the percutaneous absorption of compounds, as well as to water loss, providing most of the epidermal barrier function. It is composed of nonviable keratinocyte squames embedded in a lipid-rich matrix, making it nonpermeable and impedes the absorption of hydrophilic and lipophilic substances greater than 500 Da [131]. In addition, inflamed skin can complicate their penetration further [132]. Administration of the naked miRNA modulator will result in a poor outcome due to inefficient tissue penetration and degradation. An option to overcome this is to introduce chemical modifications that enhance their stability and delivery by increasing their resistance to degradation by the nucleases that are present in the skin. Emerging approaches for conveying small interfering RNA (siRNA) into the epidermis have been developed in recent years, mostly focusing on nonviral vectors such us liposomal or elastic vesicles, metal, liquid crystalline nanoparticles or with a peptide enhancer [133]. These studies showed the scope for the topical nanodelivery of miRNA for skin treatments (Figure 4a).

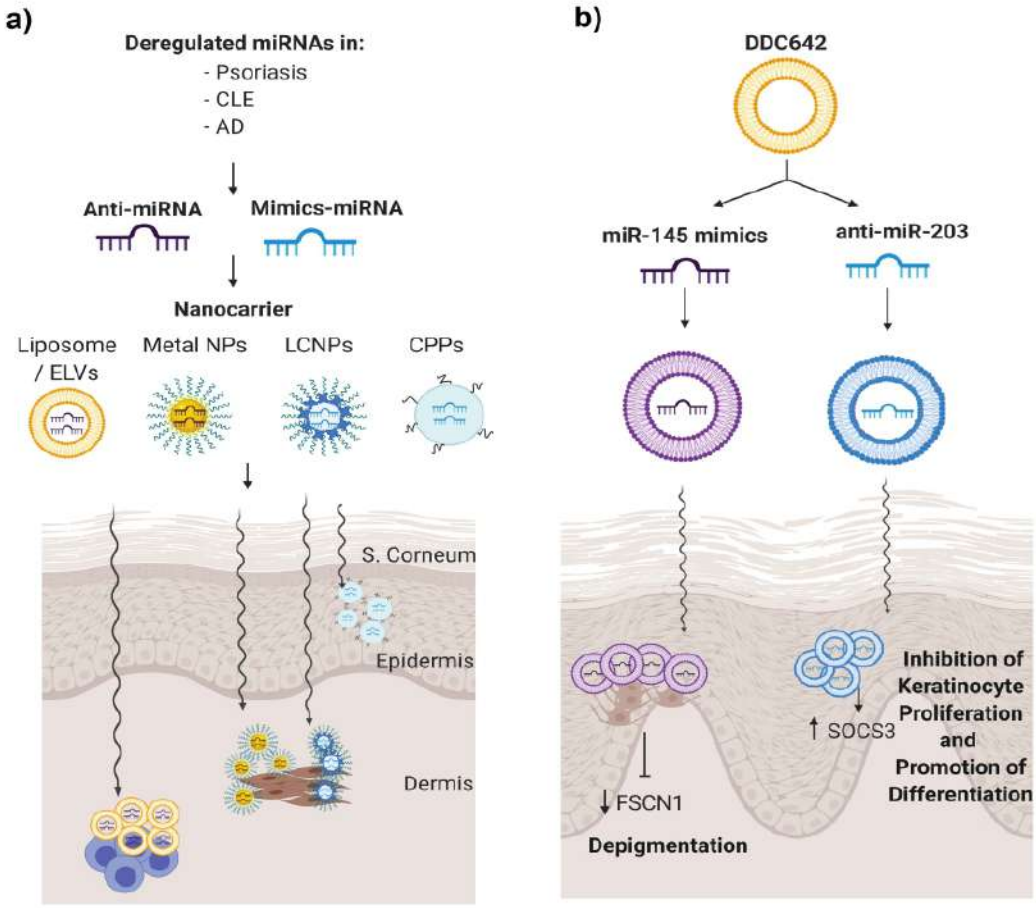

Figure 4. miRNA therapeutics for skin autoimmune diseases. (**a**) Dysregulated miRNAs in skin disorders may be potential candidates to be modulated to re-establish their expressions to normal conditions. Within this approach, anti-miRNA or mimics miRNA are encapsulated into nanovehicles to favour their penetration, avoid its degradation and be able to target the desired cells. (**b**) Deregulated miRNA in psoriasis miR-203 and miR-145 were selected, and therefore, anti-miR203 and miR-135 mimics were encapsulated in DDC624 liposome complexes, respectively, in a psoriasis tissue model.

To our knowledge, one manuscript described a type of liposomal vesicle as a nanodelivery for miRNAs in the treatment of psoriasis [134]. Liposomes are lipid-based carrier nanovehicles, stable with a high loading efficacy and low cytotoxicity. Liposome formulation implies the formation of amphiphilic phospholipid bilayers that entrap an aqueous core. In this work, Lambert et al. combined DOTAP and sodium cholate and cholesterol as a stabiliser with 30% ethanol to create surfactant-ethanol-cholesterol-osomes (SECosomes), a type of liposome with high penetration ability. This system transmitted siRNA into a skin-humanised mouse model of psoriasis to silence the expression of human beta-defensin 2 and, also, an antimicrobial peptide that is overexpressed in psoriatic skin [134]. Altering the cholesterol composition and replacing sodium cholate with 1,2-dioleoyl-sn-glycero-3-phosphoethanolamine (DOPE), they obtained a modified SECosome called DDC642 that was capable of delivering pre-miR-145 or anti-miR-203 oligonucleotides in melanocytes and keratinocytes, respectively, to modulate their target mRNA levels (Figure 4b). In addition, DDC642 complexes repress target genes in the epidermis of human 3D psoriasis skin models without targeting the dermis or circulatory system [134]. This is a proof-of-concept that elastic liposomes could be used as a topical delivery system for miRNA therapeutics in psoriasis.

6. Conclusions, Limitations and Future Perspectives

miRNA profiling studies have identified that skin immune diseases have specific miRNA signatures and that miRNAs are playing pathogenic roles when dysregulated. Studying the effects of these dysregulated miRNAs can enhance the understanding of the etiopathogenesis of psoriasis, cutaneous lupus and atopic dermatitis. Moreover, the fact that they also are dysregulated in circulation makes them candidate biomarkers for differential diagnosis, a disease severity/prognosis assessment, and they may also be able to monitor the treatment response, which is of crucial importance to patients that may be refractory to standard treatments. Since they play a role in pathogenesis, they have the potential to be used as therapeutic targets. In vivo studies support that miRNAs are able to ameliorate skin disorders after being topically or intradermally administered. Nanoparticle encapsulations may help in their delivery, degradation avoidance and, specifically, cell uptake. MicroRNA-based therapy may be able to treat refractory dermatologic immune conditions more effectively, avoiding current treatment side effects. Although many preclinical studies have been conducted exploring the role of miRNAs in autoimmune skin pathogenesis and their application as therapy, at the moment, there is only one miRNA at the clinical trial stage. Their easy degradation, possible off-target effects and toxicity need to be avoided to generate an effective, directed and safe microRNA-based therapy. Moreover, their uses as biomarkers in clinic are still conditioned by the fact that there may be variability in detection assays and nonstandardised normalisation and data statistical analysis. Therefore, further investigation needs to be performed to be able to understand their role in pathogenesis and demonstrate their application both as promising biomarkers and as an effective treatment for autoimmune dermatological conditions.

Author Contributions: Conceptualisation, C.S. and J.C.-H.; methodology, S.D. and C.S.; investigation, S.D., C.S., T.M. and B.F.; resources, J.C.-H.; data curation, S.D., C.S. and J.C.-H.; writing—original draft preparation, S.D.; writing—review and editing, C.S. and J.C.-H.; visualisation, S.D., C.S., T.M., B.F. and J.C.-H.; supervision, C.S. and J.C.-H.; project administration, C.S. and J.C.-H. and funding acquisition, J.C.-H. All authors have read and agreed to the published version of the manuscript.

Funding: This work was funded by the Instituto de Salud Carlos III (Spanish Government, PI15/02145), Catalan Lupus Foundation and A.Bosch Foundation.

Acknowledgments: We would like to acknowledge the Instituto de Salud Carlos III (Spain Government, PI15/02145), Catalan Lupus Foundation and A.Bosch Foundation for their financial support.

Conflicts of Interest: The authors declare no conflict of interest.

References

1. Ambros, V. The functions of animal microRNAs. *Nature* **2004**, *431*, 350–355. [CrossRef]
2. Baek, D.; Villén, J.; Shin, C.; Camargo, F.D.; Gygi, S.P.; Bartel, D.P. The impact of microRNAs on protein output. *Nature* **2008**, *455*, 64–71. [CrossRef] [PubMed]
3. Bartel, D.P. MicroRNAs: Genomics, biogenesis, mechanism, and function. *Cell* **2004**, *116*, 281–297. [CrossRef]
4. Vickers, K.C.; Palmisano, B.T.; Shoucri, B.M.; Shamburek, R.D.; Remaley, A.T. MicroRNAs are transported in plasma and delivered to recipient cells by high-density. *Nat. Cell Biol.* **2011**, *13*, 423–433. [CrossRef]
5. John, B.; Enright, A.J.; Aravin, A.; Tuschl, T.; Sander, C.; Marks, D.S. Human MicroRNA targets. *PLoS Biol.* **2004**, *2*, e363. [CrossRef] [PubMed]
6. Friedman, R.C.; Farh, K.K.; Burge, C.B.; Bartel, D.P. Most mammalian mRNAs are conserved targets of microRNAs. *Genome Res.* **2009**, *19*, 92–105. [CrossRef] [PubMed]
7. Vasudevan, S.; Tong, Y.; Steitz, J.A. Cell-cycle control of microRNA-mediated translation regulation. *Cell Cycle* **2008**, *7*, 1545–1549. [CrossRef] [PubMed]
8. Leung, A.K.L.; Sharp, P.A. Function and localization of microRNAs in mammalian cells. In *Cold Spring Harbor Symposia on Quantitative Biology*; Cold Spring Harbor Laboratory Press: Cold Spring Harbor, NY, USA, 2006; Volume 71, pp. 29–38.
9. Soifer, H.S.; Rossi, J.J.; Saetrom, P. MicroRNAs in disease and potential therapeutic applications. *Mol. Ther.* **2007**, *15*, 2070–2079. [CrossRef]

10. Andl, T.; Murchison, E.P.; Liu, F.; Zhang, Y.; Yunta-Gonzalez, M.; Tobias, J.W.; Andl, C.D.; Seykora, J.T.; Hannon, G.J.; Millar, S.E. The miRNA-processing enzyme dicer is essential for the morphogenesis and maintenance of hair follicles. *Curr. Biol.* **2006**, *16*, 1041–1049. [CrossRef]
11. Yi, R.; O'Carroll, D.; Pasolli, H.A.; Zhang, Z.; Dietrich, F.S.; Tarakhovsky, A.; Fuchs, E. Morphogenesis in skin is governed by discrete sets of differentially expressed miRNAs. *Nat. Genet.* **2006**, *38*, 356–362. [CrossRef]
12. Yi, R.; Fuchs, E. MicroRNA-mediated control in the skin. *Cell Death Differ.* **2010**, *17*, 229–235. [CrossRef] [PubMed]
13. Neagu, M.; Constantin, C.; Cretoiu, S.M.; Zurac, S. miRNAs in the Diagnosis and Prognosis of Skin Cancer. *Front. Cell Dev. Biol.* **2020**, *8*, 71. [CrossRef] [PubMed]
14. Sonkoly, E.; Wei, T.; Janson, P.C.; Sääf, A.; Lundeberg, L.; Tengvall-Linder, M.; Norstedt, G.; Alenius, H.; Homey, B.; Scheynius, A.; et al. MicroRNAs: Novel regulators involved in the pathogenesis of psoriasis? *PLoS ONE* **2007**, *2*, e610. [CrossRef]
15. Sonkoly, E.; Janson, P.; Majuri, M.L.; Savinko, T.; Fyhrquist, N.; Eidsmo, L.; Xu, N.; Meisgen, F.; Wei, T.; Bradley, M.; et al. MiR-155 is overexpressed in patients with atopic dermatitis and modulates T-cell proliferative responses by targeting cytotoxic T lymphocyte-associated antigen 4. *J. Allergy Clin. Immunol.* **2010**, *126*, 581–920. [CrossRef] [PubMed]
16. Solé, C.; Domingo, S.; Ferrer, B.; Moliné, T.; Ordi-Ros, J.; Cortés-Hernández, J. MicroRNA Expression Profiling Identifies miR-31 and miR-485-3p as Regulators in the Pathogenesis of Discoid Cutaneous Lupus. *J. Investig. Dermatol.* **2019**, *139*, 51–61. [CrossRef] [PubMed]
17. Parisi, R.; Symmons, D.P.; Griffiths, C.E.; Ashcroft, D.M. Identification and Management of Psoriasis and Associated ComorbidiTy (IMPACT) project team. Global epidemiology of psoriasis: A systematic review of incidence and prevalence. *J. Investig. Dermatol.* **2013**, *133*, 377–385. [CrossRef]
18. Lowes, M.A.; Suárez-Fariñas, M.; Krueger, J.G. Immunology of psoriasis. *Annu. Rev. Immunol.* **2014**, *32*, 227–255. [CrossRef]
19. Xu, Y.; Ji, Y.; Lan, X.; Gao, X.; Chen, H.D.; Geng, L. miR-203 contributes to IL-17-induced VEGF secretion by targeting SOCS3 in keratinocytes. *Mol. Med. Rep.* **2017**, *16*, 8989–8996. [CrossRef]
20. Primo, M.N.; Bak, R.O.; Schibler, B.; Mikkelsen, J.G. Regulation of pro-inflammatory cytokines TNFα and IL24 by microRNA-203 in primary keratinocytes. *Cytokine* **2012**, *60*, 741–748. [CrossRef]
21. Wei, T.; Xu, N.; Meisgen, F.; Ståhle, M.; Sonkoly, E.; Pivarcsi, A. Interleukin-8 is regulated by miR-203 at the posttranscriptional level in primary human keratinocytes. *Eur. J. Dermatol.* **2013**, *19*, 1997.
22. Xiao, Y.; Wang, H.; Wang, C.; Zeng, B.; Tang, X.; Zhang, Y.; Peng, Y.; Luo, M.; Huang, P.; Yang, Z. miR-203 promotes HaCaT cell overproliferation through targeting LXR-α and PPAR-γ. *Cell Cycle* **2020**, *19*, 1928–1940. [CrossRef] [PubMed]
23. Luan, L.; Shi, J.; Yu, Z.; Andl, T. The major miR-31 target genes STK40 and LATS2 and their implications in the regulation of keratinocyte growth and hair differentiation. *Exp. Dermatol.* **2017**, *26*, 497–504. [CrossRef] [PubMed]
24. Borska, L.; Andrys, C.; Chmelarova, M.; Kovarikova, H.; Krejsek, J.; Hamakova, K.; Beranek, M.; Palicka, V.; Kremlacek, J.; Borsky, P.; et al. Roles of miR-31 and endothelin-1 in psoriasis vulgaris: Pathophysiological functions and potential biomarkers. *Physiol. Res.* **2017**, *66*, 987–992. [CrossRef] [PubMed]
25. Yan, S.; Xu, Z.; Lou, F.; Zhang, L.; Ke, F.; Bai, J.; Liu, Z.; Liu, J.; Wang, H.; Zhu, H.; et al. NF-κB-induced microRNA-31 promotes epidermal hyperplasia by repressing protein phosphatase 6 in psoriasis. *Nat. Commun.* **2015**, *6*, 7652. [CrossRef] [PubMed]
26. Xu, N.; Meisgen, F.; Butler, L.M.; Han, G.; Wang, X.J.; Söderberg-Nauclér, C.; Ståhle, M.; Pivarcsi, A.; Sonkoly, E. MicroRNA-31 is overexpressed in psoriasis and modulates inflammatory cytokine and chemokine production in keratinocytes via targeting serine/threonine kinase 40. *J. Immunol.* **2013**, *190*, 678–688. [CrossRef] [PubMed]
27. Wang, Q.; Chang, W.; Yang, X.; Cheng, Y.; Zhao, X.; Zhou, L.; Li, J.; Li, J.; Zhang, K. Levels of miR-31 and its target genes in dermal mesenchymal cells of patients with psoriasis. *Int. J. Dermatol.* **2019**, *58*, 198–204. [CrossRef] [PubMed]
28. Xia, P.; Fang, X.; Zhang, Z.H.; Huang, Q.; Yan, K.X.; Kang, K.F.; Han, L.; Zheng, Z.Z. Dysregulation of miRNA146a versus IRAK1 induces IL-17 persistence in the psoriatic skin lesions. *Immunol. Lett.* **2012**, *148*, 151–162. [CrossRef] [PubMed]

29. Crone, S.G.; Jacobsen, A.; Federspiel, B.; Bardram, L.; Krogh, A.; Lund, A.H.; Friis-Hansen, L. microRNA-146a inhibits G protein-coupled receptor-mediated activation of NF-kappaB by targeting CARD10 and COPS8 in gastric cancer. *Mol. Cancer* **2012**, *11*, 71. [CrossRef]
30. Hung, P.S.; Liu, C.J.; Chou, C.S.; Kao, S.Y.; Yang, C.C.; Chang, K.W.; Chiu, T.H.; Lin, S.C. miR-146a enhances the oncogenicity of oral carcinoma by concomitant targeting of the IRAK1, TRAF6 and NUMB genes. *PLoS ONE* **2013**, *8*, e79926. [CrossRef]
31. Rebane, A.; Runnel, T.; Aab, A.; Maslovskaja, J.; Rückert, B.; Zimmermann, M.; Plaas, M.; Kärner, J.; Treis, A.; Pihlap, M.; et al. MicroRNA-146a alleviates chronic skin inflammation in atopic dermatitis through suppression of innate immune responses in keratinocytes. *J. Allergy Clin. Immunol.* **2014**, *134*, 836–847. [CrossRef]
32. García-Rodríguez, S.; Arias-Santiago, S.; Blasco-Morente, G.; Orgaz-Molina, J.; Rosal-Vela, A.; Navarro, P.; Magro-Checa, C.; Martínez-López, A.; Ruiz, J.C.; Raya, E.; et al. Increased expression of microRNA-155 in peripheral blood mononuclear cells from psoriasis patients is related to disease activity. *J. Eur. Acad. Dermatol. Venereol.* **2017**, *31*, 312–322. [CrossRef] [PubMed]
33. El-Komy, M.; Amin, I.; El-Hawary, M.S.; Saadi, D.; Shaker, O. Upregulation of the miRNA-155, miRNA-210, and miRNA-20b in psoriasis patients and their relation to IL-17. *Int. J. Immunopathol. Pharmacol.* **2020**, *34*, 2058738420933742. [CrossRef] [PubMed]
34. Xu, L.; Leng, H.; Shi, X.; Ji, J.; Fu, J.; Leng, H. MiR-155 promotes cell proliferation and inhibits apoptosis by PTEN signaling pathway in the psoriasis. *Biomed. Pharmacother.* **2017**, *90*, 524–530. [CrossRef] [PubMed]
35. Soonthornchai, W.; Tangtanatakul, P.; Meephansan, J.; Ruchusatsawat, K.; Reantragoon, R.; Hirankarn, N.; Wongpiyabovorn, J. Down-regulation of miR-155 after treatment with narrow-band UVB and methotrexate associates with apoptosis of keratinocytes in psoriasis. *Asian Pac. J. Allergy Immunol.* **2019**. [CrossRef]
36. Luo, Q.; Zeng, J.; Li, W.; Lin, L.; Zhou, X.; Tian, X.; Liu, W.; Zhang, L.; Zhang, X. Silencing of miR-155 suppresses inflammatory responses in psoriasis through inflammasome NLRP3 regulation. *Int. J. Mol. Med.* **2018**, *42*, 1086–1095. [CrossRef] [PubMed]
37. Wang, H.; Zhang, Y.; Luomei, J.; Huang, P.; Zhou, R.; Peng, Y. The miR-155/GATA3/IL37 axis modulates the production of proinflammatory cytokines upon TNF-α stimulation to affect psoriasis development. *Exp. Dermatol.* **2020**. [CrossRef]
38. Hou, R.X.; Liu, R.F.; Zhao, X.C.; Jia, Y.R.; An, P.; Hao, Z.P.; Li, J.Q.; Li, X.H.; Yin, G.H.; Zhang, K.M. Increased miR-155-5p expression in dermal mesenchymal stem cells of psoriatic patients: Comparing the microRNA expression profile by microarray. *Genet Mol. Res.* **2016**, *15*. [CrossRef]
39. Meisgen, F.; Xu, N.; Wei, T.; Janson, P.C.; Obad, S.; Broom, O.; Nagy, N.; Kauppinen, S.; Kemény, L.; Ståhle, M.; et al. MiR-21 is up-regulated in psoriasis and suppresses T cell apoptosis. *Exp. Dermatol.* **2012**, *21*, 312–314. [CrossRef]
40. Jia, H.Y.; Zhang, K.; Lu, W.J.; Xu, G.W.; Zhang, J.F.; Tang, Z.L. LncRNA MEG3 influences the proliferation and apoptosis of psoriasis epidermal cells by targeting miR-21/caspase-8. *BMC Mol. Cell. Biol.* **2019**, *20*, 46. [CrossRef]
41. Yang, C.; Luo, L.; Bai, X.; Shen, K.; Liu, K.; Wang, J.; Hu, D. Highly-expressed micoRNA-21 in adipose derived stem cell exosomes can enhance the migration and proliferation of the HaCaT cells by increasing the MMP-9 expression through the PI3K/AKT pathway. *Arch. Biochem. Biophys.* **2020**, *681*, 108259. [CrossRef]
42. Degueurce, G.; D'Errico, I.; Pich, C.; Ibberson, M.; Schütz, F.; Montagner, A.; Sgandurra, M.; Mury, L.; Jafari, P.; Boda, A.; et al. Identification of a novel PPARβ/δ/miR-21-3p axis in UV-induced skin inflammation. *EMBO Mol. Med.* **2016**, *8*, 919–936. [CrossRef] [PubMed]
43. Xu, N.; Brodin, P.; Wei, T.; Meisgen, F.; Eidsmo, L.; Nagy, N.; Kemeny, L.; Stahle, M.; Sonkoly, E.; Pivarcsi, A. MiR-125b, a microRNA downregulated in psoriasis, modulates keratinocyte proliferation by targeting FGFR2. *J. Investig. Dermatol.* **2011**, *131*, 1521–1529. [CrossRef] [PubMed]
44. Ichihara, A.; Jinnin, M.; Yamane, K.; Fujisawa, A.; Sakai, K.; Masuguchi, S.; Fukushima, S.; Maruo, K.; Ihn, H. microRNA-mediated keratinocyte hyperproliferatio in psoriasis vulgaris. *Br. J. Dermatol.* **2011**, *165*, 1003–1010. [CrossRef] [PubMed]
45. Jiang, M.; Sun, Z.; Dang, E.; Li, B.; Fang, H.; Li, J.; Gao, L.; Zhang, K.; Wang, G. TGFβ/SMAD/microRNA-486-3p Signaling Axis Mediates Keratin 17 Expression and Keratinocyte Hyperproliferation in Psoriasis. *J. Investig. Dermatol.* **2017**, *137*, 2177–2186. [CrossRef]

46. Feng, S.J.; Chu, R.Q.; Ma, J.; Wang, Z.X.; Zhang, G.J.; Yang, X.F.; Song, Z.; Ma, Y.Y. MicroRNA138 regulates keratin 17 protein expression to affect HaCaT cell proliferation and apoptosis by targeting hTERT in psoriasis vulgaris. *Biomed. Pharmacother.* **2017**, *85*, 169–176. [CrossRef]
47. Wang, C.; Zong, J.; Li, Y.; Wang, X.; Du, W.; Li, L. MiR-744-3p regulates keratinocyte proliferation and differentiation via targeting KLLN in psoriasis. *Exp. Dermatol.* **2019**, *28*, 283–291. [CrossRef]
48. Li, Y.; Su, J.; Li, F.; Chen, X.; Zhang, G. MiR-150 regulates human keratinocyte proliferation in hypoxic conditions through targeting HIF-1α and VEGFA: Implications for psoriasis treatment. *PLoS ONE* **2017**, *12*, e0175459. [CrossRef]
49. A, R.; Yu, P.; Hao, S.; Li, Y. MiR-876-5p suppresses cell proliferation by targeting Angiopoietin-1 in the psoriasis. *Biomed. Pharmacother.* **2018**, *103*, 1163–1169. [CrossRef]
50. Liu, T.; Zhang, X.; Wang, Y. miR-183-3p suppresses proliferation and migration of keratinocyte in psoriasis by inhibiting GAB1. *Hereditas* **2020**, *157*, 28. [CrossRef]
51. Zhao, X.; Li, R.; Qiao, M.; Yan, J.; Sun, Q. MiR-548a-3p Promotes Keratinocyte Proliferation Targeting PPP3R1 after Being Induced by IL-22. *Inflammation* **2018**, *41*, 496–504. [CrossRef]
52. Zhu, H.; Hou, L.; Liu, J.; Li, Z. MiR-217 is down-regulated in psoriasis and promotes keratinocyte differentiation via targeting GRHL2. *Biochem. Biophys. Res. Commun.* **2016**, *471*, 169–176. [CrossRef] [PubMed]
53. Chowdhari, S.; Sardana, K.; Saini, N. miR-4516, a microRNA downregulated in psoriasis inhibits keratinocyte motility by targeting fibronectin/integrin α9 signaling. *Biochim. Biophys. Acta Mol. Basis Dis.* **2017**, *1863*, 3142–3152. [CrossRef]
54. Yu, X.; An, J.; Hua, Y.; Li, Z.; Yan, N.; Fan, W.; Su, C. MicroRNA-194 regulates keratinocyte proliferation and differentiation by targeting Grainyhead-like 2 in psoriasis. *Pathol. Res. Pract.* **2017**, *213*, 89–97. [CrossRef] [PubMed]
55. Tang, L.; He, S.; Zhu, Y.; Feng, B.; Su, Z.; Liu, B.; Xu, F.; Wang, X.; Liu, H.; Chutian, L.; et al. Downregulated miR-187 contributes to the keratinocytes hyperproliferation in psoriasis. *J. Cell. Physiol.* **2019**, *234*, 3661–3674. [CrossRef] [PubMed]
56. Shen, H.; Tian, Y.; Yao, X.; Liu, W.; Zhang, Y.; Yang, Z. MiR-99a inhibits keratinocyte proliferation by targeting Frizzled-5 (FZD5) / FZD8 through β-catenin signaling in psoriasis. *Pharmazie* **2017**, *72*, 461–467.
57. Xiong, Y.; Chen, H.; Liu, L.; Lu, L.; Wang, Z.; Tian, F.; Zhao, Y. microRNA-130a Promotes Human Keratinocyte Viability and Migration and Inhibits Apoptosis Through Direct Regulation of STK40-Mediated NF-κB Pathway and Indirect Regulation of SOX9-Meditated JNK/MAPK Pathway: A Potential Role in Psoriasis. *DNA Cell Biol.* **2017**, *36*, 219–226. [CrossRef]
58. Jiang, M.; Ma, W.; Gao, Y.; Jia, K.; Zhang, Y.; Liu, H.; Sun, Q. IL-22-induced miR-122-5p promotes keratinocyte proliferation by targeting Sprouty2. *Exp. Dermatol.* **2017**, *26*, 368–374. [CrossRef]
59. Feng, S.; Wang, L.; Liu, W.; Zhong, Y.; Xu, S. MiR-126 correlates with increased disease severity and promotes keratinocytes proliferation and inflammation while suppresses cells' apoptosis in psoriasis. *J. Clin. Lab Anal.* **2018**, *32*, e22588. [CrossRef]
60. Yan, J.J.; Qiao, M.; Li, R.H.; Zhao, X.T.; Wang, X.Y.; Sun, Q. Downregulation of miR-145-5p contributes to hyperproliferation of keratinocytes and skin inflammation in psoriasis. *Br. J. Dermatol.* **2019**, *180*, 365–372. [CrossRef]
61. Zhang, W.; Yi, X.; An, Y.; Guo, S.; Li, S.; Song, P.; Chang, Y.; Zhang, S.; Gao, T.; Wang, G.; et al. MicroRNA-17-92 cluster promotes the proliferation and the chemokine production of keratinocytes: Implication for the pathogenesis of psoriasis. *Cell Death Dis.* **2018**, *9*, 567. [CrossRef]
62. Wang, Y.; Yu, X.; Wang, L.; Ma, W.; Sun, Q. miR-320b Is Down-Regulated in Psoriasis and Modulates Keratinocyte Proliferation by Targeting AKT3. *Inflammation* **2018**, *41*, 2160–2170. [CrossRef] [PubMed]
63. Xiao, Y.; Wang, C.; Zeng, B.; Tang, X.; Zhang, Y.; Xiang, L.; Mi, L.; Pan, Y.; Wang, H.; Yang, Z. miR124-3p/FGFR2 axis inhibits human keratinocyte proliferation and migration and improve the inflammatory microenvironment in psoriasis. *Mol. Immunol.* **2020**, *122*, 89–98. [CrossRef] [PubMed]
64. Roberts, J.C.; Warren, R.B.; Griffiths, C.E.; Ross, K. Expression of microRNA-184 in keratinocytes represses argonaute 2. *J. Cell. Physiol.* **2013**, *228*, 2314–2323. [CrossRef] [PubMed]
65. Zibert, J.R.; Løvendorf, M.B.; Litman, T.; Olsen, J.; Kaczkowski, B.; Skov, L. MicroRNAs and potential target interactions in psoriasis. *J. Dermatol. Sci.* **2010**, *58*, 177–185. [CrossRef]

66. Feng, C.; Bai, M.; Yu, N.Z.; Wang, X.J.; Liu, Z. MicroRNA-181b negatively regulates the proliferation of human epidermal keratinocytes in psoriasis through targeting TLR4. *J. Cell. Mol. Med.* **2017**, *21*, 278–285. [CrossRef]
67. Srivastava, A.; Pasquali, L.; Pivarcsi, A.; Sonkoly, E. MiR-1307 is upregulated in psoriasis keratinocytes and promotes keratinocyte inflammatory response. In Proceedings of the 49th Annual ESDR Meeting, Bordeaux, France, 18 September 2019.
68. Jiang, M.; Fang, H.; Dang, E.; Zhang, J.; Qiao, P.; Yu, C.; Yang, A.; Wang, G. Small extracellular vesicles containing miR-381-3p from keratinocytes promotes Th1/Th17 polarization in psoriasis. *J. Investig. Dermatol.* **2020**, *S0022-202X*, 31938–31942. [CrossRef]
69. Zhao, M.; Wang, L.T.; Liang, G.P.; Zhan, P.; Deng, X.J.; Tang, Q.; Zhai, H.; Chang, C.C.; Su, Y.W.; Lu, Q.J. Up-regulation of microRNA-210 induces immune dysfunction via targeting FOXP3 in CD4(+) T cells of psoriasis vulgaris. *Clin. Immunol.* **2014**, *150*, 22–30. [CrossRef]
70. Fu, D.; Yu, W.; Li, M.; Wang, H.; Liu, D.; Song, X.; Li, Z.; Tian, Z. MicroRNA-138 regulates the balance of Th1/Th2 via targeting RUNX3 in psoriasis. *Immunol. Lett.* **2015**, *166*, 55–62. [CrossRef]
71. Lou, C.; Xiao, M.; Cheng, S.; Lu, X.; Jia, S.; Ren, Y.; Li, Z. MiR-485-3p and miR-485-5p suppress breast cancer cell metastasis by inhibiting PGC-1α expression. *Cell Death Dis.* **2016**, *7*, e2159. [CrossRef]
72. Weidinger, S.; Beck, L.A.; Bieber, T.; Kabashima, K.; Irvine, A.D. Atopic dermatitis. *Nat. Rev. Dis. Primers* **2018**, *4*, 1. [CrossRef]
73. Nutten, S. Atopic dermatitis: Global epidemiology and risk factors. *Ann. Nutr. Metab.* **2015**, *66*, 8–16. [CrossRef] [PubMed]
74. Liu, F.T.; Goodarzi, H.; Chen, H.Y. IgE, mast cells, and eosinophils in atopic dermatitis. *Clin. Rev. Allergy Immunol.* **2011**, *41*, 298–310. [CrossRef] [PubMed]
75. Vaher, H.; Runnel, T.; Urgard, E.; Aab, A.; Carreras Badosa, G.; Maslovskaja, J.; Abram, K.; Raam, L.; Kaldvee, B.; Annilo, T.; et al. miR-10a-5p is increased in atopic dermatitis and has capacity to inhibit keratinocyte proliferation. *Allergy* **2019**, *74*, 2146–2156. [CrossRef] [PubMed]
76. Gu, C.; Li, Y.; Wu, J.; Xu, J. IFN-γ-induced microRNA-29b up-regulation contributes to keratinocyte apoptosis in atopic dermatitis through inhibiting Bcl2L2. *Int. J. Clin. Exp. Pathol.* **2017**, *10*, 10117–10126.
77. Jia, H.Z.; Liu, S.L.; Zou, Y.F.; Chen, X.F.; Yu, L.; Wan, J.; Zhang, H.Y.; Chen, Q.; Xiong, Y.; Yu, B.; et al. MicroRNA-223 is involved in the pathogenesis of atopic dermatitis by affecting histamine-N-methyltransferase. *Cell. Mol. Biol.* **2018**, *64*, 103–107. [CrossRef]
78. Chen, X.F.; Zhang, L.J.; Zhang, J.; Dou, X.; Shao, Y.; Jia, X.J.; Zhang, W.; Yu, B. MiR-151a is involved in the pathogenesis of atopic dermatitis by regulating interleukin-12 receptor β2. *Exp. Dermatol.* **2018**, *27*, 427–432. [CrossRef]
79. Jia, Q.N.; Zeng, Y.P. Rapamycin blocks the IL-13-induced deficiency of Epidermal Barrier Related Proteins via upregulation of miR-143 in HaCaT Keratinocytes. *Int. J. Med. Sci.* **2020**, *17*, 2087–2094. [CrossRef]
80. Kuhn, A.; Landmann, A. The classification and diagnosis of cutaneous lupus erythematosus. *J. Autoimmun.* **2014**, *48*, 14–19. [CrossRef]
81. Durosaro, O.; Davis, M.; Reed, K.B.; Rohlinger, A.L. Incidence of cutaneous lupus erythematosus, 1965-2005: A population-based study. *Arch. Dermatol.* **2009**, *145*, 249–253. [CrossRef]
82. Achtman, J.C.; Werth, V.P. Pathophysiology of cutaneous lupus erythematosus. *Arthritis Res. Ther.* **2015**, *17*, 182. [CrossRef]
83. Dinulovic, I.; Furrer, R.; Di Fulvio, S.; Ferry, A.; Beer, M.; Handschin, C. PGC-1α modulates necrosis, inflammatory response, and fibrotic tissue formation in injured skeletal muscle. *Skelet. Muscle* **2016**, *6*, 38. [CrossRef] [PubMed]
84. Ma, L.; Xue, H.B.; Wang, F.; Shu, C.M.; Zhang, J.H. MicroRNA-155 may be involved in the pathogenesis of atopic dermatitis by modulating the differentiation and function of T helper type 17 (Th17) cells. *Clin. Exp. Immunol.* **2015**, *181*, 142–149. [CrossRef] [PubMed]
85. Vennegaard, M.T.; Bonefeld, C.M.; Hagedorn, P.H.; Bangsgaard, N.; Løvendorf, M.B.; Ødum, N.; Woetmann, A.; Geisler, C.; Skov, L. Allergic contact dermatitis induces upregulation of identical microRNAs in humans and mice. *Contact Dermat.* **2012**, *67*, 298–305. [CrossRef] [PubMed]
86. Wang, X.; Chen, Y.; Yuan, W.; Yao, L.; Wang, S.; Jia, Z.; Wu, P.; Li, L.; Wei, P.; Wang, X.; et al. MicroRNA-155-5p is a key regulator of allergic inflammation, modulating the epithelial barrier by targeting PKIα. *Cell Death Dis.* **2019**, *10*, 884. [CrossRef] [PubMed]

87. Schwingen, J.; Kaplan, M.; Kurschus, F.C. Current concepts in inflammatory skin diseases evolved by transcriptome analysis: In-depth analysis of atopic dermatitits and psoriasis. *Int. J. Mol. Sci.* **2020**, *21*, 699. [CrossRef]
88. Choy, D.F.; Hsu, D.K.; Seshasayee, D.; Fung, M.A.; Modrusan, Z.; Martin, F.; Liu, F.; Arron, J.R. Comparative transcriptomic analyses of atopic dermatitis and psoriasis reveal shared neutrophilic inflammation. *J. Allergy Clin. Immunol.* **2012**, *130*, 1335–1343. [CrossRef]
89. Jabbari, A.; Suárez-Fariñas, M.; Fuentes-Duculan, J.; Gonzalez, J.; Cueto, I.; Franks, A.G.; Krueger, J.G. Dominant Th1 and minimal Th17 skewing in discoid lupus revealed by transcriptomic comparison with psoriasis. *J. Investig. Dermatol.* **2014**, *134*, 87–95. [CrossRef]
90. Ludwig, N.; Leidinger, P.; Becker, K.; Backes, C.; Fehlmann, T.; Pallasch, C.; Rheinheimer, S.; Meder, B.; Stähler, C.; Meese, E.; et al. Distribution of miRNA expression across human tissues. *Nucleic Acids Res.* **2016**, *44*, 3865–3877. [CrossRef]
91. Ciesla, M.; Skrzypek, K.; Kozakowska, M.; Loboda, A.; Jozkowicz, A.; Dulak, J. MicroRNAs as biomarkers of disease onset. *Anal. Bioanal. Chem.* **2011**, *401*, 2051–2061. [CrossRef]
92. Løvendorf, M.B.; Zibert, J.R.; Gyldenløve, M.; Røpke, M.A.; Skov, L. MicroRNA-223 and miR-143 are important systemic biomarkers for disease activity in psoriasis. *J. Dermatol. Sci.* **2014**, *75*, 133–139. [CrossRef]
93. Guo, S.; Zhang, W.; Wei, C.; Wang, L.; Zhu, G.; Shi, Q.; Li, S.; Ge, R.; Li, K.; Gao, L.; et al. Serum and skin levels of miR-369-3p in patients with psoriasis and their correlation with disease severity. *Eur. J. Dermatol.* **2013**, *23*, 608–613. [CrossRef] [PubMed]
94. Tsuru, Y.; Jinnin, M.; Ichihara, A.; Fujisawa, A.; Moriya, C.; Sakai, K.; Fukushima, S.; Ihn, H. miR-424 levels in hair shaft are increased in psoriatic patients. *J. Dermatol.* **2014**, *41*, 382–385. [CrossRef] [PubMed]
95. Hirao, H.; Jinnin, M.; Ichihara, A.; Fujisawa, A.; Makino, K.; Kajihara, I.; Sakai, K.; Fukushima, S.; Inoue, Y.; Ihn, H. Detection of hair root miR-19a as a novel diagnostic marker for psoriasis. *Eur. J. Dermatol.* **2013**, *23*, 807–811. [CrossRef] [PubMed]
96. Chatzikyriakidou, A.; Voulgari, P.V.; Georgiou, I.; Drosos, A.A. The role of microRNA-146a (miR-146a) and its target IL-1R-associated kinase (IRAK1) in psoriatic arthritis susceptibility. *Scand J. Immunol.* **2010**, *71*, 382–385. [CrossRef]
97. Wang, G.; Tam, L.S.; Li, E.K.; Kwan, B.C.H.; Chow, K.M.; Luk, C.C.W.; Li, P.K.T.; Szeto, C.C. Serum and urinary free microRNA level in patients with systemic lupus erythematosus. *Lupus* **2011**, *20*, 493–500. [CrossRef]
98. Méndez-Flores, S.; Furuzawa-Carballeda, J.; Hernández-Molina, G.; Ramírez-Martinez, G.; Regino-Zamarripa, N.E.; Ortiz-Quintero, B.; Jiménez-Alvarez, L.; Cruz-Lagunas, A.; Zúñiga, J. MicroRNA Expression in Cutaneous Lupus: A New Window to Understand Its Pathogenesis. *Mediat. Inflamm.* **2019**, *2019*, 5049245. [CrossRef]
99. Hashad, D.; Abdelmagid, M.; Elsherif, S. microRNA146a expression in lupus patients with and without renal complications. *J. Clin. Lab Anal.* **2012**, *26*, 35–40. [CrossRef]
100. Lv, Y.; Qi, R.; Xu, J.; Di, Z.; Zheng, H.; Huo, W.; Zhang, L.; Chen, H.; Gao, X. Profiling of serum and urinary microRNAs in children with atopic dermatitis. *PLoS ONE* **2014**, *9*, e115448. [CrossRef]
101. Meng, L.; Li, M.; Gao, Z.; Ren, H.; Chen, J.; Liu, X.; Cai, Q.; Jiang, L.; Ren, X.; Yu, Q.; et al. Possible role of hsa-miR-194-5p, via regulation of HS3ST2, in the pathogenesis of atopic dermatitis in children. *Eur. J. Dermatol.* **2019**, *29*, 603–613. [CrossRef]
102. Spuls, P.I.; Lecluse, L.; Poulsen, M.; Bos, J.; Stern, R.S.; Nijsten, T. How good are clinical severity and outcome measures for psoriasis?: Quantitative evaluation in a systematic review. *J. Investig. Dermatol.* **2010**, *130*, 933–943. [CrossRef]
103. Yang, Z.; Zeng, B.; Tang, X.; Wang, H.; Wang, C.; Yan, Z.; Huang, P.; Pan, Y.; Xu, B. MicroRNA-146a and miR-99a are potential biomarkers for disease activity and clinical efficacy assessment in psoriasis patients treated with traditional Chinese medicine. *J. Ethnopharmacol.* **2016**, *194*, 727–732. [CrossRef] [PubMed]
104. Duan, Y.; Zou, J.; Mao, J.; Guo, D.; Wu, M.; Xu, N.; Zhou, J.; Zhang, Y.; Guo, W.; Jin, W. Plasma miR-126 expression correlates with risk and severity of psoriasis and its high level at baseline predicts worse response to Tripterygium wilfordii Hook F in combination with acitretin. *Biomed. Pharmacother.* **2019**, *115*, 108761. [CrossRef] [PubMed]

105. Magenta, A.; D'Agostino, M.; Sileno, S.; Di Vito, L.; Uras, C.; Abeni, D.; Martino, F.; Barillà, F.; Madonna, S.; Albanesi, C.; et al. The Oxidative Stress-Induced miR-200c Is Upregulated in Psoriasis and Correlates with Disease Severity and Determinants of Cardiovascular Risk. *Oxid. Med. Cell. Longev.* **2019**, *2019*, 8061901. [CrossRef] [PubMed]
106. Deng, X.; Su, Y.; Wu, H.; Wu, R.; Zhang, P.; Dai, Y.; Chan, T.-M.; Zhao, M.; Lu, Q. The role of microRNAs in autoinmune diseases with skin involvement. *Scand. J. Immunol.* **2015**, *81*, 153–165. [CrossRef]
107. Chicharro, P.; Rodriguez-Jiménez, P.; Llamas-Velasco, M.; Montes, N.; Sanz-García, A.; Cibrian, D.; Vara, A.; Gómez, M.J.; Jiménez-Fernández, M.; Martínez-Fleta, P.; et al. Expression of miR-135b in Psoriatic Skin and Its Association with Disease Improvement. *Cells* **2020**, *9*, 1603. [CrossRef]
108. Albrecht, J.; Taylor, L.; Berlin, J.A.; Dulay, S.; Ang, S.; Fakharzadeh, S.; Kantor, J.; Kim, E.; Militello, G.; McGinnis, K.; et al. The CLASI (Cutaneous Lupus Erythematosus Disease Area and Severity Index): An outcome instrument for cutaneous lupus erythematosus. *J. Investig. Dermatol.* **2005**, *125*, 889–894. [CrossRef]
109. Zhou, H.; Hasni, S.A.; Perez, P.; Tandon, M.; Jang, S.I.; Zheng, C.; Kopp, J.B.; Austin, H., 3rd; Balow, J.E.; Alevizos, I.; et al. miR-150 promotes renal fibrosis in lupus nephritis by downregulating SOCS1. *J. Am. Soc. Nephrol.* **2013**, *24*, 1073–1087. [CrossRef]
110. Honda, N.; Jinnin, M.; Kira-Etoh, T.; Makino, K.; Kajihara, I.; Makino, T.; Fukushima, S.; Inoue, Y.; Okamoto, Y.; Hasegawa, M.; et al. miR-150 down-regulation contributes to the constitutive type I collagen overexpression in scleroderma dermal fibroblasts via the induction of integrin β3. *Am. J. Pathol.* **2013**, *182*, 206–216. [CrossRef]
111. Pivarcsi, A.; Meisgen, F.; Xu, N.; Ståhle, M.; Sonkoly, E. Changes in the level of serum microRNAs in patients with psoriasis after antitumour necrosis factor-α therapy. *Br. J. Dermatol.* **2013**, *169*, 563–570. [CrossRef]
112. Raaby, L.; Langkilde, A.; Kjellerup, R.B.; Vinter, H.; Khatib, S.H.; Hjuler, K.F.; Johansen, C.; Iversen, L. Changes in mRNA expression precede changes in microRNA expression in lesional psoriatic skin during treatment with adalimumab. *Br. J. Dermatol.* **2015**, *173*, 436–447. [CrossRef]
113. Mensà, E.; Recchioni, R.; Marcheselli, F.; Giuliodorri, K.; Consales, V.; Molinelli, E.; Prattichizzo, F.; Rippo, M.R.; Campanati, A.; Procopio, A.D.; et al. MiR-146a-5p correlates with clinical efficacy in patients with psoriasis treated with the tumour necrosis factor-alpha inhibitor adalimumab. *Br. J. Dermatol.* **2018**, *179*, 787–789. [CrossRef]
114. Pei, D.; Cao, J.; Qin, G.; Wang, X. Measurement of circulating miRNA-125a exhibits good value in the management of etanercept-treated psoriatic patients. *J. Dermatol.* **2020**, *47*, 140–146. [CrossRef]
115. García-Rodríguez, S.; Arias-Santiago, S.; Orgaz-Molina, J.; Magro-Checa, C.; Valenzuela, I.; Navarro, P.; Naranjo-Sintes, R.; Sancho, J.; Zubiaur, M. Abnormal levels of expression of plasma microRNA-33 in patients with psoriasis. *Actas Dermosifiliogr.* **2014**, *105*, 497–503. [CrossRef]
116. Seifeldin, N.S.; El Sayed, S.B.; Asaad, M.K. Increased MicroRNA-1266 levels as a biomarker for disease activity in psoriasis vulgaris. *Int. J. Dermatol.* **2016**, *55*, 1242–1247. [CrossRef]
117. Rupaimoole, R.; Slack, F.J. MicroRNA therapeutics: Towards a new era for the management of cancer and other diseases. *Nat. Rev. Drug Discov.* **2017**, *16*, 203–222. [CrossRef] [PubMed]
118. Rupaimoole, R.; Han, H.D.; Lopez-Berestein, G.; Sood, A.K. MicroRNA therapeutics: Principles, expectations, and challenges. *Chin. J. Cancer* **2011**, *30*, 368–370. [CrossRef]
119. Lawrence, P.; Ceccoli, J. Advances in the Application and Impact of MicroRNAs as Therapies for Skin Disease. *BioDrugs* **2017**, *31*, 423–438. [CrossRef] [PubMed]
120. Guinea-Viniegra, J.; Jiménez, M.; Schonthaler, H.B.; Navarro, R.; Delgado, Y.; Concha-Garzón, M.J.; Tshachler, E.; Obad, S.; Daudén, E.; Wagner, E.F. Targeting miR-21 to treat psoriasis. *Sci. Transl. Med.* **2014**, *6*, 225re1. [CrossRef] [PubMed]
121. Bian, J.; Liu, R.; Fan, T.; Liao, L.; Wang, S.; Geng, W.; Wang, T.; Shi, W.; Ruan, Q. miR-340 Alleviates Psoriasis in Mice through Direct Targeting of IL-17A. *J. Immunol.* **2018**, *201*, 1412–1420. [CrossRef]
122. Srivastava, A.; Nikamo, P.; Lohcharoenkal, W.; Dongquing, L.; Meisgen, F.; Landén, N.X.; Stahle, M.; Pivarcsi, A.; Sonkoly, E. MicroRNA-146a suppresses IL-17-mediated skin inflammation and is genetically associated with psoriasis. *J. Allergy Clin. Immunol.* **2017**, *139*, 550–561. [CrossRef]
123. Feng, H.; Wu, R.; Zhang, S.; Kong, Y.; Liu, Z.; Wu, H.; Wang, H.; Su, Y.; Zhao, M.; Lu, Q. Topical administration of nanocarrier miRNA-210 antisense ameliorates imiquimod-induced psoriasis-like dermatitis in mice. *J. Dermatol.* **2020**, *47*, 147–154. [CrossRef] [PubMed]

124. Lee, Y.S.; Han, S.B.; Ham, H.J.; Park, J.H.; Lee, J.S.; Hwang, D.Y.; Jung, Y.S.; Yoon, D.Y.; Hong, J.T. IL-32γ suppressed atopic dermatitis through inhibition of miR-205 expression via inactivation of nuclear factor-kappa B. *J. Allergy Clin. Immunol.* **2020**, *146*, 156–168. [CrossRef] [PubMed]
125. Li, X.; Li, D.; Wang, A.; Chu, T.; Lohcharoenkal, W.; Zheng, X.; Grünler, J.; Narayanan, S.; Eliasson, S.; Herter, E.K.; et al. MicroRNA-132 with Therapeutic Potential in Chronic Wounds. *J. Investig. Dermatol.* **2017**, *137*, 2630–2638. [CrossRef] [PubMed]
126. Zhou, Z.; Shu, B.; Xu, Y.; Liu, J.; Wnag, P.; Chen, L.; Zhao, J.; Liu, X.; Qi, S.; Xiong, K.; et al. microRNA-203 Modulates Wound Healing and Scar Formation via Suppressing Hes1 Expression in Epidermal Stem Cells. *Cell. Physiol. Biochem.* **2018**, *49*, 2333–2347. [CrossRef]
127. Maurer, B.; Stanczyk, J.; Jüngel, A.; Akhmetshina, A.; Trenkmann, M.; Brock, M.; Kowal-Bielecka, O.; Gay, R.E.; Michel, B.A.; Distle, J.H.W.; et al. MicroRNA-29, a key regulator of collagen expression in systemic sclerosis. *Arthritis Rheum.* **2010**, *62*, 1733–1743. [CrossRef]
128. Gallant-Behm, C.L.; Piper, J.; Lynch, J.M.; Seto, A.G.; Hong, S.J.; Mustoe, T.A.; Maari, C.; Pestano, L.A.; Dalby, C.M.; Jackson, A.L.; et al. A MicroRNA-29 Mimic (Remlarsen) Represses Extracellular Matrix Expression and Fibroplasia in the Skin. *J. Investig. Dermatol.* **2019**, *139*, 1073. [CrossRef]
129. Ross, K. Towards topical microRNA-directed threap for epidermal disorders. *J. Control. Release* **2018**, *269*, 13–147. [CrossRef]
130. Nastiti, C.M.R.R.; Ponto, T.; Abd, E.; Grice, J.E.; Benson, H.A.; Roberts, M.S. Topical nano and microemulsions for skin delivery. *Pharmaceutics* **2017**, *9*, 37. [CrossRef]
131. Kasting, G.B.; Barai, N.D.; Wang, T.F.; Nitsche, J.M. Mobility of water in human stratum corneum. *J. Pharm. Sci.* **2003**, *92*, 2326–2340. [CrossRef]
132. Abdel-Mottaleb, M.M.; Try, C.; Pellequer, Y.; Lamprecht, A. Nanomedicine strategies for targeting skin inflammation. *Nanomedicine* **2014**, *9*, 1727–1743. [CrossRef]
133. Liu, F.; Wang, C.; Gao, Y.; Li, X.; Tian, F.; Zhang, Y.; Fu, M.; Li, P.; Wang, Y.; Wang, F. Current transport systems and clinical applications for small interfering RNA (siRNA) drugs. *Mol. Diagn. Ther.* **2018**, *22*, 551–569. [CrossRef] [PubMed]
134. Desmet, E.; Bracke, S.; Forier, K.; Taevernier, L.; Stuart, M.C.A.; Spiegeleer, B.D.; Raemdonck, K.; Gele, M.V.; Lambert, J. An elastic liposomal formulation for RNAi-based topical treatment of skin disorders: Proof-of-concept in the treatment of psoriasis. *Int. J. Pharm.* **2016**, *500*, 268–274. [CrossRef] [PubMed]

Dermatology

Review Article

Dermatology 2020;236:467–476
DOI: 10.1159/000508672

Received: February 3, 2020
Accepted: May 11, 2020
Published online: July 13, 2020

Efficacy of Thalidomide in Discoid Lupus Erythematosus: Insights into the Molecular Mechanisms

Sandra Domingo[a] Cristina Solé[a] Teresa Moliné[b] Berta Ferrer[b]
Josep Ordi-Ros[c] Josefina Cortés-Hernández[a]

[a]Rheumatology Research Group, Lupus Unit, Vall d'Hebron University Hospital, Vall d´Hebron Research Institute (VHIR), Barcelona, Spain; [b]Departament of Pathology, Vall d'Hebron University Hospital, Barcelona, Spain; [c]Department of Internal Medicine, Vall d'Hebron University Hospital, Vall d'Hebron Research Institute (VHIR), Barcelona, Spain

Keywords
Discoid lupus erythematosus · Systemic lupus erythematosus · Thalidomide · Refractory cutaneous lupus erythematosus · First-line treatment · Mechanism of action

Abstract
Background: Thalidomide has been used successfully in a variety of chronic refractory inflammatory dermatological conditions with underlying autoimmune or infectious pathogenesis. It was first used for refractory discoid lupus erythematosus (DLE) in 1983 and has steadily grown since then. ***Method:*** In this review, we describe the therapeutic benefits of thalidomide for DLE treatment and its biological properties. We explain how new discoveries in DLE pathogenesis are relevant to understand thalidomide's mechanism of action and the need to find an alternative safe drug with similar therapeutic effects. ***Summary:*** Thalidomide's efficacy in DLE patients is significant, with 80–90% reaching clinical remission according to different studies. However, thalidomide's use is still limited by serious adverse effects such as teratogenicity, neurotoxicity, and thrombosis. In addition, there is a frequent rate of relapse and many patients require a long-term low dose of thalidomide as maintenance. The achievement of clinical response within weeks is key to avoid irreversible DLE fibrotic sequelae, making it critical to introduce thalidomide earlier in the DLE treatment algorithm. Recently, microarray and miRNA screenings demonstrated a significant CD4+ T enrichment and T-helper 1 response predominance with a dysregulation of regulatory T cell (Treg) expression in DLE lesions that induced high levels of proinflammatory, chemotaxis, and apoptotic proteins that induce the chronic inflammation response. Thalidomide's anti-inflammatory, antiangiogenic, and T-cell co-stimulatory effects may be beneficial for DLE since it promotes cytokine inhibition, inhibits macrophage activation, regulates Treg responses, inhibits angiogenesis, modulates T cells, and promotes NK cell-mediated cytotoxicity.

Introduction

Thalidomide is a derivative of glutamic acid, an oral non-barbituric drug, with sedative and antiemetic activity, introduced in the 1950s as a sedative for its rapid action and apparent safety [1]. However, teratogenicity of the drug was quickly described, estimating that 5,000–6,000 children suffered phocomelia secondary to its use during pregnancy, usually accompanied by other malfor-

karger@karger.com
www.karger.com/drm

Karger

Cristina Solé
Rheumatology Research Group, Lupus Unit
Vall d´Hebron University Hospital, Vall d´Hebron Research Institute (VHIR)
Passeig Vall d´Hebron 119-129, ES–08035 Barcelona (Spain)
cristina.sole@vhir.org

mations. It was not until Sheskin [2] that beneficial effects on erythema nodosum leprosum were reported. Since then, there have been progressively more studies demonstrating the immunomodulatory and anti-inflammatory effect of thalidomide and its possible application in immune-mediated inflammatory diseases [3] and skin disorders such as chronic refractory purigo nodularis, erythema multiforme, Behçet's syndrome, and cutaneous lupus erythematosus (CLE) [4].

CLE is an autoimmune skin disease which includes a broad range of dermatologic manifestations. It may be associated with systemic lupus erythematosus (SLE). It is important to note that the skin is the second most frequent organ affected in SLE and that around 75% of SLE patients present skin manifestations at some point during the course of the systemic disease [5]. CLE is classified into several subtypes according to histological and clinical features. Of the different clinical subtypes, discoid lupus erythematosus (DLE) is one of the most prevalent and refractory form. DLE lesions tend to appear in sun-exposed skin, may be localized or generalized, and have a chronic relapsing-remitting course over time, having an important aesthetic and psychological impact and hence an impaired quality of life.

First-line therapies for DLE include antimalarial agents and/or topical steroids, together with sun protection. Although most patients respond to this regimen, approximately 30–40% of cases will be refractory [6]. For this significant minority, there is no consensus algorithm, and a trial and error approach using multiple systemic agents has shown a variable response. Thus, there is a need for new treatments.

Rapid improvement of subacute lesions of 2 CLE patients was first observed using thalidomide as treatment in 1983 [7]. Since then, further studies in CLE have shown its efficacy [8–22]. Currently, it is used in severe CLE, especially in profundus and discoid lupus. However, despite its efficacy, its use is limited because large-scale clinical trials have not been conducted and due to the serious adverse events that include teratogenicity, peripheral neuropathy, and thrombotic events. Patients need baseline nerve conduction studies given the high risk of polyneuropathy (20–30%), which may be irreversible [23].

Thalidomide's Efficacy for DLE Treatment

The effectiveness of thalidomide has been reported by several cohort studies of more than 60 patients; however, despite its proven clinical efficacy, it is still considered second-line therapy. Our experience confirms that thalidomide is effective for the treatment of refractory DLE [14]. We reported 60 patients with refractory CLE of whom 25 were diagnosed with refractory DLE. Most patients (98%) improved following therapy and 85% achieved complete remission over a period of 8 years of follow-up. Clinical improvement was observed within the first 2 weeks of treatment, although a complete response usually occurred between weeks 4 and 8. Although no studies have established an induction and maintenance dosage for the control of skin lesions, the different studies have used between 100 and 400 mg/day. Our experience has been with an initial dose of 100 mg/day to better withstand the drowsiness that can occur, and subsequently, the dose was raised according to clinical response, not exceeding 400 mg/day [21].

Since 1983, several series of patients with different CLE subtypes have been published with good results (Table 1). The majority of the included patients were those with DLE, to a lesser extent with subacute cutaneous lupus (SCLE), and much less frequently acute lupus, profundus lupus, lupus tumidus, or non-specific lesions such as pyoderma gangrenous [21]. The response rates were significantly higher in DLE and SCLE (98%), whereas in the other CLE subtypes the response rates only reached 50%. Among patients with DLE, the generalized subtype tended to recur more than the localized one (92 vs. 73%, $p = 0.013$).

Relapse was frequent after thalidomide's withdrawal and most common in DLE. Kyriakis et al. [24] were the first to highlight the best and sustained response of patients with SCLE vs. DLE. In our series, recurrence reached 70% of all cases (35 of 50) [21], occurring mainly when decreasing or interrupting treatment [24]. Relapse occurred between 4 and 8 weeks after the interruption of thalidomide, but all cases responded to the drug reintroduction. In some cases of DLE, low-dose maintenance, 50 mg/day or even every other day, was sufficient to maintain the remission of the cutaneous disease to avoid future scars and side effects. In our studies, up to 16% of patients with DLE required long-term treatment but at lower doses.

One of the limitations of the retrospective studies has been the lack of use of validated scales to assess clinical response, such as the Cutaneous Lupus Erythematosus Disease Area and Severity Index (CLASI) that allows us to assess the extent, activity, and sequelae of skin lesions objectively during treatment [25]. This is key to evaluate the effectiveness of new drugs in future clinical trials in CLE.

Table 1. Clinical studies of thalidomide and analogue lenalidomide for refractory cutaneous lupus erythematosus

Reference	Drug	Condition	*N*	Efficacy, *n* (%)		Relapse after thalidomide withdrawal, *n* (%)
				complete response	partial response	
Knop et al. [8], 1983	Thalidomide	60 DLE	60	54/60 (90, complete/partial response)		30/41 (71)
Hasper [9], 1983	Thalidomide	7 DLE 4 SCLE	11	7/11 (64)	2/11 (18)	6/11 (54)
Naafs and Faber [10], 1985	Thalidomide	5 DLE 4 SCLE 3 disseminated CLE 1 lupus profundus 5 SLE 1 MCTD	19	17/19 (89, complete/partial response)		1/17 (6)
Atra and Sato [11], 1993	Thalidomide	20 refractory CLE	20	18/20 (90)	2/20 (10)	N.D.
Stevens et al. [12], 1997	Thalidomide	11 DLE 3 SCLE 1 SCLE/malar rash 1 chronic erythema	16	7/16 (44)	6/16 (37)	6/8 (75)
Sato et al. [13], 1998	Thalidomide	2 DLE 3 SCLE 13 rash and/or vasculitis	18	13/18 (73)	5/18 (28)	18/18 (100)
Ordi-Ros et al. [14], 2000	Thalidomide	9 DLE 7 SCLE 4 lupus profundus 2 rash	22	12/16 (75)	4/16 (25)	9/16 (65)
Thomson et al. [15], 2001	Thalidomide	20 DLE 2 SCLE 5 SLE	27	7/27 (26)	11/27 (41)	4/11 (36)
Housman et al. [16], 2003	Thalidomide	8 CCLE 1 CCLE/lupus profundus 3 SCLE 4 lupus profundus 13 SLE	29	17/23 (74)	3/23 (13)	N.D.
Briani et al. [17], 2005	Thalidomide	5 CCLE 1 CCLE/vasculitis 4 SCLE 2 SCLE/vasculitis 1 ACLE/SCLE 1 vasculitis	14	14/14 (100, complete/partial response)		N.D.
Coelho et al. [18], 2005	Thalidomide	19 DLE 15 DLE/SLE 15 SCLE 12 SCLE/SLE 3 lupus profundus 1 bullous lupus	65	63/65 (97, complete/partial response)		23/27 (85)
Cuadrado et al. [19], 2005	Thalidomide	18 DLE 6 SCLE 24 SLE	48	29/48 (60)	10/48 (21)	26/39 (67)
Lyakhovisky et al. [20], 2006	Thalidomide	10 DLE	10	9/10 (90)	1/10 (19)	5/10 (50)

Table 1 (continued)

Reference	Drug	Condition	*N*	Efficacy, *n* (%)		Relapse after thalidomide withdrawal, *n* (%)
				complete response	partial response	
Cortés-Hernández et al. [21], 2012	Thalidomide	25 DLE 18 SCLE 6 ACLE 5 lupus profundus 3 chilblain LE 2 lupus tumidus 1 pyoderma gangrenosum	60	50/59 (85)	8/59 (14)	35/50 (70)
Wang et al. [22], 2016	Thalidomide	9 DLE 12 vasculitis 48 facial rash	69	49/69 (71)	20/69 (29)	N.D.
Shah et al. [67], 2009	Lenalidomide	2 DLE	2	0/2 (0)	1/2 (50)	N.D.
Cortés-Hernández et al. [68], 2012	Lenalidomide	9 DLE 2 SCLE 1 ACLE 2 lupus profundus 1 lupus tumidus	15	12/14 (86)	2/14 (14)	9/12 (75)
Braunstein et al. [69], 2012	Lenalidomide	3 DLE 1 SCLE/lupus tumidus 1 DLE/SCLE	5	0/5 (0)	4/5 (80)	N.D.
Kindle et al. [70], 2016	Lenalidomide	6 DLE 1 SCLE 2 profundus lupus	9	5/9 (56)	2/9 (22)	N.D.
Fennira et al. [71], 2016	Lenalidomide	14 DLE 2 SCLE	16	2/14 (14)	12/14 (86)	0/13 (0)
Wu et al. [72], 2017	Lenalidomide	10 recalcitrant CLE/SLE	10	10/10 (100 complete/partial response)		N.D.

CLE, cutaneous lupus erythematosus; DLE, discoid lupus erythematosus; SCLE, subacute cutaneous lupus erythematosus; ACLE, acute cutaneous lupus erythematosus; SLE, systemic lupus erythematosus; N.D., Not detailed.

Described Biological Properties of Thalidomide

Thalidomide is known for its anti-inflammatory, antiangiogenic, and immunomodulatory properties.

Anti-inflammatory. In 1991, it was discovered that thalidomide inhibited the synthesis of tumour necrosis factor-α (TNF-α) [26]. Both soluble and membrane-bound TNF bind to 2 transmembrane receptor molecules: TNFR1 and TNFR2, which are present in almost all cells, giving the cytokine a broad function according to the tissue and/or organ where it acts. TNF-α induces an increased vascular permeability leading to a greater recruitment of inflammatory cells, immunoglobulins, and complement, as well as causing activation of T and B lymphocytes. Thalidomide's effect on TNF-α release plays an important role in its ability to modulate the immune system [27]. Activated macrophages are the main producers of TNF-α and also highly reactive to it, although it can be produced by many other cell types. It has been demonstrated that thalidomide inhibits the alternative activation of macrophages accompanied by a reduction of TNF-α, interleukin (IL)-4, IL-5, IL-13, and IL-17 [28]. It can also modulate other inflammatory cytokines such as IL-1, IL-2, IL-6, IL-8, IL-10, IL-12, and interferon-γ (IFN-γ) [29].

Antiangiogenic. It was in 1994 when the antiangiogenic effect of thalidomide was discovered [30]. Angiogenesis occurs physiologically in wound healing, bringing oxygen, nutrients, and cytokines involved in tissue repair. Using a rabbit model, it was demonstrated that thalidomide could inhibit fibroblast growth factor and vascular endothelial growth factor (VEGF) induced in angiogenesis. Due to its antiangiogenic effects, thalidomide is able to alter foetal development in pregnant women, which

leads to foetal deformity. However, at the same time this effect is one of the mechanisms for its antitumour activity [31]. In vitro and in vivo studies suggest that immunomodulatory drugs (IMiDs) may inhibit angiogenesis by antimigratory rather than antiproliferative mechanisms due to inhibiting the secretion of VEGF [32]. Thalidomide reduces metastasis by reducing the expression of proangiogenic cytokines such as VEGF that decreases both capillary density and the number of adhesion cells.

Immunomodulatory. The process of co-stimulation of lymphocytic T-cell populations is important for the activation of the immune system and the generation of antibodies against relevant antigens. In particular, to avoid immunological tolerance or anergy, activation of T cells by antigen-presenting cells (APCs) requires the interaction of the major histocompatibility complex with cellular T receptors, and other secondary molecules such as B7 (in APCs) with CD28 (in T cells). To date, immunomodulatory effect of thalidomide is poorly understood. In 1998, it was discovered that thalidomide could co-stimulate T cells independently of the secondary interaction between B7 and CD28 molecules [33]. It has been shown that thalidomide has a major effect on the immune response in T-helper 1 (Th1) diseases by shifting Th1 to a Th2 response. A potential denominator to explain thalidomide's effect in the modulation of graft vs. host, erythema nodosum leprosum, and auto-immune disorders would be the activation of T lymphocytes leading to the synthesis of IL-2, the expression of high-affinity IL-2 receptors, and the induction of lymphocyte proliferation [34]. However, Fernandez et al. [35] could not demonstrate a modulatory effect on the immune response in human leukemia cell line Jurkat cells via IL-2 production. In addition, drugs derived from thalidomide, IMiDs such as lenalidomide and pomalidomide, have been shown to have a clear co-stimulatory effect in both $CD4^+$ and in $CD8^+$ T cells [36]. IMiDs exert their effects by activating protein kinase C delta (PKC-θ) and acting on AP-1 DNA-binding activity in T cells, resulting in augmented IL-2 synthesis and activation of IL-2-dependent downstream effectors, such as natural killer cells (NK) [37]. The increment of IL-2 production by these drugs has been confirmed by several studies [38]. Moreover, in 2010, cereblon (CRBN) was discovered as the main protein target of thalidomide. CRBN forms an E3 ubiquitin ligase complex with damaged DNA binding protein 1 (DDB1) and Cul4A that is important for limb outgrowth. When thalidomide binds to CRBN, the associated ubiquitin ligase activity of CRBN is inhibited, producing teratogenic effects [39]. Subsequently, it was demonstrated that CRBN was also required for the anti-myeloma activity of thalidomide, and downstream targets of CRBN were investigated in order to understand the reason [40]. Two critical CRBN-mediated downregulation genes have been identified: transcription factor Ikaros (IKZF1) and Aiolos (IKZF3) [41]. Ikaros family genes regulate immune cell development [42] and the pathological dysregulation of c-Myc and IRF4 [43].

Plausible Biologic Mechanism in DLE

Potential Biologic Thalidomide Mechanism of Action in DLE

The pathogenesis of DLE is currently not completely understood and likely to be multifactorial, involving genetics, epigenetics, and environmental factors. The findings indicate that there is an initial trigger in order to develop the disease. UVB light is a known CLE trigger, which causes apoptosis of keratinocytes and inflammation in CLE skin. The apoptotic keratinocytes release autoantigens which are recognized by APCs, and there is an activation of autoreactive B and T cells. This promotes an immune cell recruitment and production of cytokines, chemokines, and autoantibodies [44]. Deposition of IgGs and C3 is frequently detected in DLE-affected skin. As a result, the skin is damaged and inflamed leading to the DLE lesions. Other potential DLE-described triggers are viral infections, drugs, chemicals, and smoking habits. However, further studies are required in order to obtain clear evidence concerning their role in DLE [45].

Gene expression microarray analysis of DLE have shown an increase in the IFN signalling pathway genes as well as a significant $CD4^+$ T enrichment with a Th1 response predominance [46]. In addition, an increase of the apoptotic signalling molecules CD95, TRAIL-R1, and caspase-8 has been identified by tissue microarray analysis [47]. Microarray analysis comparing lesional and non-lesional DLE areas showed an upregulation in lesioned sites of IFN, apoptosis makers, NK, dendritic cell, chemotaxis genes, and leucocyte activation [48]. DLE peripheral blood gene expression has also been studied, revealing that IFN, immune response, and stress pathways are significantly increased in comparison with healthy individuals [49]. Another study in which an miRNA screening profile was conducted in DLE showed that an overexpression of miR-31 in DLE lesional skin induced an increased production of IL-8 and IL-12 in keratinocytes, suggesting that these cytokines play a key role in the inflammatory environment of DLE lesions [50].

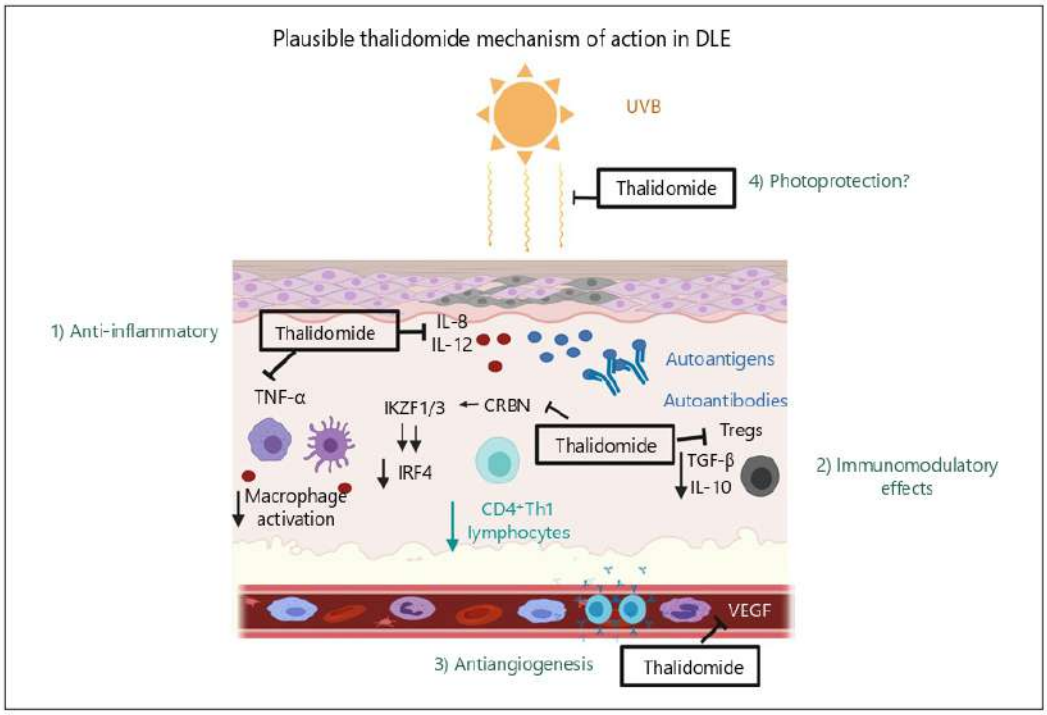

Fig. 1. Plausible thalidomide mechanism of action in discoid lupus erythematosus (DLE). 1. Anti-inflammatory: thalidomide may act as an anti-inflammatory agent by inhibiting TNF-α production that is essential for macrophage, T- and B-cell activation. It could also reduce cytokines present in DLE lesions, IL-8, and IL-12, and as a result, there may be less immune cell recruitment in the lesion site. 2. Immunomodulatory effects: thalidomide induces ubiquitination of IKZF1/3 by targeting CRBN complex resulting in their proteasomal degradation. Consequently, IRF4 transcription decreases and it could cause T-cell immunomodulatory effects and dendritic cell dysfunction. IL-10 and TGF-β in DLE are induced by regulatory T cells (Tregs) and initiate fibrosis. Thalidomide may decrease IL-10 and TGF-β Treg production. 3. Antiangiogenesis: thalidomide could improve DLE lesions, reducing erythema and telangiectasia and decreasing blood vessel formation by decreasing vascular endothelial growth (VEGF). 4. Photoprotection: thalidomide photoprotective properties could contribute to its therapeutic effects in UVB-exposed skin.

Given thalidomide's efficacy in the treatment of DLE, the inhibition of IL-8 and IL-12 might be one of the possible anti-inflammatory mechanisms of action of this drug (Fig. 1). However, no studies have assessed the effect on these cytokines in patients with DLE. Regarding TNF-α, it is unclear if thalidomide acts by inhibiting its production, since studies show contradictory results [51, 52]. In addition, anti-TNF-α drugs seem to induce cutaneous lupus lesions [53].

Thalidomide angiogenic properties may play a role in its ability to treat DLE lesions as DLE patients present high levels of VEGF in serum, and several chronic inflammatory skin diseases such as atopic dermatitis and psoriasis are characterized by altered angiogenesis and overexpression of VEGF. Moreover, one of the beneficial effects of chloroquine treatment in DLE may be due to its antiangiogenic properties reducing erythema, lowering photosensitivity and decreasing blood vessel formation and telangiectasia [54]. However, it is important to note that lesions of SCLE have been reported as a response to bevacizumab, a recombinant humanized antibody against VEGF [55], therefore it is not totally clear if the antiangiogenic properties of thalidomide could be beneficial for DLE treatment (Fig. 1).

DLE skin lesions display a significant $CD4^+$ T-cell enrichment with a high level of production of IL-2 and a relative increase of Treg response [46]. IL-2 is a relevant cytokine and induces an expansion of Tregs. Some studies show that IMiDs have an inhibitory effect on Tregs [56], and thalidomide regulates Treg activity [57]. So, a reduction or regulation of Treg response in DLE lesions may decrease IL-10 and TGF-β production and slow down the TGF-β-dependent mechanism of fibrosis, reducing scarring (Fig. 1). But restoration of abnormal immune function should be addressed more carefully in cutaneous and non-cutaneous lupus patients considering the complexity of disease pathogenesis.

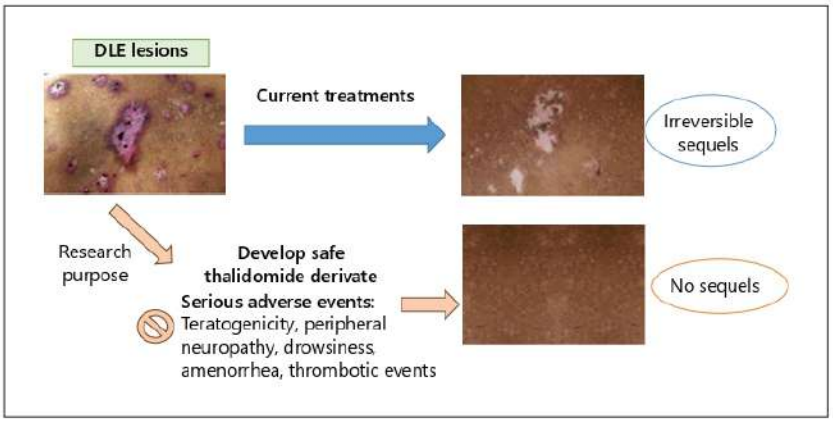

Fig. 2. Novel safety thalidomide derivate for refractory DLE treatment. Early resolution of inflammation in DLE is very relevant to avoid irreversible sequelae. In many cases, current treatments are not powerful enough to prevent scarring in refractory DLE patients. An alternative could be a thalidomide derivate with a better safety profile, avoiding serious adverse effects, such as teratogenicity, peripheral neuropathy, drowsiness, amenorrhea, and thrombotic events, but preserving anti-inflammatory and immunomodulatory thalidomide properties.

Polymorphisms in the IKZF1 and IKZF3 loci are associated with an increased risk of SLE, but their roles are still being studied [58]. On the other hand, IRF4 plays a fundamental role in dendritic cell differentiation, and it has been suggested that an IRF4-dependent pathway contributes to their dysfunction in lupus [59]. Consequently, thalidomide's T-cell modulatory properties in DLE patients could also be related to the initial binding to CRBN that induces proteasomal degradation of IKZF1/3 and inhibition of IRF4 transcription (Fig. 1). Further specific study of CRBN downstream signalling in skin biopsies will help to delineate the underlying mechanisms for thalidomide's efficacy in DLE treatment.

It has been described that thalidomide has a photoprotective effect by inhibiting acute UVB erythema in nonlesional skin of DLE (Fig. 1). However, no differences were observed in the frequency of apoptotic keratinocytes in the UVB-exposed areas before and after thalidomide treatment [60]. The authors conclude that these photoprotective properties may partly contribute to the therapeutic effect of thalidomide in cutaneous UVB-related diseases. As UVB exposure is an initial CLE trigger, this needs to be investigated in order to get more insights into the mechanism of action of thalidomide in DLE and other cutaneous diseases.

Limited Clinical Use of Thalidomide in DLE: Need of Novel Safety Analogues

Around 25–30% of DLE thalidomide-treated patients can develop minor side effects that resolve after its withdrawal or dose adjustment. Drowsiness, dizziness, flatulence, constipation, and dry skin are frequent and dose dependent. However, side effects could be more serious, such as an exfoliative dermatitis, toxic epidermolysis, and exacerbation of psoriasis, allergic vasculitis, or hereditary purpura caused by thrombocytopenia [61]. According to several studies, peripheral neuropathy incidence ranges from 20 to 30% for thalidomide-treated CLE patients [23]. Other side effects that deserve to be mentioned include ovarian toxicity and the risk of thrombotic events [62, 63]. Thalidomide could also induce a state of hypercoagulation [64], and this risk can increase significantly in the presence of concomitant oral contraceptive use and antiphospholipid antibodies [65, 66]. For this reason, thalidomide treatment is given only for refractory cases.

There is no clear definition of refractory cutaneous lupus, nor is there consensus about when thalidomide should be introduced. Thalidomide treatment always requires an accurate analysis of each case, and it is important to have its toxicity in mind. For this reason, analogues of thalidomide have been developed in order to avoid the undesired side effects. Of these, lenalidomide displayed similar efficacy and relapse rates as thalidomide [67–72], and iberdomide (CC-220) improved significantly moderate-to-severe lupus skin manifestations [73]. Lenalidomide has greater immunomodulatory properties than thalidomide, being more potent in the stimulation of T-cell proliferation and IFN-γ/IL-1 production [74]. CC-220 binds cereblon with a higher affinity than previous IMiDs, and degradation of Ikaros and Aiolos is more potent [75]. In addition, thalidomide analogues seem to be safer with less risk of developing side effects such as has been observed with lenalidomide-treated patients who seem to present a decreased risk of peripheral neuropathy [68, 76]. Regarding CC-220, frequency of side effects and its efficacy is still under investigation. IMiDs are an expensive therapeutic option compared to thalidomide. There is a need to develop novel thalidomide analogues

with a better safety profile that could be introduced at early stages in the management of DLE after failure of conventional standard therapy to avoid irreversible sequelae (Fig. 2).

Conclusion

Thalidomide is a notable drug to be used in human immune complex diseases for its potential biological effect. Its therapeutic efficacy has been described as anti-inflammatory, antiangiogenic, and T-cell co-stimulatory. In recent years, data suggest that it is a successful treatment for DLE. Its mechanism in DLE patients may be due to cytokine inhibition, inhibition of macrophage activation, Treg response regulation, inhibition of angiogenesis, T-cell modulation, and promotion of NK cell-mediated cytotoxicity. Nevertheless, serious side effects of thalidomide limited its use for refractory cases only. In DLE, where early resolution of inflammation is so important to avoid irreversible scarring and sequelae, it will be critical to introduce a safe derivate of thalidomide earlier. Further study with molecular biology techniques is required in order to get more insights into the biological mechanism of thalidomide in DLE and, therefore, be able to discover and develop novel thalidomide analogues effective for DLE, safer and without side effects.

Key Message

The recent new insights into thalidomide's mechanism of action and discoid lupus erythematosus (DLE) pathogenesis could be used to design a novel treatment for refractory DLE.

Acknowledgements

We would like to acknowledge the Instituto de Salud Carlos III (Spain Government, PI15/02145), Catalan Lupus Foundation, and A. Bosch Foundation for their financial support.

Conflict of Interest Statement

The authors declare that they have no conflict of interest regarding the publication of this article.

Funding Sources

This work was funded by the Instituto de Salud Carlos III (Spanish Government, PI15/02145), Catalan Lupus Foundation, and A. Bosch Foundation.

Author Contributions

This paper was planned and written in collaboration with all the authors.

References

1 Mellin GW, Katzenstein M. The saga of thalidomide. Neuropathy to embryopathy, with case reports of congenital anomalies. N Engl J Med. 1962 Dec;267:1184–92.
2 Sheskin J. Thalidomide in the treatment of lepra reactions. Clin Pharmacol Ther. 1965 May-Jun;6(3):303–6.
3 Baker KF, Isaacs JD. Novel therapies for immune-mediated inflammatory diseases: what can we learn from their use in rheumatoid arthritis, spondyloarthritis, systemic lupus erythematosus, psoriasis, Crohn's disease and ulcerative colitis? Ann Rheum Dis. 2018 Feb; 77(2):175–87.
4 Calderon P, Anzilotti M, Phelps R. Thalidomide in dermatology. New indications for an old drug. Int J Dermatol. 1997 Dec;36(12): 881–7.
5 Obermoser G, Sontheimer RD, Zelger B. Overview of common, rare and atypical manifestations of cutaneous lupus erythematosus and histopathological correlates. Lupus. 2010 Aug;19(9):1050–70.
6 Chang AY, Piette EW, Foering KP, Tenhave TR, Okawa J, Werth VP. Response to antimalarial agents in cutaneous lupus erythematosus: a prospective analysis. Arch Dermatol. 2011 Nov;147(11):1261–7.
7 Volc-Platzer B, Wolff K. [Treatment of subacute cutaneous lupus erythematosus with thalidomide]. Hautarzt. 1983 Apr;34(4):175–8.
8 Knop J, Bonsmann G, Happle R, Ludolph A, Matz DR, Mifsud EJ, et al. Thalidomide in the treatment of sixty cases of chronic discoid lupus erythematosus. Br J Dermatol. 1983 Apr; 108(4):461–6.
9 Hasper MF. Chronic cutaneous lupus erythematosus. Thalidomide treatment of 11 patients. Arch Dermatol. 1983 Oct;119(10): 812–5.
10 Naafs B, Faber WR. Thalidomide therapy. An open trial. Int J Dermatol. 1985 Mar;24(2): 131–4.
11 Atra E, Sato EI. Treatment of the cutaneous lesions of systemic lupus erythematosus with thalidomide. Clin Exp Rheumatol. 1993 Sep-Oct;11(5):487–93.
12 Stevens RJ, Andujar C, Edwards CJ, Ames PR, Barwick AR, Khamashta MA, et al. Thalidomide in the treatment of the cutaneous manifestations of lupus erythematosus: experience in sixteen consecutive patients. Br J Rheumatol. 1997 Mar;36(3):353–9.
13 Sato EI, Assis LS, Lourenzi VP, Andrade LE. Long-term thalidomide use in refractory cutaneous lesions of systemic lupus erythematosus. Rev Assoc Med Bras (1992). Oct-Dec 1998;44(4):289–93.
14 Ordi-Ros J, Cortés F, Cucurull E, Mauri M, Buján S, Vilardell M. Thalidomide in the treatment of cutaneous lupus refractory to conventional therapy. J Rheumatol. 2000 Jun; 27(6):1429–33.
15 Thomson KF, Goodfield MJ. Low-dose thalidomide is an effective second-line treatment in cutaneous lupus erythematosus. J Dermatolog Treat. 2001 Sep;12(3):145–7.
16 Housman TS, Jorizzo JL, McCarty MA, Grummer SE, Fleischer AB Jr, Sutej PG. Low-dose thalidomide therapy for refractory cutaneous lesions of lupus erythematosus. Arch Dermatol. 2003 Jan;139(1):50–4.
17 Briani C, Zara G, Rondinone R, Iaccarino L, Ruggero S, Toffanin E, et al. Positive and negative effects of thalidomide on refractory cutaneous lupus erythematosus. Autoimmunity. 2005 Nov;38(7):549–55.

18 Coelho A, Souto MI, Cardoso CR, Salgado DR, Schmal TR, Waddington Cruz M, et al. Long-term thalidomide use in refractory cutaneous lesions of lupus erythematosus: a 65 series of Brazilian patients. Lupus. 2005;14(6):434–9.

19 Cuadrado MJ, Karim Y, Sanna G, Smith E, Khamashta MA, Hughes GR. Thalidomide for the treatment of resistant cutaneous lupus: efficacy and safety of different therapeutic regimens. Am J Med. 2005 Mar;118(3):246–50.

20 Lyakhovisky A, Baum S, Shpiro D, Salomon M, Trau H. [Thalidomide therapy for discoid lupus erythematosus]. Harefuah. 2006 Jul;145(7):489–92.

21 Cortés-Hernández J, Torres-Salido M, Castro-Marrero J, Vilardell-Tarres M, Ordi-Ros J. Thalidomide in the treatment of refractory cutaneous lupus erythematosus: prognostic factors of clinical outcome. Br J Dermatol. 2012 Mar;166(3):616–23.

22 Wang D, Chen H, Wang S, Zou Y, Li J, Pan J, et al. Thalidomide treatment in cutaneous lesions of systemic lupus erythematosus: a multicenter study in China. Clin Rheumatol. 2016 Jun;35(6):1521–7.

23 Bastuji-Garin S, Ochonisky S, Bouche P, Gherardi RK, Duguet C, Djerradine Z, et al.; Thalidomide Neuropathy Study Group. Incidence and risk factors for thalidomide neuropathy: a prospective study of 135 dermatologic patients. J Invest Dermatol. 2002 Nov;119(5):1020–6.

24 Kyriakis KP, Kontochristopoulos GJ, Panteleos DN. Experience with low-dose thalidomide therapy in chronic discoid lupus erythematosus. Int J Dermatol. 2000 Mar;39(3):218–22.

25 Albrecht J, Taylor L, Berlin JA, Dulay S, Ang G, Fakharzadeh S, et al. The CLASI (Cutaneous Lupus Erythematosus Disease Area and Severity Index): an outcome instrument for cutaneous lupus erythematosus. J Invest Dermatol. 2005 Nov;125(5):889–94.

26 Sampaio EP, Sarno EN, Galilly R, Cohn ZA, Kaplan G. Thalidomide selectively inhibits tumor necrosis factor alpha production by stimulated human monocytes. J Exp Med. 1991 Mar;173(3):699–703.

27 Moreira AL, Sampaio EP, Zmuidzinas A, Frindt P, Smith KA, Kaplan G. Thalidomide exerts its inhibitory action on tumor necrosis factor α by enhancing mRNA degradation. J Exp Med. 1993 Jun;177(6):1675–80.

28 Lee HS, Kwon HS, Park DE, Woo YD, Kim HY, Kim HR, et al. Thalidomide inhibits alternative activation of macrophages in vivo and in vitro: a potential mechanism of anti-asthmatic effect of thalidomide. PLoS One. 2015 Apr;10(4):e0123094.

29 Meierhofer C, Dunzendorfer S, Wiedermann CJ. Theoretical basis for the activity of thalidomide. BioDrugs. 2001;15(10):681–703.

30 D'Amato RJ, Loughnan MS, Flynn E, Folkman J. Thalidomide is an inhibitor of angiogenesis. Proc Natl Acad Sci USA. 1994 Apr;91(9):4082–5.

31 Fanelli M, Sarmiento R, Gattuso D, Carillio G, Capaccetti B, Vacca A, et al. Thalidomide: a new anticancer drug? Expert Opin Investig Drugs. 2003 Jul;12(7):1211–25.

32 Dredge K, Marriott JB, Macdonald CD, Man HW, Chen R, Muller GW, et al. Novel thalidomide analogues display anti-angiogenic activity independently of immunomodulatory effects. Br J Cancer. 2002 Nov;87(10):1166–72.

33 Haslett PA, Corral LG, Albert M, Kaplan G. Thalidomide costimulates primary human T lymphocytes, preferentially inducing proliferation, cytokine production, and cytotoxic responses in the CD8+ subset. J Exp Med. 1998 Jun;187(11):1885–92.

34 Hendler SS, McCarty MF. Thalidomide for autoimmune disease. Med Hypotheses. 1983 Apr;10(4):437–43.

35 Fernandez LP, Schlegel PG, Baker J, Chen Y, Chao NJ. Does thalidomide affect IL-2 response and production? Exp Hematol. 1995 Aug;23(9):978–85.

36 Marriott JB, Clarke IA, Dredge K, Muller G, Stirling D, Dalgleish AG. Thalidomide and its analogues have distinct and opposing effects on TNF-alpha and TNFR2 during co-stimulation of both CD4(+) and CD8(+) T cells. Clin Exp Immunol. 2002 Oct;130(1):75–84.

37 Davies FE, Raje N, Hideshima T, Lentzsch S, Young G, Tai YT, et al. Thalidomide and immunomodulatory derivatives augment natural killer cell cytotoxicity in multiple myeloma. Blood. 2001 Jul;98(1):210–6.

38 Payvandi F, Wu L, Naziruddin SD, Haley M, Parton A, Schafer PH, et al. Immunomodulatory drugs (IMiDs) increase the production of IL-2 from stimulated T cells by increasing PKC-theta activation and enhancing the DNA-binding activity of AP-1 but not NF-kappaB, OCT-1, or NF-AT. J Interferon Cytokine Res. 2005 Oct;25(10):604–16.

39 Ito T, Ando H, Suzuki T, Ogura T, Hotta K, Imamura Y, et al. Identification of a primary target of thalidomide teratogenicity. Science. 2010 Mar;327(5971):1345–50.

40 Zhu YX, Kortuem KM, Stewart AK. Molecular mechanism of action of immune-modulatory drugs thalidomide, lenalidomide and pomalidomide in multiple myeloma. Leuk Lymphoma. 2013 Apr;54(4):683–7.

41 Krönke J, Hurst SN, Ebert BL. Lenalidomide induces degradation of IKZF1 and IKZF3. OncoImmunology. 2014 Jul;3(7):e941742.

42 Georgopoulos K, Winandy S, Avitahl N. The role of the Ikaros gene in lymphocyte development and homeostasis. Annu Rev Immunol. 1997;15(1):155–76.

43 Lopez-Girona A, Heintel D, Zhang LH, Mendy D, Gaidarova S, Brady H, et al. Lenalidomide downregulates the cell survival factor, interferon regulatory factor-4, providing a potential mechanistic link for predicting response. Br J Haematol. 2011 Aug;154(3):325–36.

44 Stannard JN, Kahlenberg JM. Cutaneous lupus erythematosus: updates on pathogenesis and associations with systemic lupus. Curr Opin Rheumatol. 2016 Sep;28(5):453–9.

45 Szczęch J, Samotij D, Werth VP, Reich A. Trigger factors of cutaneous lupus erythematosus: a review of current literature. Lupus. 2017 Jul;26(8):791–807.

46 Solé C, Gimenez-Barcons M, Ferrer B, Ordi-Ros J, Cortés-Hernández J. Microarray study reveals a transforming growth factor-β-dependent mechanism of fibrosis in discoid lupus erythematosus. Br J Dermatol. 2016 Aug;175(2):302–13.

47 Toberer F, Sykora J, Göttel D, Hartschuh W, Werchau S, Enk A, et al. Apoptotic signal molecules in skin biopsies of cutaneous lupus erythematosus: analysis using tissue microarray. Exp Dermatol. 2013 Oct;22(10):656–9.

48 Dey-Rao R, Smith JR, Chow S, Sinha AA. Differential gene expression analysis in CCLE lesions provides new insights regarding the genetics basis of skin vs. systemic disease. Genomics. 2014 Aug;104(2):144–55.

49 Dey-Rao R, Sinha AA. Genome-wide transcriptional profiling of chronic cutaneous lupus erythematosus (CCLE) peripheral blood identifies systemic alterations relevant to the skin manifestation. Genomics. 2015 Feb;105(2):90–100.

50 Solé C, Domingo S, Ferrer B, Moliné T, Ordi-Ros J, Cortés-Hernández J. MicroRNA expression profiling identifies miR-31 and miR-485-3p as regulators in the pathogenesis of discoid cutaneous lupus. J Invest Dermatol. 2019 Jan;139(1):51–61.

51 Aringer M, Smolen JS. Efficacy and safety of TNF-blocker therapy in systemic lupus erythematosus. Expert Opin Drug Saf. 2008 Jul;7(4):411–9.

52 Bhattacharya SN, Chattopadhaya D, Saha K. Tumor necrosis factor: status in reactions in leprosy before and after treatment. Int J Dermatol. 1993 Jun;32(6):436–9.

53 He Y, Sawalha AH. Drug-induced lupus erythematosus: an update on drugs and mechanisms. Curr Opin Rheumatol. 2018 Sep;30(5):490–7.

54 Lesiak A, Narbutt J, Kobos J, Kordek R, Sysa-Jedrzejowska A, Norval M, et al. Systematic administration of chloroquine in discoid lupus erythematosus reduces skin lesions via inhibition of angiogenesis. Clin Exp Dermatol. 2009 Jul;34(5):570–5.

55 Cleaver N, Ramirez J, Gildenberg S. Cutaneous lupus erythematosus in a patient undergoing intravitreal bevacizumab injections: case report and review of the literature. J Drugs Dermatol. 2013 Sep;12(9):1052–5.

56 Galustian C, Meyer B, Labarthe MC, Dredge K, Klaschka D, Henry J, et al. The anti-cancer agents lenalidomide and pomalidomide inhibit the proliferation and function of T regulatory cells. Cancer Immunol Immunother. 2009 Jul;58(7):1033–45.

57 Skórka K, Bhattacharya N, Własiuk P, Kowal M, Mertens D, Dmoszyńska A, et al. Thalidomide regulation of NF-κB proteins limits Tregs activity in chronic lymphocytic leukemia. Adv Clin Exp Med. 2014 Jan-Feb;23(1):25–32.

58 Hu SJ, Wen LL, Hu X, Yin XY, Cui Y, Yang S, et al. IKZF1: a critical role in the pathogenesis of systemic lupus erythematosus? Mod Rheumatol. 2013 Mar;23(2):205–9.

59 Manni M, Gupta S, Nixon BG, Weaver CT, Jessberger R, Pernis AB. IRF4-dependent and IRF4-independent pathways contribute to DC dysfunction in Lupus. PLoS One. 2015 Nov;10(11):e0141927.

60 Cummins DL, Gaspari AA. Photoprotection by thalidomide in patients with chronic cutaneous and systemic lupus erythematosus: discordant effects on minimal erythema dose and sunburn cell formation. Br J Dermatol. 2004 Aug;151(2):458–64.

61 Chasset F, Tounsi T, Cesbron E, Barbaud A, Francès C, Arnaud L. Efficacy and tolerance profile of thalidomide in cutaneous lupus erythematosus: A systematic review and meta-analysis. J Am Acad Dermatol. 2018 Feb; 78(2):342–350.e4.

62 Lenz W, Knapp K. Thalidomide embryopathy. Arch Environ Health. 1962 Aug;5(2): 100–5.

63 Ordi J, Cortes F, Martinez N, Mauri M, De Torres I, Vilardell M. Thalidomide induces amenorrhea in patients with lupus disease. Arthritis Rheum. 1998 Dec;41(12):2273–5.

64 Bennett CL, Schumock GT, Desai AA, Kwaan HC, Raisch DW, Newlin R, et al. Thalidomide-associated deep vein thrombosis and pulmonary embolism. Am J Med. 2002 Nov; 113(7):603–6.

65 Bishnoi A, Singh V, Handa S, Vinay K. Thalidomide and thromboprophylaxis for dermatologic indications: an unmet need for more evidence. J Am Acad Dermatol. 2018 Sep;79(3):e45–6.

66 Cesbron E, Bessis D, Jachiet M, Lipsker D, Cordel N, Bouaziz JD, et al.; Study Group of Systemic Diseases in Dermatology (Étude des Maladies Systémiques en Dermatologie). Risk of thromboembolic events in patients treated with thalidomide for cutaneous lupus erythematosus: A multicenter retrospective study. J Am Acad Dermatol. 2018 Jul;79(1):162–5.

67 Shah A, Albrecht J, Bonilla-Martinez Z, Okawa J, Rose M, Rosenbach M, et al. Lenalidomide for the treatment of resistant discoid lupus erythematosus. Arch Dermatol. 2009 Mar;145(3):303–6.

68 Cortés-Hernández J, Ávila G, Vilardell-Tarrés M, Ordi-Ros J. Efficacy and safety of lenalidomide for refractory cutaneous lupus erythematosus. Arthritis Res Ther. 2012 Dec; 14(6):R265.

69 Braunstein I, Goodman NG, Rosenbach M, Okawa J, Shah A, Krathen M, et al. Lenalidomide therapy in treatment-refractory cutaneous lupus erythematosus: histologic and circulating leukocyte profile and potential risk of a systemic lupus flare. J Am Acad Dermatol. 2012 Apr;66(4):571–82.

70 Kindle SA, Wetter DA, Davis MD, Pittelkow MR, Sciallis GF. Lenalidomide treatment of cutaneous lupus erythematosus: the Mayo Clinic experience. Int J Dermatol. 2016 Aug; 55(8):e431–9.

71 Fennira F, Chasset F, Soubrier M, Cordel N, Petit A, Francès C. Lenalidomide for refractory chronic and subacute cutaneous lupus erythematosus: 16 patients. J Am Acad Dermatol. 2016 Jun;74(6):1248–51.

72 Wu EY, Schanberg LE, Wershba EC, Rabinovich CE. Lenalidomide for refractory cutaneous manifestations of pediatric systemic lupus erythematosus. Lupus. 2017 May;26(6):646–9.

73 Werth V, Furie R, Gaudy A, Ye Y, Korish S, Delev N, et al. CC-220. Decreases B-Cell Subsets and Plasmacytoid Dendritic Cells in Systemic Lupus Erythematosus (SLE) Patients and Is Associated with Skin Improvement: Pharmacodynamic Results from a Phase IIa Proof of Concept Study [abstract]. Arthritis Rheumatol. Sept 2017; 69 (suppl 10).

74 Dauguet N, Fournié JJ, Poupot R, Poupot M. Lenalidomide down regulates the production of interferon-gamma and the expression of inhibitory cytotoxic receptors of human Natural Killer cells. Cell Immunol. 2010;264(2):163–70.

75 Nakayama Y, Kosek J, Capone L, Hur EM, Schafer PH, Ringheim GE. Aiolos overexpression in systemic lupus erythematosus B cell subtypes and BAFF-induced memory B cell differentiation are reduced by CC-220 modulation of cereblon activity. J Immunol. 2017 Oct;199(7):2388–407.

76 Gay F, Hayman SR, Lacy MQ, Buadi F, Gertz MA, Kumar S, et al. Lenalidomide plus dexamethasone versus thalidomide plus dexamethasone in newly diagnosed multiple myeloma: a comparative analysis of 411 patients. Blood. 2010 Feb;115(7):1343–50.

8. References

[1] Gaboriau HP, Murakami CS. Skin anatomy and flap physiology. *Otolaryngol Clin North Am*. 2001;34:555-569.

[2] Rawlings AV, Harding CR. Moisturization and skin barrier function. *Dermatol Ther*. 2004;17 Suppl 1:43-48.

[3] Boer M, Duchnik E, Maleszka R, Marchlewicz M. Structural and biophysical characteristics of human skin in maintaining proper epidermal barrier function. *Postepy Dermatol Alergol.* 2016;33:1-5.

[4] Kleczek P, Dyduch G, Graczyk-jarzynka A, A New Approach to Border Irregularity Assessment with Application in Skin Pathology. *Appl. Sci. 2019*, 1–24.

[5] Wong R, Geyer S, Weninger W, Guimberteau JC, Wong JK. The dynamic anatomy and patterning of skin. *Exp Dermatol*. 2016;25:92-98.

[6] Lai-Cheong E , McGrath JA. Structure and function of skin, hair and nails. *Med. (United Kingdom)*, 2013 41:317–320.

[7] Ramadon D, McCrudden MTC, Courtenay AJ, Donnelly RF. Enhancement strategies for transdermal drug delivery systems: current trends and applications [published online ahead of print, 2021 Jan 20]. *Drug Deliv Transl Res*. 2021;1-34.

[8] Moreci RS, Lechler T. Epidermal structure and differentiation. *Curr Biol*. 2020;30:R144-R149.

[9] Baroni A, Buommino E, De Gregorio V, Ruocco E, Ruocco V, Wolf R. Structure and function of the epidermis related to barrier properties. *Clin Dermatol.* 2012;30:257-262.

[10] Évora AS, Adams MJ, Johnson SA, Zhang Z. Corneocytes: Relationship between Structural and Biomechanical Properties. *Skin Pharmacol Physiol*. 2021;34:146-161.

[11] McLafferty E, Hendry C, Alistair F. The integumentary system: anatomy, physiology and function of skin. *Nurs Stand.* 2012;27 :35-42.

[12] Houben E, De Paepe K, Rogiers V. A keratinocyte's course of life. *Skin Pharmacol Physiol*. 2007;20:122-132.

[13] Smith EA, Fuchs E. Defining the interactions between intermediate filaments and desmosomes. *J Cell Biol*. 1998;141(5):1229-1241. doi:10.1083/jcb.141.5.1229

[14] Grove GL, Kligman AM. Age-associated changes in human epidermal cell renewal. *J Gerontol*. 1983;38:137-142.

[15] Lebre MC, van der Aar AM, van Baarsen L, et al. Human keratinocytes express functional Toll-like receptor 3, 4, 5, and 9. *J Invest Dermatol*. 2007;127:331-341.

[16] Kabashima K, Honda T, Ginhoux F, Egawa G. The immunological anatomy of the skin. *Nat Rev Immunol*. 2019;19:19-30.

[17] Gröne A. Keratinocytes and cytokines. *Vet Immunol Immunopathol*. 2002;88:1-12.

[18] Czernielewski JM, Bagot M. Class II MHC antigen expression by human keratinocytes results from lympho-epidermal interactions and gamma-interferon production. *Clin Exp Immunol*. 1986;66:295-302.

[19] Cichorek M, Wachulska M, Stasiewicz A, Tymińska A. Skin melanocytes: biology and development. *Postepy Dermatol Alergol*. 2013;30:30-41.

[20] Simon JD, Hong L, Peles DN. Insights into melanosomes and melanin from some interesting spatial and temporal properties. *J Phys Chem B*. 2008;112:13201-13217.

[21] Rajesh A, Wise L, Hibma M. The role of Langerhans cells in pathologies of the skin. *Immunol Cell Biol*. 2019;97:700-713.

[22] Clayton K, Vallejo AF, Davies J, Sirvent S, Polak ME. Langerhans Cells-Programmed by the Epidermis. *Front Immunol*. 2017;8:1676.

[23] Winkelmann RK, Breathnach AS. The Merkel cell. *J Invest Dermatol*. 1973;60:2-15.

[24] Otani T, Furuse M. Tight Junction Structure and Function Revisited [published correction appears in Trends Cell Biol. 2020 Dec;30(12):1014]. *Trends Cell Biol*. 2020;30:805-817.

[25] Daly CH. Biomechanical properties of dermis. *J. Invest. Dermatol.*,1982;79:17–20.

[26] desJardins-Park HE, Foster DS, Longaker MT. Fibroblasts and wound healing: an update. *Regen Med*. 2018;13:491-495.

[27] Epstein EH Jr, Munderloh NH. Human skin collagen. Presence of type I and type III at all levels of the dermis. *J Biol Chem*. 1978;253:1336-1337.

[28] Nguyen AV, Soulika AM. The Dynamics of the Skin's Immune System. *Int J Mol Sci*. 2019;20:1811.

[29] Rippa AL, Kalabusheva EP, Vorotelyak EA. Regeneration of Dermis: Scarring and Cells Involved. *Cells*. 2019;8:607.

[30] Nestle FO, Di Meglio P, Qin JZ, Nickoloff BJ. Skin immune sentinels in health and disease. *Nat Rev Immunol*. 2009;9::679-691.

[31] Kosaka K, Kubota Y, Adachi N, et al. Human adipocytes from the subcutaneous superficial layer have greater adipogenic potential and lower PPAR-γ DNA methylation levels than deep layer adipocytes. *Am J Physiol Cell Physiol*. 2016;311:C322-C329.

[32] Ali AT, Hochfeld WE, Myburgh R, Pepper MS. Adipocyte and adipogenesis. *Eur J Cell Biol*. 2013;92:229-236.

[33] Mathaes R, Koulov A, Joerg S, Mahler HC. Subcutaneous Injection Volume of Biopharmaceuticals-Pushing the Boundaries. *J Pharm Sci*. 2016;105:2255-2259.

[34] Gilliam JN, Sontheimer RD. Distinctive cutaneous subsets in the spectrum of lupus erythematosus. *J Am Acad Dermatol*. 1981;4:471-475.

[35] Kuhn A, Landmann A. The classification and diagnosis of cutaneous lupus erythematosus. *J Autoimmun*. 2014;48-49:14-19.

[36] Kuhn A, Wenzel J, Bijl M. Lupus erythematosus revisited. *Semin Immunopathol*. 2016;38:97-112.

[37] Okon LG, Werth VP. Cutaneous lupus erythematosus: diagnosis and treatment. *Best Pract Res Clin Rheumatol*. 2013;27:391-404.

[38] Walling HW, Sontheimer RD. Cutaneous lupus erythematosus: issues in diagnosis and treatment. *Am J Clin Dermatol*. 2009;10:365-381.

[39] Wenzel J. Cutaneous lupus erythematosus: new insights into pathogenesis and therapeutic strategies. *Nat Rev Rheumatol*. 2019;15:519-532.

[40] Sander CA, Yazdi AS , Flaig MJ , Kind P. Histologic findings in cutaneous lupus erythematosus, *Cutan. Lupus Erythematosus*, 2005. 297–303,

[41] Gilliam JN, Sontheimer RD. Subacute cutaneous lupus erythematosus. *Clin Rheum Dis*. 1982;8:343-352.

[42] Parodi A, Caproni M, Cardinali C, et al. Clinical, histological and immunopathological features of 58 patients with subacute cutaneous lupus erythematosus. A review by the Italian group of immunodermatology. *Dermatology*. 2000;200:6-10.

[43] Deng JS, Sontheimer RD, Gilliam JN. Relationships between antinuclear and anti-Ro/SS-A antibodies in subacute cutaneous lupus erythematosus. *J Am Acad Dermatol*. 1984;11:494-499.

[44] Tebbe B, Mansmann U, Wollina U, et al. Markers in cutaneous lupus erythematosus indicating systemic involvement. A multicenter study on 296 patients. *Acta Derm Venereol*. 1997;77:305-308.

[45] Cruz-Tapias P, Castiblanco J, Anaya JM. HLA Association with Autoimmune Diseases. In: Anaya JM, Shoenfeld Y, Rojas-Villarraga A, et al., editors. Autoimmunity: From Bench to Bedside [Internet]. Bogota (Colombia): El Rosario University Press; 2013 Jul 18. Chapter 17. Available from: https://www.ncbi.nlm.nih.gov/books/NBK459459/

[46] Borucki R, Werth VP. Cutaneous lupus erythematosus induced by drugs - novel insights. *Expert Rev Clin Pharmacol*. 2020;13:35-42.

[47] Nieboer C, Tak-Diamand Z, Van Leeuwen-Wallau HE. Dust-like particles: a specific direct immunofluorescence pattern in sub-acute cutaneous lupus erythematosus. *Br J Dermatol*. 1988;118:725-729.

[48] O'Brien JC, Chong BF. Not Just Skin Deep: Systemic Disease Involvement in Patients With Cutaneous Lupus. *J Investig Dermatol Symp Proc*. 2017;18:S69-S74.

[49] Haber JS, Merola JF, Werth VP. Classifying discoid lupus erythematosus: background, gaps, and difficulties. *Int J Womens Dermatol*. 2017;3:S62-S66.

[50] Garza-Mayers AC, McClurkin M, Smith GP. Review of treatment for discoid lupus erythematosus. *Dermatol Ther*. 2016;29:274-283.

[51] Kuhn A, Sticherling M, Bonsmann G. Clinical manifestations of cutaneous lupus erythematosus. *J Dtsch Dermatol Ges*. 2007;5:1124-1137.

[52] Callen JP, Fowler JF, Kulick KB. Serologic and clinical features of patients with discoid lupus erythematosus: relationship of antibodies to single-stranded deoxyribonucleic acid and of other antinuclear antibody subsets to clinical manifestations. *J Am Acad Dermatol*. 1985;13:748-755.

[53] Wieczorek IT, Propert KJ, Okawa J, Werth VP. Systemic symptoms in the progression of cutaneous to systemic lupus erythematosus. *JAMA Dermatol*. 2014;150:291-296.

[54] Baltaci M, Fritsch P. Histologic features of cutaneous lupus erythematosus. *Autoimmun Rev*. 2009;8:467-473.

[55] Crowson AN, Magro C. The cutaneous pathology of lupus erythematosus: a review. *J Cutan Pathol*. 2001;28:1-23.

[56] Fabbri P, Cardinali C, Giomi B, Caproni M. Cutaneous lupus erythematosus: diagnosis and management. *Am J Clin Dermatol*. 2003;4:449-465.

[57] Uva L, Miguel D, Pinheiro C, Freitas JP, Marques Gomes M, Filipe P. Cutaneous manifestations of systemic lupus erythematosus. *Autoimmune Dis*. 2012;2012:834291.

[58] Kulkarni S, Kar S, Madke B, Krishnan A, Prasad K. A rare presentation of verrucous/hypertrophic lupus erythematosus: A variant of cutaneous LE. *Indian Dermatol Online J*. 2014;5:87-88.

[59] Zhao YK, Wang F, Chen WN, et al. Lupus Panniculitis as an Initial Manifestation of Systemic Lupus Erythematosus: A Case Report. *Medicine (Baltimore)*. 2016;95:e3429.

[60] Patel S, Hardo F. Chilblain lupus erythematosus. *BMJ Case Rep*. 2013; 2013:bcr2013201165.

[61] Filotico R, Mastrandrea V. Cutaneous lupus erythematosus: clinico-pathologic correlation. *G Ital Dermatol Venereol*. 2018;153:216-229.

[62] Choonhakarn C, Poonsriaram A, Chaivoramukul J. Lupus erythematosus tumidus. *Int J Dermatol*. 2004;43:815-818.

[63] Grönhagen CM, Nyberg F. Cutaneous lupus erythematosus: An update. *Indian Dermatol Online J*. 2014;5:7-13.

[64] Jarukitsopa S, Hoganson DD, Crowson CS, et al. Epidemiology of systemic lupus erythematosus and cutaneous lupus erythematosus in a predominantly white population in the United States. *Arthritis Care Res (Hoboken)*. 2015;67:817-828.

[65] Durosaro O, Davis MD, Reed KB, Rohlinger AL. Incidence of cutaneous lupus erythematosus, 1965-2005: a population-based study. *Arch Dermatol*. 2009;145:249-253.

[66] Grönhagen CM, Fored CM, Granath F, Nyberg F. Cutaneous lupus erythematosus and the association with systemic lupus erythematosus: a population-based cohort of 1088 patients in Sweden. *Br J Dermatol*. 2011;164:1335-1341.

[67] Baek YS, Park SH, Baek J, Roh JY, Kim HJ. Cutaneous lupus erythematosus and its association with systemic lupus erythematosus: A nationwide population-based cohort study in Korea. *J Dermatol*. 2020;47:163-165.

[68] Petersen MP, Möller S, Bygum A, Voss A, Bliddal M. Epidemiology of cutaneous lupus erythematosus and the associated risk of systemic lupus erythematosus: a nationwide cohort study in Denmark. *Lupus*. 2018;27:1424-1430.

[69] Jarrett P, Thornley S, Scragg R. Ethnic differences in the epidemiology of cutaneous lupus erythematosus in New Zealand. *Lupus*. 2016;25:1497-1502.

[70] Deligny C, Clyti E, Sainte-Marie D, et al. Incidence of chronic cutaneous lupus erythematosus in French Guiana: a retrospective population-based study. *Arthritis Care Res (Hoboken)*. 2010;62:279-282.

[71] Jarrett P, Werth VP. A review of cutaneous lupus erythematosus: improving outcomes with a multidisciplinary approach. *J Multidiscip Healthc*. 2019;12:419-428.

[72] Kole AK, Ghosh A. Cutaneous manifestations of systemic lupus erythematosus in a tertiary referral center. *Indian J Dermatol*. 2009;54:132-136.

[73] Cojocaru M, Cojocaru IM, Silosi I, Vrabie CD. Manifestations of systemic lupus erythematosus. *Maedica (Bucur)*. 2011;6:330-336.

[74] Grönhagen CM, Gunnarsson I, Svenungsson E, Nyberg F. Cutaneous manifestations and serological findings in 260 patients with systemic lupus erythematosus [published correction appears in Lupus. 2011;20(3):336]. *Lupus*. 2010;19(10):1187-1194.

[75] Petri M, Orbai AM, Alarcón GS, et al. Derivation and validation of the Systemic Lupus International Collaborating Clinics classification criteria for systemic lupus erythematosus. *Arthritis Rheum*. 2012;64(8):2677-2686. doi:10.1002/art.34473

[76] Chong BF, Song J, Olsen NJ. Determining risk factors for developing systemic lupus erythematosus in patients with discoid lupus erythematosus. *Br J Dermatol*. 2012;166:29-35.

[77] Callen JP. Subacute cutaneous lupus erythematosus versus systemic lupus erythematosus. *J Am Acad Dermatol*. 1999;40:129-131.

[78] Provost TT. The Relationship Between Discoid and Systemic Lupus Erythematosus. *Arch Dermatol.* 1994;130:1308–1310.

[79] Patsinakidis N, Kautz O, Gibbs BF, Raap U. Lupus erythematosus tumidus: clinical perspectives. *Clin Cosmet Investig Dermatol*. 2019;12:707-719.

[80] Klein R, Moghadam-Kia S, Taylor L, et al. Quality of life in cutaneous lupus erythematosus. *J Am Acad Dermatol*. 2011;64:849-858.

[81] Fanouriakis A, Kostopoulou M, Alunno A, et al. 2019 update of the EULAR recommendations for the management of systemic lupus erythematosus. *Ann Rheum Dis*. 2019;78:736-745.

[82] Elston DM, Stratman EJ, Miller SJ. Skin biopsy: Biopsy issues in specific diseases [published correction appears in J Am Acad Dermatol. 2016 Oct;75(4):854]. *J Am Acad Dermatol*. 2016;74:1-18.

[83] Garelli CJ, Refat MA, Nanaware PP, Ramirez-Ortiz ZG, Rashighi M, Richmond JM. Current Insights in Cutaneous Lupus Erythematosus Immunopathogenesis. *Front Immunol*. 2020;11:1353.

[84] M. Meurer, “Immunopathology of Cutaneous Lupus Erythematosus Immunofluorescence Techniques in Cutaneous Lupus Erythematosus,” *Springer*, vol. Chapter 22, 2005.

[85] Albrecht J, Taylor L, Berlin JA, et al. The CLASI (Cutaneous Lupus Erythematosus Disease Area and Severity Index): an outcome instrument for cutaneous lupus erythematosus. *J Invest Dermatol*. 2005;125:889-894.

[86] Osmola A, Namysł J, Jagodziński PP, Prokop J. Genetic background of cutaneous forms of lupus erythematosus: update on current evidence. *J Appl Genet*. 2004;45:77-86.

[87] Little AJ, Vesely MD. Cutaneous Lupus Erythematosus: Current and Future Pathogenesis-Directed Therapies. *Yale J Biol Med*. 2020;93:81-95.

[88] Patel J, Borucki R, Werth VP. An Update on the Pathogenesis of Cutaneous Lupus Erythematosus and Its Role in Clinical Practice. *Curr Rheumatol Rep*. 2020;22:69.

[89] Rice G, Newman WG, Dean J, et al. Heterozygous mutations in TREX1 cause familial chilblain lupus and dominant Aicardi-Goutieres syndrome. *Am J Hum Genet*. 2007;80:811-815.

[90] Günther C, Berndt N, Wolf C, Lee-Kirsch MA. Familial chilblain lupus due to a novel mutation in the exonuclease III domain of 3' repair exonuclease 1 (TREX1). *JAMA Dermatol*. 2015;151:426-431.

[91] Colasanti T, Maselli A, Conti F, et al. Autoantibodies to estrogen receptor α interfere with T lymphocyte homeostasis and are associated with disease activity in systemic lupus erythematosus. *Arthritis Rheum*. 2012;64:778-787.

[92] Fisher J, Patel M, Miller M, Burris K. Anastrozole-induced subacute cutaneous lupus erythematosus. *Cutis*. 2016;98:E22-E26.

[93] Liang Y, Tsoi LC, Xing X, et al. A gene network regulated by the transcription factor VGLL3 as a promoter of sex-biased autoimmunee diseases. *Nat Immunol*. 2017;18:152-160.

[94] Fischer GF, Pickl WF, Faé I, Anegg B, Milota S, Volc-Platzer B. Association between chronic cutaneous lupus erythematosus and HLA class II alleles. *Hum Immunol*. 1994;41:280-284.

[95] Millard LG, Rowell NR, Rajah SM. Histocompatibility antigens in discoid and systemic lupus erythematosus. *Br J Dermatol*. 1977;96:139-144.

[96] Järvinen TM, Hellquist A, Koskenmies S, et al. Tyrosine kinase 2 and interferon regulatory factor 5 polymorphisms are associated with discoid and subacute cutaneous lupus erythematosus. *Exp Dermatol*. 2010;19:123-131.

[97] Sontheimer RD. Subacute cutaneous lupus erythematosus: 25-year evolution of a prototypic subset (subphenotype) of lupus erythematosus defined by characteristic cutaneous, pathological, immunological, and genetic findings. *Autoimmun Rev*. 2005;4:253-263.

[98] Millard TP, Kondeatis E, Cox A, et al. A candidate gene analysis of three related photosensitivity disorders: cutaneous lupus erythematosus, polymorphic light eruption and actinic prurigo. *Br J Dermatol*. 2001;145:229-236.

[99] Agnello V, Gell J, Tye MJ. Partial genetic deficiency of the C4 component of complement in discoid lupus erythematosus and urticaria/angioedema. *J Am Acad Dermatol*. 1983;9:894-898.

[100] Richardson B, Scheinbart L, Strahler J, Gross L, Hanash S, Johnson M. Evidence for impaired T cell DNA methylation in systemic lupus erythematosus and rheumatoid arthritis. *Arthritis Rheum*. 1990;33:1665-1673.

[101] Renauer P, Coit P, Jeffries MA, et al. DNA methylation patterns in naïve CD4+ T cells identify epigenetic susceptibility loci for malar rash and discoid rash in systemic lupus erythematosus. *Lupus Sci Med*. 2015;2:e000101.

[102] Luo Y, Zhang X, Zhao M, Lu Q. DNA demethylation of the perforin promoter in CD4(+) T cells from patients with subacute cutaneous lupus erythematosus. *J Dermatol Sci*. 2009;56:33-36.

[103] Luo Y, Zhao M, Lu Q. Demethylation of promoter regulatory elements contributes to CD70 overexpression in CD4+ T cells from patients with subacute cutaneous lupus erythematosus. *Clin Exp Dermatol*. 2010;35(:425-430.

[104] Relle M, Weinmann-Menke J, Scorletti E, Cavagna L, Schwarting A. Genetics and novel aspects of therapies in systemic lupus erythematosus. *Autoimmun Rev*. 2015;14:1005-1018.

[105] Wang Z, Chang C, Peng M, Lu Q. Translating epigenetics into clinic: focus on lupus. *Clin Epigenetics*. 2017;9:78.

[106] White CA, Pone EJ, Lam T, et al. Histone deacetylase inhibitors upregulate B cell microRNAs that silence AID and Blimp-1 expression for epigenetic modulation of antibody and autoantibody responses. *J Immunol*. 2014;193:5933-5950.

[107] Ceribelli A, Yao B, Dominguez-Gutierrez PR, Chan EK. Lupus T cells switched on by DNA hypomethylation via microRNA?. *Arthritis Rheum*. 2011;63:1177-1181.

[108] Ceribelli A, Yao B, Dominguez-Gutierrez PR, Nahid MA, Satoh M, Chan EK. MicroRNAs in systemic rheumatic diseases. *Arthritis Res Ther*. 2011;13:229.

[109] Sang W, Sun C, Zhang C, et al. MicroRNA-150 negatively regulates the function of CD4(+) T cells through AKT3/Bim signaling pathway. *Cell Immunol*. 2016;306-307:35-40.

[110] Baek D, Villén J, Shin C, Camargo FD, Gygi SP, Bartel DP. The impact of microRNAs on protein output. *Nature*. 2008;455:64-71.

[111] O'Brien J, Hayder H, Zayed Y, Peng C. Overview of MicroRNA Biogenesis, Mechanisms of Actions, and Circulation. *Front Endocrinol (Lausanne)*. 2018;9:402.

[112] Vickers KC, Palmisano BT, Shoucri BM, Shamburek RD, Remaley AT. MicroRNAs are transported in plasma and delivered to recipient cells by high-density lipoproteins [published correction appears in Nat Cell Biol. 2015 Jan;17(1):104]. *Nat Cell Biol*. 2011;13:423-433.

[113] Yi R, Fuchs E. MicroRNA-mediated control in the skin. *Cell Death Differ*. 2010;17:229-235.

[114] Neagu M, Constantin C, Cretoiu SM, Zurac S. miRNAs in the Diagnosis and Prognosis of Skin Cancer. *Front Cell Dev Biol*. 2020;8:71.

[115] Sonkoly E, Wei T, Janson PC, et al. MicroRNAs: novel regulators involved in the pathogenesis of psoriasis?. *PLoS One*. 2007;2:e610.

[116] Gerasymchuk M, Cherkasova V, Kovalchuk O, Kovalchuk I. The Role of microRNAs in Organismal and Skin Aging. *Int J Mol Sci*. 2020;21:5281.

[117] Millard TP, Hawk JL, McGregor JM. Photosensitivity in lupus. *Lupus*. 2000;9:3-10.

[118] Wang PW, Hung YC, Lin TY, et al. Comparison of the Biological Impact of UVA and UVB upon the Skin with Functional Proteomics and Immunohistochemistry. *Antioxidants (Basel)*. 2019;8:569.

[119] Skopelja-Gardner S, An J, Tai J, et al. The early local and systemic Type I interferon responses to ultraviolet B light exposure are cGAS dependent. *Sci Rep*. 2020;10:7908.

[120] Sarkar MK, Hile GA, Tsoi LC, et al. Photosensitivity and type I IFN responses in cutaneous lupus are driven by epidermal-derived interferon kappa. *Ann Rheum Dis*. 2018;77:1653-1664.

[121] Kreuter A, Lehmann P. Relevant new insights into the effects of photoprotection in cutaneous lupus erythematosus. *Exp Dermatol*. 2014;23:712-713.

[122] Piette EW, Foering KP, Chang AY, et al. Impact of smoking in cutaneous lupus erythematosus [published correction appears in Arch Dermatol. 2012 Dec;148(12):1369]. *Arch Dermatol*. 2012;148:317-322.

[123] Chasset F, Francès C, Barete S, Amoura Z, Arnaud L. Influence of smoking on the efficacy of antimalarials in cutaneous lupus: a meta-analysis of the literature [published correction appears in J Am Acad Dermatol. 2015 Aug;73(2):353]. *J Am Acad Dermatol*. 2015;72:634-639.

[124] Szczęch J, Samotij D, Werth VP, Reich A. Trigger factors of cutaneous lupus erythematosus: a review of current literature. *Lupus*. 2017;26:791-807.

[125] Lowe GC, Henderson CL, Grau RH, Hansen CB, Sontheimer RD. A systematic review of drug-induced subacute cutaneous lupus erythematosus [published correction appears in Br J Dermatol. 2014 Apr;170(4):999. Lowe, G [corrected to Lowe, G C]]. *Br J Dermatol*. 2011;164:465-472.

[126] Vaglio A, Grayson PC, Fenaroli P, et al. Drug-induced lupus: Traditional and new concepts. *Autoimmun Rev*. 2018;17:912-918.

[127] Kim JW, Kwok SK, Choe JY, Park SH. Recent Advances in Our Understanding of the Link between the Intestinal Microbiota and Systemic Lupus Erythematosus. *Int J Mol Sci*. 2019;20:4871.

[128] Greiling TM, Dehner C, Chen X, et al. Commensal orthologs of the human autoantigen Ro60 as triggers of autoimmunity in lupus. *Sci Transl Med*. 2018;10:eaan2306.

[129] Gallucci S, Matzinger P. Danger signals: SOS to the immune system. *Curr Opin Immunol*. 2001;13:114-119.

[130] Kuhn A, Wenzel J, Weyd H. Photosensitivity, apoptosis, and cytokines in the pathogenesis of lupus erythematosus: a critical review. *Clin Rev Allergy Immunol*. 2014;47:148-162.

[131] Zahn S, Rehkämper C, Ferring-Schmitt S, Bieber T, Tüting T, Wenzel J. Interferon-α stimulates TRAIL expression in human keratinocytes and peripheral blood mononuclear cells: implications for the pathogenesis of cutaneous lupus erythematosus. *Br J Dermatol*. 2011;165:1118-1123.

[132] Sáenz-Corral CI, Vega-Memíje ME, Martínez-Luna E, et al. Apoptosis in chronic cutaneous lupus erythematosus, discoid lupus, and lupus profundus. *Int J Clin Exp Pathol*. 2015;8:7260-7265.

[133] Scholtissek B, Zahn S, Maier J, et al. Immunostimulatory Endogenous Nucleic Acids Drive the Lesional Inflammation in Cutaneous Lupus Erythematosus. *J Invest Dermatol*. 2017;137:1484-1492.

[134] Saadeh D, Kurban M, Abbas O. Update on the role of plasmacytoid dendritic cells in inflammatory/autoimmune skin diseases. *Exp Dermatol*. 2016;25:415-421.

[135] Papayannopoulos V. Neutrophil extracellular traps in immunity and disease. *Nat Rev Immunol*. 2018;18:134-147.

[136] Safi R, Al-Hage J, Abbas O, Kibbi AG, Nassar D. Investigating the presence of neutrophil extracellular traps in cutaneous lesions of different subtypes of lupus erythematosus. *Exp Dermatol*. 2019;28:1348-1352.

[137] Mande P, Zirak B, Ko WC, et al. Fas ligand promotes an inducible TLR-dependent model of cutaneous lupus-like inflammation. *J Clin Invest*. 2018;128:2966-2978.

[138] Lood C, Arve S, Ledbetter J, Elkon KB. TLR7/8 activation in neutrophils impairs immune complex phagocytosis through shedding of FcgRIIA. *J Exp Med*. 2017;214:2103-2119.

[139] Chong BF, Tseng LC, Hosler GA, et al. A subset of CD163+ macrophages displays mixed polarizations in discoid lupus skin. *Arthritis Res Ther*. 2015;17:324.

[140] Yu C, Chang C, Zhang J. Immunologic and genetic considerations of cutaneous lupus erythematosus: a comprehensive review. *J Autoimmun*. 2013;41:34-45.

[141] Shipman WD, Chyou S, Ramanathan A, et al. A protective Langerhans cell-keratinocyte axis that is dysfunctional in photosensitivity. *Sci Transl Med*. 2018; 10:eaap9527.

[142] Solé C, Gimenez-Barcons M, Ferrer B, Ordi-Ros J, Cortés-Hernández J. Microarray study reveals a transforming growth factor-β-dependent mechanism of fibrosis in discoid lupus erythematosus. *Br J Dermatol*. 2016;175:302-313.

[143] Achtman JC, Werth VP. Pathophysiology of cutaneous lupus erythematosus. *Arthritis Res Ther*. 2015;17:182.

[144] Antonelli A, Ferrari SM, Giuggioli D, Ferrannini E, Ferri C, Fallahi P. Chemokine (C-X-C motif) ligand (CXCL)10 in autoimmune diseases. *Autoimmun Rev*. 2014;13:272-280.

[145] Oh SH, Roh HJ, Kwon JE, et al. Expression of interleukin-17 is correlated with interferon-α expression in cutaneous lesions of lupus erythematosus. *Clin Exp Dermatol*. 2011;36:512-520.

[146] Tanasescu C, Balanescu E, Balanescu P, et al. IL-17 in cutaneous lupus erythematosus. *Eur J Intern Med*. 2010;21:202-207.

[147] Jabbari A, Suárez-Fariñas M, Fuentes-Duculan J, et al. Dominant Th1 and minimal Th17 skewing in discoid lupus revealed by transcriptomic comparison with psoriasis [published correction appears in J Invest Dermatol. 2014 Jun;134(6):1780]. *J Invest Dermatol*. 2014;134:87-95.

[148] Zeidi M, Chen KL, Desai K, et al. AB003. Increased CD69+ tissue-resident memory T cells and STAT3 expression in cutaneous lupus erythematosus patients recalcitrant to antimalarials. *Ann Transl Med*. 2021;9:AB003.

[149] Wenzel J, Uerlich M, Wörrenkämper E, Freutel S, Bieber T, Tüting T. Scarring skin lesions of discoid lupus erythematosus are characterised by high numbers of skin-homing cytotoxic lymphocytes associated with strong expression of the type I interferon-induced protein MxA. *Br J Dermatol*. 2005;153:1011-1015.

[150] Taylor A, Verhagen J, Blaser K, Akdis M, Akdis CA. Mechanisms of immune suppression by interleukin-10 and transforming growth factor-beta: the role of T regulatory cells. *Immunology*. 2006;117:433-442

[151] Franz B, Fritzsching B, Riehl A, et al. Low number of regulatory T cells in skin lesions of patients with cutaneous lupus erythematosus. *Arthritis Rheum*. 2007;56:1910-1920.

[152] Liu Y, Xu M, Min X, et al. TWEAK/Fn14 Activation Participates in Ro52-Mediated Photosensitization in Cutaneous Lupus Erythematosus. *Front Immunol*. 2017;8:651.

[153] Casciola-Rosen LA, Anhalt G, Rosen A. Autoantigens targeted in systemic lupus erythematosus are clustered in two populations of surface structures on apoptotic keratinocytes. *J Exp Med*. 1994;179:1317-1330.

[154] Cozzani E, Drosera M, Gasparini G, Parodi A. Serology of Lupus Erythematosus: Correlation between Immunopathological Features and Clinical Aspects. *Autoimmune Dis*. 2014;2014:321359.

[155] Abernathy-Close L, Lazar S, Stannard J, et al. B Cell Signatures Distinguish Cutaneous Lupus Erythematosus Subtypes and the Presence of Systemic Disease Activity. *Front Immunol*. 2021;12:775353.

[156] Erkeller-Yuksel FM, Lydyard PM, Isenberg DA. Lack of NK cells in lupus patients with renal involvement. *Lupus*. 1997;6:708-712.

[157] Hofmann SC, Bosma A, Bruckner-Tuderman L, et al. Invariant natural killer T cells are enriched at the site of cutaneous inflammation in lupus erythematosus. *J Dermatol Sci*. 2013;71:22-28.

[158] Braunstein I, Klein R, Okawa J, Werth VP. The interferon-regulated gene signature is elevated in subacute cutaneous lupus erythematosus and discoid lupus erythematosus

and correlates with the cutaneous lupus area and severity index score. *Br J Dermatol*. 2012;166:971-975.

[159] Teijaro JR. Type I interferons in viral control and immune regulation. *Curr Opin Virol*. 2016;16:31-40.

[160] Bertolotti A, Boniface K, Vergier B, et al. Type I interferon signature in the initiation of the immune response in vitiligo. *Pigment Cell Melanoma Res*. 2014;27:398-407.

[161] Hile GA, Gudjonsson JE, Kahlenberg JM. The influence of interferon on healthy and diseased skin. *Cytokine*. 2020;132:154605.

[162] Robinson ES, Werth VP. The role of cytokines in the pathogenesis of cutaneous lupus erythematosus. *Cytokine*. 2015;73:326-334.

[163] Fetter T, Wenzel J. Cutaneous lupus erythematosus: The impact of self-amplifying innate and adaptive immune responses and future prospects of targeted therapies. *Exp Dermatol*. 2020;29:1123-1132.

[164] Oke V, Vassilaki I, Espinosa A, et al. High Ro52 expression in spontaneous and UV-induced cutaneous inflammation. *J Invest Dermatol*. 2009;129:2000-2010.

[165] Barkauskaite V, Ek M, Popovic K, Harris HE, Wahren-Herlenius M, Nyberg F. Translocation of the novel cytokine HMGB1 to the cytoplasm and extracellular space coincides with the peak of clinical activity in experimentally UV-induced lesions of cutaneous lupus erythematosus. *Lupus*. 2007;16:794-802.

[166] Martinotti S, Patrone M, Ranzato E. Emerging roles for HMGB1 protein in immunity, inflammation, and cancer. *Immunotargets Ther*. 2015;4:101-109.

[167] Means TK, Latz E, Hayashi F, Murali MR, Golenbock DT, Luster AD. Human lupus autoantibody-DNA complexes activate DCs through cooperation of CD32 and TLR9. *J Clin Invest*. 2005;115:407-417.

[168] Kuo PT, Zeng Z, Salim N, Mattarollo S, Wells JW, Leggatt GR. The Role of CXCR3 and Its Chemokine Ligands in Skin Disease and Cancer. *Front Med (Lausanne)*. 2018;5:271.

[169] Pothinamthong P, Janjumratsang P. A comparative study in efficacy and safety of 0.1% tacrolimus and 0.05% clobetasol propionate ointment in discoid lupus erythematosus by modified cutaneous lupus erythematosus disease area and severity index. *J Med Assoc Thai*. 2012;95:933-940.

[170] Jemec GB, Ullman S, Goodfield M, et al. A randomised controlled trial of R-salbutamol for topical treatment of discoid lupus erythematosus. *Br J Dermatol*. 2009;161:1365-1370.

[171] Kuhn A, Ruland V, Bonsmann G. Cutaneous lupus erythematosus: update of therapeutic options part I. *J Am Acad Dermatol*. 2011;65:e179-e193.

[172] Stiefel C, Schwack W. Photoprotection in changing times - UV filter efficacy and safety, sensitization processes and regulatory aspects. *Int J Cosmet Sci*. 2015;37:2-30.

[173] Chang AY, Werth VP. Treatment of cutaneous lupus. *Curr Rheumatol Rep*. 2011;13:300-307.

[174] Coondoo A, Phiske M, Verma S, Lahiri K. Side-effects of topical steroids: A long overdue revisit. *Indian Dermatol Online J*. 2014;5:416-425.

[175] Sticherling M. Update on the use of topical calcineurin inhibitors in cutaneous lupus erythematosus. *Biologics*. 2011;5:21-31.

[176] Kuhn A, Gensch K, Haust M, et al. Efficacy of tacrolimus 0.1% ointment in cutaneous lupus erythematosus: a multicenter, randomised, double-blind, vehicle-controlled trial. *J Am Acad Dermatol*. 2011;65:54-64.e642.

[177] Winkelmann RR, Kim GK, Del Rosso JQ. Treatment of Cutaneous Lupus Erythematosus: Review and Assessment of Treatment Benefits Based on Oxford Centre for Evidence-based Medicine Criteria. *J Clin Aesthet Dermatol*. 2013;6:27-38.

[178] Kuhn A, Aberer E, Bata-Csörgő Z, et al. S2k guideline for treatment of cutaneous lupus erythematosus - guided by the European Dermatology Forum (EDF) in cooperation with the European Academy of Dermatology and Venereology (EADV). *J Eur Acad Dermatol Venereol*. 2017;31:389-404.

[179] Yokogawa N, Eto H, Tanikawa A, et al. Effects of Hydroxychloroquine in Patients With Cutaneous Lupus Erythematosus: A Multicenter, Double-Blind, Randomised, Parallel-Group Trial. *Arthritis Rheumatol*. 2017;69:791-799.

[180] Ruiz-Irastorza G, Ramos-Casals M, Brito-Zeron P, Khamashta MA. Clinical efficacy and side effects of antimalarials in systemic lupus erythematosus: a systematic review. *Ann Rheum Dis*. 2010;69:20-28.

[181] Shipman WD, Vernice NA, Demetres M, Jorizzo JL. An update on the use of hydroxychloroquine in cutaneous lupus erythematosus: A systematic review. *J Am Acad Dermatol*. 2020;82:709-722.

[182] Oliveira-Santos M, Verani JF, Klumb EM, Albuquerque EM. Evaluation of adherence to drug treatment in patients with systemic lupus erythematosus in Brazil. *Lupus*. 2011;20:320-329.

[183] Costedoat-Chalumeau N, Amoura Z, Hulot JS, et al. Low blood concentration of hydroxychloroquine is a marker for and predictor of disease exacerbations in patients with systemic lupus erythematosus. *Arthritis Rheum*. 2006;54:3284-3290.

[184] Kuznik A, Bencina M, Svajger U, Jeras M, Rozman B, Jerala R. Mechanism of endosomal TLR inhibition by antimalarial drugs and imidazoquinolines. *J Immunol*. 2011;186:4794-4804.

[185] Yusuf IH, Sharma S, Luqmani R, Downes SM. Hydroxychloroquine retinopathy. *Eye (Lond)*. 2017;31(6):828-845.

[186] Eldeeb M, Chan EW, Omar A. Case Report: Hydroxychloroquine Retinopathy. *Optom Vis Sci*. 2018;95:545-549.

[187] Melles RB, Marmor MF. The risk of toxic retinopathy in patients on long-term hydroxychloroquine therapy [published correction appears in JAMA Ophthalmol. 2014 Dec;132(12):1493]. *JAMA Ophthalmol*. 2014;132:1453-1460.

[188] Murray JJ, Lee MS. Re: Marmor et al.: American Academy of Ophthalmology Statement: Recommendations on screening for chloroquine and hydroxychloroquine

retinopathy (2016 Revision). (Ophthalmology 2016;123:1386-1394). *Ophthalmology*. 2017;124:e28-e29.

[189] Feldmann R, Salomon D, Saurat JH. The association of the two antimalarials chloroquine and quinacrine for treatment-resistant chronic and subacute cutaneous lupus erythematosus. *Dermatology*. 1994;189:425-427.

[190] Sigges J, Biazar C, Landmann A, et al. Therapeutic strategies evaluated by the European Society of Cutaneous Lupus Erythematosus (EUSCLE) Core Set Questionnaire in more than 1000 patients with cutaneous lupus erythematosus. *Autoimmun Rev*. 2013;12:694-702.

[191] Kuhn A, Ruland V, Bonsmann G. Cutaneous lupus erythematosus: update of therapeutic options part II. *J Am Acad Dermatol*. 2011;65:e195-e213.

[192] Wenzel J, Brähler S, Bauer R, Bieber T, Tüting T. Efficacy and safety of methotrexate in recalcitrant cutaneous lupus erythematosus: results of a retrospective study in 43 patients. *Br J Dermatol*. 2005;153:157-162.

[193] Gammon B, Hansen C, Costner MI. Efficacy of mycophenolate mofetil in antimalarial-resistant cutaneous lupus erythematosus. *J Am Acad Dermatol*. 2011;65:717-721.e2.

[194] Chang AY, Ghazi E, Okawa J, Werth VP. Quality of life differences between responders and nonresponders in the treatment of cutaneous lupus erythematosus. *JAMA Dermatol*. 2013;149:104-106.

[195] Wozel G, Blasum C. Dapsone in dermatology and beyond. *Arch Dermatol Res*. 2014;306:103-124.

[196] Manzi S, Sánchez-Guerrero J, Merrill JT, et al. Effects of belimumab, a B lymphocyte stimulator-specific inhibitor, on disease activity across multiple organ domains in patients with systemic lupus erythematosus: combined results from two phase III trials. *Ann Rheum Dis*. 2012;71:1833-1838.

[197] McArdle A, Baker JF. A case of "refractory" lupus erythematosus profundus responsive to rituximab [case report]. *Clin Rheumatol*. 2009;28:745-746.
[198] Kieu V, O'Brien T, Yap LM, et al. Refractory subacute cutaneous lupus erythematosus successfully treated with rituximab. *Australas J Dermatol*. 2009;50:202-206.

[199] Morand EF, Furie R, Tanaka Y, et al. Trial of Anifrolumab in Active Systemic Lupus Erythematosus. *N Engl J Med*. 2020;382:211-221.

[200] Domingo S, Solé C, Moliné T, Ferrer B, Ordi-Ros J, Cortés-Hernández J. Efficacy of Thalidomide in Discoid Lupus Erythematosus: Insights into the Molecular Mechanisms. *Dermatology*. 2020;236:467-476.

[201] Franks ME, Macpherson GR, Figg WD. Thalidomide. *Lancet*. 2004;363:1802-1811.

[202] Vargesson N. Thalidomide-induced teratogenesis: history and mechanisms. *Birth Defects Res C Embryo Today*. 2015;105:140-156.

[203] Sheskin J. Thalidomide in the treatment of lepra reactions. *Clin Pharmacol Ther*. 1965;6:303-306.

[204] Londoño F. Thalidomide in the treatment of actinic prurigo. *Int J Dermatol*. 1973;12:326-328.

[205] Aguh C, Kwatra SG, He A, Okoye GA. Thalidomide for the treatment of chronic refractory prurigo nodularis. *Dermatol Online J*. 2018;24:13030/qt44n0k1xm.

[206] Grinspan D. Significant response of oral aphthosis to thalidomide treatment. *J Am Acad Dermatol*. 1985;12(1 Pt 1):85-90.

[207] Barba Rubio J, Franco Gonzalez F,. Discoid lupus erythematosus and thalidomide. Preliminary report [LUPUS ERITEMATOSO DISCOIDE Y TALIDOMINA. INFORME PRELIMINAR], 1975. [Online]. Available: https://riudg.udg.mx//handle/20.500.12104/68043.

[208] Amato RJ. Thalidomide: an antineoplastic agent. *Curr Oncol Rep*. 2002;4:56-62.
[209] Palumbo A, Facon T, Sonneveld P, et al. Thalidomide for treatment of multiple myeloma: 10 years later. *Blood*. 2008;111:3968-3977.

[210] Chasset F, Tounsi T, Cesbron E, Barbaud A, Francès C, Arnaud L. Efficacy and tolerance profile of thalidomide in cutaneous lupus erythematosus: A systematic review and meta-analysis. *J Am Acad Dermatol*. 2018;78:342-350.e4.

[211] Cortés-Hernández J, Torres-Salido M, Castro-Marrero J, Vilardell-Tarres M, Ordi-Ros J. Thalidomide in the treatment of refractory cutaneous lupus erythematosus: prognostic factors of clinical outcome. *Br J Dermatol*. 2012;166:616-623.

[212] Cuadrado MJ, Karim Y, Sanna G, Smith E, Khamashta MA, Hughes GR. Thalidomide for the treatment of resistant cutaneous lupus: efficacy and safety of different therapeutic regimens. *Am J Med*. 2005;118:246-250.

[213] Gordon JN, Goggin PM. Thalidomide and its derivatives: emerging from the wilderness. *Postgrad Med J*. 2003;79:127-132.

[214] Ito T, Ando H, Suzuki T, et al. Identification of a primary target of thalidomide teratogenicity. *Science*. 2010;327:1345-1350.

[215] Gandhi AK, Kang J, Havens CG, et al. Immunomodulatory agents lenalidomide and pomalidomide co-stimulate T cells by inducing degradation of T cell repressors Ikaros and Aiolos via modulation of the E3 ubiquitin ligase complex CRL4(CRBN.). *Br J Haematol*. 2014;164:811-821.

[216] Bjorklund CC, Lu L, Kang J, et al. Rate of CRL4(CRBN) substrate Ikaros and Aiolos degradation underlies differential activity of lenalidomide and pomalidomide in multiple myeloma cells by regulation of c-Myc and IRF4. *Blood Cancer J*. 2015;5:e354.

[217] Cytlak U, Resteu A, Bogaert D, et al. Ikaros family zinc finger 1 regulates dendritic cell development and function in humans. *Nat Commun*. 2018;9:1239.

[218] Fionda C, Abruzzese MP, Zingoni A, et al. The IMiDs targets IKZF-1/3 and IRF4 as novel negative regulators of NK cell-activating ligands expression in multiple myeloma. *Oncotarget*. 2015;6:23609-23630.

[219] Powell MD, Read KA, Sreekumar BK, Oestreich KJ. Ikaros Zinc Finger Transcription Factors: Regulators of Cytokine Signaling Pathways and $CD4^+$ T Helper Cell Differentiation. *Front Immunol*. 2019;10:1299.

[220] Thomas RM, Chen C, Chunder N, et al. Ikaros silences T-bet expression and interferon-gamma production during T helper 2 differentiation. *J Biol Chem*. 2010;285:2545-2553.

[221] Petzold G, Fischer ES, Thomä NH. Structural basis of lenalidomide-induced CK1α degradation by the CRL4(CRBN) ubiquitin ligase. *Nature*. 2016;532:127-130.

[222] Matyskiela ME, Lu G, Ito T, et al. A novel cereblon modulator recruits GSPT1 to the CRL4(CRBN) ubiquitin ligase. *Nature*. 2016;535:252-257.

[223] Asatsuma-Okumura T, Ando H, De Simone M, et al. p63 is a cereblon substrate involved in thalidomide teratogenicity. *Nat Chem Biol*. 2019;15:1077-1084.

[224] Matyskiela ME, Couto S, Zheng X, et al. SALL4 mediates teratogenicity as a thalidomide-dependent cereblon substrate. *Nat Chem Biol*. 2018;14:981-987.

[225] Sampaio EP, Sarno EN, Galilly R, Cohn ZA, Kaplan G. Thalidomide selectively inhibits tumor necrosis factor alpha production by stimulated human monocytes. *J Exp Med*. 1991;173:699-703.

[226] Jang DI, Lee AH, Shin HY, et al. The Role of Tumor Necrosis Factor Alpha (TNF-α) in Autoimmune Disease and Current TNF-α Inhibitors in Therapeutics. *Int J Mol Sci*. 2021;22:2719.

[227] Lee HS, Kwon HS, Park DE, et al. Thalidomide inhibits alternative activation of macrophages in vivo and in vitro: a potential mechanism of anti-asthmatic effect of thalidomide. *PLoS One*. 2015;1:e0123094.

[228] Meierhofer C, Dunzendorfer S, Wiedermann CJ. Theoretical basis for the activity of thalidomide. *BioDrugs*. 2001;15:681-703.

[229] Haslett PA, Corral LG, Albert M, Kaplan G. Thalidomide costimulates primary human T lymphocytes, preferentially inducing proliferation, cytokine production, and cytotoxic responses in the CD8+ subset. *J Exp Med*. 1998;187):1885-1892.

[230] Marriott JB, Clarke IA, Dredge K, Muller G, Stirling D, Dalgleish AG. Thalidomide and its analogues have distinct and opposing effects on TNF-alpha and TNFR2 during co-stimulation of both CD4(+) and CD8(+) T cells. *Clin Exp Immunol*. 2002;130:75-84.

[231] Payvandi F, Wu L, Naziruddin SD, et al. Immunomodulatory drugs (IMiDs) increase the production of IL-2 from stimulated T cells by increasing PKC-theta activation and enhancing the DNA-binding activity of AP-1 but not NF-kappaB, OCT-1, or NF-AT. *J Interferon Cytokine Res*. 2005;25:604-616.

[232] D'Amato RJ, Loughnan MS, Flynn E, Folkman J. Thalidomide is an inhibitor of angiogenesis. *Proc Natl Acad Sci U S A*. 1994;91:4082-4085.

[233] Kowalski TW, Fraga LR, Tovo-Rodrigues L, et al. Angiogenesis-related genes and thalidomide teratogenesis in humans: an approach on genetic variation and review of past in vitro studies. *Reprod Toxicol*. 2017;70:133-140.

[234] Wang L, Wang S, Xue A, Shi J, Zheng C, Huang Y. Thalidomide Inhibits Angiogenesis via Downregulation of VEGF and Angiopoietin-2 in Crohn's Disease. *Inflammation*. 2021;44:795-807.

[235] Komorowski J, Jerczyńska H, Siejka A, et al. Effect of thalidomide affecting VEGF secretion, cell migration, adhesion and capillary tube formation of human endothelial EA.hy 926 cells. *Life Sci*. 2006;78:2558-2563.

[236] Shortt J, Hsu AK, Johnstone RW. Thalidomide-analogue biology: immunological, molecular and epigenetic targets in cancer therapy. *Oncogene*. 2013;32:4191-4202.

[237] David-Bajar KM, Bennion SD, DeSpain JD, Golitz LE, Lee LA. Clinical, histologic, and immunofluorescent distinctions between subacute cutaneous lupus erythematosus and discoid lupus erythematosus. *J Invest Dermatol*. 1992;99:251-257.

[238] Méndez-Flores S, Hernández-Molina G, Enríquez AB, et al. Cytokines and Effector/Regulatory Cells Characterization in the Physiopathology of Cutaneous Lupus Erythematous: A Cross-Sectional Study. *Mediators Inflamm*. 2016;2016:7074829.

[239] Keyes E, Jobanputra A, Grinnell M, Feng R, Vazquez T, Diaz D, Werth V. An Analysis of Medication Responsiveness Based on Subtype and Race Within a Cohort of Cutaneous Lupus Erythematosus Patients [abstract]. Arthritis Rheumatol. 2021; 73 (suppl 10). https://acrabstracts.org/abstract/an-analysis-of-medication-responsiveness-based-on-subtype-and-race-within-a-cohort-of-cutaneous-lupus-erythematosus-patients/.

[240] Kuhn A, Rondinone R, Doria A, Shoenfeld Y. 1st International Conference on Cutaneous Lupus Erythematosus Düsseldorf, Germany, September 1-5, 2004. *Autoimmun Rev*. 2005;4(1):66-78.

[241] Reed SI. The ubiquitin-proteasome pathway in cell cycle control. *Results Probl Cell Differ*. 2006;42:147-181.

[242] Li C, Wang X, Song Q. MicroRNA 885-5p Inhibits Hepatocellular Carcinoma Metastasis by Repressing AEG1. *Onco Targets Ther*. 2020;13:981-988.

[243] Morgan EL, Chen Z, Van Waes C. Regulation of NFκB Signalling by Ubiquitination: A Potential Therapeutic Target in Head and Neck Squamous Cell Carcinoma?. *Cancers (Basel)*. 2020;12:2877.

[244] Oyoshi MK, Barthel R, Tsitsikov EN. TRAF1 regulates recruitment of lymphocytes and, to a lesser extent, neutrophils, myeloid dendritic cells and monocytes to the lung airways following lipopolysaccharide inhalation. *Immunology*. 2007;120:303-314.

[245] Pivarcsi A, Meisgen F, Xu N, Ståhle M, Sonkoly E. Changes in the level of serum microRNAs in patients with psoriasis after antitumour necrosis factor-α therapy. *Br J Dermatol*. 2013;169:563-570.

[246] Raaby L, Langkilde A, Kjellerup RB, et al. Changes in mRNA expression precede changes in microRNA expression in lesional psoriatic skin during treatment with adalimumab. *Br J Dermatol*. 2015;173:436-447.

[247] Tsoi LC, Hile GA, Berthier CC, et al. Hypersensitive IFN Responses in Lupus Keratinocytes Reveal Key Mechanistic Determinants in Cutaneous Lupus. *J Immunol*. 2019;202:2121-2130.

[248] Stannard JN, Reed TJ, Myers E, et al. Lupus Skin Is Primed for IL-6 Inflammatory Responses through a Keratinocyte-Mediated Autocrine Type I Interferon Loop. *J Invest Dermatol*. 2017;137:115-122.

[249] Gambichler T, Genc Z, Skrygan M, et al. Cytokine and chemokine ligand expression in cutaneous lupus erythematosus. *Eur J Dermatol*. 2012;22:319-323.

[250] Valastyan S, Weinberg RA. miR-31: a crucial overseer of tumor metastasis and other emerging roles. *Cell Cycle*. 2010;9:2124-2129.

[251] Stepicheva NA, Song JL. Function and regulation of microRNA-31 in development and disease. *Mol Reprod Dev*. 2016;83:654-674.

[252] Li D, Li XI, Wang A, et al. MicroRNA-31 Promotes Skin Wound Healing by Enhancing Keratinocyte Proliferation and Migration. *J Invest Dermatol*. 2015;135:1676-1685.

[253] Luan L, Shi J, Yu Z, Andl T. The major miR-31 target genes STK40 and LATS2 and their implications in the regulation of keratinocyte growth and hair differentiation. *Exp Dermatol*. 2017;26:497-504.

[254] Xiuli Y, Honglin W. miRNAs Flowing Up and Down: The Concerto of Psoriasis. *Front Med (Lausanne)*. 2021;8:646796.

[255] Yan S, Xu Z, Lou F, et al. NF-κB-induced microRNA-31 promotes epidermal hyperplasia by repressing protein phosphatase 6 in psoriasis. *Nat Commun*. 2015;6:7652.

[256] Xu N, Meisgen F, Butler LM, et al. MicroRNA-31 is overexpressed in psoriasis and modulates inflammatory cytokine and chemokine production in keratinocytes via targeting serine/threonine kinase 40. *J Immunol*. 2013;190:678-688.

[257] Yoshimura T. Discovery of IL-8/CXCL8 (The Story from Frederick). *Front Immunol*. 2015;6:278.

[258] Janssens AS, Lashley EE, Out-Luiting CJ, Willemze R, Pavel S, de Gruijl FR. UVB-induced leucocyte trafficking in the epidermis of photosensitive lupus erythematosus patients: normal depletion of Langerhans cells. *Exp Dermatol*. 2005;14:138-142.

[258] Xu N, Meisgen F, Butler LM, et al. MicroRNA-31 is overexpressed in psoriasis and modulates inflammatory cytokine and chemokine production in keratinocytes via targeting serine/threonine kinase 40. *J Immunol*. 2013;190:678-688.

[259] Chakir H, Wang H, Lefebvre DE, Webb J, Scott FW. T-bet/GATA-3 ratio as a measure of the Th1/Th2 cytokine profile in mixed cell populations: predominant role of GATA-3. *J Immunol Methods*. 2003;278:157-169.

[260] Gambichler T, Pätzholz J, Schmitz L, Lahner N, Kreuter A. FOXP3+ and CD39+ regulatory T cells in subtypes of cutaneous lupus erythematosus. *J Eur Acad Dermatol Venereol*. 2015;29(:1972-1977.

[261] Taherdangkoo K, Kazemi Nezhad SR, Hajjari MR, Tahmasebi Birgani M. miR-485-3p suppresses colorectal cancer via targeting TPX2. *Bratisl Lek Listy*. 2020;121:302-307.

[262] Koh HS, Lee S, Lee HJ, et al. Targeting MicroRNA-485-3p Blocks Alzheimer's Disease Progression. *Int J Mol Sci*. 2021;22:13136.

[263] Gu J, Zhang J, Huang W, et al. Activating miRNA-mRNA network in gemcitabine-resistant pancreatic cancer cell associates with alteration of memory $CD4^+$ T cells. *Ann Transl Med*. 2020;8:279.

[264] Han SH, Wu MY, Nam BY, et al. PGC-1*α* Protects from Notch-Induced Kidney Fibrosis Development. *J Am Soc Nephrol*. 2017;28:3312-3322.

[265] Lou C, Xiao M, Cheng S, et al. MiR-485-3p and miR-485-5p suppress breast cancer cell metastasis by inhibiting PGC-1α expression. *Cell Death Dis*. 2016;7:e2159.

[266] Wolf SJ, Estadt SN, Gudjonsson JE, Kahlenberg JM. Human and Murine Evidence for Mechanisms Driving Autoimmune Photosensitivity. *Front Immunol*. 2018;9:2430.

[267] Foering K, Chang AY, Piette EW, Cucchiara A, Okawa J, Werth VP. Characterization of clinical photosensitivity in cutaneous lupus erythematosus. *J Am Acad Dermatol*. 2013;69(:205-213.

[268] Zhou X, Yan J, Lu Q, Zhou H, Fan L. The pathogenesis of cutaneous lupus erythematosus: The aberrant distribution and function of different cell types in skin lesions. *Scand J Immunol*. 2021;93:e12933.

[269] Liang X, Qin C, Yu G, et al. Circular RNA circRAB31 acts as a miR-885-5psponge to suppress gastric cancer progressionvia the PTEN/PI3K/AKT pathway. *Mol Ther Oncolytics*. 2021;23:501-514.

[270] Zu Y, Wang Q, Wang H. Identification of miR-885-5p as a Tumor Biomarker: Regulation of Cellular Function in Cervical Cancer. *Gynecol Obstet Invest*. 2021;86:525-532.

[271] Jiang Z, Cui H, Zeng S, Li L. miR-885-5p Inhibits Invasion and Metastasis in Gastric Cancer by Targeting Malic Enzyme 1. *DNA Cell Biol*. 2021;40:694-705.

[272] Shou J, Gao H, Cheng S, Wang B, Guan H. LncRNA HOXA-AS2 promotes glioblastoma carcinogenesis by targeting miR-885-5p/RBBP4 axis. *Cancer Cell Int*. 2021;21:39.

[273] Lixin S, Wei S, Haibin S, Qingfu L, Tiemin P. miR-885-5p inhibits proliferation and metastasis by targeting IGF2BP1 and GALNT3 in human intrahepatic cholangiocarcinoma. *Mol Carcinog*. 2020;59:1371-1381.

[274] de Jong EM, van Erp PE, Ruiter DJ, van de Kerkhof PC. Immunohistochemical detection of proliferation and differentiation in discoid lupus erythematosus. *J Am Acad Dermatol*. 1991;25:1032-1038.

[275] Nandi D, Tahiliani P, Kumar A, Chandu D. The ubiquitin-proteasome system. *J Biosci*. 2006;31:137-155.

[276] Vangala JR, Dudem S, Jain N, Kalivendi SV. Regulation of PSMB5 protein and β subunits of mammalian proteasome by constitutively activated signal transducer and activator of transcription 3 (STAT3): potential role in bortezomib-mediated anticancer therapy. *J Biol Chem*. 2014;289:12612-12622.

[277] Glickman MH, Ciechanover A. The ubiquitin-proteasome proteolytic pathway: destruction for the sake of construction. *Physiol Rev*. 2002;82:373-428.

[278] Lalani AI, Zhu S, Gokhale S, Jin J, Xie P. TRAF molecules in inflammation and inflammatory diseases. *Curr Pharmacol Rep*. 2018;4:64-90.

[279] Wang CY, Mayo MW, Korneluk RG, Goeddel DV, Baldwin AS Jr. NF-kappaB antiapoptosis: induction of TRAF1 and TRAF2 and c-IAP1 and c-IAP2 to suppress caspase-8 activation. *Science*. 1998;281:1680-1683.

[280] Yamamoto H, Ryu J, Min E, et al. TRAF1 Is Critical for DMBA/Solar UVR-Induced Skin Carcinogenesis. *J Invest Dermatol*. 2017;137:1322-1332.

[281] Xie P. TRAF molecules in cell signaling and in human diseases. *J Mol Signal*. 2013;8:7.

[282] McPherson AJ, Snell LM, Mak TW, Watts TH. Opposing roles for TRAF1 in the alternative versus classical NF-κB pathway in T cells. *J Biol Chem*. 2012;287:23010-23019.

[283] Zhang XF, Zhang R, Huang L, et al. TRAF1 is a key mediator for hepatic ischemia/reperfusion injury. *Cell Death Dis*. 2014;5:e1467.

[284] Missiou A, Köstlin N, Varo N, et al. Tumor necrosis factor receptor-associated factor 1 (TRAF1) deficiency attenuates atherosclerosis in mice by impairing monocyte recruitment to the vessel wall. *Circulation*. 2010;121:2033-2044.

[285] Méndez-Flores S, Furuzawa-Carballeda J, Hernández-Molina G, et al. MicroRNA Expression in Cutaneous Lupus: A New Window to Understand Its Pathogenesis. *Mediators Inflamm*. 2019;2019:5049245.

[286] Nasca MR, O'Toole EA, Palicharla P, West DP, Woodley DT. Thalidomide increases human keratinocyte migration and proliferation. *J Invest Dermatol*. 1999;113:720-724.

[287] Keller M, Sollberger G, Beer HD. Thalidomide inhibits activation of caspase-1. *J Immunol*. 2009;183:5593-5599.

[288] Zhu M, Ma Y, Tan K, et al. Thalidomide with blockade of co-stimulatory molecules prolongs the survival of alloantigen-primed mice with cardiac allografts. *BMC Immunol*. 2020;21:19.

[289] Kim EJ, Lee JG, Kim JY, et al. Enhanced immune-modulatory effects of thalidomide and dexamethasone co-treatment on T cell subsets. *Immunology*. 2017;152:628-637.

[290] Navarini AA, Kerl K, French LE, Trüeb RM. Control of widespread hypertrophic lupus erythematosus with T-cell-directed biologic efalizumab. *Dermatology*. 2010;220:249-253.

[291] Song W, van der Vliet HJ, Tai YT, et al. Generation of antitumor invariant natural killer T cell lines in multiple myeloma and promotion of their functions via lenalidomide: a strategy for immunotherapy. *Clin Cancer Res*. 2008;14:6955-6962.

[292] Gadola SD, Dulphy N, Salio M, Cerundolo V. Valpha24-JalphaQ-independent, CD1d-restricted recognition of alpha-galactosylceramide by human CD4(+) and CD8alphabeta(+) T lymphocytes. *J Immunol*. 2002;168:5514-5520.

[293] Elkhal A, Pichavant M, He R, et al. CD1d restricted natural killer T cells are not required for allergic skin inflammation. *J Allergy Clin Immunol*. 2006;118(6):1363-1368.

[294] Goubier A, Vocanson M, Macari C, et al. Invariant NKT cells suppress CD8(+) T-cell-mediated allergic contact dermatitis independently of regulatory CD4(+) T cells. *J Invest Dermatol*. 2013;133:980-987.

[295] Tanno H, Kawakami K, Ritsu M, et al. Contribution of Invariant Natural Killer T Cells to Skin Wound Healing. *Am J Pathol*. 2015;185:3248-3257.

[296] Tanno H, Kawakami K, Kanno E, et al. Invariant NKT cells promote skin wound healing by preventing a prolonged neutrophilic inflammatory response. *Wound Repair Regen*. 2017;25:805-815.

[297] Godó M, Sessler T, Hamar P. Role of invariant natural killer T (iNKT) cells in systemic lupus erythematosus. *Curr Med Chem*. 2008;15:1778-1787.

[298] Verbon A, Juffermans NP, Speelman P, et al. A single oral dose of thalidomide enhances the capacity of lymphocytes to secrete gamma interferon in healthy humans. *Antimicrob Agents Chemother*. 2000;44:2286-2290.

[299] McHugh SM, Rifkin IR, Deighton J, et al. The immunosuppressive drug thalidomide induces T helper cell type 2 (Th2) and concomitantly inhibits Th1 cytokine production in mitogen- and antigen-stimulated human peripheral blood mononuclear cell cultures. *Clin Exp Immunol*. 1995;99:160-167.

[300] Gause WC, Wynn TA, Allen JE. Type 2 immunity and wound healing: evolutionary refinement of adaptive immunity by helminths. *Nat Rev Immunol*. 2013;13:607-614.

[301] Iborra-Egea O, Gálvez-Montón C, Roura S, et al. Mechanisms of action of sacubitril/valsartan on cardiac remodeling: a systems biology approach. *NPJ Syst Biol Appl*. 2017;3:12.

[302] Iborra-Egea O, Santiago-Vacas E, Yurista SR, et al. Unraveling the Molecular Mechanism of Action of Empagliflozin in Heart Failure With Reduced Ejection Fraction With or Without Diabetes. *JACC Basic Transl Sci*. 2019;4:831-840.

[303] Cheng J, Guo J, North BJ, Tao K, Zhou P, Wei W. The emerging role for Cullin 4 family of E3 ligases in tumorigenesis. *Biochim Biophys Acta Rev Cancer*. 2019;1871:138-159.

[304] Amare GG, Meharie BG, Belayneh YM. A drug repositioning success: The repositioned therapeutic applications and mechanisms of action of thalidomide. *J Oncol Pharm Pract*. 2021;27:673-678.

[305] Mori T, Ito T, Liu S, et al. Structural basis of thalidomide enantiomer binding to cereblon. *Sci Rep*. 2018;8:1294.

[306] Kowalski TW, Gomes JDA, Garcia GBC, et al. CRL4-Cereblon complex in Thalidomide Embryopathy: a translational investigation. *Sci Rep*. 2020;10:851.

[307] Ni A, Chen H, Wu Y, Li W, Chen S, Li J. Expression of IRF-4 and IBP in skin lesions of patients with psoriasis vulgaris. *J Huazhong Univ Sci Technolog Med Sci*. 2012;32:287-290.

[308] Nam S, Lim JS. Essential role of interferon regulatory factor 4 (IRF4) in immune cell development. *Arch Pharm Res*. 2016;39:1548-1555.

[309] Rodríguez-Carrio J, López P, Alperi-López M, Caminal-Montero L, Ballina-García FJ, Suárez A. IRF4 and IRGs Delineate Clinically Relevant Gene Expression Signatures in Systemic Lupus Erythematosus and Rheumatoid Arthritis. *Front Immunol*. 2019;9:3085.

[310] Zhu YX, Kortuem KM, Stewart AK. Molecular mechanism of action of immune-modulatory drugs thalidomide, lenalidomide and pomalidomide in multiple myeloma. *Leuk Lymphoma*. 2013;54:683-687.

[311] Watanabe T, Asano N, Meng G, et al. NOD2 downregulates colonic inflammation by IRF4-mediated inhibition of K63-linked polyubiquitination of RICK and TRAF6. *Mucosal Immunol*. 2014;7:1312-1325.

[312] Herzig S, Shaw RJ. AMPK: guardian of metabolism and mitochondrial homeostasis. *Nat Rev Mol Cell Biol*. 2018;19:121-135.

[313] Lee KM, Jo S, Kim H, Lee J, Park CS. Functional modulation of AMP-activated protein kinase by cereblon. *Biochim Biophys Acta*. 2011;1813:448-455.

[314] Yang SJ, Jeon SJ, Van Nguyen T, Deshaies RJ, Park CS, Lee KM. Ubiquitin-dependent proteasomal degradation of AMPK gamma subunit by Cereblon inhibits AMPK activity. *Biochim Biophys Acta Mol Cell Res*. 2020;1867:118729.

[315] Kwon E, Li X, Deng Y, Chang HW, Kim DY. AMPK is down-regulated by the CRL4A-CRBN axis through the polyubiquitination of AMPKα isoforms. *FASEB J*. 2019;33:6539-6550.

[316] Sawamura N, Yamada M, Fujiwara M, et al. The Neuroprotective Effect of Thalidomide against Ischemia through the Cereblon-mediated Repression of AMPK Activity. *Sci Rep*. 2018;8:2459.

[317] Zhang HX, Yuan J, Li YF, Li RS. Thalidomide decreases high glucose-induced extracellular matrix protein synthesis in mesangial cells via the AMPK pathway. *Exp Ther Med*. 2019;17:927-934.

[318] Kwon E, Li X, Deng Y, Chang HW, Kim DY. AMPK is down-regulated by the CRL4A-CRBN axis through the polyubiquitination of AMPKα isoforms. *FASEB J*. 2019;33:6539-6550.

[319] Cibrian D, de la Fuente H, Sánchez-Madrid F. Metabolic Pathways That Control Skin Homeostasis and Inflammation. *Trends Mol Med*. 2020;26:975-986.

[320] Karagianni F, Pavlidis A, Malakou LS, Piperi C, Papadavid E. Predominant Role of mTOR Signaling in Skin Diseases with Therapeutic Potential. *Int J Mol Sci*. 2022;23:1693.

[321] Dai J, Jiang C, Chen H, Chai Y. Rapamycin Attenuates High Glucose-Induced Inflammation Through Modulation of mTOR/NF-κB Pathways in Macrophages. *Front Pharmacol.* 2019;10:1292.

[322] Qian G, Liu T, Zhou C, Zhang Y. Successful treatment of recalcitrant granulomatous rosacea with oral thalidomide and topical pimecrolimus. *J Dermatol*. 2015;42:539-540.

[323] Chen M, Xie H, Chen Z, et al. Thalidomide ameliorates rosacea-like skin inflammation and suppresses NF-κB activation in keratinocytes. *Biomed Pharmacother*. 2019;116:109011.

[324] DiDonato JA, Mercurio F, Karin M. NF-κB and the link between inflammation and cancer. *Immunol Rev*. 2012;246:379-400.

[325] Pomerantz JL, Baltimore D. Two pathways to NF-kappaB. *Mol Cell*. 2002;10:693-695.

[326] Chen ZJ. Ubiquitin signalling in the NF-kappaB pathway. Nat Cell Biol. 2005;7:758-765.

[327] Bell S, Degitz K, Quirling M, Jilg N, Page S, Brand K. Involvement of NF-kappaB signalling in skin physiology and disease. *Cell Signal*. 2003;15:1-7.

[328] Liu T, Zhang L, Joo D, Sun SC. NF-κB signaling in inflammation. *Signal Transduct Target Ther*. 2017;2:17023.

[329] Xu N, Brodin P, Wei T, et al. MiR-125b, a microRNA downregulated in psoriasis, modulates keratinocyte proliferation by targeting FGFR2. *J Invest Dermatol*. 2011;131(7):1521-1529.

[330] Zheng F, Zhu J, Zhang W, Fu Y, Lin Z. Thal protects against paraquat-induced lung injury through a microRNA-141/HDAC6/IκBα-NF-κB axis in rat and cell models. *Basic Clin Pharmacol Toxicol*. 2021;128:334-347.

[331] Graudejus O, Ponce Wong RD, Varghese N, Wagner S and Morrison B (2019). Bridging the gap between in vivo and in vitro research: Reproducing in vitro the mechanical and electrical environment of cells in vivo. *Conference Abstract: MEA Meeting 2018 | 11th International Meeting on Substrate Integrated Microelectrode Arrays.*

[332] Goers L, Freemont P, Polizzi KM. Co-culture systems and technologies: taking synthetic biology to the next level. *J R Soc Interface*. 2014;11:20140065.

[333] Lee J, Koehler KR. Skin organoids: A new human model for developmental and translational research. *Exp Dermatol*. 2021;30:613-620.

[334] Condrat CE, Thompson DC, Barbu MG, et al. miRNAs as Biomarkers in Disease: Latest Findings Regarding Their Role in Diagnosis and Prognosis. *Cells*. 2020;9:276.

[335] Rupaimoole R, Han HD, Lopez-Berestein G, Sood AK. MicroRNA therapeutics: principles, expectations, and challenges. *Chin J Cancer*. 2011;30:368-370.

[336] Lawrence P, Ceccoli J. Advances in the Application and Impact of MicroRNAs as Therapies for Skin Disease. *BioDrugs*. 2017;31:423-438. 0243-4

[337] Yu H, Lin L, Zhang Z, Zhang H, Hu H. Targeting NF-κB pathway for the therapy of diseases: mechanism and clinical study. *Signal Transduct Target Ther*. 2020;5:209.

[338] Bacher S, Schmitz ML. The NF-kappaB pathway as a potential target for autoimmune disease therapy. *Curr Pharm Des*. 2004;10:2827-2837.

[339] Andrés RM, Montesinos MC, Navalón P, Payá M, Terencio MC. NF-κB and STAT3 inhibition as a therapeutic strategy in psoriasis: in vitro and in vivo effects of BTH. *J Invest Dermatol*. 2013;133:2362-2371.

[340] Tanaka A, Muto S, Jung K, Itai A, Matsuda H. Topical application with a new NF-kappaB inhibitor improves atopic dermatitis in NC/NgaTnd mice. *J Invest Dermatol*. 2007;127:855-863.

ACKNOWLEGMENTS - AGRAÏMENTS

El camí no ha estat gens fàcil i sense tots vosaltres no hagués arribat mai fins aquí.

Primer de tot agrair a la meva directora de Tesi, la **Dra**. **Fina Cortés**, per donar-me l'oportunitat de realitzar la tesi a la unitat del Lupus. Perquè de tu aprenc la perseverança, l'esforç i el treball. Gràcies per apostar sempre per la recerca en el Lupus i també per donar-me l'oportunitat d'entrar al món d'assaigs clínics com a coordinadora i formar-me en aquest últim any de tesi.

Gràcies a la meva tutora **Dra. Anna Meseguer** per acceptar la tutoria de la tesi i la seva disponibilitat i amabilitat durant tot el procés.

A la **Dra. Cristina Solé**, la meva companya imprescindible i incondicional. Gràcies perquè sense tu aquesta tesi no hagués estat possible. Gràcies per estar-hi SEMPRE. Perquè aquest any passat 2021 ha sigut un any molt dur per a tu i has estat en tot moment ajudant-me en el que calgués. Perquè m'has ensenyat molt no només en la vessant investigadora, sempre curiosa per buscar el perquè de les coses i inconformista sinó també a nivell personal amb la teva actitud sempre optimista lluitadora. *Pels padelsitos, el teu amor als Westerns i recent promoció a IP Investigadora principal!*

Al **Dr. Ordi** per transmetre'm la seva gran passió per el Lupus Eritematós tant a nivell clínic com a nivell de recerca biomèdica i aprendre de vostè dia rere dia durant el temps que vam coincidir.

Als **pacients amb Lupus**, per donar mostres de manera desinteressada i animar-nos a fer difusió de tot el que fem els investigadors a través de l'associació per a la investigació del lupus eritematós sistèmic (AILES).

Als que ha passat durant aquest temps pel Lupus Team, la **Ana Maria**, la **Mireia**, i el **Eloi**. Gràcies per fomentar un ambient genial de treball. Gràcies a la **Laura** per incorporar-te en l'últim tram, i per continuar amb el projecte presentat en aquesta tesi. A la **Montse** pels millors dinars de nadal: *un dels millors records que tinc.... al Ritz ajajaja.*

Gràcies als companys d'altres laboratoris del VHIR: **Laura, Vanesa, Paula, Ingrid, Lorena, Laura, Noelia**...és un plaer compartir estones amb vosaltres. **Maite** perquè recordo quan vam començar a parlar, tenia problemes amb els cultius i parlant amb tu em vas ajudar un munt a no donar-me per vençuda i a seguir lluitant i endavant. Perquè m'emporto una gran amistat i moltes ganes de noves aventures amb totes vosaltres: *California here we go?!.* **Núria** vas arribar quan més et necessitava.

Al personal de la UAT: **Marta, Pilar i Maria**. Als zeladors i al personal de coordinació **Helena i Fátima**. A la **Tresa Moliné** i la dra. **Berta Ferrer** d'anatomia patològica. A les infermeres de la USIC: **Carla** i **Gisela** Per la vostra amabilitat i ajuda.

Als meus amics **Gala**, que tu també estàs passant pel mateix, molts ànims futura doctora!. **Ainhoa, Eli** gracias por vuestros audios de whatsapp que dan la vida jaajjaj. **Cris Bierge**

por estar a mi lado y apoyarme siempre! **Silvia i Cris** per tot. **Uri i Pol** perquè el viatge a Bilbao em va donar moments molt feliços :)

Thanks to **Karin Loré** and **Liz** from Karolinska Institutet, because with you I learned a lot of immunology and I enjoyed a lot working in the lab and for this reason, I ended performing a phD.

Sheila por tu comprensión hoy entrego la tesis también gracias a ti.

A tu **Pau**, perquè has viscut tot de aquest camí de ben a prop. I perquè tinc moltes ganes de seguir creixent i compartint moments junts agafats de la mà. T'estimo!

Als meus pares, per confiar en mi i veure que si que seria capaç. Per animar-me sempre a no conformar-me i a voler millorar i augmentar el meu coneixement, formar-me, a tenir inquietuds i aspiracions. A **tota la meva família** per alegrar-se sempre dels meus petits èxits.

Em sento molt afortunada. Gràcies a tots!